Appendix F
Attainment Demonstration

Appendix F-1

Baltimore Nonattainment Area Ozone Modeling Protocol

Ozone Modeling Protocol

For Regulatory Photochemical Air Quality Modeling For the Baltimore Nonattainment Area

Prepared for:

The Environmental Protection Agency - Region 3

1650 Arch Street

Philadelphia, PA 19103-2029

Prepared by:

The Maryland Department of the Environment

1800 Washington Blvd, Ste. 730

Baltimore, MD 21230-1720

June 2006

(Final Draft)

PROTOCOL
For Regulatory Photochemical Air Quality Modeling
Of The Baltimore Nonattainment Area

TABLE OF CONTENTS

Appendix A - Modeling Schedules
Appendix B - Conceptual Model Information
Appendix C - Boundaries of the Modeling Domain
Appendix D - Diagnostic and Sensitivity Tests for 12-km and 4-km Horizontal Grid Resolutions
Appendix E - Horizontal Grid Definitions for MM5 and CMAQ Modeling Domains
Appendix F - Vertical Layer Definitions for MM5 and CMAQ Modeling Domains
Appendix G- MM5 Meteorological Model Configuration
Appendix H – SMOKE Emissions Model Configuration
Appendix I - CMAQ Air Quality Model Configuration
Appendix J - Supplemental Analyses and Weight of Evidence Techniques

I. MODELING STUDY DESIGN

A. Background and Objectives

In 1997, the ozone National Ambient Air Quality Standard was reviewed, and the Environmental Protection Agency (EPA) recommended that the ozone standard be changed from 0.12 parts per million (ppm) of ozone measured over one hour to a standard of 0.08 ppm measured over eight hours, with the average fourth highest concentration over a three-year period determining whether an area is in compliance. The revised standard recognizes current scientific view that the previous ozone standard of 0.12 ppm was not sufficiently protective of public health.

The State of Maryland is defined as four separate ozone nonattainment areas and one early action compact area. Cecil County is part of the Philadelphia, Wilmington, Trenton Non-Attainment Area (NAA). The Baltimore NAA includes Anne Arundel, Baltimore, Carroll, Harford, and Howard Counties and Baltimore City. The Washington, DC-MD-VA NAA includes Calvert, Charles, Frederick, Montgomery, and Prince George's Counties. Kent and Queen Anne's Counties are there own non-attainment area. Washington County is an early action compact area. This modeling protocol document deals only with the Baltimore NAA.

The Baltimore NAA has been classified as moderate for the 8-hour ozone standard with an attainment date of June 15, 2010. In making designations and classifications, EPA uses the most recent 3 years of monitoring data. The current designations and classifications are based on monitoring data collected in 2001-2003.

Table 1 identifies all jurisdictions within Maryland as designated by EPA.

Table 1. Maryland's Designations for the 8-Hour Ozone Standard

Area	Maryland Counties	Classification	Attainment Date
Philadelphia, Wilmington, Trenton Non-Attainment Area	Cecil	Moderate	June 2010
Baltimore Non-Attainment Area	Anne Arundel Baltimore (Baltimore City) Carroll Harford Howard	Moderate	June 2010
Washington, DC-MD-VA	Calvert Charles Frederick Montgomery Prince George's	Moderate	June 2010
Kent & Queen Anne's Counties	Kent Queen Anne's	Marginal	June 2007
Washington County	Washington	Early Action Compact (EAC) Area	December 2007
Other Maryland Counties	Allegany Caroline Dorchester Garrett Somerset St. Mary's Talbot Wicomico Worcester	Unclassifiable	NA

Figure 1 provides a graphical representation of the Maryland region.

Figure 1. Maryland's 8-Hour Ozone Non-Attainment Designations

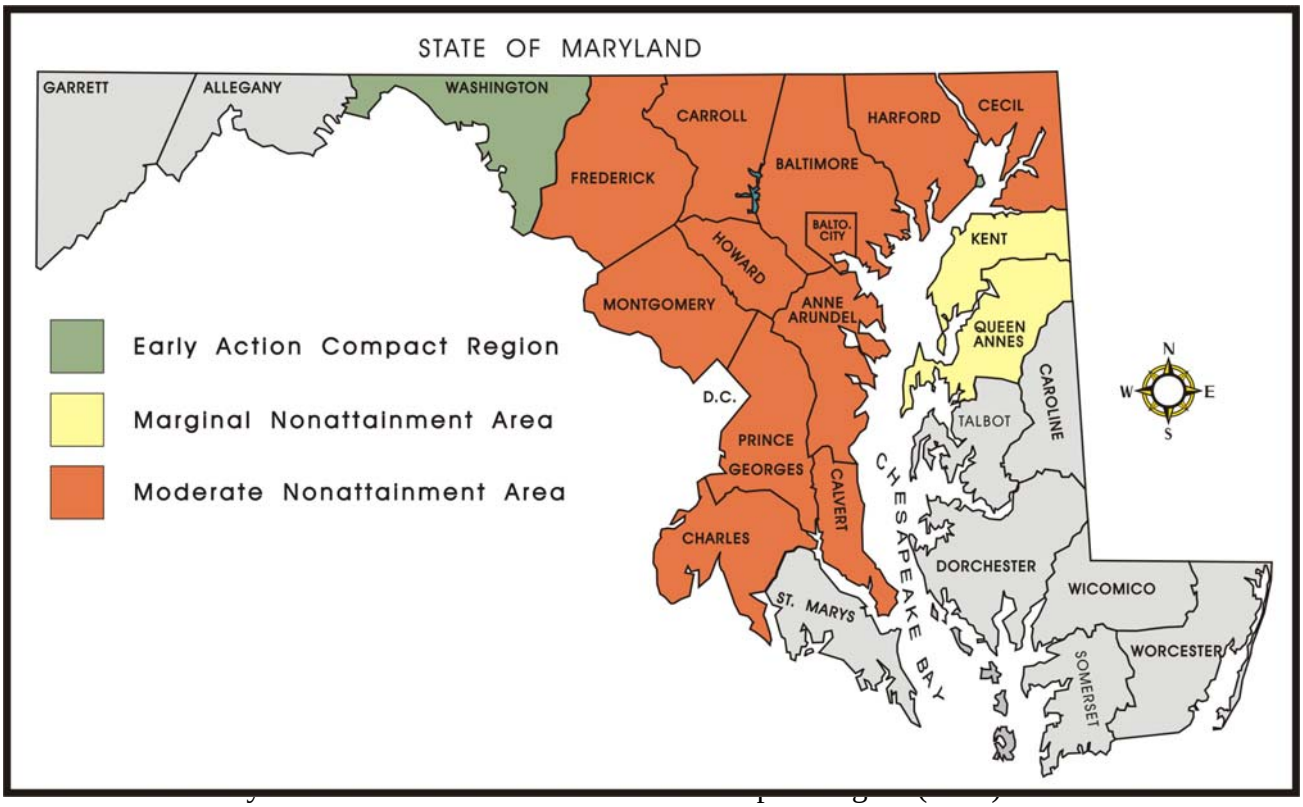

The Ozone Transport Commission (OTC) was tasked with the assignment of preparing an ozone modeling platform that all the Ozone Transport Region (OTR) states could use to demonstrate compliance with the 8-hour ozone standard. It is the responsibility of the Maryland Department of the Environment (MDE) for preparing this attainment demonstration for the Baltimore NAA.

The objective of this ozone modeling analyses is to enable the MDE to analyze the effectiveness of various control strategies, and to demonstrate that the measures adopted as part of the State Implementation Plan (SIP) will result in attainment of the 8-hour ozone standard by June 15, 2010. The procedures set forth in this modeling protocol have been developed in accordance with the Guidance on the Use of Models and Other Analyses in Attainment Demonstrations for the 8-hour Ozone NAAQS (EPA-454/R-05-002, October 2005).

The Baltimore NAA modeling analyses will directed by the MDE with modeling assistance from the University of Maryland at College Park (UMD). Upon completion of the draft modeling protocol it shall be submitted to EPA Region III for approval. Submission of the protocol and its subsequent approval by EPA Region III does not preclude future changes in the document deemed necessary by MDE. These changes may reflect evolving EPA

guidance, or the development or refinement of existing procedures.

B. Schedule and Deliverables

The CMAQ modeling for the Baltimore NAA will be a collaborative effort involving the other members of the OTR. The OTC has tasked the New York Department of Conservation (NYDEC) with completing the CMAQ 8-hour ozone modeling for the OTR. After the final CMAQ modeling is completed for the OTR, the MDE will determine if additional CMAQ modeling is necessary for the Baltimore NAA domain. If additional CMAQ modeling is required it will be completed by the UMD under contract with the MDE.

Installation of the models at NYDEC and UMD has been completed and diagnostic procedures have been run successfully. The NYDEC and UMD models have been properly benchmarked against each other and other modeling centers located within the OTR.

The modeling schedule for the Baltimore NAA attainment demonstration is provided in Appendix A. This appendix also provides the regional modeling schedule for the OTR. This schedule will periodically be updated during the modeling process.

The key deliverables for the CMAQ modeling effort are as follows:

- Select Ozone Episodes.
- Prepare Meteorological Fields.
- Prepare 2002 Emission Inventories for each OTC State.
- Acquire 2002 Emission Inventories for non-OTC States in OTR Domain.
- Prepare 2002 Emission Input Files for the OTR Domain.
- Complete 2002 Model Performance Evaluation for the OTR Domain.
- Prepare 2009 CAA Emission Inventories for each OTC State.
- Prepare 2009 CAA Emission Input Files for the OTR Domain.
- Complete Modeling Runs for 2009 CAA Scenarios.
- Design Control Strategy for the OTR Modeling Domain.
- Prepare 2009 Emission Input Files for OTR Control Strategy.
- Complete Modeling Runs for 2009 for Control Strategy.
- Complete Evaluation Report for 2009 Control Strategy.

C. Management Structure and Committees

OTC Oversight Committee
OTC Air Directors will serve as the OTR Oversight Committee. The Air Directors will ensure that 2002 and 2009 Clean Air Act (CAA) emission inventories are prepared for each OTC state in the OTR domain, and will also be responsible for obtaining emission inventories for OTR states that are not members of the OTC. The Air Directors will oversee the design of ozone control strategies for the OTR, and will make the final decision on any funding needed to develop the OTC SIP quality modeling system. The Air Directors will review all OTC SIP quality modeling system documentation before it is released to interested parties.

OTC Modeling Committee
The state members of the OTC Modeling Committee will provide policy and day to day technical guidance for the development of the OTC SIP quality modeling system. The modeling committee will recommend (to the OTC Air Directors) what tasks need to be funded in order to develop the OTC SIP quality modeling system in a timely fashion.

OTR Photochemical Modeling Workgroup
The OTR Photochemical Modeling Workgroup will be responsible for preparing the modeling assessment of the 8-hour ozone NAAQS in the OTR. The Workgroup will be responsible for collecting and processing model input data, setting up all model input files, performing model runs, and interpreting and documenting the results of the modeling analyses for the OTR domain. The Workgroup will prepare and submit all OTR SIP quality modeling system documentation to the OTC Air Directors. Gopal Sistla, NY DEC will serve as the lead for this group.

OTR Meteorological Modeling Workgroup
The OTR Meteorological Modeling Workgroup will be responsible for preparing and assessing MM5 meteorological fields for the OTR domain. The OTR Meteorological Modeling Workgroup will work with the OTR Photochemical Modeling Workgroup to prepare all meteorological input files for the OTC SIP quality modeling system. Michael Woodman, MDE, will serve as the lead for this group.

OTR Emission Inventory Development Workgroup
The OTR Emission Inventory Development Workgroup will be responsible for obtaining or developing guidance for preparing 2002 and 2009 state emission inventories for all states in the OTR. Ray Malenfant, DE DNREC, will serve as the lead for this group.

OTR Control Strategy Development Workgroup
The OTR Control Strategy Development Workgroup will be responsible for designing an ozone control strategy for the OTR Domain that will attain the ozone NAAQS by 2010 in moderate non-attainment areas. The Workgroup will work with OTR states and the OTC stationary and mobile source committees to design an effective ozone control strategy for the OTR domain. Jeff Underhill, NH DES, will serve as the lead for this group.

The lead-modeling agency for the OTR will be the NYDEC, but members of the OTR states within the framework of the OTC will manage the modeling project jointly. The MDE is responsible for conducting and submitting to EPA by June 15, 2007 the Baltimore NAA regional modeling attainment demonstration.

Table 2. OTC Technical Workgroup Leads

Lead	Workgroup
Gopal Sistla NYDEC 625 Broadway Albany, NY 12233 Email: gsistla@dec.state.ny.us Office: 518-402-8402 Fax: 518-402-9035	Photochemical
Michael Woodman MDE 1800 Washington Blvd Baltimore, MD 21230 Email: mwoodman@mde.state.md.us Office: 410-537-3229 Fax: 410-537-3202	Meteorological Modeling
Ray Malenfant DDNREC Division of Air & Waste Management Air Quality Management Section 156 South State Street Dover, DE 19901 Email: raymond.malenfant@state.de.us Phone: 302-739-9405 Fax: 302-739-9405	Emissions Inventory
Jeff Underhill NHDES 29 Hazen Drive Concord, NH 03302 Email: junderhill@des.state.nh.us Phone: 603-271-1370 Fax: 603-271-1381	Control Strategy

The role of the photochemical and meteorological modeling, emissions inventory and control strategy workgroups will be to assemble the necessary modeling inputs in the

proper format, to recommend the meteorological episodes and report on the effectiveness of control strategies that are modeled.

The workgroup leads will update the OTC Air Directors who will evaluate the recommended episodes and strategies, and the overall modeling methodology to ensure that these are appropriate and consistent with the directions of the OTR participating state agencies and EPA guidance.

The workgroup leads will prepare progress reports, either written or verbal, to the OTC Air Directors highlighting the status of tasks in the schedule shown in Appendix A, identifying significant conflicts or decisions, and recommending actions.

The workgroup leads, in conjunction with the OTR State members, will obtain information from the Technical Information Providers identified by their respective agencies as responsible for providing the air monitoring, meteorological, emission inventory and control strategy information necessary to perform the modeling described in this protocol.

Contractual Advisors will provide detailed technical advice on episode selection, sensitivity analyses, and the interpretation of meteorological output data from the model.

Table 3. Technical Information Providers

Organization	Contact Information
Mid-Atlantic Regional Air Management Association (MARAMA)	Patrick Davis Environmental Specialist Mid-Atlantic Regional Air Management Association 711 West 40th Street Suite 312 Baltimore, MD 21211-2109 Phone: (410) 467-0170 Email: pdavis@marama.org
Ozone Transport Commission (OTC)	Doug Austin Program Manager Ozone Transport Commission Hall of the States, 444 North Capitol St., Suite 638; Washington, DC 20001. USA (202) 508-3827 Email: daustin@otcair.org

Table 4. Contractual Advisors

Organization	Contact Information
University of Maryland Department of Atmospheric & Oceanic Science	Dale Allen Assistant Research Scientist University of Maryland Department of Atmospheric & Oceanic Science College Park, Maryland 20742-2425 Phone: 301-405-7629 Email: allen@atmos.umd.edu
University of Maryland Department of Atmospheric & Oceanic Science	Jeff Stehr Assistant Research Scientist University of Maryland Department of Atmospheric & Oceanic Science College Park, Maryland 20742-2425 Phone: 301-405-7638 Email: stehr@atmos.umd.edu
University of Maryland Department of Atmospheric & Oceanic Science	Charles Piety Faculty Research Assistant University of Maryland Department of Atmospheric & Oceanic Science College Park, Maryland 20742-2425 Phone: 301-405-7668 Email: charles@atmos.umd.edu
University of Maryland Department of Chemical Engineering (Emissions)	Sheryl Ehrman Department of Chemical Engineering 1223C Building 090 (office) 2113 Building 090 (mailing address) Department of Chemical Engineering University of Maryland College Park, MD 20742 Phone: (301) 405-1917 E-mail: sehrman@eng.umd.edu
University of Maryland Department of Atmospheric & Oceanic Science (Meteorology)	Da-Lin Zhang Professor University of Maryland Department of Atmospheric & Oceanic Science College Park, Maryland 20742-2425 Phone: 301-405-2018 Email: dalin@atmos.umd.edu
University of Maryland Department of Atmospheric & Oceanic Science (Meteorology)	Shunli Zhang Research Associate (postdoc) University of Maryland Department of Atmospheric & Oceanic Science College Park, Maryland 20742-2425 Phone: (301) 405-5321 Email: shunli@atmos.umd.edu

D. Committee/Participant Interaction

The lead agency for coordinating the running of the model and performing the modeling runs for the OTR will be the NYDEC. The lead agency for coordinating the running of the model and performing the modeling runs for the Baltimore NAA will be the MDE with the actual modeling being completed by the UMD under a contract with the MDE.

The workgroup leads will develop a process to recommend strategies to be modeled and to evaluate the benefits of the recommended strategies in accordance with a schedule developed by the Air Directors of the OTR.

E. Participating Organizations

The workgroup leads will obtain information from the individuals identified by each of the OTR agencies as responsible for providing the air monitoring, meteorological, emission inventory and control strategy information necessary to perform the modeling described in this protocol. The Control Strategy Workgroup will develop control strategies other than those mandated by the Clean Air Act. The Workgroup Lead will gather the necessary data to model both the required and selected control strategies and compile the results for review by the OTC Air Directors.

The Photochemical Modeling Workgroup Lead will present the modeling results to the OTC modeling committee for evaluation. The OTC modeling committee will then update and make a recommendation to the OTC Air Directors according to their established procedures. Further analysis may be necessary as determined by the involved committees or the OTC Air Directors for incorporation into the OTC air quality modeling plan may recommend other strategies. Insofar as resources permit, sufficient model runs will be completed to evaluate any policy option a state wishes to implement.

In general, the OTC Committees will attempt to avoid conflict regarding technical modeling issues by holding joint meetings and building consensus among the OTR members. The modeling shall in all cases be consistent with established EPA policies. In cases of policy disputes, the State Air Directors and Secretaries or their equivalents may be consulted for guidance. The State Air Directors will seek to resolve policy and technical issues at their level whenever possible before elevating the problem to the State Secretaries.

F. Relationship to Regional Modeling Protocols

The state of Maryland is a member of the OTC and this modeling protocol will follow the analyses being performed by the OTC.

G. Conceptual Model

EPA recommends that a conceptual description of the area's ozone problem be developed prior to the initiation of any air quality modeling study. A "conceptual description" is a qualitative way of characterizing the nature of an area's nonattainment problem. Within the conceptual description of a particular modeling exercise, it is recommended that the specific meteorological parameters that influence air quality be identified and qualitatively ranked in

importance.

The conceptual model for this study consists of the following components as provided in Appendix B:

1. A Conceptual Model for Ozone Transport, Prepared by Dr. Robert Hudson, Department of Atmospheric & Science, UMD, Date: January 24, 2006.

2. Determination of Representativeness of 2002 Ozone Season for Ozone Transport Region SIP Modeling Prepared for OTC, Prepared by Environ, June 2005.

3. Where Does Our Air Pollution Come From and What Do We Need To Do To Fix It, A Simplified Conceptual Model For the OTR, June 7, 2005.

4. Qualitative Episode Analysis of the 2002 Ozone Season (Ryan and Piety, 2002).

II. DOMAIN AND DATABASE ISSUES

A. Episode Selection

The procedures for selecting 8-hr ozone modeling episodes seek to achieve a balance between good science and regulatory needs and constraints. Modeling episodes, once selected, influence technical and policy decisions for many years. Clearly, both the direct and implicit procedures used in selecting episodes warrant full consideration.

Historically, ozone attainment demonstrations have been based on a limited number of episodes consisting of several days each. In the past, the number of days modeled has been limited by the speed of computers and the ability to store the model output files. With the advancement in computer technology over the past decade, computer speed and storage issues are no longer an impediment to modeling long time periods.

Additionally, recent research has shown that model performance evaluations and the response to emissions controls need to consider modeling results from long time periods, in particular full synoptic cycles or even full ozone seasons. In order to examine the response to ozone control strategies, it may not be necessary to model a full ozone season (or seasons), but EPA recommends it to model "longer" episodes that encompass full synoptic cycles.

The policy and technical criteria that influenced episode selection for this study include:

1. Choose a mix of episodes reflecting a variety of meteorological conditions that frequently correspond with observed 8-hour daily maxima greater than or equal to 85 ppb at multiple monitoring sites.
2. Model periods in which observed 8-hour daily maximum concentrations are close to the average 4th high 8-hour daily maximum ozone concentrations.
3. Model periods for which extensive air quality/meteorological data bases exist.
4. Model a sufficient number of days so that the modeled attainment test applied at each monitor violating the NAAQS is based on at least several days (i.e., 10 days).

A two-tiered approach will be applied in the selection of modeling episodes. It is intended that the entire 2002 ozone season (May 1 to September 30) will be simulated in the final SIP modeling analysis. However, it might be necessary to model smaller episode periods during the control strategy evaluation process as to maximize the number of control strategies that can be modeled. Therefore, individual modeling episodes may also be evaluated as part of this modeling process.

It is anticipated the total number of days examined under this two-tiered approach would far exceed EPA recommendations, and would also provide for better assessment of the simulated pollutant fields.

The individual smaller episode selection process will give preference to episodes occurring during the current average design value period. Additionally, multi-day episodes will be given preference to attempt to ensure that there are several days with monitored ozone

concentrations near the site-specific design value at each monitoring site in the nonattainment area.

The rationale for distinguishing among individual modeled episodes was conducted using a qualitative analysis (Ryan and Piety 2002) (Appendix B) and a quantitative analysis conducted by the consultant for the OTC (Environ 2005) (Appendix B).

The qualitative analysis was conducted through an evaluation of weather maps (surface and aloft) and air quality measurements, in order to distinguish between individual episodes with distinctively different meteorological regimes. Specifically, the qualitative analysis involved the evaluation of phenomenological variables, some of which are present during each high ozone weather pattern in Baltimore NAA. These include, but are not limited to, the following:

1. The presence of a migrating continental surface high pressure.
2. The strength and location of the upper air (500 mb) ridge.
3. Warm air advection in boundary layer prior to the episode onset.
4. Residual layer of high ozone aloft indicating transport of ozone and ozone precursors.
5. Appalachian Lee Trough (ALT) associated with a pollutant convergence zone east of the Appalachians.
6. Easterly Flow Reversal indicating transport from Northeast Corridor.
7. Low-Level Jet indicating transport from a southerly direction.
8. Re-circulation and frontal boundaries.

The result of this process produced the following seven proposed individual episodes:

1. Episode of June 9-12, 2002
2. Episode June 21-25, 2002
3. Episode of July 1-4, 2002
4. Episode of July 17-23, 2002
5. Episode of July 31-August 5, 2002
6. Episode of August 10-14, 2002
7. Episode of September 9-10, 2002

The selected individual episodes will be run in a “hot start” mode. Therefore, no “spin-up” days are required. The initial and boundary conditions for the individual episodes shall be obtained from the annual simulation.

To encompass these seven individual episodes, the following three individual episode “periods” were selected:

1. Episode of June 6-July 5, 2002
2. Episode of July 14-August 14, 2002
3. Episode of September 6-12, 2002

B. Size of the Modeling Domain

The boundaries of the OTC CMAQ modeling domain are provided in Appendix C. It is intended that the final SIP modeling analysis will utilize the modeling domain boundaries established by OTC.

C. Horizontal Grid Size

The OTC platform will provide the basic platform for the Baltimore NAA modeling analysis and will utilize a coarse grid continental United States (US) domain with a 36-km horizontal grid resolution. The CMAQ domain is nested in the MM5 domain. A larger MM5 domain was selected for the MM5 simulation to provide a buffer of several grid cells around each boundary of the CMAQ 36 km domain. This is designed to eliminate any errors in the meteorology from boundary effects in the MM5 simulation at the interface of the MM5 model. The buffer regions that will be used in the OTC simulations exceed the EPA suggestion of at least a 5 grid cell buffer at each boundary.

The horizontal grid size for the regional modeling domain is 12-km. As part of this modeling exercise and to address EPA recommendations, diagnostic and sensitivity tests were conducted by the VADEQ for both 12-km and 4-km grid resolutions in the Washington, D.C. region (see Appendix D). The results of these analyses resulted in the following conclusions:

1. The modeling results with 12-km grid cell size are slightly better than the modeling results using a 4-km grid resolution.
2. The increased computer costs, run times and data base management needs associated with the finer grid scales in combination with the performance results do not support the use of 4-km grid resolution modeling.

Appendix E contains the horizontal grid definitions for the MM5 and CMAQ modeling domains used in the OTC/MANE-VU modeling analyses.

D. Vertical Resolution

The vertical grid used in the MM5 modeling primarily defines the CMAQ vertical structure. The MM5 model employed a terrain following coordinate system defined by pressure. The layer averaging scheme adopted for CMAQ is designed to reduce the computational cost of the CMAQ simulations. The effects of layer averaging have a relatively minor effect on the model performance metrics when compared to ambient monitoring data.

Appendix E contains the vertical layer definitions for the MM5 and CMAQ modeling domains used in the OTC regional modeling analyses.

E. Initial and Boundary Conditions

The influence of boundary conditions shall be minimized to the extent possible. The modeling domains for the OTC are large enough to allow the use of clean or relatively

clean boundary conditions.

Prior experiences have shown that a 3-day ramp-up period is sufficient to establish pollutant levels that are encountered in the beginning of the ozone episode. The initial conditions at the startup would be for "clean" conditions.

In prior studies attempts have been made to include any information that is available from ozonesonde and from monitors that are near the boundaries of the modeling domain. For this study, similar attempts will be made to obtain pollutant data at the boundaries. In the absence of reliable boundary condition data, "clean conditions" will be assumed for boundary conditions.

F. Meteorological Model Selection and Configuration

The Pennsylvania State University/National Center for Atmospheric Research (PSU/NCAR) Mesoscale Meteorological Model (MM5) was selected for application in the OTC modeling analysis. The MM5 is a non-hydrostatic, prognostic meteorological model routinely used for urban- and regional-scale photochemical regulatory modeling studies.

Results of detailed performance evaluations of the MM5 modeling system in regulatory air quality application studies have been widely reported in the literature (i.e., Emery et al. 1999; Tesche et al., 2000, 2003) and many have involved comparisons with other prognostic models such as RAMS and SAIMM. The MM5 enjoys a far richer application history in regulatory modeling studies compared with RAMS or other models. Furthermore, in evaluations of these models in over 60 recent regional scale air quality application studies since 1995, it has been generally found that MM5 model tends to produce somewhat better photochemical model inputs than alternative models. For these reasons MM5 was selected as the meteorological modeling system for this modeling application.

The final SIP modeling analysis for the Baltimore NAA will utilize the MM5 data set developed by UMD in conjunction with OTC. The MM5 Setup has been described by Zhang (2000) for generating meteorological fields that are based on modified Blackadar scheme for the boundary layer. Provided in Appendix G are the MM5 configurations as selected by the OTC.

G. Emissions Model Selection and Configuration

The Sparse Matrix Operator Kernel Emissions (SMOKE) Emissions Processing System was selected for application in the OTR and Baltimore NAA modeling analysis. SMOKE is principally an emission processing system and not a true emissions inventory preparation system in which emissions estimates are simulated from 'first principles'. This means that, with the exception of mobile and biogenic sources, its purpose is to provide an efficient, modern tool for converting emissions inventory data into the formatted emission files required by an air quality simulation model. SMOKE is the

fastest emissions processing tool currently available to the air quality modeling community. The sparse matrix approach utilized throughout SMOKE permits both rapid and flexible processing of emissions data. The processing is rapid because SMOKE utilizes a series of matrix calculations instead of less efficient algorithms used in previous systems. The processing is flexible because the processing steps of temporal projection, controls, chemical speciation, temporal allocation, and spatial allocation have been separated into independent operations wherever possible. The results from these steps are merged together at a final stage of processing.

SMOKE supports area, mobile, fire, point and biogenic sources emission processing. The model can take on a variety of input formats from other emissions processing systems, including the Inventory Data Analyzer (IDA), Emissions Modeling System - 2003 (EMS-2003), and the Emissions Preprocessor System 2.x (EPS2.x). For biogenic emissions, SMOKE supports both gridded land use and county total land use data.

SMOKE (Version 2.1) will be used for the OTR and Baltimore NAA modeling demonstration. 2002 base case and 2009 future base case emissions data files will be provided by MANE-VU and other RPOs. Wherever possible, the mobile source emission inventory (in VMT format) will be replaced with SCC-specific county level emissions to more accurately reflect actual emissions for typical ozone season day.

Detailed SMOKE configurations are provided in Appendix H.

It is expected that the final SIP modeling analysis will be performed using the most current 2009 emissions inventory that is available from the MANE-VU RPO and other RPO's. Significant coordination efforts currently exist between RPOs in the development of these emissions inventories.

H. Air Quality Model Selection and Configuration

EPA's Models-3/Community Multi-scale Air Quality (CMAQ) modeling system is a 'One-Atmosphere' photochemical grid model capable of addressing ozone at regional scale and is considered one of the preferred models for regulatory modeling applications. The model is recommended by the Guidance on the Use of Models and Other Analyses in Attainment Demonstrations for the 8-hour Ozone NAAQS (EPA-454/R-05-002, October 2005).

CMAQ is generally considered by the scientific community to meet the following prerequisites for photochemical modeling applications:

1. It has been received and been revised in response to a scientific peer review.
2. It is appropriate for the specific application on a theoretical basis.
3. It shall be used with a data base that is adequate to support its application.
4. It has been shown to perform well in past ozone modeling applications.

5. It will be applied consistently with a protocol on methods and procedures.

Furthermore, several factors were considered as criteria for choosing CMAQ as a qualifying air quality model to support the Baltimore NAA modeling demonstration for the 8-hour ozone NAAQS. These factors are:

1. Documentation and past track record of in similar applications;
2. Advanced science and technical features available in the modeling system;
3. Experience of staff; and
4. Required time and resources versus available time and resources.

Lastly, CMAQ will be thoroughly validated and tested for this modeling application to ensure acceptable performance. The model evaluation shall be conducted in accordance with EPA guidance.

Detailed CMAQ configurations for the OTC modeling platform is provided in Appendix I.

I. Quality Assurance

All air quality, emissions, and meteorological data will be reviewed to ensure completeness, accuracy, and consistency before proceeding with modeling. Any errors, missing data or inconsistencies, will be addressed using appropriate methods that are consistent with standard practices. All modeling shall be benchmarked through the duplication of a set of standard modeling results.

Quality Assurance (QA) activities will be carried out for the various emissions, meteorological, and photochemical modeling components of the modeling study. Emissions inventories obtained from the RPO's will be examined through the use of quality assurance software, algorithms, and plotting routines to check for errors in the emissions estimates. When such errors are discovered, the problems in the input data files shall be corrected.

The MM5 meteorological and CMAQ air quality model inputs and outputs will be plotted and examined to ensure accurate representation of the observed data in the model-ready fields, and temporal and spatial consistency and reasonableness. Both MM5 and CMAQ will undergo an operational/scientific evaluation and this will facilitate, among other things, the quality assurance review of the meteorological and air quality modeling procedures. Data sets available to support this quality assurance of the aerometric inputs include the routine synoptic-scale data sets from the NWS 12-hourly rawinsondes and 3-hourly surface observations. These data include the horizontal wind components (u and v), temperature (T), and relative humidity (q) at the standard pressure levels, plus sea-level pressure (SLP) and ground temperature (Tg).

III. MODEL PERFORMANCE EVALUATION

A. Overview

The results of a model performance evaluation shall be considered prior to using modeling to support the attainment demonstration. The performance of CMAQ shall be evaluated using two methods:

1. Operational Evaluation - The model's ability to replicate observed concentrations of ozone and/or precursors (surface and aloft), and
2. Diagnostic Evaluation - The model's accuracy with respect to characterizing the sensitivity of ozone to changes in emissions (i.e., relative reduction factors).

B. Operational Evaluation

This section describes the statistical measures and other analytical techniques that shall be utilized to evaluate ozone model performance.

The following three statistical measures at a minimum shall be calculated for hourly ozone and 8-hourly maxima over the episode days in the attainment demonstration:

1. Mean Normalized Bias (MNB): This performance statistic averages the model/observation residual, normalized by observation, over all monitor times/locations.
2. Mean Normalized Gross Error (MNGE): This performance statistic averages the absolute value of the model/observation residual, normalized by observation, over all monitor times/locations.
3. Average Peak Prediction Accuracy: This is a measure of model performance that assesses only the ability of the model to predict daily peak 1-hour and 8-hour ozone.

The three metrics above shall be calculated two ways:

1. For pairs in which the 1-hour or 8-hour observed concentrations are greater than 60 ppb, and
2. For all pairs (no threshold).

In terms of pairing model predictions with monitored observations, the grid cell value in which the monitor resides shall be used for the calculations. Bi-linear interpolation of model predictions to specific monitoring locations may also be selected as an option if deemed necessary.

The three metrics shall be calculated for individual days (averaged over all sites) and individual sites (averaged over all days). Raw statistical results shall be aggregated into meaningful subregions or subperiods, as applicable. Other statistics may also be used (i.e., fractional bias, fractional error, root mean square error, and correlation coefficients) to the extent that they provide meaningful information. Wherever possible, these types of

performance measures shall be calculated for ozone precursors and related gas-phase oxidants (NOx, NOy, CO, HNO3, H2O2, VOCs and VOC species, etc.) and ozone (and precursors) aloft.

The following graphical display sets shall also be prepared and included as part of the performance analysis:

1. Time series plots of model and predicted hourly ozone for each monitoring location in the Baltimore NAA. Other sites may be included as deemed necessary.
2. Scatter plots of predicted and observed ozone at each site within the Baltimore NAA. These plots shall be completed using: a) all hours within the modeling period for hourly ozone, and b) all 8-hour daily maxima within the modeling period.
3. Daily tile plots of predicted ozone across the modeling domain with the actual observations as an overlay. Plots shall be completed for both daily 1-hour maxima and daily 8-hour maxima.
4. Animations of predicted hourly ozone concentrations for selected episode days as deemed necessary to evaluate transport patterns.

C. Diagnostic Evaluation

To aid the interpretation of simulation results, predicted and observed ozone concentration maps will be constructed. These concentration maps will present spatial information on the structure of the ozone plume. The following information shall be provided:

1. Maps of concentrations at one or two hour intervals will be constructed over periods of most interest, including recirculation, stagnation and transport conditions.
2. Maps depicting the highest predicted daily maximum ozone value for each grid cell will be prepared.
3. Predicted concentration to be used in the time-series plot will be consistent with a four-cell weighted average using bilinear interpolation of the prediction from the four adjacent grid cells nearest to the monitor location. Time-series plots will also be developed for NO, NO_2, and VOC species at selected locations, including comparisons between modeled and observed ratios of indicator species (i.e., O_3/NOy, O_3/HNO_3), particularly for cases in which ozone time-series or mapping results do not appear consistent with observations.
4. Comparison of ozone precursors will be done for concentration levels above the monitoring equipment's detectable limits.

Any modifications and diagnostic steps will be documented to avoid misinterpretation of model performance results.

IV. ATTAINMENT DEMONSTRATION

A. Overview

The modeled attainment demonstration consists of analyses that estimate whether selected emissions reductions will result in ambient concentrations that meet the 8-hour ozone NAAQS, and an identified set of control measures that will result in the required emissions reductions. The attainment demonstration estimates the amount of emission reduction needed to demonstrate attainment by using the modeled attainment test. Additional analyses may also be performed to indicate that a proposed emission reduction will lead to attainment of the NAAQS. The modeled attainment test predicts whether or not all estimated future design values will be less than or equal to the concentration level specified in the ozone NAAQS under meteorological conditions similar to those which have been simulated.

B. Modeling Attainment Test

The modeled attainment test applied at each monitor shall be performed using the following equation:

$(DVF)_I = (RRF)_I (DVC)_I$

Where:

$(DVC)_I$ = the baseline concentration monitored at site I, in ppb
$(RRF)_I$ = the relative reduction factor, calculated near site I
$(DVF)_I$ = the estimated future design value for the time attainment is required, in ppb.

Current design values shall be calculated using the average of the three design value periods that include the baseline inventory year. Specifically, the average design value shall be calculated using the 2000-2002, 2001-2003, and 2002-2004 periods.

In the event that there is less than five years of available data at a monitoring site the following procedure shall be used:

1. 4 years of data - The current design value will be based on an average of two design value periods.
2. 3 years of data - The current design value will be based on a single design value.
3. Less than 3 years of data – The site shall not be used in the attainment test.

A 3x3 array of grid cells surrounding each monitor shall be used in the modeled attainment test as recommended for 12-km grid resolution modeling to calculate RRFs.

The predicted 8-hour daily maximum concentrations from each modeled day shall be

used in the modeled attainment test with the nearby grid cell with the highest predicted 8-hour daily maximum concentration with baseline emissions for each day considered in the test, and the grid cell with the highest predicted 8-hour daily maximum concentration with the future emissions for each day in the test.

The RRFs used in the modeled attainment test shall be computed by taking the ratio of the mean of the 8-hour daily maximum predictions in the future to the mean of the 8-hour daily maximum predictions with baseline emissions, over all relevant days.

To avoid overestimates of future design values and provide for more robust RRFs and future design values, the following rules shall be applied to determine the number of days and the minimum threshold at each ozone monitor:

1. If there are 10 or more days with daily maximum 8-hour average modeled ozone > 85 ppb an 85 ppb threshold shall be used.
2. If there are less than 10 days with daily maximum 8-hour average modeled ozone > 85 ppb the threshold shall be reduced to as low as 70 ppb until there are 10 days in the mean RRF calculation.
3. If there are less than 10 days with daily maximum 8-hour average modeled ozone > 70 ppb then all days > 70 ppb shall be used.
4. No RRF calculations shall be performed for sites with less than 5 days > 70 ppb.

Table 5 provides the monitors that will be used for calculating RRFs in the Baltimore NAA.

Table 5. Monitors for Calculating RRFs in the Baltimore Nonattainment Area

AIRS ID	Monitor Name	County
24-003-0014	Davidsonville	Anne Arundel
24-003-0019	Ft. Meade	
25-005-1007	Padonia	Baltimore
24-005-3001	Essex	
24-013-0001	South Carroll	Carroll
24-025-1001	Edgewood	Harford
24-025-9001	Aldino	

C. Unmonitored Area Analysis

In the event that it is necessary to estimate design values at unmonitored locations within the Baltimore NAA, an "unmonitored area analysis" using model adjusted spatial fields shall be performed. The basic steps of this process are as follows:

1. Interpolate ambient ozone design value data to create a set of spatial fields.
2. Adjust the spatial fields using gridded model output gradients (base year values).
3. Apply gridded model RRFs to the model adjusted spatial fields.

4. Determine if any unmonitored areas are predicted to exceed the NAAQS in the future.

Recommended EPA guidance shall be utilized in the "unmonitored area analysis".

D. Emissions Inventories

For areas with an attainment date of no later than June 15, 2010, the emission reductions need to be implemented no later than the beginning of the 2009 ozone season. A determination of attainment will likely be based on air quality monitoring data collected in 2007, 2008, and 2009. Therefore, the year to project future emissions should be no later than the last year of the three-year monitoring period; in this case 2009.

The 2002 base year emissions inventory shall be projected to 2009 using standard emissions projection techniques. 2009 MANE-VU emission inventory shall be used in the attainment demonstration.

Emission inventory guidance documents will be followed for developing projection year inventories for point, area, mobile, and biogenic emissions. These procedures address projections of spatial, temporal, and chemical composition change between the base year and projection year.

The alternative control strategies for evaluation in the Baltimore NAA attainment demonstration will be selected by the MDE. These will be selected from groups of strategies developed by the technical staff responsible for identifying and developing the regulations and/or control measures.

Consideration will be given to maintaining consistency with control measures likely to be implemented by other modeling domains that may be involved in region-wide analysis. Also, technology-based emission reduction requirements mandated by the Clean Air Act will be included in the future year model runs.

E. Additional Analyses

Corroboratory evidence shall accompany the modeled attainment demonstration. EPA guidance for supplemental analyses and weight of evidence demonstrations shall be followed.

The weight of evidence submittal, if necessary, shall describe the analyses performed, databases used, key assumptions and outcomes of each analysis, and why the evidence, viewed as a whole, supports a conclusion that the Baltimore NAA will attain the NAAQS despite the model predicted future design value, or conversely, demonstrate that reaching attainment is not likely despite passing the model attainment test.

Table 6 provides guidelines for the supplemental analyses and weight of evidence determinations.

Table 6. Guidelines for Supplemental Analyses And Weight of Evidence Determinations

Results of Modeled Attainment Test	Supplemental Analyses
Future Design Value < 82 ppb, all monitor sites	Basic supplemental analyses should be completed to confirm the outcome of the modeled attainment test.
Future Design Value 82 - 87 ppb, at one or more sites/grid cells	A weight of evidence demonstration should be conducted to determine if aggregate supplemental analyses support the modeled attainment test.
Future Design Value > 88 ppb, at one or more sites/grid cells	More qualitative results are unlikely to support a conclusion differing from the outcome of the modeled attainment test.

A list of potential supplemental analyses and weight of evidence techniques are provided in Appendix J.

V. PROCEDURAL REQUIREMENTS

A. Reporting

Documents, technical memorandums, and data bases developed in the OTC study will be submitted to all parties of the OTR for review and subsequent distribution as appropriate. The various work products developed in preceding tasks will be synthesized and integrated to produce a draft Technical Support Document (TSD) that describes the full range of technical and modeling activities performed during the study. This report will contain the essential methods and results of the conceptual model, episode selection, modeling protocol, base case model development and performance testing, future year and control strategy modeling, quality assurance, weight of evidence analyses, and calculation of 8-hr ozone attainment via EPA's relative reduction factor (RRF) methodology.

The MDE is the state agency responsible for conducting and submitting to EPA a regional CMAQ modeling attainment demonstration that shows the Baltimore NAA in attainment for the 8-hour ozone NAAQS as of June 15, 2010 to EPA.

B. Data Archival and Transfer of Modeling Files

All relevant data sets, model codes, scripts, and related software required by any OTC project participant necessary to corroborate the study findings (e.g., performance evaluations, control strategy runs) will be provided in an electronic format. The MDE will be responsible for the archival of all modeling data relevant to the Baltimore NAA. Transfer of data may be facilitated through the combination of a website and the transfer of large databases via overnight mail. Database transfers will be accomplished using an

ftp protocol for smaller datasets, and the use of IDE and Firewire disk drives for larger data sets that allow the transfer of hundreds of gigabytes of data quickly and efficiently.

GENERAL REFERENCES

Ryan, W.F., Piety, C. (2002) Summary of 2002 Pollution Episodes in the Mid-Atlantic. The Pennsylvania State University Department of Meteorology, State College, Pennsylvania and the University of Maryland Department of Meteorology, College Park, Maryland.

Stoeckenius, T., Kemball-Cook, S. (2005) Ozone Episode Classification Project for Ozone Transport Commission (Task 2b), ENVIRON International Corporation, Novato, California.

Hudson, Dr. Robert (2006) A Conceptual Model for Ozone Transport. Department of Atmospheric & Oceanic Science, University of Maryland, College Park, Maryland.

Where Does Our Air Pollution Come From and What Do We Need To Do To Fix It?, A Simplified Conceptual Model for the OTR, OTC Annual Meeting, June 2005.

A Modeling Protocol for the OTC SIP Quality Modeling System For Assessment of the Ozone National Ambient Air Quality Standard in the Ozone Transport Region, The Modeling Committee of the Ozone Transport Commission.

EPA GUIDANCE DOCUMENTS

Guidance on the Use of Models and Other Analyses in Attainment Demonstrations for the 8-hour Ozone NAAQS (EPA-454/R-05-002, October 2005). U.S. Environmental Protection Agency, Research Triangle Park, N.C.

APPENDIX A

Modeling Schedules

MDE Timeline for the 8-Hour Ozone SIP

Modeling Tasks	Responsible Parties	Dates															
		2003 Fall	2003-04 Winter	2004 Spring	2004 Summer	2004 Fall	2004-05 Winter	2005 Spring	2005 Summer	2005 Fall	2005-06 Winter	2006 Spring	2006 Summer	2006 Fall	2006-07 Winter	2007 Spring	2007 Summer
Initial Planning																	
Prepare work plan	OTC	**Completed**						**Revised**									
Modeling protocol	MDE											**Completed**					
Conceptual Model	OTC/ENVIRON								**Completed**								
	MDE										**Completed**						
2002 Meteorological Processing and Evaluation																	
MM5 Modeling	UMD								**Completed**								
MCIP Processing for CMAQ Input	UMD,OTC/NYDEC								**Completed**								
Emissions Inventory Preparation																	
2002 Base Case V3	MARAMA												**Completed**				
2009 Future Base Case V3	MARAMA												**Completed**				
2009 Control Cases V3	MARAMA												**Completed**				
Emission Inventory Processing - SMOKE																	
2002 Base Case	OTC/NYDEC												**Completed**				
2009 Future Base Case	OTC/NYDEC												**Completed**				
2009 Control Cases	OTC/NYDEC												**Completed**				
CMAQ Modeling																	
2002 Base Case	OTC/NYDEC												**Completed**				
2002 Base Case Model Performance Evaluation	MDE/UMD												**Completed**				
	OTC/NYDEC												**Completed**				
Sensitivity runs for control measures	MDE/UMD												**Completed**				
	OTC/NYDEC												**Completed**				
CAIRplus Scenarios	OTC/NYDEC												**Completed**				
2009 CAA scenarios (OTB &OTW)	OTC/NYDEC																
2002 Final Base Case	OTC/NYDEC													**Completed**			
2009 Final Base Case	OTC/NYDEC													**Completed**			
2009 Final Control Case	OTC/NYDEC													**Completed**			
Additional Modeling Analyses																	
Weight of evidence	MDE/UMD														**Completed**		
Modeling technical support	NYDEC, MDE/UMD														**Completed**		
Control Strategy Development																	
CALGRID screening runs	OTC/NHDES												**Completed**				
Control strategy design	OTC												**Completed**				
Reports																	
Technical reports														**Completed**			

Appendix A

Work plan for the Development and Application of the OTC SIP Quality Modeling System[†]
Revised by S.Dennis and Gopal Sistla May 25, 2005

Task No.	Activity or Task	Initial Target Date	Organization(s) Performing Task	Remarks and Status Notes and Revised Anticipated Completion Dates (See
	Initial Planning			
1	Prepare a Work plan and a Modeling Protocol for the development of the OTC SIP quality modeling system to address ozone non-attainment problems in the OTR.	Nov 03	NY, MA	Completed
	Meteorology			
2	Complete MM5 modeling for 2002 (May thru Sep)	Dec 04	MD (UMD), NY	Completed
3	Episode evaluation and assessment	Dec 04	Environ	Completed
4	Evaluate MM5 data and process for photochemical models.	Dec 04	MD (UMD), NY	Completed
	Emissions Inventories			
5	Prepare 2002 emission inventories for MANEVU states in the OTR Domain.	Jan 05	MARAMA	Completed
6	Obtain 2002 emission inventories for non-MANEVU states in the OTR Domain.	Jan 05	MARAMA	Completed
7	Prepare 2009 CAA emission inventories for MANEVU states in the OTR Domain.	Aug 05	MARAMA	
8	Obtain 2009 CAA emission inventories for non-MANEVU states in the OTR Domain.	Aug 05	MARAMA	
	Emission Input files			
9	Prepare 2002 emission files for the OTR domain with SMOKE and /or EMS2001, and QA emissions data.	Nov 04	NY	Completed
10	Prepare 2009 CAA emission files for the OTR domain with SMOKE and /or EMS2001, and QA emissions data.	Nov 05	NY	
11	Prepare 2009 emission files for OTR control strategy with SMOKE and /or EMS2001, and QA emissions data.	Nov 05	NY	

Task No.	Activity or Task	Initial Target Date	Organization(s) Performing Task	Status Notes and Revised Anticipated Completion Dates (See any footnotes for any additional discussion)
	Modeling			
12	Complete 2002 model performance evaluation for OTR Domain.	May 06	NY	36 and 12 km grid CMAQ modeling on-going
13	Test model sensitivity to NOx, VOC reductions and potential control measure options.	Jul 06	NY	
14	Complete modeling runs for 2009 CAA scenarios.	Jul 06	NY	
15	Complete modeling runs for 2009 OTR control strategy	Jul 06	NY	
	OTR Control Strategy Development			
16	Perform screening runs with OTC CALGRID modeling system	May 06	OTR Control Strategy Development Workgroup	
17	Review air quality and emission databases to help identify potential sources of ozone in the OTR.	May 06	OTR Control Strategy Development Workgroup	
18	Design Control Strategy for the OTR Domain	May 06	OTR Control Strategy Development Workgroup	
	Reports			
19	Complete technical support documents presenting regional OTR modeling and air quality/emission database analyses. (These two documents will provide technical support for state ozone SIPs.	July 06	NY, other OTC states?	.
	Management			
20	Day-to-day management and coordination.	on-going	OTC Modeling Committee	
21	Provide direction, oversight, and obtain any necessary funding.	on-going	OTC Air Directors	

[†] To be used as needed for Ozone SIPs in the OTR. Based on EPA draft guidance, Ozone SIPs expected submission by April 2007.

APPENDIX B

Conceptual Model Information

A Conceptual Model for Ozone Transport

Prepared by:

Dr. Robert Hudson

Department of Atmospheric & Oceanic Science

University of Maryland

College Park, MD 20742

January 24, 2006

1. Introduction

Locations downwind of urban areas with high ozone (O_3) levels and substantial ozone precursors can be subject to high ozone exposure because winds carry VOCs and NO_x, as well as ozone itself, from their original sources. Ozone transport can occur at ground level on surface winds, or ozone can be transported long distances on wind currents above the atmospheric mixing layer. Whether the transported pollutants travel long distances or short distances, the transport phenomenon makes ozone a regional problem. It can geographically separate the source of the pollution from the location of high ozone levels and poor air quality.

For more than a quarter of a century, states in the eastern United States have been designing and implementing programs to attain the air quality standard for ground level ozone. Although much progress has been made to improve air quality, many areas have yet to attain the EPA ozone standard. Progress in attaining the health-based ozone standard has been limited by ozone transport. Traditional programs that primarily focus on controls in the vicinity of the ozone standard violation are not adequate for many areas. It has become apparent that, to attain the standard, it is necessary to also develop control programs that reduce ozone-forming pollutants that are emitted many miles upwind of the area of violation.

This report summarizes the current knowledge of the meteorological processes that impact ozone levels which occur in the Ozone Transport Region (OTR).

2. Temperature inversions

An important element in the production of severe ozone events is the ability of the atmosphere through temperature inversions to inhibit the mixing processes which under normal conditions would lead to dilution of the emitted pollutants. One can identify two major classes of temperature inversions, (1) nocturnal (radiative) and (2) subsidence.

2.1 Nocturnal inversions

Land surfaces are far more efficient at radiating heat than the atmosphere above, hence at night, the Earth's surface cools more rapidly than the air. That temperature drop is then conveyed to the lowest hundred meters of the atmosphere. The air above this layer

cools more slowly, and a temperature inversion forms. The inversion divides the atmosphere into two layers which do not mix. Below the inversion the surface winds are weak, and any pollutants emitted overnight accumulate. Above the inversion, winds continue through the night and can even become stronger as the inversion isolates the winds from the friction of the rough surface.

In the morning, the sun warms the Earth's surface, and conduction and convection transfer heat upward to warm the air near the surface. By about 10:00 – 11:00 am the temperature of the surface has risen sufficiently to remove the inversion. Air from above and below the inversion can then mix freely. Depending on whether the air above the inversion is cleaner or more polluted than the air at the surface, this mixing can either lower or increase air pollution levels. Figure 1 shows a temperature profile taken over Fort Meade, MD, on June 19, 2001. The nocturnal inversion is marked on the figure.

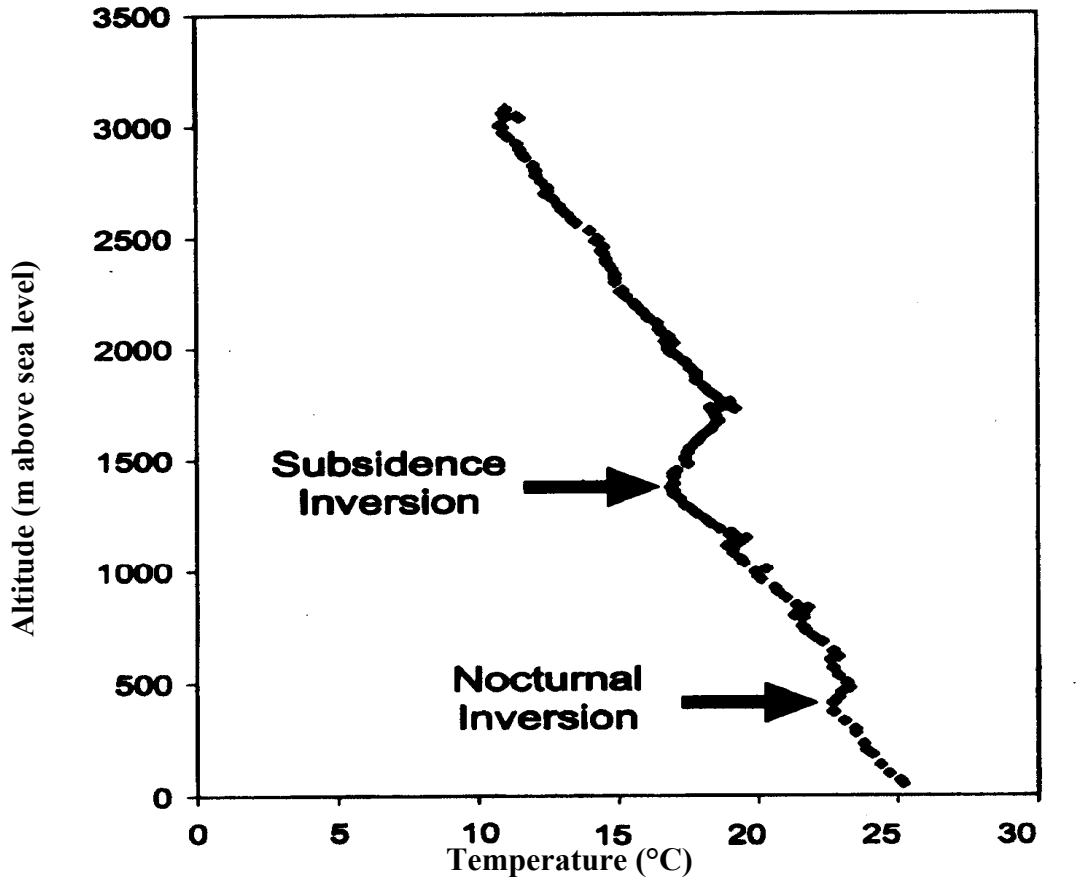

Figure 1. Temperature profile taken over Fort Meade, MD, on June 19, 2001

2.2 Subsidence inversions

Severe ozone events are usually associated with high pressure systems. In the upper atmosphere, the winds around a high pressure system move in a clockwise direction. However at the ground, friction between the ground and the winds, turn the winds away from the center of the system and divergence occurs. This divergence gives rise to subsidence in the atmosphere, which in turn causes the air to warm as it moves downward and is compressed. As the warmer air meets the colder air below, an inversion is formed. A subsidence inversion is particularly strong, since it is associated with this large scale downward motion of the atmosphere. The subsidence inversion caps pollution at a higher altitude in the atmosphere (typically from 1200 to 2000 meters, or about 4000 to 6500 feet), and it is far more difficult to remove than the nocturnal inversion. Hence the subsidence inversion limits vertical mixing in the middle of the day during an air pollution episode. An example of a subsidence inversion is also shown in Figure 1.

3. Transport processes

3.1 Introduction

The classic synoptic weather pattern associated with severe ozone episodes within the OTR is shown in Figure 2. A slow moving high pressure system lies over the Mid-Atlantic States with an associated clockwise circulation. The winds are usually light. In addition, as discussed above, the high pressure system produces subsidence, which in turn induces a subsidence inversion, and cloud free skies. However, the picture shown in Figure 2 is true only at pressure levels above about 925 mb. Close to the surface the Appalachian Mountain range interferes with this classic picture. First it acts as a physical barrier; secondly it can induce local effects such as mountain and valley breezes, the lee-side trough, and the low level jet, all of which can overcome the weak winds of the synoptic system. The proximity of the OTR states to the Atlantic Ocean also produces another interference, notably the sea and land breezes. The combination of these local effects can produce severe stagnation, and winds that do not follow the synoptic flow, indeed at many times the surface flow can be in the opposite direction to that of the synoptic flow. The surface flow pattern for any day depends on the relative speeds of the

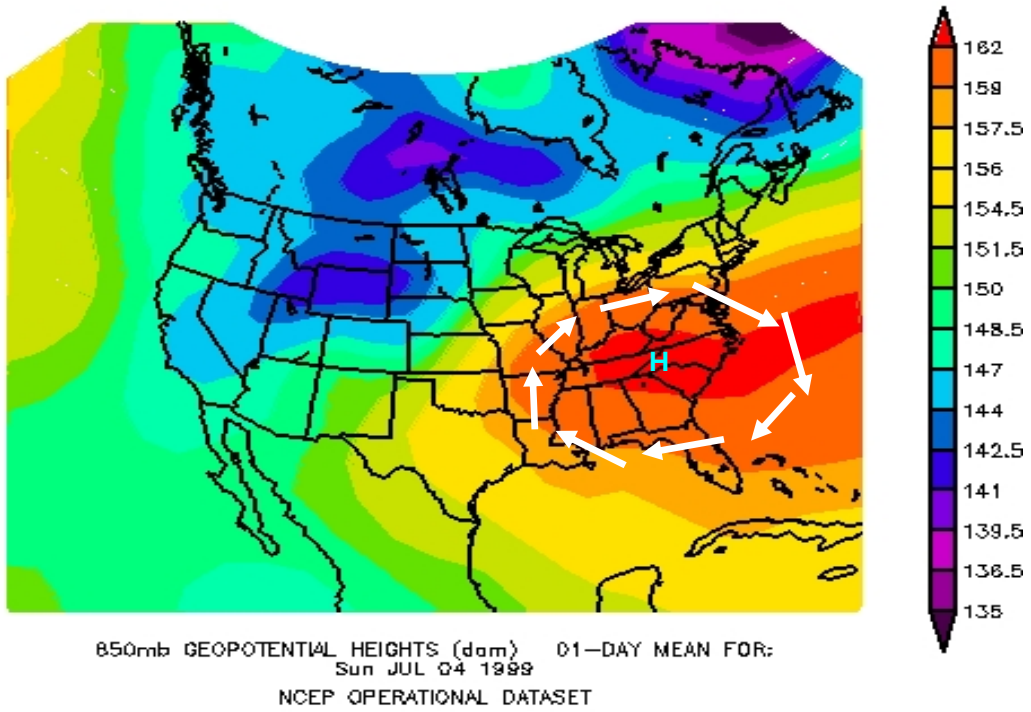

Figure 2. Schematic of a typical weather pattern associated with severe ozone episodes

winds induced by the local and synoptic flow. It therefore depends on the position of the high pressure system.

Transport processes for the OTR can roughly be broken down into three levels, surface, mid and upper. In the following sections the winds associated with these three levels will be discussed in more detail.

3.2 Surface level winds

3.2.1 Land, sea, mountain and valley breeze

In the Mid-Atlantic Region, land and sea breezes, and mountain and valley breezes can have an important influence on local air quality. These local winds are driven by a difference in temperature that produces a difference in pressure. Figure 3 shows a schematic of the formation of a sea breeze. The sea breeze forms in the afternoon when the land is considerably hotter than the ocean or bay. Air then flows from the high pressure over the ocean toward the low pressure over land. At night, the opposite may

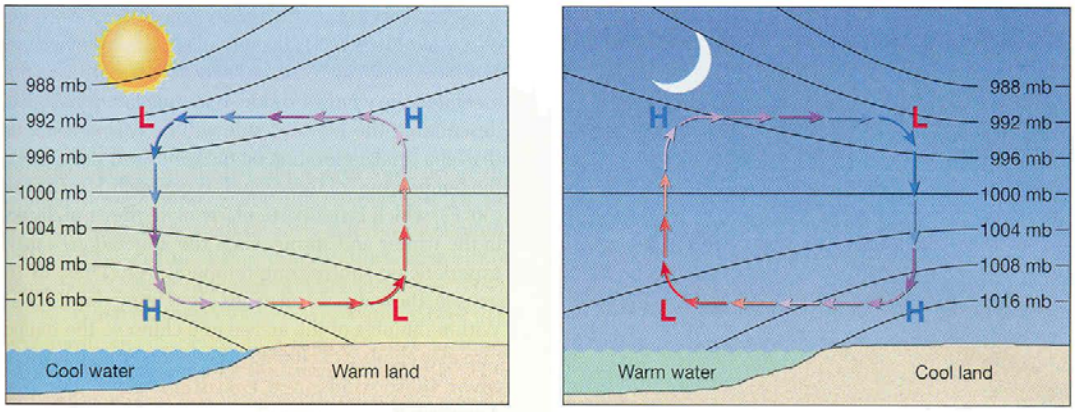

a) Sea Breeze **b) Land Breeze**

Figure 3. Illustration of a sea breeze and a land breeze. (*Lutgens and Tarbuck*, 2001)

happen as the land cools to below the ocean's temperature, and a land breeze blows out to sea. Since the nighttime land and water temperature differences are usually much smaller than in the day, the land breeze is weaker than the sea breeze. Sea breezes typically only penetrate a few kilometers inland, since they are driven by temperature contrasts which disappear inland. Air quality is affected by sea and bay breezes in coastal cities because the sea breeze can bring a city's polluted air back over the city. Figure 4 shows the average 2000-2002 wind direction frequency for elevated 1 hour ozone in the vicinity of Maine's Kennebec and Penobscot rivers. There is a clear maximum of pollution in the direction of the sea breeze.

Mountain and Valley breezes are also driven by a temperature contrast. In the daytime the side of the mountain will heat up more quickly than the valley, and hence a flow from the valley to the mountain results. At night this flow is reversed as the mountain side cools more quickly than the valley.

3.2.2 Appalachian lee-side trough

The Appalachian lee side trough forms on the leeward (downwind) side of the Appalachian Mountains. An example can be seen in Figure 5. In a sense, it is the daytime companion to the low level jet, since it forms under similar, stagnant conditions; however the mechanism for its formation is different. The lee side trough forms when

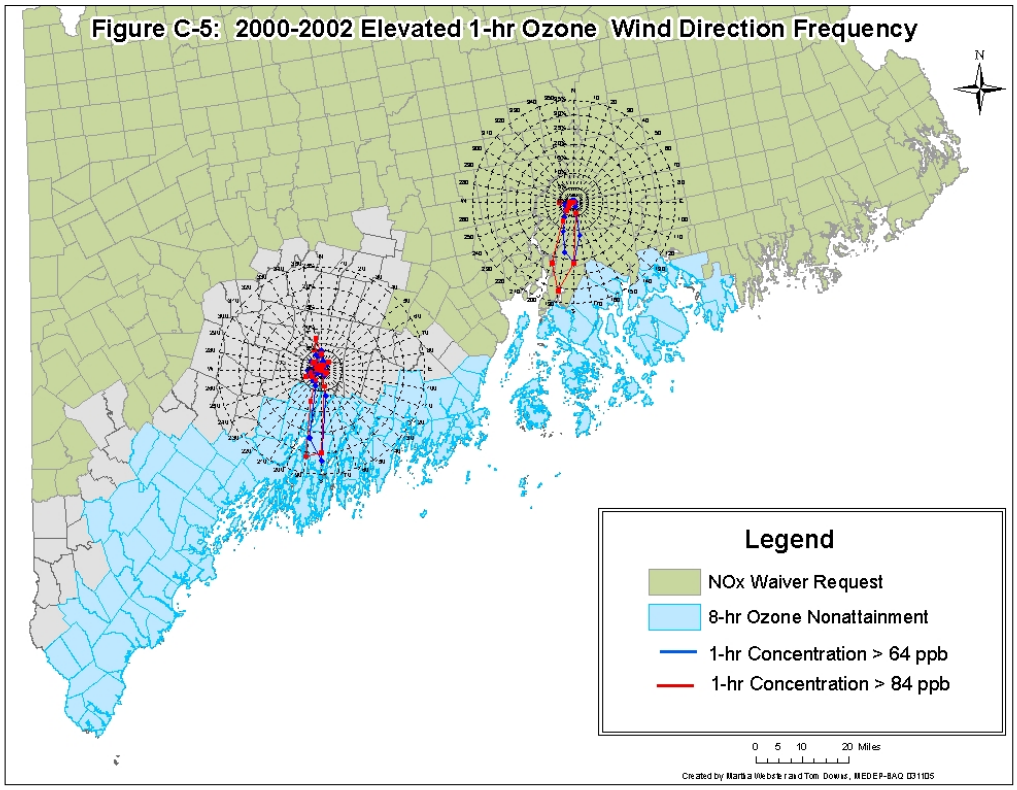

Figure 4. Average 2000 – 2002 wind direction frequency associated with elevated one-hour ozone levels in Maine

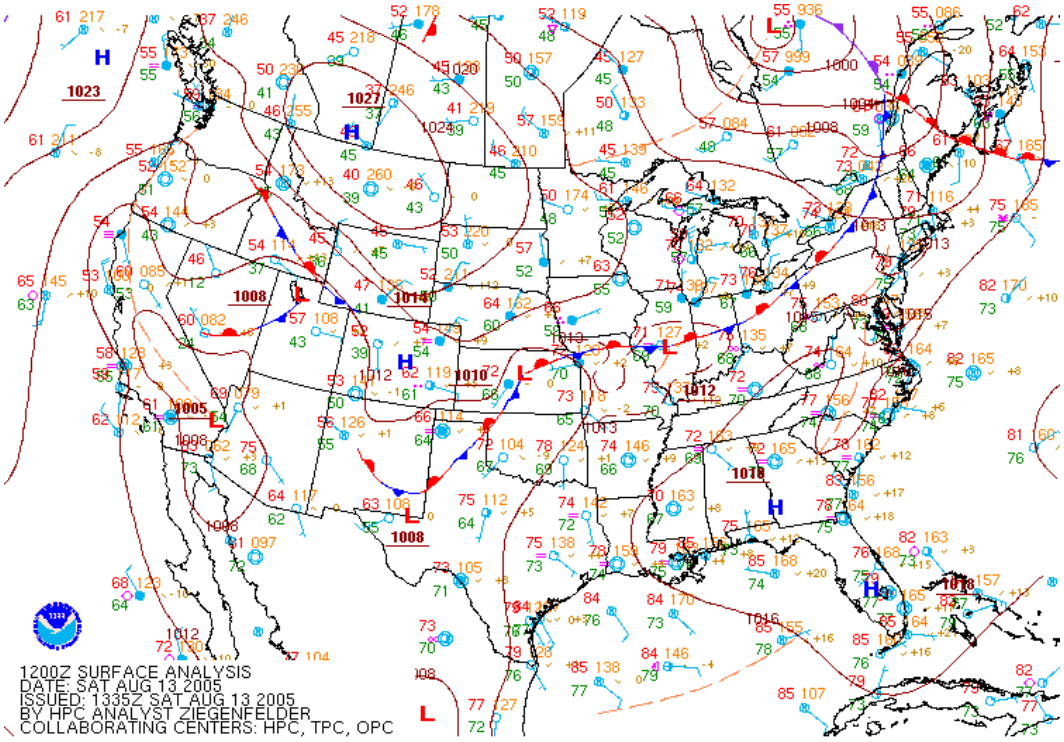

Figure 5. 1200Z Surface analysis for 13 August 2003. The Appalachian lee side trough can be observed in isobars over Maryland, Virginia, North Carolina, and South Carolina

westerly winds blow over the mountains and down to the coastal plain. As these winds descend, the air is compressed, warming it, leading to a broad area of low pressure at the surface (a trough). This, in turn, causes the surface and mid-level winds to shift their direction towards the northeast along the coastal plain. In figure 5 the trough can be seen over Maryland, Virginia, North Carolina, and South Carolina.

3.3 Mid-level winds

3.3.1 Low level jets

A low level jet (LLJ) is typically defined as a wind speed maximum of more than 12 m s^{-1} between 500-1500 m (1600-5000 ft) above the ground level (AGL), and it is primarily a nocturnal phenomenon that occurs more frequently during the spring and summer seasons. This phenomenon was first noted in late 1930's over Africa (*Farquharson*, 1939), and later frequently reported over North and South Americas, Australia, Asia, Antarctica and elsewhere (*Zemba and Friehe*, 1987; *Bonner*, 1968; *Enfield*, 1981; *Parish*, 1988). The generation mechanisms of LLJs and their effects on many meteorological problems have been extensively studied in theory, observations, and numerical models (*Buajitti and Blackadar*, 1957; *Wexler*, 1961; *Holton*, 1967; *Paegle and McLawhorn*, 1983), particularly for the LLJs that occur frequently over the Great Plains states (*Hoecker*, 1963; *Fast and McCorcle*, 1990; *Zhong et al*., 1996).

Despite the considerable attention paid to LLJ's during the past five decades, little is known about the development of LLJ's along the east coastal region of the United States during the spring and summer seasons. As compared to the Great Plains states where the Rocky Mountains are located to the west, the east coastal region is situated to the east of the Appalachian Mountains and to the west of the Atlantic Ocean. Although the Mid-Atlantic LLJ is much weaker and less extensive than that over the Great Plains states, it has a width of 300-400 km (or about 180- 250 miles, to its half peak value) and a length scale of more than 1500 km (or about 930 miles), following closely the orientation of the Appalachians Mountains. Moreover, LLJs could play an important role in transporting chemical constituents trapped in the residual layer at night. *Zhang et al*., 2005, recently performed a study of the Mid-Atlantic LLJ and its associated characteristics during the warm seasons of 2001 and

2002 using both wind-profiler data and the daily real-time model forecast products from the MM5 model. Figure 6 shows wind profiler data for the period 10 August, 2002 to 12 August 2002, from the Fort Meade station. The red symbols (high winds) are at the position of the low level jet.

A case study with three model sensitivity simulations was performed to gain insight into the three-dimensional structures and evolution of a LLJ and the mechanisms by which it developed. Results from the MM5 simulations showed that the Mid-Atlantic LLJ, ranged from 8 to 23 m s^{-1}, appeared at an average altitude of 670 m (2200 ft), and on 15 – 25 days of each month. About 90% of the 160 observed LLJ events occurred between 0000 and 0600 LST; and about 60% had south to westerly directions. Statistically, the real-time forecasts capture most of the LLJ events with nearly the right timing, intensity, and altitude although individual forecasts may not correspond to observations.

For a selected southwesterly LLJ case, both the observations and the control simulation exhibit a pronounced diurnal cycle of horizontal winds in the lowest 1.5 km (~5000 ft). The simulation shows that the Appalachians tend to produce a sloping mixed layer with northeasterly thermal winds during the daytime and reversed thermal winds after midnight. With additional thermal contrast effects associated with the Chesapeake Bay and the Atlantic Ocean, the daytime low-level winds vary significantly from the east coast to the mountainous regions. The LLJ after midnight tends to be peaked preferentially around 77.5°W near the middle portion of the sloping terrain and it decreases eastward as a result of the opposite thermal gradient across the coastline from the mountain-generated.

3.4 Upper level winds

Theoretical and numerical model simulations have suggested for some time that there is a strong regional component to urban air quality in the northeastern United States (*Liu et al*., 1987; *Sillman et al*., 1990; *McKeen et al*., 1990). The first aircraft observations, undertaken by UMD (The University of Maryland) with MDE ARMA (Maryland Department of Energy – Air and Radiation Management Administration) funding for limited periods in 1992 and 1993, were not made during extreme regional

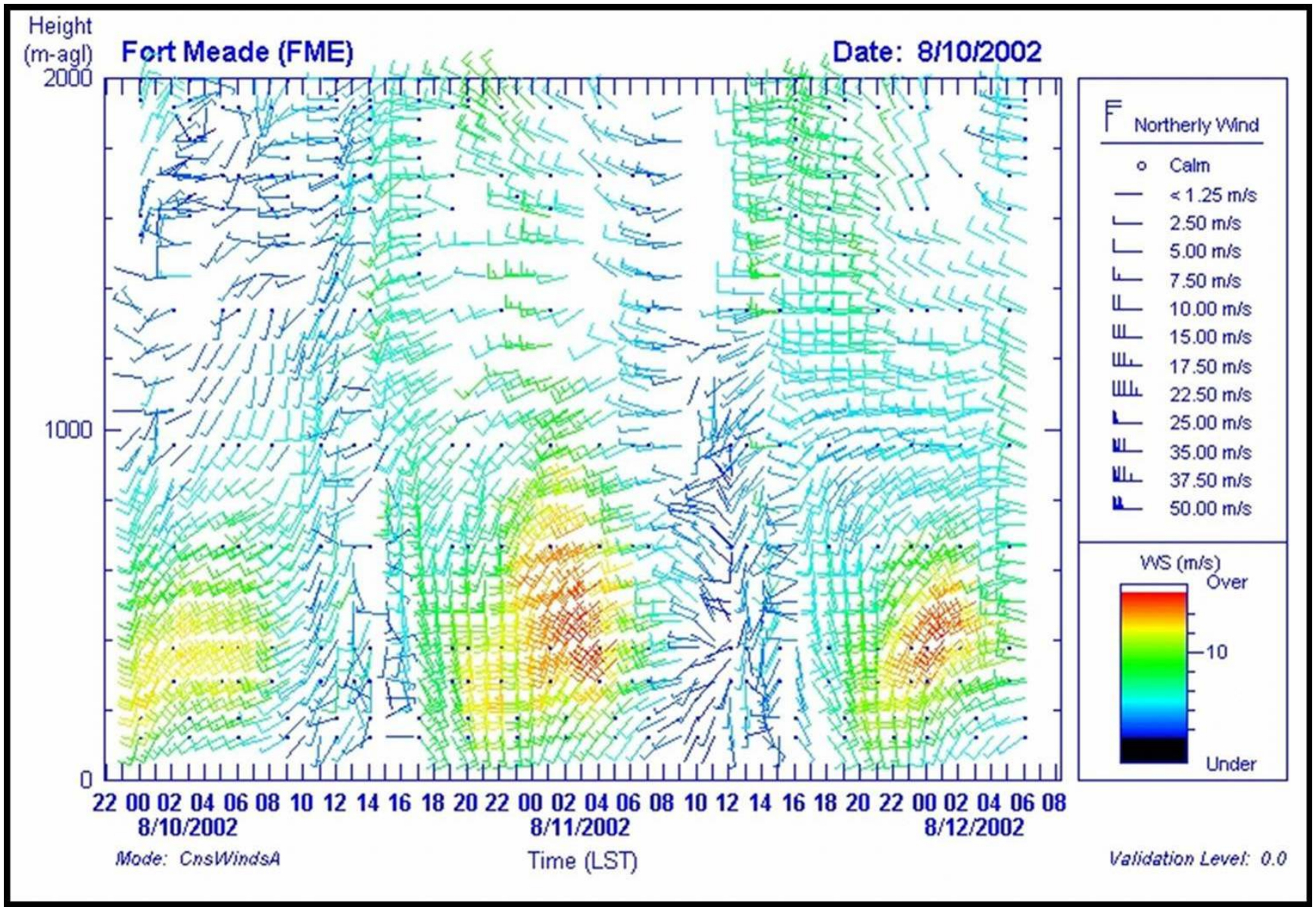

Figure 6. Wind profiler data from 10 August 2002 to 12 August 2002, from the Fort Meade, MD station

ozone events. However, these results suggested that the ozone upwind of the Baltimore area was enhanced during higher than average ozone periods.

Since 1992 over 300 aircraft flights have been made to measure vertical profiles of ozone, the nitrogen oxides, carbon dioxide, sulfur dioxide, and more recently aerosol particles during high ozone episodes. These measurements were made as part of the University of Maryland RAMMPP (Regional Atmospheric Measurement and Modeling and Prediction Program) program under the sponsorship of MDE-ARMA, MARAMA (Mid-Atlantic Region Air Management Association), VADEQ (Virginia Department of Environmental Quality), and NCDEQ (North Carolina Department of Environmental Quality). Figure 7 shows the results of profiles taken over central Virginia on 15 July 1995, at about 9:00 am on the last day of a four day severe ozone episode. During this episode, winds measured at Sterling, Virginia (IAD) in the 500-3000 m (1600-9800 ft) layer, where ozone was at a maximum, were consistently from the west to the north. This was particularly true on 15 July. There were no periods of stagnation or reversal of wind direction during this period.

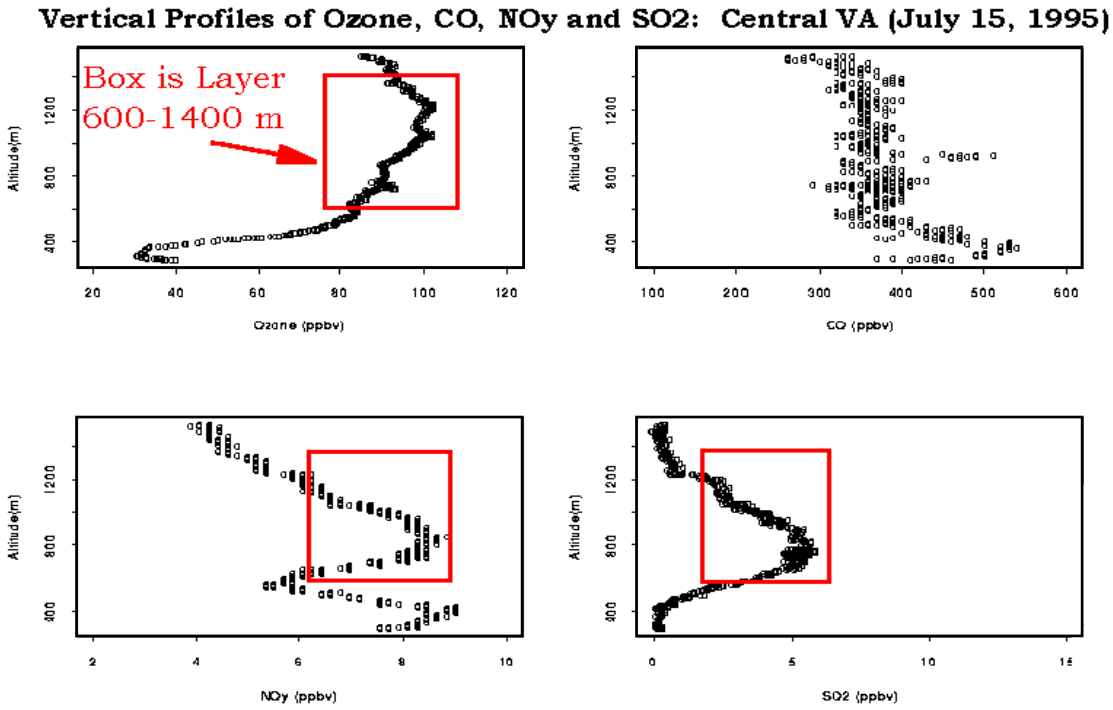

Figure 7. Altitude profiles for ozone, carbon dioxide, NO_y, and SO_2 taken on 15 July 1995

An examination of the data in Figure 7 shows that the ozone mixing ratio above the boundary layer is much larger than that at the ground, peaking at about 1200 m (4000 ft). It should be noted that while both automobiles and power plants emit NO, automobiles emit CO but not SO_2, while power plants emit SO_2 but not CO. The CO profile is not correlated well with the ozone data, indicating that the source of the carbon monoxide is not from local sources (automobiles). The peak in the NO_y profile at around 800 m (2600 ft) is due to 'aged' air, and is also unlikely to come from local sources (automobiles). Finally the peak in the SO_2 profile is also unlikely to come from local sources. Indeed the presence of the SO_2 leads to the conclusion that the air is coming from power plants west of the Appalachian Mountains.

4. The ozone reservoir

4.1 Introduction

Consider a typical day, starting at sunset, for a severe ozone event associated with a high pressure system. As the temperature of the earth drops, a nocturnal inversion forms, isolating the surface from stronger winds only a few hundred feet overhead. Ozone near the surface cannot mix with ozone above and is destroyed as it reacts with the Earth's surface. In a city, fresh NO_x emissions react with ozone, further reducing its concentration by NO_x titration, so that by morning, very little ozone is left below the nocturnal inversion. At this time, the nocturnal inversion is at its strongest, and winds at the surface are typically calm.

Above the nocturnal inversion, the situation is quite different. Ozone, and its precursors, both from the previous day's local emissions and from transport remain largely intact. There are no surfaces to react with the ozone and a large reservoir of ozone remains above the inversion. At mid-morning, when the nocturnal inversion breaks down, the ozone and precursors that were above the inversion can now mix with the air near the surface. The result of this mixing is a sudden change in ozone. Figure 8 shows median ozone profiles for morning and afternoon flights from 1996 – 2003. One can clearly see the breakdown of the nocturnal inversion throughout the day.

Pollutants that do not react with the Earth's surface as readily as ozone do not show such a marked diurnal cycle, but the same mixing mechanism also affects their

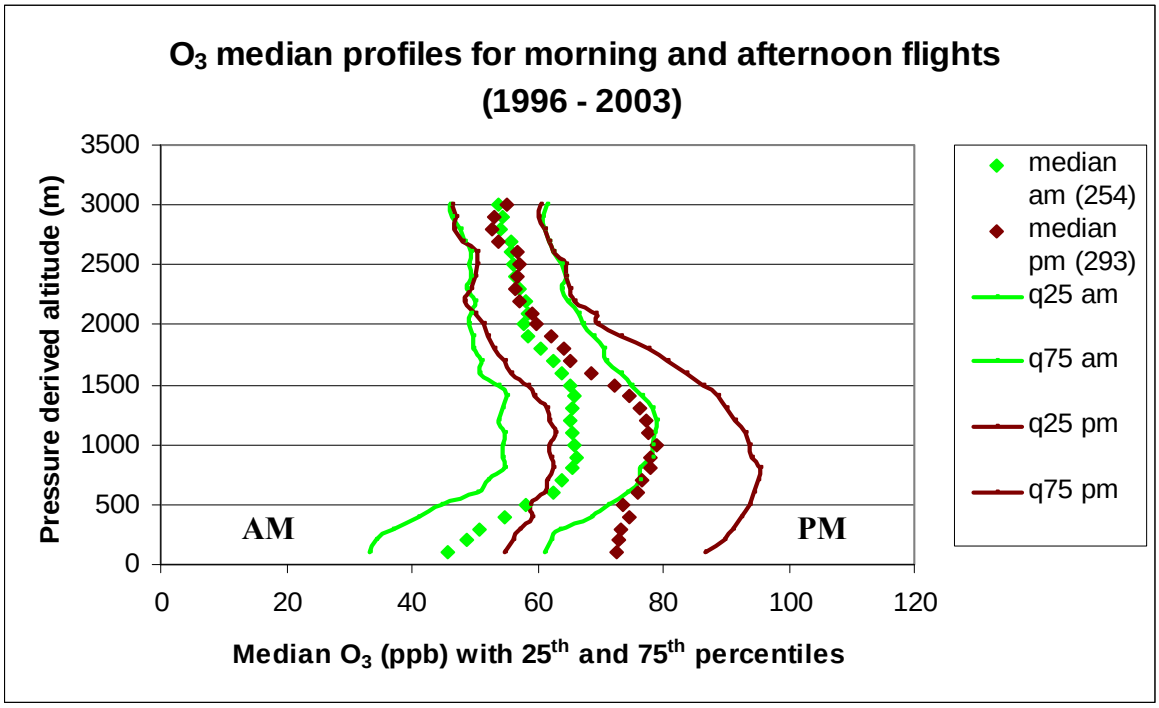

Figure 8. Median ozone profiles for morning and afternoon flights from 1996 – 2003

concentrations. Nighttime emissions of trace gases and particles can build up under the nocturnal inversion, leading to higher levels in the early morning. In the summertime, regional sulfate levels above the inversion can combine with local emissions as the inversion breaks up. In the winter, with less direct sunshine, it's harder to break the inversion, and local emissions can continue to build unless washed out by precipitation or dispersed by winds.

4.2 Contributions to the ozone reservoir

Contributions to the ozone reservoir can come from two sources. The first is from the residual ozone and precursors in the atmosphere at sunset. The second is from transport of ozone and precursors from outside of the local region. An analysis of the complete set of aircraft flights undertaken by RAMMPP between 1992 and 2003 has recently been made by *Taubman et al.*, 2005 to identify these outside sources. Initially, the data were divided into morning and afternoon profiles to identify diurnal patterns. Little diurnal variation was observed in the carbon monoxide and sulfur dioxide profiles. The ozone values were greater in the afternoon than the morning, while ozone in the

lower free troposphere (i.e. above the boundary level), where long range transport is possible, was consistently ~55 ppbv. Transport patterns and source regions during summertime haze and ozone episodes were analyzed with a cluster analysis of back trajectory data. Eight clusters were identified, which were then divided into morning and afternoon profiles. Table 1 lists the characteristics of each cluster. Figures 9 and 10 show the trajectory densities for each cluster. When the greatest trajectory density lay over the northern Ohio River Valley, which has large NO_x and sulfur dioxide sources, the result were large ozone values, a large SO_2/CO ratio, large, scattering particles, and high aerosol optical depth over the Mid-Atlantic U.S. In contrast, relatively clean conditions over the Mid-Atlantic occurred when the greatest trajectory density lay over the southern Ohio River Valley and nearly missed many large NO_x and SO_2 sources. The greatest afternoon ozone values occurred during periods of stagnation that were most conducive to photochemical production. The least pollution occurred when flow from the north-northwest was too fast for pollution to accumulate and when flow was from the north, where there are few urban or industrial sources.

Ozone transport over several hundred kilometers into the Mid-Atlantic U.S. was estimated by calculating the ratio of the residual layer ozone in the upwind morning profiles to the downwind afternoon boundary layer values. The greatest ozone transport (69-82%) occurred when the maximum trajectory density lay over the southern and northern Ohio River Valley (~59% of the total profiles). The least ozone transport (55-58%) was associated with fast southwesterly flow (~3% of the total profiles), clean northerly flow (~6% of the total profiles), and stagnant, polluted conditions (~27% of the total profiles). The average ozone transport to the Baltimore Washington Urban corridor is 64%, if the background ozone is removed, then this value is lowered to 55%.

In Figures 9 and 10 specific source regions were identified by overlaying the trajectory density plots on maps with the largest annual NO_x and SO_2 emitters. The results indicate that the areas of maximum trajectory density together with wind speed are effective predictors of regional pollution and loadings. Additionally, due to the Lagrangian nature of the dataset, the regionally transported contribution to the total afternoon boundary layer column ozone content in each cluster could be quantified.

5.0 Conclusion

This report has summarized current knowledge of the meteorological processes that impact local ozone levels within the OTR. A conceptual model of transport within the OTR can be divided into three principle components, transport aloft, transport by the low-level jet, and ground level transport. Transport aloft is dominated by the anti-cyclonic flow around a high pressure system, which can lead to transport from States that lie outside the OTR. Ground level transport is the result of interaction between the synoptic flow, and local effects, such as the sea breeze and the Appalachian lee side trough. All three modes of transport depend on the location of the high pressure system.

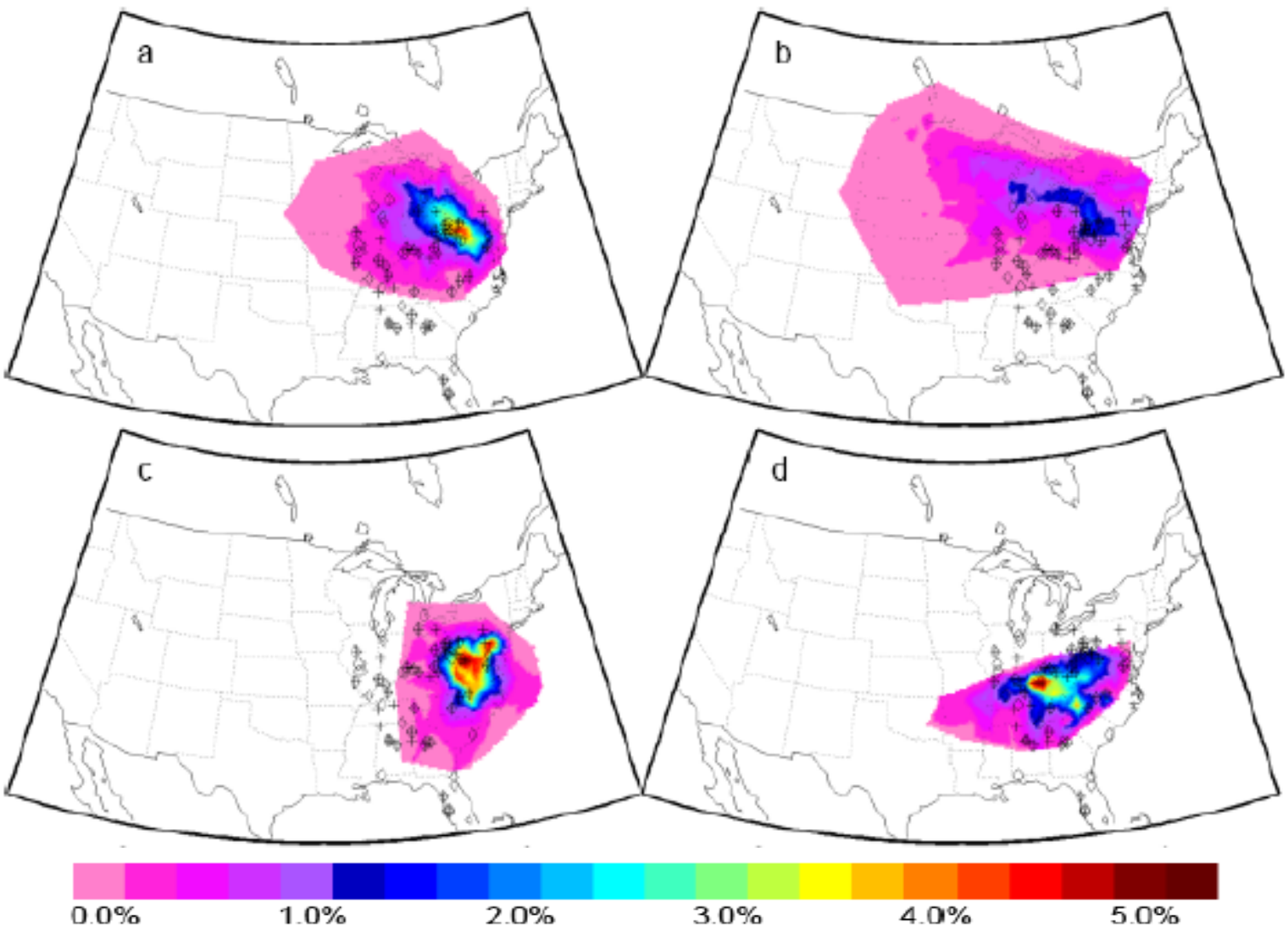

Figure 9. Trajectory density maps for a) cluster 1, b) cluster 2, c) cluster 3, d) cluster 4. The plots were generated using a 39 linear interpolation method between the trajectory end points. They indicate the relative density (%) of air parcels over the total area described by the spaghetti plots. Also pictured are the locations of the top 0.3% emitters annually of NOx (diamonds) and SO2 (crosses) in the eastern U.S. Taken from Figure 4 of *Taubman et al.*, 2005.

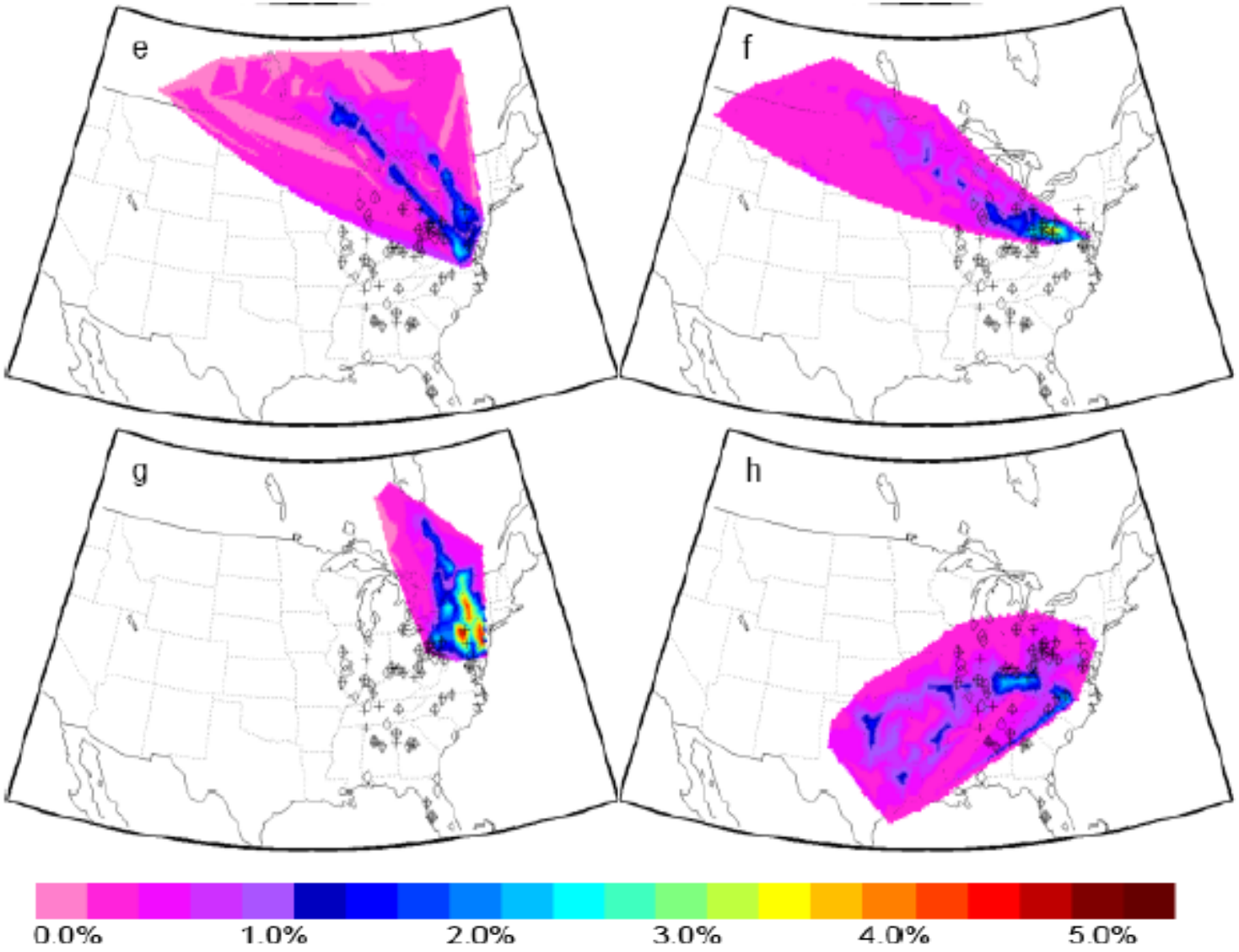

Figure 10. Trajectory density maps for e) cluster 5, f) cluster 6, g) cluster 7, h) cluster 8. The plots were generated using a 39 linear interpolation method between the trajectory end points. They indicate the relative density (%) of air parcels over the total area described by the spaghetti plots. Also pictured are the locations of the top 0.3% emitters annually of NOx (diamonds) and SO2 (crosses) in the eastern U.S. Taken from Figure 4 of *Taubman et al*., 2005.

Table 1.

Cluster	Description	Region
1	Large ozone, large SO_2/CO ratio, moderate northeasterly flow - aged point source air	Northern Ohio river valley
2	Large ozone, large SO_2/CO ratio, high wind speeds than cluster 1- aged point source air	Northern Ohio river valley, extending into the Great lakes region
3	Stagnant conditions with light southerly flow. Small SO_2/CO ratio	Central Mid-Atlantic region
4	Moderate southeasterly flow, small pollution loading. SO_2/CO ratio is small – low point sources.	Southern Ohio river valley
5	Fairly fast north-northwesterly flow, over the Northern Great Lakes. Transports little ozone into the region	Northern Great lakes into Mid-Atlantic region
6	Northwesterly flow, but faster wind speeds than (2). Crosses several large SO_2 and NO_x sources.	Northern Ohio valley
7	Least pollution of any of the clusters. Flow is out of the North. Cool, dry continental air	Northern states
8	Fast flow. Very few trajectories	Texas

References

Bonner, W. D. (1968), Climatology of the low level jet, *Mon. Weather Rev., 96,* 833–850.

Buajitti, K., and Blackadar, A. K. (1957) Theoretical studies of diurnal wind-structure variations in the planetary boundary layer, *Q. J. R. Meteorol. Soc., 83,* 486-500.

Enfield, D. B. (1981) Thermally driven wind variability in the planetary boundary layer above Lima, Peru, *J. Geophys. Res., 86,* 2005–2016.

Farquharson, J. S. (1939) The diurnal variation of wind over tropical Africa, *Q. J. R. Meteor. Soc., 65,* 165–183.

Fast, J. D., McCorcle, M. D. (1990) A 2-dimensional numerical sensitivity study of the Great Plains low-level jet, *Mon. Weather Rev., 118,* 151–163.

Hoecker, W. H. (1963) Three southerly low-level jet systems delineated by the Weather Bureau special PIBAL network of 1961, *Mon. Weather. Rev., 91,* 573–582.

Holton, J.R. (1967) Trapping of unstable baroclinic waves, *J. Atmos. Sci., 31,* 2220-2222.

Liu, S. C., M. Trainer, F. C. Fehsenfeld, D. D. Parrish, E. J. Williams, D. W. Fahey, G. Hubler, and P. C. Murphy (1987) Ozone production in the rural troposphere and the implications for regional and global ozone distributions, *J. Geophys. Res., 92,* 4191–4207.

Lutgens, F., and E. Tarbuck (2001), *The Atmosphere: An Introduction to Meteorology*, 8th ed., 512 pp., Prentice Hall, Upper Saddle River, New Jersey.

McKeen, S. A., M. Trainer, E. Y. Hsie, R. K. Tallamraju, S. C. Liu (1990) On the indirect determination of atmospheric OH radical concentrations from reactive hydrocarbon measurements, *J. Geophys. Res., 95,* 7493–7500.

Paegle, J., and D. W. McLawhorn (1983) Numerical modeling of diurnal convergence oscillations above sloping terrain, *Mon. Weather Rev., 111,* 67–85.

Parish, T.R. (1988) Surface Winds over the Antarctic continent – A Review, *Rev. Geophys., 26,* 169–180.

Sillman, S., J. A. Logan, S. C. Wofsy (1990) A regional scale model for ozone in the United States with subgrid representation of urban and power plant plumes, *J. Geophys. Res., 95,* 5731–5748.

Taubman, B. F., J. C. Hains, A. M. Thompson, L. T. Marufu, B. G. Doddridge, J. W. Stehr, C. A. Peity, and R. R. Dickerson (2005) Aircraft vertical profiles of trace gas and

aerosol pollution over the Mid-Atlantic U.S.: Statistics and meteorological cluster analysis, (submitted to *J. Geophys. Res.*).

Wexler, W. H. (1961) A boundary layer interpretation of the low-level jet, *Tellus*, *13*, 368–378.

Zemba, J., and C. A. Friehe (1987) The marine atmospheric boundary layer jet in the Coastal Ocean Dynamics Experiment, *J. Geophys. Res. - Oceans*, 92, 1489–1496.

Zhang, D.-L., et al. (2005) Low-Level jets over the Mid-Atlantic region: Warm-season climatology and a case study", *J. Applied Meteor.*, in review.

Zhong, S. Y., J. D. Fast, X. D. Bian (1996) A case study of the Great Plains low-level jet using wind profiler network data and a high-resolution mesoscale model, *Mon. Weather Rev.*, *124*, 785–806.

Where Does Our Air Pollution Come From and What Do We Need To Do To Fix It?

A Simplified Conceptual Model for the OTR

OTC Annual Meeting

June 7, 2005

Topics Covered

- Primer on transport
  - The simplified conceptual model
- How do OTC strategies address the different components of our air pollution problem
  - Local strategies
  - Regional power plant controls
  - Level-the-playing field initiatives

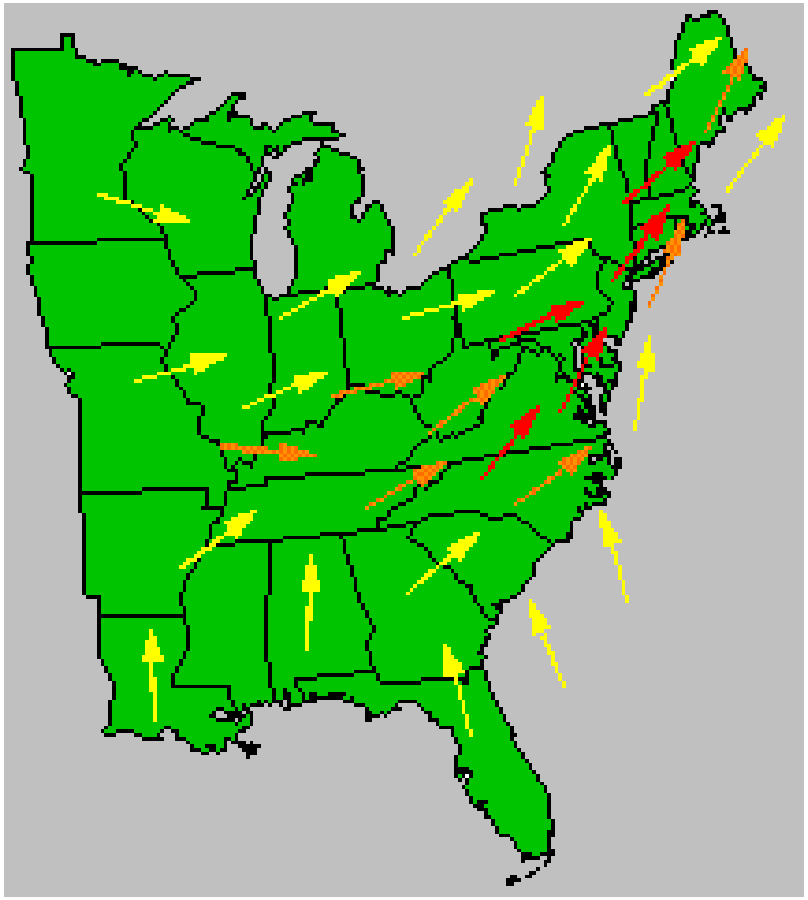

A Simplified Conceptual Model

- Or … Where does our air pollution come from?
- Developed based upon 20 years of science
- Presented multiple times over the past year
- Much Thanks to:
  - UMD
  - NH, CT, ME, VA
  - NESCAUM
  - MARAMA
  - OTC

Blending Science and Policy

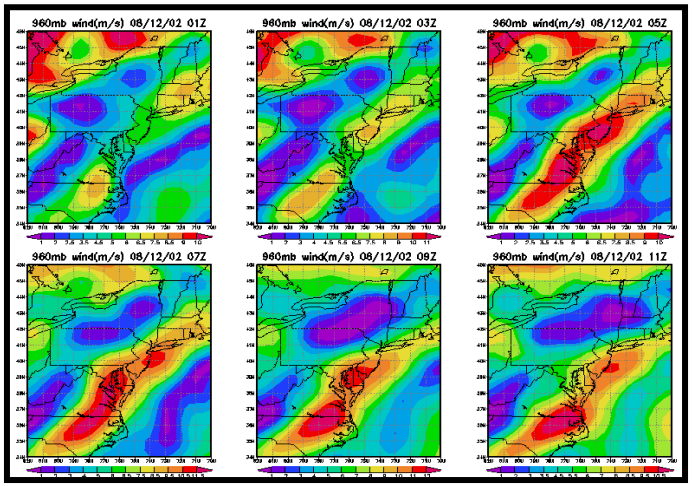

- Air pollution is complicated!!!
- This presentation boils down years of technical work and hundreds of technical papers into simple conclusions about the most important things that need to be done to clean up the the air in the OTR.
- Many details and nuances are left out
- There is however, considerable support from the scientific community that the conclusions reached in this presentation are accurate.

Where Does Our Air Pollution Come From?

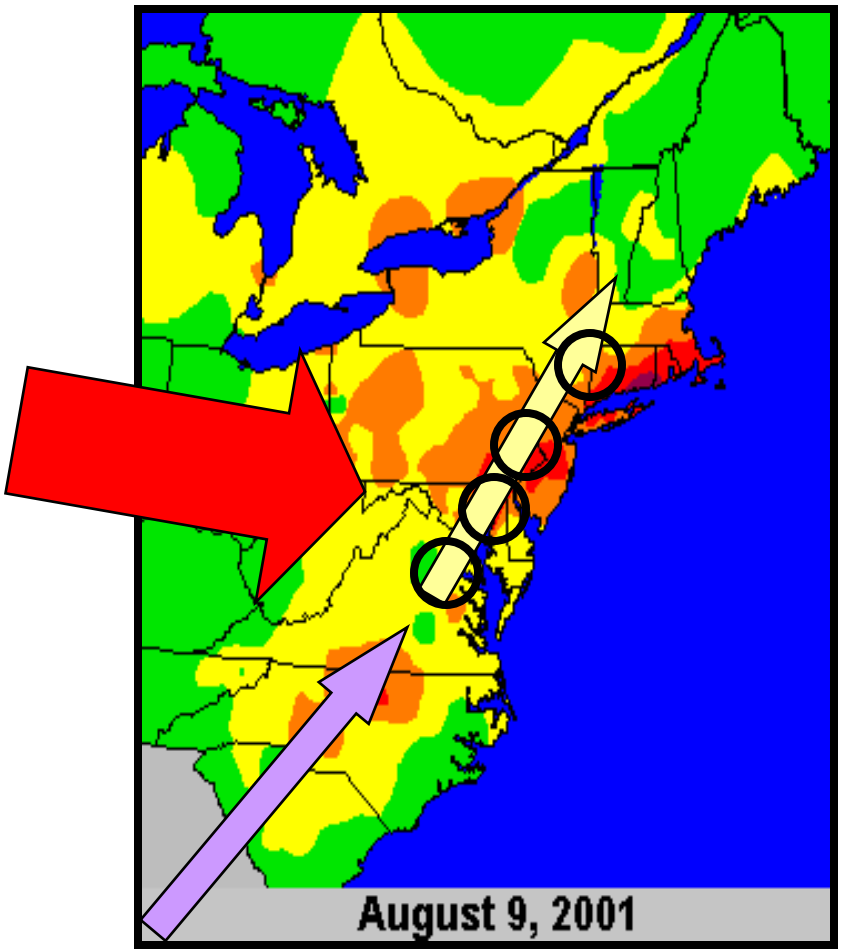

Four Distinct Parts

- Emissions from within each Nonattainment Area (NAA)
- Three types of transport
  - Short range
    - "Ground level" transport
    - VA to MD to PA to NJ to NY to MA to NH.
  - Long range (synoptic scale)
    - "Aloft" transport
    - 100s of miles
    - Generally from W or NW
  - Low Level Night-Time Jets
    - "Aloft" transport at night
    - 100s of miles
    - SW to NE along the Atlantic

Different Types of Transport

Not Really a New Concept

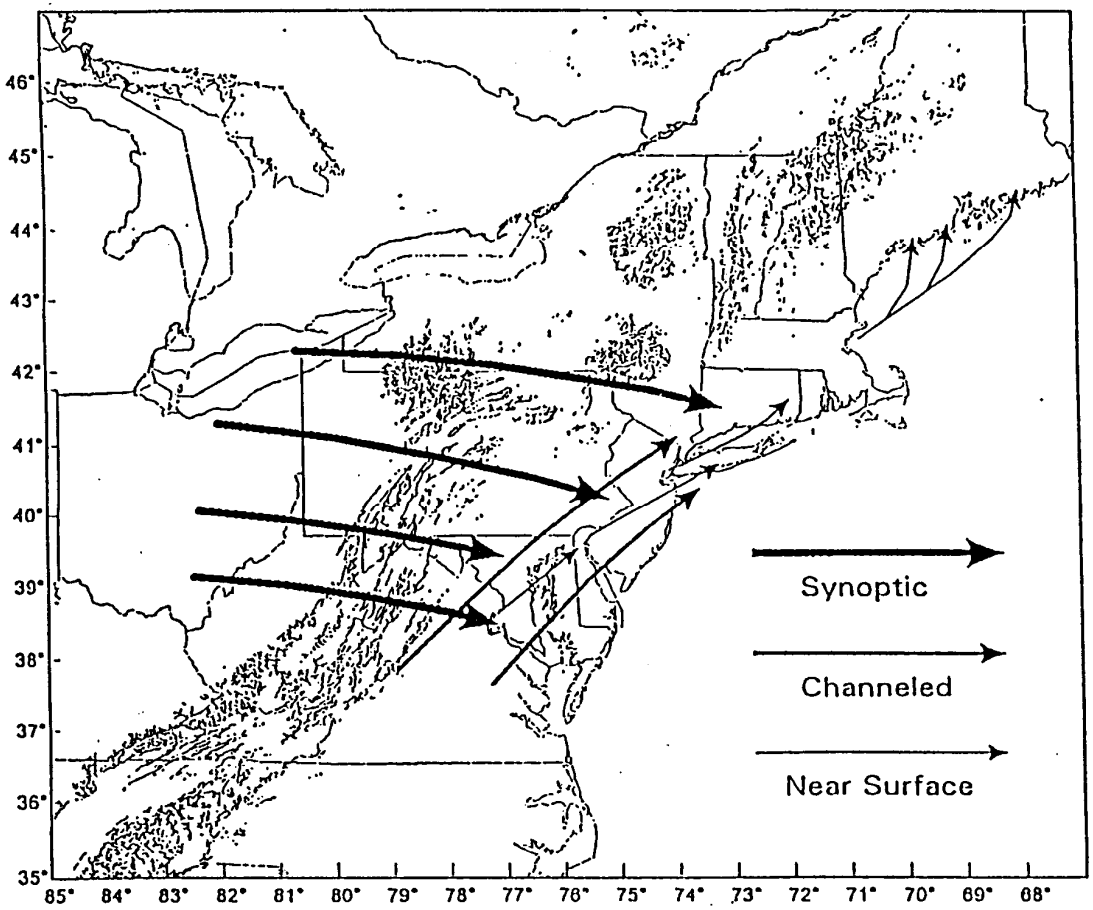

Transport Regimes Observed During NARSTO-Northeast

1998

How Much Is Transport?

- Changes from day to day as the weather changes
- However … On our worst days we use airplanes to routinely measure ozone at 80 to 110 parts per billion (ppb) floating into the OTR from the West and South
  - Standard is 85 ppb
- Best guess … something like
  - 30 to 40 percent long range (westerly) transport
  - 10 to 20 percent short range transport
  - 10 to 20 percent Low Level Jet (LLJ) transport
  - 10 to 20 percent local

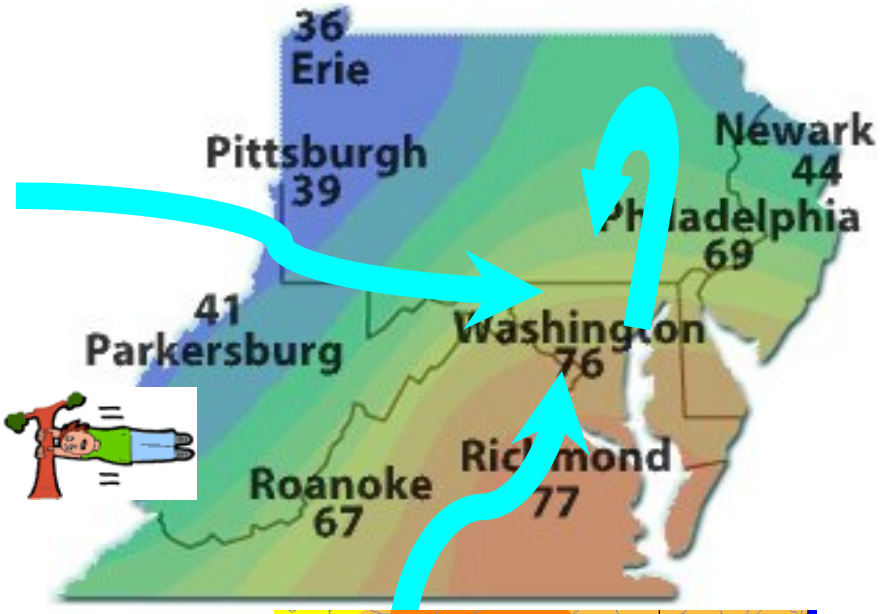

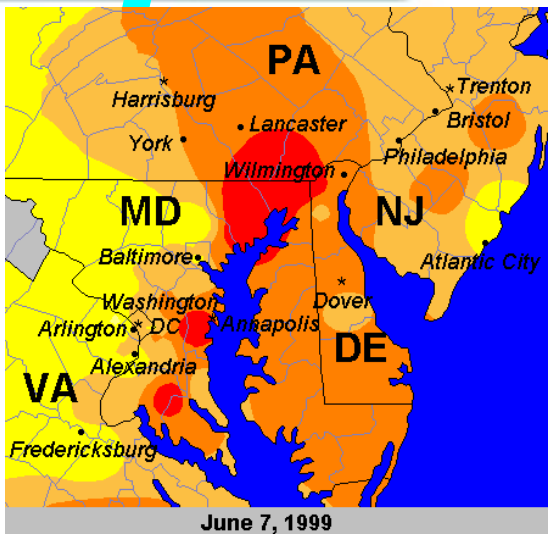

The Phases of a Bad Ozone Day

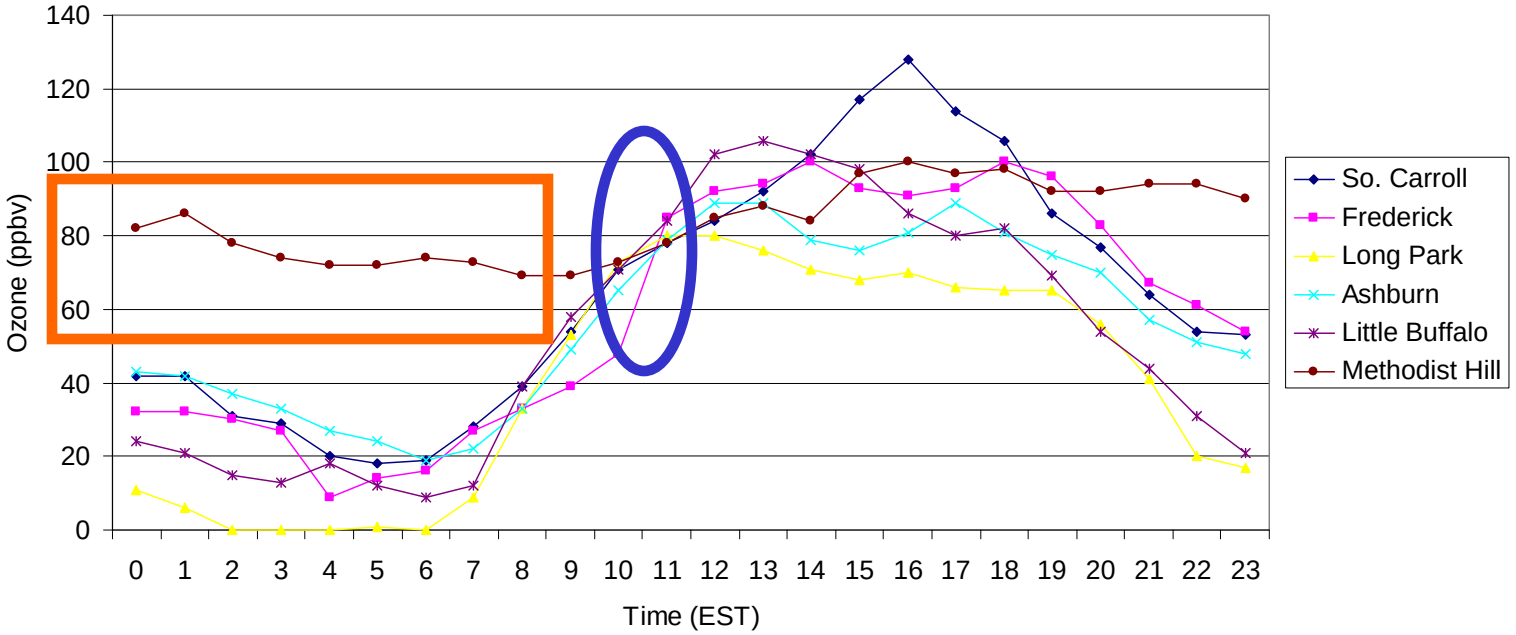

Three Stages of a Severe Regional Ozone Event

- **Up to around 10 - The "elevated reservoir"**
- **10 to 12 – Inversion breaks – the "regional" signal**
- **Afternoon – Local and regional pollution combine**

The Elevated Ozone Reservoir

Early Morning Ozone in Maryland

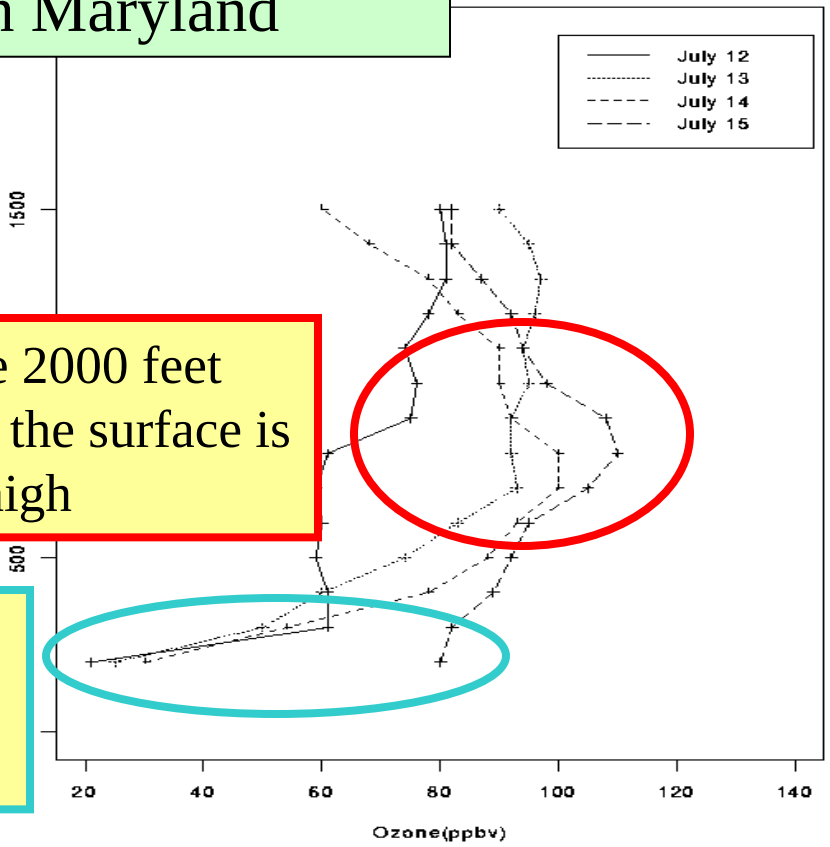

Ozone 2000 feet above the surface is very high

Surface ozone is very low

- On most bad ozone days, before any new ozone has been formed, a large reservoir of ozone and ozone precursors sits above the OTR waiting to mix down.
- Ozone levels in the reservoir can reach 80 to 100 ppb

Maryland Data

How Big is the Reservoir?

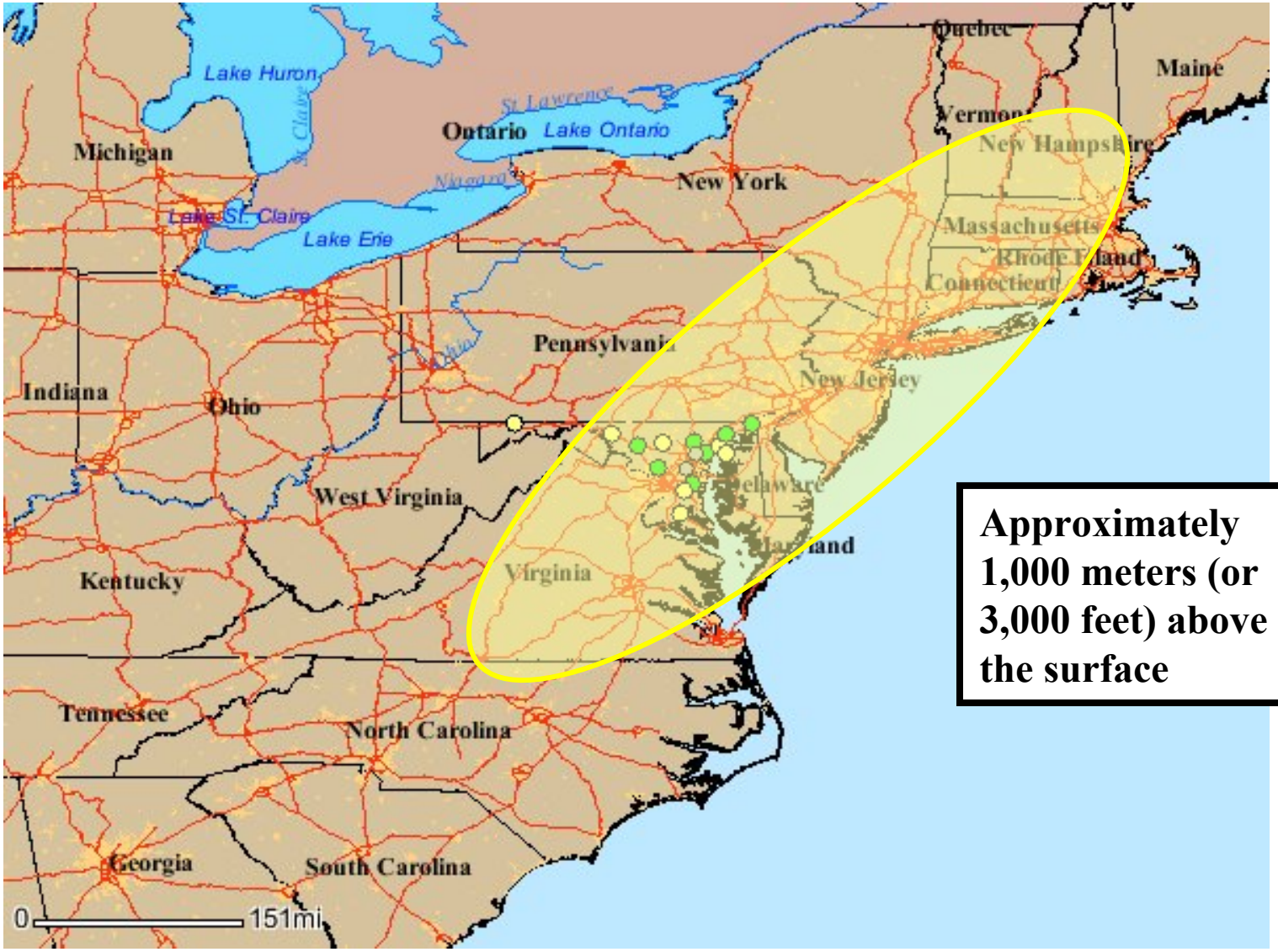

Approximately 1,000 meters (or 3,000 feet) above the surface

What Creates the Reservoir?

- At night the earth cools and a “nocturnal inversion” is created several hundred meters above the surface
- Ozone, created earlier in the day is trapped above the inversion and moved to the north by night-time jets.
- Ozone below the inversion drops to very low levels.

Filling the Reservoir

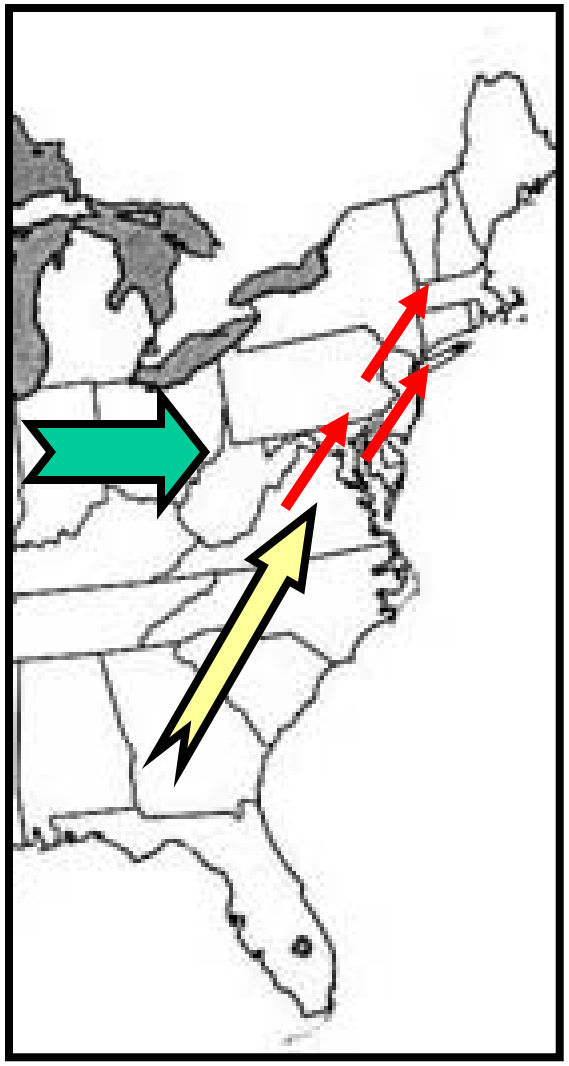

- What's over MD on Tuesday started off in Ohio and North Carolina on Monday.
  - MD's pollution soup floats to New Jersey and New York
  - New York's pollution floats to New England
- Power plants, cars, trucks and other sources are all contributors to the elevated pollutant reservoir.
- Filled with ozone and ozone precursors.

Recap: The Different Types of Transport

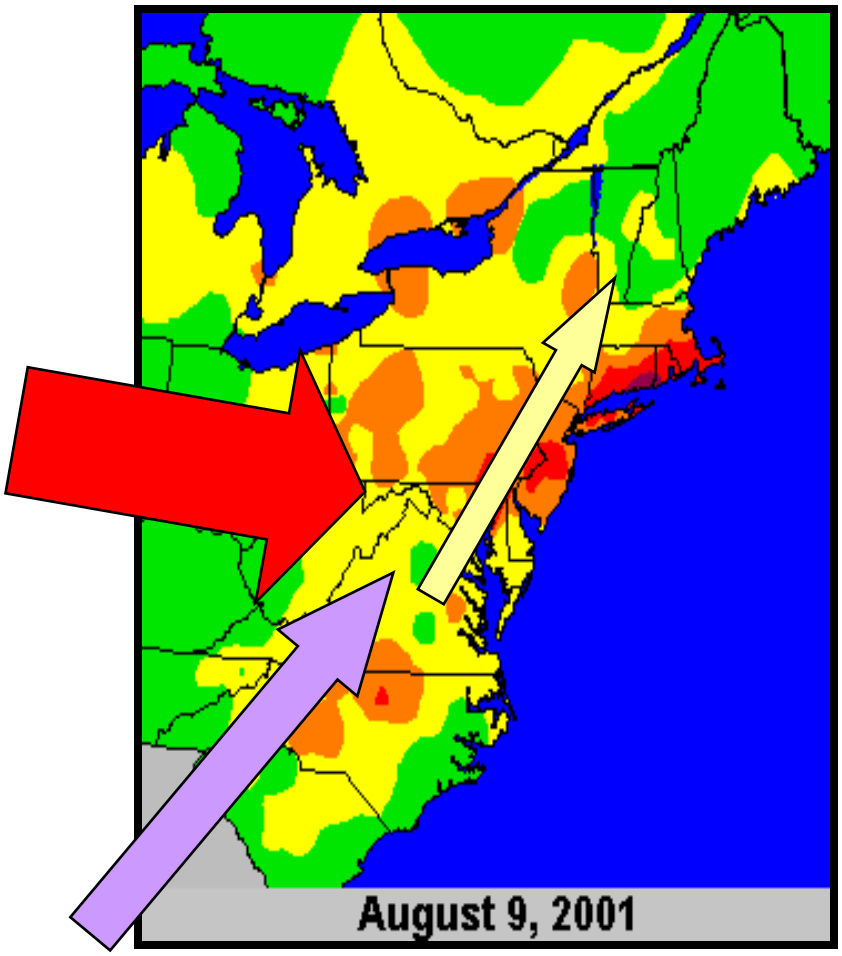

- Long range westerly transport
  - West to east “aloft” transport
  - Primarily power plants
- Low Level Night-Time Jets
  - SW to NE “aloft” transport at night
  - Mobile, area and stationary sources
- Short range transport
  - SW to NE “ground level” transport
  - Mobile, area and stationary sources
- The “perfect storm”
  - Three types of transport and local emissions = code red

Westerly Transport

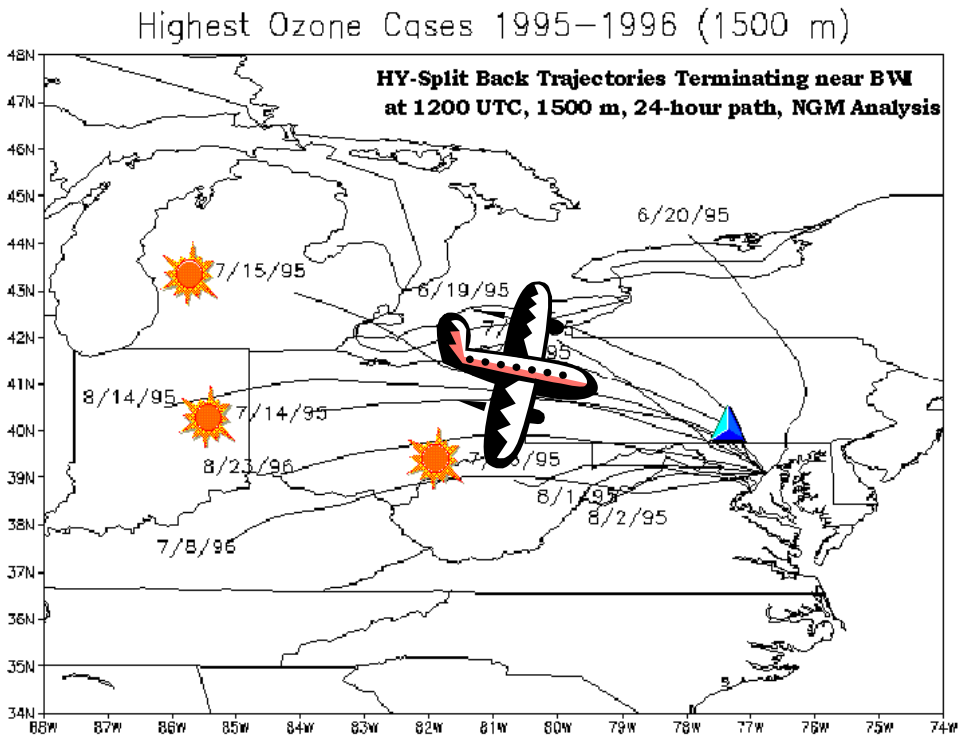

- On the worst ozone days “westerly transport” plays a significant role in creating high ozone.

Classic Ozone Weather in the Mid-Atlantic

- **The OTR states see very high ozone levels during the summer when high pressure sets up over the southern Appalachians.**
- **Air aloft circulates clockwise around the High**

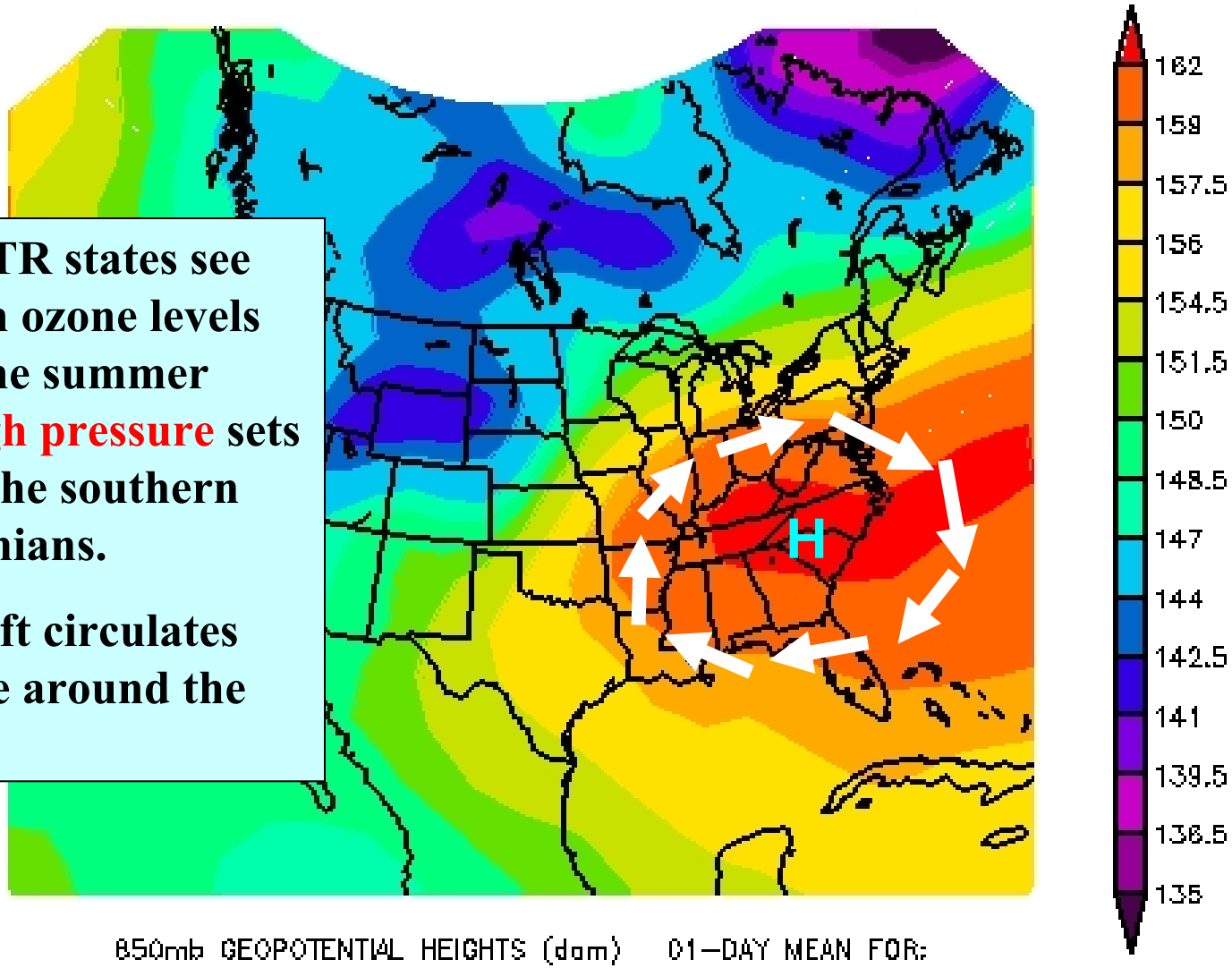

850mb GEOPOTENTIAL HEIGHTS (dam) 01-DAY MEAN FOR:
Sun JUL 04 1999
NCEP OPERATIONAL DATASET

Power Plant Emissions

- Very large power plant emissions are concentrated along the Ohio River valley
- Again, air aloft circulates clockwise around the high

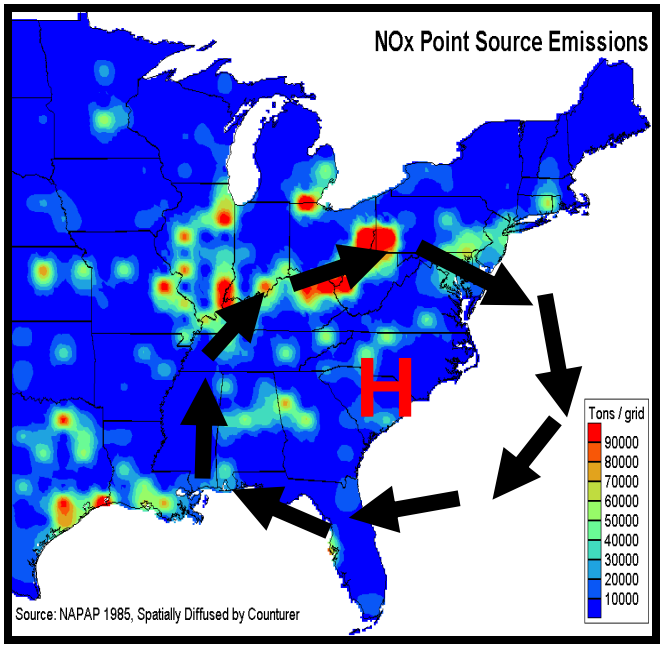

Westerly Transport – What Does the Data Tell us About Its Origin?

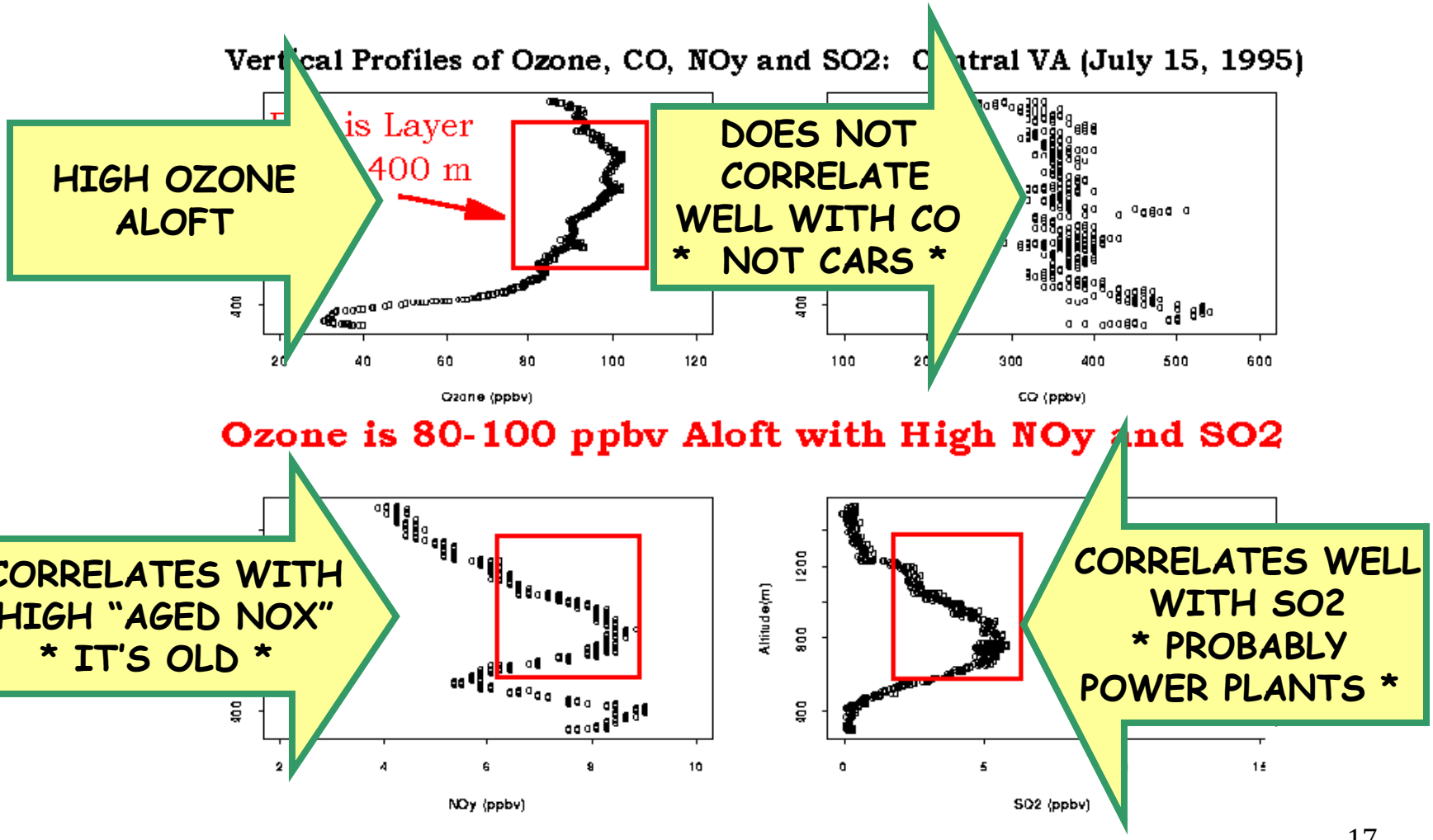

Low Level Jet

- Night time transport that moves air from NC to MD, MD to NJ, and northward
- The LLJ is funneled northward with the Appalachians on the west and the Atlantic on the east
- Wind speeds up to 40 miles per hour can move pollution hundreds of miles overnight
- Recent PSU/UMD findings
  - LLJ is routine not occasional
  - Almost always a 2 to 5 hr LLJ for MD Orange or Red days
  - Precursor transport – not just O3

How Much Ozone May be in the LLJ?

- Still analyzing this issue
- Theory and recent work by Penn State around Philadelphia (using laser technology called LIDAR) indicates that the low level jet can carry 80 to 90 ppb ozone.
- It’s not just ozone but precursors too!

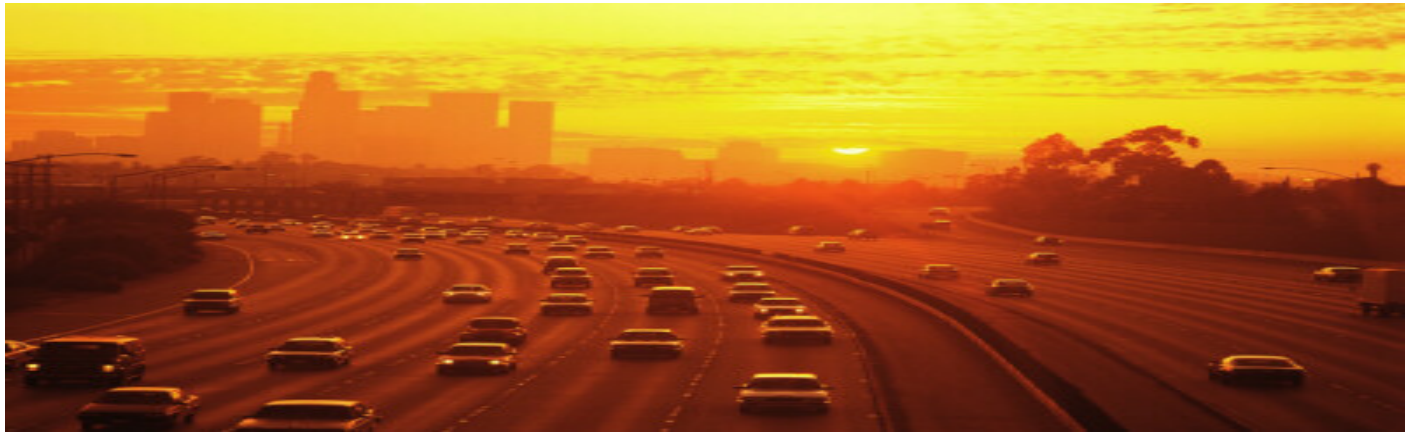

Low Level Jet Recorded Above Fort Meade Maryland

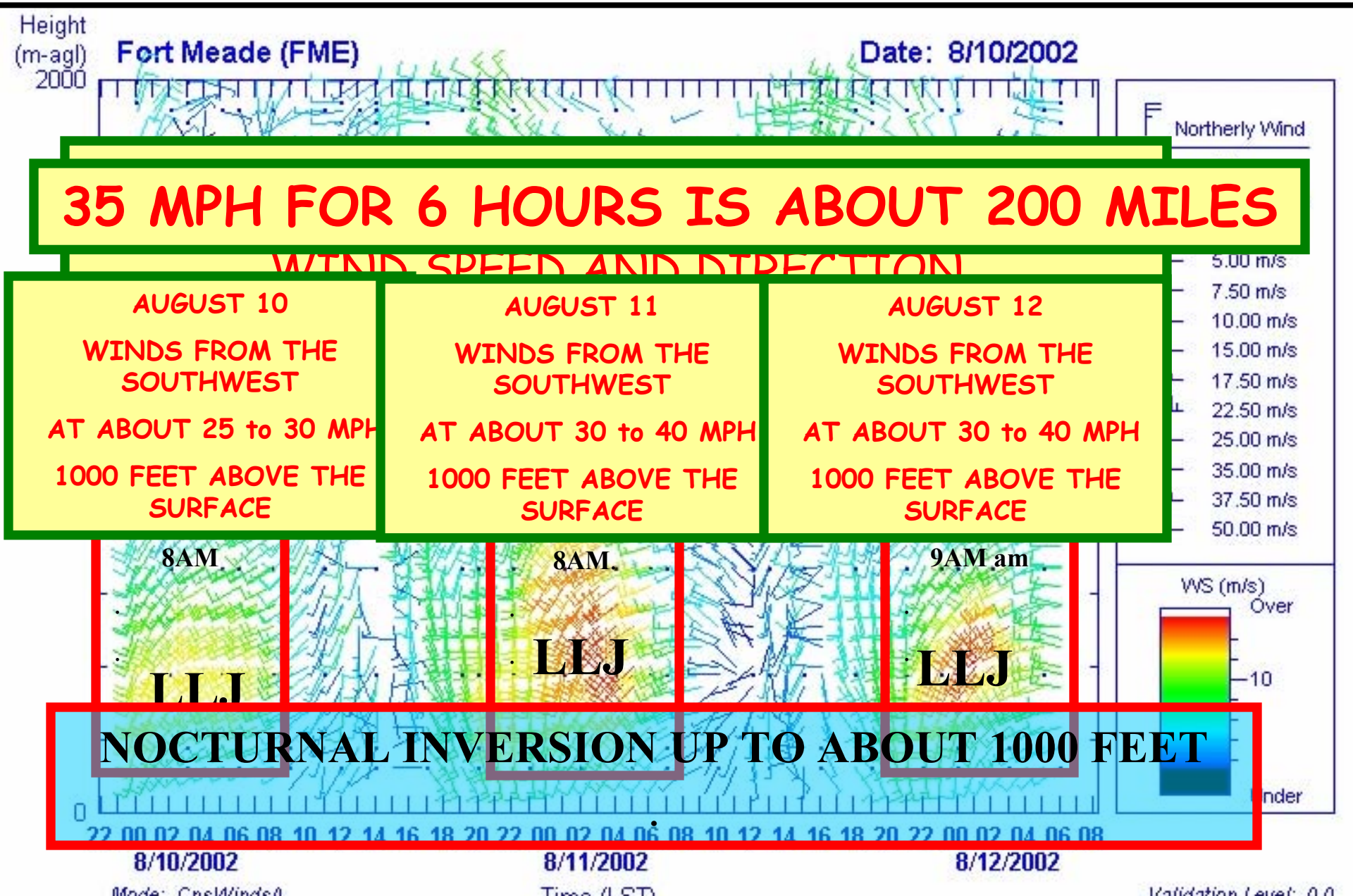

Meteorological Model Depiction of the LLJ

A Worst Case Scenario - High Wind Speeds In Red

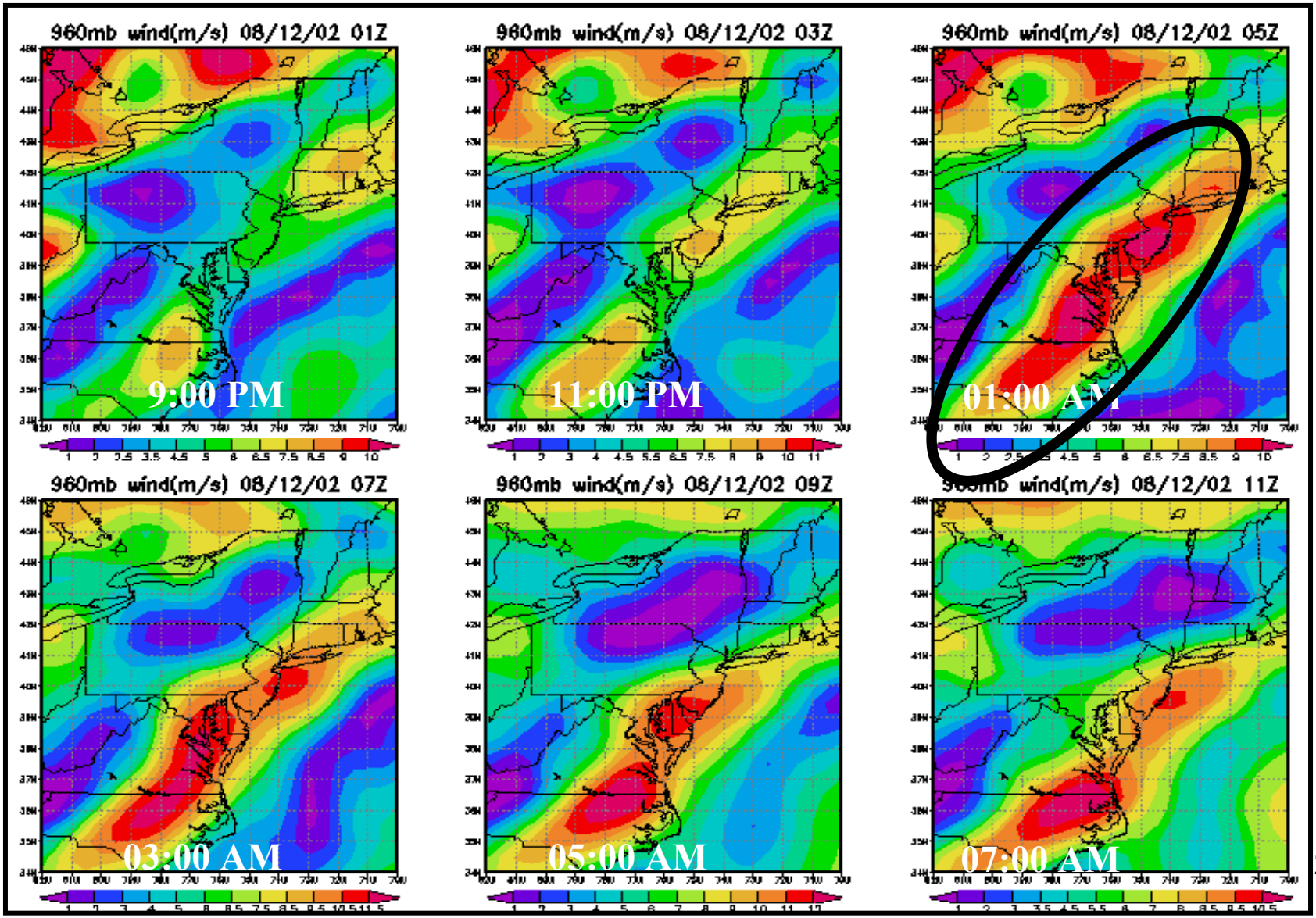

Short Range Transport

- Ground level (not aloft) transport
  - DC to Baltimore
  - Baltimore to Philly
  - Philly to NJ/NY, etc.
- Ground level winds can push pollution about 100 miles in a day
  - Ground level winds generally from southwest to the northeast
  - On some days, pollution can actually re-circulate back to the south from the north
  - Emissions from cars, area sources and stationary sources

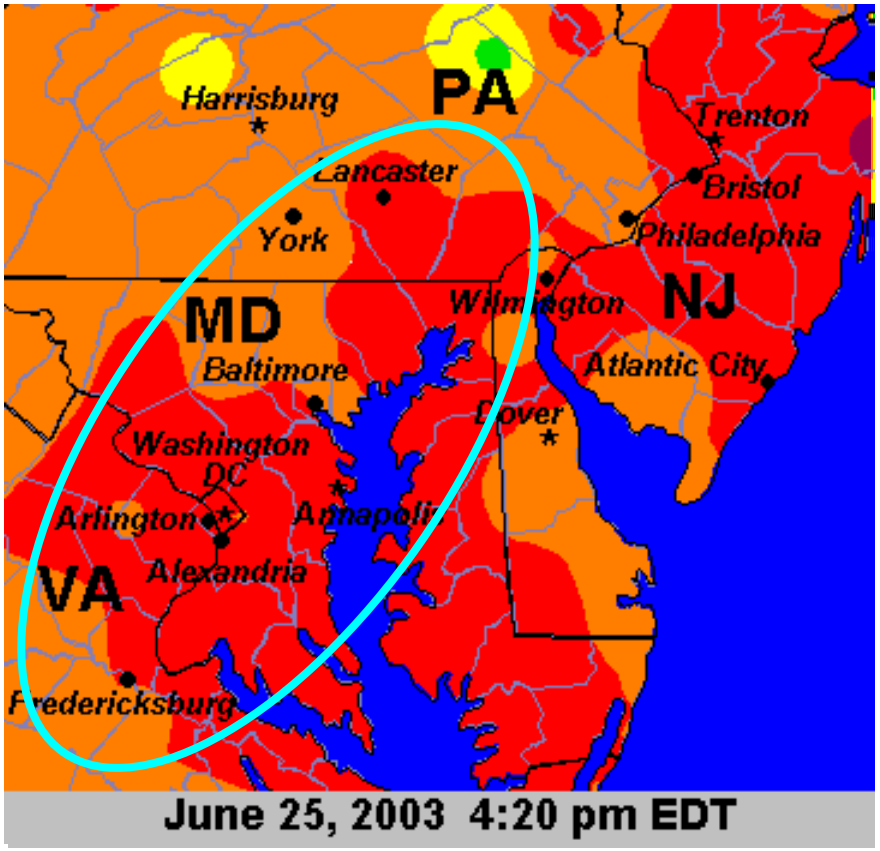

The Transport “Crossroads”

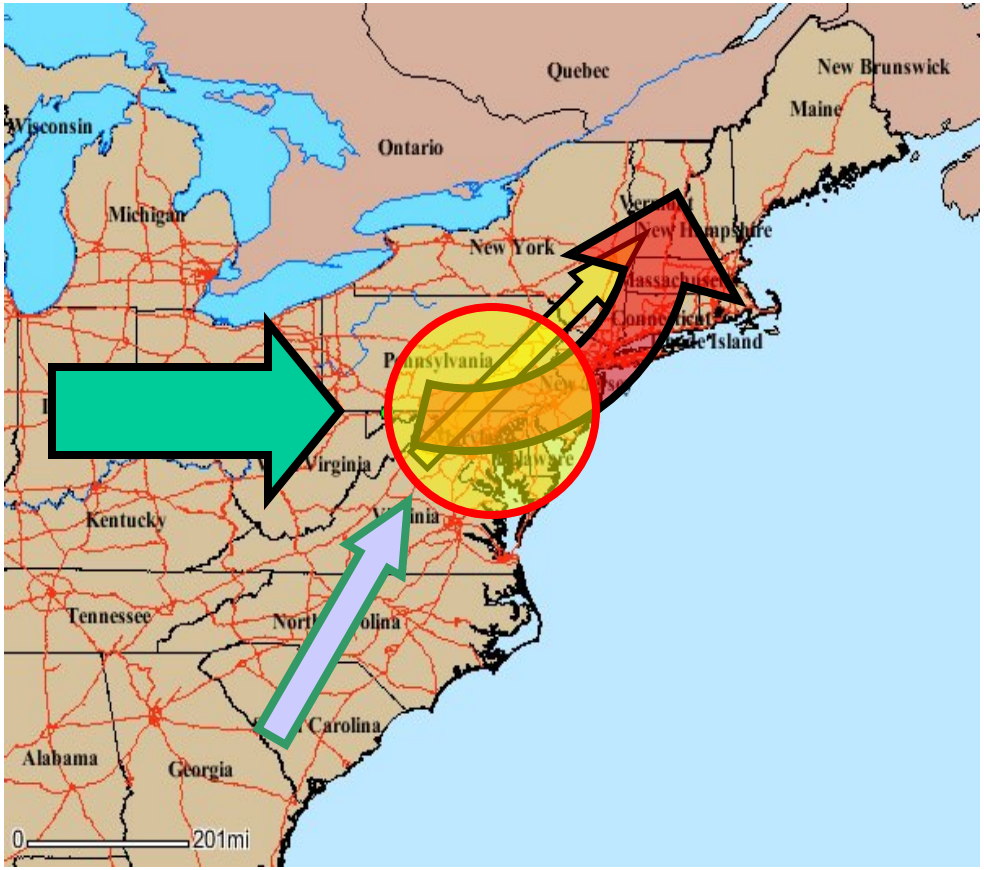

- The Mid-Atlantic “Crossroads”
- Westerly, LLJ and local transport converge on the Mid-Atlantic area
- Jets, sea breezes, the lee-side trough and other coastal meteorology all turn pollution northward at the Mid-Atlantic crossroads

A Worst Case Day in Connecticut

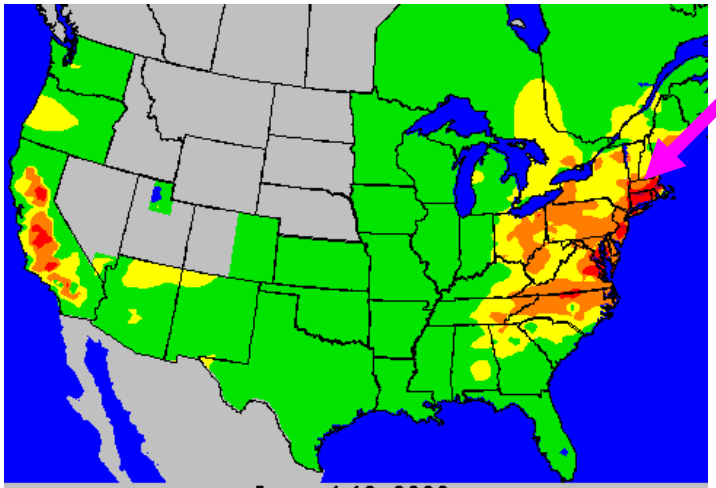

High Ozone

Westerly Transport

Low Level Jets

Coastal Meteorology

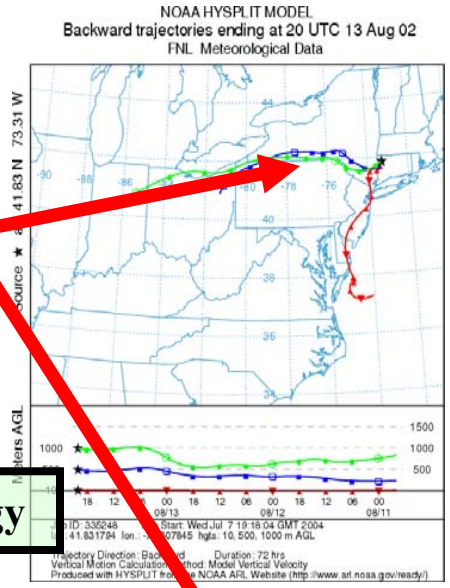

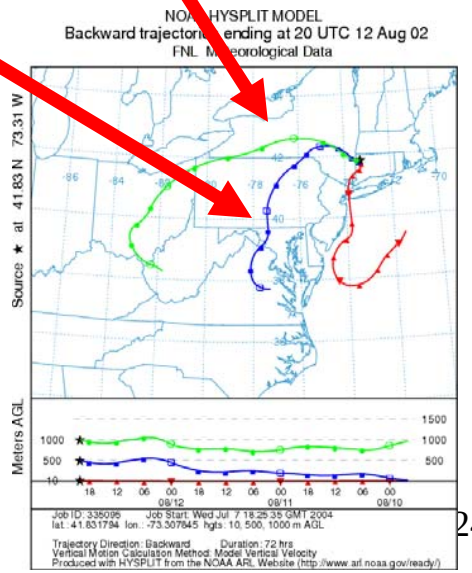

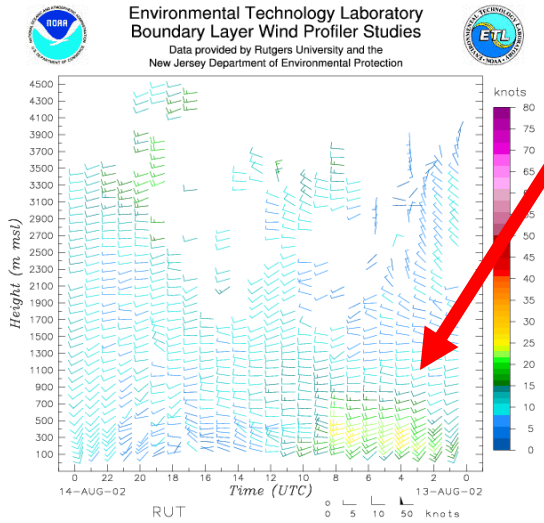

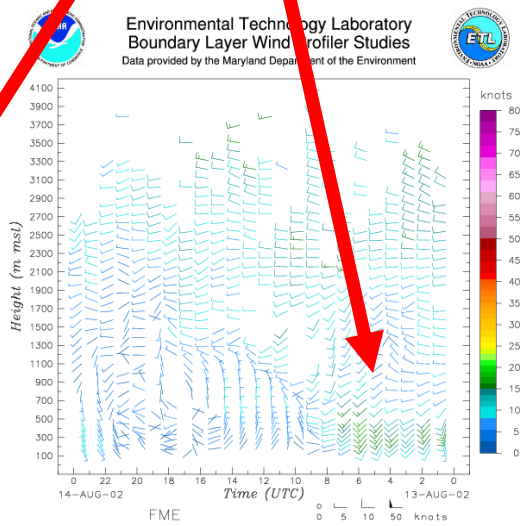

OTC Policies

How do they address the different types of transport?

- Short Range Transport
  - Addressed by historical "inside the OTR" strategy and regional model rule development work
- Long Range Westerly Transport
  - Addressed by OTC NOx Budget, Program, the SIP Call and the OTC Multipollutant Position
- Low Level Night-Time Jet Transport
  - Just beginning to address this issue
    - Part of CAAAC effort pushing for more "regional" control programs through national rules
    - OTC Control Measure Workgroup "level-playing-field" effort

Beginning to Address Transport

- The NOx SIP Call is working
- Significant NOx reductions from regional power plants between 2002 and 2005
- Billions of dollars being invested in “Selective Catalytic Reduction” (SCR) technology to reduce power plant NOx emissions
- New tougher ozone and fine particle standards
  - More reductions needed

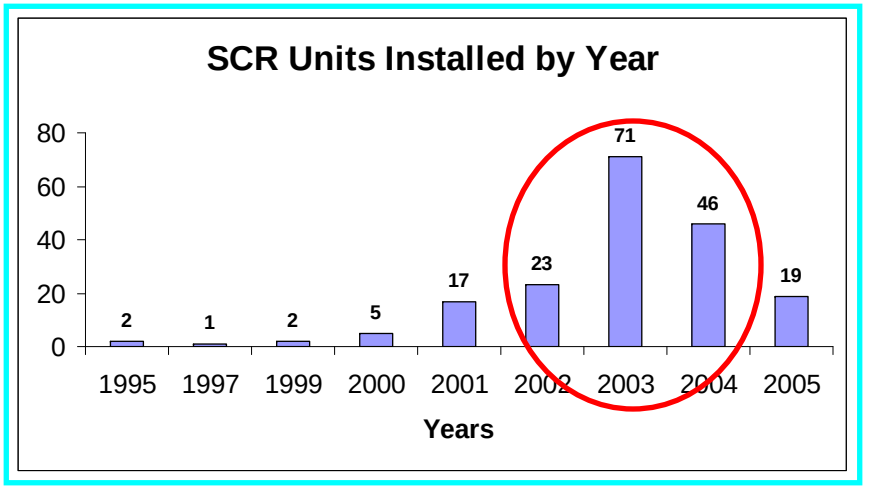

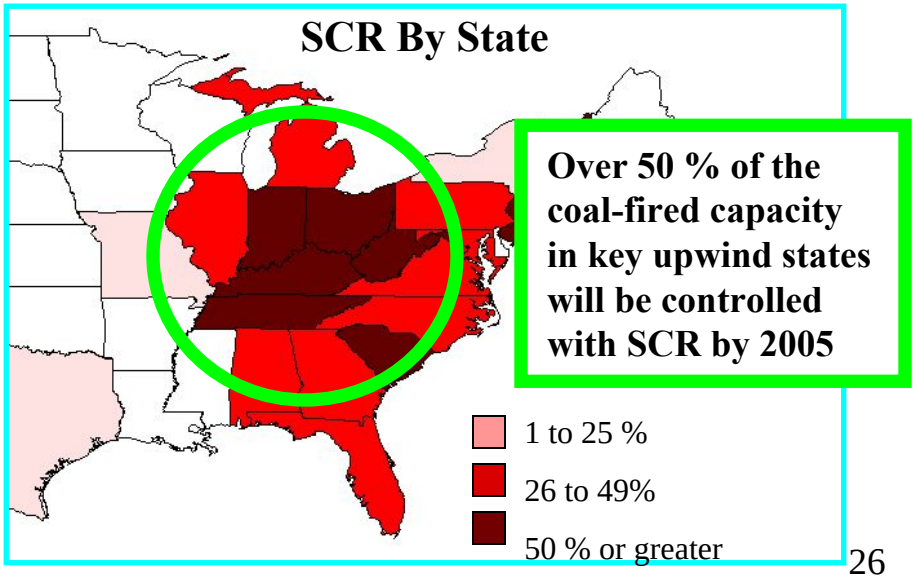

Next Steps

- Develop technical report on the conceptual model as part of OTC modeling effort
- Use simplified conceptual model to guide strategy development and resource allocations
- Blend in fine particle and haze work now underway in states and MANEVU
- Outreach to various audiences

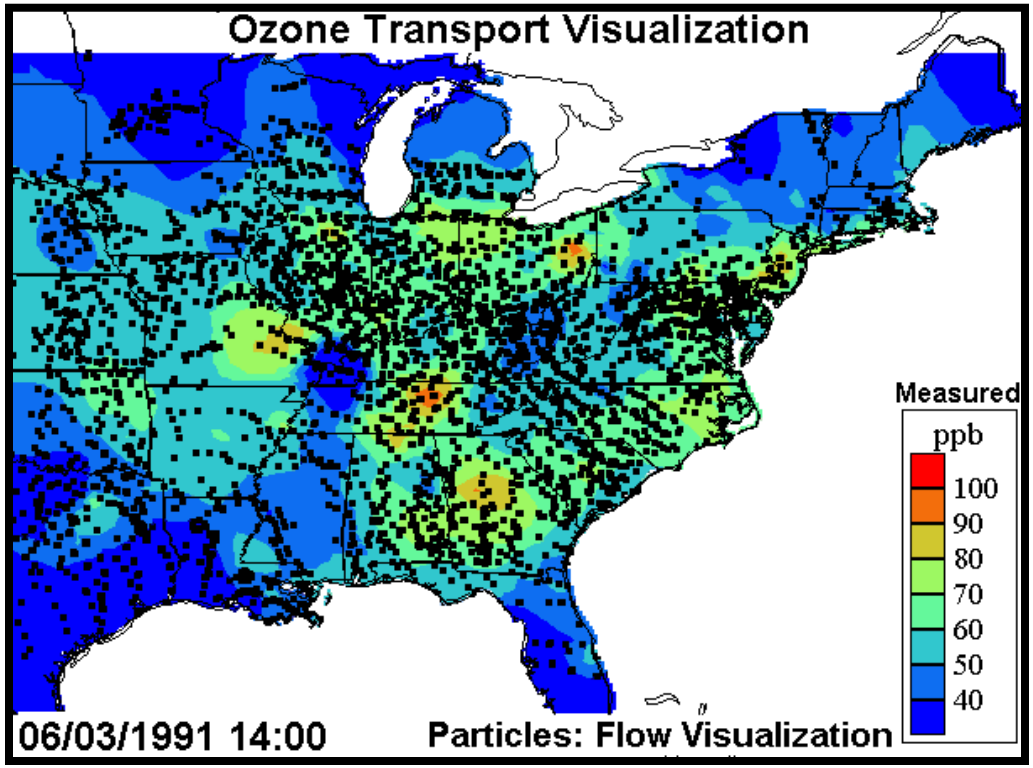

FINAL REPORT

DETERMINATION OF REPRESENTATIVENESS OF 2002 OZONE SEASON FOR OZONE TRANSPORT REGION SIP MODELING

Prepared for

Tom Frankiewicz
Ozone Transport Commission
444 North Capitol St., NW, Suite 638
Washington, DC 20001

Prepared by

Till Stoeckenius
Sue Kemball-Cook
ENVIRON International Corporation
101 Rowland Way, Suite 220
Novato, CA 94945

June 3, 2005

TABLE OF CONTENTS

APPENDICES

TABLES

FIGURES

1. INTRODUCTION

The Ozone Transport Commission is coordinating a photochemical modeling study of the Ozone Transport Region (OTR) in support of State Implementation Plan development for certain areas recently designated by the United States Environmental Protection Agency (U.S. EPA) as being in nonattainment of the 8-hour ozone National Ambient Air Quality Standard (NAAQS). The OTR is comprised of 12 states (DC, CT, DE, ME, MD, MA, NH, NJ, NY, PA, RI, VT) and that portion of Virginia contained within the Washington DC Consolidated Metropolitan Statistical Area (see Figure 1-1). Areas within the OTR designated nonattainment for the 8-hour ozone NAAQS are shown in Figure 1-2; detailed attainment demonstrations are required for the nonattainment areas within the OTR classified as "moderate".

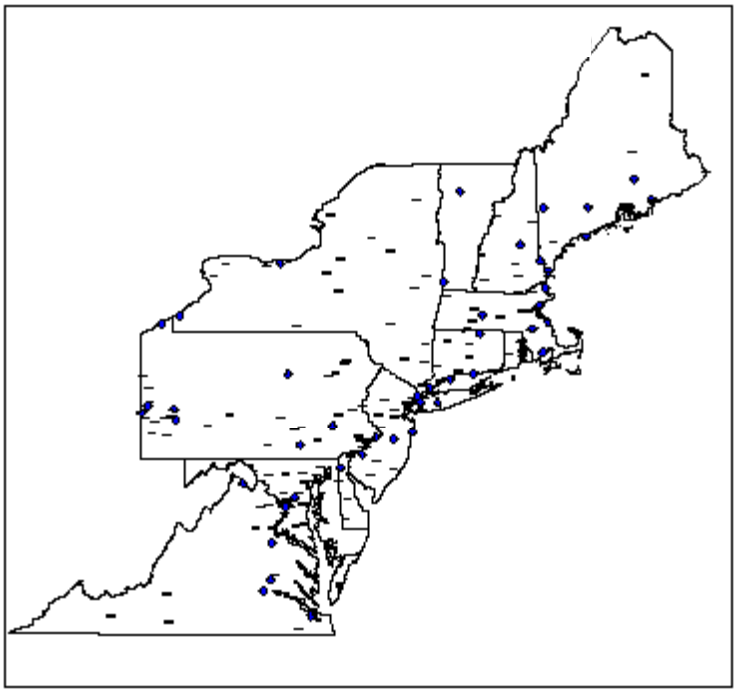

Figure 1-1. Ozone monitoring sites in the Ozone Transport Region which is comprised of DC, CT, DE, ME, MD, MA, NH, NJ, NY, PA, RI, VT, and that portion of Virginia contained within the DC Consolidated Metropolitan Statistical Area.

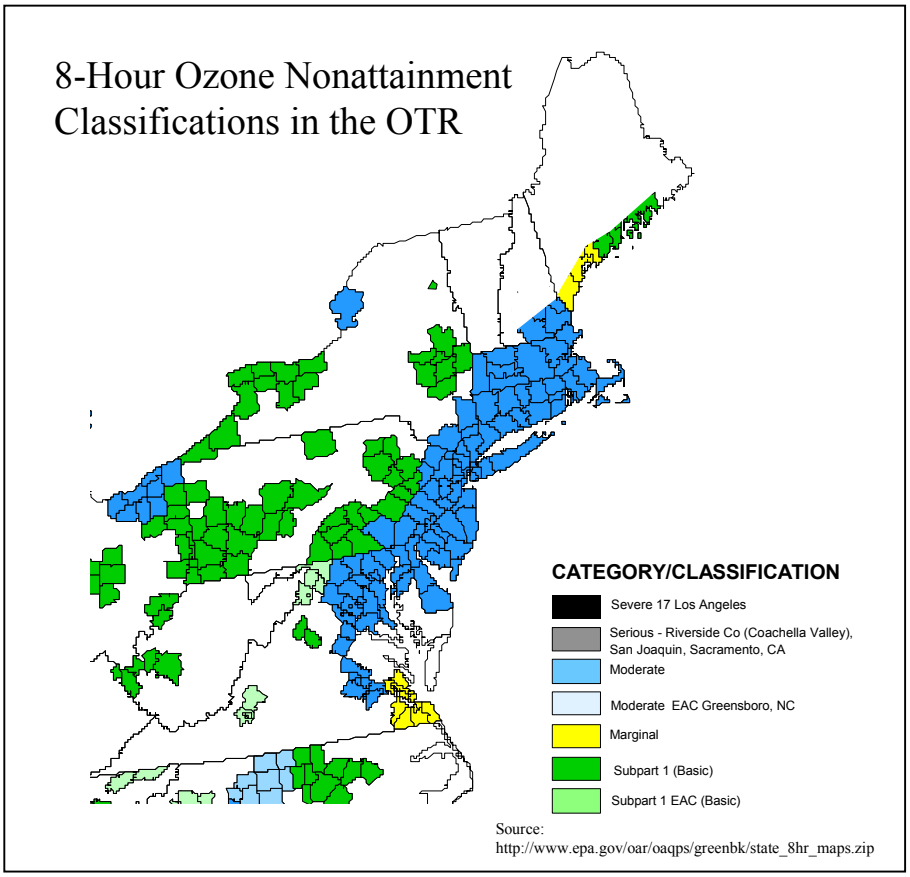

Figure 1-2. 8-hour ozone nonattainment classifications in the OTR and adjacent areas.

Development of effective 8-hour ozone attainment strategies requires application of photochemical models to a set of episodes that adequately represent the range of meteorological conditions associated with violations of the ambient standard. EPA's 8-hour ozone NAAQS modeling guidance (EPA, 1999) lists four criteria for episode selection:

1. Select episodes that both represent a variety of meteorological conditions and frequently correspond to exceedances of the 8-hour ozone standard.
2. Select episodes during which the daily maximum 8-hour ozone averages are close to the 8-hour ozone design value, i.e., the average annual 4th highest daily maximum 8-hour ozone average.
3. Select episodes for which extensive meteorological and air quality data sets are available.
4. Select a sufficient number of episode days for modeling so that the modeled attainment test specified in EPA's guidance is based on several days.

In practice, it is difficult, if not impossible, to meet all of these criteria simultaneously. In general, it is important to include episodes that represent as completely as possible the full range of meteorological conditions associated with exceedances of the ozone standard. Differences among episode types are important in so far as they influence the predicted effectiveness of alternative emission control strategies.

Because the OTR is a large region that experiences a wide variety of weather patterns associated with 8-hour ozone NAAQS exceedances, the OTC has decided to perform ozone SIP modeling of the full 2002 ozone season, May 15 - September 15, to incorporate a fairly large number of episode days in different portions of the OTR. Thus, there should be a good chance that all of the important episode types are covered within this period. However, the 2002 season includes some of the most prolonged and severe ozone episodes in recent years, raising the possibility that one or more episode types of interest are not adequately represented within the 2002 season. The goal of this study, therefore, is to assess the representativeness of conditions during the 2002 season with respect to exceedance events that have occurred in other years and determine if there are any types of episodes that are not adequately represented within the 2002 season.

EPA's 1999 draft guidance recommends joint use of subjective and statistical methods for characterizing and classifying 8-hr ozone episodes. Subjective methods include "typing" of episode meteorological conditions in which episodes are classified via inspection on the basis of similarities in meso- and synoptic-scale weather patterns. In contrast, statistical methods can produce objective classifications either by use of tree models[1] or and various forms of cluster analysis (often in conjunction with a principal components analysis). A predictive classification procedure such as a classification tree model (which can be viewed as a non-parametric form of least-squares regression) does not actually classify episodes, although it can be used to identify potential episodes with common meteorological features. This information can then be used to inform the episode selection process. A cluster analysis, on the other hand, is designed to identify natural groupings of conditions within the set of candidate episodes. In either case, considerable expert judgment is required in variable selection, selection of different modeling methods, and interpretation of results so even the statistical methods are not wholly objective. Nevertheless, these approaches are well suited to the development of valid, defensible episode classification schemes that are sufficiently robust to explain the major characteristics of ozone episode types.

In this study, we apply a combination of exploratory statistical techniques, cluster analyses, and classification tree building algorithms to ozone and meteorological data from the OTR to assess the representativeness of 8-hour ozone episodes occurring during the 2002 season. Data sources and preliminary analyses are described in Section 2. Procedures and results used to identify the major Northeastern U.S. ozone episode types and their key characteristics are presented in Section 3 along with a comparison of the frequency of occurrence and features of each episode type in 2002 versus those in other recent years. Our conclusions regarding the representativeness of the 2002 season are detailed in Section 4.

[1] A commonly used tree modeling approach is based on the CART methodology (Breiman et al., 1984).

2. DATA GATHERING AND INITIAL ANALYSIS

DATA

Daily ozone and meteorological data required for the episode representativeness analysis were obtained from a variety of sources. To capture the full range of OTR episode characteristics and insure statistical significance, a seven year period (1997 – 2003) was chosen for analysis. Data prior to 1997 were not used to avoid any confounding influences of long-term air quality trends. For purposes of this study, data from the warm season months (May – September) were used to capture most if not all high ozone events during the year.

Ozone and meteorological data were separated into two groups: data from 1997 – 2001 and 2003 were treated as the "historical" period and were used to define the types of ozone episode conditions occurring in the OTR. Data from 2002 were treated as an independent data set with data in this year to be compared against the types of conditions found in the historical period.

Hourly ozone concentrations at monitoring sites throughout the OTR for the period 1997-2003 were provided by the New York State Department of Environmental Conservation. Stations missing more than one year of data were excluded from the study, leaving a total of 158 stations with nearly complete data. Daily maximum 8-hour averages were calculated from the hourly data using the data handling conventions specified in 40 CFR 50, Appendix I. Because the spatial pattern analysis procedure requires a complete data set, missing daily maxima were set to the station mean daily maximum (this conforms to the procedure used by Cox, 1997).

Hourly surface meteorological data (winds, temperature, etc.) from airports and other locations in the OTR were obtained from the National Center for Atmospheric Research (NCAR) as dataset ds472. Upper air data were extracted from the ETA Data Assimilation System (EDAS) files available from the National Climatic Data Center. EDAS contains 3-hourly objective analysis initialization and forecast fields from the National Center for Environmental Prediction's (NCEP) ETA model at 40 km resolution. By using the EDAS data, we were able to obtain a consistent set of surface and upper air variables covering the entire eastern half of the U.S. at high temporal resolution.

IDENTIFICATION OF OZONE MONITORING SUB-REGIONS

Monitoring sub-regions were defined within the OTR to emphasize the spatial ozone patterns associated with different types of ozone episodes and to reduce the number of variables required to describe the spatial ozone distribution under different episode patterns. Sub-regions were defined by combining results of a station clustering analysis with information on typical ozone concentration patterns provided by air quality analysts from several OTR states. A variable clustering procedure (VARCLUS) based on principal components analysis was used to group the OTR ozone monitoring sites into disjoint geographic clusters (Sarle, 1990, Harrell 1999). This procedure essentially divides the monitoring stations into groups of highly correlated sites. Station clusters are selected to explain most of the day-to-day variation in ozone levels over the OTR using a small number of station groups. VARCLUS works by performing a principal components analysis on the ozone values in each candidate cluster and seeks to find the set of

clusters that maximize the total (across clusters) of the variance explained by the first principal components.

Required input for the VARCLUS procedure is the number of clusters to be formed. As with any clustering procedure, this introduces an element of subjectivity that can be minimized by repeating the analysis several times, each time varying the number of clusters to be formed and examining the robustness of the cluster memberships as the number of requested clusters (k) changes.

Application of the clustering algorithm for various values of k showed that, for a given value of k, the VARCLUS procedure produced several spatially coherent clusters as well as other clusters which were not spatially coherent. Clusters which were not spatially coherent were always made up of just 5 or fewer member stations. For example, setting k=5 produced 2 coherent clusters (clusters 1 and 2) and 3 smaller clusters (clusters 3-5) whose members tended to be widely separated in space (see Figure 2-1). The version of VARCLUS used for our analysis assigns the lowest cluster identification numbers to the "tightest" (i.e., most easily identifiable and robust) clusters. As the results in Figure 2-1 show, these lowest numbered clusters (in this case Clusters 1 and 2) turned out to also be the most spatially coherent (note that the clustering is based on ozone correlations only – the locations of each monitoring site are not an input to the clustering algorithm). This is consistent with our expectation that sites located close to one another will be highly correlated. Clusters 1 and 2 are similar to the two northeast clusters found by Cox (1997), who used a similar analysis technique applied over the entire eastern U.S.. Successive increases in k over the range 6-10 produced additional coherent clusters which subdivided the two large clusters seen in Figure 2-1. The smaller, non-contiguous clusters remained largely unchanged for all values of k.

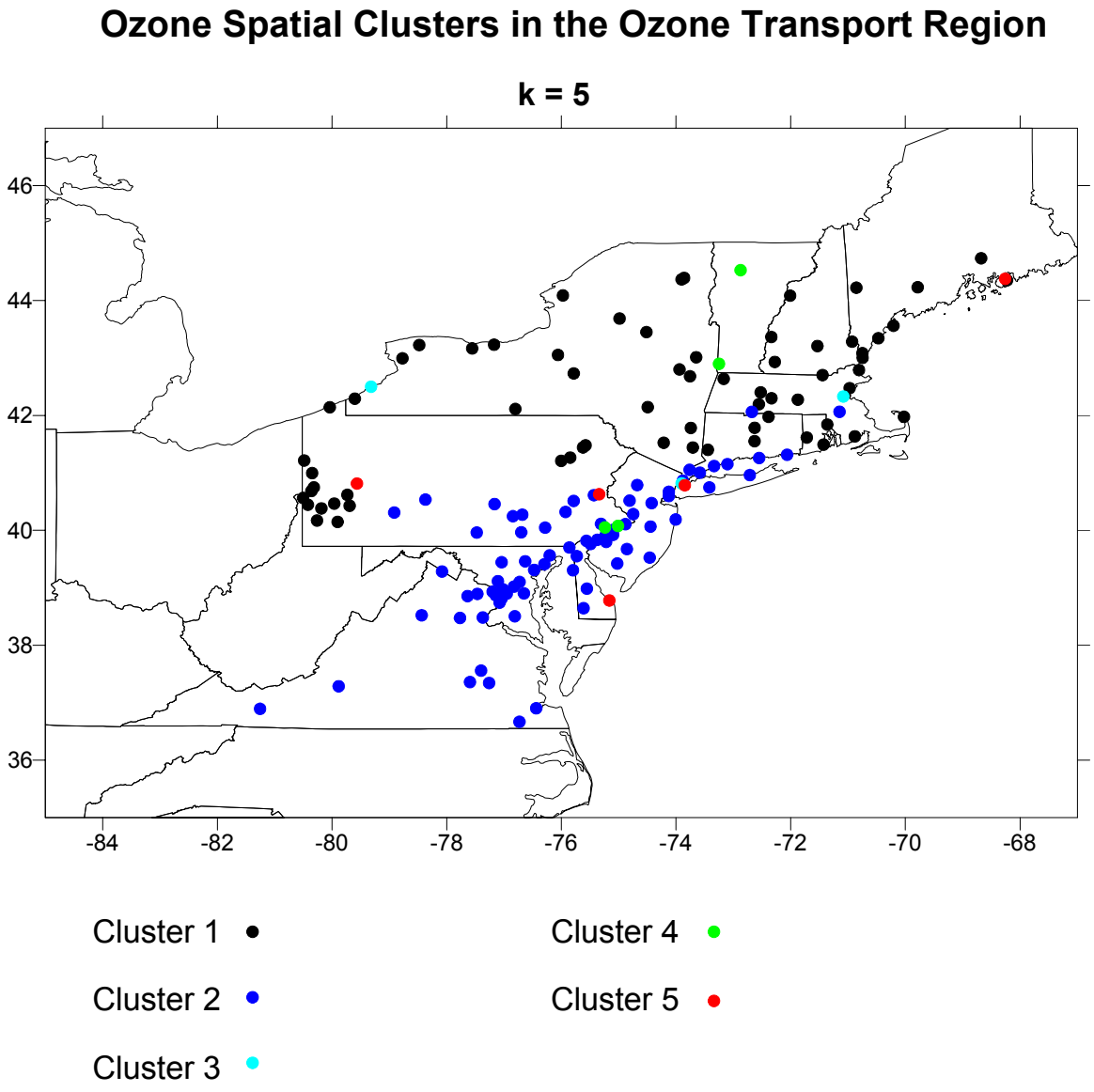

Figure 2-1. Ozone monitoring station cluster assignments for k = 5 clusters.

With k = 10, VARCLUS produced 6 spatially coherent clusters, and 4 smaller, non-coherent clusters (Figure 2-2)[2]. As in the k=5 case, the spatially coherent clusters are the lowest numbered clusters, 1-5, and the non-contiguous clusters are 6-8, and 10. The k=10 case is unusual because cluster 9 (located on the Rhode Island/Massachusetts coast) turned out to be spatially coherent, even though the lower numbered clusters 6-8 were not. We investigated the possibility that cluster 9 should be treated as a separate sub-region. After examining the way exceedances in cluster 9 vary with those in surrounding clusters, however, we concluded that this area could be adequately treated by including it in with cluster 4 (along the Washington – New York City corridor). In order to use only the clusters which seemed robust under variations in k, we therefore based the final ozone monitoring sub-regions largely on the first five clusters obtained under the k=9 scenario (which were slightly more coherent than those under the k=10 case).

[2]Ask was increased beyond 10, the coherent clusters produced were judged to be too small in spatial dimension to be useful in classifying ozone exceedance regimes.

However, the RI – MA coastal sites were associated with the New York City metropolitan area sites rather than the other MA sites based both on the k=10 result described above and input from several state air quality analysts. In addition, all stations on the ME coast were assigned to the southern New England group (Cluster 1) based on input from state air quality analysts. Stations from the other higher numbered, non-contiguous clusters were integrated into the surrounding clusters; there were no such stations for which the appropriate cluster assignment was ambiguous.

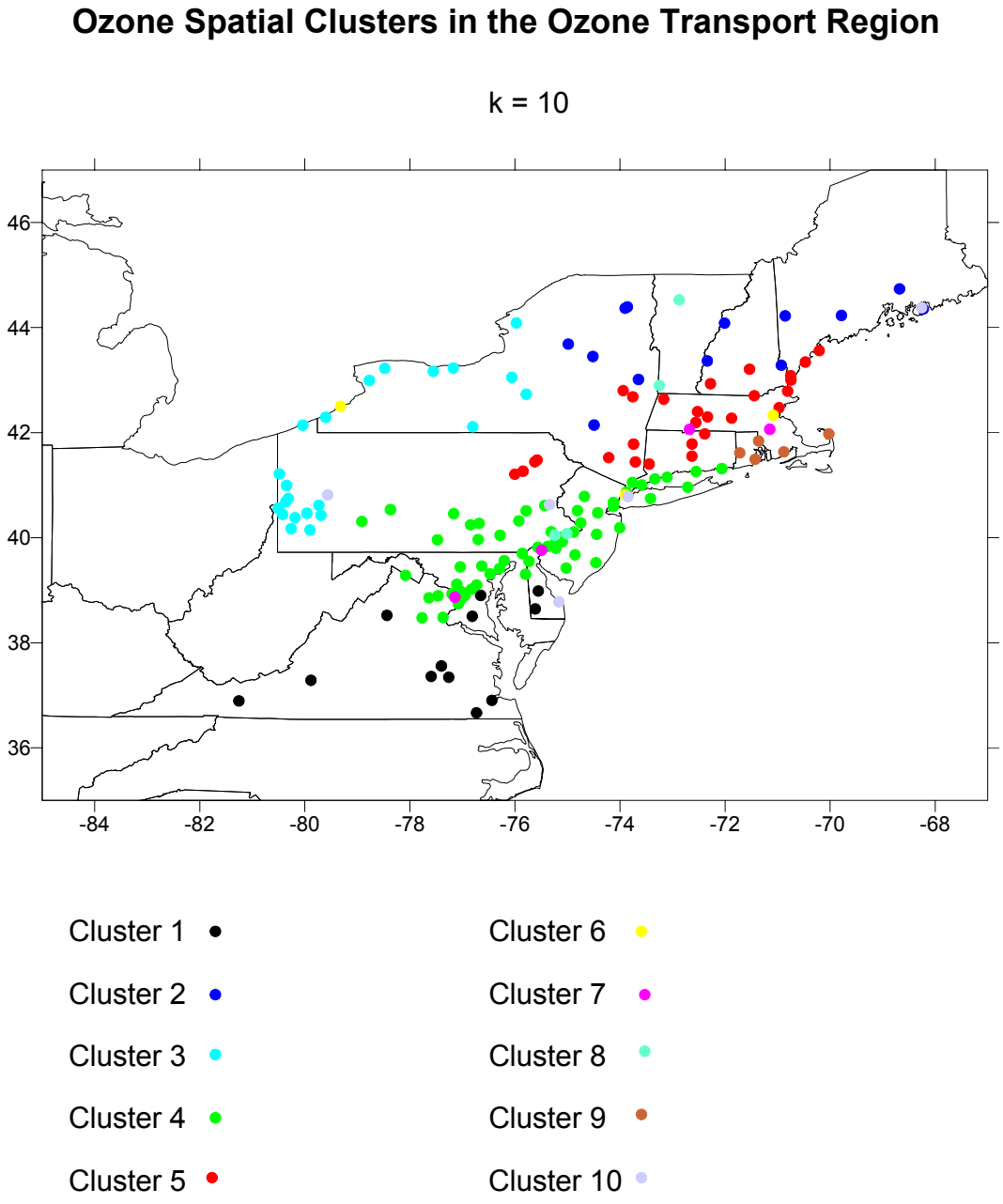

Figure 2-2. Ozone monitoring station cluster assignments for k = 10 clusters.

Another adjustment to the VARCLUS results was made along the Philadelphia – New York corridor. Figure 2-3 shows the number of 8-hour exceedances at each monitoring site during the period analyzed. Exceedance events in the Washington – Philadelphia corridor are more frequent than within and downwind (northeast) of the New York City metropolitan area. Furthermore, based on our discussions with state ozone forecasters in the OTR, we expect transport of ozone and ozone precursors along the I-95 corridor to play an important role in exceedance events. This suggests that leaving the entire Washington to New York City cluster intact might cause our final episode classification scheme to overlook events in which transport northeast from Washington-Baltimore-Philadelphia to New York is an important feature. We therefore decided to split this cluster into two parts as shown in the final ozone monitoring sub-region assignments presented in Figure 2-4. Cluster 5 extends from the Washington area through Trenton and a new cluster 6 covers the New York City-Long Island-Southern Connecticut region. A list of the monitoring sites assigned to each cluster is provided in Appendix D.

Number of 8-Hour Station Ozone Exceedances for 1997-2003 Excluding 2002

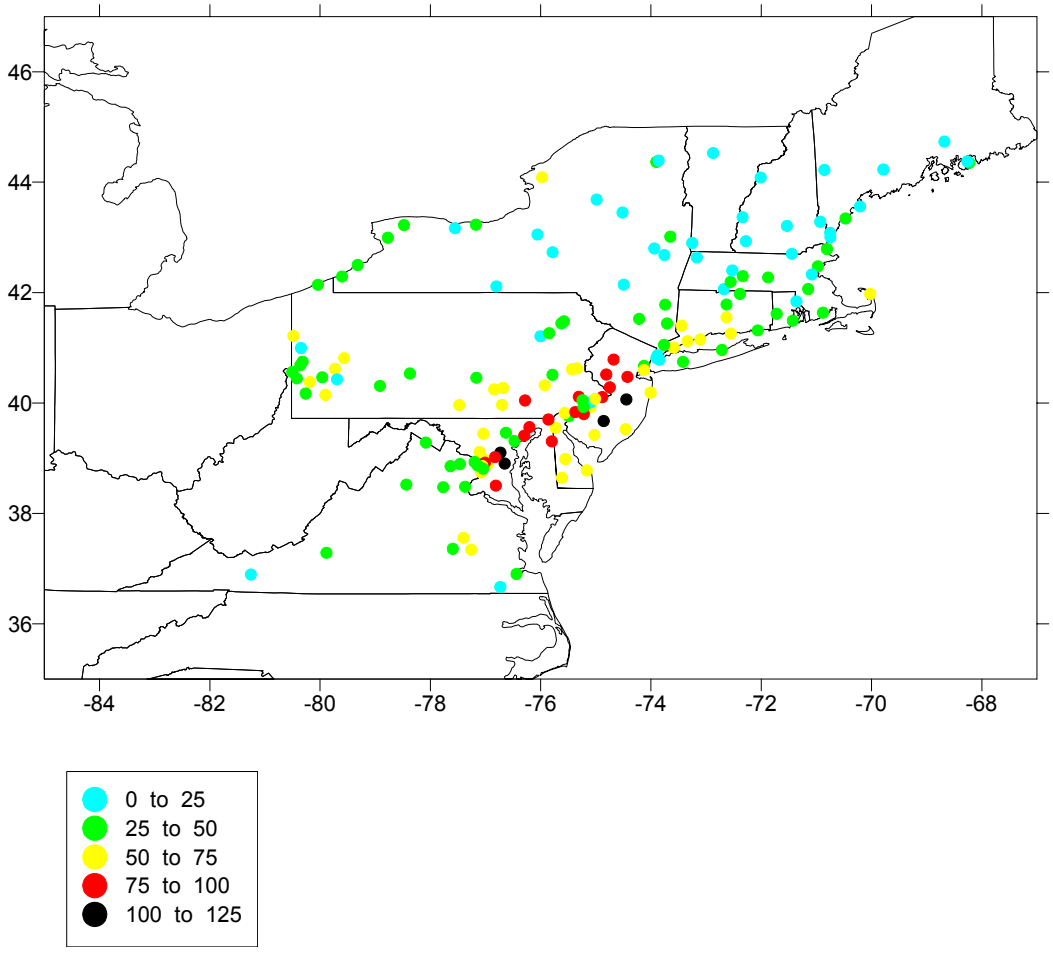

Figure 2-3. Number of 8-hour ozone NAAQS exceedance days at each monitoring site during the study period (1997 – 2001 and 2003).

Ozone Spatial Clusters in the Ozone Transport Region

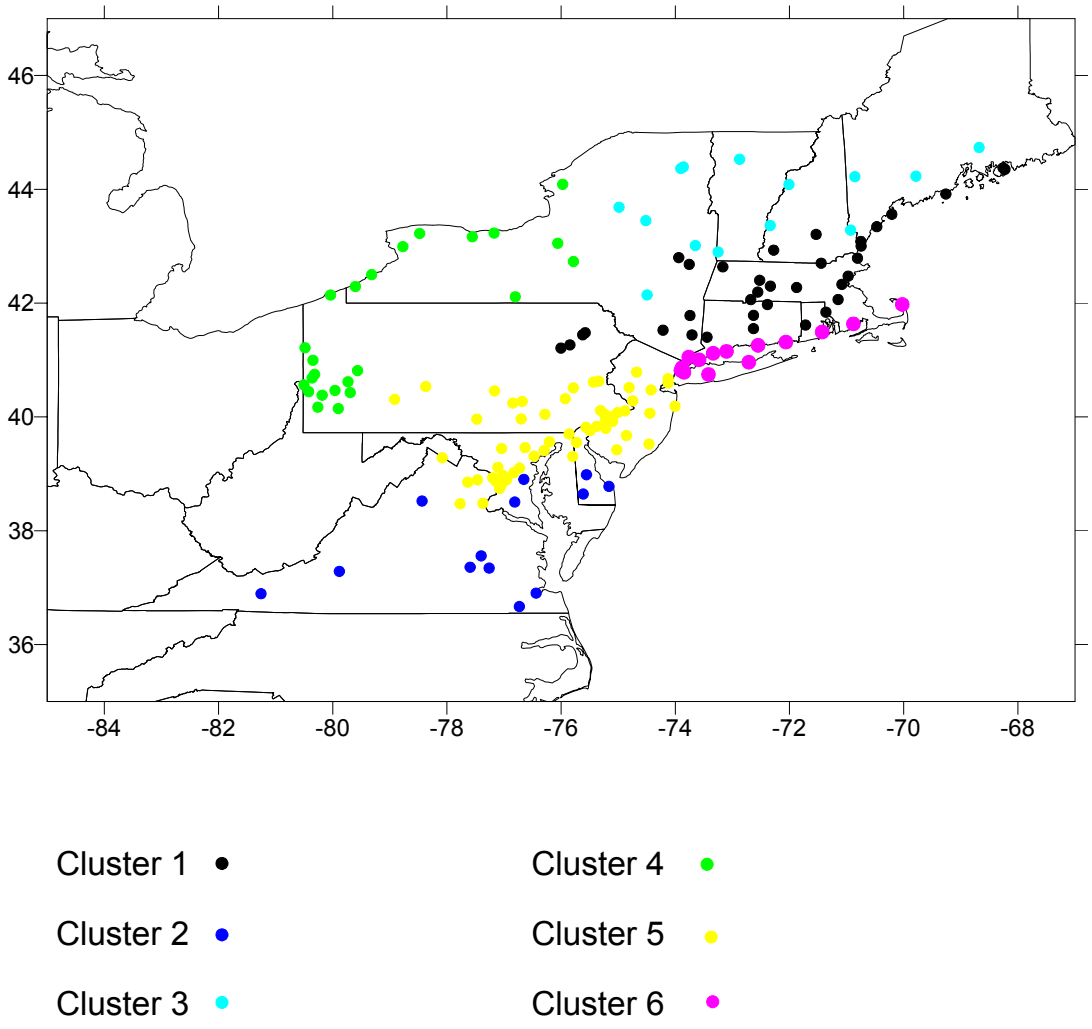

Figure 2-4. Ozone monitoring sub-regions in the OTR.

SPATIAL OZONE PATTERN ANALYSIS

An initial analysis of episode patterns was performed based on 8-hour ozone concentrations within the sub-regions (spatial clusters) described above. For each day, a cluster was determined to be in exceedance if any one monitoring site in the cluster recorded an exceedance. We then counted the number of joint exceedance events between each pair of clusters and examined exceedance patterns across all six clusters. Detailed results from this analysis were provided in a technical memorandum to the OTC (Stoeckenius and Kemball-Cook, 2004) but are not repeated here because this approach was eventually discarded in favor of an integrated analysis approach in which the daily ozone levels in each sub-region were combined with daily meteorological data to determine the key characteristics of the major types of ozone episodes occurring in the OTR.

METEOROLOGICAL VARIABLE SELECTION

The extensive amount of meteorological data collected for this study was reduced to allow processing of days into groups with similar conditions as described in Section 3. Selection of key meteorological variables that best represent conditions across the OTR on exceedance days was based on a review of previous studies (Deuel and Douglas, 1996; McHenry et al., 2004) and on discussions with state and local agency air quality personnel involved in ozone forecast programs within the OTR. Key variables focused on both surface conditions (maximum temperature, morning and afternoon average wind direction and speed, pressure) and conditions aloft (500 and 850 mb heights, temperatures, and winds). The final selected set of key daily meteorological parameters are:

Surface resultant wind speed and direction computed for both morning (05:00 – 10:00 EST) and afternoon (12:00 – 17:00 EST) hours at New York City (LaGuardia), NY; Philadelphia, PA; Boston, MA; Buffalo, NY; Albany, NY; Washington, DC; Portland, ME, Atlantic City, NJ; Islip (Long Island), NY; Hyannis (Cape Cod), MA; Worcester, MA; and Hartford, CT.[3]

Surface daily maximum temperatures at New York City (LaGuardia), NY; Philadelphia, PA; Boston, MA; Buffalo, NY; Albany, NY; Washington, DC; Portland, ME, Atlantic City, NJ; Islip (Long Island), NY; Hyannis (Cape Cod), MA; Worcester, MA; and Hartford, CT.[3]

Temperatures, heights, and winds at 850 mb pressure surface at Washington, DC; New York, NY; Boston, MA; Pittsburgh, PA; Buffalo, NY; and Portland, ME.

Surface pressure gradients across the OTR computed as pressure differences between:

Washington, DC and New York City, NY;
Washington, DC and Boston, MA;
Washington, DC and Pittsburgh, PA;
Pittsburgh, PA and Buffalo, NY;
Buffalo, NY and Boston, MA.

[3]Surface wind and temperature data from Concord, NH and New Haven, CT were also examined but these sites had a high frequency of missing data which prevented their use in this analysis.

3. EPISODE CLASSIFICATION ANALYSIS

In this section we describe a series of clustering and exploratory analyses performed on the ozone and meteorological data discussed in Section 2. Clustering was performed with data from the historical (1997 – 2001 and 2003) period to identify the major types of ozone episodes in the OTR and their key characteristics. Once the key episode types were identified, we developed a decision rule for classifying any given day into one of the identified episode types based on ozone levels and meteorological conditions. This decision rule was then used to classify days during the 2002 ozone season by episode type. The resulting distribution of episode types and the ozone and meteorological conditions occurring within each type in 2002 were subsequently compared with results from the historical period to determine the representativeness of the 2002 with respect to conditions during the historical period.

CLUSTERING ANALYSIS

Clustering was performed with data for the 329 days in the 1997-2001/2003 historical period on which an 8-hour ozone exceedance was recorded at one or more of the monitoring sites shown in Figure 2-4. As the clustering algorithms require numerical variables, wind directions were decomposed into u (east-west) and v (north-south) components. Meteorological data were prepared for clustering by first filling in missing values with exceedance day means. This step was necessary as the clustering procedures cannot process any days that have missing values for one or more variables. While the fraction of data that are missing for any individual variable is fairly small, roughly two-thirds of the 329 8-hour ozone exceedance days in our historical dataset had at least one missing value, so it was important to impute the missing values in some fashion even though the clustering results are not likely to be too sensitive to the exact method of imputation. All of the data were then standardized by computing z-scores (i.e., subtracting the mean and dividing by the standard deviation) prior to clustering so that variables with different scales of measure are given equal weight.

Ozone data were also prepared for use in the clustering analysis. Two daily ozone summary statistics, AvgEx08 and AvgEx00 were computed for each monitoring sub-region shown in Figure 2-4. AvgEx08 was defined as the average, over all sites in a given sub-region, of the amount by which the daily maximum 8-hour average exceeded 0.08 ppm (with values for sites below 0.08 ppm set equal to zero). AvgEx00 is identical to AvgEx08 but with the exceedance threshold set to 0 ppm. As with the meteorological data, z-scores were computed for the daily AvgEx08 in each sub-region for use in the clustering analysis. Preliminary clustering analyses were performed using the methods described below with first the AvgEx08 measure and then the AvgEx00 measure. Of the two, cluster results based on the AvgEx00 measure were chosen, as they were more robust and physically meaningful then results based on the AvgEx08 measure.

Initially, clustering was applied to the meteorological variables only. Both agglomerative and divisive hierarchical clustering techniques were used. Classifications of days under the resulting meteorological clusters were compared with the classification of days by ozone exceedance pattern, which had previously been reported (Stoeckenius and Kemball-Cook, 2004). These comparisons showed that, while some pairs of exceedance and meteorological patterns showed a dominant one-to-one relationship, others did not. In other words, some of the exceedance

patterns were typically associated with more than one meteorological pattern and some meteorological patterns were typically associated with more than one exceedance pattern. This result was found to be robust in the sense that it occurred under a variety of clustering approaches. We interpreted this to mean that at least some of the ozone exceedance patterns described by Stoeckenius and Kemball-Cook were not sufficiently unique from a meteorological perspective to serve as adequate archetypes of different types of ozone episodes. Given this result, we decided to examine clustering approaches based on using both the meteorological and ozone (AvgEx00) data simultaneously.

Before proceeding further, we performed a principal components analysis (PCA) on the combined ozone and meteorological data set prior to clustering to determine if it would be possible to reduce the number of variables required for the analysis. Preliminary results showed, however, that the first four components only explained 14% of the total variance. As a result, we did not pursue the PCA any further but simply retained all of the key variables in the clustering analysis.

Several different clustering procedures were applied to the data. Application of single and complete linkage hierarchical agglomerative clustering methods (Venables and Ripley, 1994) to the combined ozone and meteorological data resulted in the formation of one large cluster containing most of the days in the dataset and a large number of additional clusters containing at most a few days each. Use of Ward's method (Ward, 1963) produced a more even distribution of cluster membership at each stage of the agglomeration but with fairly evenly spaced reductions in deviance (see resulting dendrogram in Figure 3-1). In other words, these results did not provide much guidance as to what would constitute a reasonable number of clusters to use in describing the data.

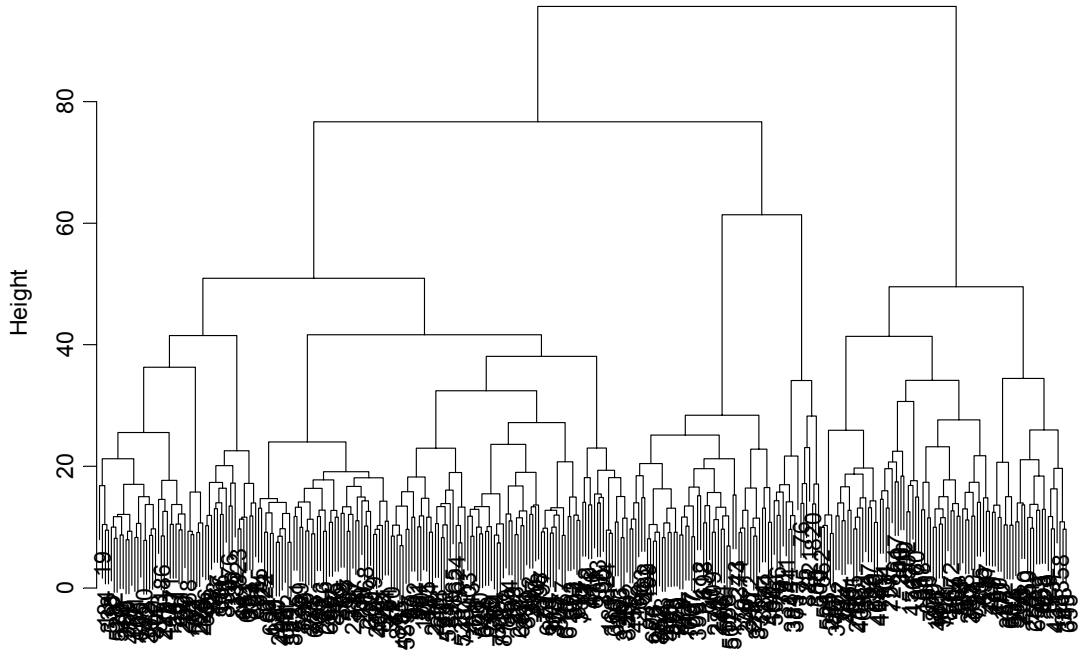

Figure 3-1. Dendrogram from application of Ward's hierarchical agglomerative clustering to the combined daily ozone and meteorological data. Each leaf at the bottom of the figure represents one day; the vertical height at which pairs of leaves (or pairs of clusters of leaves) are joined represents a measure of the distance between the leaves (or cluster centroids) in the multivariate data space.

Based on the agglomerative clustering results, we decided to apply Hartigan's k-means clustering algorithm (Hartigan, 1979) several times, specifying a different value for the number of clusters to form in each application. Under the k-means algorithm, data are arranged into a pre-specified number of clusters so as to minimize the total within-cluster sum of squares. Initial cluster centroids are determined via agglomerative hierarchical clustering. After this initial step, each day is assigned to the nearest cluster centroid where "nearest" is in this case defined as the minimum least squares distance computed over all of the standardized variables. After this initial assignment phase, the algorithm iteratively reassigns days to different clusters until the sum of the within-cluster sums of squares is minimized.[4]

Due to the large number of variables used in the clustering procedure, it is difficult to obtain a complete picture of the meteorological and air quality conditions associated with days falling in each cluster, especially when looking at several alternative cluster configurations. As one of the most important features of each cluster is the spatial ozone distribution, we tabulated the mean

[4]As finding the global minimum of this objective function is not computationally feasible, Hartigan's algorithm actually finds a local minimum such that switching any single observation from one cluster to another does not reduce the objective. As a result, the final cluster assignments may be sensitive to the selection of initial cluster centroids.

values of the ozone measure described above (AvgExc00) for each sub-region within each cluster identified by the k-means algorithm when the data are divided into between 4 and 7 clusters (see Table 3-1). We also examined similar sets of results for each key meteorological variable. Inspection of these results revealed the presence of five distinct sets of ozone and meteorological conditions that are robust in the sense that they show up consistently whether the data are divided into 4, 5, 6 or 7 clusters.

Table 3-1. Mean z-scores for the AvgEx00 ozone summary statistic within each monitoring sub-region under four different candidate sets of cluster designations. The episode pattern ID in the far right-hand column is keyed to the episode patterns described in the text.

a) 4 clusters							**Episode Pattern**
Cluster #	**Sub-Region 1**	**Sub-Region 2**	**Sub-Region 3**	**Sub-Region 4**	**Sub-Region 5**	**Sub-Region 5a**	**ID**
1	0.51	0.08	0.40	-0.08	0.26	0.56	C
2	-0.86	0.49	-0.86	-0.40	-0.15	-0.37	B
3	0.27	0.05	0.22	0.30	0.30	0.20	A
4	-0.72	-0.57	-0.45	-0.31	-0.93	-0.96	E
b) 5 clusters							
Cluster #	**Sub-Region 1**	**Sub-Region 2**	**Sub-Region 3**	**Sub-Region 4**	**Sub-Region 5**	**Sub-Region 5a**	
1	-0.74	0.07	-0.40	-0.58	-0.34	-0.78	E
2	-0.70	0.45	-0.73	-0.37	-0.06	-0.17	B
3	0.45	0.16	0.32	0.35	0.45	0.46	A
4	-0.49	-0.97	-0.35	0.22	-1.07	-0.91	D
5	0.54	-0.04	0.47	-0.10	0.17	0.42	C
c) 6 clusters							
Cluster #	**Sub-Region 1**	**Sub-Region 2**	**Sub-Region 3**	**Sub-Region 4**	**Sub-Region 5**	**Sub-Region 5a**	
1	-0.83	0.47	-0.88	-0.47	-0.17	-0.27	B
2	0.38	0.21	0.23	0.44	0.49	0.46	A
3	0.05	-1.62	0.17	0.58	-1.32	-0.86	D
4	-1.13	-0.17	-0.91	-0.52	-0.89	-1.10	E1
5	0.49	0.03	0.43	-0.10	0.21	0.48	C
6	-0.19	-0.14	0.11	-0.39	-0.17	-0.48	E2
d) 7 clusters							
Cluster #	**Sub-Region 1**	**Sub-Region 2**	**Sub-Region 3**	**Sub-Region 4**	**Sub-Region 5**	**Sub-Region 5a**	
1	0.59	-0.30	0.56	-0.39	-0.02	-0.01	C
2	0.08	0.02	0.02	0.32	0.32	0.10	D1
3	0.08	-1.77	0.21	0.65	-1.52	-1.00	D2
4	-1.17	-0.15	-0.97	-0.54	-0.88	-1.11	E1
5	0.60	0.44	0.39	0.45	0.60	1.03	A
6	-0.38	-0.12	-0.03	-0.45	-0.27	-0.58	E2
7	-0.89	0.47	-0.89	-0.47	-0.19	-0.39	B

We prepared summaries of the meteorological characteristics of each of these five episode types as follows:

1) Composite maps of surface and upper air (850 mb) meteorological variables for each cluster,

2) Side-by-side box plots comparing the distributions of selected key meteorological variables within each cluster, and

3) Tables of morning and afternoon resultant wind direction frequencies within each cluster.

Full results of items 1 – 3 above are presented in Appendix A, B, and C, respectively. By way of example, we show the 850 mb height and wind fields, 850 mb temperature, surface pressure, and surface daily maximum temperature and 10 m wind fields composited for each episode type in Figures 3-2 to 3-5, respectively. Comparing these composite fields for different episode types reveals that each episode type is characterized by a distinct meteorological pattern and these patterns are consistent with the ozone patterns noted in Table 3-1. Key characteristics of the five episode types are presented in Table 3-2. In the description of each episode type, "average" refers to averages over all OTR exceedance days used in the cluster analysis.

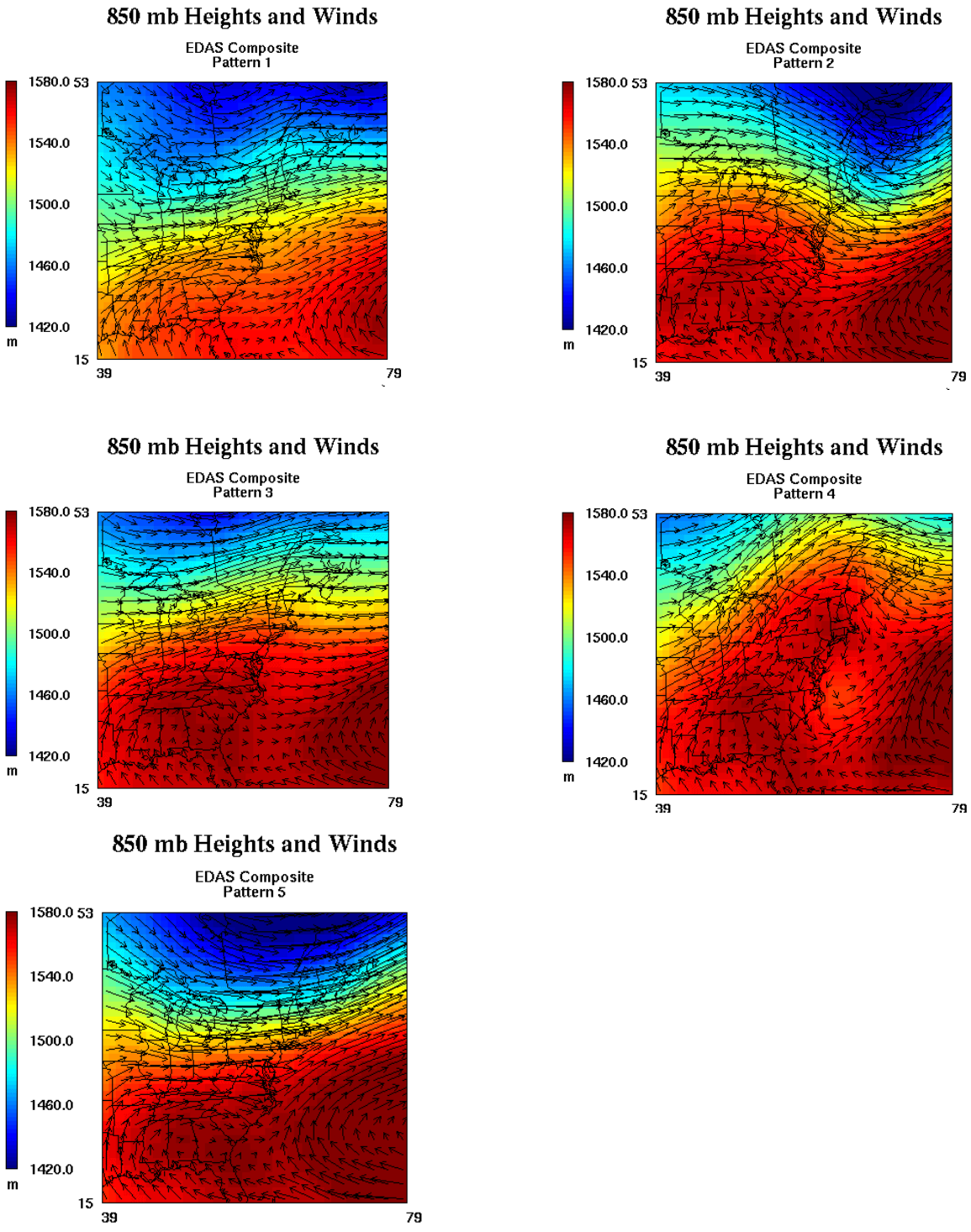

Figure 3-2. Average 850 mb height and wind fields for each episode (pattern) type (pattern numbers refer to the episode types listed in Table 3-2): Pattern 1 = Episode Type E, 2 = B, 3 = A, 4 = D, 5 = C).

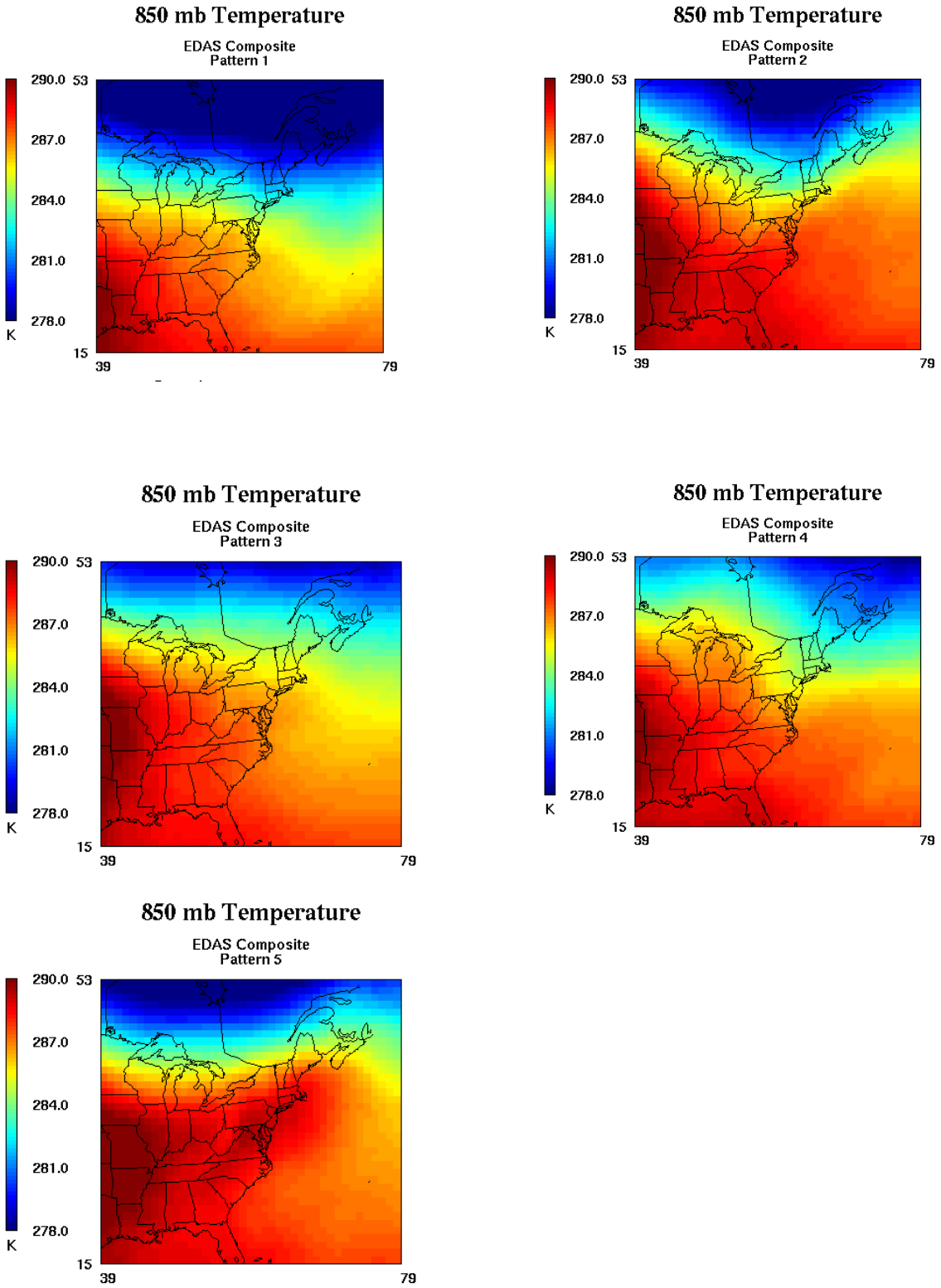

Figure 3-3. Average 850 mb temperature fields for each episode (pattern) type (pattern numbers refer to the episode types listed in Table 3-2): Pattern 1 = Episode Type E, 2 = B, 3 = A, 4 = D, 5 = C).

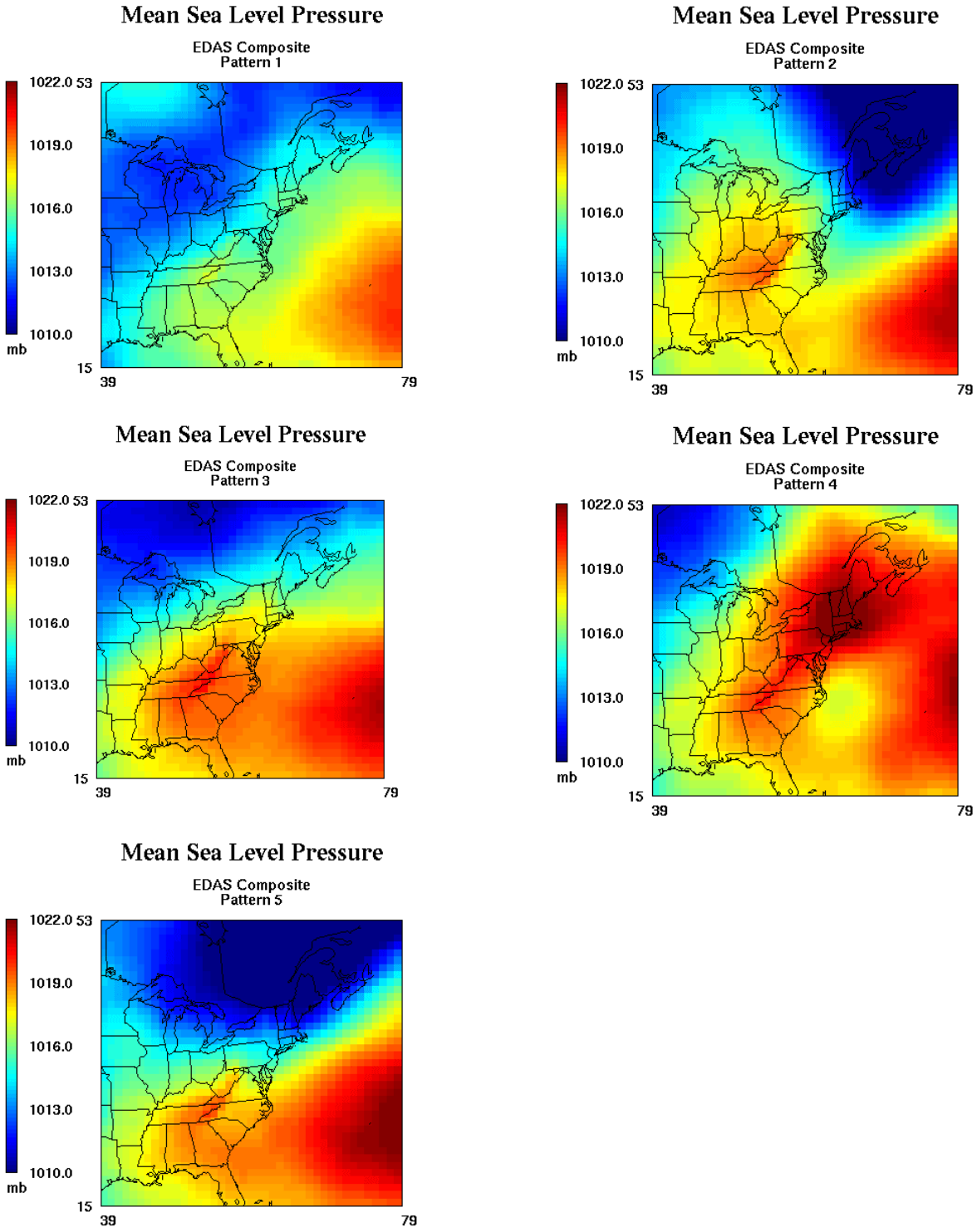

Figure 3-4. Average surface sea level pressure for each episode (pattern) type (pattern numbers refer to the episode types listed in Table 3-2). Pattern 1 = Episode Type E, 2 = B, 3 = A, 4 = D, 5 = C).

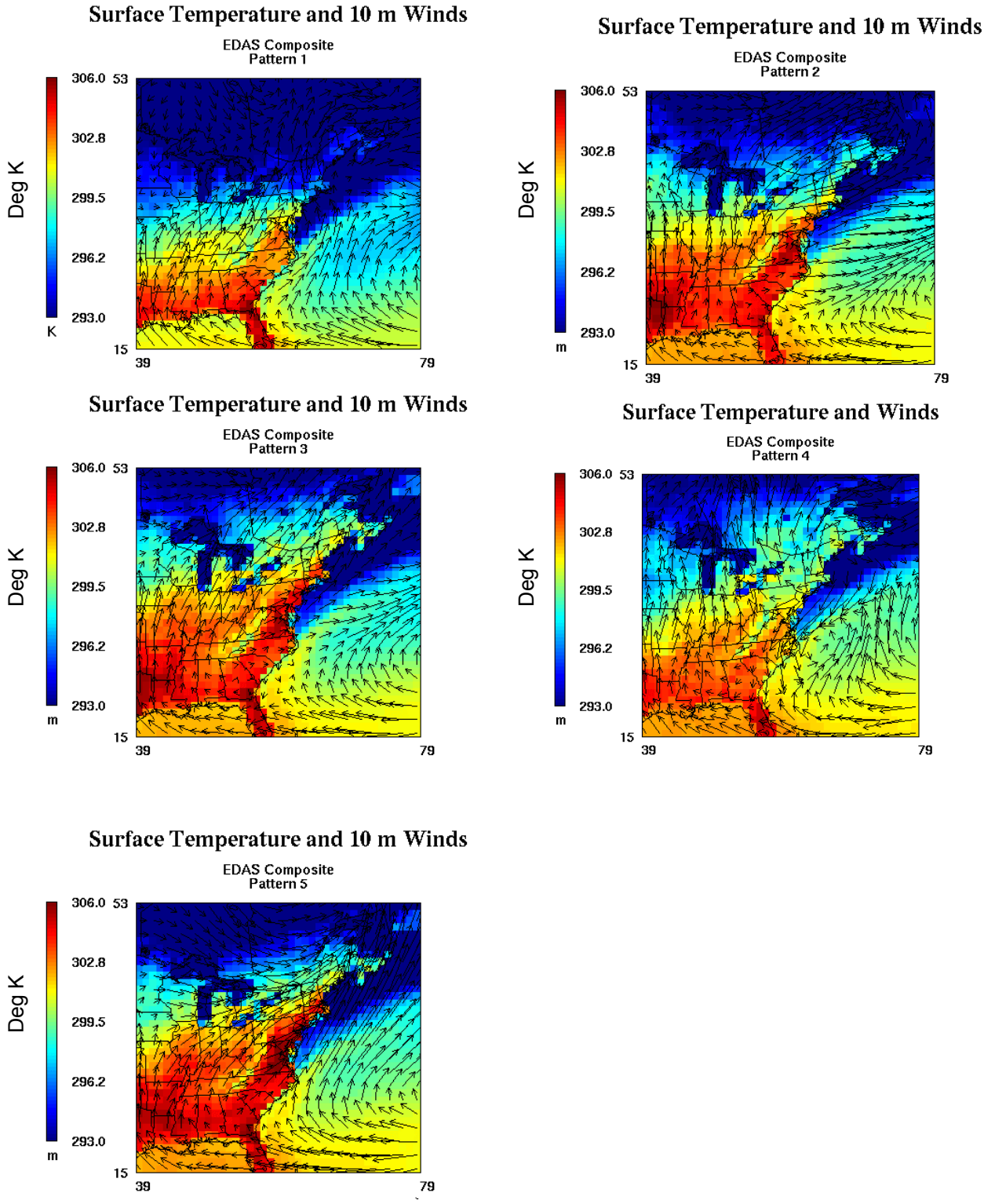

Figure 3-5. Average surface temperature and 10 m wind fields for each episode (pattern) type (pattern numbers refer to the episode types listed in Table 3-2). Pattern 1 = Episode Type E, 2 = B, 3 = A, 4 = D, 5 = C).

Table 3-2. Key characteristics of each OTR episode type.

Episode Type	Pattern No.	Description
A	3	*High ozone throughout the OTR.* This pattern is characterized by strong high pressure over the southeastern states extending from the surface to 500 mb with high temperatures extending into New England and southwest surface winds throughout the OTR. 850 mb temperatures and heights, and surface temperatures are above average at all locations except Washington DC; winds are SW to W throughout the OTR except more variable at LaGuardia and magnitudes of resultant wind vectors are higher than average (indicative of a fairly steady, well defined flow regime), E-W surface pressure gradients are near neutral but SW-NE gradients both along the I-95 corridor and in the west (Pittsburgh to Buffalo) are positive which is consistent with the SW flow. Ozone formation under these conditions is promoted throughout the OTR by the stable air mass and high temperatures.
B	2	*High ozone confined to the extreme southeastern OTR.* This pattern is characterized by an upper-level trough offshore of the OTR and a surface high centered over Kentucky. This results in cooler air advection over nearly all of the OTR with northwest flow aloft and a more westerly flow at the surface. 850 mb heights are lower than average (especially in New England) and surface winds are more frequently from NW along the I-95 corridor than under Type A. Temperatures at 850 mb along the I-95 corridor are only slightly cooler than under Type A but inland temperatures, especially in the north, are much cooler (e.g., at Buffalo); similarly, surface temperatures along the I-95 corridor are about the same as under Type A but temperatures are cooler in Buffalo and Albany. Type B events have the strongest positive W – E surface pressure gradients of any category, consistent with the NW winds but gradients from Washington to New York and Boston are positive. The cooler air over the western OTR and westerly to northwesterly flow result in the higher ozone levels being confined to just the extreme southern portion of the OTR under this pattern.
C	5	*High ozone along I-95 corridor and northern New England.* This pattern is characterized by an extension of the semi-permanent Bermuda high into the southeastern U.S. and an area of high surface and 850 mb temperatures extending from Maryland to Maine; the 500 mb pattern is nearly zonal (east – west flow) while flow at the surface is generally from the SW. 850 mb heights intermediate between Type A and Type B but 850 mb temperatures are very high along the I-95 corridor and slightly cooler further inland. Winds are more consistently S - SW at all sites than under other episode types and almost no NW-N-NE winds are seen at LaGuardia in contrast to other types. Resultant wind vector magnitudes are much higher than average, consistent with the steady SW flow. SW – NE pressure gradients along I-95 corridor and from Pittsburgh to Buffalo are positive, consistent with the SW flow. Average E-W pressure gradients are near zero. These conditions result in above average ozone levels all along the I-95 corridor with advection north into coastal and interior New England. Ozone levels are slightly below average in the extreme southeastern and western OTR (subregions 2 and 4).

Episode Type	Pattern No.	Description
D	4	*High ozone in the western OTR*. This pattern is characterized by an area of mean upper level divergence with associated cut-off low at 850 mb off the Outer Banks of North Carolina. A relatively vigorous mean low pressure center can be seen at the surface. An east-west temperature gradient across the OTR is evident at 850 mb. Surface temperatures along the I-95 corridor and in Albany are below average but surface temperature is above average at Buffalo. 850 mb heights are the highest of any episode type due to a strong ridge over New England. Surface winds are mostly E - NE along I-95 corridor from DC to NY but more variable further north. In contrast to episode types A, B, or C, SW – NE pressure gradients along the I-95 corridor are negative, consistent with the NE surface winds. W – E pressure gradients are flat. These conditions result in below average ozone in the eastern OTR (sub-regions 1, 2, 3, 5, and 6) due to the on-shore flow in the north and cyclonic conditions in the south but above average ozone levels in the western OTR (sub-region 4) due to stable, warm conditions with light winds.
E	1	*Generally low ozone throughout OTR*. This category includes days with moderately low to lowest average ozone readings of all OTR exceedance days included in the cluster analysis. The Bermuda high is shifted east relative to the other types and flow over the southeastern U.S. is only weakly anti-cyclonic with a nearly zonal flow pattern at the 850 and 500 mb levels over the OTR. Temperatures at the surface and aloft are the coolest of any episode type. While winds aloft are nearly westerly, surface winds are generally S – SE over most of the OTR. SW – NE pressure gradients are negative along the I-95 corridor and E-W gradients are positive, consistent with the SE flow. These conditions result in below average ozone throughout the OTR due to the relatively low temperatures and southeasterly onshore flow at coastal locations.

The five episode types described in Table 3-2 exhibit characteristics, which are largely consistent across the different cluster allocations noted in Table 1 (4, 5, 6 or 7 clusters). When four clusters are specified, the Type D events are subsumed into the remaining four episode types. Finer division of days into six clusters results in a split of the Type E events into two groups (denoted as E1 and E2 in Table 1) with generally very similar meteorological conditions but distinguished in part by E-W pressure gradient anomalies that are slightly greater under type E2. Further division into seven clusters appears to preserve the Type A, B, and, to a lesser extent, Type C events along with the Type E1 and E2 events found in the seven cluster result while the Type D events are split into two new categories (denoted D1 and D2 in Table 1). Both D1 and D2 events are associated with high ozone in the west (sub-region 4) under S – SW flow as is typical of Type D but differ in the surface wind pattern, and hence ozone anomalies, along the I-95 corridor.

It is important to keep in mind that there is no *a priori* expectation that all ozone exceedance events in the OTR fall into one of a finite number of distinct patterns: daily conditions differ from one another to varying degrees and some days will always have characteristics that cross over any predetermined classification boundaries. This means that an episode classification system will always have a certain degree of arbitrariness to it and division of days into bins will always result in some days that do not fit particularly well into any single bin. Nevertheless, for purposes of this study, we seek a reasonable classification system based on a handful of pattern types each of which is uniquely identifiable by a set of characteristics related to ozone formation

across the *entire* OTR.[5] Based on the clustering results described above, it appears that the episode Types A – E meet these requirements reasonably well. Frequencies of occurrence for these five types are shown in Table 3-3.

Table 3-3. Frequencies of occurrence of OTR episode types.

	Type A	Type B	Type C	Type D	Type E
No. Days	123	50	66	44	46
Pct.	37%	15%	20%	13%	14%

DEVELOPMENT OF AN OBJECTIVE CLASSIFICATION PROCEDURE

In order to complete our analysis, we needed to develop a final episode classification rule based on results of the above analysis of the 1997 – 2001 and 2003 data which can then be applied to the 2002 data to determine the classification of episodes in 2002 to the five ozone event types described above. A classification tree model was created for this purpose using the ozone and meteorological data from 1997-2001 and 2003 as predictors and the episode pattern type as the response variable. In the classification tree model, data from all exceedance days start out together in the root node of the tree and are then split into two daughter nodes based on the value of one of the predictor variables. For example, a split might consist of sending all days with resultant afternoon wind speed at Hartford, CT less than 4.8 m/s to one node and all remaining days to the other. The variable and value of that variable used to perform a split is determined by examining all possible splits and finding the one which results in the greatest reduction in deviance in the response variable (deviance is a measure of the degree of heterogeneity of the response variable in a node). The splitting process is then repeated for each resulting daughter node and so on until a stopping criterion is reached. The daughter nodes resulting from the last split along each branch of the tree are referred to as *terminal* nodes. The resulting classification tree, grown using the 1997-2001/2003 data as the *learning* dataset, can then be applied to the 2002 data for which the episode classifications are unknown by running the 2002 daily data down the tree, separating days at each node according to the previously determined splitting criteria. Each day from the 2002 data will fall into one of the terminal nodes of the tree, and the probability of that day belonging to the ith episode type is estimated from the fraction of days from the learning dataset in the terminal node belonging to the ith episode type. The *predicted* episode type for days in 2002 falling in the terminal node is taken to be the episode type with the highest probability of occurrence.

Initially, the classification tree was grown by making successive splits until only a small number of days (in this case five) ends up in each terminal node. This results in a relatively large tree with many terminal nodes, each of which will typically be very homogeneous: most of the days in any one terminal node will belong to the same episode type. This large tree represents an over fit to the data in the learning dataset. In other words, if the tree were to be validated against an independent set of days for which the episode types are known (i.e., a test dataset) the frequency of misclassification will generally be higher than the low misclassification frequency determined

[5]It is worth reiterating here that we are seeking a general classification system applicable to the whole of the OTR. More precise classification systems could be developed for individual sub-regions within the OTR but the resulting two dimensional system (consisting of a unique set of episode types for each of several sub-regions) would not only be very time-consuming to develop but would lead to results from which it would most likely be very difficult to draw any conclusions regarding the representativeness of a single season with respect to conditions over the whole of the OTR.

by applying the full tree against the learning dataset. Thus, a smaller tree (one with fewer splits and therefore fewer terminal nodes), is likely to perform at least as well against a test dataset as the initial, large tree. We therefore applied a recursive tree-pruning algorithm known as *cost-complexity pruning* to the large tree (Venables and Ripley, 1994). This results in a sequence of trees, each of which can be characterized by the number of terminal nodes and the cost-complexity parameter, which is a measure of the trade off between growth in tree size and reduction in deviance. The resulting tree sequence is shown in Figure 3-6. As this figure shows, there is a diminishing return in deviance reduction as the size of the tree increases beyond about 5 terminal nodes.

To further evaluate the relative value of different size trees, we performed a ten-fold cross-validation using the learning dataset. The ten-fold cross-validation consists of setting aside 1/10th of the days in the learning sample as a test sample, building a tree using the remaining 90% of days, and evaluating the deviance reduction using the reserved days. This process is repeated 10 times with a different set days set aside in each case. Results from the cross-validation (Figure 3-7) suggests that the residual deviance is minimized at a tree size of about five or six terminal nodes. These results, together with an examination of the misclassification rates from the learning dataset for the pruned tree sequence shows that the 6 terminal node tree is about the optimal size.

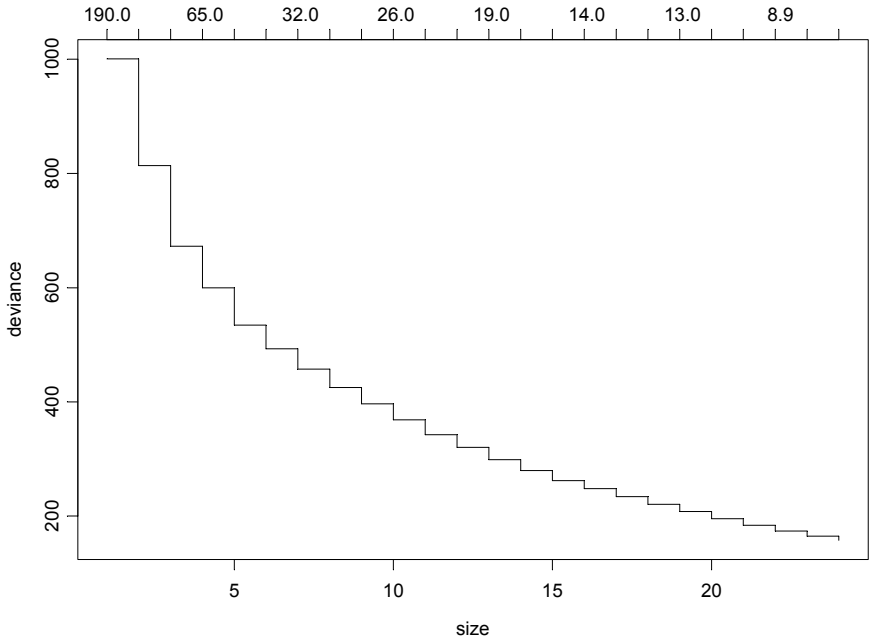

Figure 3-6. Deviance as a function of tree size (number of terminal nodes) for sequence of trees generated by the pruning algorithm.

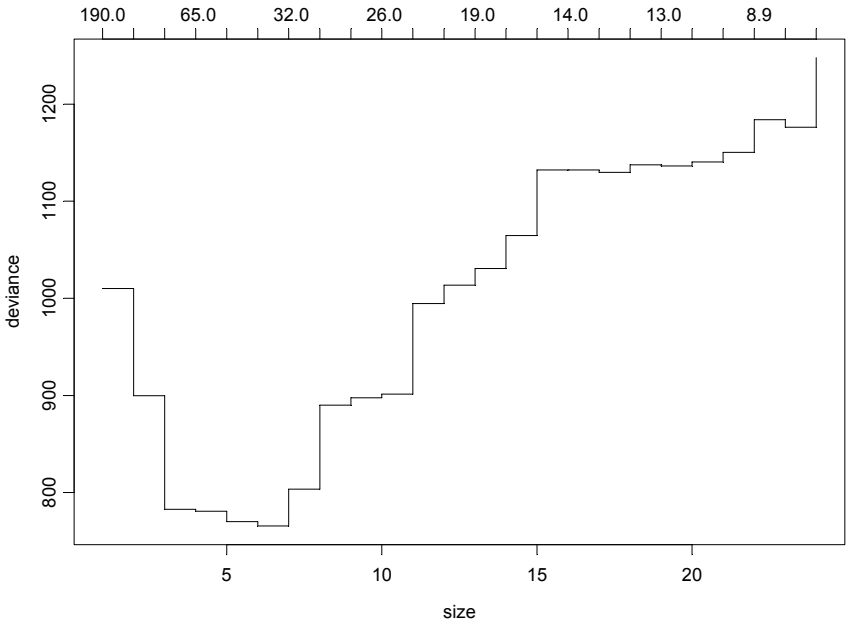

Figure 3-7. Deviance from 10-fold cross-validation as a function of tree size (number of terminal nodes) for sequence of trees generated by pruning algorithm.

The selected classification tree is shown in Figure 3-8; Table 3-4 summarizes the distribution of days by episode type in each terminal node. Two nodes are made up of predominantly Type E days, each of the rest are most representative of one of the four other episode types. Each terminal node has a dominant episode type accounting for between 64 and 81% of days assigned to the node. To use the classification tree for assigning an episode type to a previously unclassified day, we define the *predicted* episode type for all days reaching a given terminal node as the dominant episode type for the node as shown by the shaded boxes in Table 3-4. When this rule is applied to the 329 episode days during the historical period, a comparison of the predicted episode types with the episode types assigned by the cluster analysis shows an overall misclassification rate of 23%.

Table 3-4. Distribution of episode types during the 1997-2001/2003 historical period (as determined via the clustering analysis) for days in each terminal node of the classification tree shown in Figure 3-8.

	Episode Type					
Node No.	**A**	**B**	**C**	**D**	**E**	**Total**
4	6	3	0	0	16	25
5	100	16	9	1	0	126
7	5	3	53	0	5	66
8	1	25	3	0	2	31
10	5	0	0	4	19	28
11	6	3	1	39	4	53
Total	123	50	66	44	46	329

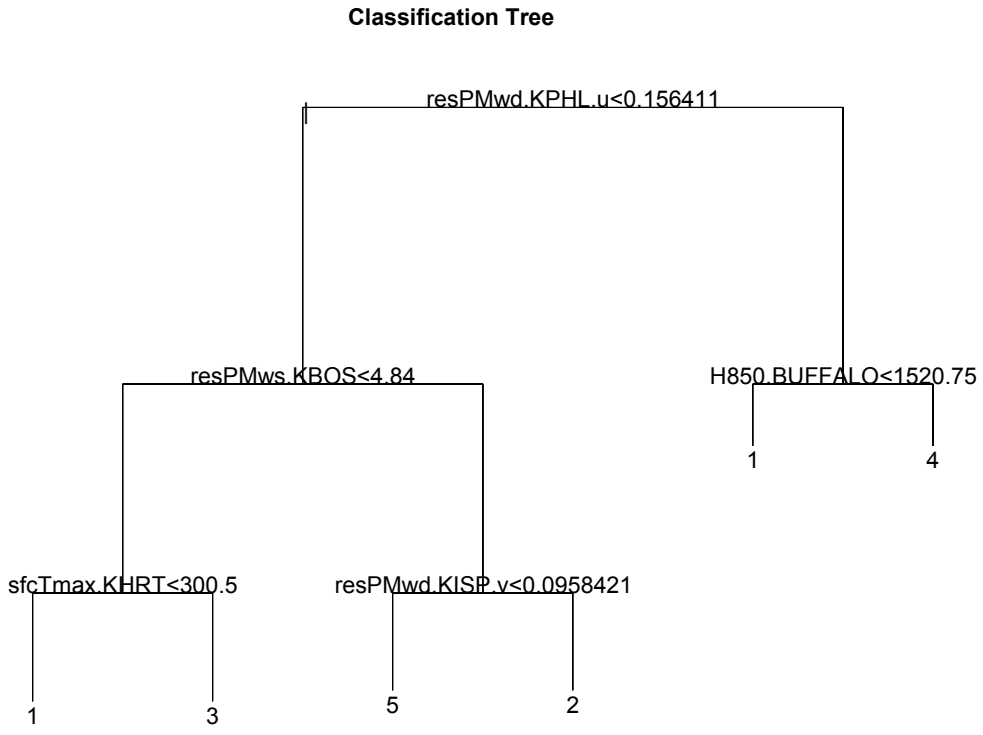

Figure 3-8. Classification tree used to group days by episode type. Variable names and values used to divide data at each splitting node are shown: days meeting the specified criterion are moved down the left branch in each case (resPMwd.KPHL.u = easterly component of the resultant afternoon wind direction at Philadelphia [m/s]; resPMws.KBOS = resultant afternoon wind speed at Boston [m/s]; H850.BUFFALO = 850 mb pressure height at Buffalo [m]; sfcTmax.KHRT = daily maximum surface temperature at Hartford, CT [K]; resPMwd.KISP.v = northerly component of afternoon wind direction at Islip, NY [m/s]). Terminal nodes are numbered 1 – 5 and are keyed to the summary in Table 3-4.

CLASSIFICATION OF 2002 OZONE EPISODES

Data from the 2002 ozone season were analyzed using the classification tree described above to yield a division of the ozone exceedance days into the five episode types. The resulting frequency distribution of episode types in 2002 was then compared with the historical episode type frequency distribution shown in Table 3-4, thereby providing an indication of the degree to which conditions during 2002 are representative of conditions observed in other years. We also compared ozone concentration distributions and composite meteorological fields by episode type in 2002 with those during the historical period as a way of further evaluating the representativeness of conditions during the 2002 ozone season.

Episode Type Classification

We applied the 6-node tree shown in Figure 3-8 to all 8-hour ozone exceedance days in 2002. Of the 71 exceedance days, 69 could be assigned to terminal nodes on the tree; missing data prevented classification of two of the days. Examination of the classification results showed that

if surrogate splits[6] were used to assign these two days to one of the terminal nodes, the number of days falling into the node would change by no more than 3 percentage points, so the two days with missing data were simply ignored. The predicted episode type for each exceedance day in 2002 was taken to be the predominant episode type in the terminal node to which it was assigned (as indicated by the shaded boxes in Table 3-4). Appendix E lists the resulting episode type associated with each exceedance day in 2002. The resulting distributions of days by episode type for the 2002 season and the 1997-2001/2003 historical period are shown in Figure 3-9.[7] For the historical days, both the episode type assignments based on the classification tree and the episode types as originally assigned in the clustering analysis are shown. The overall pattern of episode type occurrence frequencies for the historical period is similar between the classification tree and the clustering analysis, as we would expect. Frequencies of occurrence of the episode types are within two percentage points of each other except for Type D events (slightly more Type D days assigned by the classification tree) and Type B events (about a third fewer Type B days determined by the classification tree).

Comparison of the occurrence frequencies over the historical period with the 2002 data also suggest a generally similar pattern of episode types. Note that the error bars in Figure 3-9 show the 10^{th} and 90^{th} percentile range in the frequencies of occurrence of each episode type observed within individual years during the historical period: an individual year would be expected to fall within this range with 80% probability. The 2002 type frequencies generally fall within these error bars except for a somewhat higher frequency of Type C events and a lower frequency of Type E events. As Type E events are characterized by below average ozone (relative to all exceedance days) throughout all but the southernmost OTR, this difference reflects the higher frequency of exceedance days in 2002 relative to the historical period as noted above. If we ignore the Type E events and renormalize (see Figure 3-10), the occurrence frequencies in 2002 of the remaining episode types are found to be similar to those in the historical period and fall within the 10^{th} to 90^{th} percentile range in each case. Thus, each of the event types A – D appear to be well represented within the 2002 season.

[6]Surrogate splitting uses the best alternative splits (based on the non-missing variable that produces nearly the same split as the primary splitting variable).

[7]The bars in this figure are scaled to the fraction of OTR exceedance days assigned to each episode type. Thus, these comparisons are not effected by the above average number of exceedance days in 2002 noted earlier.

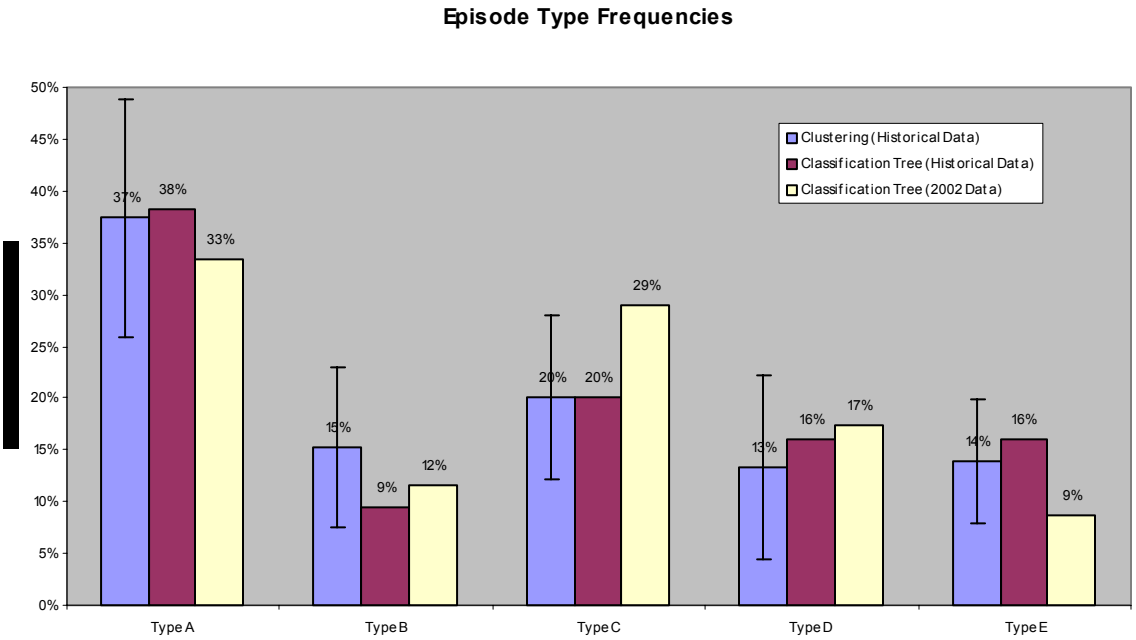

Figure 3-9. Percent of episode days by type in the 1997 – 2001/2003 historical period (as determined by the cluster analysis and by the classification tree) and in 2002; error bars show 10th and 90th percentiles of annual frequencies of occurrence during 1997-2001&2003.

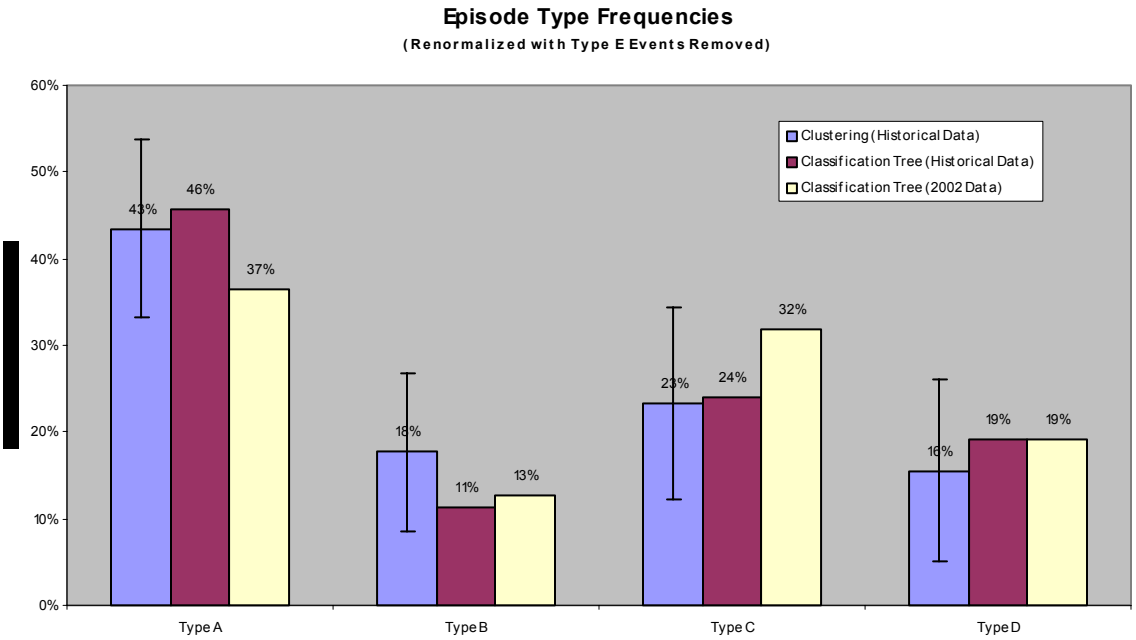

Figure 3-10. Percent of episode days by type in the 1997 – 2001/2003 historical period (as determined by the cluster analysis and by the classification tree) and in 2002 with Type E events removed and frequencies re-normalized; error bars show 10th and 90th percentiles of annual frequencies of occurrence during 1997-2001&2003.

Ozone Concentration levels

An exceedance of the 8-hour ozone standard occurred at one or more sites in the study region on 71 days during 2002, representing 46% of the 153 days during the May – September season analyzed in this study. For the 1997 – 2001/2003 historical period, the corresponding percentage was 36% so exceedances were more frequent during 2002. The greater frequency of ozone exceedance events was distributed throughout the OTR as shown by the comparison by monitoring sub-region in Table 3-5. Exceedances occurred with 20 – 50% greater frequency in 2002 in all sub-regions (100% greater in sub-region 3). This difference in the frequency of exceedances in 2002 as compared to the historical period does not necessarily mean, however, that the exceedance events themselves have characteristics that significantly differ from those seen during the historical period.

Table 3-5. Number of days during May-September with 8-hour daily maximum ozone greater than 0.08 ppm in each monitoring sub-region averaged over the 1997-2001/2003 historical period and in 2002.

	Sub-Region					
	1	2	3	4	5	6
>0.08 ppm						
1997-2001/2003	22.3	31.0	8.5	27.3	42.0	30.8
2002	34	38	17	39	58	44
Pct. Difference	52%	23%	100%	43%	38%	43%

Distributions of daily maximum 8-hour average ozone concentrations averaged over monitors in each sub-region (the AvgExc00 statistic) in 2002 and the historical period are compared for each event type in Figures 3-12(a-e), a key to the boxplot symbols used to summarize the ozone distribution is shown in Figure 3-11. Overall, the range of ozone under each event type in 2002 is similar to that under the corresponding event type in the historical period. The most notable exceptions are higher ozone levels during Type D events in 2002 along the Washington – New York City corridor (sub-regions 2, 5, and 6). This is consistent with a less pronounced low pressure center off the NC coast in the 2002 Type D events as compared to the historical period (see further discussion below). Aside from this difference, the overall ozone levels during the 2002 exceedance events were generally very consistent with those observed during the historical period, not withstanding the fact that exceedance days were more frequent during 2002.

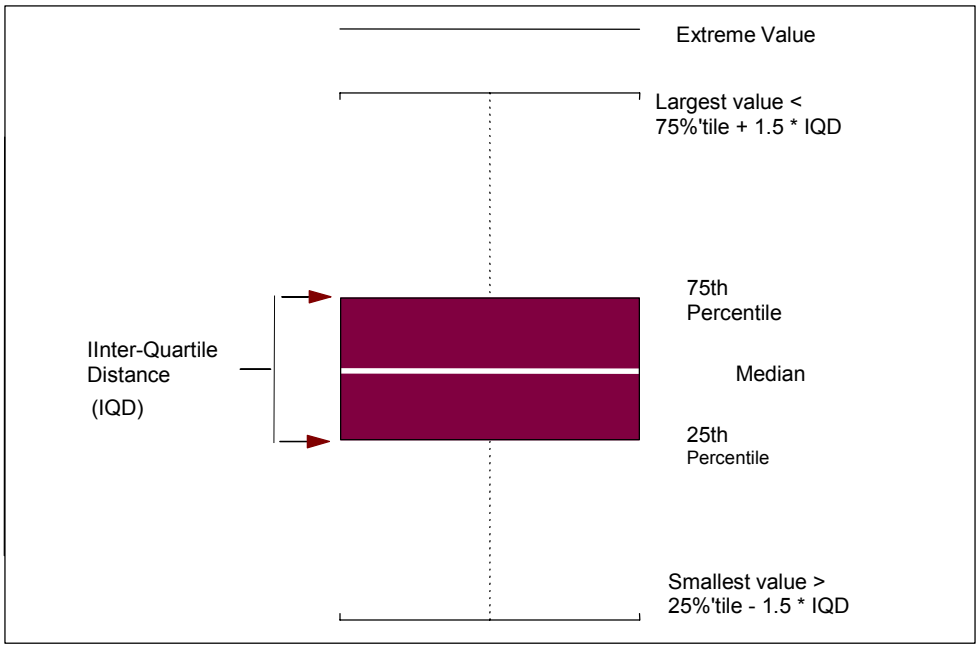

Figure 3-11. Key to boxplot symbols.

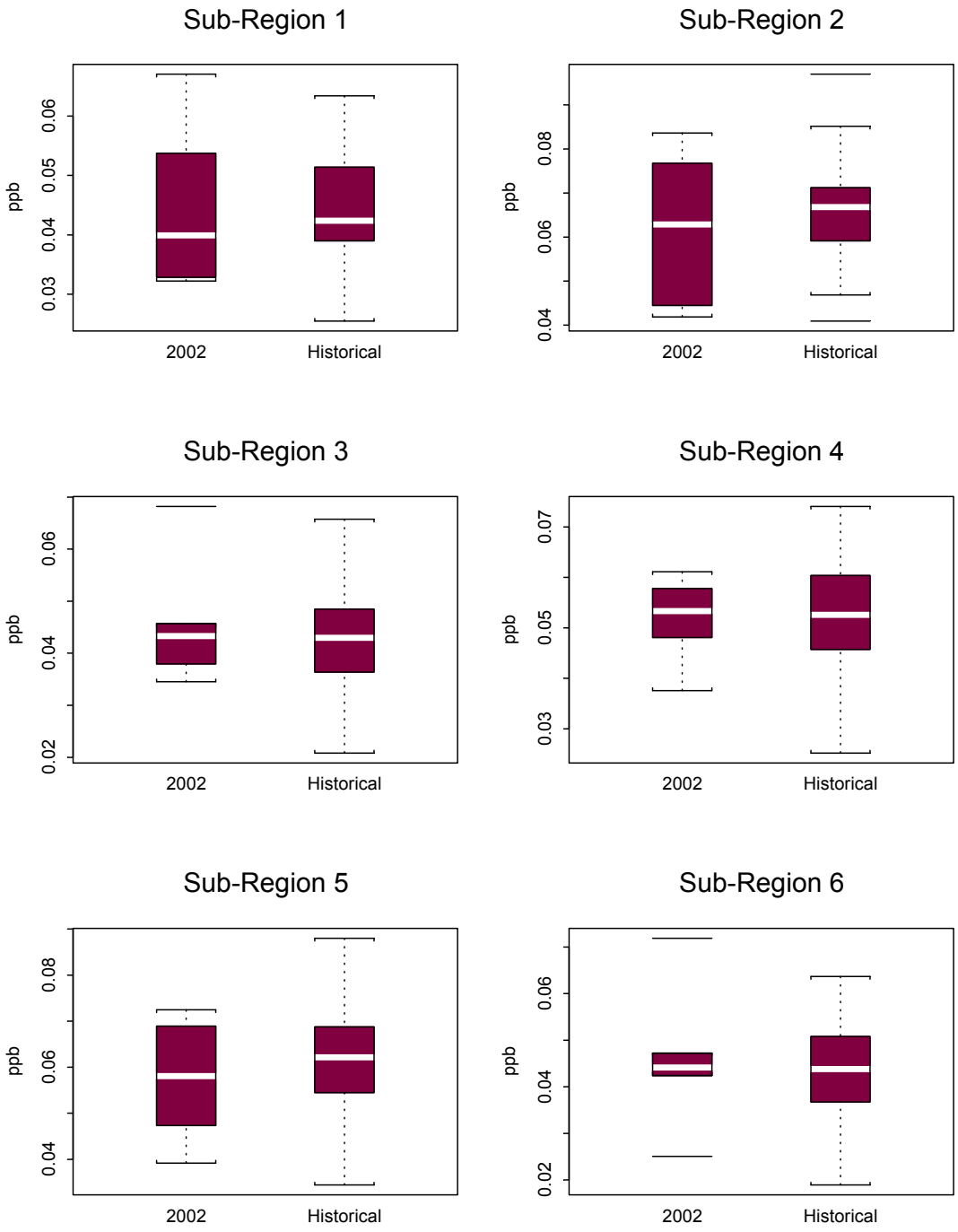

Figure 3-12a. Boxplots of average 8-hour daily maximum ozone (ppb) in each monitoring sub-region during 2002 and during the 1997-2001 and 2003 "historical" period: Type E (Pattern No. 1) events.

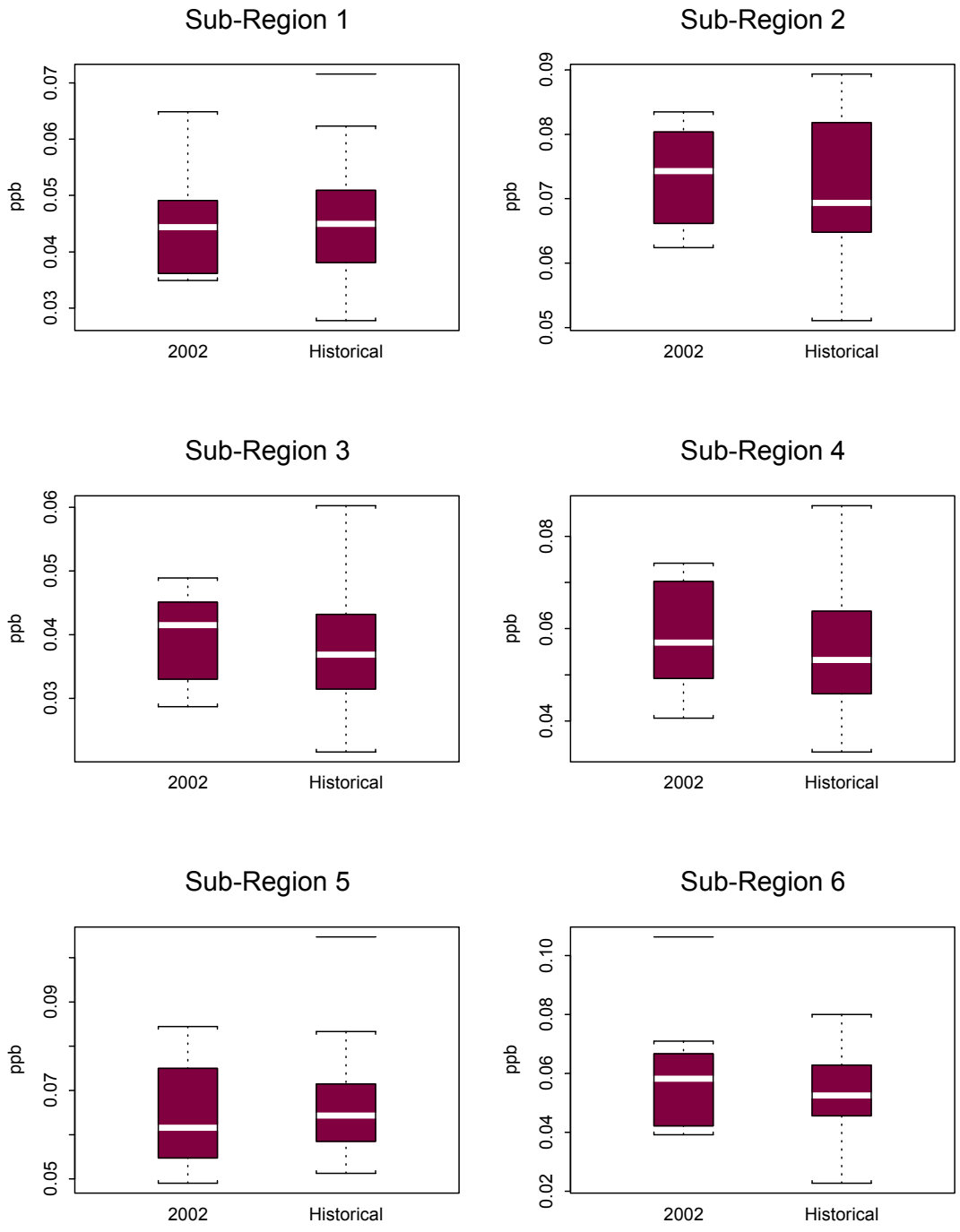

Figure 3-12b. Boxplots of average 8-hour daily maximum ozone (ppb) in each monitoring sub-region during 2002 and during the 1997-2001 and 2003 "historical" period: Type B (Pattern No. 2) events.

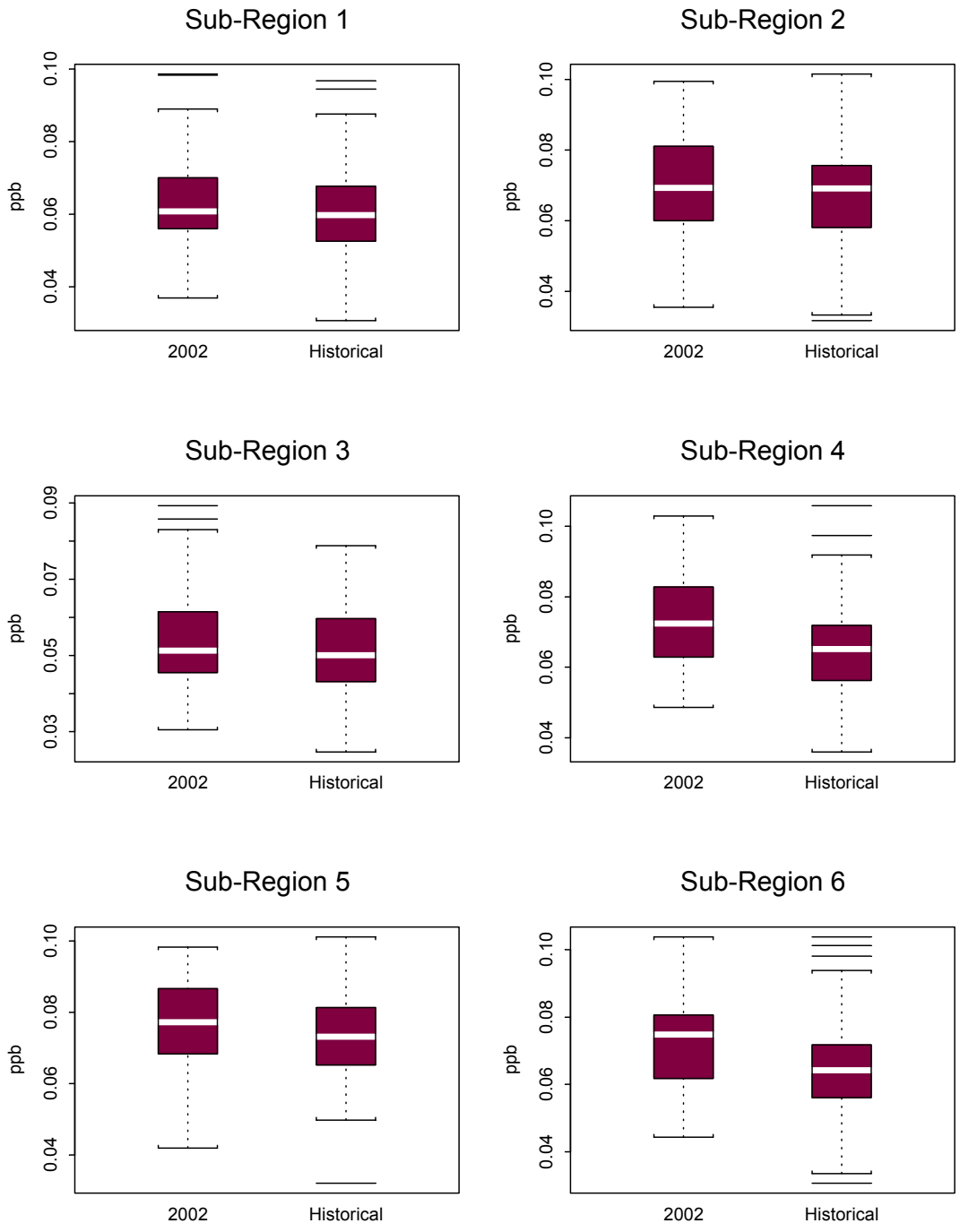

Figure 3-12c. Boxplots of average 8-hour daily maximum ozone (ppb) in each monitoring sub-region during 2002 and during the 1997-2001 and 2003 "historical" period: Type A (Pattern No. 3) events.

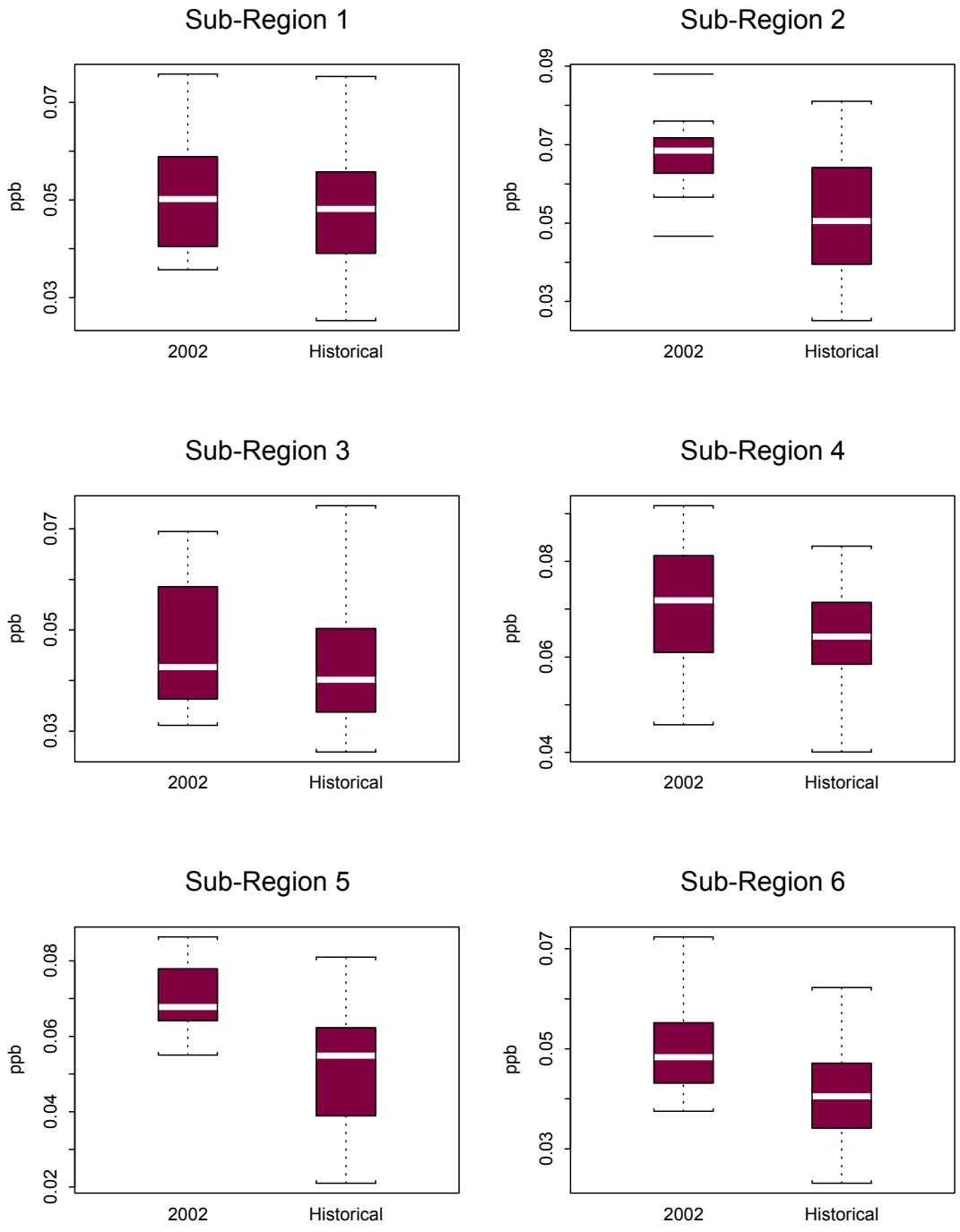

Figure 3-12d. Boxplots of average 8-hour daily maximum ozone (ppb) in each monitoring sub-region during 2002 and during the 1997-2001 and 2003 "historical" period: Type D (Pattern No. 4) events.

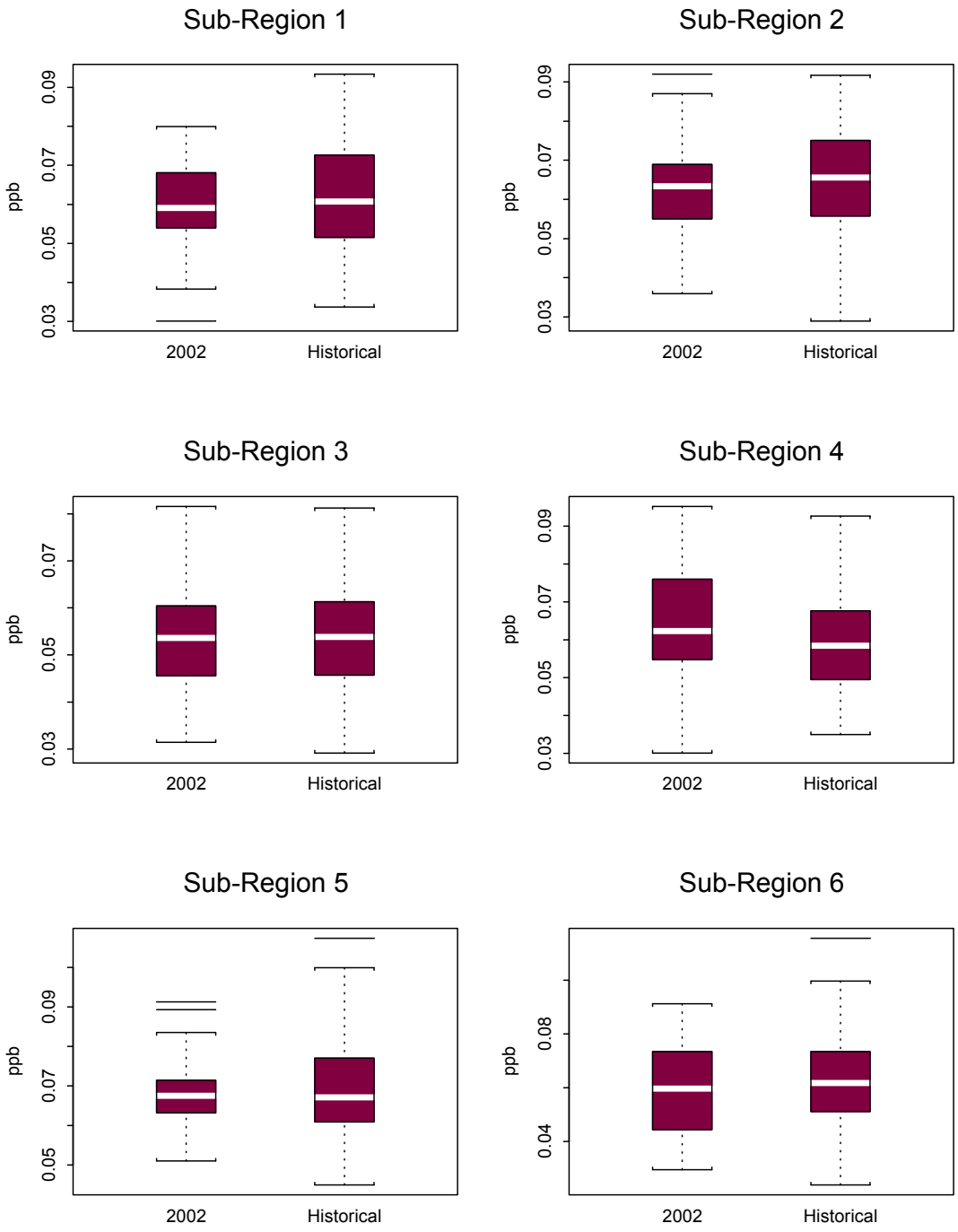

Figure 3-12e. Boxplots of average 8-hour daily maximum ozone (ppb) in each monitoring sub-region during 2002 and during the 1997-2001 and 2003 "historical" period: Type C (Pattern No. 5) events.

Meteorological Conditions

Selected composite meteorological fields for each episode type in 2002 as predicted by application of the classification tree were computed and displayed for comparison with the historical period composite fields. Results are shown in Figure 3-13 through 3-16. Comparing of these results with those for the historical period (Figures 3-2 to 3-5), we see a remarkable degree of similarity:[8] the surface and upper air meteorological patterns for a given episode type in 2002 are very similar to those for the same episode type observed in the historical period. In other words, the key characteristics of each type observed in the historical dataset are reproduced within the 2002 data. Perhaps the most significant difference is the less pronounced low pressure center off the NC coast under Type D events in 2002 which allowed for the formation of higher ozone concentrations along the Washington – New York City corridor for these event types in 2002 as compared to the historical period. Overall, however, the close match in weather patterns associated with each event type in 2002 and the historical period strongly supports the conclusion that the 2002 ozone episodes, although more numerous than in other years, are of substantially similar character.

[8] In making these comparisons, note that different color and wind vector scales had to be used in some plots of the 2002 data.

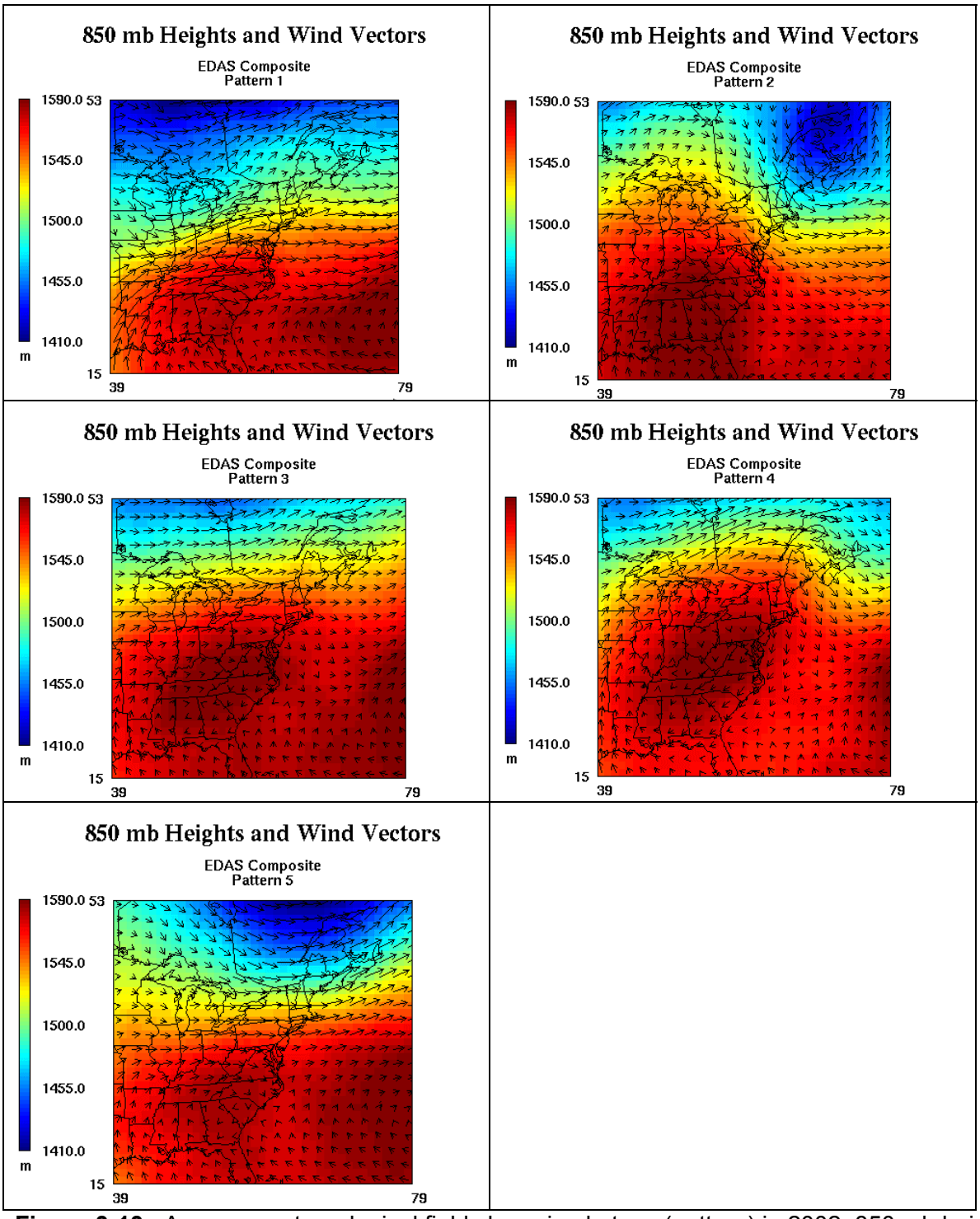

Figure 3-13. Average meteorological fields by episode type (pattern) in 2002: 850 mb heights and winds. Pattern numbers refer to the episode types listed in Table 3-2: Pattern 1 = Episode Type E, 2 = B, 3 = A, 4 = D, 5 = C).

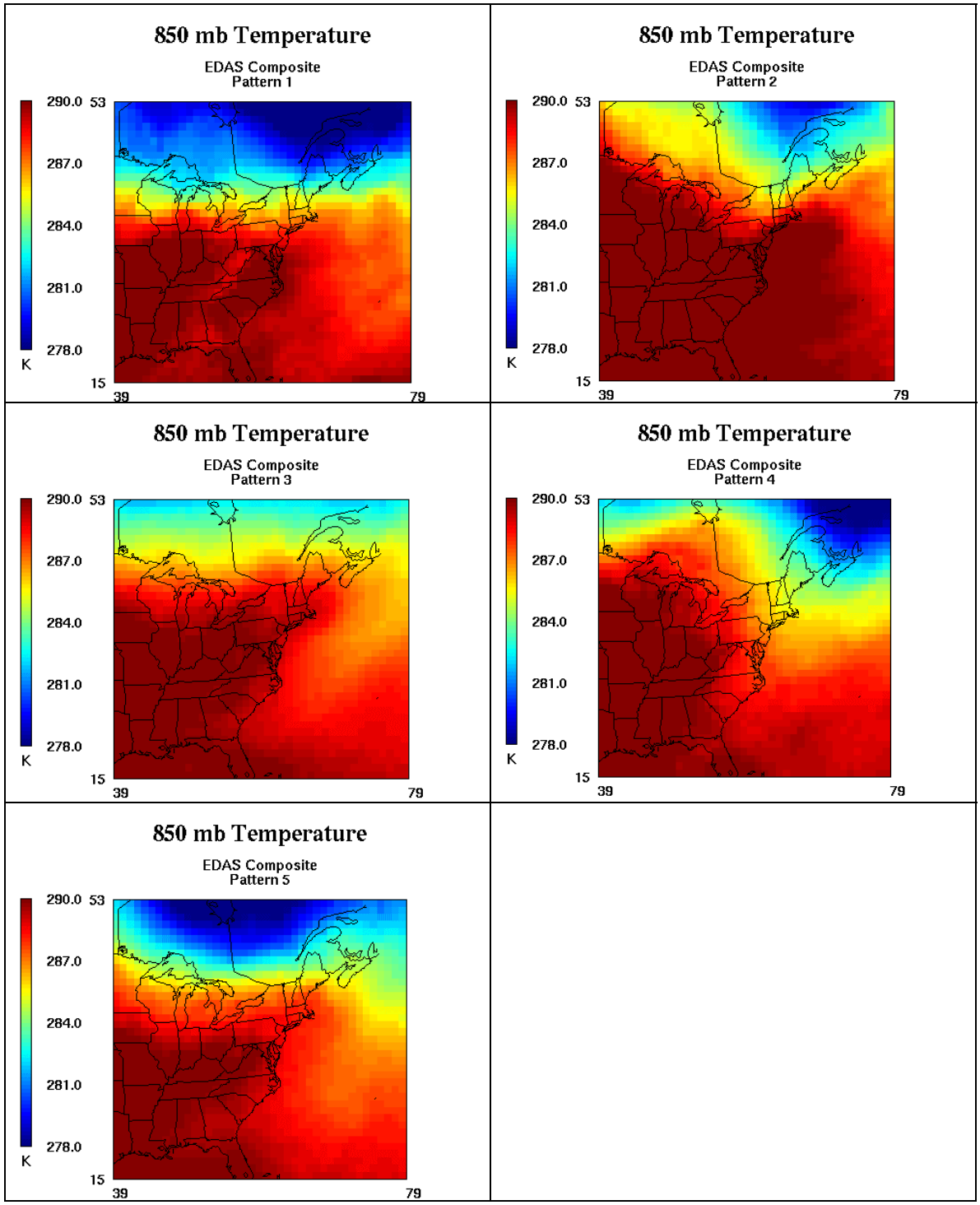

Figure 3-14. Average meteorological fields by episode type (pattern) in 2002: 850 mb temperature. Pattern numbers refer to the episode types listed in Table 3-2: Pattern 1 = Episode Type E, 2 = B, 3 = A, 4 = D, 5 = C).

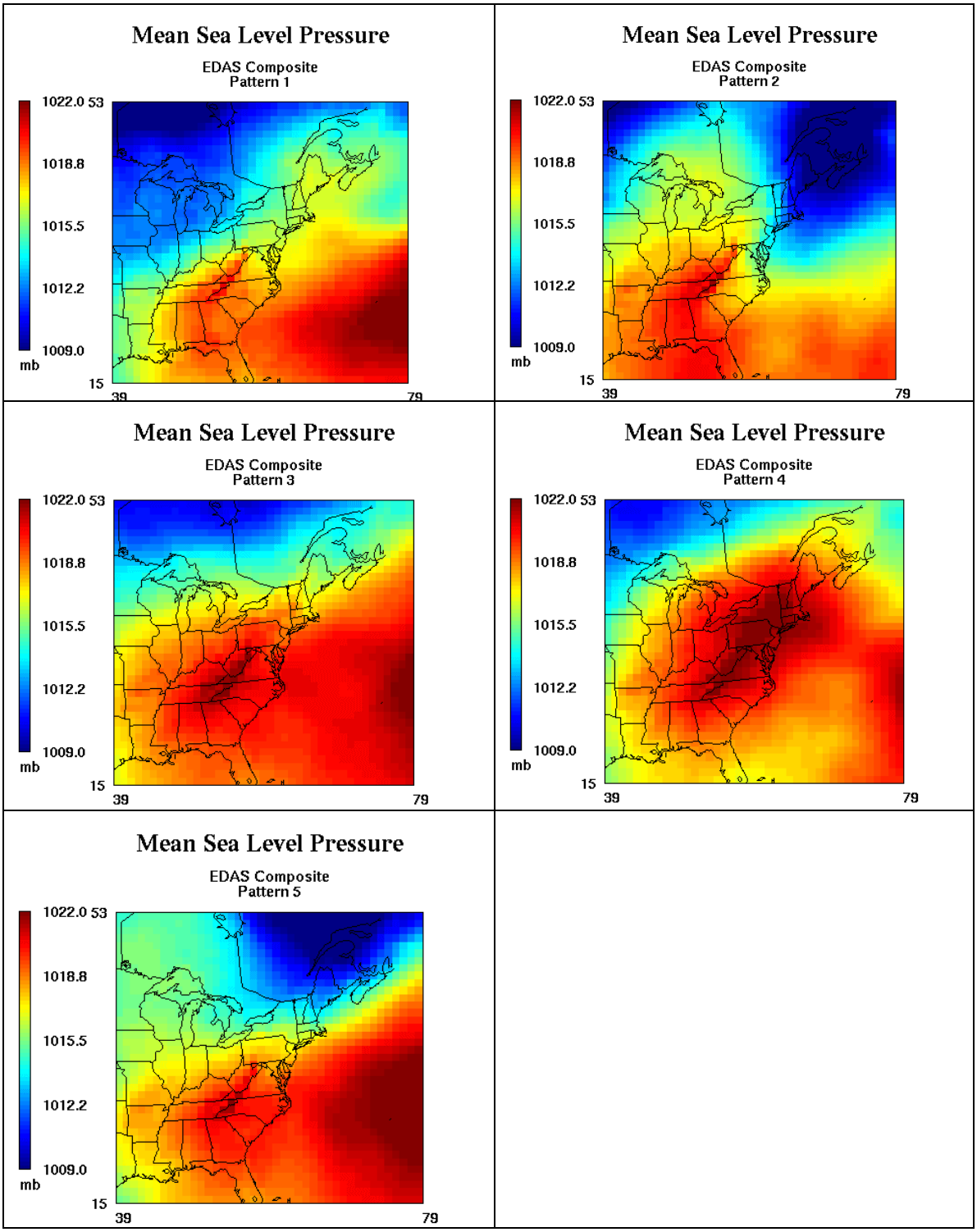

Figure 3-15. Average meteorological fields by episode type (pattern) in 2002: sea level pressure. Pattern numbers refer to the episode types listed in Table 3-2: Pattern 1 = Episode Type E, 2 = B, 3 = A, 4 = D, 5 = C).

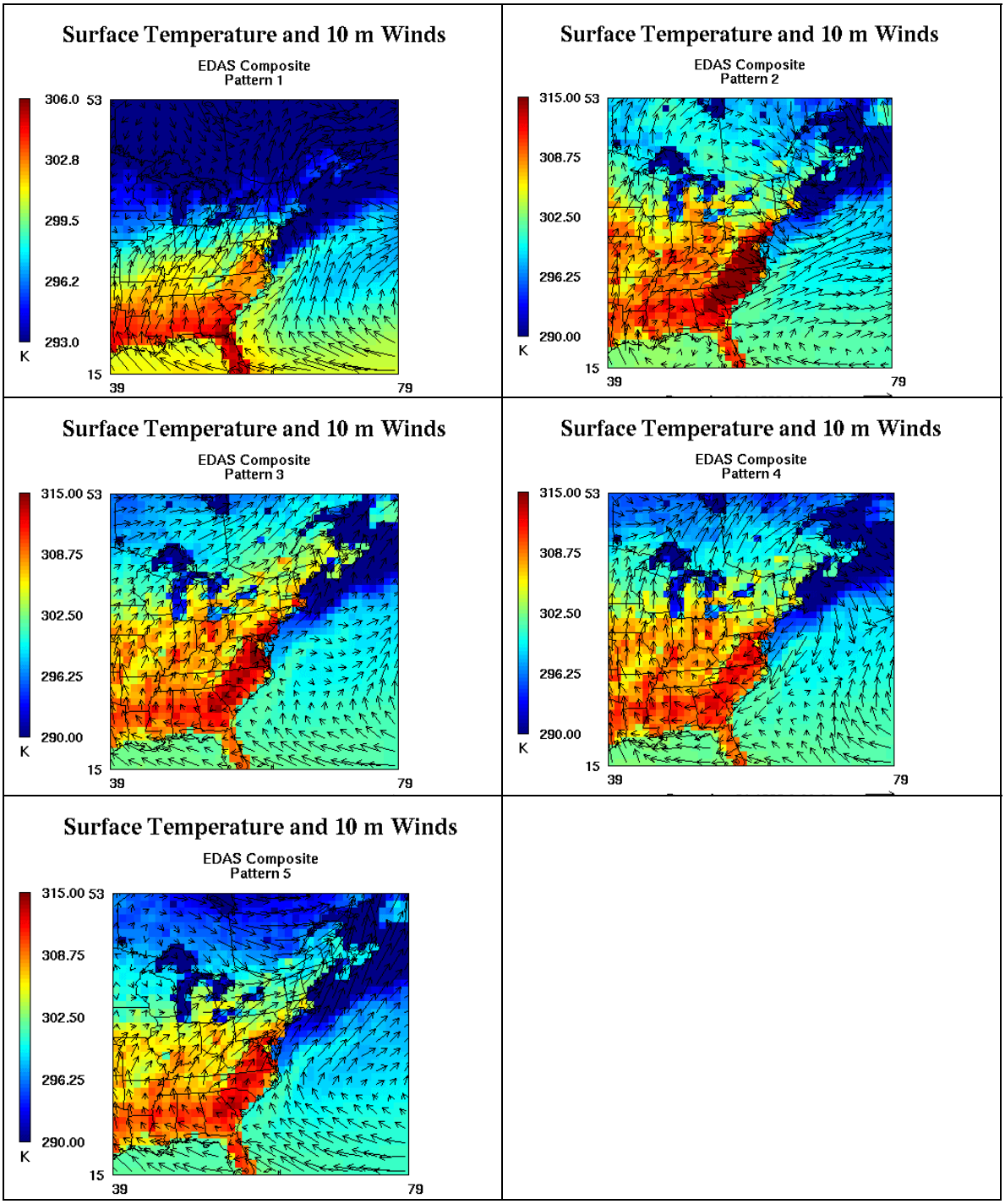

Figure 16. Average meteorological fields by episode type (pattern) in 2002: surface temperature and 10 m winds. Pattern numbers refer to the episode types listed in Table 3-2: Pattern 1 = Episode Type E, 2 = B, 3 = A, 4 = D, 5 = C).

4. CONCLUSIONS AND RECOMMENDATIONS

Results from the application of statistical clustering analyses presented in Section 3 show that regional ozone episode conditions over the OTR can be reasonably well described by a set of five different episode types. Our examination of mean ozone and meteorological conditions shows that each of these episode types is associated with a unique set of distinguishing characteristics. While we would not expect every exceedance day to exhibit all of the characteristics of one type or another, our results provide no clear evidence for the existence of any other additional sufficiently unique types that occur frequently enough to be distinguishable within the six year historical period analyzed.

Data from the 2002 ozone season were analyzed within the framework of the five identified episode types with respect to: a) frequencies of occurrence of each type and b) characteristics of the ozone and meteorological conditions within each type in 2002 as compared to the 1997 – 2001/2003 historical period.

A key feature of the 2002 season is that ozone episodes (defined as an exceedance of the 8-hour ozone NAAQS at one or more monitoring sites within the OTR) occurred more frequently than during the historical period (71 exceedance days during the May – September season in 2002 as compared to an average of 55 days per season during the historical period). Taken by itself, however, this difference does not necessarily mean that region-wide meteorological and ozone concentration patterns *during exceedance days* were significantly different in 2002 as compared to other years: the greater number of exceedance days in 2002 may just reflect a lower than average frequency of days with meteorological conditions not conducive to ozone formation in 2002. The higher than average exceedance rate in 2002 is by itself not an indication of any lack of representativeness of the 2002 exceedance events.

Our examination of conditions during exceedance days in 2002 showed that:

- Except for the Type E events during which ozone exceedances are typically confined to the extreme southeastern corner of the OTR, each of the five episode types identified in the historical period was found to occur on about as many days in 2002 as one would expect based on their rate of occurrence during the historical record. Thus the meteorological conditions on episode days in 2002 exhibit a normal range of variation and each of the five types of episodes are well represented.
- Type E events are under represented in the 2002 season. This is consistent with the higher than average frequency of exceedance days in 2002. The relative lack of Type E events in 2002 should not be of concern from a SIP modeling standpoint, however, as these events are characterized by relatively low ozone levels throughout nearly all of the OTR (except the Washington and Virginia area).
- The distribution of daily maximum 8-hour average ozone levels during each event type in 2002 is generally very similar to that within the same event type during the historical period. The only significant exception is higher ozone along the Washington – New York City corridor under Type D events in 2002 as compared to the historical average.
- Regional-scale meteorological conditions during each event type in 2002 exhibit the same key characteristics as observed for the event types during the historical period. A less

pronounced low pressure center off of the NC coast under the 2002 Type D events appears to be responsible for the higher Washington – New York City ozone levels under this event type noted in the previous bullet.

In summary, while ozone exceedances were more frequent during 2002, conditions during the 2002 exceedance events were for the most part very similar to those found to occur in other years. This leads us to conclude that the 2002 season can be considered to be representative for purposes of photochemical modeling in support of SIP development.

REFERENCES

Breiman, L., J.H. Friedman, R.A. Olshen and C.J. Stone, 1984. Classification and Regression Trees. Wadsworth, Belmont, CA

Cox, W.M., 1997. Spatial Clustering of Ambient Ozone in Eastern U.S., Draft, U.S. Environmental Protection Agency, January (available at http://www.epa.gov/ttn/naaqs/ozone/areas/misc/ozclus2a.htm)

Deuel, H.P. and S.G. Douglas, 1996. "Regional Ozone Patterns in the Eastern U.S. 1985-1995: Statistical Pattern Analysis and Classification and Regression Tree (CART) Analysis in Support of the Ozone Transport and Assessment Group (OTAG) Modeling Effort." Systems Applications Inc. San Rafael, CA October.

EPA, 1999. "Draft Guidance on the Use of Models and Other Analyses in Attainment Demonstrations for the 8-Hour Ozone NAAQS." EPA-54/R-99-004, U.S. Environmental Protection Agency, May.

Harrell, F.E., 1999. Hmisc S-PLUS function library. Programs available from lib.stat.cmu.edu.

Hartigan, J. A. and M.A. Wong, 1979. A k-means clustering algorithm. *Applied Statistics 28*, 100-108.

McHenry, J.N., W.F. Ryan, N.L. Seaman, C.J. Coats, J. Pudykiewicz, S. Arunachalam and J.M. Vukovich, 2004. A real-time Eulerian photochemical model forecast system: Overview and initial ozone forecast performance in the northeastern U.S. corridor. *Bulletin of the American Meteorological Society*, 85(4), April.

Sarle, WS: The VARCLUS Procedure. SAS/STAT User's Guide, 4th Edition, 1990. Cary NC: SAS Institute, Inc.

Stoeckenius, T.E. and S. Kemball-Cook, 2004. Ozone episode classification project: spatial ozone pattern analysis (Task 2a). Memo to T. Frankiewicz, Ozone Transport Comission, 21 September.

Venables, W.N. and B.D. Ripley, 1994. "Modern Applied Statistics with S-Plus." Springer-Verlag, New York.

Ward, J.H., 1963. Hierarchical groupings to optimize an objective function. *J. Amer. Statistical Assoc.*, 58:236-244.

Appendix A

Composites Representing Mean Meteorological Conditions During Each Ozone Episode Pattern

Composites Representing Mean Meteorological Conditions During Each Ozone Episode Pattern

Mean meteorological fields were computed over days falling into each of the five ozone episode patterns in the Ozone Transport Region defined in the text. The five episode patterns and their composite pattern identifiers are:

Composite Pattern	Episode Type
3	Type A: High ozone throughout the OTR
2	Type B: High ozone confined to extreme southeastern OTR
5	Type C: High ozone along I-95 corridor and northern New England
4	Type D: High ozone in the western OTR
1	Type E: Generally low ozone throughout the OTR

Mean fields were computed for the following parameters extracted from the EDAS data:

Parameter ID	Description
H850	850 mb height
850 mb Wind	Resultant wind vector at 850 mb
T(850 mb)	850 mb temperature (deg K)
MSLP	Mean sea level pressure (mb)
TSFC	Surface temperature (deg K)
10m Wind	Resultant wind vector at 10 m height
w_500	w (vertical) component of 500 mb wind vector
H500	500 mb heights

850 mb Heights and Winds

EDAS Composite
Pattern 1

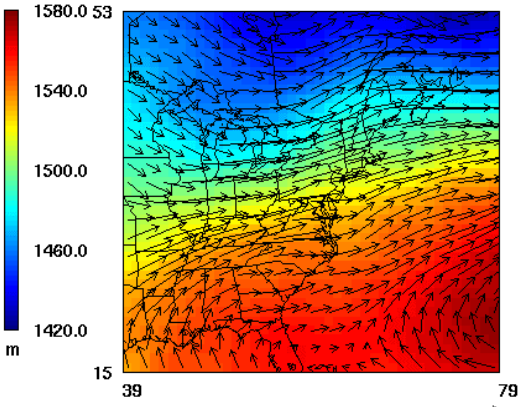

850 mb Heights and Winds

EDAS Composite
Pattern 2

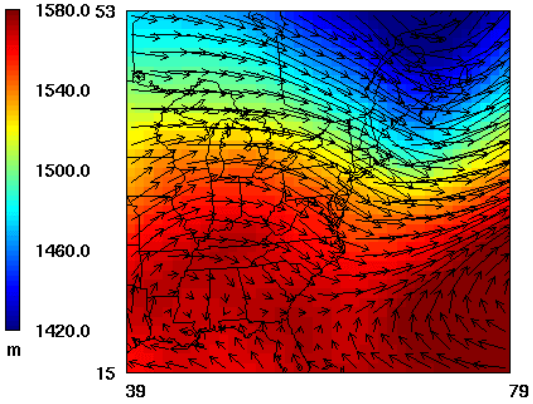

850 mb Heights and Winds

EDAS Composite
Pattern 3

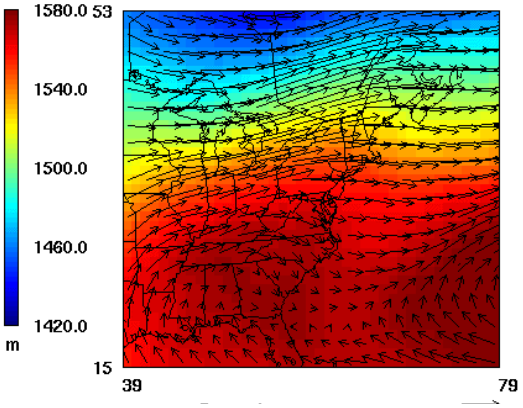

850 mb Heights and Winds

EDAS Composite
Pattern 4

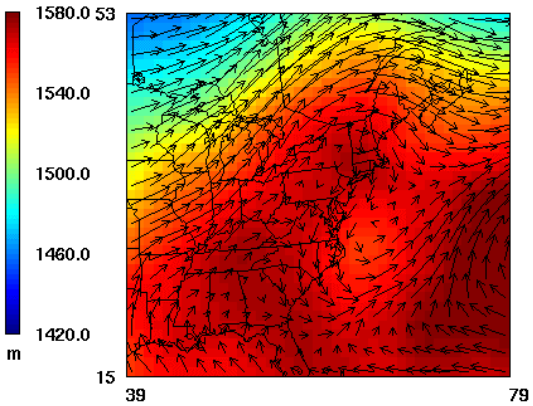

850 mb Heights and Winds

EDAS Composite
Pattern 5

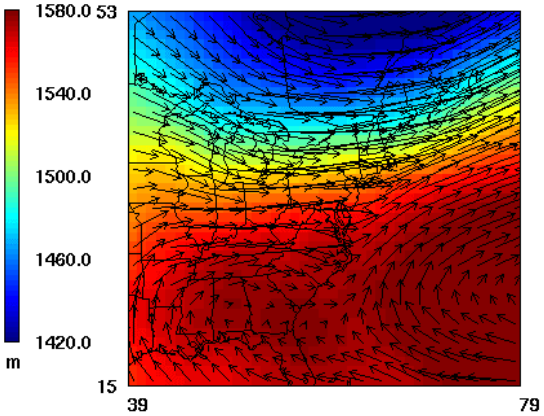

850 mb Temperature

EDAS Composite
Pattern 1

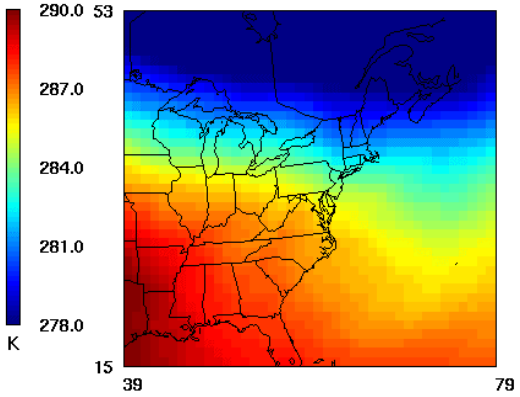

850 mb Temperature

EDAS Composite
Pattern 2

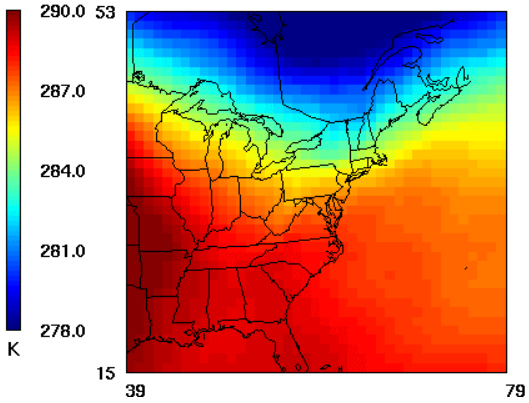

850 mb Temperature

EDAS Composite
Pattern 3

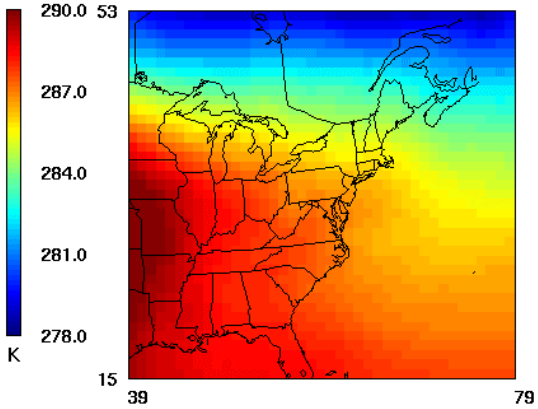

850 mb Temperature

EDAS Composite
Pattern 4

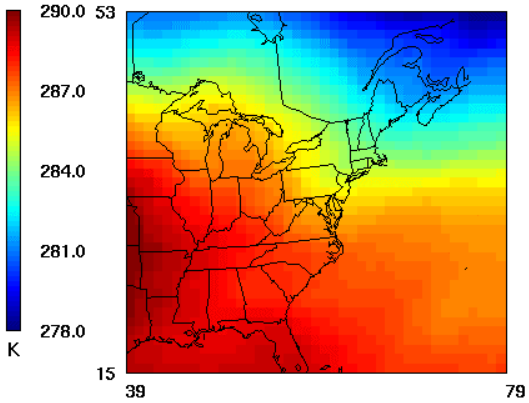

850 mb Temperature

EDAS Composite
Pattern 5

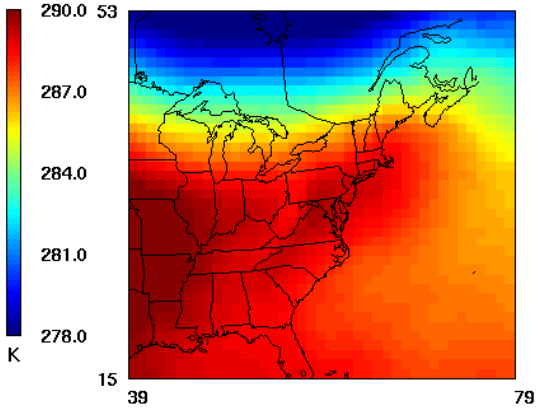

Mean Sea Level Pressure

EDAS Composite
Pattern 1

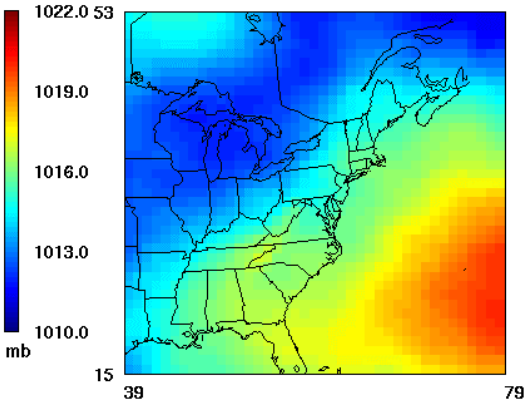

Mean Sea Level Pressure

EDAS Composite
Pattern 2

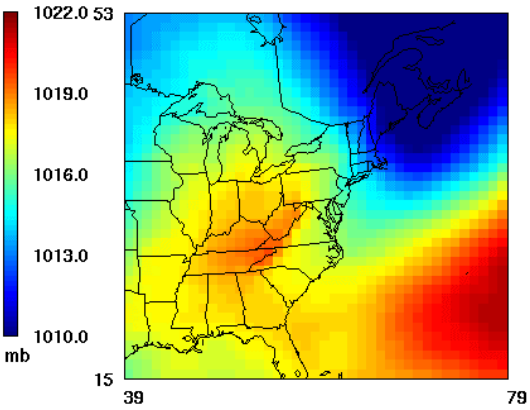

Mean Sea Level Pressure

EDAS Composite
Pattern 3

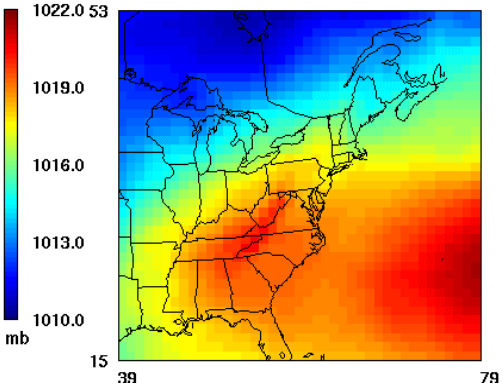

Mean Sea Level Pressure

EDAS Composite
Pattern 4

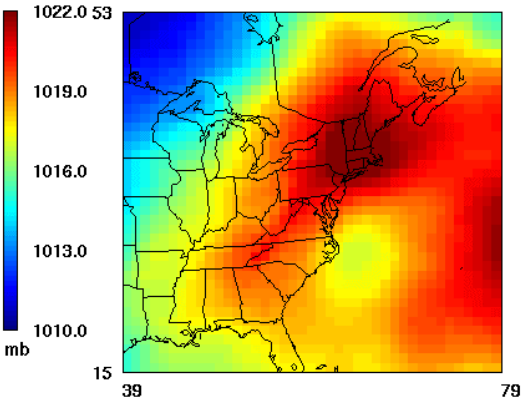

Mean Sea Level Pressure

EDAS Composite
Pattern 5

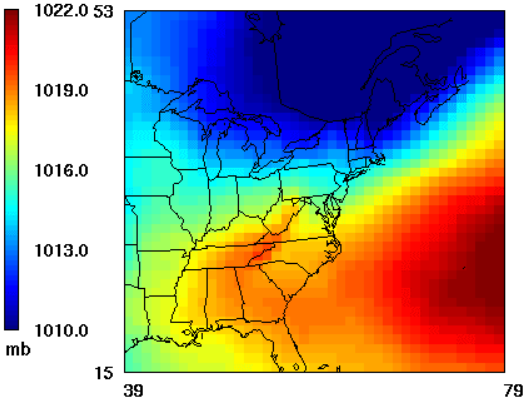

Surface Temperature and 10 m Winds

EDAS Composite
Pattern 1

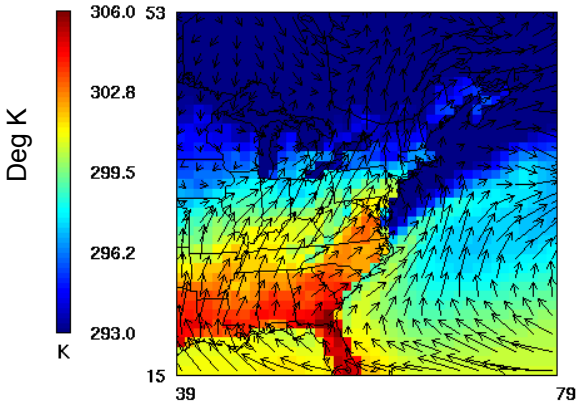

Surface Temperature and 10 m Winds

EDAS Composite
Pattern 2

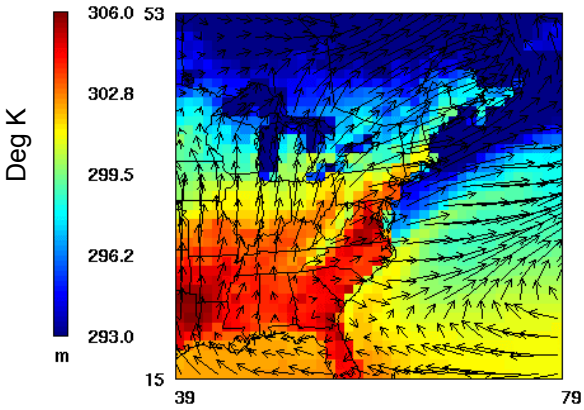

Surface Temperature and 10 m Winds

EDAS Composite
Pattern 3

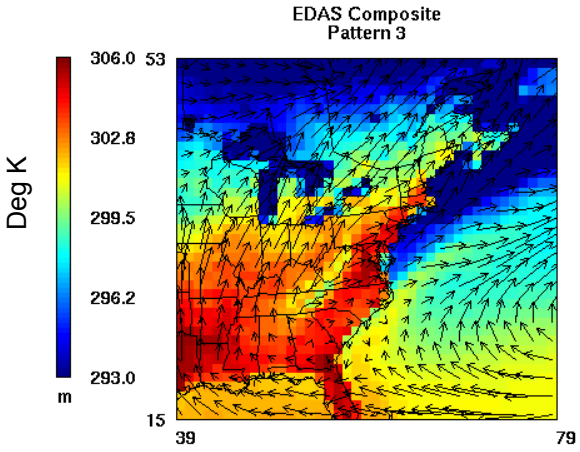

Surface Temperature and Winds

EDAS Composite
Pattern 4

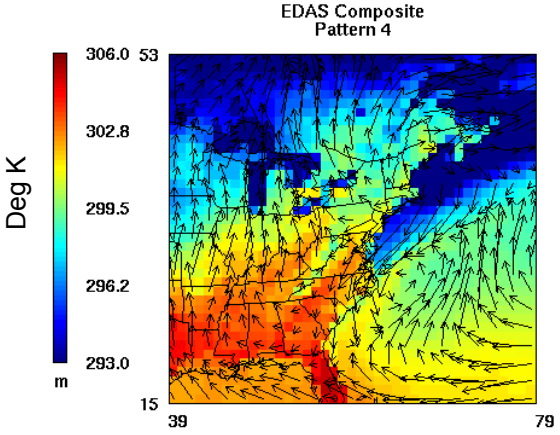

Surface Temperature and 10 m Winds

EDAS Composite
Pattern 5

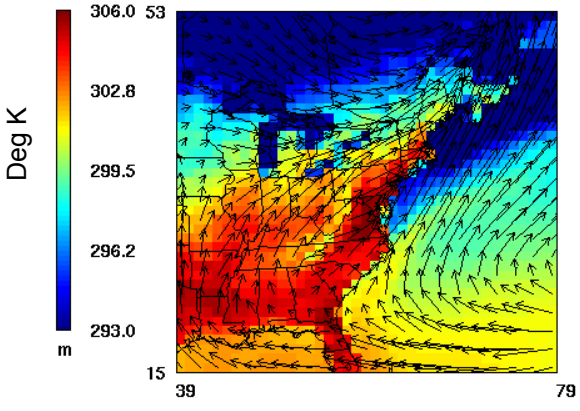

500 mb Vertical Velocity

EDAS Composite
Pattern 1

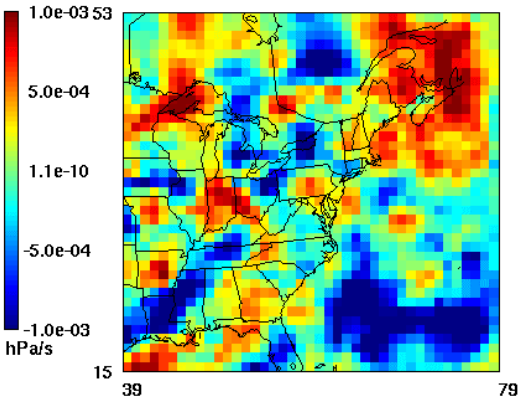

500 mb Vertical Velocity

EDAS Composite
Pattern 2

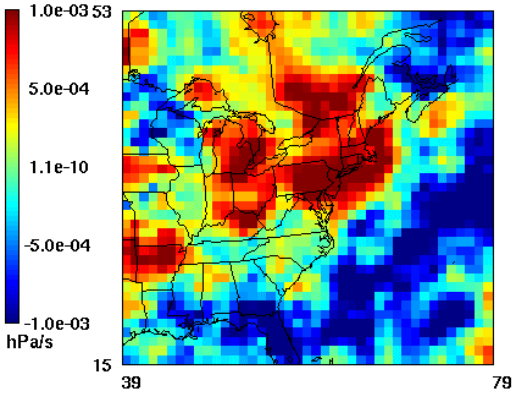

500 mb Vertical Velocity

EDAS Composite
Pattern 3

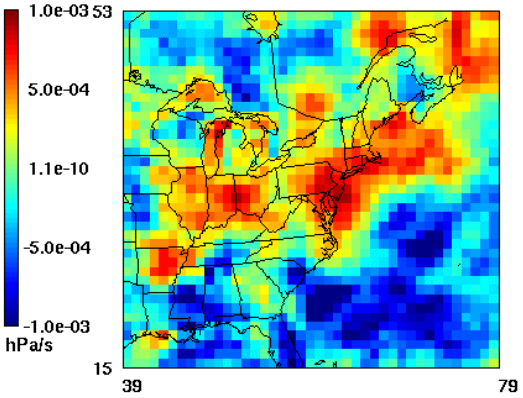

500 mb Vertical Velocity

EDAS Composite
Pattern 4

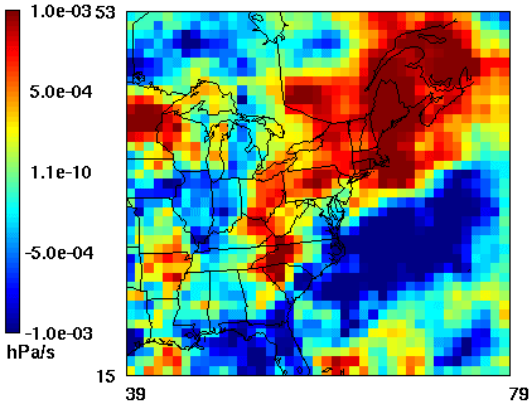

500 mb Vertical Velocity

EDAS Composite
Pattern 5

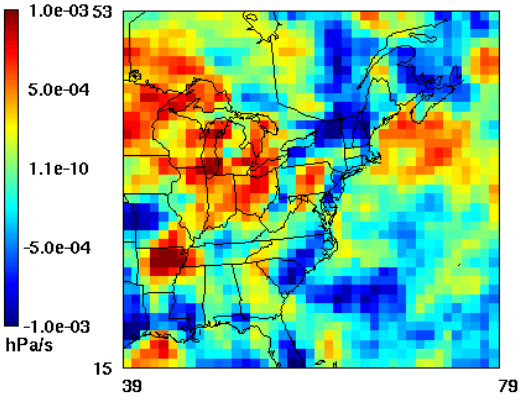

500 mb Heights

EDAS Composite
Pattern 1

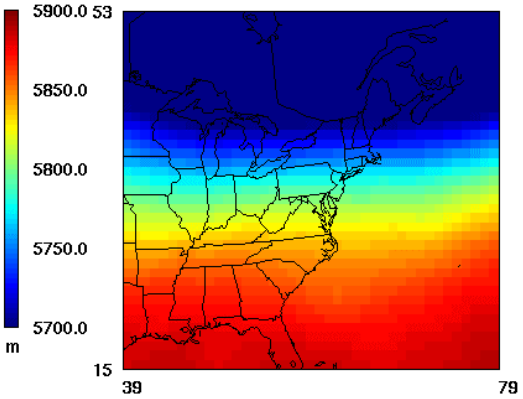

500 mb Heights

EDAS Composite
Pattern 2

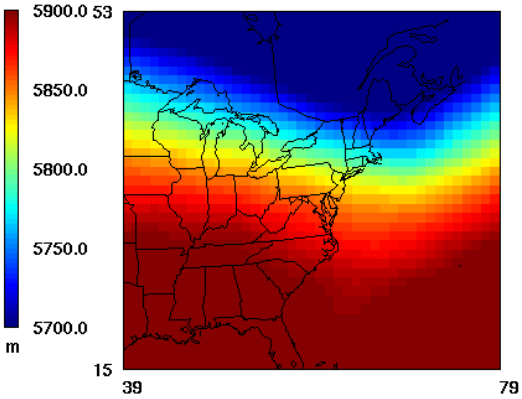

500 mb Heights

EDAS Composite
Pattern 3

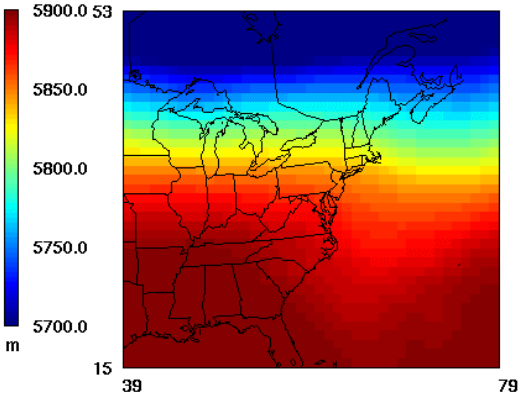

500 mb Heights

EDAS Composite
Pattern 4

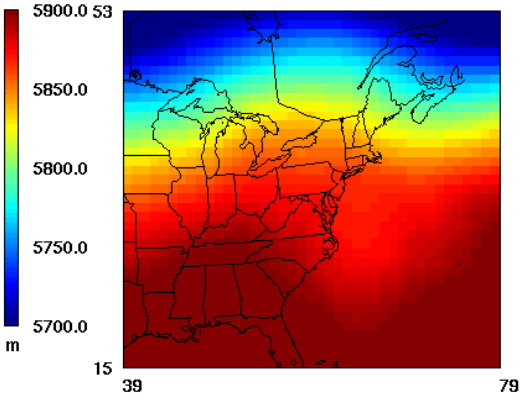

500 mb Heights

EDAS Composite
Pattern 5

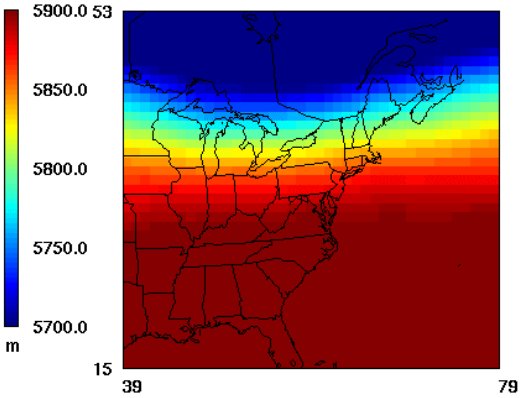

Appendix B

Boxplots of Key Meteorological Variables

Boxplots Of Key Meteorological Variables

Boxplots in this Appendix summarize distributions of the sub-regional ozone summary statistic, AvgEx00, described in the text along with selected key daily meteorological variables by episode pattern membership for the five cluster case. Pattern membership identifiers ("Met Cluster") used in these plots correspond to the episode types described in the text as follows:

Met Cluster	Episode Type
1	Type E
2	Type B
3	Type A
4	Type D
5	Type C

Ozone and meteorological variables are:

Variable	Description
clnx	AvgEx00 ozone summary statistic for ozone monitoring cluster x (x = 1,2…6; see Figure 1 in text)
DelPsfc.edas.DCtoNYC	Surface pressure gradient: Washington DC – New York City
DelPsfc.edas.DCtoBOSTON	Surface pressure gradient: Washington DC to Boston
DelPsfc.edas.DCtoPITTSBURGH	Surface pressure gradient: Washington DC to Pittsburgh
DelPsfc.edas.BUFFALOtoBOSTON	Surface pressure gradient: Buffalo to Boston
DelPsfc.edas.PITTSBURGHtoBUFFALO	Surface pressure gradient: Pittsburgh to Buffalo
H850.DC	850 mb height: Washington DC
H850.BOSTON	850 mb height: Boston
H850.PITTSBURGH	850 mb height: Pittsburgh
H850.BUFFALO	850 mb height: Buffalo
H850.PORTLAND	850 mb height: Portland, ME
H850.NYC	850 mb height: New York City
T850.DC	850 mb temperature: Washington DC
T850.BOSTON	850 mb temperature: Boston
T850.PITTSBURGH	850 mb temperature: Pittsburgh
T850.BUFFALO	850 mb temperature: Buffalo
T850.PORTLAND	850 mb temperature: Portland, ME
T850.NYC	850 mb temperature: New York City
sfcTmax.KLGA	Daily max surface temperature: La Guardia
sfcTmax.KPHL	Daily max surface temperature: Philadelphia
sfcTmax.KBOS	Daily max surface temperature: Boston
sfcTmax.KBUF	Daily max surface temperature: Buffalo
sfcTmax.KALB	Daily max surface temperature: Albany
sfcTmax.KDCA	Daily max surface temperature: Washington DC

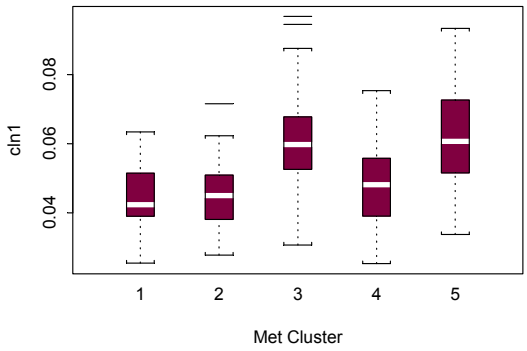
cln1
0.04
0.06
0.08
1
2
3
4
5
Met Cluster

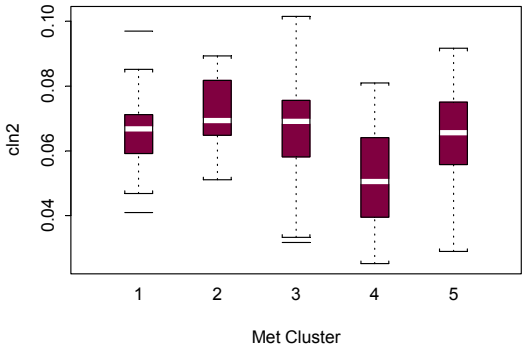
cln2
0.04
0.06
0.08
0.10
1
2
3
4
5
Met Cluster

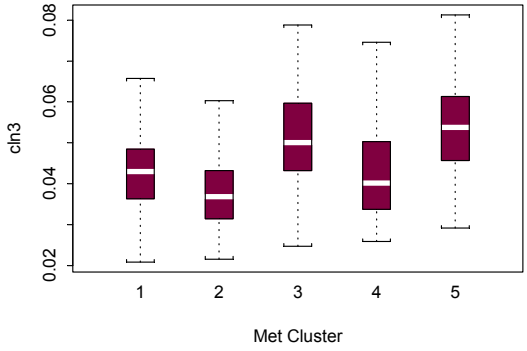
cln3
0.02
0.04
0.06
0.08
1
2
3
4
5
Met Cluster

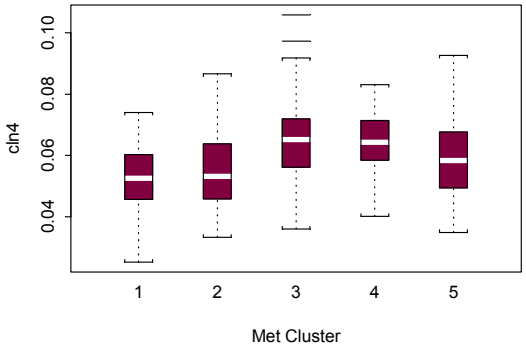
cln4
0.04
0.06
0.08
0.10
1
2
3
4
5
Met Cluster

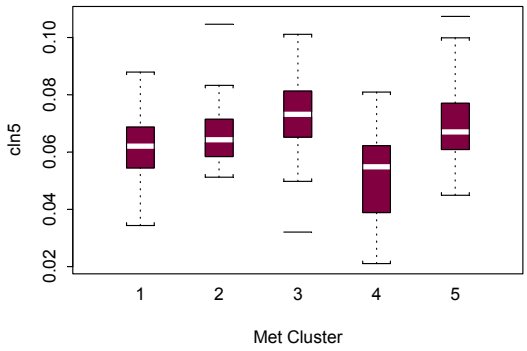
cln5
0.02
0.04
0.06
0.08
0.10
1
2
3
4
5
Met Cluster

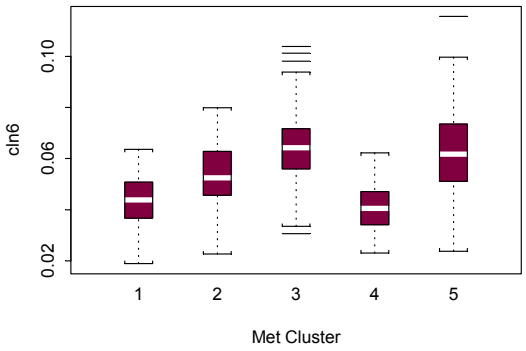
cln6
0.02
0.06
0.10
1
2
3
4
5
Met Cluster

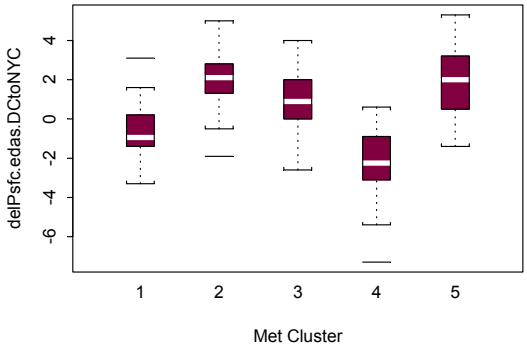
delPsfc.edas.DCtoNYC
-6
-4
-2
0
2
4
1
2
3
4
5
Met Cluster

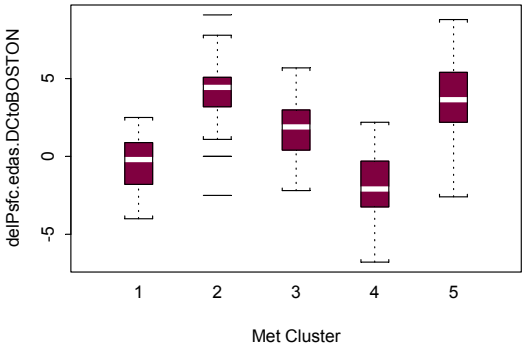
delPsfc.edas.DCtoBOSTON
-5
0
5
1
2
3
4
5
Met Cluster

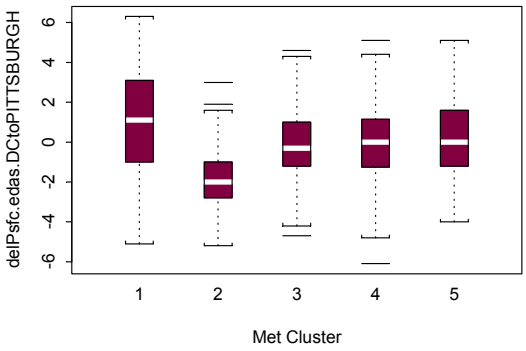
delPsfc.edas.DCtoPITTSBURGH
6
4
2
0
-2
-4
-6
1
2
3
4
5
Met Cluster

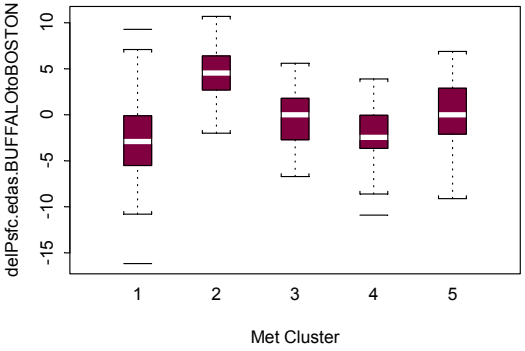
delPsfc.edas.BUFFALOtoBOSTON
10
5
0
-5
-10
-15
1
2
3
4
5
Met Cluster

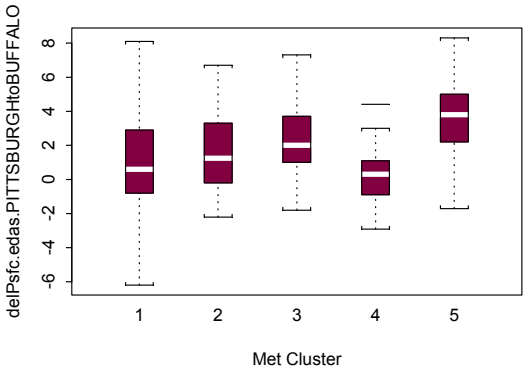
delPsfc.edas.PITTSBURGHtoBUFFALO
8
6
4
2
0
-2
-4
-6
1
2
3
4
5
Met Cluster

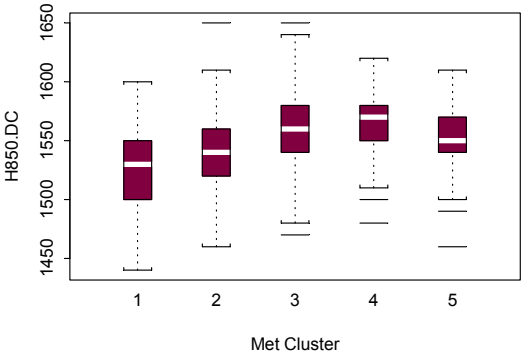
H850.DC
1650
1600
1550
1500
1450
1
2
3
4
5
Met Cluster

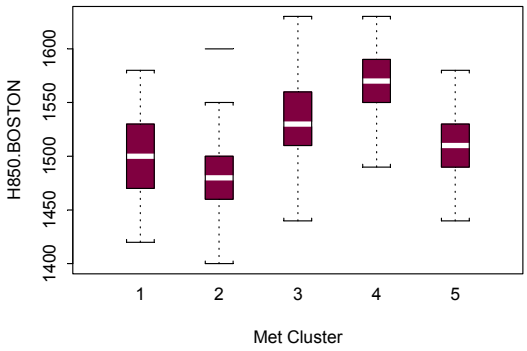
H850.BOSTON
1400
1450
1500
1550
1600
1
2
3
4
5
Met Cluster

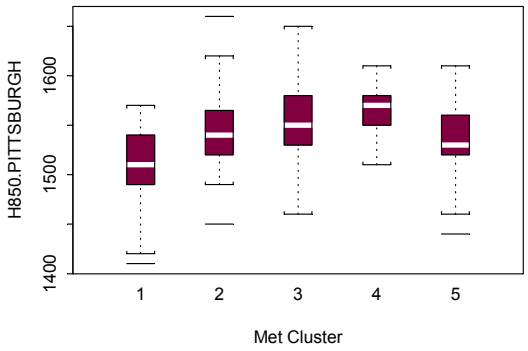
H850.PITTSBURGH
1400
1500
1600
1
2
3
4
5
Met Cluster

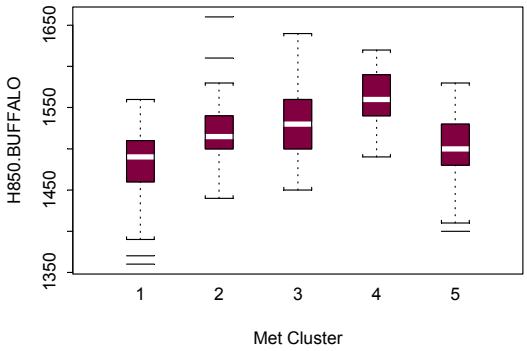
H850.BUFFALO
1350
1450
1550
1650
1
2
3
4
5
Met Cluster

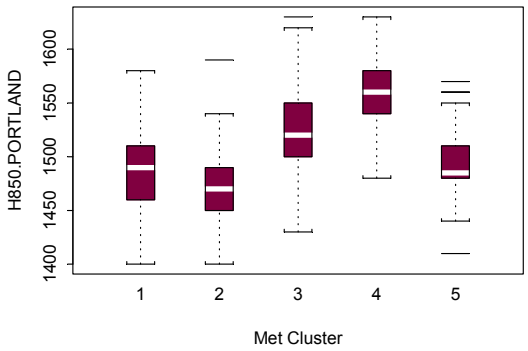
H850.PORTLAND
1400
1450
1500
1550
1600
1
2
3
4
5
Met Cluster

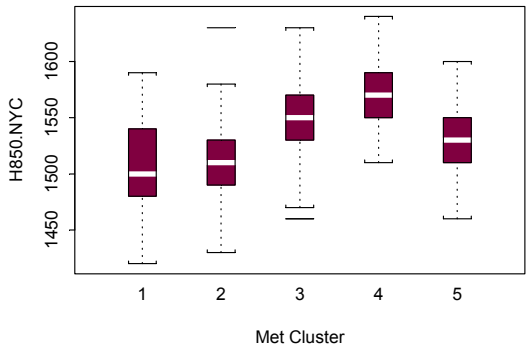
H850.NYC
1450
1500
1550
1600
1
2
3
4
5
Met Cluster

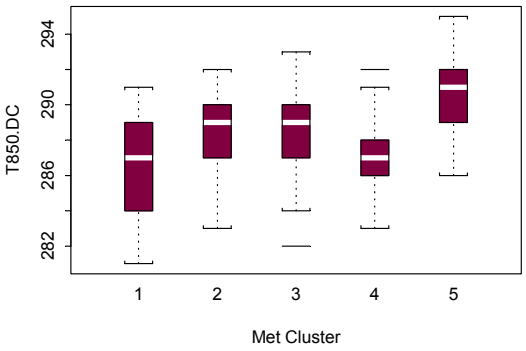
T850.DC
282
286
290
294
1
2
3
4
5
Met Cluster

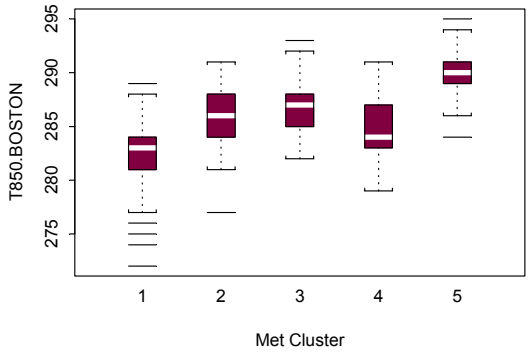
T850.BOSTON
275
280
285
290
295
1
2
3
4
5
Met Cluster

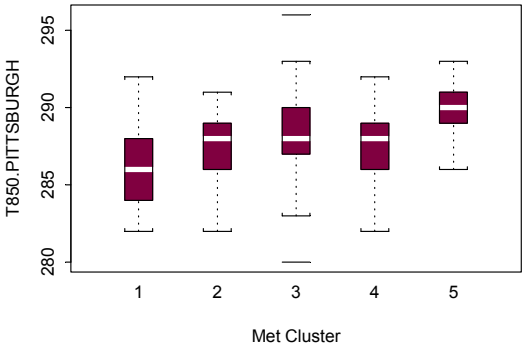
T850.PITTSBURGH
280
285
290
295
1
2
3
4
5
Met Cluster

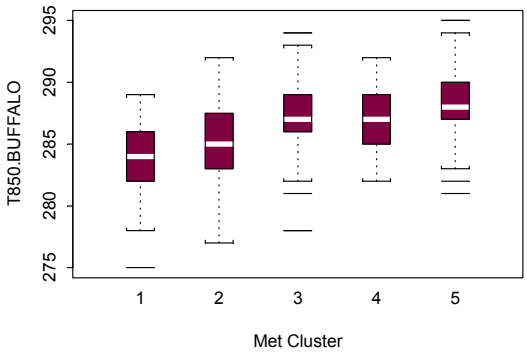
T850.BUFFALO
275
280
285
290
295
1
2
3
4
5
Met Cluster

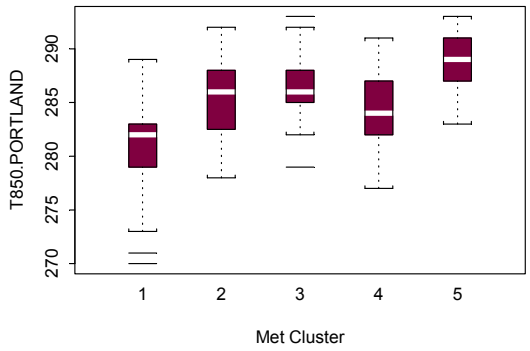
T850.PORTLAND
270
275
280
285
290
1
2
3
4
5
Met Cluster

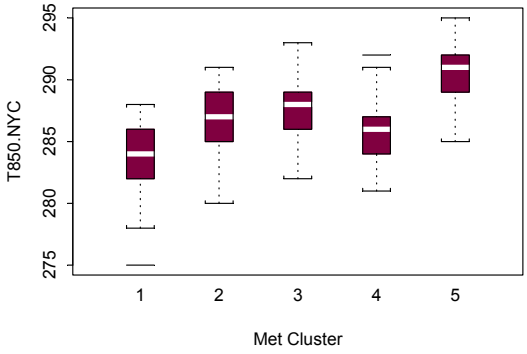
T850.NYC
275
280
285
290
295
1
2
3
4
5
Met Cluster

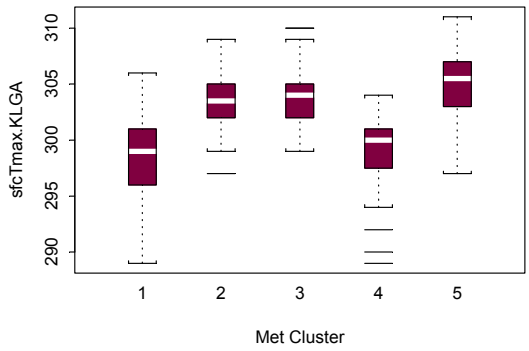
sfcTmax.KLGA
290
295
300
305
310
1
2
3
4
5
Met Cluster

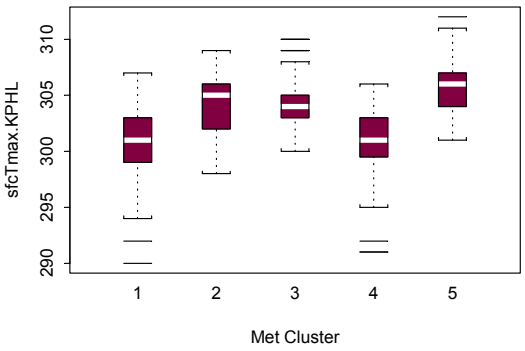
sfcTmax.KPHL
290
295
300
305
310
1
2
3
4
5
Met Cluster

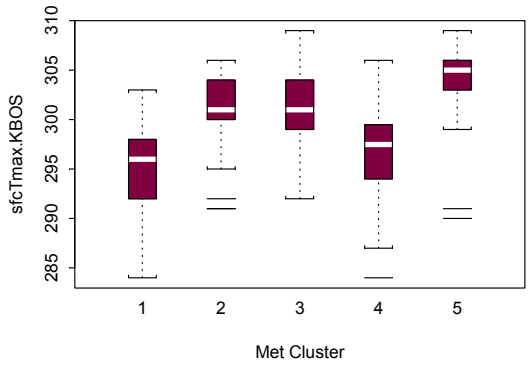
sfcTmax.KBOS
285
290
295
300
305
310
1
2
3
4
5
Met Cluster

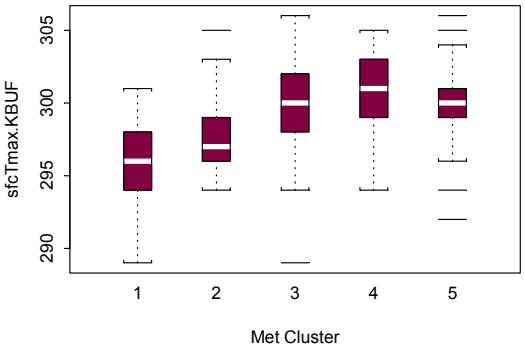
sfcTmax.KBUF
290
295
300
305
1
2
3
4
5
Met Cluster

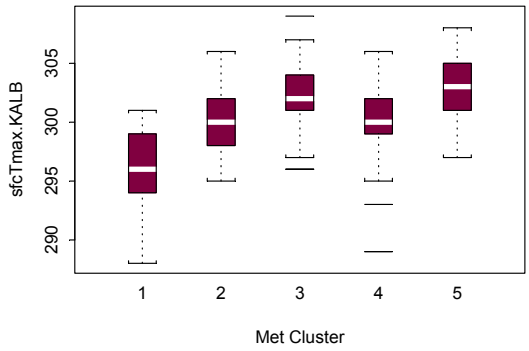
sfcTmax.KALB
290
295
300
305
1
2
3
4
5
Met Cluster

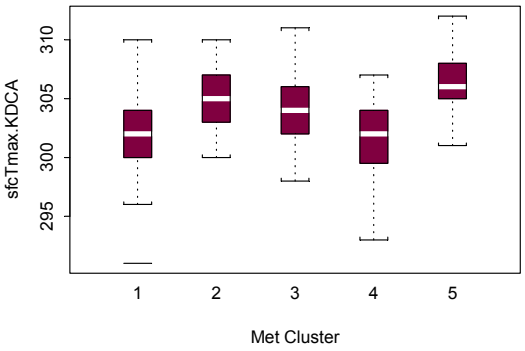
sfcTmax.KDCA
295
300
305
310
1
2
3
4
5
Met Cluster

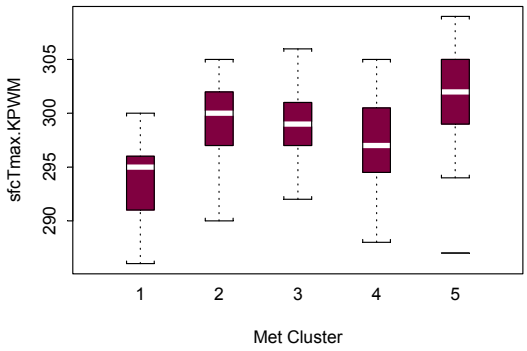
sfcTmax.KPWM
290
295
300
305
1
2
3
4
5
Met Cluster

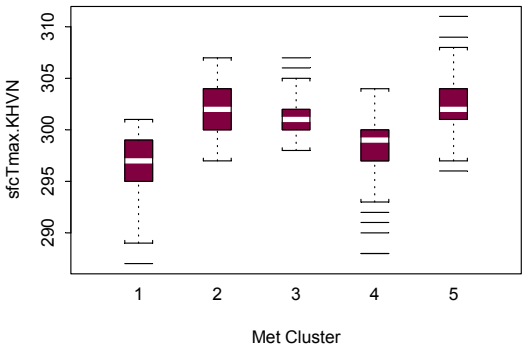
sfcTmax.KHVN
290
295
300
305
310
1
2
3
4
5
Met Cluster

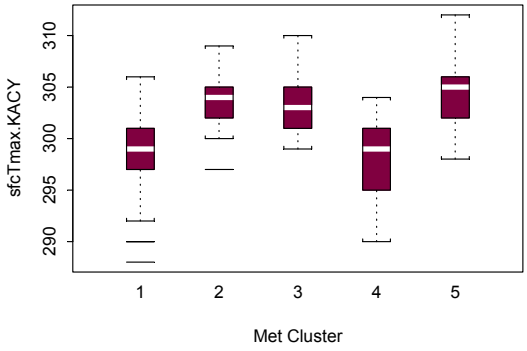
sfcTmax.KACY
290
295
300
305
310
1
2
3
4
5
Met Cluster

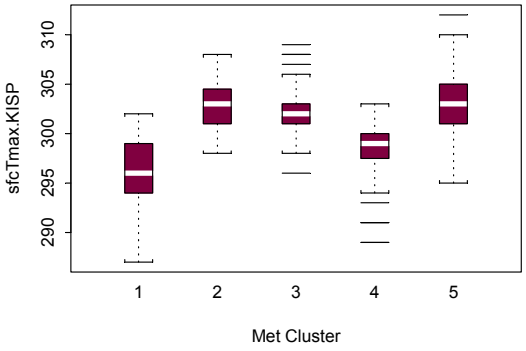
sfcTmax.KISP
290
295
300
305
310
1
2
3
4
5
Met Cluster

Appendix C

Wind Direction Frequency Tables

Wind Direction Frequency Tables

Contingency tables showing resultant surface wind direction frequencies were prepared for the five cluster membership cases. These results show relative frequency of days with the indicated wind direction in each cluster, i.e., the values for each cluster (column) sum to 100%. Tabulations are shown for both morning (AM) and afternoon (PM) resultant wind direction. Site location codes referenced in these tables are shown below.

Site Code	Location
KLGA	LaGuardia airport, New York, NY
KPHL	Philadelphia, PA
KBOS	Boston, MA
KBUF	Buffalo, NY
KALB	Albany, NY
KDCA	Washington, DC
KPWM	Portland, ME
KHVN	New Haven, CT
KACY	Atlantic City, NJ
KISP	Islip, Long Island, NY
KHYA	Hayannis, Cape Cod, MA
KWOR	Worcester, MA (KORH)
KHRT	Hartford, CT (KHFD)

Table B-1. Morning and afternoon daily resultant wind direction frequencies (%) by cluster membership for the five cluster case (columns sum to 100%). Header row for each table indicates AM or PM and four letter site ID as described in text (e.g., KLGA = LaGuardia, NY). Cluster identifier (A, B, C, D, E) is shown in first row of each table.

a) Morning wind directions

$resAMwd.KLGA:

	E	B	A	D	C
E	2	2	5	47	3
N	4	4	1	0	0
NE	27	4	7	35	0
NW	7	42	10	0	0
S	33	6	12	5	6
SE	11	0	7	7	2
SW	16	10	34	2	76
W	0	32	23	5	14

$resAMwd.KPHL:

	E	B	A	D	C
E	9	0	2	32	2
N	4	4	1	2	0
NE	7	0	0	34	0
NW	4	28	4	5	0
S	24	4	17	9	29
SE	20	0	4	7	2
SW	26	34	55	9	64
W	7	30	17	2	5

$resAMwd.KBOS:

	E	B	A	D	C
E	2	0	4	9	2
N	2	0	1	0	0
NE	9	4	1	14	0
NW	9	22	13	20	0
S	17	8	11	16	11
SE	15	2	2	7	3
SW	22	26	43	20	77
W	24	38	25	14	8

$resAMwd.KBUF:

	E	B	A	D	C
E	16	2	3	16	0
N	0	0	1	0	0
NE	13	0	0	5	3
NW	0	10	0	0	5
S	31	29	44	16	17
SE	24	0	24	57	6
SW	16	40	25	7	59
W	0	19	2	0	11

$resAMwd.KALB:

	E	B	A	D	C
E	2	0	8	6	0
N	10	7	5	20	2
NE	2	0	1	3	0
NW	10	20	4	3	0
S	34	20	55	49	87
SE	15	0	9	6	3
SW	20	26	12	9	8
W	7	28	5	6	0

$resAMwd.KDCA:

	E	B	A	D	C
E	4	0	0	26	0
N	2	14	2	2	0
NE	7	0	1	28	0
NW	9	24	5	5	0
S	46	24	38	16	68
SE	4	0	5	16	2
SW	22	28	45	2	29
W	7	10	5	5	2

$resAMwd.KPWM:

	E	B	A	D	C
E	10	8	3	2	3
N	2	0	1	7	0
NE	7	2	0	0	2
NW	12	17	14	17	2
S	12	8	11	5	27
SE	2	4	7	2	5
SW	15	8	16	29	50
W	39	52	49	38	12

$resAMwd.KACY:

	E	B	A	D	C
E	7	0	1	26	0
N	2	2	2	10	0
NE	5	0	1	23	0
NW	5	22	7	10	0
S	29	0	17	10	41
SE	12	2	6	8	3
SW	22	29	45	8	52
W	17	45	22	5	5

$resAMwd.KISP:

	E	B	A	D	C
E	9	0	5	14	0
N	9	9	6	19	0
NE	9	0	7	36	0
NW	0	34	10	5	0
S	32	2	8	2	11
SE	14	0	3	14	2
SW	11	21	44	7	80
W	16	34	18	2	8

$resAMwd.KHYA:

	E	B	A	D	C
E	6	0	0	8	0
N	3	13	3	14	0
NE	11	2	1	43	0
NW	6	20	6	0	0
S	14	7	6	11	3
SE	8	4	6	3	0
SW	31	22	41	19	60
W	22	33	38	3	37

$resAMwd.KWOR:

	E	B	A	D	C
E	5	2	0	7	0
N	0	4	3	10	0
NE	10	0	1	15	2
NW	5	23	10	17	0
S	5	2	0	5	2
SE	5	0	2	7	0
SW	33	4	19	12	62
W	38	65	65	27	35

$resAMwd.KHRT:

	E	B	A	D	C
E	5	5	5	19	0
N	5	2	2	6	0
NE	8	2	2	9	0
NW	3	7	0	0	0
S	51	36	71	41	94
SE	5	12	13	16	3
SW	19	19	2	6	3
W	3	17	5	3	0

Table B-1 (concl).

b) Afternoon wind directions

$resPMwd.KLGA:

	E	B	A	D	C
E	9	0	7	20	0
N	0	6	1	0	0
NE	30	0	15	68	0
NW	4	68	26	0	8
S	30	6	12	2	8
SE	13	2	8	7	0
SW	11	6	17	0	48
W	2	12	14	2	36

$resPMwd.KPHL:

	E	B	A	D	C
E	13	2	4	57	0
N	0	8	2	0	0
NE	4	0	0	32	0
NW	2	40	5	0	2
S	22	0	20	2	8
SE	26	4	3	9	2
SW	30	22	50	0	73
W	2	24	16	0	17

$resPMwd.KBOS:

	E	B	A	D	C
E	20	2	13	34	5
NE	9	2	2	9	0
NW	4	30	2	0	0
S	17	4	23	18	8
SE	15	2	20	25	0
SW	26	10	24	7	65
W	9	50	16	7	23

$resPMwd.KBUF:

	E	B	A	D	C
E	7	2	3	19	0
N	0	2	0	0	0
NE	11	4	1	5	5
NW	2	6	6	0	8
S	28	12	20	33	3
SE	11	6	2	16	0
SW	37	51	61	28	68
W	4	16	7	0	17

$resPMwd.KALB:

	E	B	A	D	C
E	2	0	3	8	0
N	2	2	2	11	0
NE	4	2	2	3	0
NW	7	41	6	0	2
S	59	2	45	50	58
SE	15	2	5	18	2
SW	7	20	17	8	24
W	4	31	20	3	15

$resPMwd.KDCA:

	E	B	A	D	C
E	7	4	5	23	0
N	0	4	2	2	0
NE	9	6	2	48	0
NW	2	34	4	0	5
S	57	14	53	9	59
SE	11	6	9	11	3
SW	11	6	17	2	21
W	4	26	8	5	12

$resPMwd.KPWM:

	E	B	A	D	C
E	11	8	17	20	5
N	0	4	2	0	0
NE	13	2	2	7	2
NW	11	42	11	0	2
S	20	6	24	27	29
SE	20	4	16	25	6
SW	16	14	15	14	33
W	9	20	13	7	24

$resPMwd.KACY:

	E	B	A	D	C
E	15	2	3	42	0
N	0	6	1	2	0
NE	7	4	1	47	0
NW	2	48	11	0	0
S	33	4	21	0	23
SE	24	0	10	9	0
SW	13	8	26	0	55
W	7	28	27	0	22

$resPMwd.KISP:

	E	B	A	D	C
E	11	0	6	36	0
N	2	10	5	2	0
NE	11	0	3	36	0
NW	2	52	11	2	3
S	38	0	17	2	14
SE	20	0	8	18	0
SW	11	8	39	2	68
W	4	29	13	0	15

$resPMwd.KHYA:

	E	B	A	D	C
E	16	11	7	9	0
N	0	9	2	7	0
NE	9	4	5	27	0
NW	0	11	6	0	0
S	13	9	12	20	5
SE	18	6	8	20	0
SW	38	21	48	16	75
W	7	30	11	0	20

$resPMwd.KWOR:

	E	B	A	D	C
E	14	4	3	17	2
N	5	4	1	2	0
NE	14	4	4	22	0
NW	9	35	9	2	0
S	9	0	7	22	5
SE	5	0	3	10	0
SW	37	4	28	7	54
W	7	49	44	17	40

$resPMwd.KHRT:

	E	B	A	D	C
E	11	2	16	16	0
N	4	9	3	3	0
NE	0	4	7	22	0
NW	2	22	1	0	0
S	56	13	43	22	52
SE	13	11	18	24	2
SW	11	11	9	11	35
W	2	28	4	3	11

Appendix D

Ozone Monitoring Stations by Sub-Region

Cluster	Site ID	State	City	Location
6	90010017	Connecticut	GREENWICH	GREENWICH POINT PARK
1	90011123	Connecticut	DANBURY	TRAILER, W. CONNECTICUT STATE UNIVERSITY
6	90013007	Connecticut	STRATFORD	USCG LIGHTHOUSE, PROSPECT STREET
6	90019003	Connecticut	WESTPORT	SHERWOOD ISLAND STATE PARK
1	90031003	Connecticut	EAST HARTFORD	MCAULIFFEE PARK
1	90070007	Connecticut	MIDDLETOWN	CONN. VALLEY HOSP., SHEW HALL, EASTERN D
6	90093002	Connecticut	MADISON	HAMMONASSET STATE PARK
6	90110008	Connecticut	GROTON	UNIVERSITY OF CONNECTICUT, AVERY POINT
1	90131001	Connecticut	STAFFORD	ROUTE 190, SHENIPSIT STATE FOREST
2	100010002	Delaware	NOT IN A CITY	STATE ROAD 384
5	100031003	Delaware	NOT IN A CITY	RIVER ROAD PARK, BELLEFONTE
5	100031007	Delaware	NOT IN A CITY	LUMS POND STATE PARK
5	100031010	Delaware	NOT IN A CITY	BRANDYWINE CREEK STATE PARK
2	100051002	Delaware	SEAFORD	350 VIRGINIA AVE SEAFORD
2	100051003	Delaware	LEWES	UNIV. OF DE COLLEGE OF MARINE STUDIES
5	110010025	Washington DC	NOT IN A CITY	TAKOMA SC. PINEY BRANCH RD & DAHLIA ST N
5	110010041	Washington DC	NOT IN A CITY	34TH. AND DIX STREETS, N.E.
5	110010043	Washington DC	NOT IN A CITY	S.E. END MCMILLIAN RESERVOIR, WASH. DC.
1	230052003	Maine	CAPE ELIZABETH	TWO LIGHTS STATE PARK
1	230090102	Maine	BAR HARBOR	TOP OF CADILLAC MOUNTAIN
1	230090103	Maine	BAR HARBOR	MCFARLAND HILL-DISPRO SITE
3	230112005	Maine	GARDINER	PRAY STREET SCHOOL
1	230130004	Maine	NOT IN A CITY	PORT CLYDE, MARSHALL POINT LIGHTHOUSE
3	230173001	Maine	NOT IN A CITY	ROUTE 5, NORTH LOVELL DOT
3	230194008	Maine	NOT IN A CITY	SUMMIT OF RIDER BLUFF (WLBZ TRANSMITTER)
1	230312002	Maine	NOT IN A CITY	OCEAN AVE/PARSONS WAY, KENNEBUNKPORT
1	230313002	Maine	KITTERY	FRISBEE SCHOOL, GOODSOE ROAD
2	240030014	Maryland	NOT IN A CITY	QUEEN ANNE AND WAYSON ROADS
5	240030019	Maryland	FORT MEADE	9001 'Y'STREET, FT. MEADE, ANNE ARUNDEL MD
5	240051007	Maryland	COCKEYSVILLE	GREENSIDE DRIVE, COCKEYSVILLE MD
5	240053001	Maryland	ESSEX	WOODWARD & DORSEY RDS, ESSEX MD
5	240130001	Maryland	NOT IN A CITY	1300 W. OLD LIBERTY ROAD, WINFIELD, MD
5	240150003	Maryland	NOT IN A CITY	RTE.273, FAIR HILL, CEIL CO., MARYLAND
2	240170010	Maryland	NOT IN A CITY	SO MD CORRECTIONAL CAMP, HUGHESVILLE MD
5	240251001	Maryland	EDGEWOOD	EDGEWOOD ARMY CHEM CENTER EDGEWOOD MD
5	240259001	Maryland	NOT IN A CITY	3538 ALDINO ROAD, HARFORD COUNTY MARYLAND
5	240290002	Maryland	NOT IN A CITY	KENT COUNTY; MILLINGTON
5	240313001	Maryland	ROCKVILLE	LOTHROP E SMITH ENV.ED CENTER ROCKVILLE
5	240330002	Maryland	GREENBELT	GODDARD SPACE FLIGHT CENTER
6	250010002	Massachusetts	TRURO	FOX BOTTOM AREA-CAPE COD NAT'L SEASHORE
1	250034002	Massachusetts	ADAMS	MT. GREYLOCK SUMMIT
6	250051002	Massachusetts	FAIRHAVEN	LEROY WOOD SCHOOL
1	250051005	Massachusetts	EASTON	1 BORDERLAND ST.
1	250092006	Massachusetts	LYNN	390 PARKLAND AVE. (LYNN WATER TREATMENT)
1	250094004	Massachusetts	NEWBURY	SUNSET BOULEVARD
1	250130003	Massachusetts	AGAWAM	152 SOUTH WESTFIELD STREET, FEEDING HILL

Cluster	Site ID	State	City	Location
1	250130008	Massachusetts	CHICOPEE	ANDERSON ROAD AIR FORCE BASE
1	250150103	Massachusetts	AMHERST	NORTH PLEASANT ST. U. MASS PATHOLOGY DEPT
1	250154002	Massachusetts	WARE	QUABBIN SUMMIT
1	250250042	Massachusetts	BOSTON	HARRISON AVENUE
1	250270015	Massachusetts	WORCESTER	WORCESTER AIRPORT
1	330050007	New Hampshire	KEENE	RAILROAD STREET
3	330090008	New Hampshire	HAVERHILL	HAVERHILL ARMORY, RT 116, HAVERHILL, NH
1	330111010	New Hampshire	NASHUA	SANDERS ASSOCIATES, PARKING LOT D
1	330130007	New Hampshire	CONCORD	STORRS STREET
1	330150012	New Hampshire	RYE	RYE HARBOR STATE PARK OCEAN BLVD, RTE. 1A
3	330173002	New Hampshire	ROCHESTER	ROCHESTER HILL ROAD, ROCHESTER
3	330190003	New Hampshire	CLAREMONT	SOUTH STREET
5	340010005	New Jersey	NOT IN A CITY	BRIGANTINE WILDLIFE REFUGE, NACOTE CREEK
5	340070003	New Jersey	NOT IN A CITY	COPEWOOD E. DAVIS STS; TRAILER
5	340071001	New Jersey	NOT IN A CITY	ANCORA STATE HOSPITAL, ANCORA
5	340110007	New Jersey	NOT IN A CITY	LINCOLN AVE.&HIGHWAY 55,NE OF MILLVILLE
5	340150002	New Jersey	NOT IN A CITY	CLARKSBORO, SHADY LANE REST HOME
5	340170006	New Jersey	BAYONNE	VETERANS PARK ON NEWARK BAY
5	340190001	New Jersey	FLEMINGTON	RARITAN STP, RTE.613S, THREE BRIDGES
5	340210005	New Jersey	NOT IN A CITY	RIDER COLLEGE; LAWRENCE TOWNSHIP
5	340230011	New Jersey	NOT IN A CITY	R.U. VEG RESEARCH FARM 3,RYDERS LN, NEWB
5	340250005	New Jersey	WEST LONG BRANC	MONMOUTH COLLEGE, WEST LONG BRANCH
5	340273001	New Jersey	NOT IN A CITY	BLDG.#1, BELL LABS, OFF ROUTE 513
5	340290006	New Jersey	NOT IN A CITY	COLLIERS MILLS, JACKSON TOWNSHIP
1	360010012	New York	ALBANY	LOUDONVILLE RESERVOIR
6	360050083	New York	NEW YORK CITY	200TH STREET AND SOUTHERN BLVD
6	360050110	New York	NEW YORK CITY	E 156TH ST BET DAWSON AND KELLY
4	360130006	New York	DUNKIRK	STP LAKESIDE BLD DUNKIRK
4	360130011	New York	NOT IN A CITY	TOWN OF WESTFIELD
4	360150003	New York	ELMIRA	SULLIVAN ST., WATER TR. PL.
1	360270007	New York	NOT IN A CITY	VILLAGE OF MILLBROOK
4	360290002	New York	AMHERST	AUDUBON GOLF COURSE, MAPLE ROAD
3	360310002	New York	NOT IN A CITY	SUMMIT, WHITEFACE MTN, WEATHER STATION
3	360310003	New York	NOT IN A CITY	BASE WHITEFACE MTN, ASRC, SUNY
3	360410005	New York	NOT IN A CITY	PISECO LAKE AIRPORT
3	360430005	New York	NOT IN A CITY	NICKS LAKE CAMPGROUND
4	360450002	New York	NOT IN A CITY	VADAI ROAD, PERCH RIVER, BROWNVILLE
4	360530006	New York	NOT IN A CITY	TOWN OF GEORGETOWN
4	360551004	New York	NOT IN A CITY	TRAILER, WEST END OF FARMINGTON ROAD
4	360631006	New York	NOT IN A CITY	MIDDLEPORT STP, NORTH HARTLAND RD
4	360671015	New York	NOT IN A CITY	5895 ENTERPRISE PARKWAY,
1	360715001	New York	NOT IN A CITY	1175 ROUTE 17K, MONTGOMERY
1	360790005	New York	NOT IN A CITY	NYSDEC FIELD HQTRS GYPSY TRAIL ROAD
6	360810098	New York	NEW YORK CITY	120-07 15TH AVE
5	360850067	New York	NEW YORK CITY	SUSAN WAGNER HS, BRIELLE AVE.& MANOR RD,
3	360910004	New York	NOT IN A CITY	SARATOGA NATIONAL HISTORICAL PARK
1	360930003	New York	SCHENECTADY	MT.PLEASANT HS, NORWOOD AVE.& FOREST RD.

Cluster	Site ID	State	City	Location
6	361030002	New York	BABYLON	EAST FARMINGDALE WATER DIST., GAZZA BLVD.
6	361030004	New York	RIVERHEAD	39 SOUND AVENUE, RIVERHEAD
3	361111005	New York	NOT IN A CITY	BELLEAYRE MOUNTAIN
4	361173001	New York	NOT IN A CITY	WAYNE EDUCATIONAL CENTER, WILLIAMSON
6	361192004	New York	WHITE PLAINS	WHITE PLAINS PUMP STATION, ORCHARD STREET
4	420030008	Pennsylvania	PITTSBURGH	BAPC 301 39TH STREET BLDG #7
4	420030067	Pennsylvania	NOT IN A CITY	OLD OAKDALE ROAD SOUTH FAYETTE
4	420031005	Pennsylvania	NOT IN A CITY	CALIFORNIA & 11TH, HARRISON TWP
4	420050001	Pennsylvania	KITTANNING	GLADE DR. & NOLTE RD. KITTANNING
4	420070002	Pennsylvania	NOT IN A CITY	ROUTE 168 & TOMLINSON ROAD
4	420070005	Pennsylvania	NOT IN A CITY	1015 SEBRING ROAD
4	420070014	Pennsylvania	BEAVER FALLS	EIGHT STREET AND RIVER ALLEY
5	420110001	Pennsylvania	KUTZTOWN	KUTZTOWN UNIVERSITY - GRIM SCIENCE BLDG
5	420110009	Pennsylvania	READING	UGI CO MONGANTOWN RD AND PROSPECT ST
5	420130801	Pennsylvania	ALTOONA	2ND AVE & 7TH ST
5	420170012	Pennsylvania	BRISTOL (BOROUG	ROCKVIEW LANE
5	420210011	Pennsylvania	NOT IN A CITY	MILLER AUTO SHOP 1 MESSENGER ST
5	420430401	Pennsylvania	HARRISBURG	1833 UPS DRIVE HARRISBURG PA
5	420431100	Pennsylvania	HERSHEY	SIPE AVE & MAE STREET
5	420450002	Pennsylvania	CHESTER	FRONT ST & NORRIS ST
4	420490003	Pennsylvania	NOT IN A CITY	10TH AND MARNE STREETS
5	420550001	Pennsylvania	NOT IN A CITY	FOREST ROAD - METHODIST HILL
1	420690101	Pennsylvania	NOT IN A CITY	WILSON FIRE CO. ERIE & PLEASANT
1	420692006	Pennsylvania	SCRANTON	GEORGE ST TROOP AND CITY OF SCRANTON
5	420710007	Pennsylvania	LANCASTER CITY	ABRAHAM LINCOLN JR HIGH GROFFTOWN RD
4	420730015	Pennsylvania	NEW CASTLE	CROTON ST & JEFFERSON ST.
5	420770004	Pennsylvania	ALLENTOWN	STATE HOSPITAL REAR 1600 HANOVER AVE
1	420791100	Pennsylvania	NANTICOKE	255 LOWER BROADWAY (NEXT TO LEON&EDDY'S)
1	420791101	Pennsylvania	WILKES-BARRE	CHILWICK & WASHINGTON STS
4	420850100	Pennsylvania	NOT IN A CITY	PA518 (NEW CASTLE ROAD) & PA418
5	420910013	Pennsylvania	NORRISTOWN	STATE ARMORY - 1046 BELVOIR RD
5	420950025	Pennsylvania	NOT IN A CITY	WASHINGTON & CAMBRIA STS. FREEMANSBURG
5	420990301	Pennsylvania	NOT IN A CITY	ROUTE 34 LITTLE BUFFALO STATE PARK
5	421010004	Pennsylvania	PHILADELPHIA	1501 E LYCOMING AVE AMS LAB
5	421010014	Pennsylvania	PHILADELPHIA	ROXY WATER PUMP STA EVA-DEARNLEY STS
5	421010024	Pennsylvania	PHILADELPHIA	GRANT-ASHTON ROADS PHILA NE AIRPORT
5	421010136	Pennsylvania	PHILADELPHIA	AMTRAK, 5917 ELMWOOD AVENUE
4	421250005	Pennsylvania	CHARLEROI	CHARLER01 WASTE TREATMENT PLANT
4	421250200	Pennsylvania	WASHINGTON	MCCARRELL AND FAYETTE STS
4	421255001	Pennsylvania	NOT IN A CITY	HILLMAN STATE PARK - KINGS CREEK ROAD
4	421290006	Pennsylvania	NOT IN A CITY	OLD WILLIAM PENN HWY & SARDIS AVE
5	421330008	Pennsylvania	YORK	HILL ST.
1	440030002	Rhode Island	NOT IN A CITY	W. ALTON JONES CAMPUS URI PARKERFIELD WE
1	440071010	Rhode Island	EAST PROVIDENCE	FRANCIS SCHOOL, 64 BOURNE AVE
6	440090007	Rhode Island	NARRAGANSETT	TARWELL ROAD, NARRAGANSETT
3	500030004	Vermont	BENNINGTON	AIRPORT RD, BENNINGTON, VERMONT
3	500070007	Vermont	UNDERHILL	PROCTOR MAPLE RESEARCH FARM

Cluster	Site ID	State	City	Location
5	510130020	Virginia	NOT IN A CITY	S 18TH AND HAYES ST
2	510360002	Virginia	NOT IN A CITY	SHIRLEY PLANTATION, ROUTE 5
2	510410004	Virginia	NOT IN A CITY	BEACH, INTERSECTION OF CO.ROADS 655 & 654
5	510590005	Virginia	NOT IN A CITY	CUBRUN LEE RD CHANT, (CUBRUN TREAT PLANT)
5	510590018	Virginia	NOT IN A CITY	MT.VERNON 2675 SHERWOOD HALL LANE
5	510591004	Virginia	SEVEN CORNERS	6100 ARLINGTON BLVD MONTG WARD
5	510595001	Virginia	MC LEAN	LEWINSVILLE 1437 BALLS HILL RD
5	510610002	Virginia	NOT IN A CITY	RT651 C PHELPS WILDLIFE MANAGEMENT AREA
5	510690010	Virginia	NOT IN A CITY	RTE 669, BUTLER MANUF. CO NEAR REST VA
2	510870014	Virginia	NOT IN A CITY	2401 HARTMAN STREET MATH & SCIENCE CTR
2	511130003	Virginia	NOT IN A CITY	SHENANDOAH NP BIG MEADOWS
5	511530009	Virginia	NOT IN A CITY	JAMES S. LONG PARK
2	511611004	Virginia	VINTON	EAST VINTON ELEMENTARY SCHOOL
5	511790001	Virginia	NOT IN A CITY	WIDEWATER ELEM. SCH., DEN RICH ROAD
2	511970002	Virginia	NOT IN A CITY	16-B RURAL RETREAT SEWAGE DISPOSAL
5	515100009	Virginia	ALEXANDRIA	517 N SAINT ASAPH ST, ALEXANDRIA HEALTH
2	518000004	Virginia	SUFFOLK	TIDEWATER COMM. COLLEGE, FREDERIC CAMPUS
2	518000005	Virginia	SUFFOLK	TIDEWATER RESEARCH STATION, HARE ROAD

Appendix E

Episode Types Associated with 8-Hour Ozone Exceedance Days in 2002

Episode Pattern	Year	Month	Day
5	2002	5	16
3	2002	5	24
1	2002	5	25
5	2002	6	1
5	2002	6	5
5	2002	6	6
5	2002	6	9
4	2002	6	10
5	2002	6	11
1	2002	6	12
4	2002	6	20
5	2002	6	21
3	2002	6	22
3	2002	6	23
2	2002	6	24
4	2002	6	25
5	2002	6	26
5	2002	6	27
5	2002	6	29
3	2002	6	30
5	2002	7	1
3	2002	7	2
3	2002	7	3
3	2002	7	4
2	2002	7	5
3	2002	7	7
3	2002	7	8
5	2002	7	9
4	2002	7	12
3	2002	7	13
3	2002	7	14
5	2002	7	15
2	2002	7	16
3	2002	7	17
2	2002	7	18
3	2002	7	19
4	2002	7	20
4	2002	7	21
5	2002	7	22
5	2002	7	23
1	2002	7	27
1	2002	7	28
2	2002	7	29
2	2002	7	30
2	2002	7	31

Episode Pattern	Year	Month	Day
3	2002	8	1
4	2002	8	2
3	2002	8	3
3	2002	8	4
5	2002	8	5
4	2002	8	9
3	2002	8	10
3	2002	8	11
3	2002	8	12
3	2002	8	13
3	2002	8	14
5	2002	8	15
3	2002	8	16
3	2002	8	17
3	2002	8	18
1	2002	8	19
4	2002	8	21
5	2002	8	22
2	2002	8	23
3	2002	9	7
4	2002	9	8
4	2002	9	9
5	2002	9	10
5	2002	9	13
1	2002	9	14
4	2002	9	18

Qualitative Episode Analysis for 2002 Ozone Season

Episode of June 10-12, 2002

***June 10*:** At 0000 UTC, at cold front is analyzed in northern PA. This boundary drifts slightly south and becomes stationary along a Dover-Baltimore-Pittsburgh line by 1200 UTC. Visible images show clear skies with hints of haze at 1600 UTC with only shallow cumulus developing by 1800 UTC. Surface reports at 1800 UTC have scattered reports of haze in the Washington area and more widespread reports west of the Appalachians. The upper air pattern is conducive to the development of a high ozone period with high pressure at 850 mb centered over KY and a modest ridge west of the region at 500 mb. The forecast back trajectories are consistent with standard high ozone cases with westerly flow. Upstream ozone at 1500 UTC at the source of the back trajectories on June 9 is strongly enhanced – in the 70-80 ppb (1-hour average) range. Widespread Code Orange concentrations are found south of the frontal boundary.

June 11: The slow moving/near stationary frontal boundary has now taken the form of a retreating warm front and is well into New England at 1800 UTC with an Appalachian lee trough (ALT) analyzed from Baltimore to northern NC. A broad ridge at 850 mb stretches from AL to the Delmarva with the 500 mb ridge axis remaining just west of the mid-Atlantic. High ozone concentrations are reported right along the I-95 Corridor with scattered Code Red concentrations. The forecast back trajectories show a shift from west-northwesterly flow to along-Corridor. The 1200 UTC sounding at Dulles Airport, VA (IAD) showed continuing westerly flow through the depth of the boundary layer with a very strong cap at 660 mb. A residual mixed layer, often found in association with high ozone cases, is also seen.

June 12: Ozone concentrations fall region-wide on June 12 with strong southwest winds observed. Forecast back trajectories suggest very fast flow backing further to the southwest than the previous two days. Convection develops by afternoon across central PA with a substantial cirrus cloud shield moving into the mid-Atlantic in advance of the rain.

Episode of June 22-26:

During this episode, the mid-Atlantic is sandwiched between two systems. First, a vigorous low that crosses southern Canada on June 20-21 and, second, an upper level low that develops over the southeastern US and then drifts westward with time. A small area of high pressure is wedged between the systems and the highest ozone concentrations are found beneath this high pressure wedge.

***June 22*:** The strong system that crossed Canada earlier in the period has now weakened and moved just northeast of ME (500 mb). A sprawling area of high pressure at 850 mb is found from IN east to just south of Long Island. At the surface at 1200 UTC, high pressure is located over WV. The frontal boundary associated with the departing Canadian system is quasi-stationary over New England and northern NY. Further south,

the upper level low over the eastern Gulf of Mexico has resulted in the development of a coastal trough with sustained easterly winds reaching as far north as NC. The ozone pattern this day follows the synoptic situation closely with good air quality north of the frontal boundary and south across VA and NC where the maritime inflow is strongest. In the Washington, DC area a wide range of concentrations is found. Concentrations range from Code Green in the northwest suburbs to upper Code Orange in the near southern suburbs.

Skies are generally clear across the Washington region with some shallow cumulus developing by afternoon. The 1200 UTC IAD sounding showed light southwest winds beneath the surface based inversion with easterly flow aloft and a very strong cap at 820 mb. The air mass is relatively dry for the season (62-63 $^{\circ}$F).

***June 23*:** Areas of good air quality (Code Green) are again found in the Washington area with no 8-hour ozone violations on this day. The very clean maritime air mass associated with the coastal trough and associated upper level low is seen over VA. The forecast back trajectories show a complex transport pattern with an offshore component at 500 m. Back trajectories based on analysis field are roughly similar with a weaker maritime component. The morning IAD sounding again has a strong inversion based at 850 mb with light and variable winds beneath it.

June 24: By mid-afternoon on June 23, low pressure develops along a frontal boundary north of the Washington area. This system develops quickly so that, by 1200 UTC on June 24, a reinforced cold front has pushed to just north of New York City. By 1800 UTC, the boundary is quasi-stationary across northern NJ and central PA with scattered convection occurring across central PA. Scattered haze is reported south of this frontal boundary in the morning hours, persisting into afternoon. The 1200 UTC IAD sounding shows a residual inversion present at 800 mb though much weaker than the two previous days. An elevated mixed layer is evident just beneath the inversion. The highest ozone concentrations are organized in a west-to-east band across OH and PA into NJ and MD. Scattered Code Red concentrations are found east and northeast of Washington, DC.

***June 25*:** The frontal boundary that was driven southward on June 24 reaches as far as southern NJ by 1200 UTC before returning northward by mid-afternoon. Scattered Code Red concentrations are present in the Washington area. The most unusual aspect of the ozone field on this day is the presence of Code Red concentrations over the urban center of Washington. Haze reports are widespread and forecast back trajectories are less complex than previous days with standard west-northwest flow within the boundary layer.

***June 26*:** The episode ends on June 26 when the upper level ridge begins to flatten. This allows for increased boundary layer winds and a much more unstable atmosphere. The 1200 UTC IAD sounding is nearly dry adiabatic on June 26 in the boundary layer with strong SW winds throughout (10-15 knots range). The unstable air mass results in convection developing along the Blue Ridges by 1900 UTC with widespread convection later in the afternoon.

Episode of July 1-3, 2002

A relatively mild ozone episode with strong local peaks on July 2, 2002. The peak 1-hour ozone concentration in the Washington area was 158 ppbv in the Washington area on July 2, 2002. Widespread one-hour exceedances on July 2, 2002 were reported near Washington, DC. Throughout the episode, the highest concentrations were found along and east of the I-95 Corridor with lower concentrations further west.

The high ozone event of June 22-26, 2002 ended with an upper level trough crossing the northeastern US. The trough exited the region fairly rapidly but the transition to a ridging pattern was complicated by a small "cut off" low left behind by the trough over New England. This low drifted only slowly eastward to near Nova Scotia by July 2, 2002. Surface winds were north to northeast on June 29, 2002 becoming southwest early on June 30, 2002.

July 1: The 1200 UTC surface analysis shows a fairly standard high ozone pattern. The center of high pressure is located in western VA with a very weak pressure gradient across the region. At 850 mb, high pressure is centered further west over western TN with a weak trough exiting New England. A similar pattern is present at 500 mb although the presence of a lingering closed low just east of Maine suggests that the pattern will remain stationary in the short term not allowing the ridge to build quickly east.

Ozone concentrations in the Washington, DC region were relatively high (86-87 ppbv 8-hour average) on the preceding day (June 30), and back trajectories suggested slow transport along and slightly west of the I-95 Corridor. Peak 1-hour ozone concentrations rose into the 87-99 ppbv range in the Washington area. The bulk of the monitors exceeding the 8-hour standard were in the 90-100 ppbv range, reflecting a rising regional ozone load.

The morning IAD sounding showed a layer of strong southwest winds and the Fort Meade, MD profiler showed steady WSW winds through the day. As reflected in the afternoon visible image, there was significant boundary layer overturning producing widespread, though shallow, cumulus beneath a subsidence inversion based at ~ 770 mb. The 0000 UTC IAD sounding for July 2 shows a residual mixed layer to ~ 800 mb corroborating that deep boundary layer mixing occurred.

***July 2*:** The most unusual aspect of this day was the abrupt decrease in visibility beginning in the late morning and continuing through the afternoon and the speed with which the haze layer moved northeastward into New England. Typically, visibility reaches its maximum with mixing and increased winds in the afternoon and then reaches a minimum just before sunrise. This occurred in the context of continuing brisk southwest winds with 10-13 knots reported by afternoon. The regional surface wind field was complex with variable winds through the early afternoon becoming southeast.

The upper level analyses at 850 mb and 500 mb are barely distinguishable from the

previous day. Of most interest is the position of high pressure at 850 mb that is slightly further north over IL at 1200 UTC. Unlike the standard mid-Atlantic pollution case, however, this continental high has not linked up with the semi-permanent Bermuda High as a lingering trough is present along the Eastern Seaboard. As a result, 850 mb winds reported at IAD were north to north-northwest early on July 2, 2002. At IAD, this flow pattern is consistent to the base of a strong capping inversion at ~ 800 mb. The IAD sounding at 0000 UTC on July 3 showed the boundary layer was further suppressed during the day with mixing only to ~ 1500 m. As a result, only shallow cumulus develops over the mid-Atlantic during the afternoon with the exception of scattered strong convective activity across western PA south into WV.

Back trajectories, and regional surface observations, suggest transport of pollutants from locations northwest of the I-95 Corridor. Upstream ozone at 1600 UTC across northwestern PA was on the order of 70-80 ppbv.

***July 3*:** Although temperatures continued very warm in the upper 90's $^{\circ}$F, the characteristics of the air mass appear to change rapidly yet again. Ozone concentrations fell across the region with peaks reaching the Code Orange range.

Forecast back trajectories for July 3 were quite similar to the preceding day and verify well with analysis trajectories. Ozone concentrations upstream, however, ran ~ 10 ppbv lower than on the preceding day. The morning sounding for July 3 was more unstable with a much reduced cap from the previous day although only shallow cumulus formed during the afternoon hours.

The ALT, which was analyzed along the I-95 Corridor for much of July 2, slips slowly eastward and the region of highest ozone concentrations is roughly aligned with its later afternoon position.

Episode of July 31-August 5

***July 31*:** Scattered Code Orange reported in the southern mid-Atlantic. Generally moderate ozone is reported along the I-95 Corridor. Forecast back trajectories suggest fairly fast boundary layer flow with the air mass origination in southern Ontario. Ozone concentrations at 1600 UTC on July 30th in that region were about average (45-50 ppbv). The cold front, located near Norfolk, VA at 0000 UTC, drifts a bit further south by 1200 UTC and then dissipates by 1800 UTC.

***August 1*:** Ozone concentrations rise region-wide. Forecast back trajectories show a strong anti-cyclonic curvature from near Lake Ontario through northern NJ. Again, upstream ozone is relatively low (40-50 ppbv) in southern Canada and northern PA but emissions along the path are likely quite high as the air parcels cross the metropolitan New York area. An ALT is analyzed overnight along and east of the I-95 Corridor. By 1200 UTC, high pressure is centered over WV a climatologically favored location for high ozone in the I-95 Corridor. A very strong low-level inversion is observed with northeast winds in the layer beneath 800 mb.

***August 2*:** Highest O3 concentrations are reported right along the I-95 Corridor with scattered Code Red observations in the Washington area. The highest ozone concentrations are found south and west of Washington DC. Forecast back trajectories show a good deal of variability. At 1200 UTC, a back door front is analyzed near NYC with surface high pressure still centered near WV. As on August 1, the sounding at IAD shows a strong low-level inversion. Early morning observations show haze along the I-95 Corridor with the most numerous observations in VA and NC. As afternoon mixing occurs, only widely scattered haze reports by afternoon.

***August 3*:** High ozone levels are concentrated along the I-95 Corridor again on August 3. The forecast back trajectories are the standard west-northwest flow although mid-day ozone across northern OH on the preceding day was not extreme (47-56 ppbv). This likely reflects difficulties in the trajectory model in the vicinity of a frontal boundary which reaches central PA by 0000 UTC and then just N of PHL by 1200 UTC where it stalls. Scattered haze is reported across PA, MD and VA lingering into the early afternoon hours.

***August 4*:** Ozone increases along a band from just north of Washington, DC to just north of New York City with widespread Code Red concentrations in a pattern characterized by re-circulation and stagnation. The cold front that reached into eastern PA on the previous day becomes stationary along a line from Portland, ME to just north of New York City and then across central PA to near Pittsburgh. This boundary washes out by 1200 UTC with surface high pressure remaining in place over WV and an ALT analyzed along the I-95 Corridor at 1800 UTC.

***August 5*:** Scattered Code Red ozone concentrations near Washington DC. The presence of significant cloud cover north of the Mason Dixon Line reduces peak ozone in that region. The frontal boundary has washed out over New England with remnants still quasi-stationary over northern PA. The next cold front reaches northwestern PA by 1200 UTC. Again there is considerable vertical shear noted by the forecast back trajectories with southerly flow at the lowest (500 m) layer.

<u>Episode of August 10-14</u>

***August 10*:** High pressure is directly over the mid-Atlantic with dew points in the mid-50's $^{\circ}$F, and clear skies. Temperatures are generally in the upper 80s across the Washington, D.C. region. With high pressure overhead, the forecast back trajectories indicate very light winds and recirculation. Highly variable ozone field with concentrations are present on August 10th in the Washington, D.C area. Scattered Code Orange peaks were reported along the I-95 Corridor. While the Dulles, Virginia (IAD) sounding at 1200 UTC did not show a very strong low-level inversion, with 950 mb temperatures only 21°C, there was a very strong cap at 805 mb with absolutely stable conditions above this level. The presence of a deep residual layer (975-805 mb) suggests the presence of stagnation. Peak eight-hour average ozone exceedances in the Washington, DC region ranged from 87 ppbv (Arlington and Loudoun Counties, VA) to

93 ppbv (Fairfax County, Annandale, VA).

***August 11*:** Surface high pressure drops slowly southeastward across the mid-Atlantic with the center analyzed in western NC at 1200 UTC drifting to coastal SC by 1800 UTC. The upper level ridge has also moved east and is located over the mid-Atlantic at 1200 UTC. The ozone map for the Washington area shows another day of highly variable peak ozone. A peak concentration of 120 ppbv occurred along the I-95 Corridor northeast of Washington DC. Again, a very clear day in the mid-Atlantic. Winds are generally south to southwest as is reflected in the boundary layer back trajectories. The key factor driving local ozone production appears to be a very stable boundary layer. The 1200 UTC sounding at IAD shows a very strong low-level inversion from 950-900 mb with a deep residual layer beneath a continuing strong subsidence inversion, now based at 760 mb. Peak eight-hour average exceedances ranged from 88 ppbv (Prince Georges County, MD) to 106 ppbv (Washington, D.C., McMillan).

***August 12*:** The upper level ridge remains quasi-stationary with its axis over the mid-Atlantic. The center of high pressure at 850 mb is over NC/GA. At the surface, the characteristic Appalachian lee trough (ALT) is analyzed at 0000 UTC and remains in place through 1800 UTC, continuing into August 13. Clear skies remain, although haze is seen in the 1600 UTC visible image. The surface observations show a rapid and widespread decrease in visibility west and northwest of the I-95 Corridor, shifting further east by early afternoon. The 1200 UTC IAD sounding is similar to the preceding in several respects: a slightly deeper and continuing strong low level inversion, now from 975-925 mb with a strong cap at ~ 770 mb. Winds are fairly strong from the NW. This is reflected in the forecast back trajectories that show a shift to westerly transport. The upwind O3 concentrations at 1600 UTC on August 11 in the vicinity of the origin of the forecast back trajectories is enhanced, on the order of 78-86 ppbv. Ozone concentrations fall this day west of the Appalachians but increase markedly across the mid-Atlantic with widespread Code Red observations from NC to Boston. Widespread exceedances are found in the Washington area, ranging from 85 ppbv (Rockville, MD) to 114 ppbv (Arlington County, VA).

***August 13*:** Periods of calm winds are reported overnight. Significant haze has now spread all along the I-95 Corridor and remains into the afternoon hours. The regional ozone map shows an extensive episode. Skies are again clear with shallow convection developing later in the afternoon. The 1200 UTC IAD sounding showed a continuing strong low level inversion with a residual mixed layer to 850 mb ending just beneath a weak secondary inversion. The cap aloft has lifted to ~ 630 mb and the sounding is more unstable compared to previous day's between the two inversion layers. In addition to a very stable, and hazy, boundary layer, the surface analyses show that the ALT continues in place from late on August 12, to a position slightly further east at 1200 UTC and then backing west at 1800 UTC. As is typically the case, the highest ozone concentrations are found in proximity to this boundary. Eight-hour exceedances ranged from 87 ppbv (Loudoun County, VA) to 125 ppbv (Fairfax County, Mt. Vernon, VA).

***August 14*:** Back trajectories forecast fairly fast flow along the I-95 Corridor. The increase in southerly wind component results as the upper level ridge axis finally moves offshore. On the back side of the upper level ridge, low level southerly winds increase as the Bermuda High circulation pushes maritime air northward. The haze reports corroborate a slow clean out from south to north with morning haze reported north of Washington, D.C. This episode ends in a very different manner than the standard high ozone episode. Instead of the passage of a sharp cold front, this episode ends gradually as cleaner air sweeps north, winds increase and the atmosphere steadily destabilizes. On August 15, concentrations fall across the region as low level flow becomes more southeast and the Bermuda high fills in westward. Cloud cover spreads over the region on August 16 with ozone concentration continuing to decrease. Peak eight-hour exceedances ranged from 87 ppbv (Arlington County, VA) to 101 ppbv (Fort Meade, MD).

Episode of September 9-10

Summary: A two-day ozone episode with northeasterly flow due to high pressure to the north and west and Tropical Storm Gustav to the southeast. Strong subsidence occurs over the region as Gustav approached and moves along the North Carolina coast. Northeasterly winds occurs due to clockwise flow around high pressure over the Ohio Valley and counter-clockwise flow around Gustav as it neared the Outer Banks. Highest ozone concentrations on September 9th occur in central Pennsylvania, northeast of Baltimore, near Annapolis, MD and west of Fairfax County, VA. A sharp ozone gradient was evident on the 10th with low concentrations east of a Baltimore-Rockville, MD-Fairfax City, VA line while eight-hour exceedances occurred in counties immediately west and south of Fairfax.

September 9: At 1200 UTC, Tropical Storm Gustav is southeast of Cape Hatteras, NC with high pressure was over Ohio and Indiana. Widespread surface haze observed in Ohio, Michigan, Indiana, and Illinois. Very warm air aloft over Pennsylvania and West Virginia enhanced stable atmospheric dispersion conditions. The upper air pattern indicates a large ridge over the eastern half of the US, with a closed low associated with Gustav off the southeast coast. Strong subsidence occurs over Mid-Atlantic region, centered over south-central Pennsylvania. Forecast back trajectories indicate flow from the northeast megalopolis (Philadelphia to New York City). Code Orange concentrations are observed throughout much of New Jersey, northeast Maryland, and the western Virginia suburbs of Washington, DC. Code Red was reached northeast of Baltimore. Code Green conditions occurred in coastal southern Delaware and Maryland due to the influence of clean air from Gustav.

September 10: Tropical Storm Gustav nearer Cape Hatteras with heavy precipitation along the Outer Banks. Widespread surface haze was again observed throughout the Ohio Valley into Indiana, Illinois, and Michigan. As Gustav moves closer to the North Carolina coast, the region of strong subsidence moves further west, along and to the west of the Appalachians. Forecast back trajectories indicate the influence from Gustav as the flow was generally from the east. The maritime tropical air from Gustav reaches as far inland as Washington, D.C. but stable, continental air is quite close to the west as

indicated by the 8-hour ozone peak concentration map. A very sharp ozone gradient is evident. Conditions range from Code Green to Code Red just several miles apart in Fairfax County, VA. Code Orange conditions occur west of Baltimore and in the western Virginia suburbs of DC while Code Green conditions occur along I-95 and eastward. Code Red conditions occur just west of I-95 at three Virginia locations in the Washington, D.C. region.

Appendix C
Boundaries of the Modeling Domain

OTC CMAQ 12km Modeling Domain

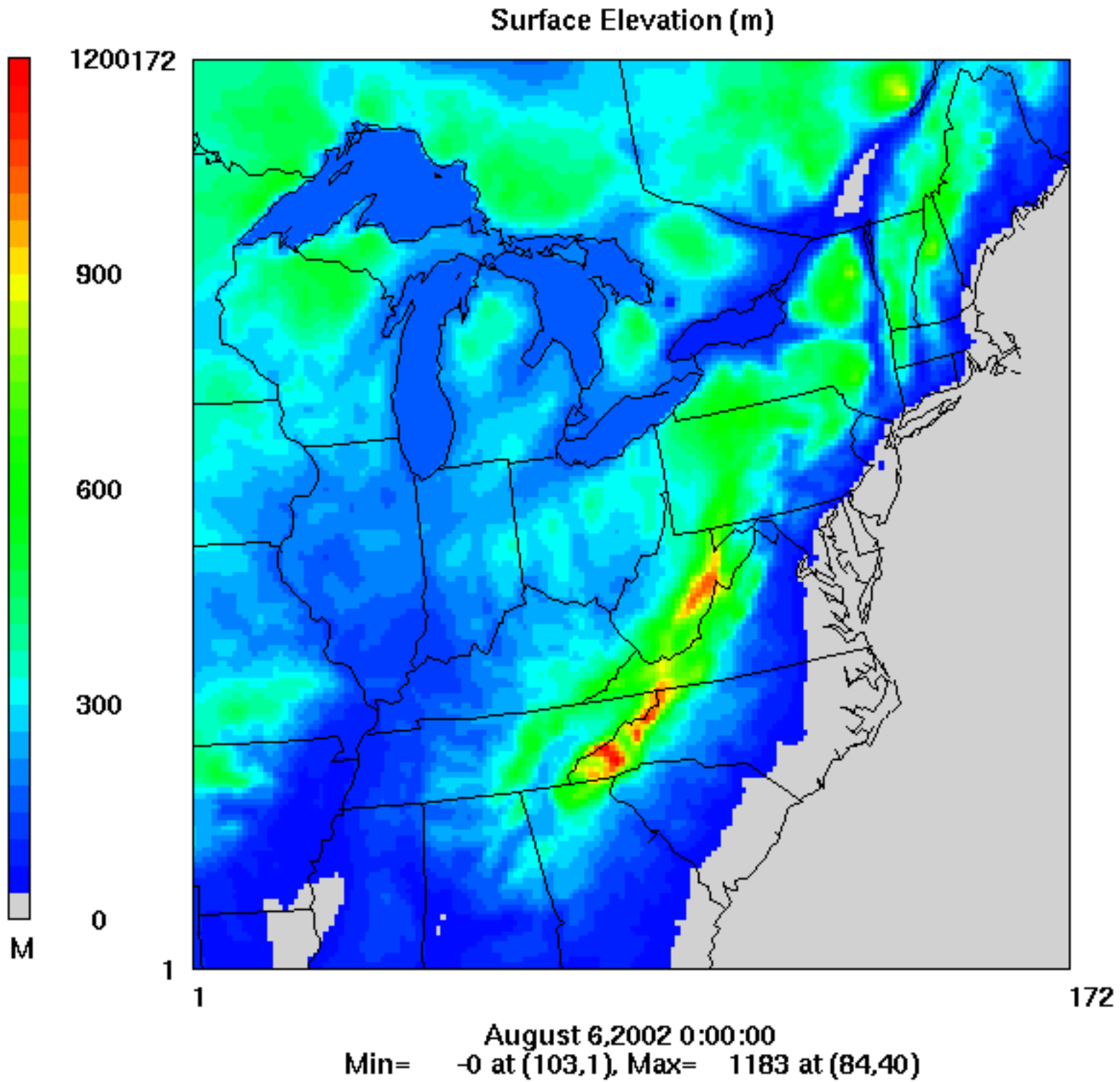

Appendix D
Diagnostic and Sensitivity Tests for 12-km and 4-km Horizontal Grid Resolutions

8-Hour Ozone Modeling for the Washington, D.C. Area

Attainment Modeling Committee Meeting

August 22, 2005

Topics of Discussion

- Review of 2002 Base Case Modeling Results
  - Modeling Domains & Grid Resolution
  - MM5 Model Options
    - VISTAS versus UMD
  - Emissions Inventory Comparison (Pre-SMOKE)
    - VISTAS versus MANE-VU
  - CMAQ Model Performance Evaluation
    - VADEQ 12-km & 4-km Resolutions
    - OTC 12-km Resolution
  - Summary and Conclusions

2002 Base Case Modeling Runs

Modeling Center	Grid Resolutions (km)	Meteorology (MM5)	Emissions Inventory
VADEQ	36, 12 & 4	VISTAS	VISTAS
OTC	36 & 12	UMD	MANE-VU

VADEQ Modeling Domain

- Portion of VISTAS domain
- 36 km course grid
- 12 km interim grid **(in Yellow)**
- 4 km fine grid **(in Red)**

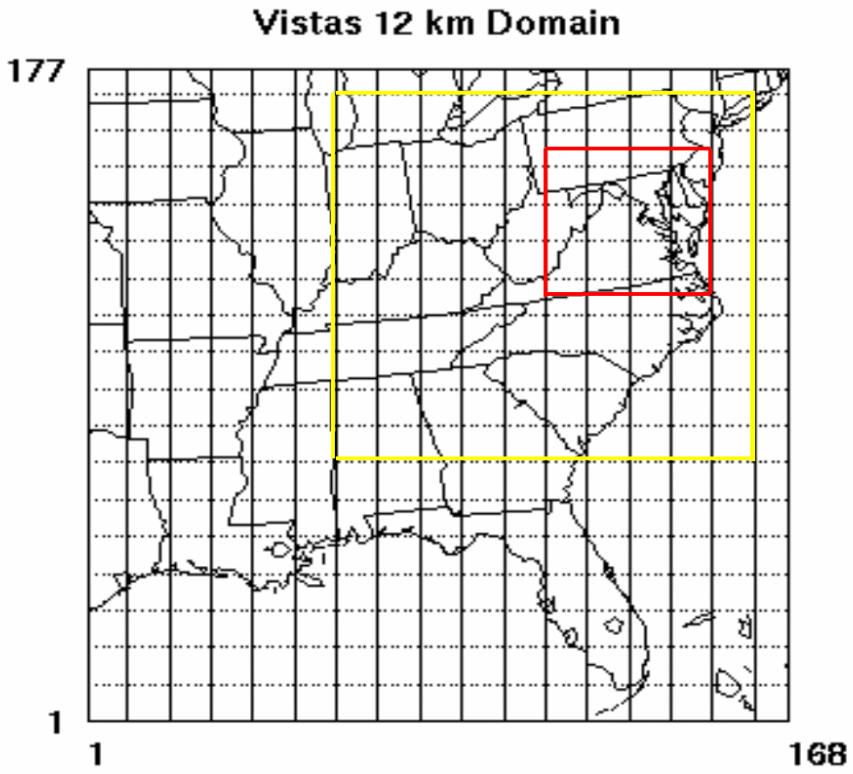

OTC Modeling Domain

- 36 km course grid
- 12 km fine grid

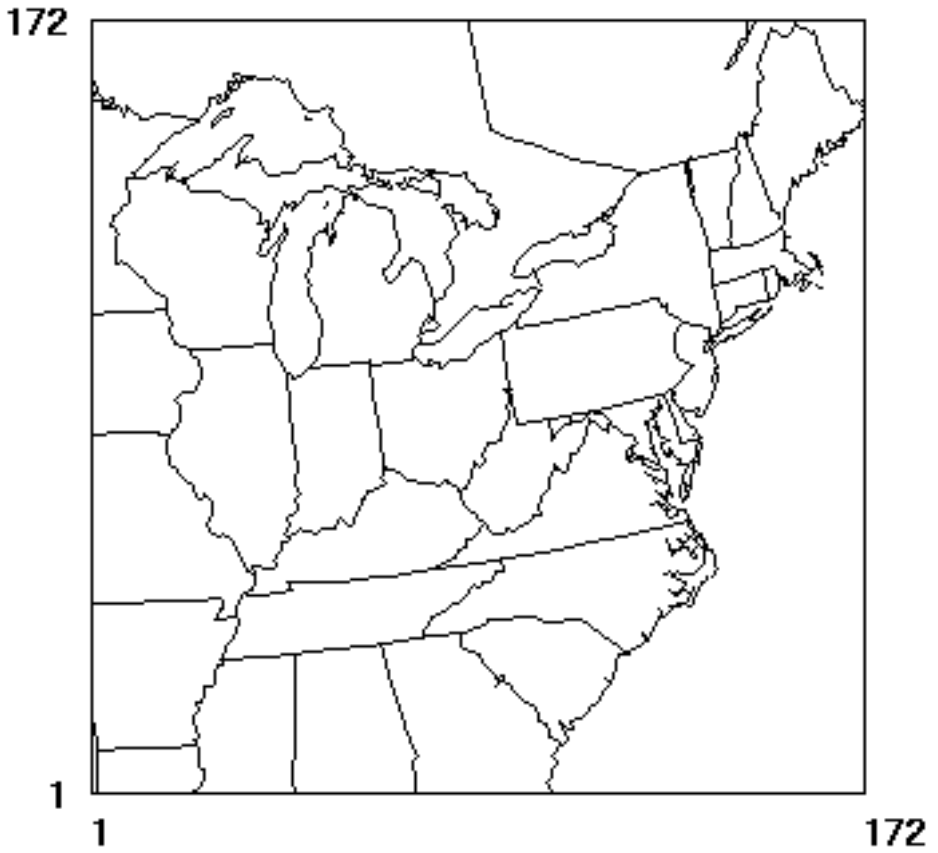

VISTAS & UMD MM5 Configurations

MODEL OPTIONS	VADEQ	OTC
Number of Vertical Layers	34 (Layer 1 ~38 meters)	34 (Layer 1 ~29 meters)
Soil/Land Surface Model	Pleim-Xiu	Five-Layer Soil model
PBL Scheme	Asymmetric Convective Mixing	Modified Blackadar PBL scheme (Zhang)
Radiation	Rapid Radiative Transfer Model (RRTM)	Simple cooling
Clouds	Kain-Fritsch 2 cumulus parameterization	Kain-Fritsch cumulus parameterization
Microphysics	Reisner 1 (mixed phase)	Simple Ice
Sea Surface Temperatures	EDAS 24-hr averaged skin temperatures	EDAS 24-hr averaged skin temperatures

MANE-VU & VISTAS Emissions Inventories (MANE-VU – Yellow, VISTAS - Peach)

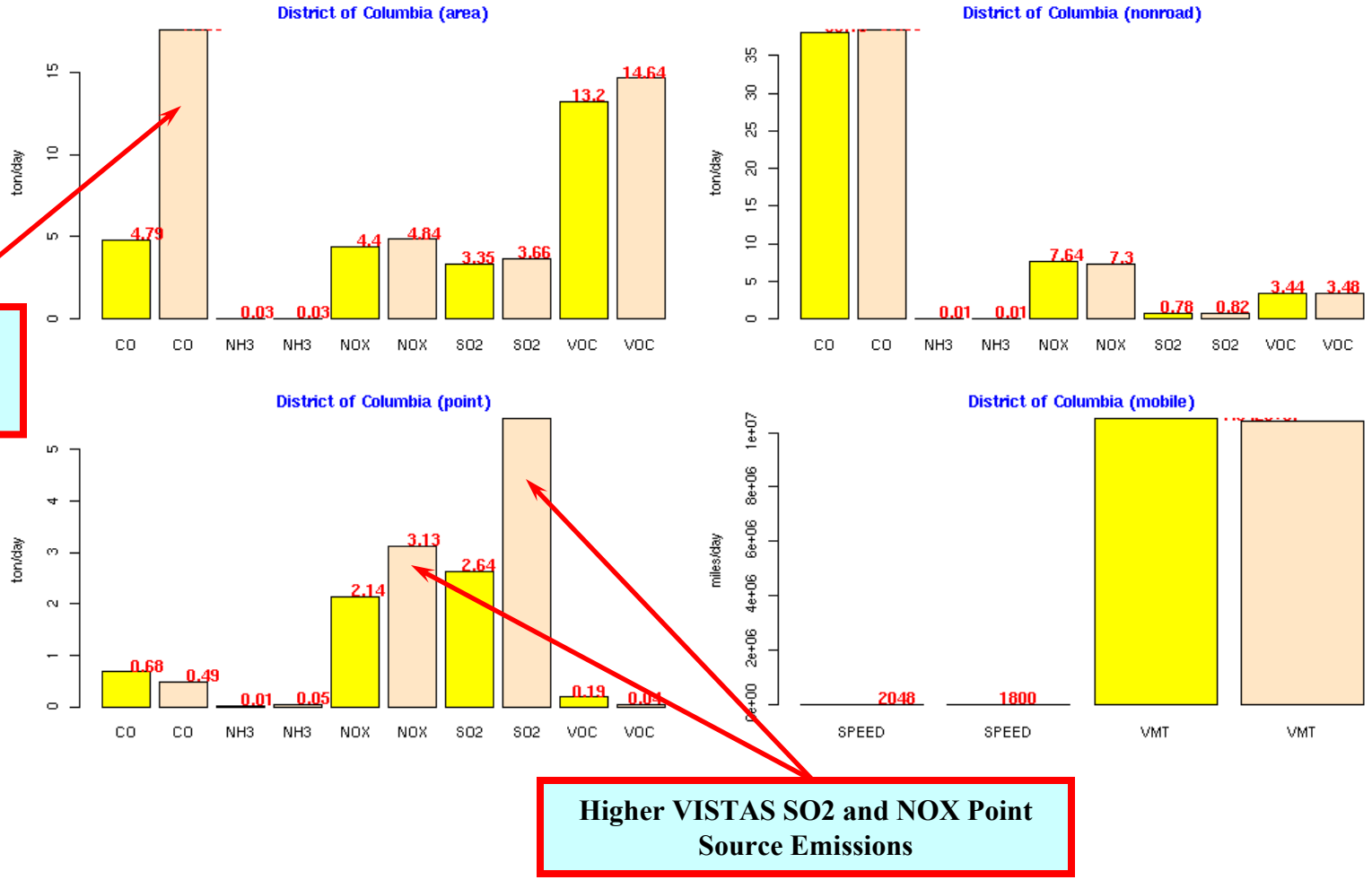

Higher VISTAS CO Area Source Emissions

Higher VISTAS SO2 and NOX Point Source Emissions

MANE-VU & VISTAS Emissions Inventories (MANE-VU – Yellow, VISTAS - Peach)

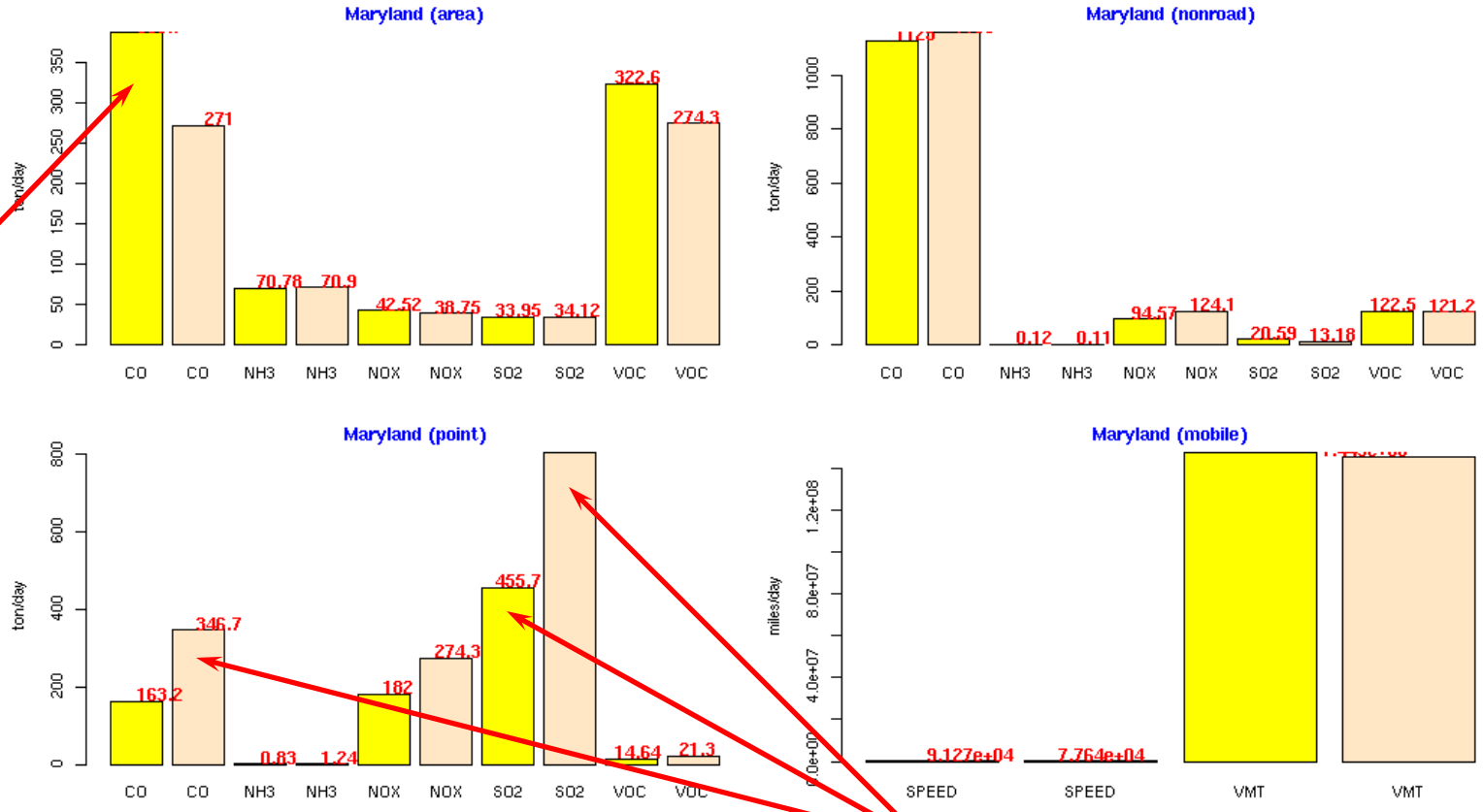

Higher OTC CO Area Source Emissions

Higher VISTAS CO, SO2 and NOX Point Source Emissions

MANE-VU & VISTAS Emissions Inventories (MANE-VU – Yellow, VISTAS - Peach)

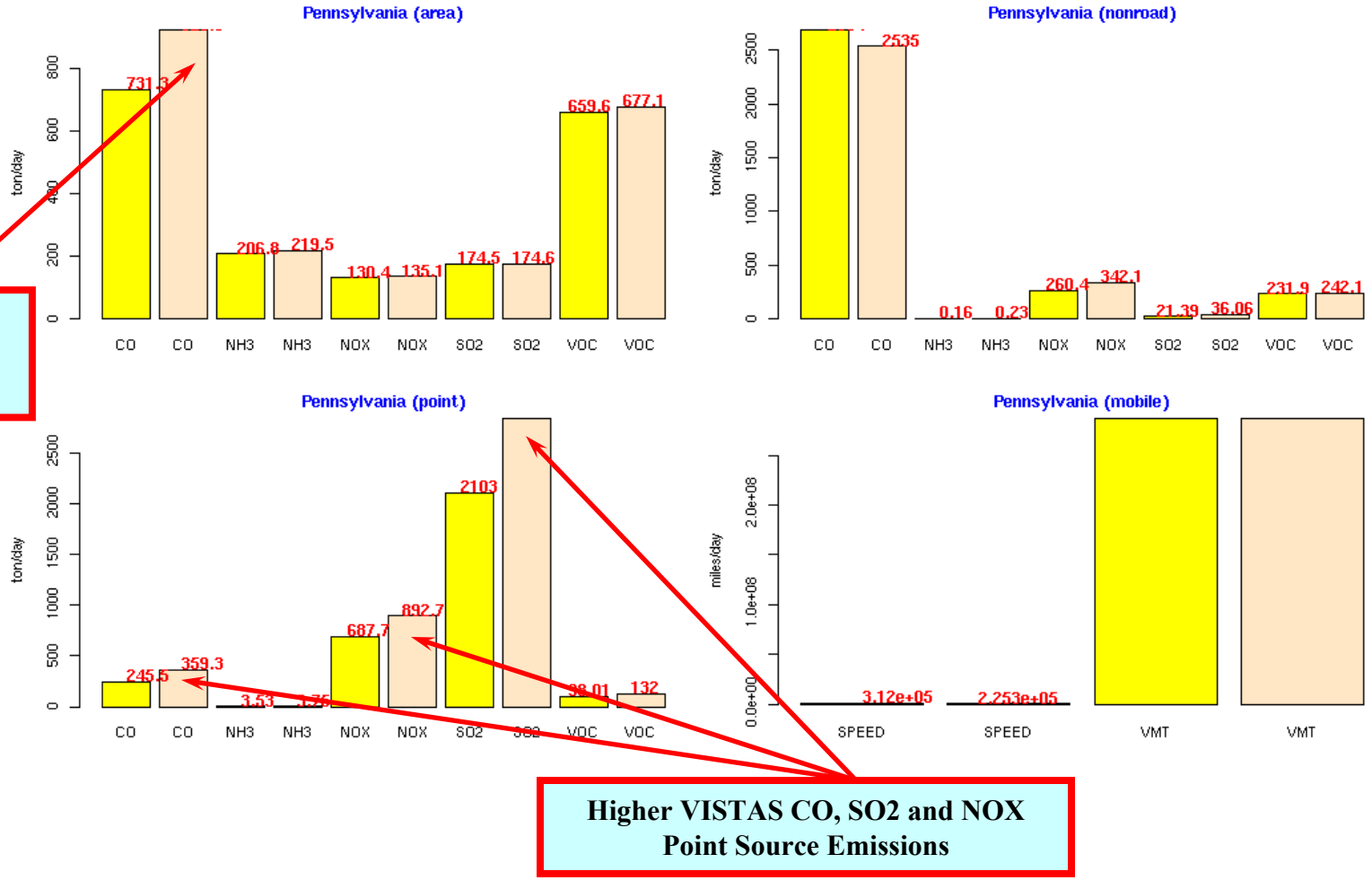

Higher VISTAS CO Area Source Emissions

Higher VISTAS CO, SO2 and NOX Point Source Emissions

MANE-VU & VISTAS Emissions Inventories (MANE-VU – Yellow, VISTAS - Peach)

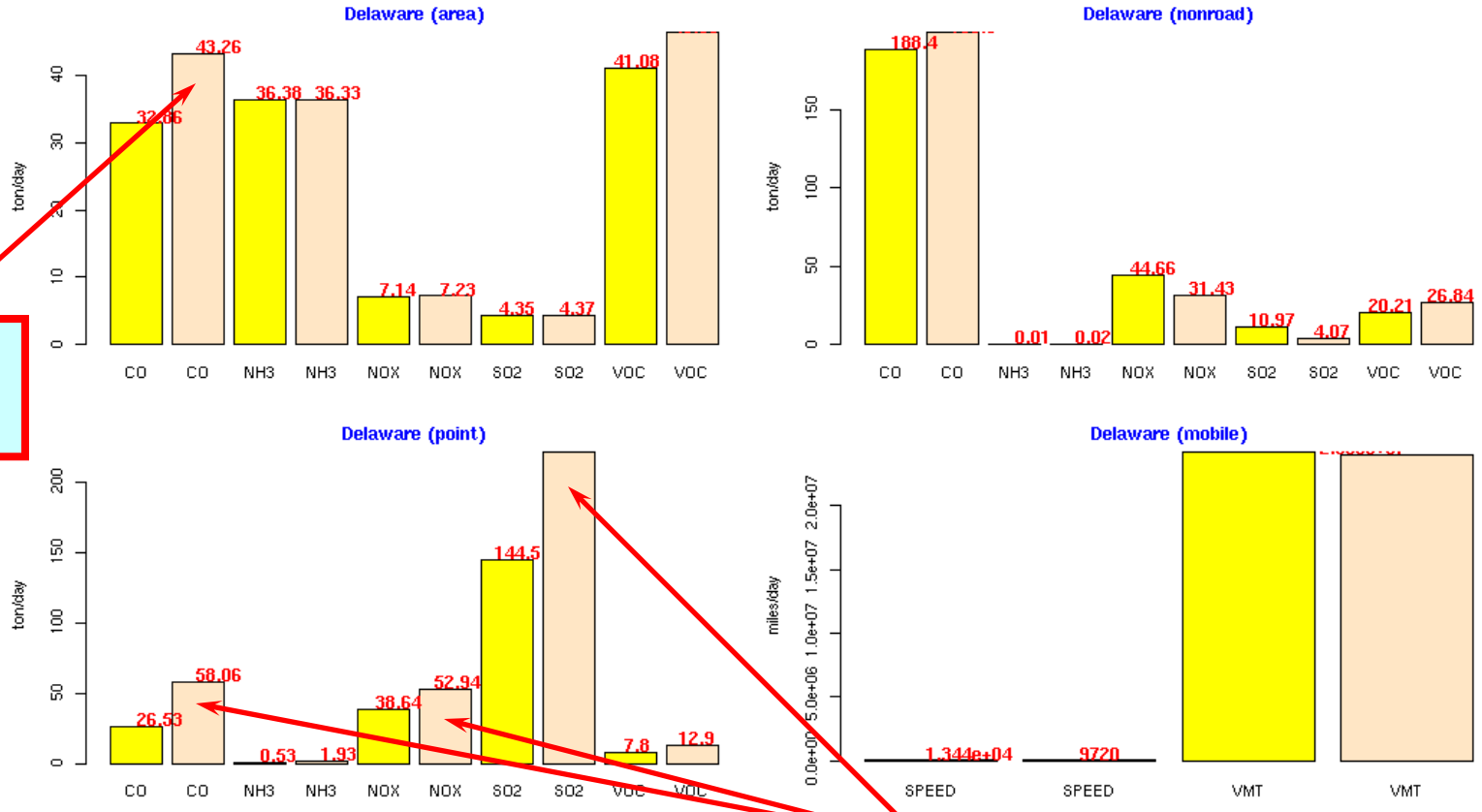

Higher VISTAS CO Area Source Emissions

Higher VISTAS CO, SO2 and NOX Point Source Emissions

MANE-VU & VISTAS Emissions Inventories (MANE-VU – Yellow, VISTAS - Peach)

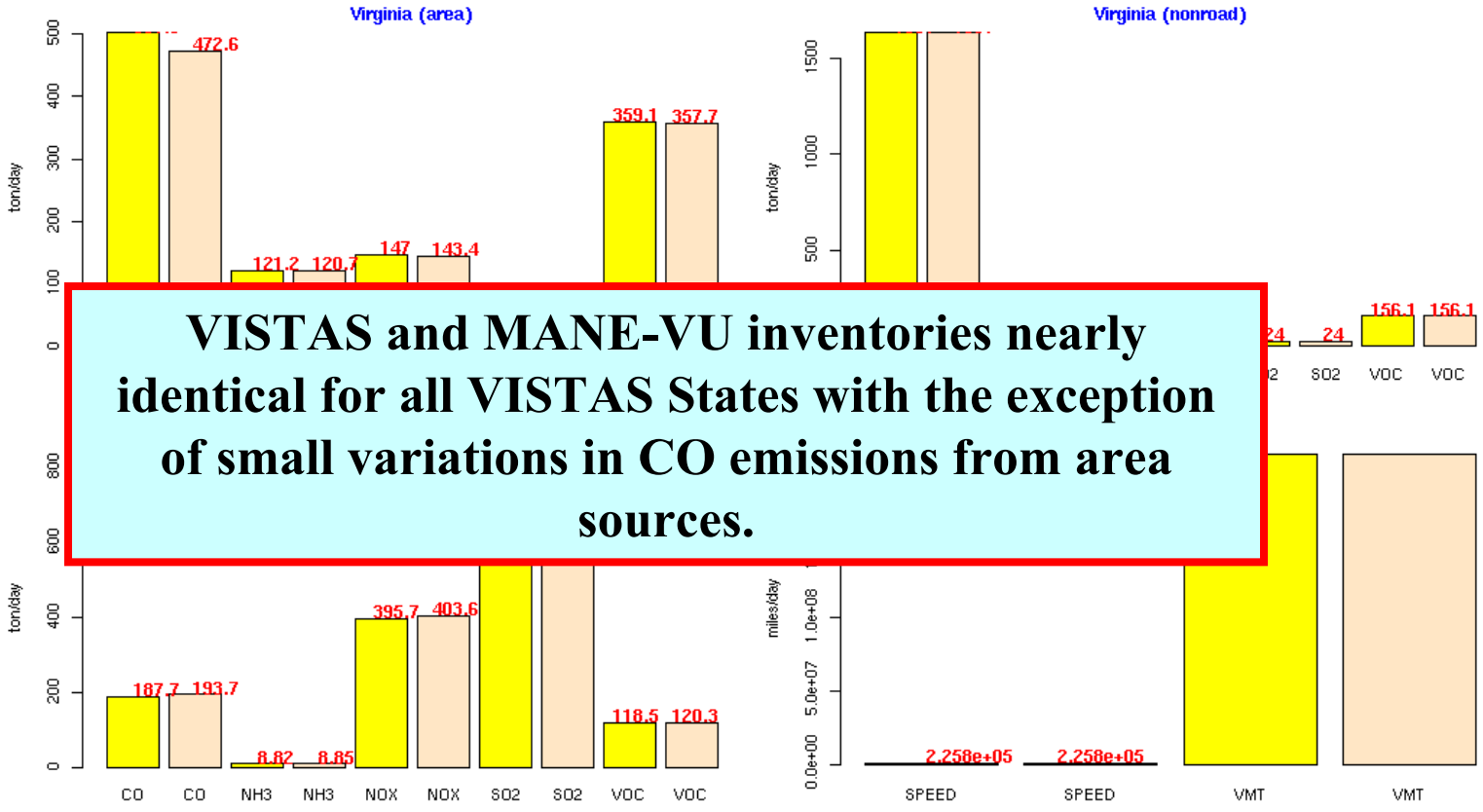

VISTAS and MANE-VU inventories nearly identical for all VISTAS States with the exception of small variations in CO emissions from area sources.

MANE-VU & VISTAS Emissions Inventories (MANE-VU – Yellow, VISTAS - Peach)

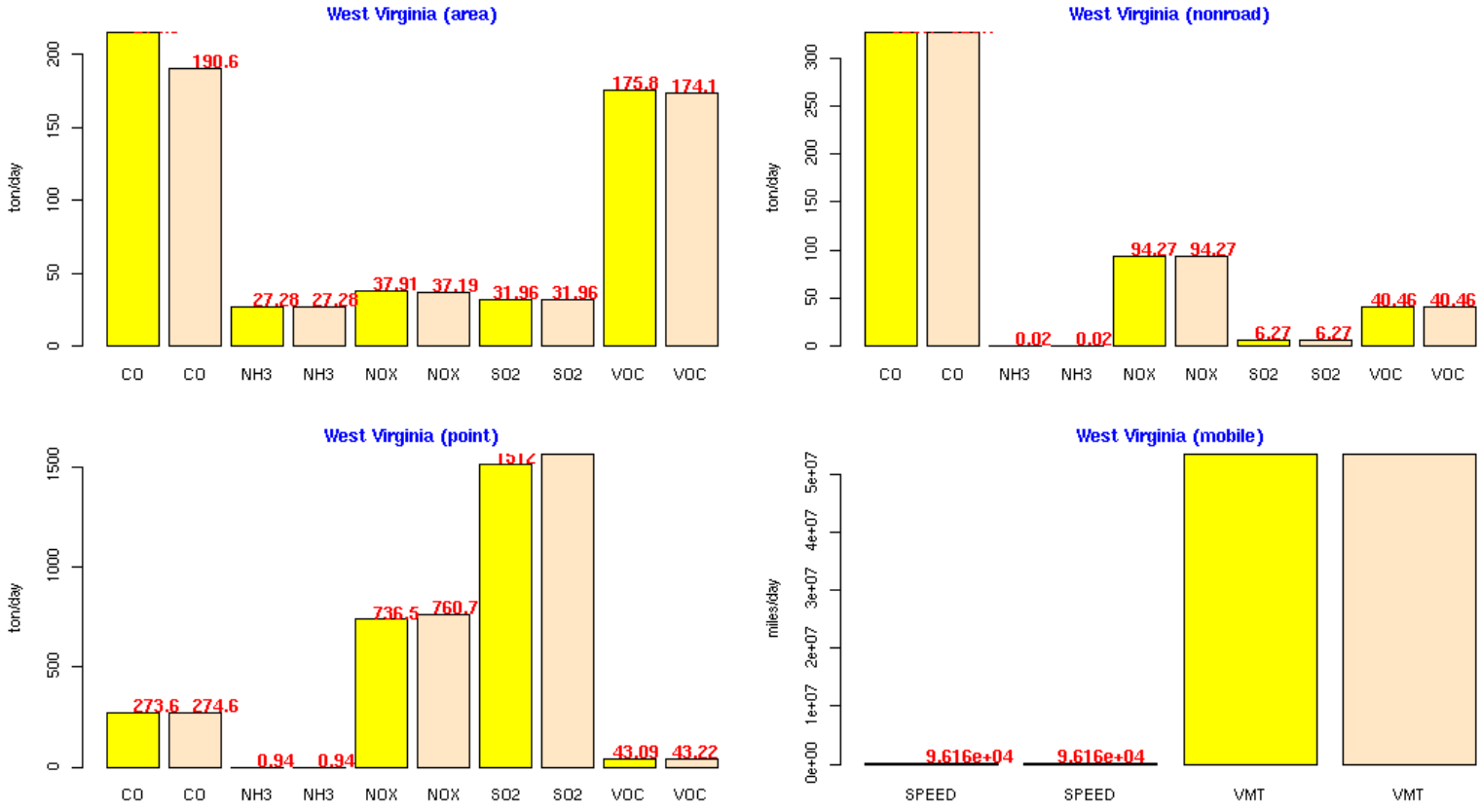

MANE-VU & VISTAS Emissions Inventories (MANE-VU – Yellow, VISTAS - Peach)

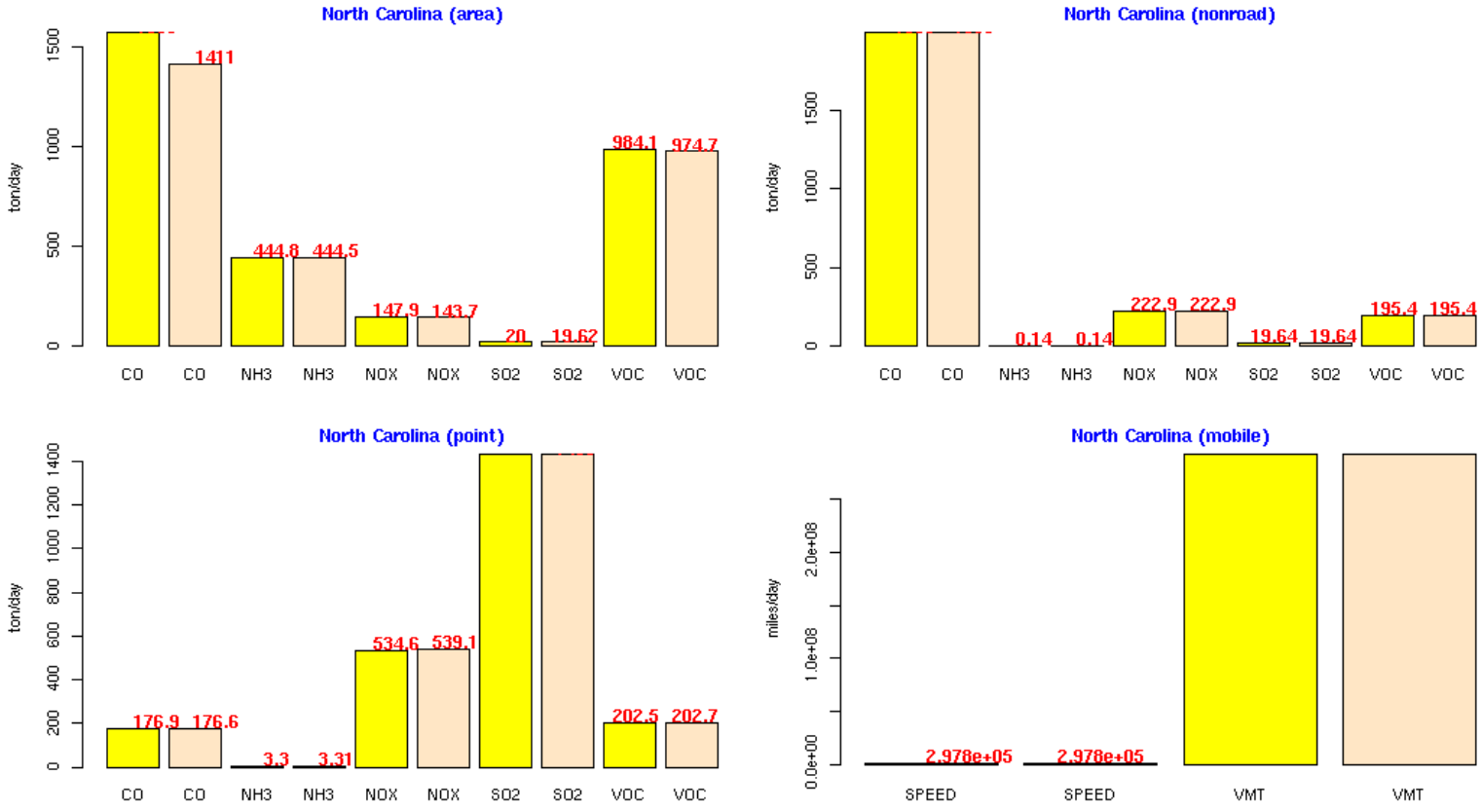

MANE-VU & VISTAS Emissions Inventories

- Conclusions
  - Inventories nearly identical for all VISTAS States
  - Inventory differences for several MANE-VU States
    - CO, NOx and SO2 point source emissions used by VISTAS (2002 NEI) generally higher than MANE-VU
    - CO area source emissions
  - Updated RPO inventories due this Fall
    - Revisions should eliminate major differences

VADEQ & OTC CMAQ Model Performance

- 2002 Ozone Episode Periods
  - June 6 - July 5
    - Includes all 5 Synoptic Patterns from Environ Report
  - July 27 - August 16
    - Includes all 5 Synoptic Patterns from Environ Report
  - September 5 – 12
    - Includes Synoptic Patterns 3 & 4 from Environ Report
- VADEQ CMAQ modeling based on VISTAS platform.

VADEQ CMAQ Model Performance
June 11, 2002
(12-km Versus 4-km Resolution)

12-km run does better job than 4-km run at capturing magnitude of peak ozone concentrations in I-95 corridor and Richmond.

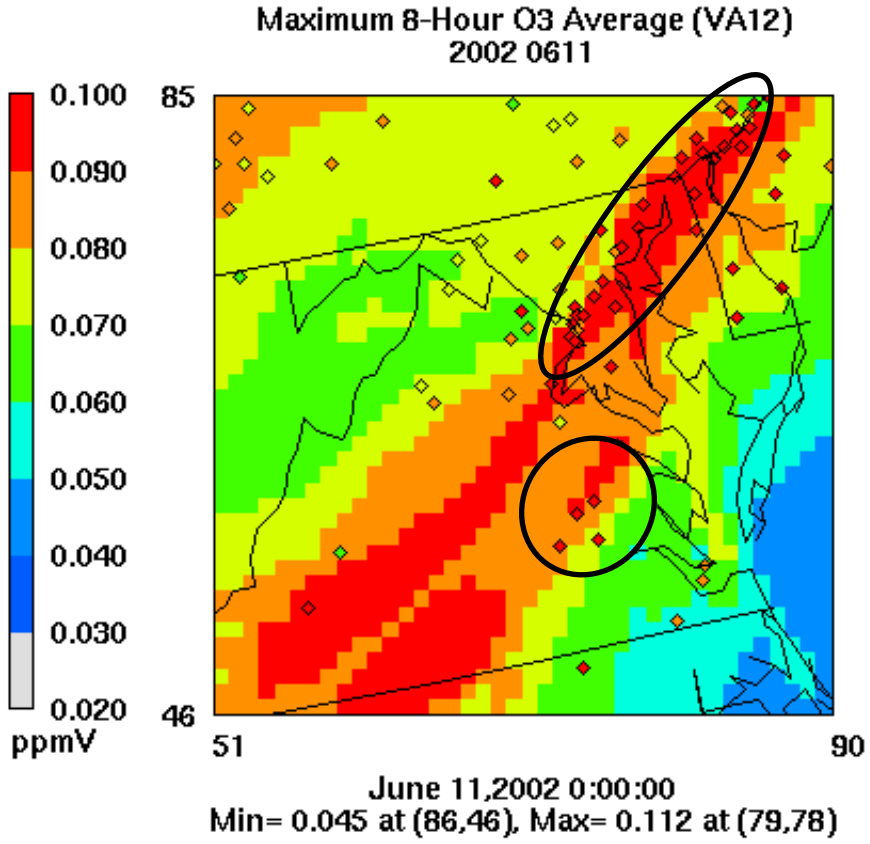

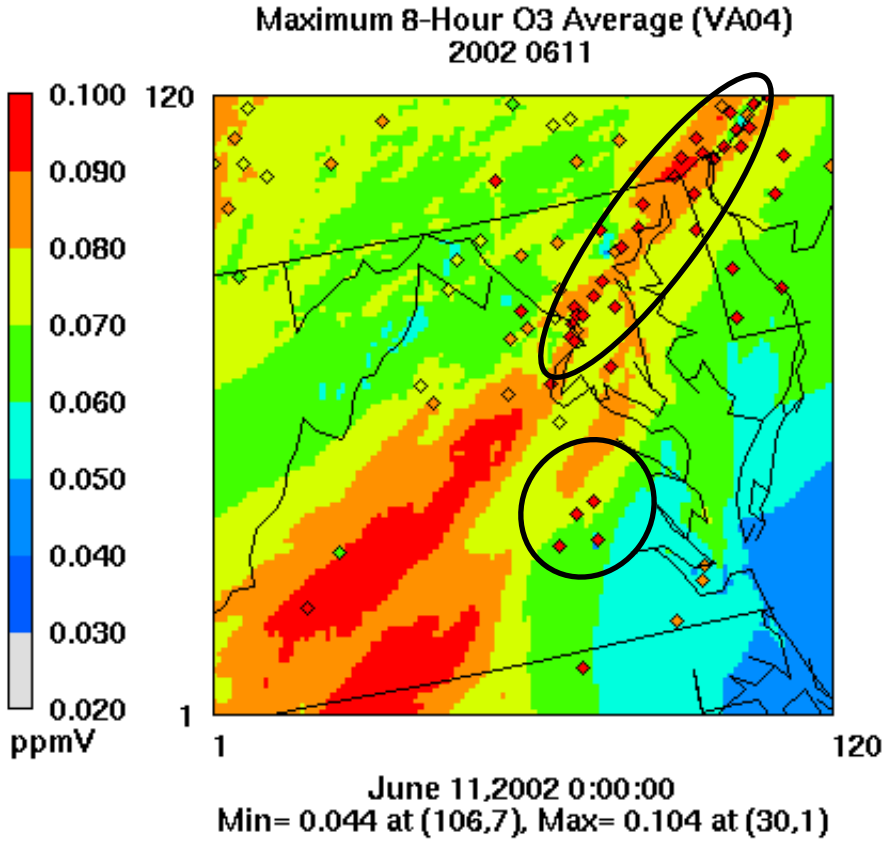

VADEQ CMAQ Model Performance
June 11, 2002
(12-km Versus 4-km Resolution)
(Predicted O3 – Observed O3)

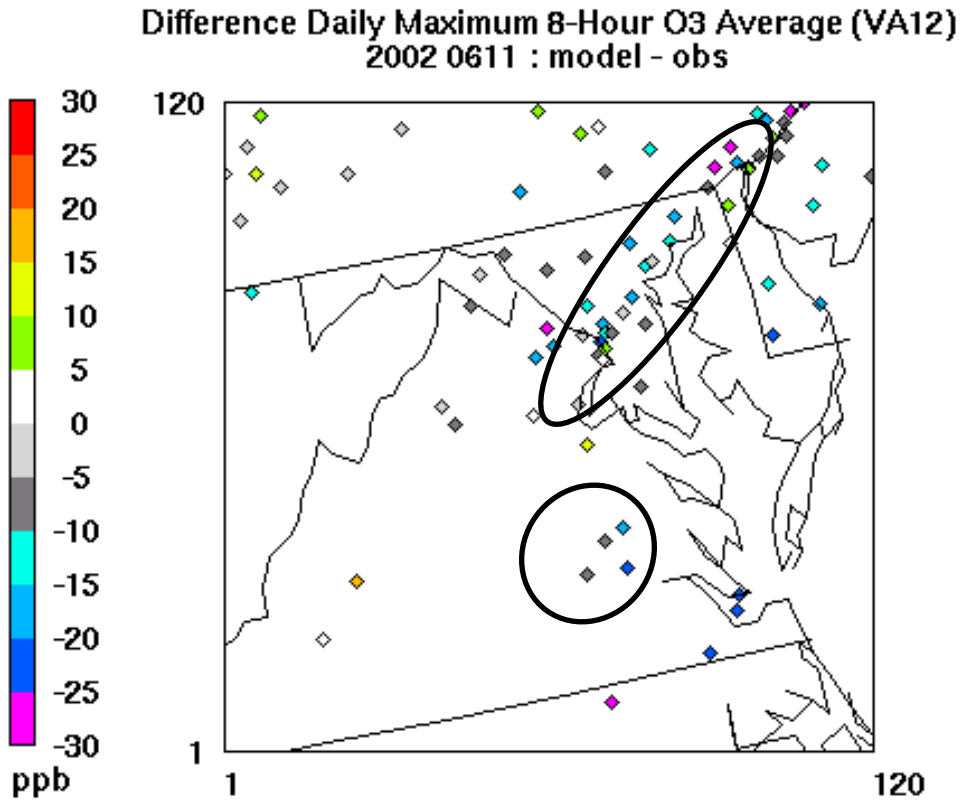

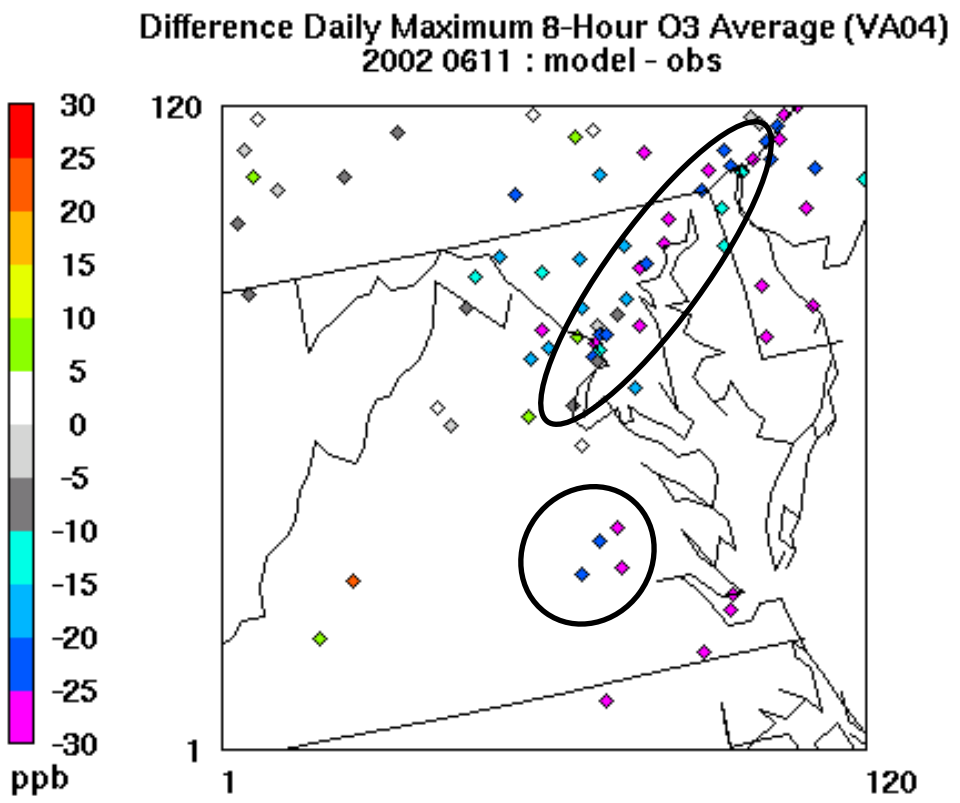

VADEQ CMAQ Model Performance
June 25, 2002
(12-km Versus 4-km Resolution)

12-km run does slightly better job at capturing magnitude of peak ozone concentrations in D.C. and Maryland.

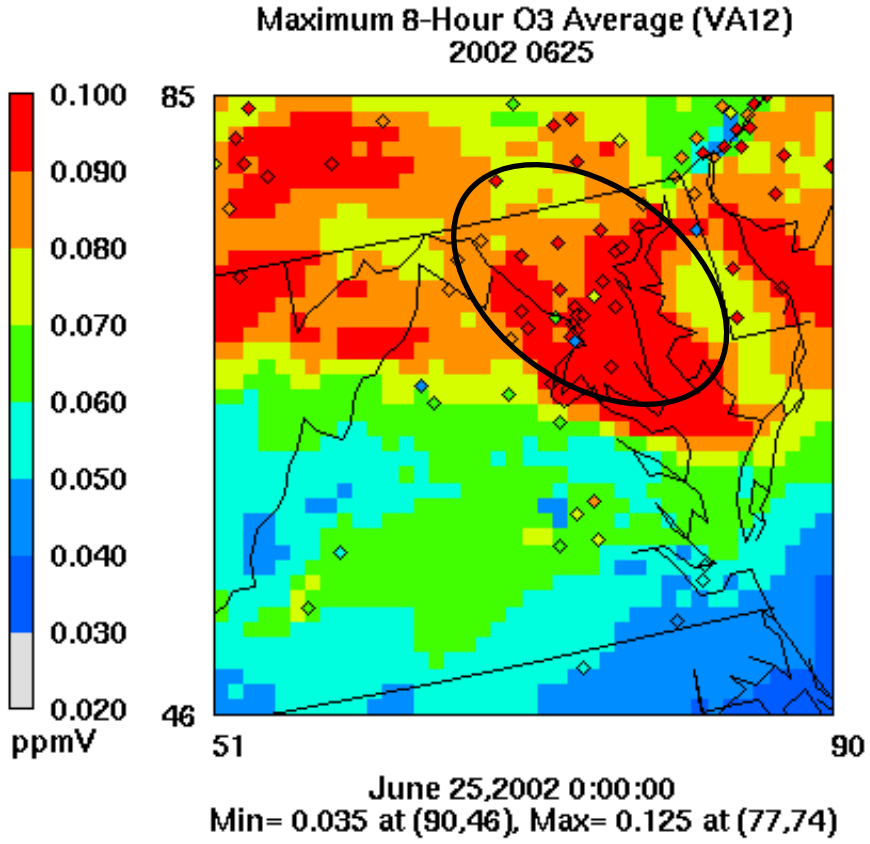

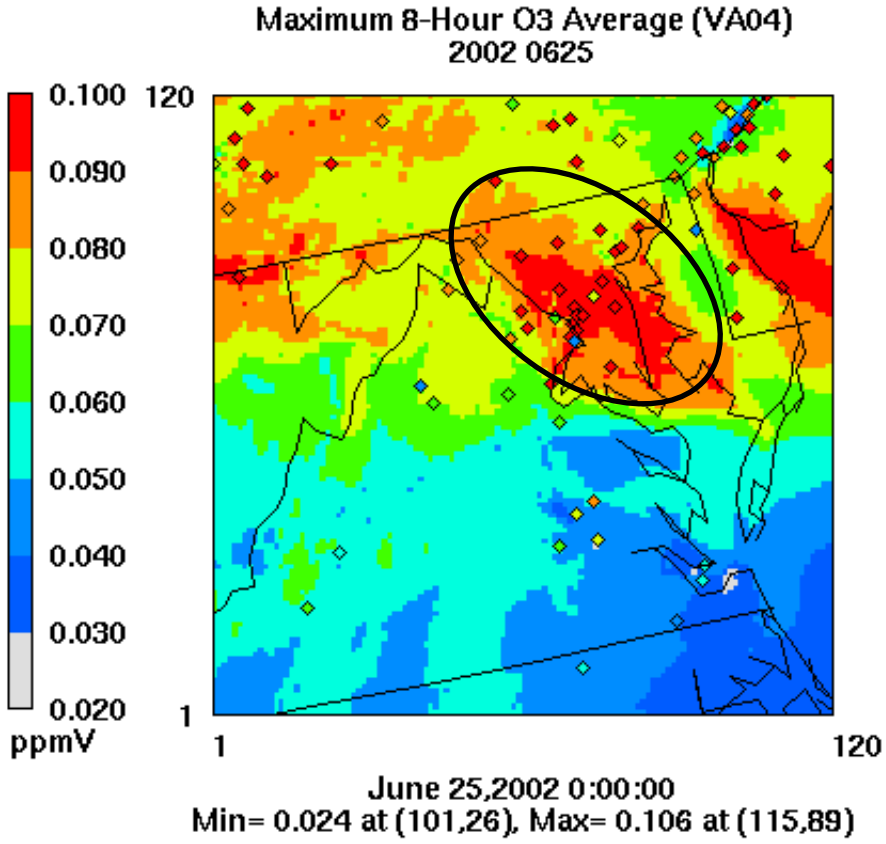

VADEQ CMAQ Model Performance
June 25, 2002
(12-km Versus 4-km Resolution)
(Model Predicted O3 – Observed O3)

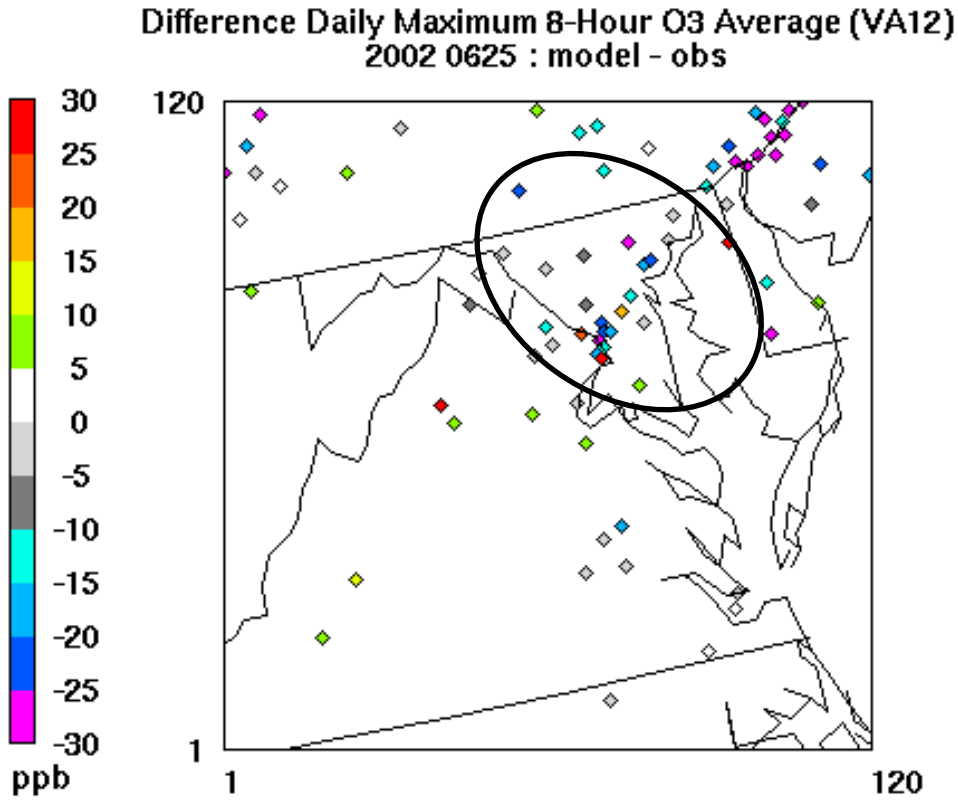

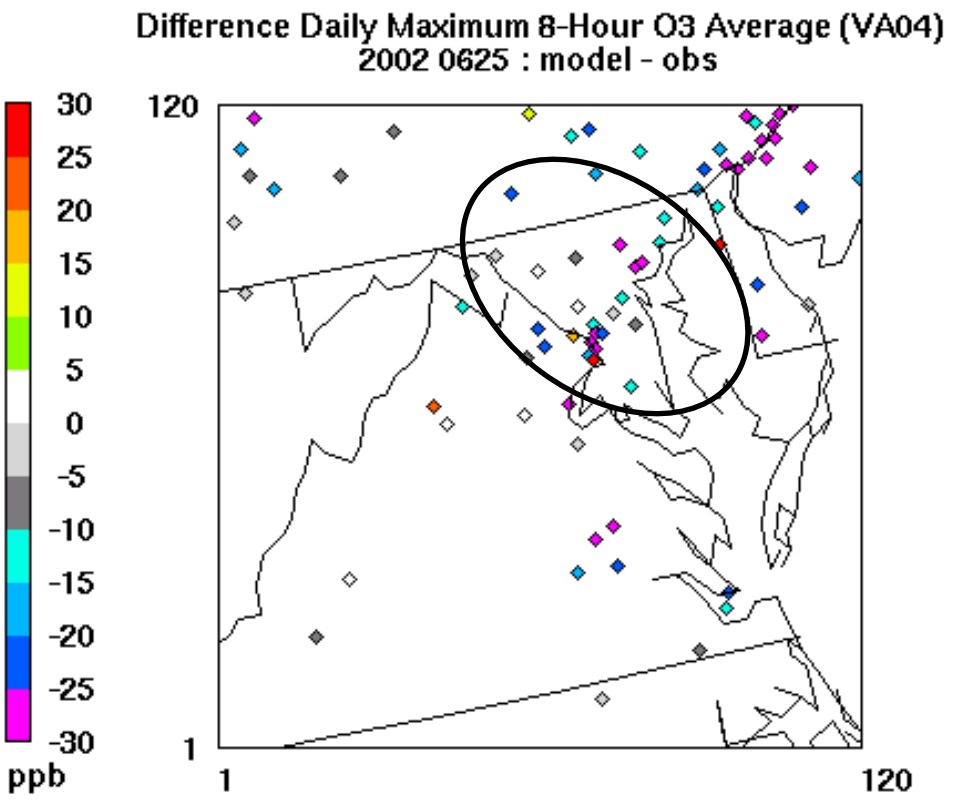

VADEQ CMAQ Model Performance
July 2, 2002
(12-km Versus 4-km Resolution)

12-km run performs slightly better than 4-km run in I-95 corridor. Poorer performance for both runs in Delaware and southeast NJ.

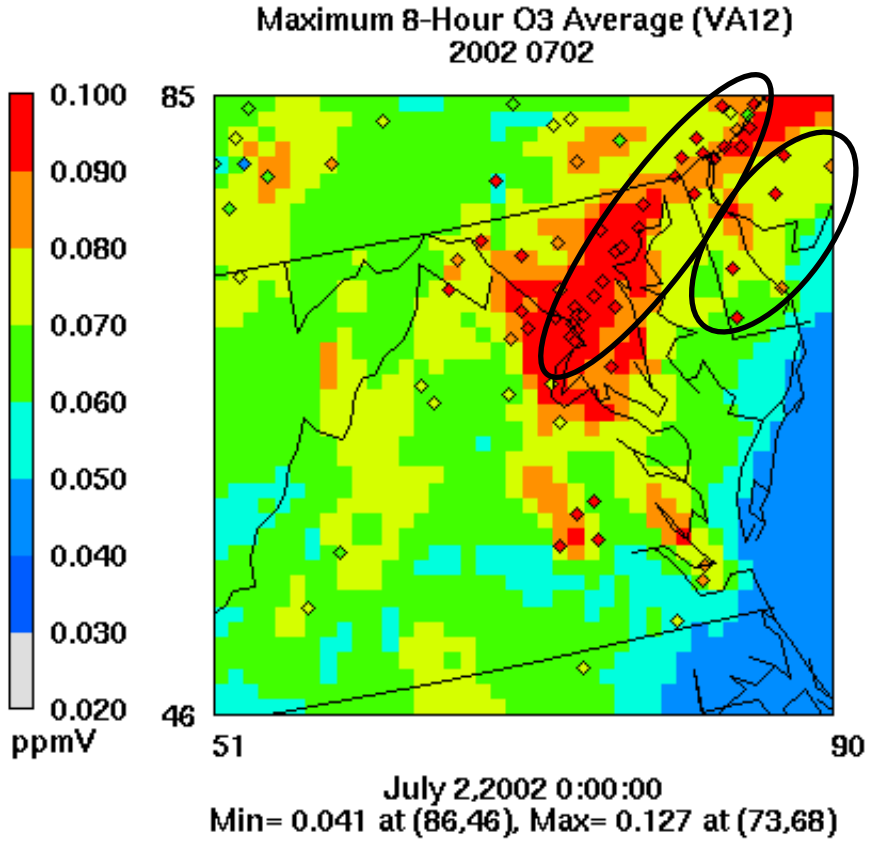

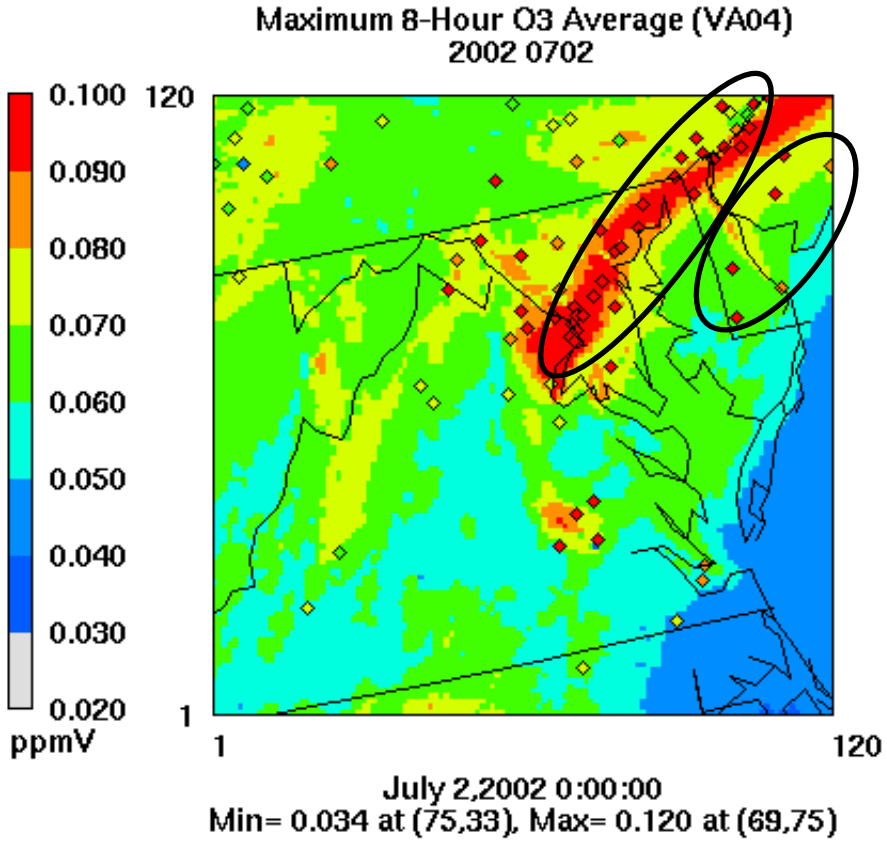

VADEQ CMAQ Model Performance
July 2, 2002
(12-km Versus 4-km Resolution)
(Model Predicted O3 – Observed O3)

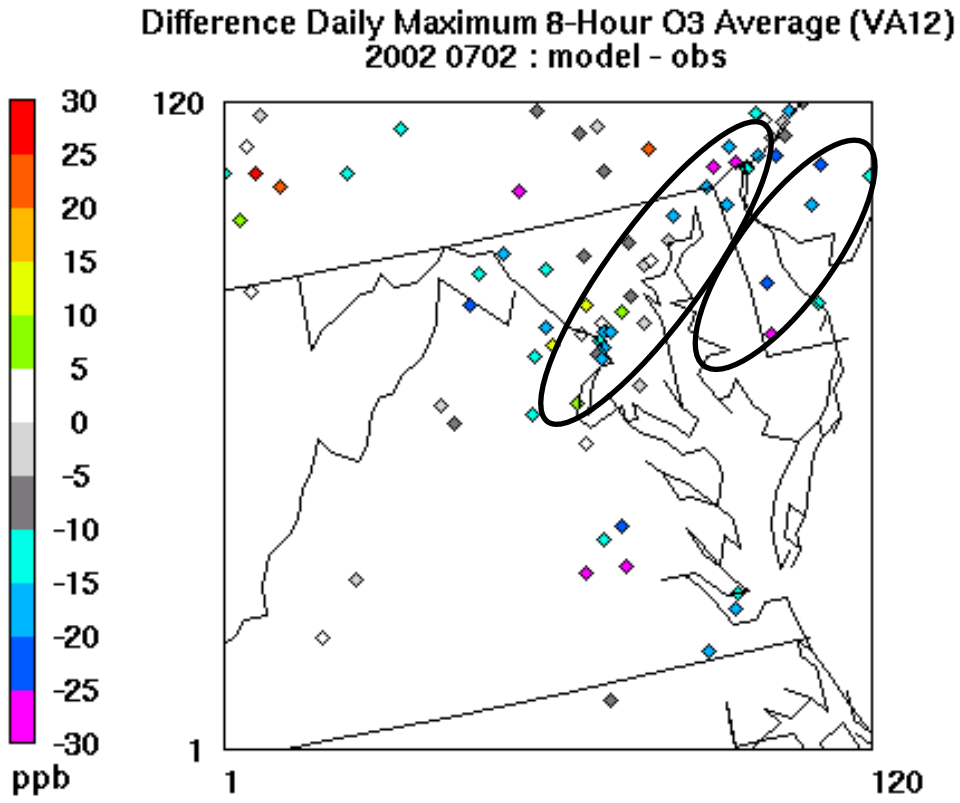

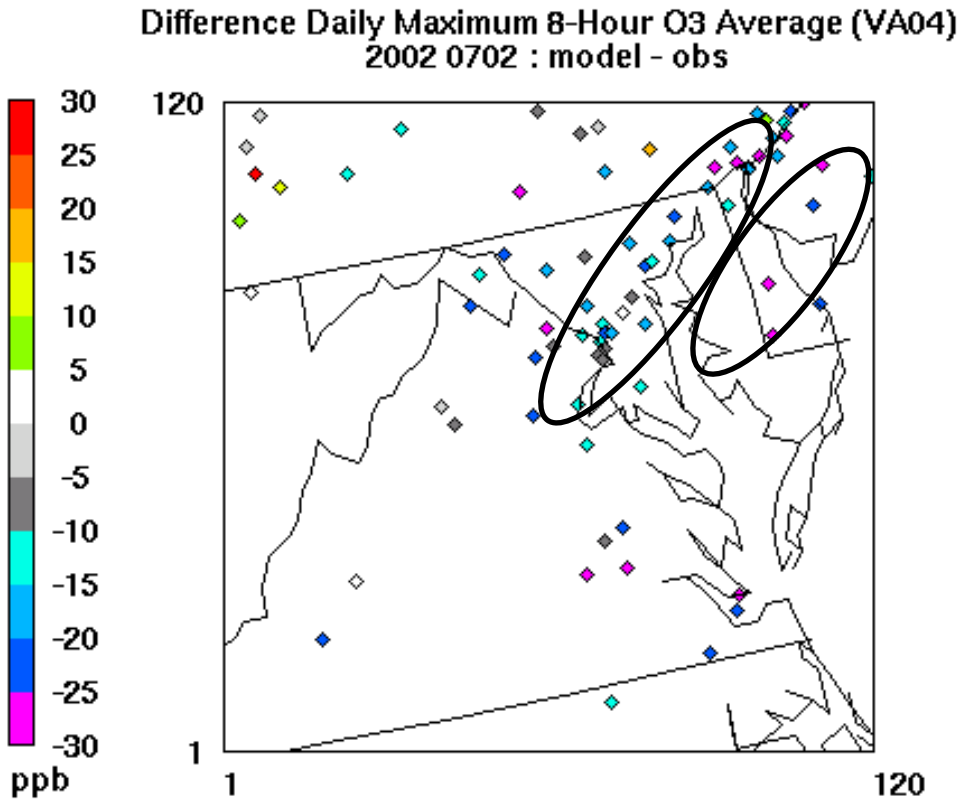

VADEQ CMAQ Model Performance
August 2, 2002
(12-km Versus 4-km Resolution)

Both 12-km and 4-km resolution runs completely fail domain-wide on this ozone episode day as a result of an error found in the JPROC preprocessor.

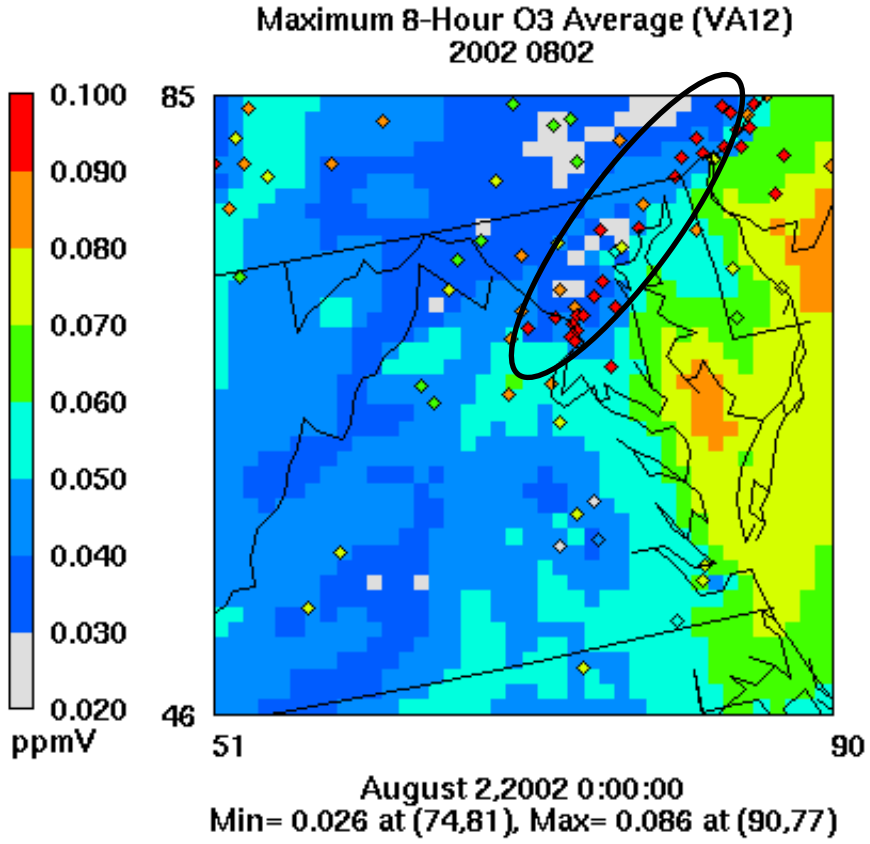

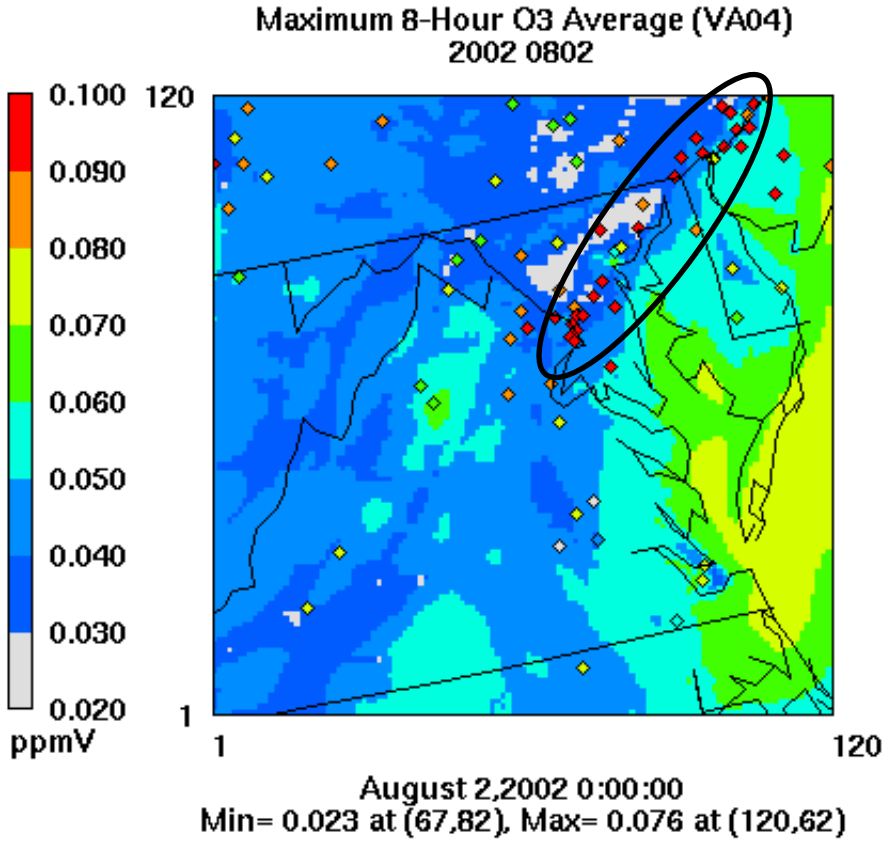

VADEQ CMAQ Model Performance
August 2, 2002
(12-km Versus 4-km Resolution)
(Model Predicted O3 – Observed O3)

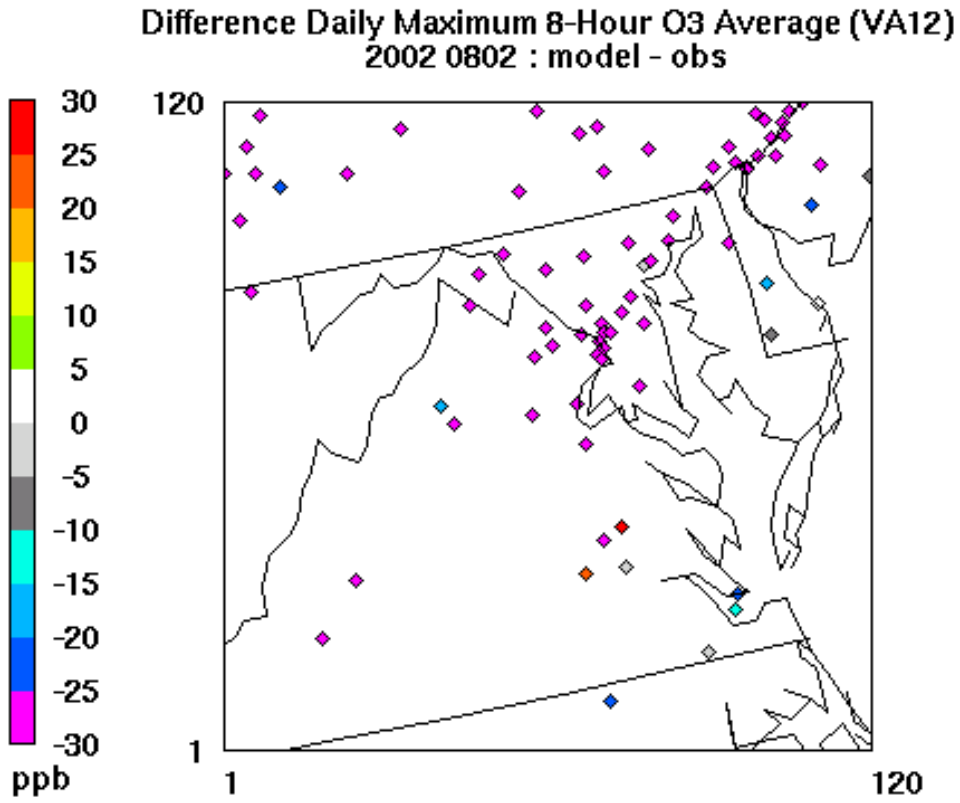

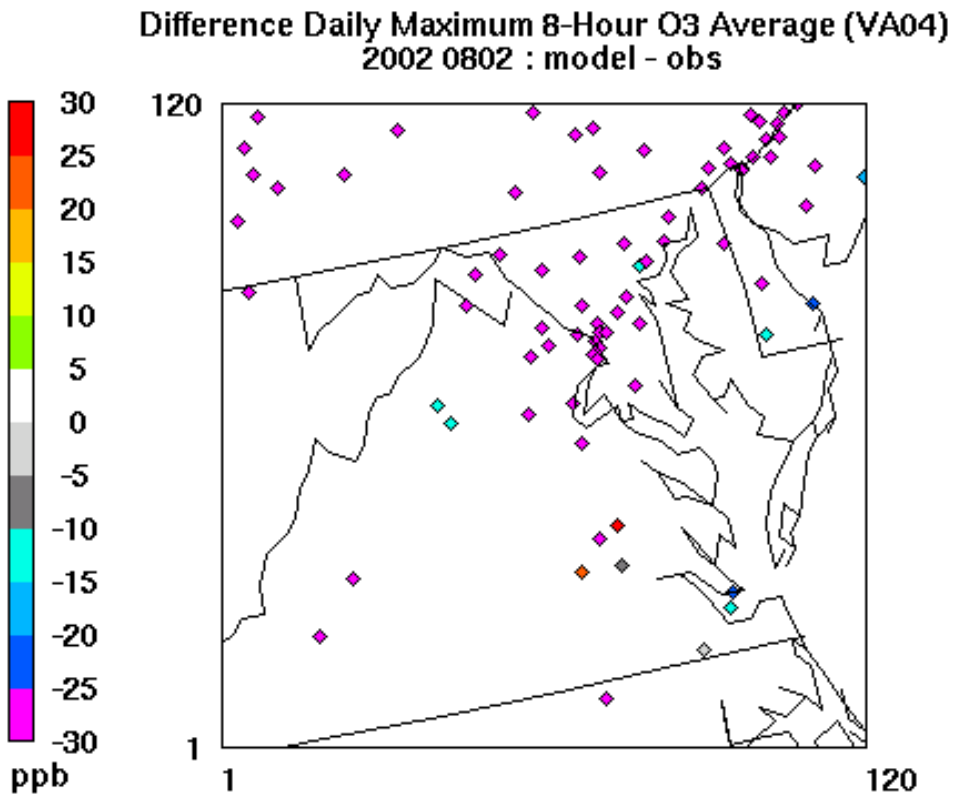

VADEQ CMAQ Model Performance
August 2, 2002
(Revised JPROC Values - 12-km Resolution)

VISTAS notified of JPROC issue and plans to correct issue with Base F modeling. VADEQ test run with revised JPROC values shows marked improvement in performance.

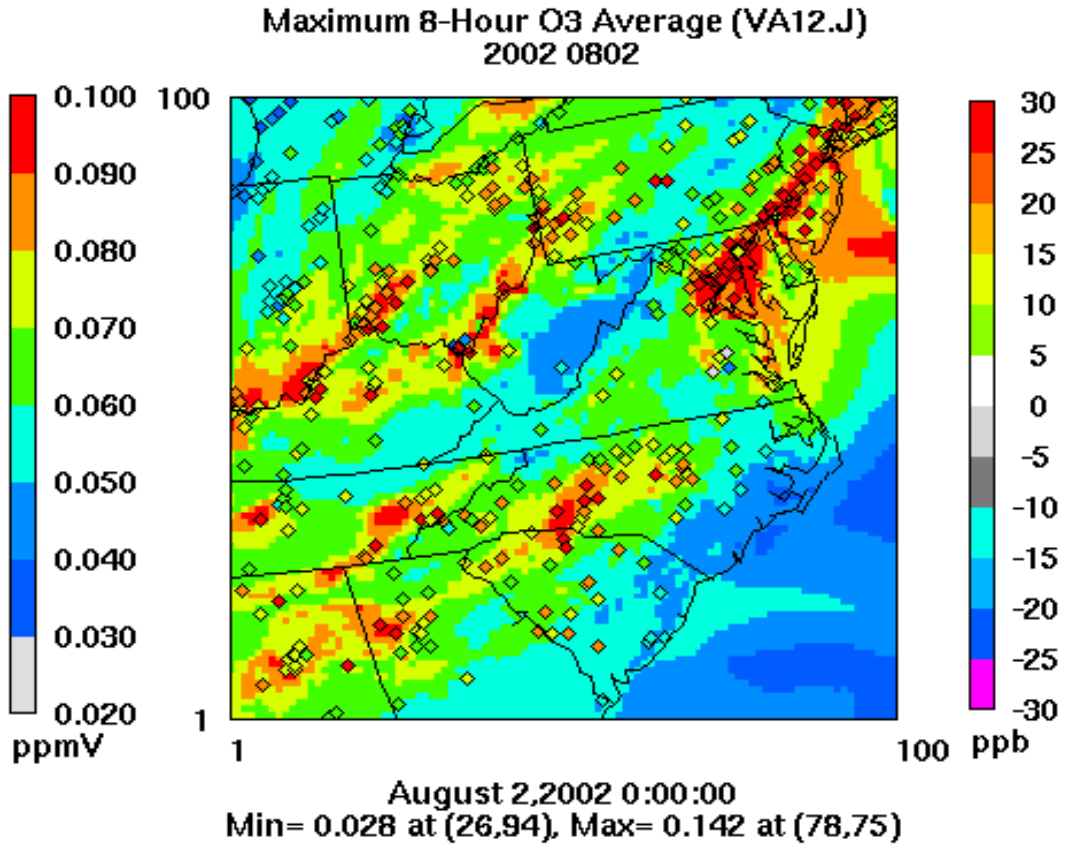

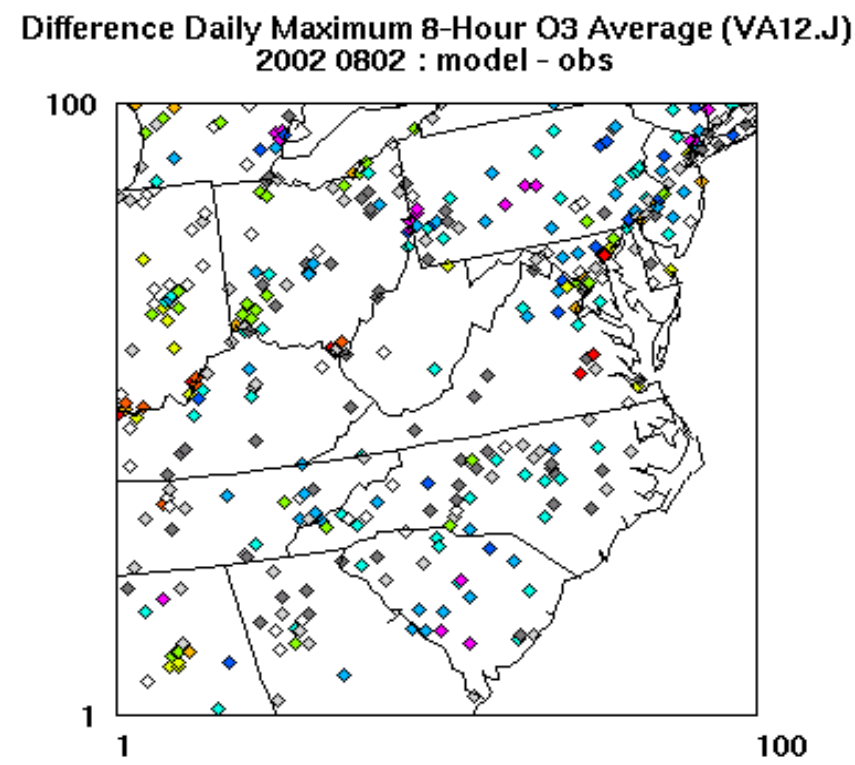

VADEQ CMAQ Model Performance
August 13, 2002
(12-km Versus 4-km Resolution)

12-km run does better job than 4-km run at capturing magnitude of peak ozone concentrations in I-95 corridor.

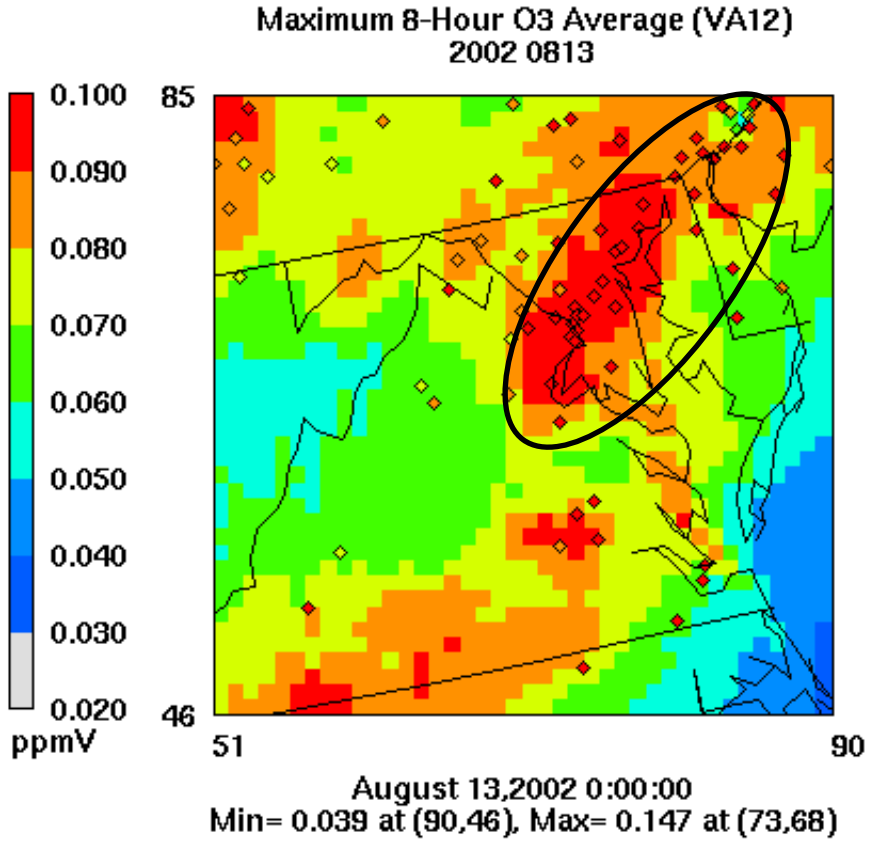

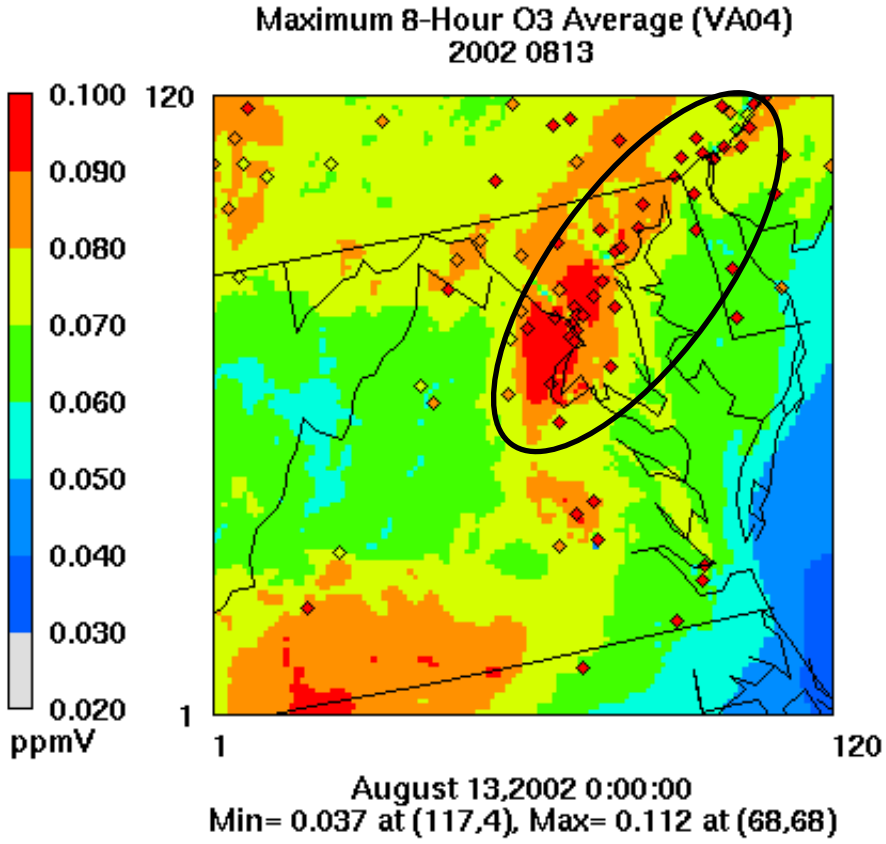

VADEQ CMAQ Model Performance
August 13, 2002
(12-km Versus 4-km Resolution)
(Model Predicted O3 – Observed O3)

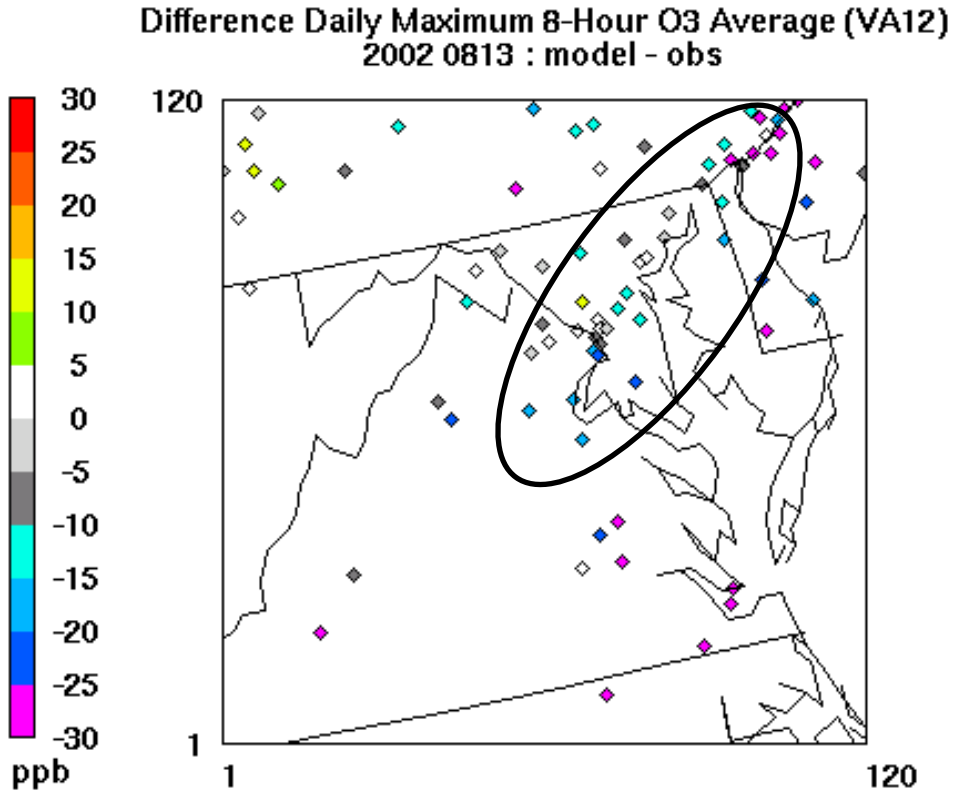

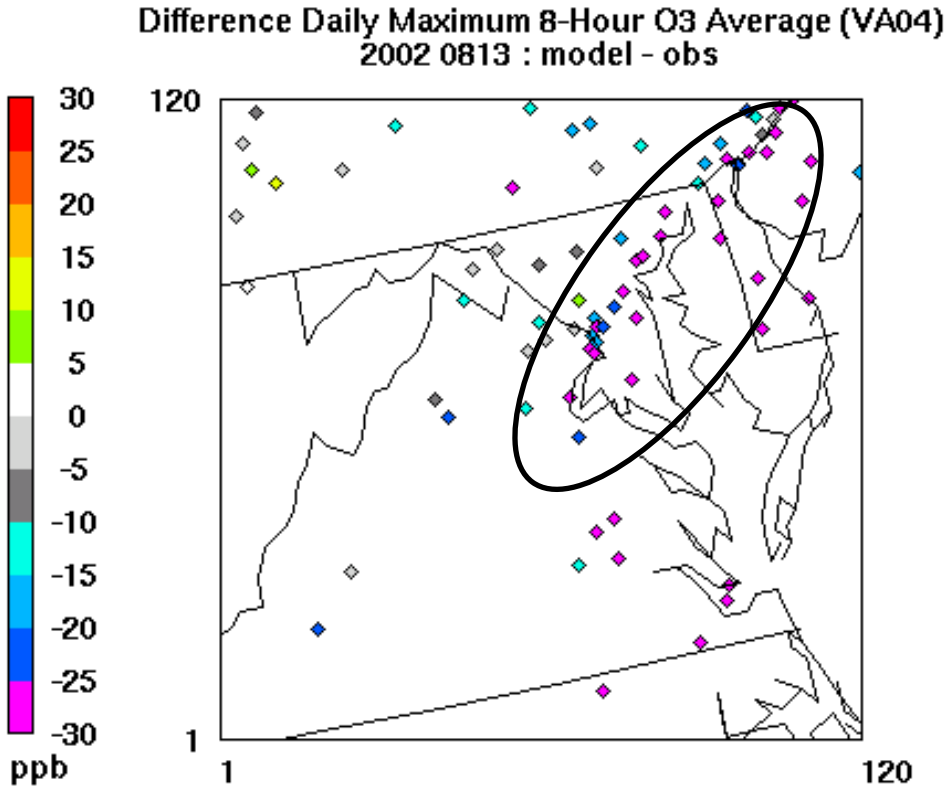

VADEQ CMAQ Model Performance
September 9, 2002
(12-km Versus 4-km Resolution)

Another example of a day with poor model performance for both runs. May also be the result of errors in the JPROC preprocessing.

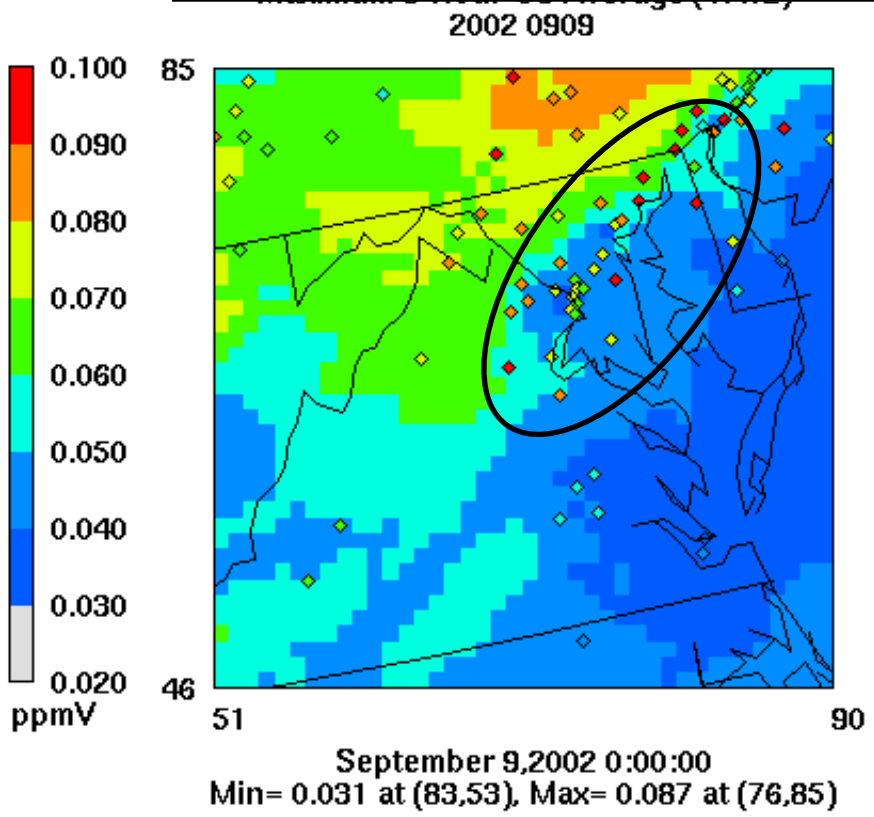

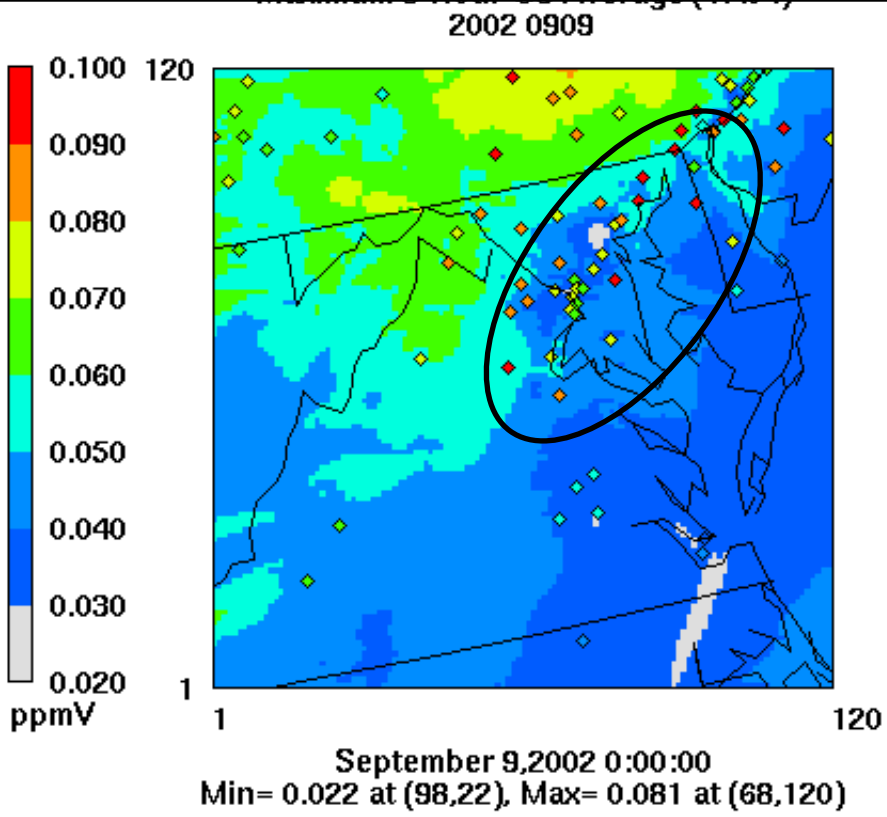

VADEQ CMAQ Model Performance
September 9, 2002
(12-km Versus 4-km Resolution)
(Model Predicted O3 – Observed O3)

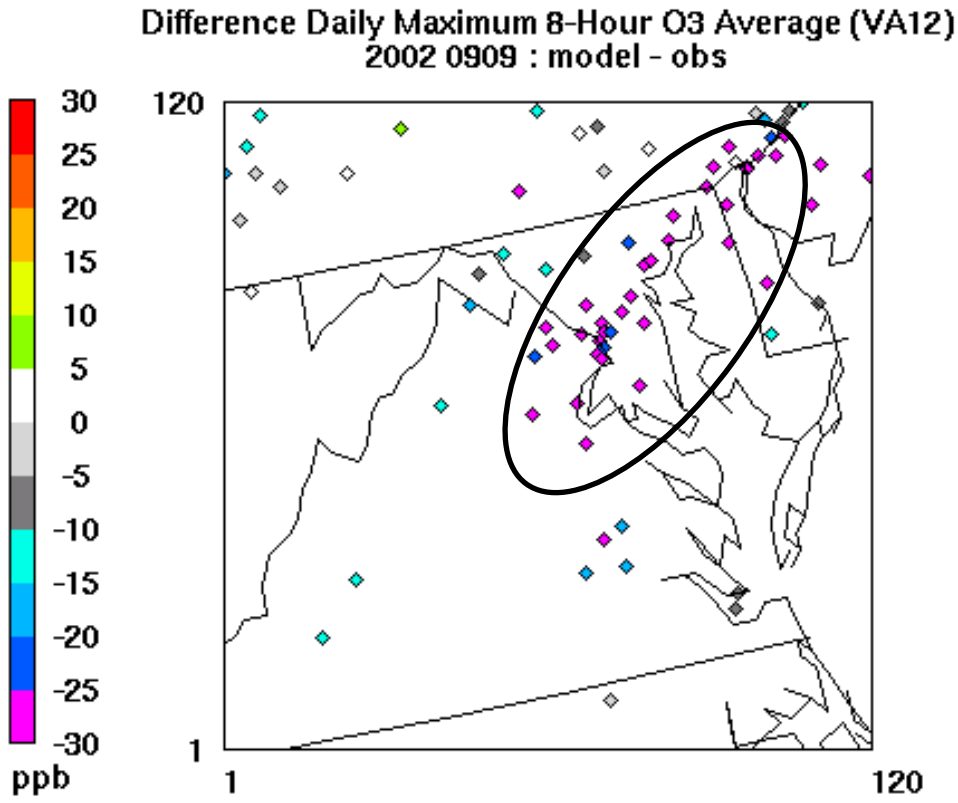

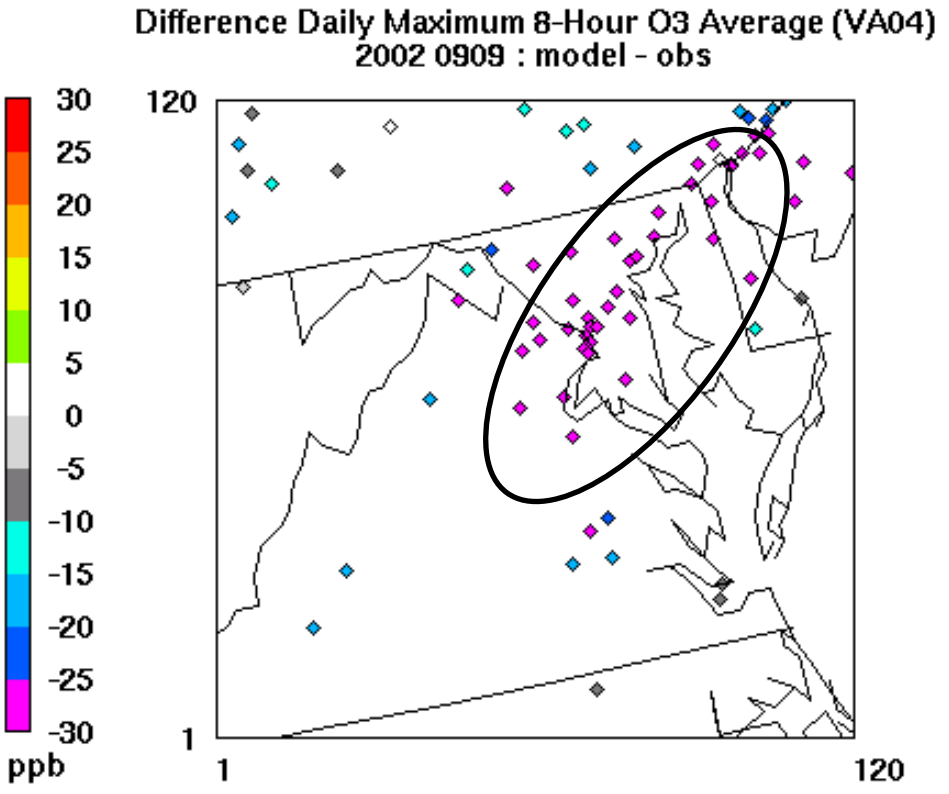

VADEQ CMAQ Model Performance September 9, 2002 (12-km Versus 4-km Resolution)

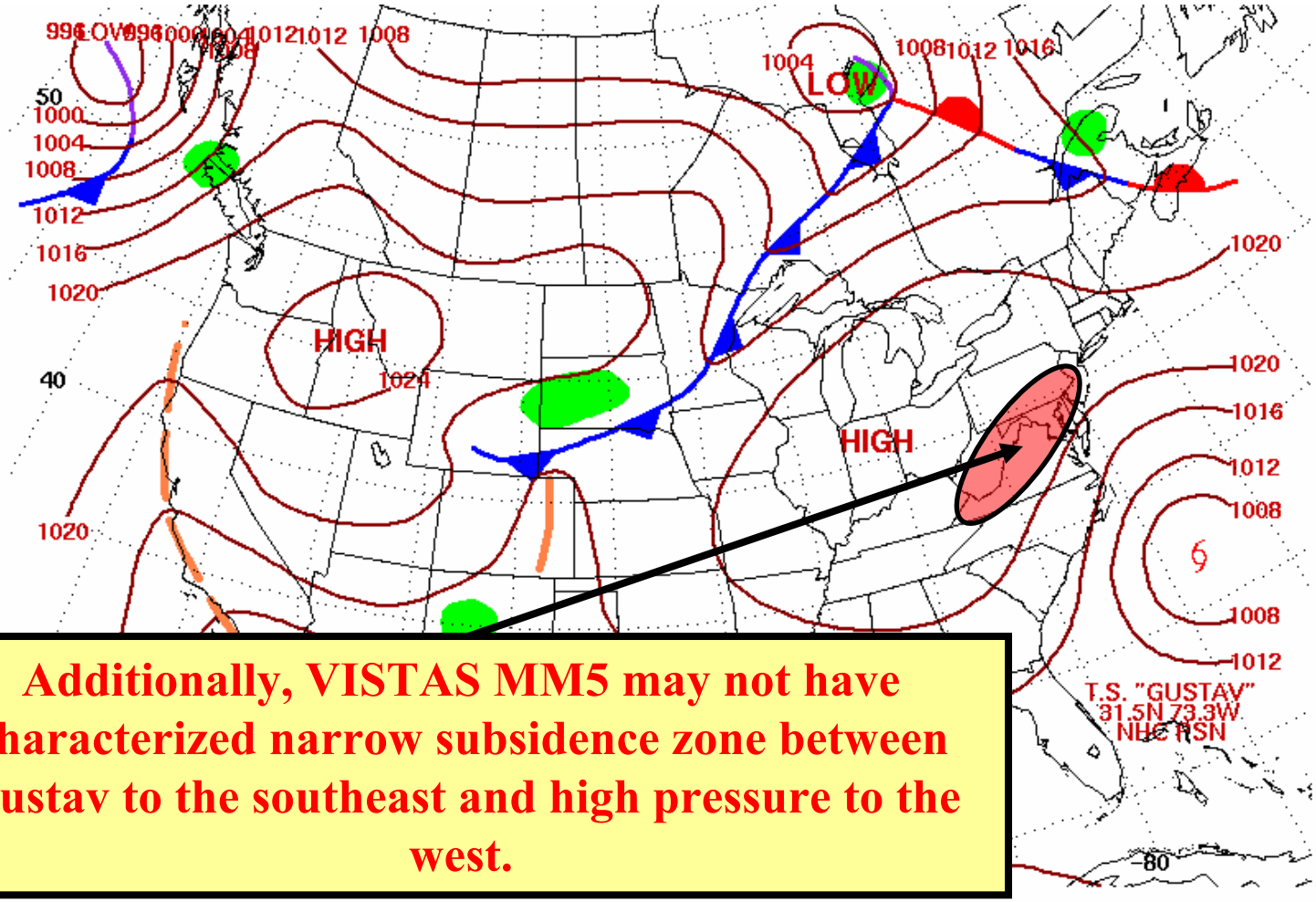

Additionally, VISTAS MM5 may not have characterized narrow subsidence zone between Gustav to the southeast and high pressure to the west.

Surface Weather Map at 7:00 A.M. E.S.T.

VADEQ & OTC CMAQ Model Performance June 11, 2002 (12-km Resolution)

Both 12-km runs similar in the spatial pattern of the maximum ozone concentrations. OTC run slightly better in predicting the magnitude of the impacts.

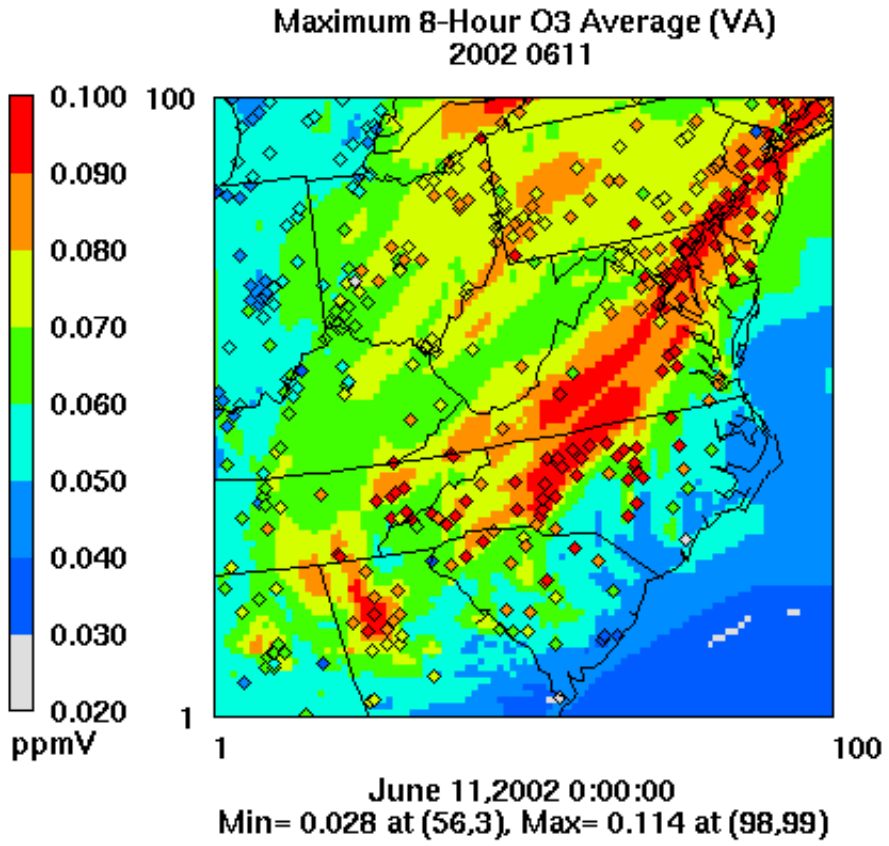

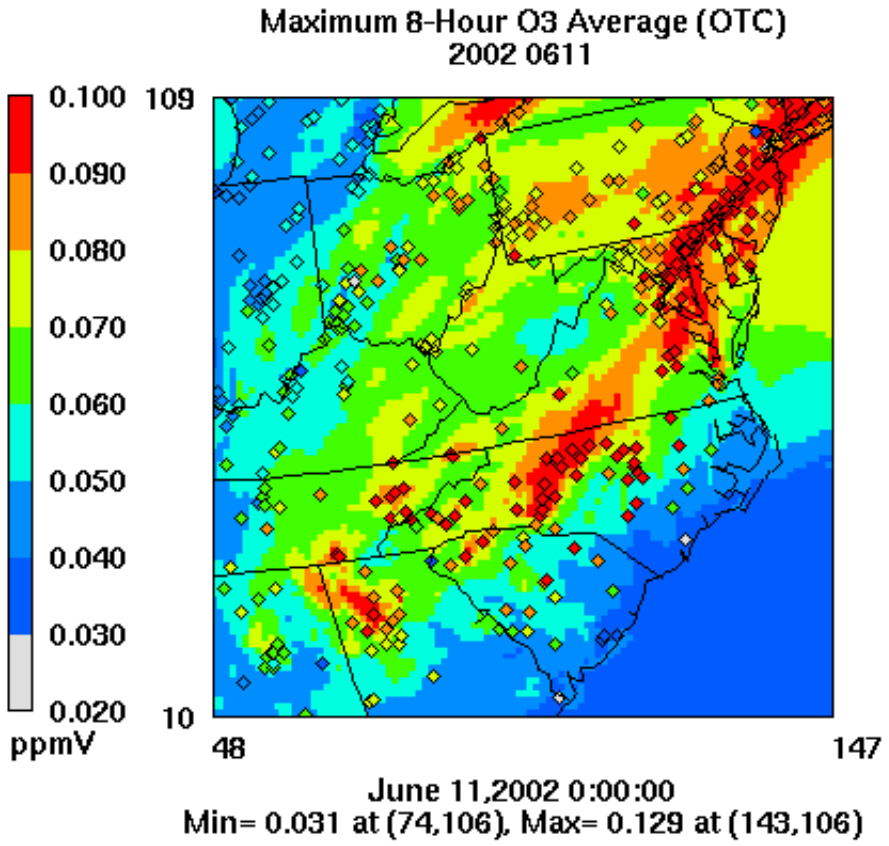

VADEQ & OTC CMAQ Model Performance
June 11, 2002
(12-km Resolution)
(Model Predicted O3 – Observed O3)

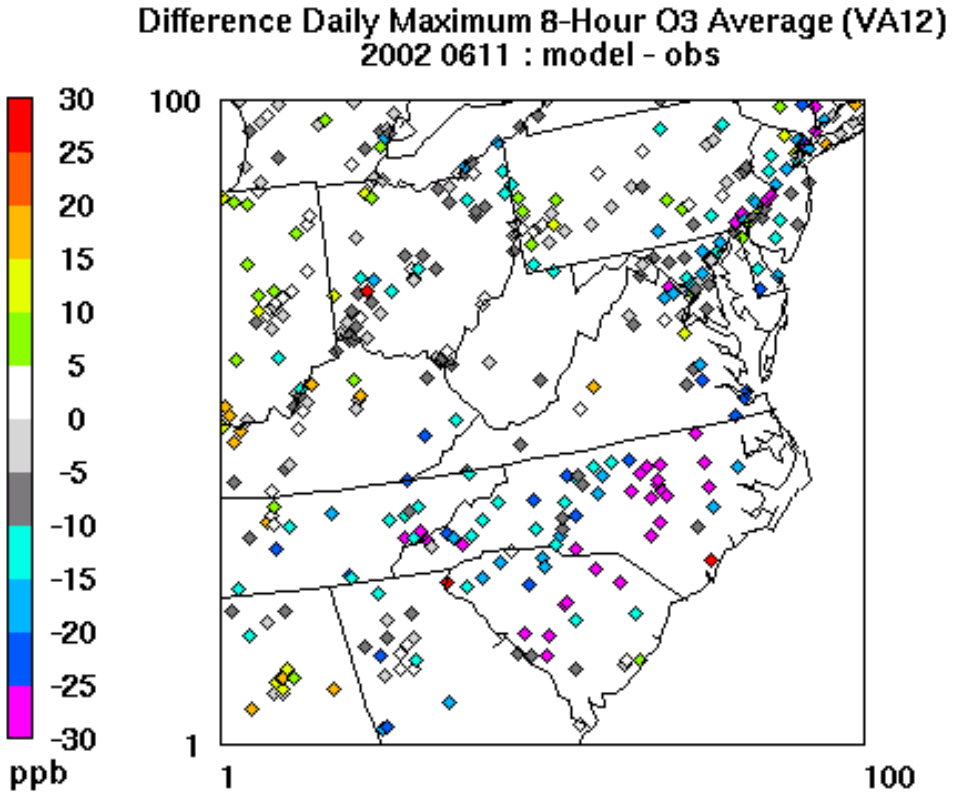

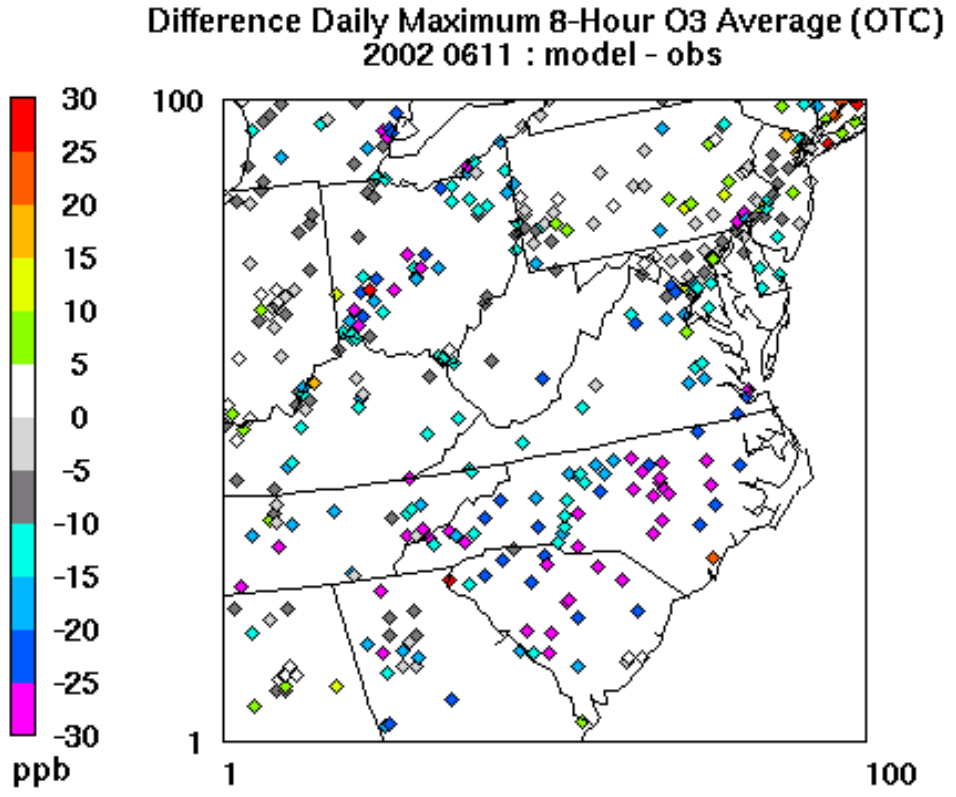

VADEQ & OTC CMAQ Model Performance June 25, 2002 (12-km Resolution)

Both 12-km runs similar in the spatial pattern of the maximum ozone concentrations. OTC run slightly better in predicting the magnitude of the impacts.

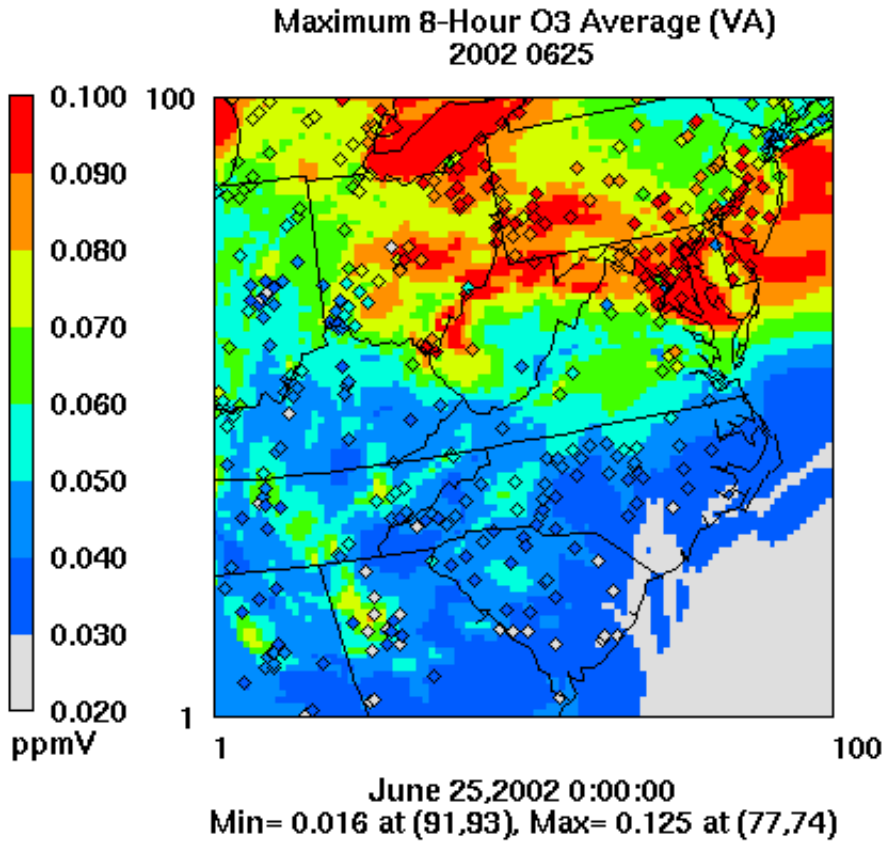

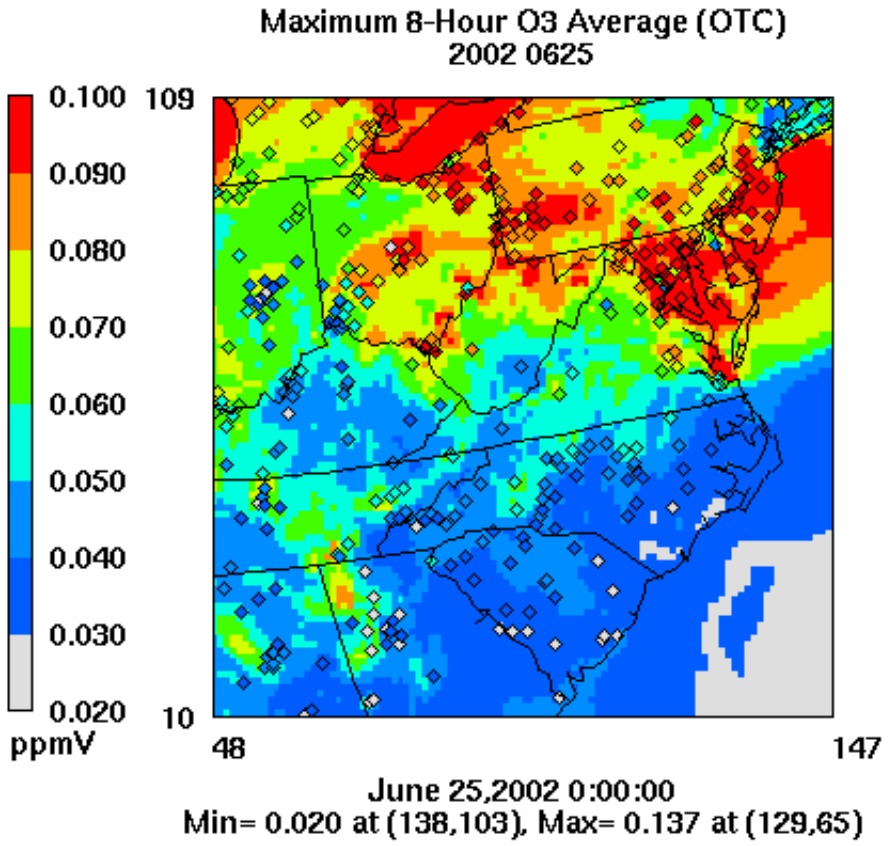

VADEQ & OTC CMAQ Model Performance
June 25, 2002
(12-km Resolution)
(Model Predicted O3 – Observed O3)

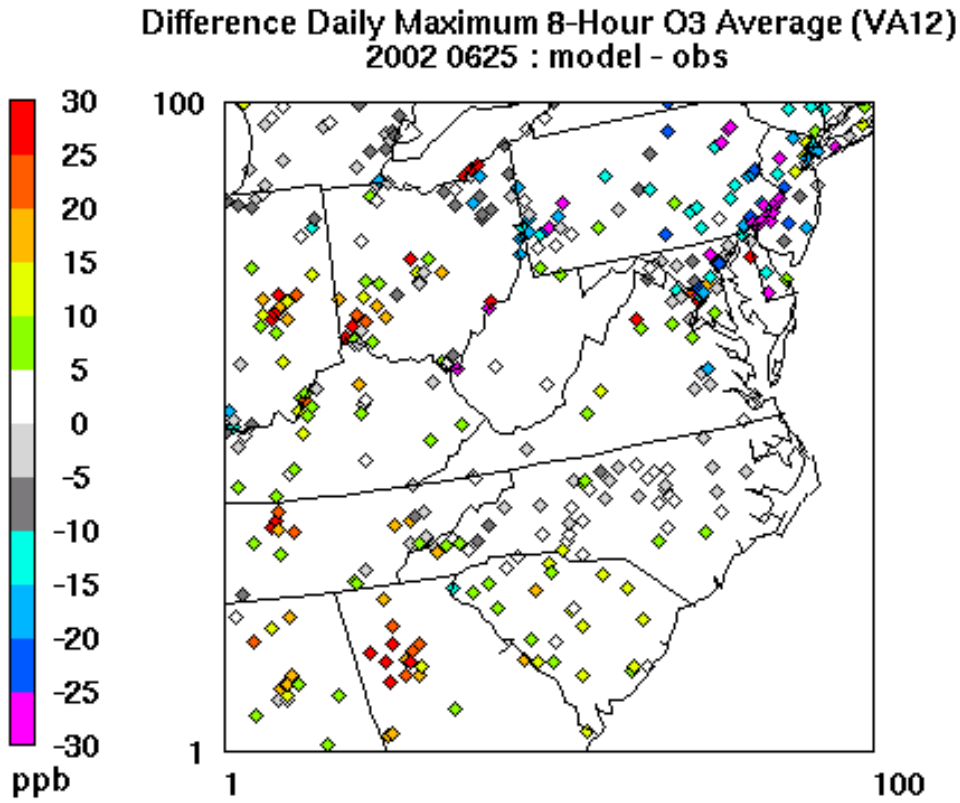

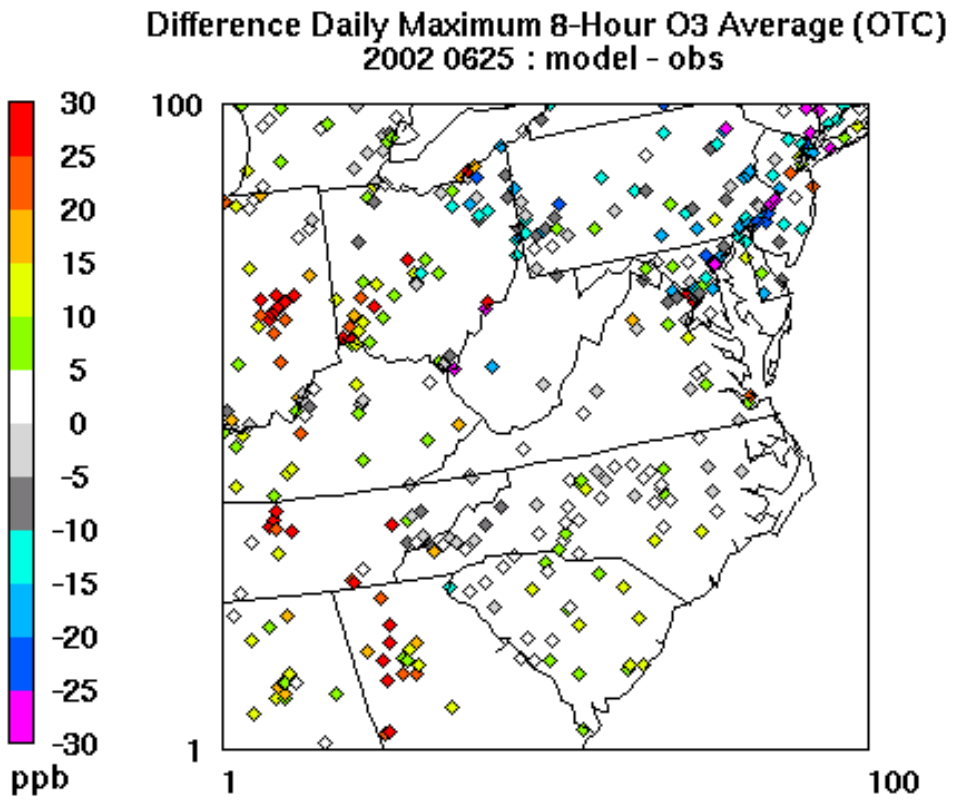

VADEQ & OTC CMAQ Model Performance July 2, 2002 (12-km Resolution)

Both 12-km runs similar in the spatial pattern of the maximum ozone concentrations. OTC run slightly better in predicting the magnitude of the impacts.

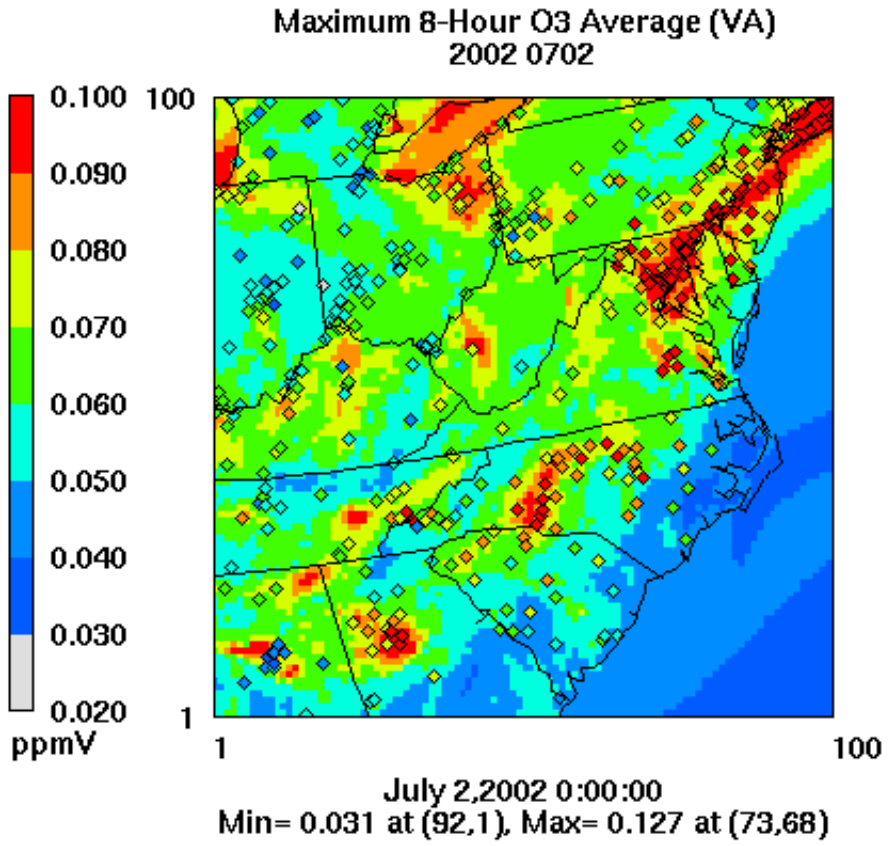

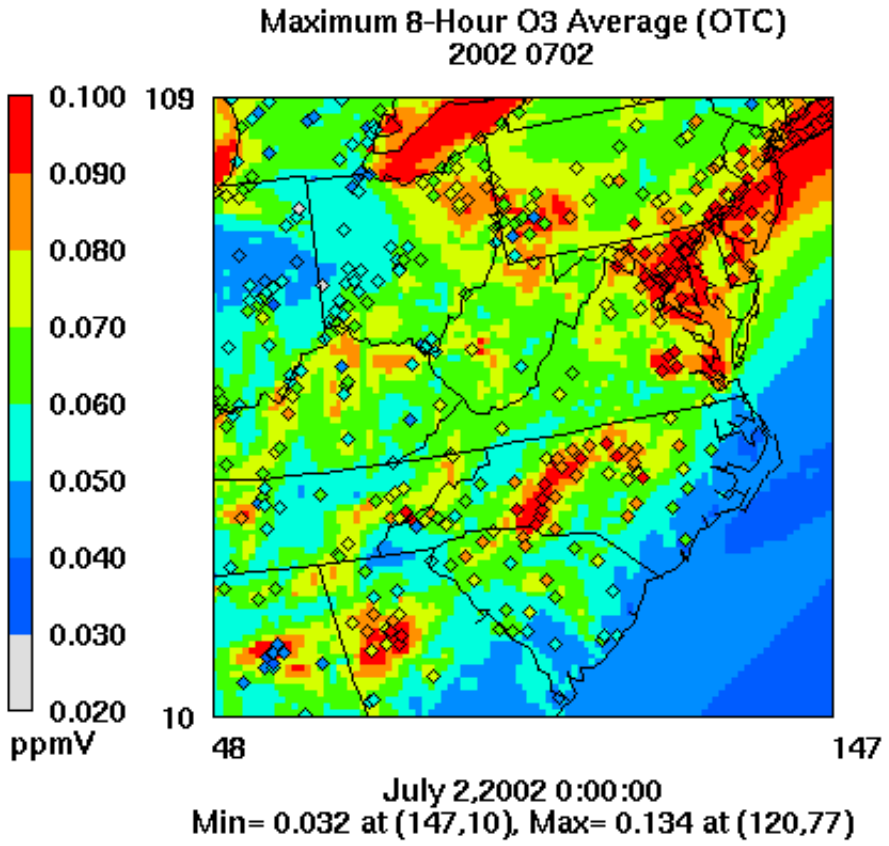

VADEQ & OTC CMAQ Model Performance
July 2, 2002
(12-km Resolution)
(Model Predicted O3 – Observed O3)

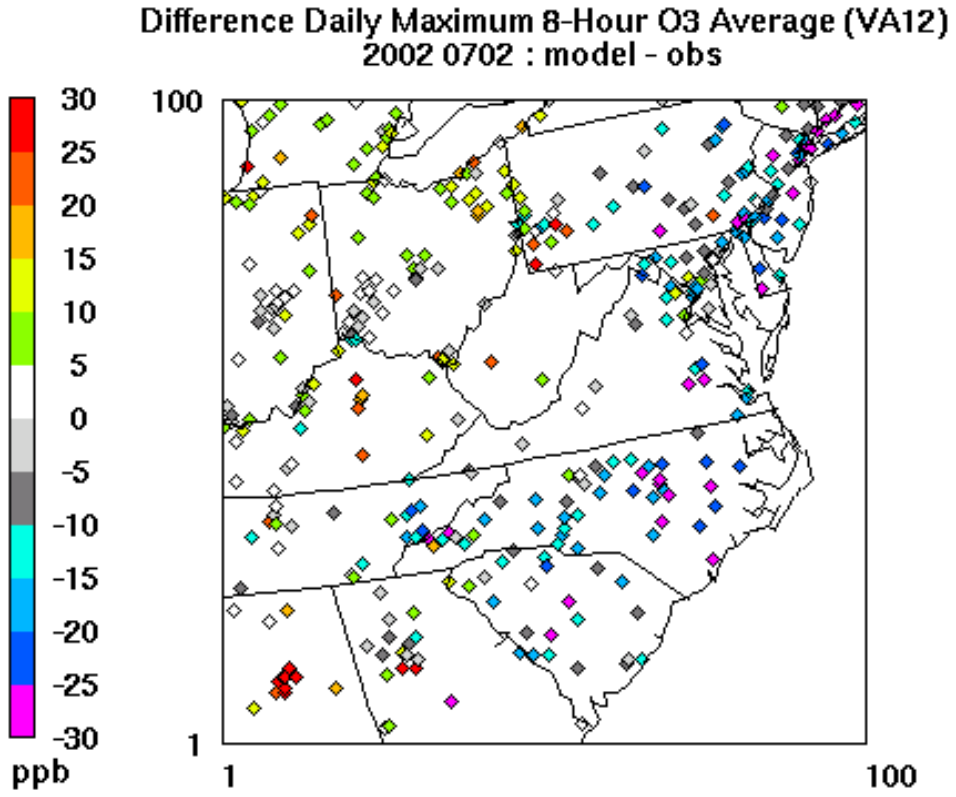

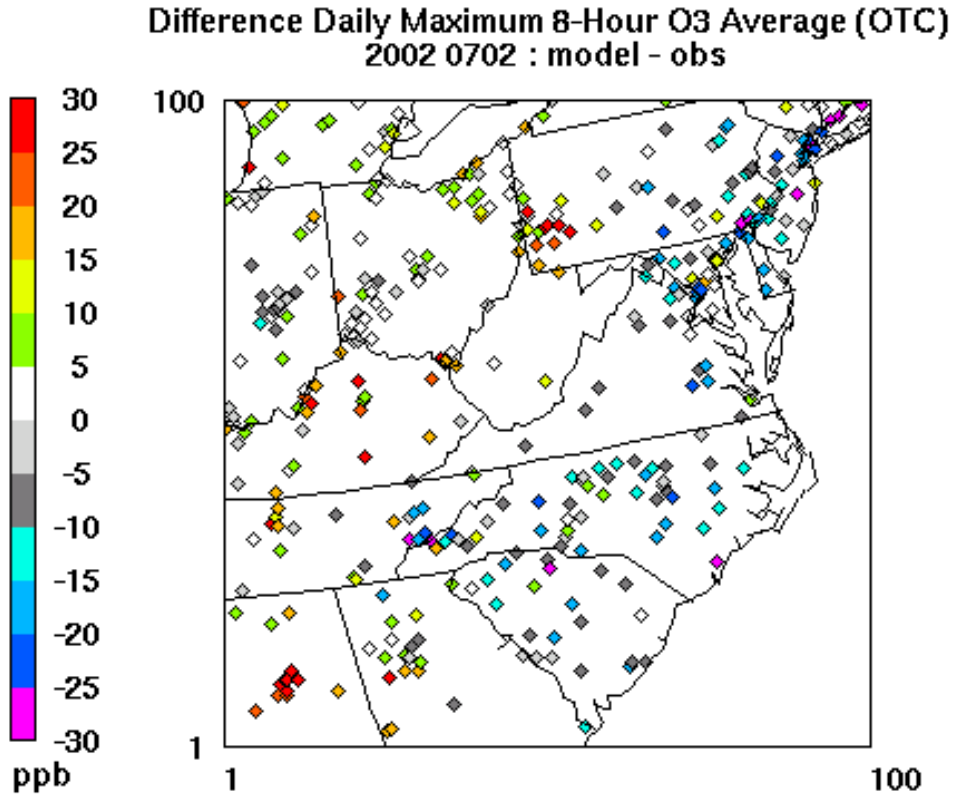

VADEQ & OTC CMAQ Model Performance August 2, 2002 (12-km Resolution)

OTC run clearly outperforms VADEQ run for this episode day due to VISTAS JPROC preprocessing error.

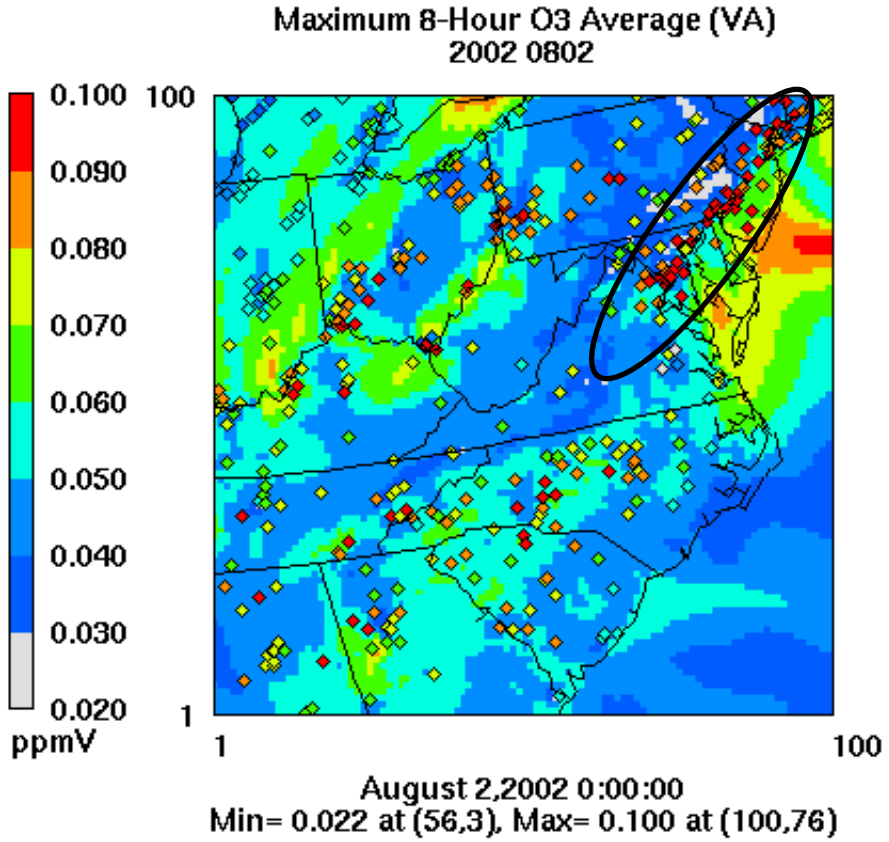

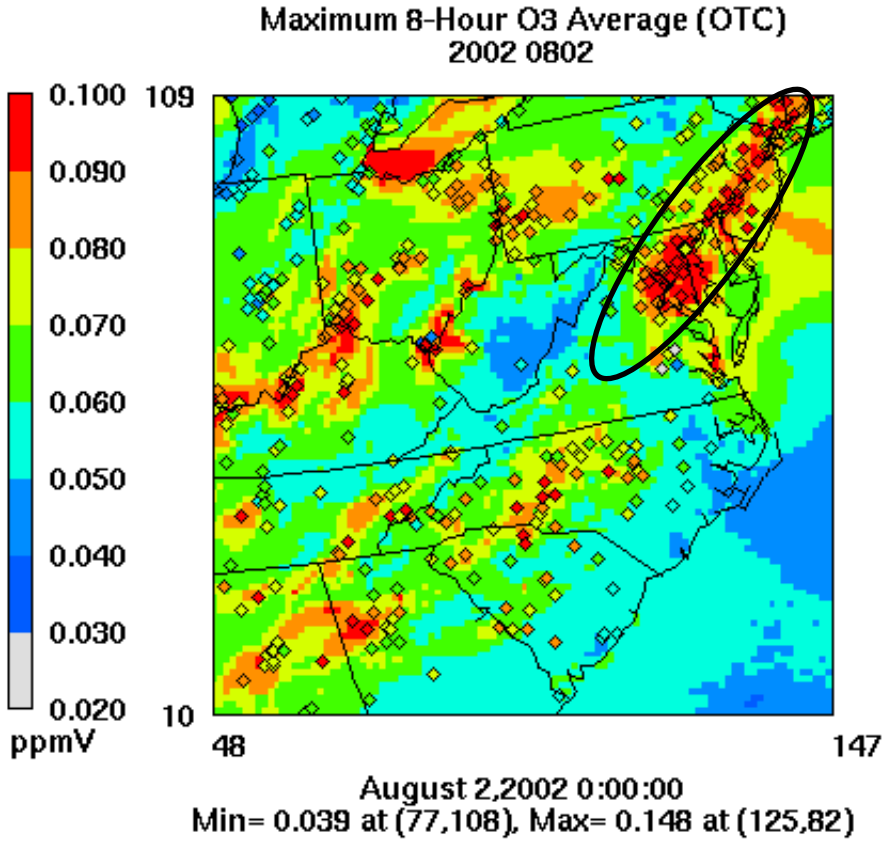

VADEQ & OTC CMAQ Model Performance
August 2, 2002
(12-km Resolution)
(Model Predicted O3 – Observed O3)

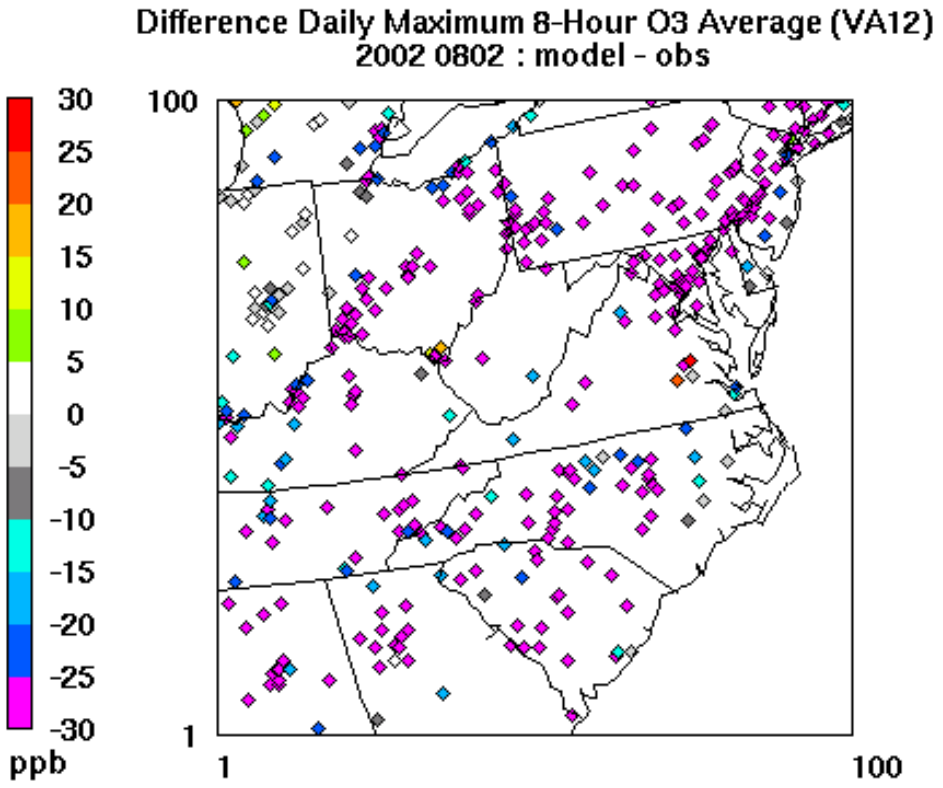

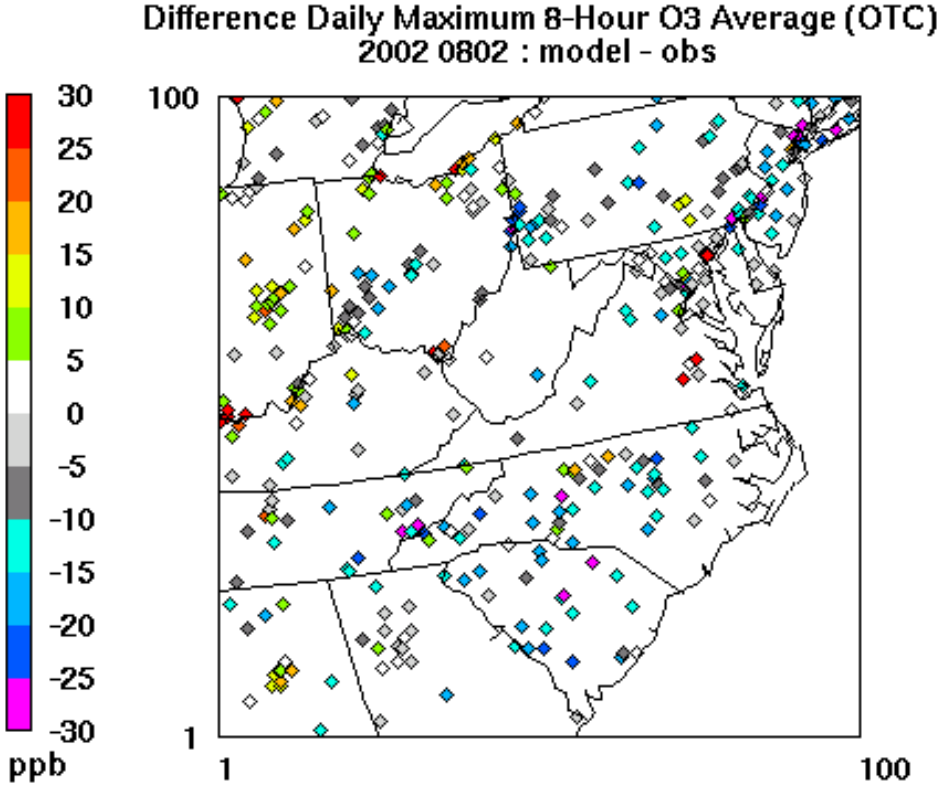

VADEQ & OTC CMAQ Model Performance August 13, 2002 (12-km Resolution)

Both 12-km runs similar in the spatial pattern of the maximum ozone concentrations. VADEQ run slightly better in predicting the magnitude of the impacts. Both runs show large negative bias of 30+ ppb at many locations.

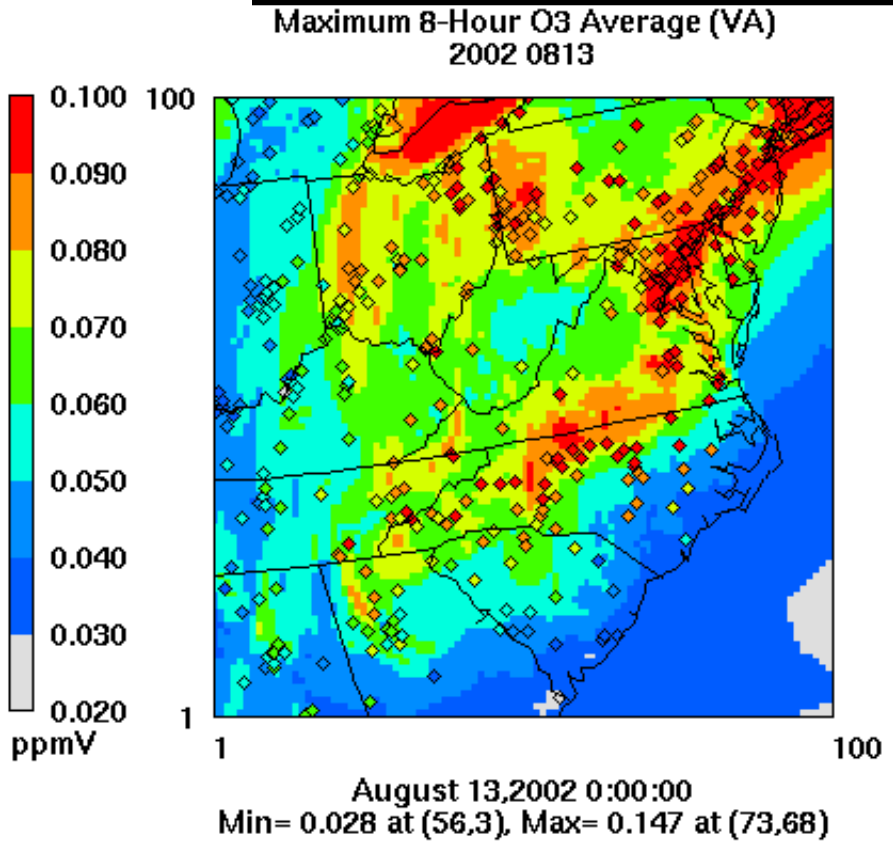

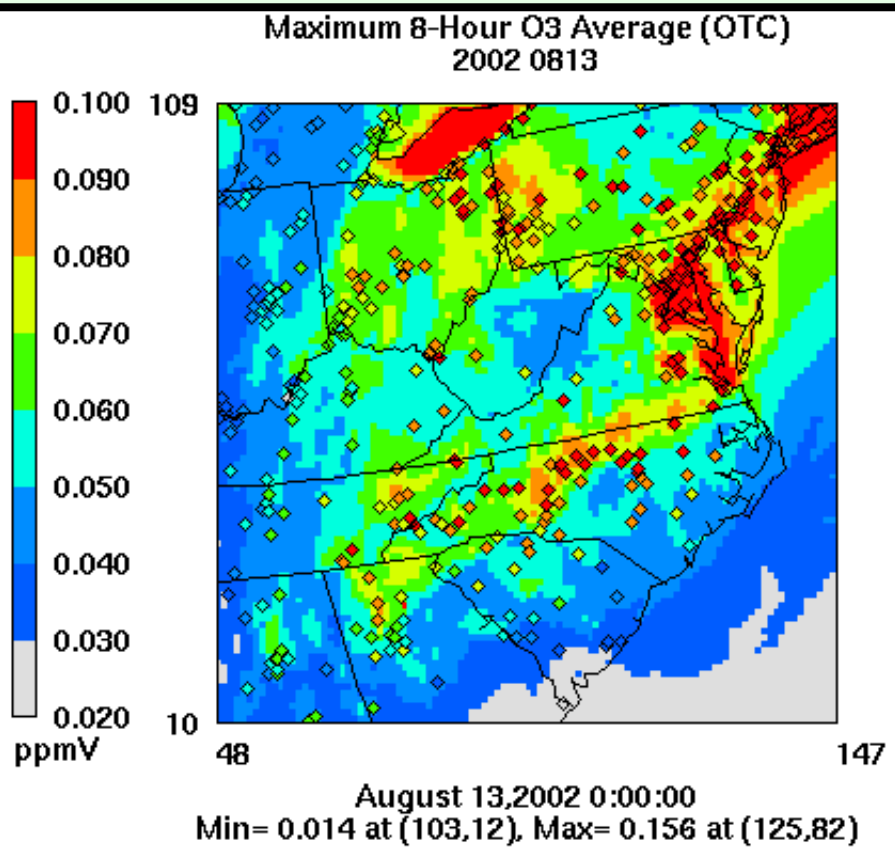

VADEQ & OTC CMAQ Model Performance
August 13, 2002
(12-km Resolution)
(Model Predicted O3 – Observed O3)

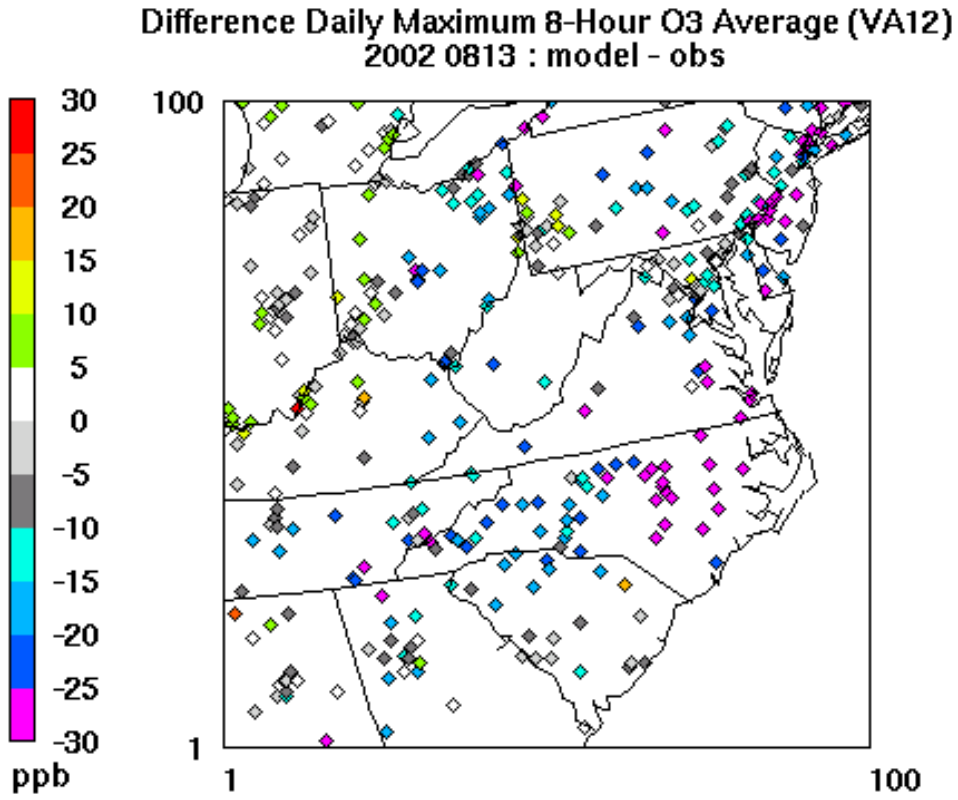

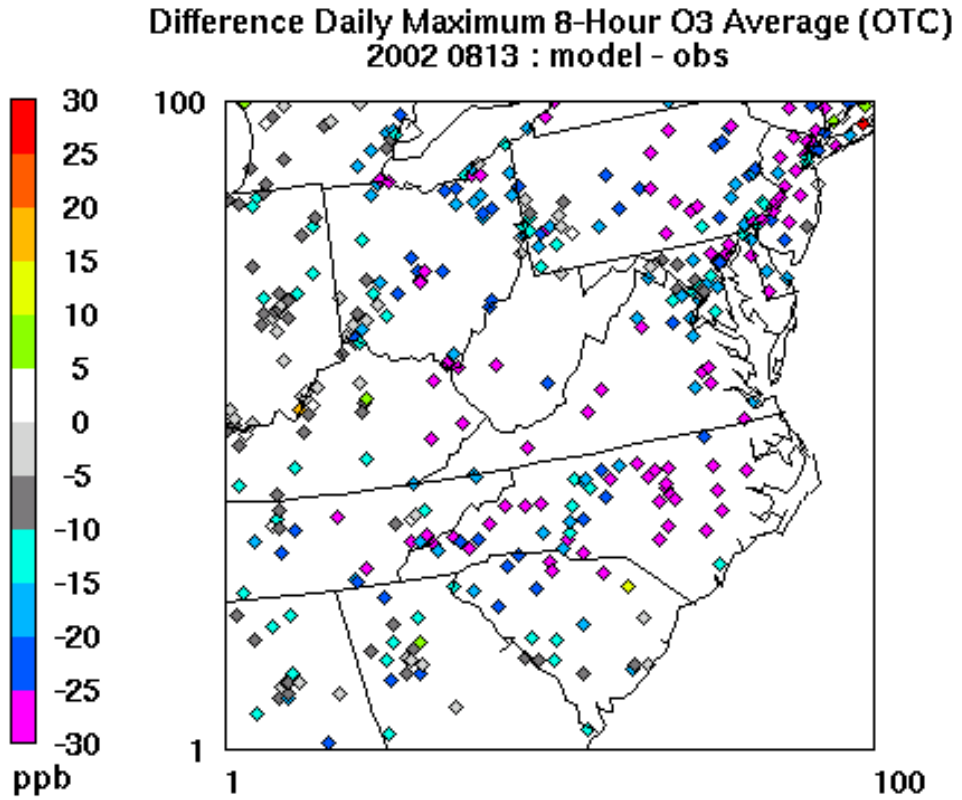

VADEQ & OTC CMAQ Model Performance September 9, 2002 (12-km Resolution)

OTC run outperforms VADEQ run for this episode day. UMD MM5 run may have characterized subsidence zone. JPROC preprocessor error may also be present although not conclusive based on VADEQ preliminary examination of this day.

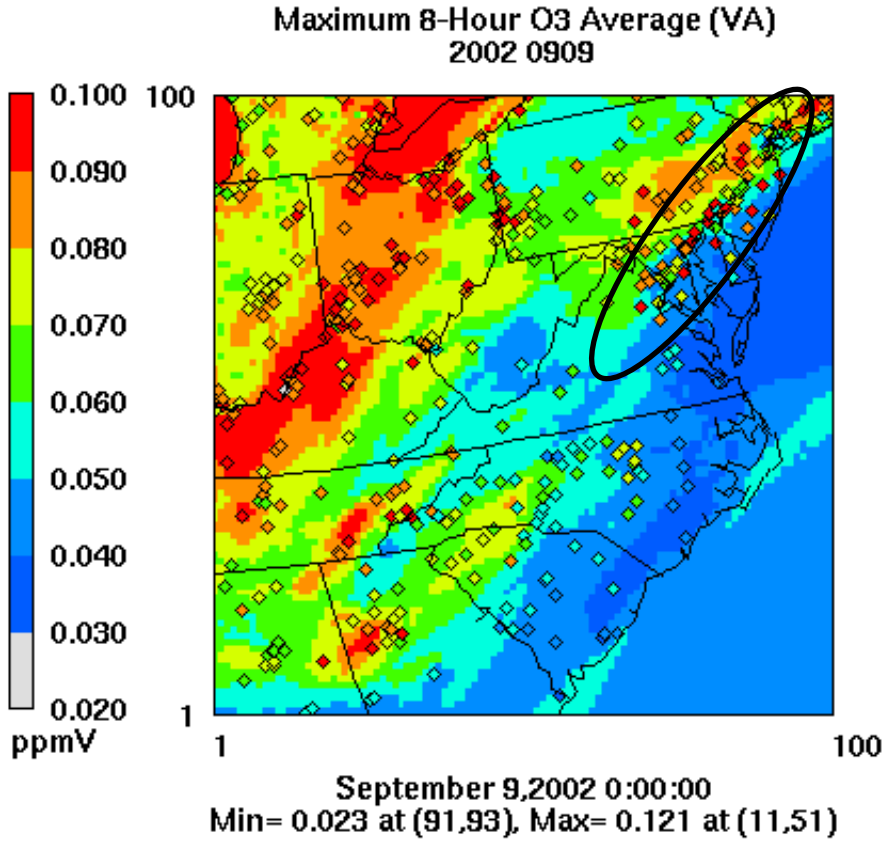

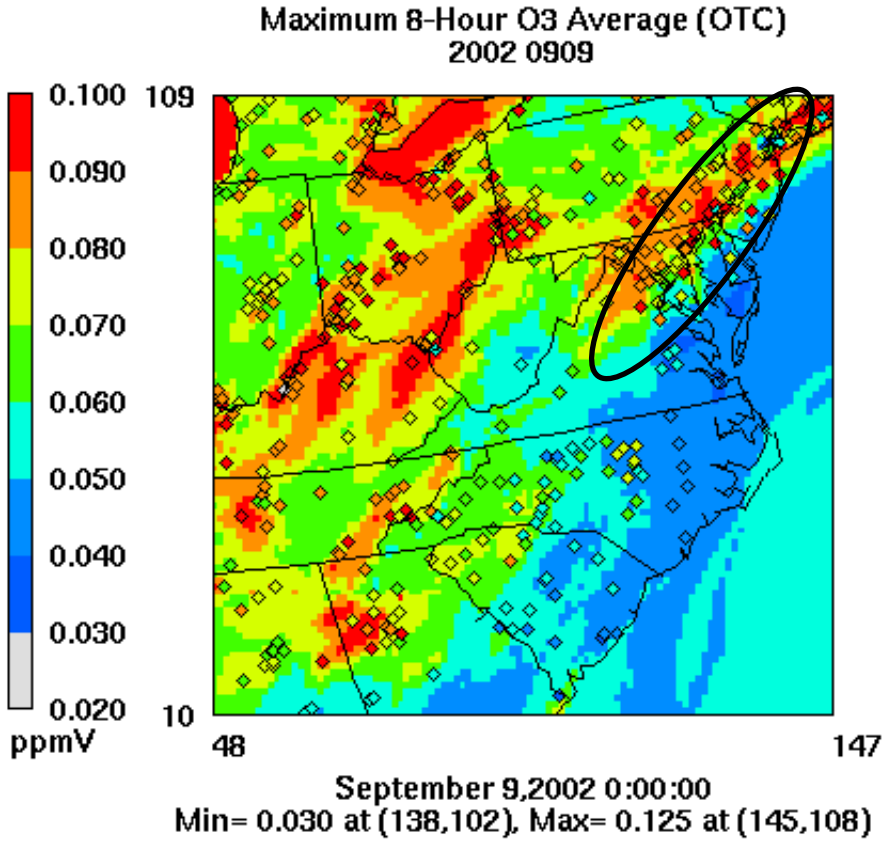

VADEQ & OTC CMAQ Model Performance
September 9, 2002
(12-km Resolution)
(Model Predicted O3 – Observed O3)

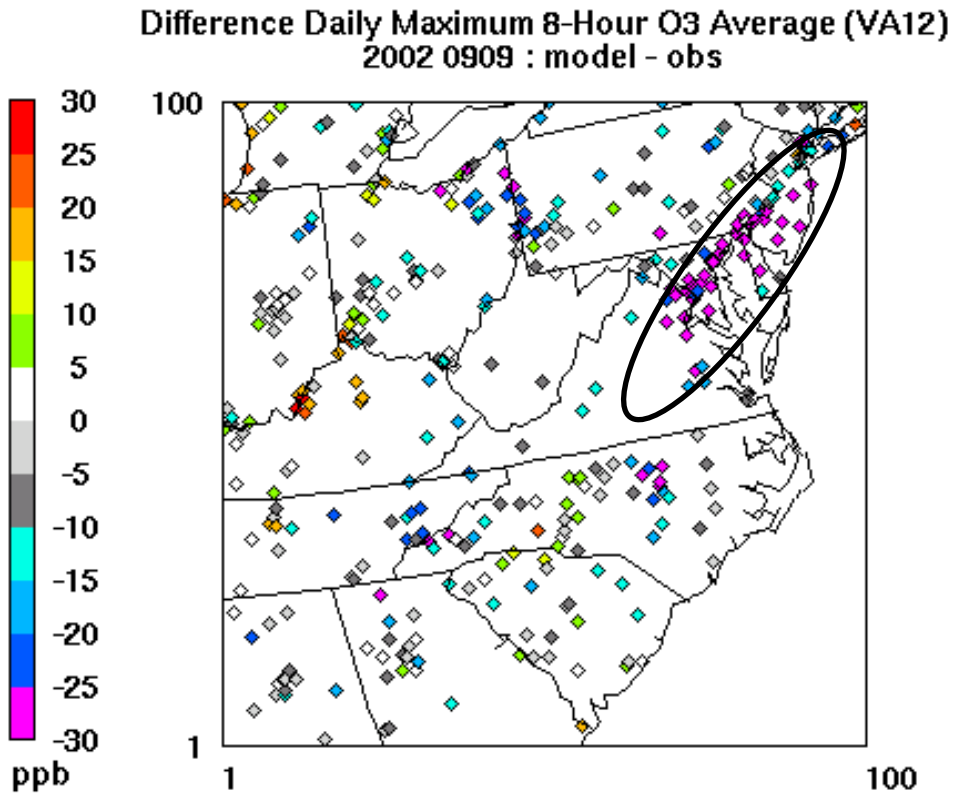

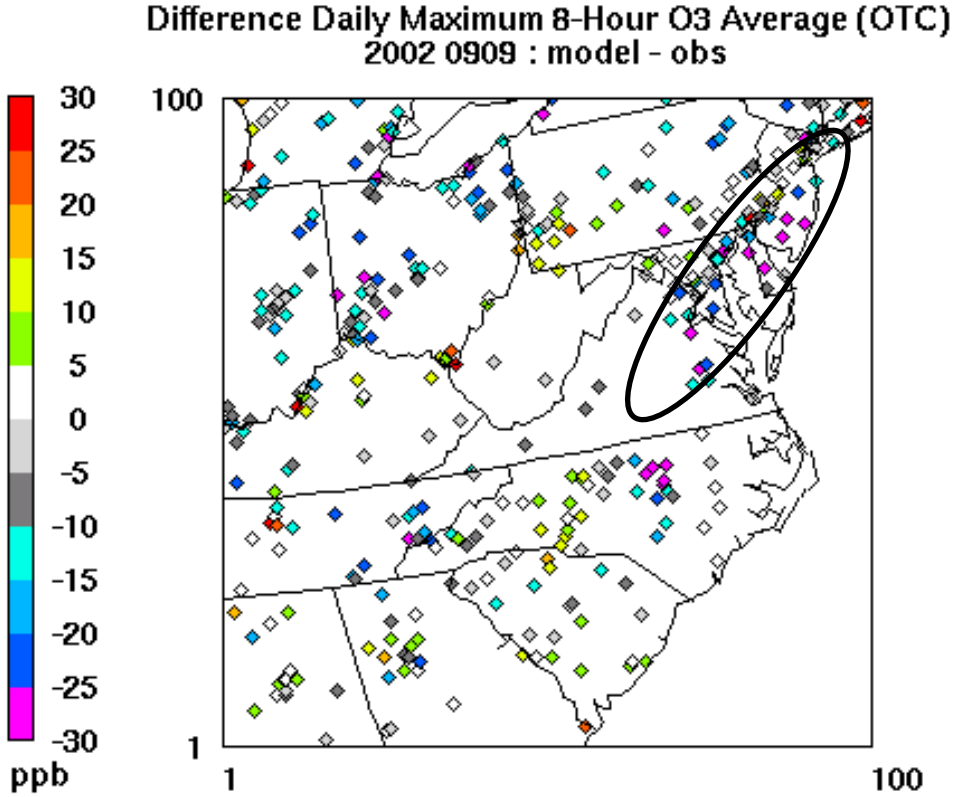

Ozone Time Series Plot
Baltimore, Maryland (24-005-1007)
CMAQ Results versus Observations
June 6, 2002 - July 5, 2002

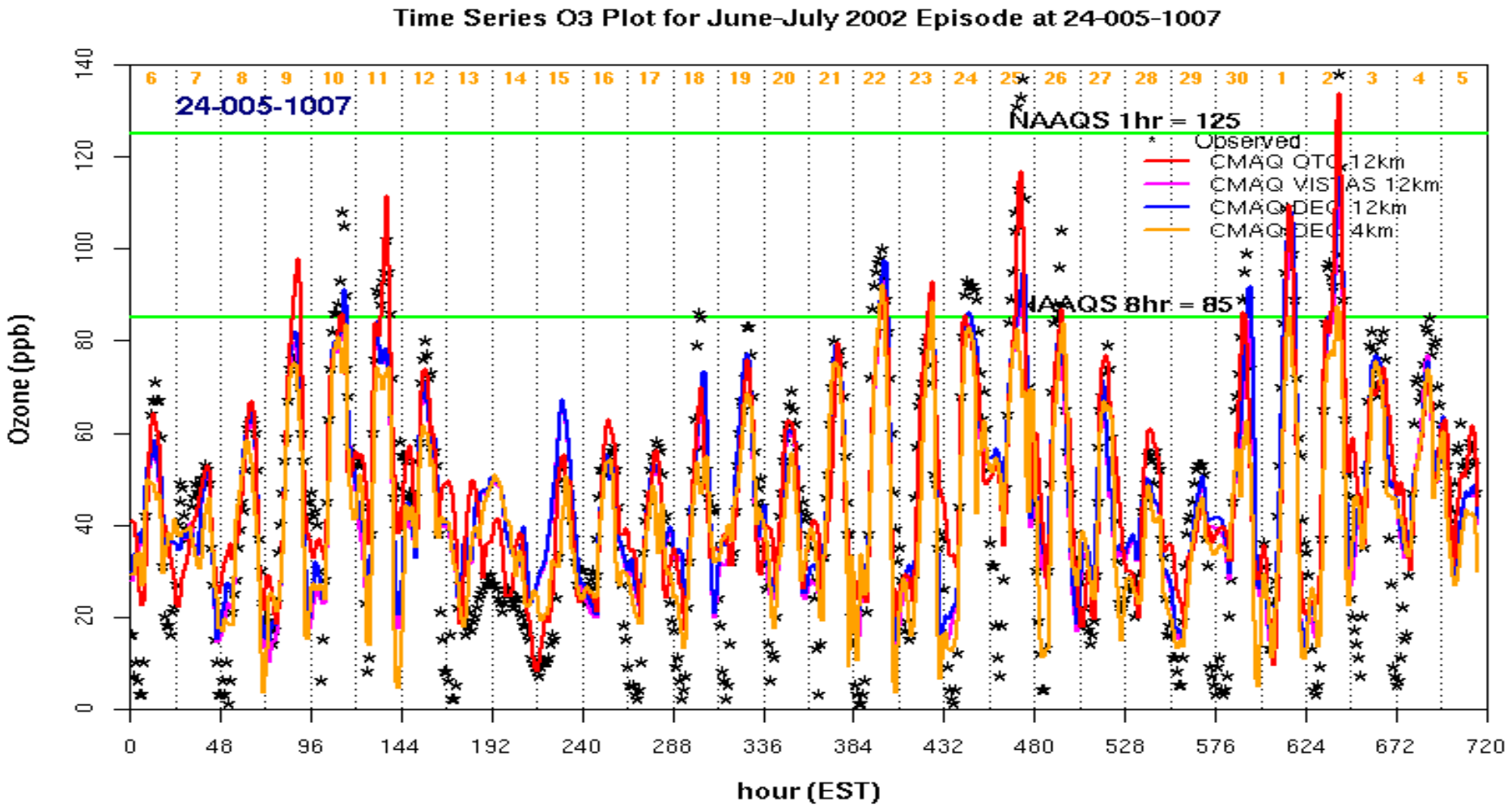

Ozone Time Series Plot
Rockville, Maryland (24-031-3001)
CMAQ Results versus Observations
June 6, 2002 - July 5, 2002

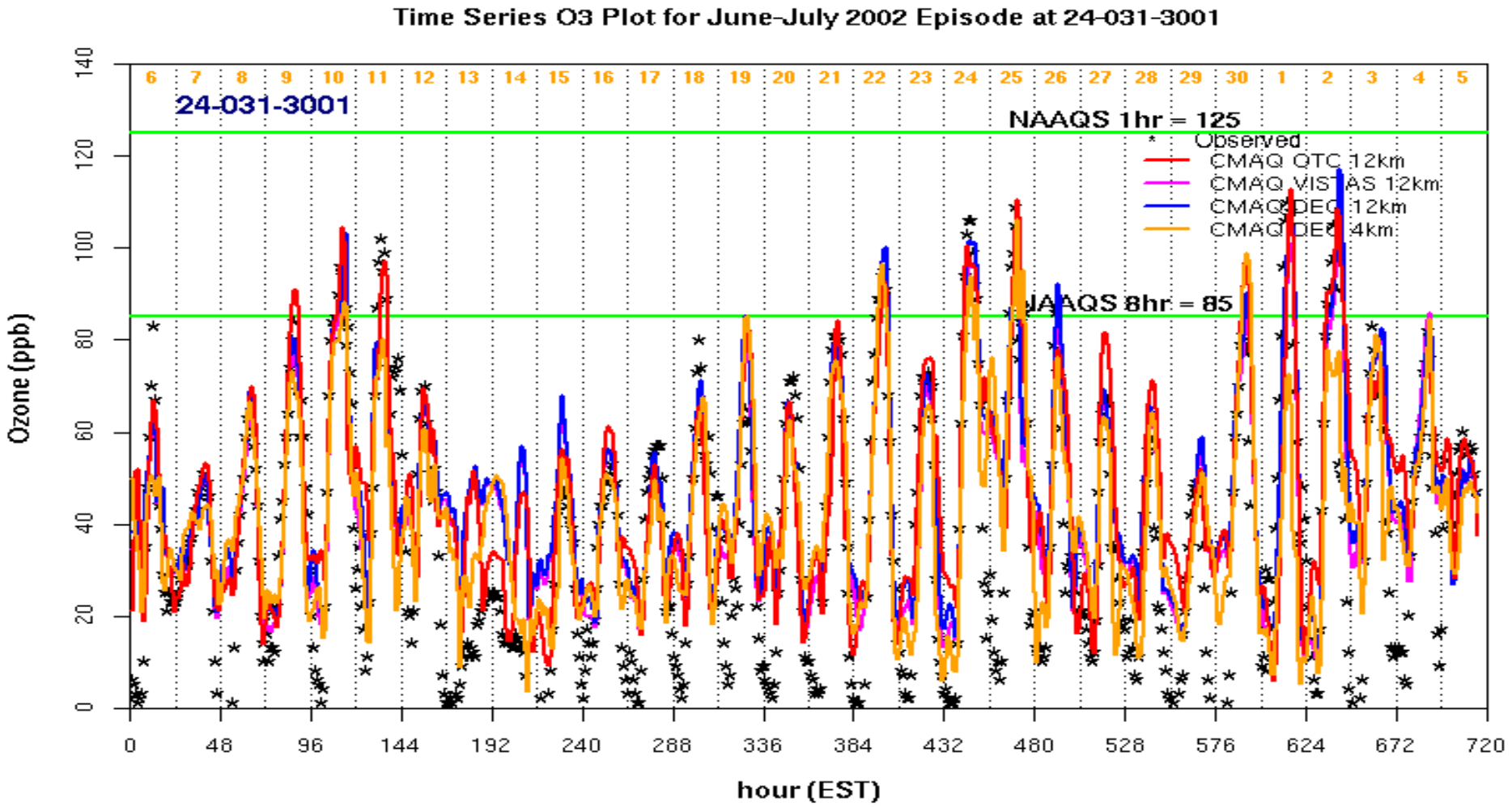

Ozone Time Series Plot
District of Columbia (11-001-0041)
CMAQ Results versus Observations
June 6, 2002 - July 5, 2002

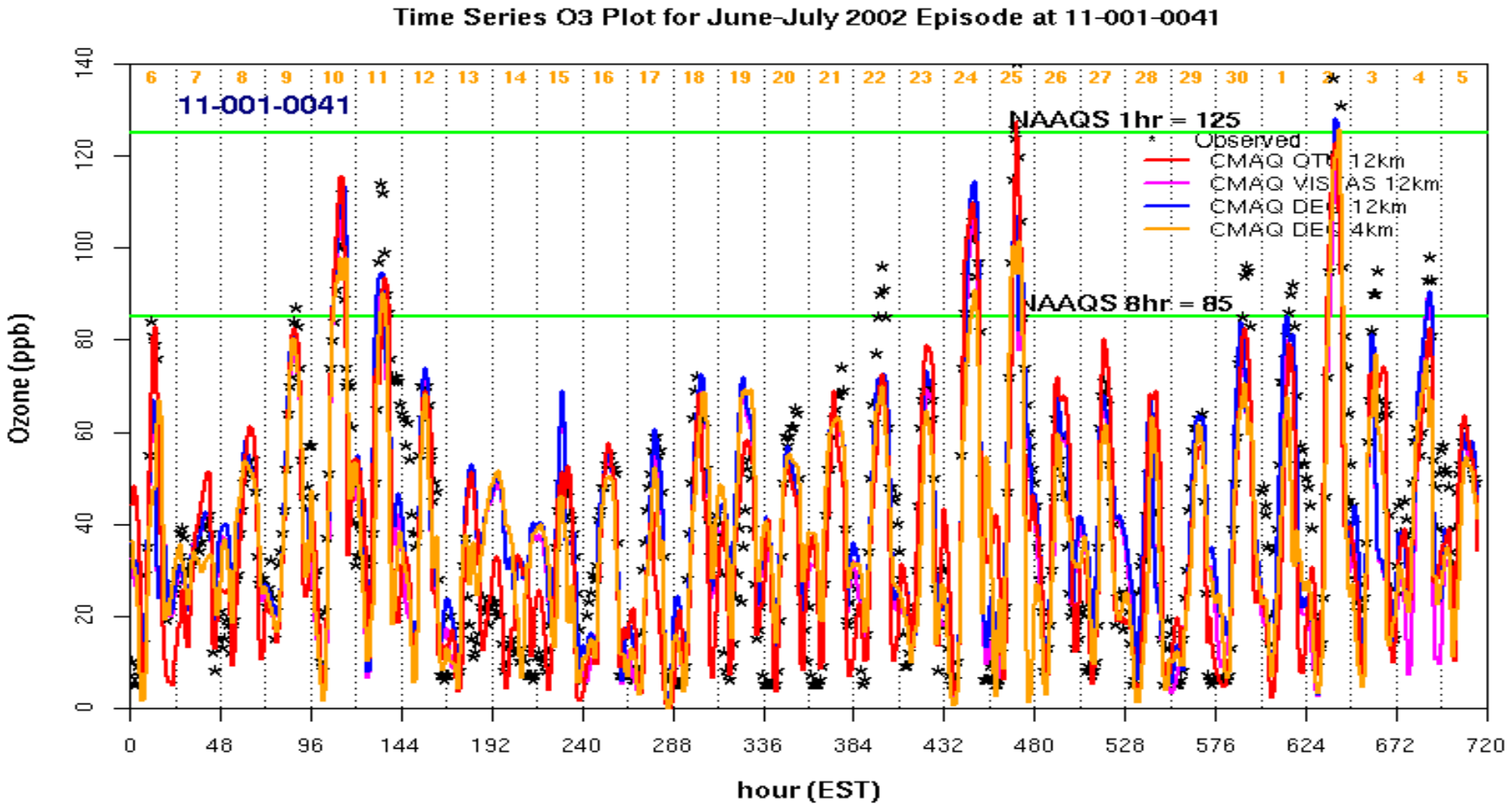

Ozone Time Series Plot
Baltimore, Maryland (24-005-1007)
CMAQ Results versus Observations
July 27, 2002 – August 16, 2002

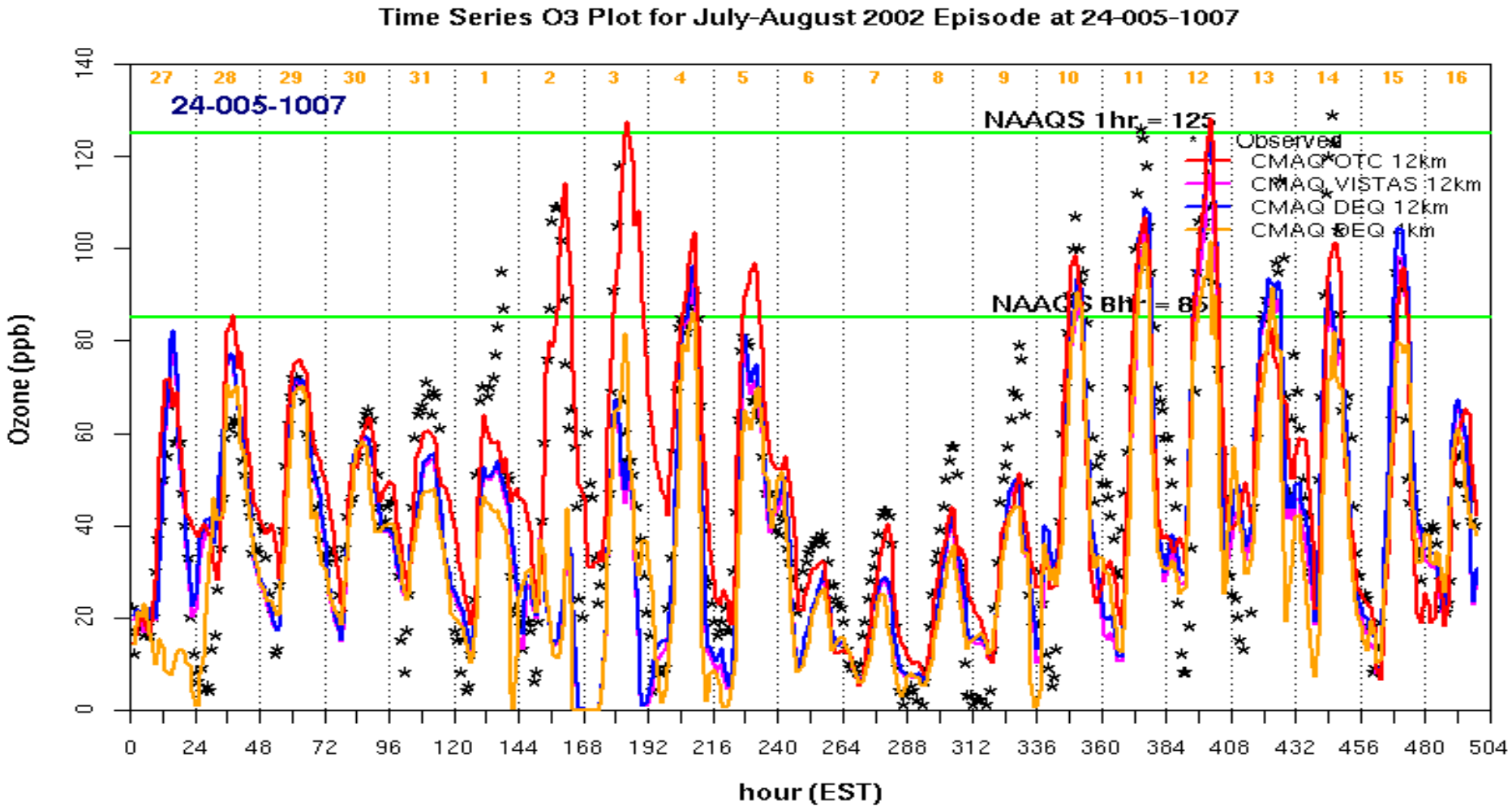

Ozone Time Series Plot
Rockville, Maryland (24-031-3001)
CMAQ Results versus Observations
July 27, 2002 – August 16, 2002

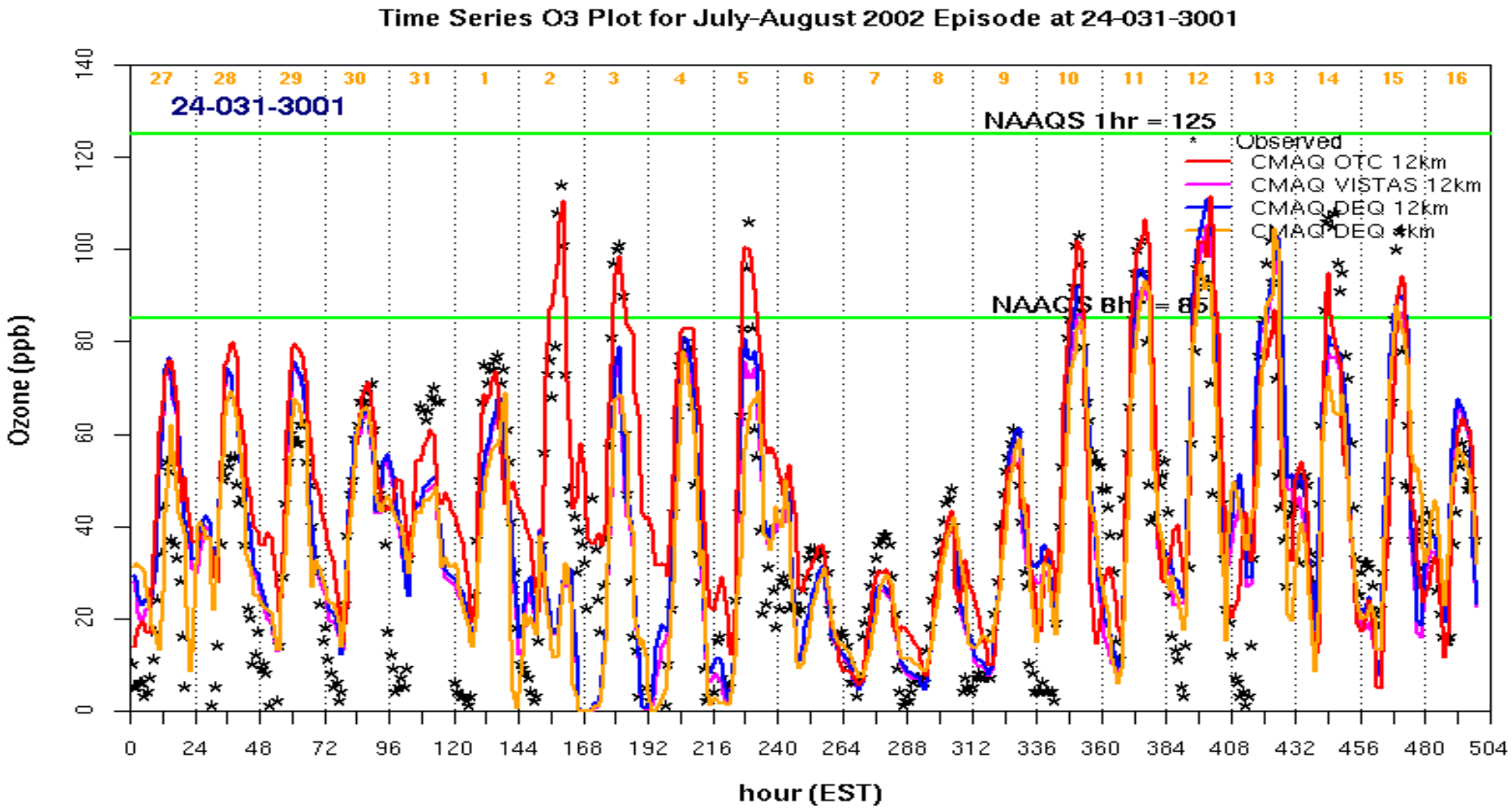

Ozone Time Series Plot
District of Columbia (11-001-0025)
CMAQ Results versus Observations
July 27, 2002 – August 16, 2002

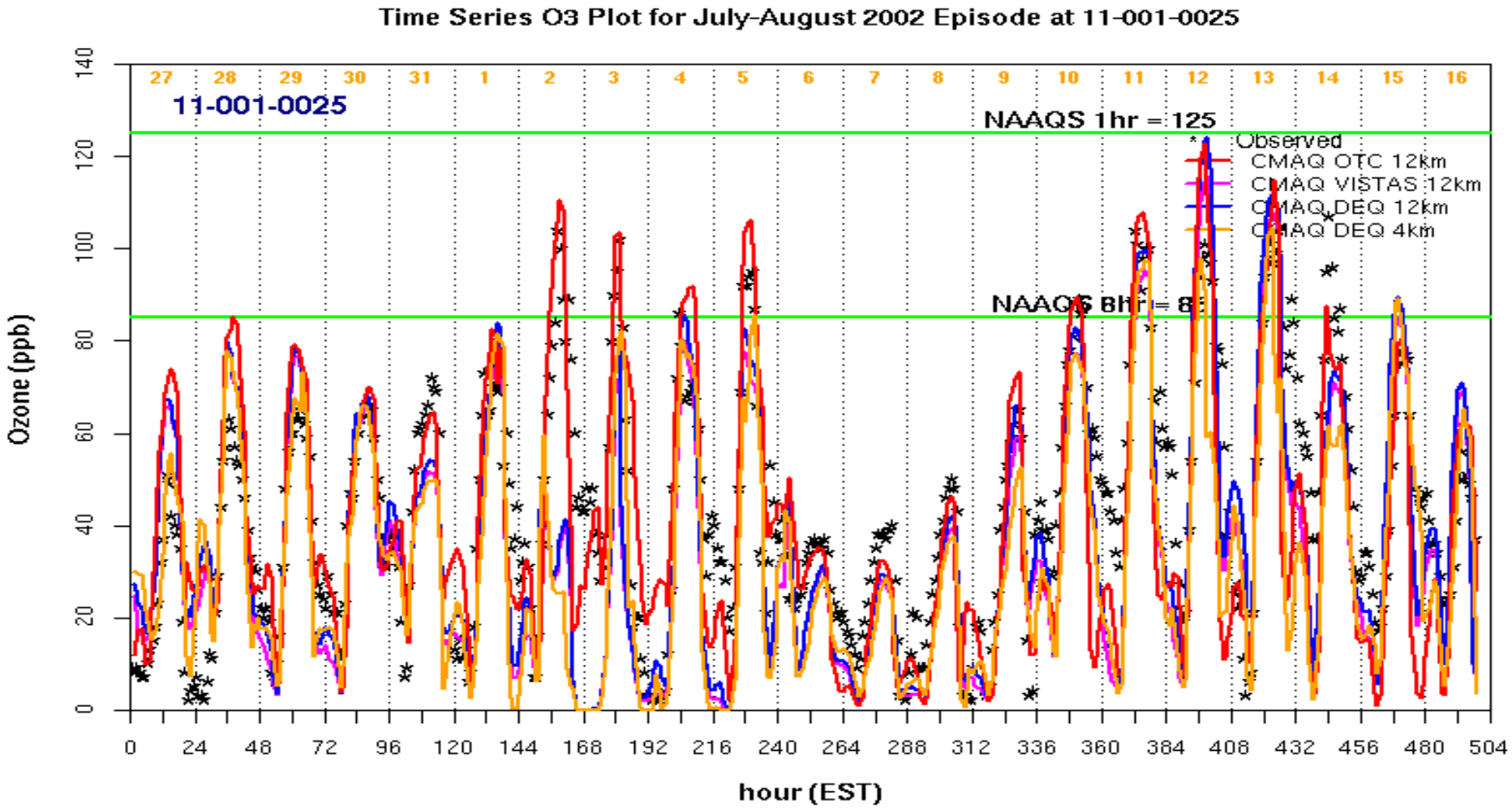

VADEQ & OTC CMAQ Model Performance Mean Normal Bias (%) for All Episode Days (12-km Resolution)

Both 12-km runs similar with respect to the magnitude and spatial pattern of bias. Generally a negative bias of ~5-20% across monitors in the D.C. area. VADEQ run has larger negative bias across PA and NJ. Emissions issue???

VADEQ 12-km

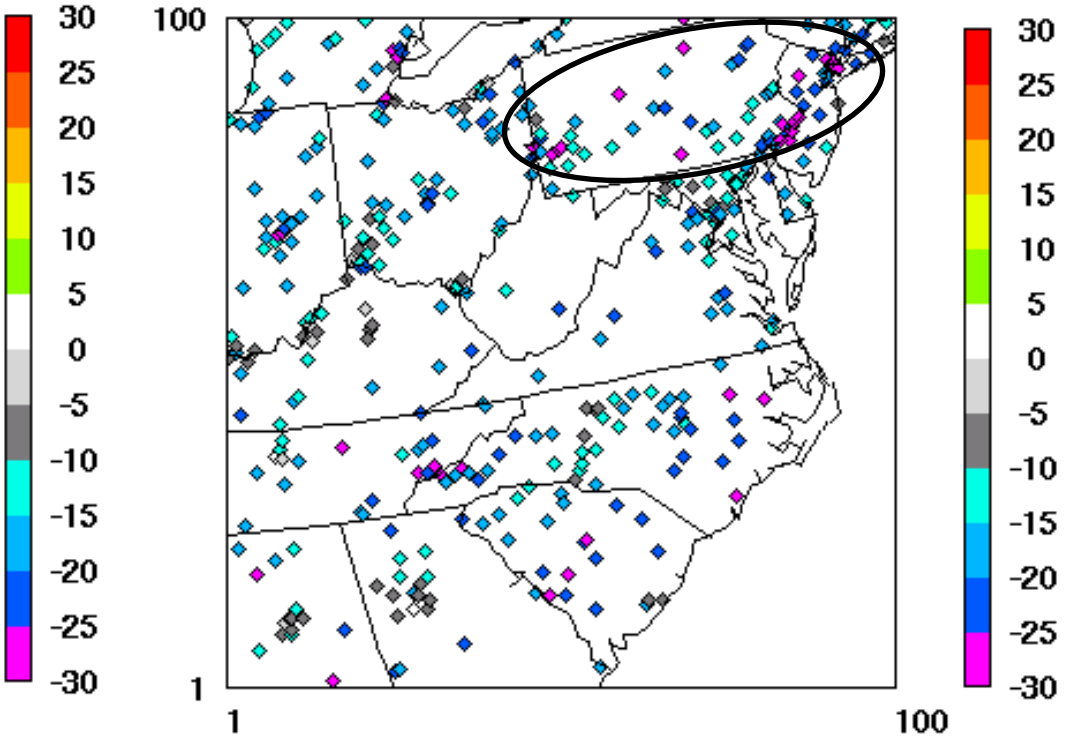

OTC 12-km

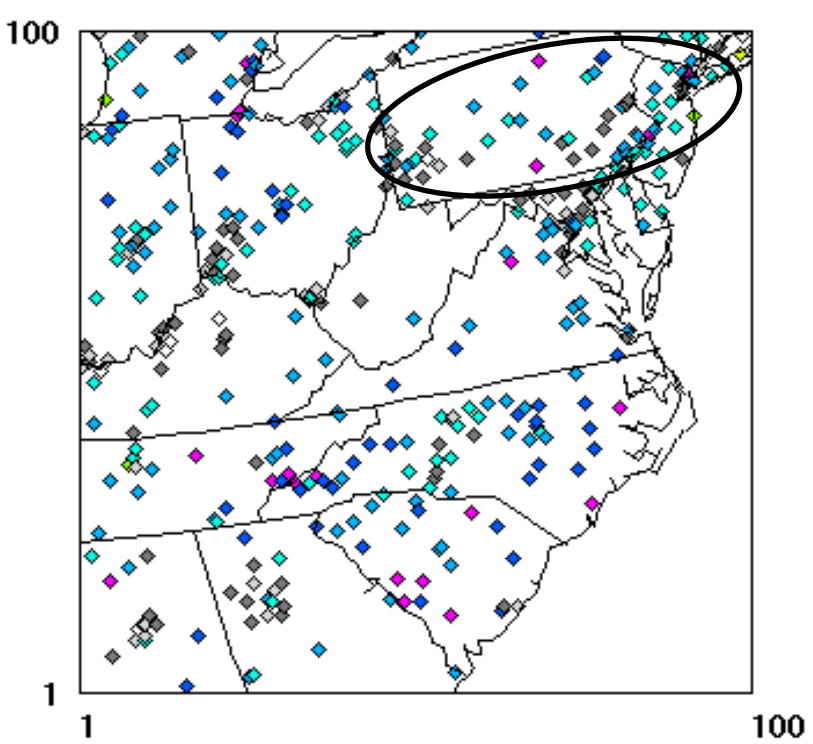

VADEQ & OTC CMAQ Model Performance (12-km Resolution)

(O3 Concentrations >60 ppb)

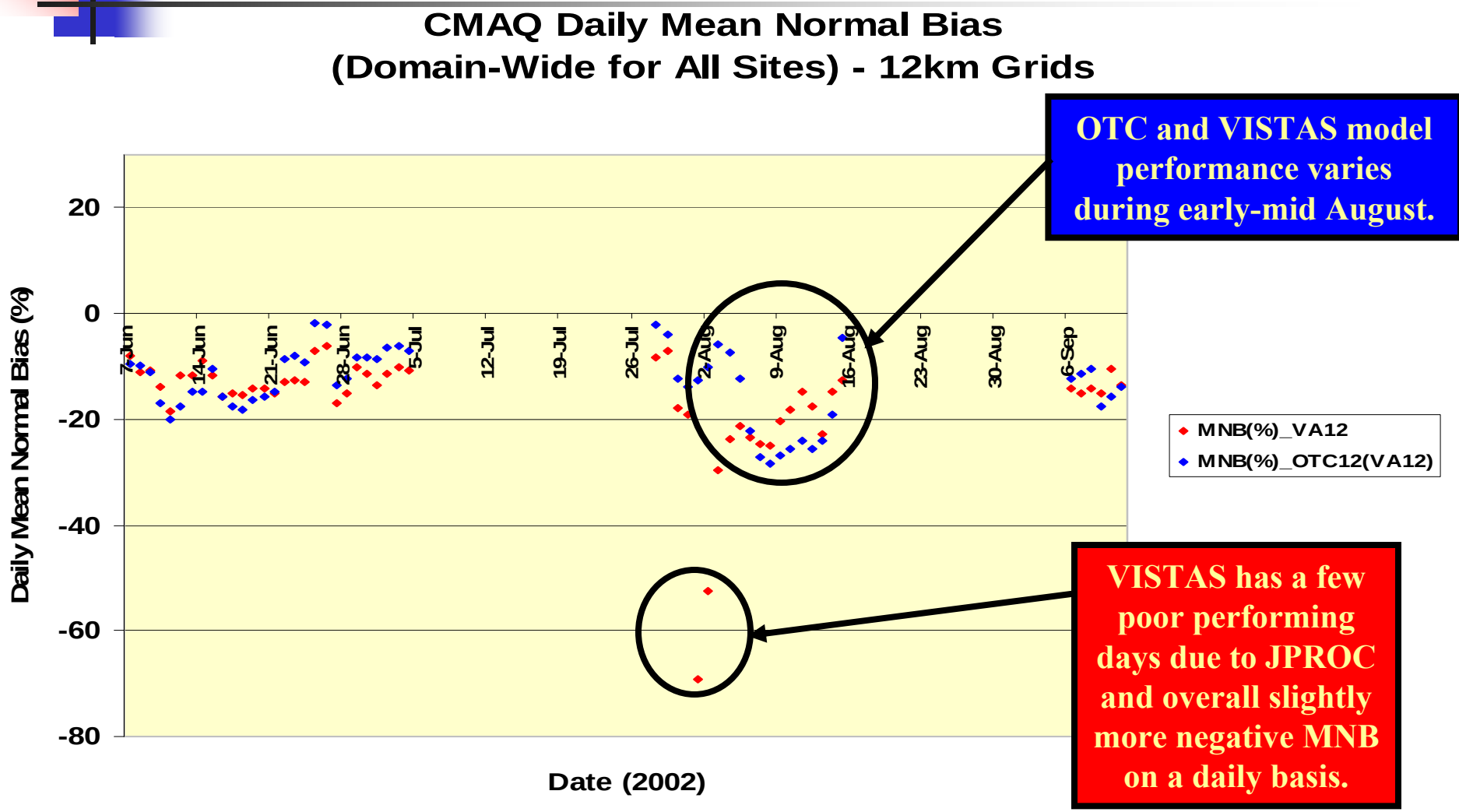

VADEQ & OTC CMAQ Model Performance (12-km Resolution)

(O3 Concentrations >60 ppb)

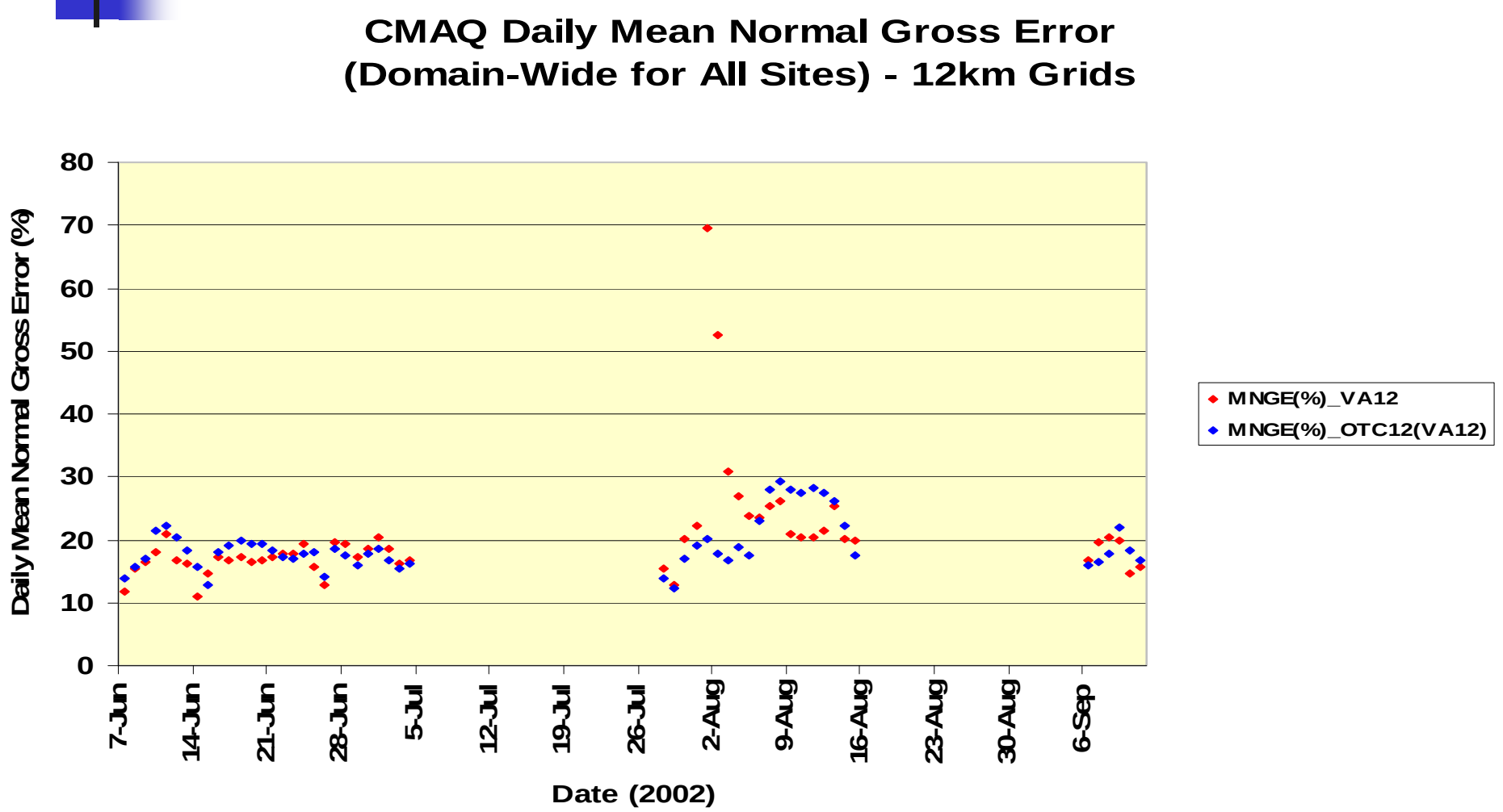

VADEQ & OTC CMAQ Model Performance Summary and Conclusions

- VADEQ 12-km run performed as well or slightly better than VADEQ 4-km run on most ozone episode days
- VADEQ & OTC 12-km runs comparable for June 6 - July 5, 2002 Period with OTC having slightly less negative MNB
- OTC 12-km run outperformed VADEQ 12-km run significantly for small number of episode days during the July 27 - August 16 and September 5 – 12 Periods due to error in JPROC preprocessing. VISTAS to correct problem.

Appendix E
Horizontal Grid Definitions for MM5 and CMAQ Modeling Domains

Table E-1. OTC Grid Definitions for MM5 and CMAQ

Model	Columns Dot (nx)	Rows Dot (ny)	X-Origin (km)	Y-Origin (km)
MM5 36-km	149	129	-2664	-2304
CMAQ 36-km	145	102	-2628	-1728
MM5 12-km	175	175	252	-900
CMAQ 12-km	172	172	264	-888

Appendix F
Vertical Layer Definitions for MM5 and CMAQ Modeling Domains

Table F-1 OTC Vertical Layer Definition for MM5 Simulations and Approach For Reducing CMAQ Layers By Collapsing Multiple MM5 Layers

MM5					CMAQ				
Layer	Sigma	Pres(mb)	Height(m)	Depth(m)	Layer	Sigma	Pres(mb)	Height(m)	Depth(m)
29	0.000	50	18600	2145	23	0.000	50	18600	4290
28	0.040	88.5	16450	2145					
27	0.080	127.1	14300	1460	21	0.080	127.1	14300	2920
26	0.123	168.5	12800	1460					
25	0.168	211.8	11400	1200	20	0.168	211.8	11400	2390
24	0.218	260.0	10200	1200					
23	0.268	308.1	8990	934	19	0.268	308.1	8990	1870
22	0.318	356.3	8060	934					
21	0.368	404.5	7120	772	18	0.368	404.5	7120	1540
20	0.418	452.6	6350	772					
19	0.468	500.8	5580	662	17	0.468	500.8	5580	1320
18	0.518	549.0	4920	662					
17	0.568	597.1	4250	581	16	0.568	597.1	4250	1160
16	0.618	645.3	3670	581					
15	0.668	693.4	3090	532	15	0.668	693.4	3090	532
14	0.718	741.6	2560	455	14	0.781	741.6	2560	455
13	0.763	785.0	2110	388	13	0.763	785.0	2110	388
12	0.803	823.5	1720	337	12	0.803	823.5	1720	337
11	0.839	858.2	1380	290	11	0.839	858.2	1380	290
10	0.871	889.0	1090	247	10	0.871	889.0	1090	247
9	0.899	916.0	844	207	9	0.899	916.0	844	207
8	0.923	939.1	637	169	8	0.923	939.1	637	169
7	0.943	958.3	468	133	7	0.943	958.3	468	133
6	0.959	973.7	334	107	6	0.959	973.7	334	107
5	0.972	986.3	227	82	5	0.972	986.3	227	82
4	0.982	995.9	145	57	4	0.982	995.9	145	57
3	0.989	1002.6	89	40	3	0.989	1002.6	89	40
2	0.994	1007.5	48	27	2	0.994	1007.5	48	27
1	0.9974	1010.7	21	21	1	0.9974	1010.7	21	21
0	1.000	1013.24	0	0	0	1.000	1013.24	0	0

Note: Layer-top pressures assume a surface pressure of 1013.24 hPa. Layer-top heights are determined by averaging MM5 (CMAQ)-calculated layer-top heights over time (August 2002) and space (the entire 172x172 domain).

Appendix G
MM5 Meteorological Model Configuration

Table G-1. OTC MM5 Meteorological Model Configuration

Science Options	Configuration	Details/Comments
Model Code	MM5 Version 3.6	
Horizontal Grid Mesh	36km/12km	
36-km grid	149x129 cells	
12-km grid	175x175 cells	
Vertical Grid Mesh	29 layers	
Grid Interaction	No feedback	Two-way nesting
Initialization	Eta first guess fields/LittleR	
Boundary Conditions	Eta first guess fields/LittleR	
Microphysics	Simple Ice	
Cumulus Scheme	Kain-Fritsch	36km/12km grids
Planetary Boundary Layer	High-resolution Blackadar PBL	
Radiation	Simple cooling	
Vegetation Data	USGS	24 Category Scheme
Land Surface Model	Five-Layer Soil model	
Shallow Convection	None	
Sea Surface Temperature	Do not update SST	
Thermal Roughness	Default	
Snow Cover Effects	None	
4D Data Assimilation	Analysis Nudging: 36km/12km	
Integration Time Step	75 seconds	
Simulation Periods	2002	
Platform	Linux Cluster	Done at UMD

Appendix H
SMOKE Emissions Model Configuration

Emission Processing for the 2002 OTC Regional and Urban 12 km and 36 km Base Case Simulations

Bureau of Air Quality Analysis and Research
Division of Air Resources
New York State Department of Environmental Conservation

May 24, 2005

1. Overview

All emissions processing for the 2002 OTC regional and urban 12 km and 36 km base case simulations was performed with SMOKE2.1 compiled on a Red Hat 9.0 Linux operating system with the Portland group fortran compiler version 5.1. The emissions processing was performed on a month-by-month and RPO-by-RPO basis, i.e. SMOKE processing was performed for the months of May, June, July, August, and September for each of the RPOs (MANE-VU, VISTAS, CENRAP, MRPO, WRAP) individually as well as for Canada and Mexico. Note the processing of WRAP and Mexican emissions was necessary for use with the 36 km grid modeling only. For each month/RPO combination, a separate SMOKE ASSIGNS file was created, and the length of the episode in each of these ASSIGNS files was set to the entire month. Also, as discussed in Section 3, there was no difference between "episode-average" temperatures and "monthly-average" temperatures for the Mobile6 simulations that used the option of temperature averaging.

This document is structured as follows: A listing of all emission inventories is given in Section 2, organized by RPO and source category. Section 3 discusses the Mobile6 processing approach employed for the different RPOs, while Section 4 describes the processing of biogenic emissions with BEIS3.12. Finally, Sections 5 through7 describe the temporal allocation, speciation, and spatial allocation of the emissions inventories, respectively.

2. Emission Inventories

2.1 MANE-VU

The emissions inventory data were obtained from the MANEVU archive in February 2005. This inventory was deemed acceptable for the current work, although it is possible that there may be revisions forthcoming based upon further state review.

2.1.1 Area Sources

- File: MANEVU_AREA_SMOKE_INPUT_ANNUAL_SUMMERDAY_011705.txt prepared by PECHAN, was downloaded from **ftp.marama.org** (username mane-vu, password exchange)
- Fugitive dust correction: This was applied as county-specific correction factors for SCC's listed at http://www.epa.gov/ttn/chief/emch/invent/index.html#dust; the correction factors were obtained from http://www.epa.gov/ttn/chief/emch/invent/transportfractions.xls; this adjustment was performed outside of SMOKE with in-house Fortran programs

2.1.2 Nonroad Sources

- Files: CT_NRD2002.IDA, DC_NRD2002.IDA, DE_NRD2002.IDA, MA_NRD2002.IDA, MD_NRD2002.IDA, ME_NRD2002.IDA, NH_NRD2002.IDA, NJ_NRD2002.IDA, NY_NRD2002.IDA,

PA_NRD2002.IDA, RI_NRD2002.IDA, and VT_NRD2002.IDA contained in the "MANE-VU Nrd SMOKE files.zip" file prepared by PECHAN were downloaded from **ftp.marama.org** (username mane-vu, password exchange)

2.1.3 Mobile Sources

- VMT/Speed: MANEVU_2002_mbinv.txt prepared by PECHAN were downloaded from **ftp.marama.org** (username mane-vu, password exchange)

2.1.4 Point Sources

- File: MANEVU_Point_SMOKE_INPUT_ANNUAL_SUMMERDAY_122004.txt prepared by PECHAN were downloaded from **ftp.marama.org** (username mane-vu, password exchange)
- Fugitive dust correction: This was applied as county-specific correction factors for SCC's listed at http://www.epa.gov/ttn/chief/emch/invent/index.html#dust; the correction factors were obtained from http://www.epa.gov/ttn/chief/emch/invent/transportfractions.xls; this adjustment was performed outside of SMOKE with in-house Fortran programs
- Emission corrections were made for "THE HARTFORD STEAM CO" in Connecticut, Plant ID P0250.

2.2 CENRAP

The inventory data were obtained from CENRAP website in January and February 2005.

2.2.1 Area Sources

- Files:
  - CENRAP_AREA_SMOKE_INPUT_ANN_STATES_120704.txt
  - CENRAP_AREA_MISC_SMOKE_INPUT_ANN_STATE_120704.txt
  - CENRAP_AREA_BURNING_SMOKE_INPUT_ANN_TX_AR_NELI_120704.txt
  - CENRAP_AREA_MISC_SMOKE_INPUT_NH3_MONTH_{MMM}_120304.txt where {MMM} is MAY, JUN, JUL, AUG, or SEP
  - CENRAP_AREA_SMOKE_INPUT_NH3_MONTH_{MMM}_120304.txt where {MMM} is MAY, JUN, JUL, AUG, or SEP
  - All files were downloaded from the CENRAP website http://www.cenrap.org/emission_document.asp
- Fugitive dust correction: This was applied as county-specific correction factors for SCC's listed at http://www.epa.gov/ttn/chief/emch/invent/index.html#dust; the correction factors were obtained from http://www.epa.gov/ttn/chief/emch/invent/transportfractions.xls; this adjustment was performed outside of SMOKE with in-house Fortran programs

2.2.2 Nonroad Sources

- File: CENRAP_NONROAD_SMOKE_INPUT_ANN_120704.txt downloaded from the CENRAP website http://www.cenrap.org/emission_document.asp

2.2.3 Mobile Sources

- VMT/Speed files: mbinv02_vmt_cenrap_ce.ida, mbinv02_vmt_cenrap_no.ida, mbinv02_vmt_cenrap_so.ida, and mbinv02_vmt_cenrap_we.ida, downloaded from the CENRAP website http://www.cenrap.org/emission_document.asp

2.2.4 Point Sources

- Files:
    - Annual: CENRAP_Point_SMOKE_INPUT_ANN_121004.txt
    - Hour-specific CEM: pthour.{QQ}.{ST}.txt where {QQ} is the quarter (q1, q2, q3, or q4) and {ST} is the state (AR, IA, KS, LA, MN, MO, NE, OK, TX)
    - All files were downloaded from the CENRAP website http://www.cenrap.org/emission_document.asp
- Fugitive dust correction: This was applied as county-specific correction factors for SCC's listed at http://www.epa.gov/ttn/chief/emch/invent/index.html#dust; the correction factors were obtained from http://www.epa.gov/ttn/chief/emch/invent/transportfractions.xls; this adjustment was performed outside of SMOKE with in-house Fortran programs

2.3 VISTAS

All VISTAS emission files were obtained from Greg Stella of VISTAS. These files contained emissions for the entire country and were then split by RPOs and renamed accordingly. For example, the file ida_ar_2002_rev_29sep04.emis obtained from Greg Stella was split into ida_ar_2002_rev_29sep04.vistas.emis, ida_ar_2002_rev_29sep04.cenrap.emis, ida_ar_2002_rev_29sep04.manevu.emis, ida_ar_2002_rev_29sep04.wrap.emis, and ida_ar_2002_rev_29sep04.mrpo.emis, and only the "vistas" portion was utilized.

2.3.1 Area Sources

- Files:
    - ida_ar_2002_rev_29sep04.vistas.emis
    - arinv_2002_ncnox_01apr05.emis
    - ida_ar_fire_typ_29nov04.vistas.emis
    - ida_ar_dust_2002_wfac_27nov04.vistas.emis
- All files were obtained from Greg Stella (VISTAS) and were processed to extract VISTAS-only emissions as described above.
- Note: the header lines of these files indicate that the fugitive dust correction was already applied, so no further correction was performed.

2.3.2 Nonroad Sources

File: ida_nr_2002_rev_01oct.vistas.emis was obtained from Greg Stella (VISTAS) and processed to extract VISTAS-only emissions as described above.

2.3.3 Mobile Sources

- VMT/Speed file: mbinv_2002_ida_vmt_22sep04.vistas.txt, obtained from Greg Stella (VISTAS) and was processed to extract VISTAS-only VMT as described above.

2.3.4 Point Sources

- Files:
    - Annual: ptinv_2002typ_28nov04.vistas.ida and ptinv_fires_{MM}_typ.vistas.txt where {MM} is 01, 02, 03, etc. depending on the month
    - Hour-specific: pthour_rev2002typ_{MMM}_08nov04.vistas.ems and pthour_fires_{MM}_typ.vistas.ida where {MMM} is jan, feb, mar, etc. and {MM} is 01, 02, 03, etc. depending on the month
- All files were obtained from Greg Stella (VISTAS) and were processed to extract VISTAS-only emissions as described above.
- Note: the header lines of these files indicate that the fugitive dust correction was already applied, so no further correction was performed.

2.4 MRPO

MRPO emissions were obtained from Greg Stella (utilized for the VISTAS revised Phase II modeling) because MRPO BaseI emissions in IDA format were not yet available for all source categories when the current emissions processing was performed. As noted above, all VISTAS emission files obtained from Greg Stella contained emissions for the entire country. After obtaining these original files, we then split them by state groups into emission inventories for the different RPOs and were renamed accordingly. For example, the file ida_ar_2002_rev_29sep04.emis obtained from Greg Stella was split into ida_ar_2002_rev_29sep04.vistas.emis, ida_ar_2002_rev_29sep04.cenrap.emis, ida_ar_2002_rev_29sep04.manevu.emis, ida_ar_2002_rev_29sep04.wrap.emis, and ida_ar_2002_rev_29sep04.mrpo.emis and only the “mrpo” portion was utilized for the MRPO emissions processing.

2.4.1 Area Sources

- Files:
    - ida_ar_2002_rev_29sep04.mrpo.emis
    - ida_ar_fire_typ_29nov04.mrpo.emis
    - ida_ar_dust_2002_wfac_27nov04.mrpo.emis
- All files were obtained from Greg Stella (VISTAS) and processed to extract MRPO-only emissions as described above.

- Note: the header lines of these files indicate that the fugitive dust correction was already applied, so no further correction was performed.

2.4.2 Nonroad Sources

File: ida_nr_2002_rev_01oct.wrap.emis, obtained from Greg Stella (VISTAS) and processed to extract WRAP-only emissions as described above.

2.4.3 Mobile Sources

- VMT/Speed file: mbinv_2002_ida_vmt_22sep04.mrpo.txt, obtained from Greg Stella (VISTAS) and were processed to extract MRPO-only VMT as described above in the VISTAS section.
- Note: Per email exchange between Gopal Sistla, Mark Janssen and Jeff Vukovich, it was determined that the VMT information used by VISTAS for their revised Phase II modeling reflects the latest MRPO information. Therefore, the MRPO-portion of the mobile source files obtained from Greg Stella (VISTAS), were used in this work.

2.4.4 Point Sources

- Files:
    - Annual: ptinv_2002typ_28nov04.mrpo.ida and ptinv_fires_{MM}_typ.mrpo.txt where {MM} is 01, 02, 03, etc. depending on the month
    - Hour-specific: pthour_rev2002typ_{MMM}_08nov04.mrpo.ems and pthour_fires_{MM}_typ.mrpo.ida where {MMM} is jan, feb, mar, etc. and {MM} is 01, 02, 03, etc. depending on the month
- All files were obtained from Greg Stella (VISTAS) and processed to extract MRPO-only emissions as described above.
- Note: the header lines of these files indicate that the fugitive dust correction was already applied, so no further correction was performed

2.5 WRAP

WRAP emissions are only needed for the 36 km modeling grid, which will provide boundary conditions for the 12 km modeling grid. Therefore, it was decided that the WRAP-portion of the files obtained from Greg Stella (utilized for the VISTAS revised Phase II modeling) would be sufficient rather than obtaining data from WRAP directly. As noted above all VISTAS emission files obtained from Greg Stella contained emissions for the entire country. After obtaining these original files, we then split them by state groups into emission inventories for the different RPOs and were renamed accordingly. For example, the file ida_ar_2002_rev_29sep04.emis obtained from Greg Stella was split into ida_ar_2002_rev_29sep04.vistas.emis, ida_ar_2002_rev_29sep04.cenrap.emis, ida_ar_2002_rev_29sep04.manevu.emis, ida_ar_2002_rev_29sep04.wrap.emis, and ida_ar_2002_rev_29sep04.mrpo.emis and only the “wrap” portion was utilized for the WRAP emissions processing.

2.5.1 Area Sources

- Files:
  - ida_ar_2002_rev_29sep04.wrap.emis
  - ida_ar_fire_typ_29nov04.wrap.emis
  - ida_ar_dust_2002_wfac_27nov04.wrap.emis
- All files were obtained from Greg Stella (VISTAS) and processed to extract WRAP-only emissions as described above.
- Note: the header lines of these files indicate that the fugitive dust correction was already applied, so no further correction was performed.

2.5.2 Nonroad Sources

File: ida_nr_2002_rev_01oct.wrap.emis, obtained from Greg Stella (VISTAS) and processed to extract WRAP-only emissions as described above.

2.5.3 Mobile Sources

- VMT/Speed file: mbinv_2002_ida_vmt_22sep04.wrap.txt, obtained from Greg Stella (VISTAS) and processed to extract WRAP-only VMT as described above.

2.5.4 Point Sources

- Files:
  - Annual: ptinv_2002typ_28nov04.wrap.ida and ptinv_fires_{MM}_typ.wrap.txt where {MM} is 01, 02, 03, etc. depending on the month
  - Hour-specific: pthour_rev2002typ_{MMM}_08nov04.wrap.ems and pthour_fires_{MM}_typ.wrap.ida where {MMM} is jan, feb, mar, etc. and {MM} is 01, 02, 03, etc. depending on the month
- All files were obtained from Greg Stella (VISTAS) and processed to extract WRAP-only emissions as described above.
- Note: the header lines of these files indicate that the fugitive dust correction was already applied, so no further correction was performed.

2.6 Canada

2.6.1 Area Sources

- File: AS2000_SMOKEready.txt obtained from ftp://ftp.epa.gov/EmisInventory/canada_2000inventory
- Fugitive dust correction: We applied “divide-by-four” correction for SCC’s listed at http://www.epa.gov/ttn/chief/emch/invent/index.html#dust; this adjustment was performed outside SMOKE with in-house Fortran programs. No county/province-specific correction factors were available for Canada

2.6.2 Nonroad Sources

- File: NONROAD2000_SMOKEready.txt obtained from ftp://ftp.epa.gov/EmisInventory/canada_2000inventory

2.6.3 Mobile Sources

- File: MOBILE2000_SMOKEready.txt obtained from ftp://ftp.epa.gov/EmisInventory/canada_2000inventory
- Fugitive dust correction: applied "divide-by-four" correction for SCC's listed at http://www.epa.gov/ttn/chief/emch/invent/index.html#dust; this adjustment was performed outside of SMOKE with in-house Fortran programs. No county/province-specific correction factors were available for Canada.

2.6.4 Point Sources

There has long been difficulty in obtaining an up-to-date Canadian criteria emissions inventory for point sources. This is due largely to confidentiality rights afforded to Canadian facilities. Thus far, the most recent inventory of Canadian point sources is rooted in the 1985 NAPAP data and is close to two decades old. Because there are a number of high emitting industrial facilities in southern Canada it is of particular importance to have a reasonably accurate inventory of these sources especially when modeling air quality over the Northeast and Midwest United States. Toward this end, an effort was made to obtain more recent Canadian point source data and incorporate it into an inventory database, which could then be used for the 2002 OTC air quality modeling.

Perhaps the most accurate and publicly accessible source of Canadian pollutant data is now available from the National Pollutant Release Inventory (NPRI) database. This database contains 268 substances. Facilities that manufacture, process or otherwise use one of these substances and that meet reporting thresholds are required to report these emissions to Environment Canada on an annual basis. The NPRI data are available at Environment Canada's website and can be found at the link http://www.ec.gc.ca/pdb/npri/npri_home_e.cfm. The page hosts an on-line search engine where one can locate emissions by pollutant or location. In addition, the entire database is available for download as an MS Access or Excel file. The NPRI database contains numerous pages with a rather comprehensive list of information. Detailed information is available about each facility, including location, activity and annual emissions. In addition, facilities having stacks with a height of 50 meters or more are required to report stack parameters.

Unfortunately, one of the limitations of the NPRI database for modeling purposes is that the data are only available at the facility level. Emissions models require process level information, so in order to use this data, a few generalizations had to be made. Each facility has a Standard Industrial Classification (SIC) code associated with it; however, emissions models require Source Classification Codes (SCC's). SCC's are of critical importance as the emissions models use these codes for assignment of temporal and

speciation profiles. SIC codes describe the general activity of a facility while SCC codes describe specific processes taking place at each facility. While no direct relationship exists between these two codes, a general albeit subjective association can be made.

For the purposes of creating a model-ready inventory file it was necessary to obtain the whole NPRI database. After merging all the necessary components from the NPRI database required in the SMOKE inventory file, the SIC code from each facility was examined and assigned an SCC code. In most cases, only a SCC3 level code was assigned with confidence. While this is admittedly a less than desirable process, it does allow for the use of the most recent emissions from the NPRI database to be used in modeling. Furthermore, having some level of SCC associated with these emissions will ensure that they will be assigned a temporal and speciation profile by the model, other than the default. Once the model-ready inventory file was developed, it was processed through SMOKE.

2.7 Mexico

2.7.1 Area Sources / Nonroad Sources / Mobile Sources

- File: arinv.mx.ver7.txt, includes combined area/nonroad/mobile sources for 1999, obtained from EPA's CAIR NODA ftp site airmodelingftp.com (password protected)

2.7.2 Point Sources

- File: ptinv_mx_dat.bravo.txt, obtained from EPA's CAIR NODA ftp site airmodelingftp.com (password protected)

3. Mobile6 Processing

3.1 MANE-VU

3.1.1 Mobile6 input files

- Month-specific input files contained in the file "MANEVU_2002_SMOKE_M6_InputFiles_12032004.zip", prepared by PECHAN and were downloaded from **ftp.marama.org** (username mane-vu, password exchange)
- Added the line "REBUILD EFFECTS :0.10" to each file before the SCENARIO record to override the Mobile6 default setting of 0.9 (90%) for the "chip reflash" effectiveness

3.1.2 SMOKE/Mobile6 auxiliary files

- SMOKE/Mobile6 auxiliary files were contained in the file "MANEVU_2002_SMOKE_M6_ExternalFiles.zip", prepared by PECHAN and were downloaded from **ftp.marama.org** (username mane-vu, password

exchange). Furthermore, the SMOKE MCREF, MVREF, SPDREF, SPDPRO, and MCODES files were also obtained from this ftp site.

3.1.3 Temperature averaging

- Following the setting in the MANEVU_2002_mvref.txt files, the following procedures were used by SMOKE for temporal and spatial temperature averaging in the calculation of emission factors:
    - Spatial averaging: temperatures were averaged over all counties that share a common reference county (i.e. Mobile6 input file)
    - Temporal averaging: no temporal averaging was used, i.e. day-specific temperatures were used to calculate emission factors for each day.

3.2 CENRAP

3.2.1 Mobile6 input files

- Mobile6 input files for the CENRAP region for January and July were contained in the files central_M6_{MMM}.zip, north_M6_{MMM}.zip, south_M6_{MMM}.zip, west_M6_{MMM}.zip where {MMM} is either jan or jul. Only the July input files were used for the current emissions processing that was performed for the time period from May through September 2002.
- All files were downloaded from the CENRAP website http://www.cenrap.org/emission_document.asp

3.2.2 SMOKE/Mobile6 auxiliary files

- SMOKE/Mobile6 auxiliary files were contained in the files central_M6_RD.zip, north_M6_RD.zip, south_M6_RD.zip, west_M6_RD.zip, prepared by PECHAN and downloaded from **ftp.marama.org** (username mane-vu, password exchange). Furthermore, the SMOKE MCREF, MVREF, and MCODES files were also obtained. The MCREF and MVREF files were combined for the different regions ("central", "east", "west", "north")
- All files were downloaded from the CENRAP website http://www.cenrap.org/emission_document.asp

3.2.3 Temperature averaging

- The following procedures were used by SMOKE for temporal and spatial temperature averaging in the calculation of emission factors according to the setting in the mvref files:
    - Spatial averaging: no spatial averaging of temperatures, i.e. the temperatures for the reference county is used to calculate emission factors for all counties that share this reference county (i.e. Mobile6 input file)
    - Temporal averaging: Temporal averaging over the duration of the episode (i.e. the entire month, see introduction) was used, i.e. monthly average temperatures were used to calculate the emission factors.

3.3 VISTAS, MRPO, and WRAP

The VISTAS, MRPO, and WRAP portions of the national Mobile6 files obtained from Greg Stella (utilized for the VISTAS revised Phase II modeling) were utilized for these RPOs

3.3.1 Mobile6 input files

- Month-specific Mobile6 input files for the entire U.S. utilized in the VISTAS revised Phase II modeling were obtained from Greg Stella (VISTAS) and were reorganized by RPO; the input files for the VISTAS, WRAP, and MRPO regions were utilized for the OTC emission processing.

3.3.2 SMOKE/Mobile6 auxiliary files

- SMOKE/Mobile6 auxiliary files utilized in the VISTAS revised Phase II modeling were obtained from Greg Stella (VISTAS) and utilized for the OTC emission processing for the VISTAS, WRAP, and MRPO regions. Furthermore, the mcref_vistas2_txt_revised.ag, mvref_vista_pIIrev_091504.ag, and mcodes.txt files were also obtained from Greg Stella.

3.3.3 Temperature averaging

- The following procedures were used by SMOKE for the temporal and spatial temperature averaging in the calculation of emission factors according to the setting in the mvref_vista_pIIrev_091504.ag file:
    - Spatial averaging: temperatures averaged over all counties that share a common reference county (i.e. Mobile6 input file)
    - Temporal averaging: Temporal averaging over the duration of the episode (i.e. the entire month, see introduction) was used, i.e. monthly average temperatures were used to calculate the emission factors.

4. Biogenic Emission Processing

Hourly gridded biogenic emissions for the 12 km and 36 km modeling domains were calculated by BEIS3.12 through SMOKE, using MCIP-processed MM5 fields for temperature ("TA", layer-1 temperature), solar radiation ("RGRND"), surface pressure ("PRES"), and precipitation ("RN" and "RC").

5. Temporal Allocation

5.1 MANE-VU

5.1.1 Area and nonroad sources

- amptpro.m3.us+can.manevu.030205.txt
- amptref.m3.manevu.012405.txt
- downloaded from **ftp.marama.org** (username mane-vu, password exchange)

5.1.2 Mobile sources

- MANEVU_2002_mtpro.txt
- MANEVU_2002_mtref.txt
- Generated by PECHAN, and were downloaded from **ftp.marama.org** (username mane-vu, password exchange), part of the "2002 MANE-VU Onroad/FINAL_SMOKE_FILES" directory

5.1.3 Point Sources

- Based on the same files as for the MANE-VU area and nonroad temporal files listed above, but added the VISTAS-generated CEM-based 2002 state-specific temporal profiles and cross-references for EGU sources for the MANE-VU states
- No CEM-based hour-specific EGU emissions were utilized

5.2 CENRAP

The following temporal profiles and cross-reference files were used for all source categories:

- amptpro.m3.us_can.cenrap.010605.txt
- amptref.m3.cenrap.010605.txt
- These files were downloaded from the CENRAP website http://www.cenrap.org/emission_document.asp
- For point sources, the CEM-based hour-specific EGU emissions described in Section 2.2.4 were utilized to override the annual-total based emissions whenever a match could be established by SMOKE

5.3 VISTAS, WRAP and MRPO

The following month-specific temporal profiles and cross-reference files were used for all source categories:

- amptpro_typ_us_can_{MMM}_vistas_27nov04.txt where {MMM} is jan, feb, mar, etc.
- amptref_2002_us_can_vistas_17dec04.txt
- These files were obtained from Greg Stella (VISTAS)
- For point sources (EGU and fires), the hour-specific emission files described in Sections 2.3.4 and 2.5.4 were utilized for the VISTAS and WRAP states to override the annual-total based emissions whenever a match could be established by SMOKE

5.4 Canada and Mexico

For Canada and Mexico, the SMOKE2.1 default temporal profiles and cross-reference files (amptpro.m3.us+can.txt and amptref.m3.us+can.txt) were utilized.

6. Speciation

The same speciation profiles (gspro.cmaq.cb4p25.txt) and cross-references (gsref.cmaq.cb4p25.txt) were utilized for all regions and all source categories. Different versions of these files were obtained (SMOKE2.1 default, EPA-CAIR modeling, VISTAS, CENRAP and MANE-VU) and compared. After comparing the creation dates and header lines of these files, it was determined that the EPA-CAIR and MANE-VU files had the most recent updates, and consequently the final speciation profile and cross-reference files used for all regions and source categories was based on the EPA-CAIR files with the addition of MANE-VU specific updates.

7. Spatial Allocation

7.1 U.S.

The spatial surrogates for the 12 km and 36 km domains were extracted from the national grid 12 km and 36 km U.S. gridding surrogates posted at EPA's website at http://www.epa.gov/ttn/chief/emch/spatial/newsurrogate.html
The gridding cross-references were also obtained from this website, but for the processing of MANE-VU area source emissions, MANE-VU specific cross-reference entries posted on the MARAMA ftp site were added.

7.2 Canada

The spatial surrogates for Canadian emissions for the 12 km and 36 km domains were extracted from the national grid 12 km and 36 km Canadian gridding surrogates posted at EPA's website at http://www.epa.gov/ttn/chief/emch/spatial/newsurrogate.html
The gridding cross-references were also obtained from this website.

7.3 Mexico

The spatial surrogates for Mexican emissions the 36 km domain were extracted from the national 36 km gridding surrogates used by EPA in the CAIR modeling. These files were obtained from EPA's CAIR NODA ftp site http://www.airmodelingftp.com
(password protected). The gridding cross-references were also obtained from this ftp site.

Appendix I
CMAQ Air Quality Model Configuration

Table I-1. OTC CMAQ Air Quality Model Configuration

Science Options	Configuration	Details/Comments
Model	CMAQ Version 4.5	
Horizontal Grid Mesh	36km/12km	
36-km grid	145x102 cells	
12-km grid	172x172 cells	
Vertical Grid Mesh	22 Layers	
Grid Interaction	One-way nesting	
Boundary Conditions	GEOS-CHEM	
Emissions		
Baseline Emissions Processing	SMOKE (Version 2.1) model configuration	MM5 meteorology input to SMOKE & CMAQ
Sub-grid-scale Plumes	No Plume –in-Grid (PinG)	
Chemistry		
Gas Phase Chemistry	CBM-IV	
Aerosol Chemistry	AE3/ISORROPIA	
Secondary Organic Aerosols	Secondary Organic Aerosol Model (SORGAM)	
Aerosol Mass Conservation Patch	Yes	Schell et. al., (2001)
Cloud Chemistry	RADM-type aqueous chemistry	Includes sub-grid cloud processes
N_2O_5 Reaction Probability	0.01-0.001	
Meteorological Processor	MCIP Version 3.0	
Horizontal Transport		
Eddy Diffusivity Scheme	K-theory with Kh grid size dependence	Multi-scale Smagorinsky (1963) approach
Vertical Transport		
Eddy Diffusivity Scheme	K-theory	
Diffusivity Lower Limit	Kzmin = 1.0	
Planetary Boundary Layer	No Patch	
Deposition Scheme	M3dry	Directly linked to Pleim-Xiu Land Surface Model parameters
Numerics		
Gas Phase Chemistry Solver	Euler Backward Iterative (EBI) solver	Hertel et. Al. (1993) EBI solver ~2x faster than MEBI
Horizontal Advection Scheme	Piecewise Parabolic Method (PPM) scheme	
Simulation Periods	2002	
Platform	Linux Cluster	

Appendix J
Supplemental Analyses and Weight of Evidence Techniques

	Attainment Demonstration			Pollution Apportionment			Transport (more general)			
WOE Techique	O3	PM mass	PM species/H	O3	PM mass	PM species/Haze	O3	PM mass	PM species/Haze	O3
Grid Models										
CMAQ modeling	**OTC/MV**	**OTC/MV**	**OTC/MV**				**P(movie)**	**P(movie)**	**MV(movies)**	
CMAQ with DDM				**P**	**?**	**?**	**P**			**?**
REMSAD Tagged Species Model		**P**	**MV**		**P**	**MV**		**P**	**MV(movies)**	
CALGRID	**OTC**	**OTC**	**P**	**P**	**P**	**P**	**OTC(movies)**	**OTC(movies)**		**?**
CAMx										
CAMx with PSAT/OSAT										
EPA CAIR Modeling	**P**	**P**					**P**	**P**		
Dispersion Models										
CALPUFF (NWS obs) [cannot be used for O3]		**P**	**MV**		**P**	**MV**		**P(movies)**	**P(movies)**	
CALPUFF (MM5) [cannot be used for O3]		**P**	**MV**		**P**	**MV**		**P(movies)**	**P(movies)**	
Trajectory & Met Data Analysis Techniques										
Everyday probability of good days/bad days								**MV**	**MV**	
Incremental Probability (HYSPLIT: 200, 500, 1000 m)				**P**	**MV**	**MV**	**P**	**MV**	**MV**	
Incremental Probability (ATAD)				**P**	**P**	**P**	**P**	**P**	**P**	
Cluster Weighted Probability (HYSPLIT: 200, 500, 1000 m)				**P**	**MV**	**MV**	**P**	**MV**	**MV**	
Wind direction frequency analysis (local)							**P-ES: ME**	**P-ES: ME**		
Forward trajectories from source regions							**P-ES: ME**	**P**	**P**	
Interannual Variability of Trajectory Clusters										
Low altitude 24-hour trajectories(local transport)							**P-ES: ME**	**P**	**P**	
Trajectory analyses using profiler data compared with HYSPLIT trajectories							**P**	**P**		
Source Apportionment/Factor Analysis Receptor Methods										
Multi-site analysis of Inc. Prob. For various factors				**?**	**MV+**	**MV+**		**MV+**	**MV+**	
Historical Analysis of Factors Over Time?		**?**	**?**							
%time upwind x %emissions				**P**	**P**	**MV**				
Kenski Metric Analysis					**P**	**P**		**P**	**P**	
Monitoring Data/Inventory Analysis										
Trends in DVs										
Monitor Exceedances										
Trends in NO2-NO-NOx-NOy-CO										
meteorologically adjusted trend analysis										
Historical Trends Analysis (PAMS)										
Historical Trends Analysis (IMPROVE)										
Historical Trends Analysis (FRM/TEOMs?)										
Spatial analysis of FRM/TEOM data (MARAMA)					**MARAMA**					
Emissions Inventory Trends				**P**	**P**	**MV**				
Compare 2002 versus 2004 PAMS & STN data--> effect of NOx SIP Call							**P**	**P**		
Aged vs fresh air mass analysis (benzene/toulene ratios & benzene/xylene ratios)							**P**			
Emissions divided by Distance, compare to CALPUFF results	**?**		**MV**	**?**		**MV**				
Historical trend of use of SO2 credits										
NOx vs VOC limited analysis							**P**			
RAIN Data Analysis								**MV**	**MV**	
Literature Review / Other										
Low level jet analyses							**MD**	**?**		

	Attainment Demonstration			Pollution Apportionment			Transport (more general)			
WOE Techique	O3	PM mass	PM species/H	O3	PM mass	PM species/Haze	O3	PM mass	PM species/Haze	O3
Blackout paper							**UMD**			
Additional measures not modeled: retrofits, energy conservation, Supplemental Environmental Projects										**P-ES**
OTC = doing analysis; **MV** = doing analysis **P** = Analysis Possibily **P** = Priority Analysis Possibily **P-ES** = Analysis Possible, state-by-state basis										

	Small measures		Historical control effectiveness (Trends Analysis)		
WOE Techique	PM mass	PM species/Haze	O3	PM mass	PM species/Haze
Grid Models					
CMAQ modeling					
CMAQ with DDM					
REMSAD Tagged Species Model					
CALGRID	**?**				
CAMx					
CAMx with PSAT/OSAT					
EPA CAIR Modeling					
Dispersion Models					
CALPUFF (NWS obs) [cannot be used for O3]					
CALPUFF (MM5) [cannot be used for O3]					
Trajectory & Met Data Analysis Techniques					
Everyday probability of good days/bad days					
Incremental Probability (HYSPLIT: 200, 500, 1000 m)					
Incremental Probability (ATAD)					
Cluster Weighted Probability (HYSPLIT: 200, 500, 1000 m)					
Wind direction frequency analysis (local)					
Forward trajectories from source regions					
Interannual Variability of Trajectory Clusters			**P**	**P**	**P**
Low altitude 24-hour trajectories(local transport)					
Trajectory analyses using profiler data compared with HYSPLIT trajectories					
Source Apportionment/Factor Analysis Receptor Methods					
Multi-site analysis of Inc. Prob. For various factors					
Historical Analysis of Factors Over Time?				**?**	**?**
%time upwind x %emissions					
Kenski Metric Analysis					
Monitoring Data/Inventory Analysis					
Trends in DVs			**P-ES**	**P-ES**	
Monitor Exceedances			**P-ES**	**P-ES**	
Trends in NO2-NO-NOx-NOy-CO			**P-ES:NH**	**P-ES:NH**	
meteorologically adjusted trend analysis			**P:ME/MD?**	**P**	**P**
Historical Trends Analysis (PAMS)			**P-ES: ME/MA/CT**		
Historical Trends Analysis (IMPROVE)				**P**	**MV**
Historical Trends Analysis (FRM/TEOMs?)				**?**	
Spatial analysis of FRM/TEOM data (MARAMA)					
Emissions Inventory Trends			**P-ES**	**P-ES**	
Compare 2002 versus 2004 PAMS & STN data--> effect of NOx SIP Call					
Aged vs fresh air mass analysis (benzene/toulene ratios & benzene/xylene ratios)					
Emissions divided by Distance, compare to CALPUFF results					
Historical trend of use of SO2 credits				**P**	
NOx vs VOC limited analysis			**P**		
RAIN Data Analysis					
Literature Review / Other					
Low level jet analyses					

	Small measures		Historical control effectiveness (Trends Analysis)		
WOE Techique	PM mass	PM species/Haze	O3	PM mass	PM species/Haze
Blackout paper			**UMD**		
Additional measures not modeled: retrofits, energy conservation, Supplemental Environmental Projects	**P-ES**				
OTC = doing analysis; **MV** = doing analysis **P** = Analysis Possibily **P** = Priority Analysis Possibily **P-ES** = Analysis Possible, state-by-state basis					

Appendix F-2

Conceptual Description

The Nature of the Ozone Air Quality Problem in the Ozone Transport Region: A Conceptual Description

Prepared for the Ozone Transport Commission

Prepared by NESCAUM
Boston, MA

Final
October 2006

Contributing Authors

Tom Downs, Maine Department of Environmental Protection
Richard Fields, Massachusetts Department of Environmental Protection
Prof. Robert Hudson, University of Maryland
Iyad Kheirbek, NESCAUM
Gary Kleiman, NESCAUM
Paul Miller, NESCAUM
Leah Weiss, NESCAUM

Acknowledgements

NESCAUM thanks the Mid-Atlantic Regional Air Management Association for providing the foundational basis of this report.

NESCAUM also thanks the following people for their comments and input during the development of this report:

Tad Aburn, Maryland Department of the Environment
Michael Geigert, Connecticut Department of Environmental Protection
Kurt Kebschull, Connecticut Department of Environmental Protection
Tonalee Key, New Jersey Department of Environmental Protection
Mohammed A. Majeed, Delaware Department of Natural Resources and Environmental Conservation
Charles Pietarinen, New Jersey Department of Environmental Protection
Jeff Underhill, New Hampshire Department of Environmental Services
David Wackter, Connecticut Department of Environmental Protection
Martha Webster, Maine Department of Environmental Protection
Danny Wong, New Jersey Department of Environmental Protection
Jung-Hun Woo, NESCAUM
Michael Woodman, Maryland Department of the Environment

TABLE OF CONTENTS

FIGURES

TABLES

Executive Summary

The Ozone Transport Region (OTR) of the eastern United States covers a large area that is home to over 62 million people living in Connecticut, Delaware, the District of Columbia, Maine, Maryland, Massachusetts, New Hampshire, New Jersey, New York, Pennsylvania, Rhode Island, Vermont, and northern Virginia. Each summer, the people who live within the OTR are subject to episodes of poor air quality resulting from ground-level ozone pollution that affects much of the region. During severe ozone events, the scale of the problem can extend beyond the OTR's borders and include over 200,000 square miles across the eastern United States. Contributing to the problem are local sources of air pollution as well as air pollution transported hundreds of miles from distant sources outside the OTR.

To address the ozone problem, the Clean Air Act Amendments require states to develop State Implementation Plans (SIPs) detailing their approaches for reducing ozone pollution. As part of this process, states are urged by the U.S. Environmental Protection Agency (USEPA) to include in their SIPs a conceptual description of the pollution problem in their nonattainment areas. This document provides the conceptual description of the ozone problem in the OTR states, consistent with the USEPA's guidance.

Since the late 1970s, a wealth of information has been collected concerning the regional nature of the OTR's ground-level ozone air quality problem. Scientific studies have uncovered a rich complexity in the interaction of meteorology and topography with ozone formation and transport. The evolution of severe ozone episodes in the eastern U.S. often begins with the passage of a large high pressure area from the Midwest to the middle or southern Atlantic states, where it assimilates into and becomes an extension of the Atlantic (Bermuda) high pressure system. During its passage east, the air mass accumulates air pollutants emitted by large coal-fired power plants and other sources located outside the OTR. Later, sources within the OTR make their own contributions to the air pollution burden. These expansive weather systems favor the formation of ozone by creating a vast area of clear skies and high temperatures. These two prerequisites for abundant ozone formation are further compounded by a circulation pattern favorable for pollution transport over large distances. In the worst cases, the high pressure systems stall over the eastern United States for days, creating ozone episodes of strong intensity and long duration.

One transport mechanism that has fairly recently come to light and can play a key role in moving pollution long distances is the nocturnal low level jet. The jet is a regional scale phenomenon of higher wind speeds that often forms during ozone events a few hundred meters above the ground just above the stable nocturnal boundary layer. It can convey air pollution several hundreds of miles overnight from the southwest to the northeast, directly in line with the major population centers of the Northeast Corridor stretching from Washington, DC to Boston, Massachusetts. The nocturnal low level jet can extend the entire length of the corridor from Virginia to Maine, and has been observed as far south as Georgia. It can thus be a transport mechanism for bringing ozone and other air pollutants into the OTR from outside the region, as well as move locally formed air pollution from one part of the OTR to another.

Other transport mechanisms occur over smaller scales. These include land, sea, mountain, and valley breezes that can selectively affect relatively local areas. They play a vital role in drawing ozone-laden air into some areas, such as coastal Maine, that are far removed from major source regions.

With the knowledge of the different transport scales into and within the OTR, a conceptual picture of bad ozone days emerges. After sunset, the ground cools faster than the air above it, creating a nocturnal temperature inversion. This stable boundary layer extends from the ground to only a few hundred meters in altitude. Above this layer, a nocturnal low level jet can form with higher velocity winds relative to the surrounding air. It forms from the fairly abrupt removal of frictional forces induced by the ground that would otherwise slow the wind. Absent this friction, winds at this height are free to accelerate, forming the nocturnal low level jet. Ozone above the stable nocturnal inversion layer is likewise cut off from the ground, and thus it is not subject to removal on surfaces or chemical destruction from low level emissions. Ozone in high concentrations can be entrained in the nocturnal low level jet and transported several hundred kilometers downwind overnight. The next morning as the sun heats the Earth's surface, the nocturnal boundary layer begins to break up, and the ozone transported overnight mixes down to the surface where concentrations rise rapidly, partly from mixing and partly from ozone generated locally. By the afternoon, abundant sunshine combined with warm temperatures promotes additional photochemical production of ozone from local emissions. As a result, ozone concentrations reach their maximum levels through the combined effects of local and transported pollution.

Ozone moving over water is, like ozone aloft, isolated from destructive forces. When ozone gets transported into coastal regions by bay, lake, and sea breezes arising from afternoon temperature contrasts between the land and water, it can arrive highly concentrated.

During severe ozone episodes associated with high pressure systems, these multiple transport features are embedded within a large ozone reservoir arriving from source regions to the south and west of the OTR. Thus a severe ozone episode can contain elements of long range air pollution transport from outside the OTR, regional scale transport within the OTR from channeled flows in nocturnal low level jets, and local transport along coastal shores due to bay, lake, and sea breezes.

From this conceptual description of ozone formation and transport into and within the OTR, air quality planners need to develop an understanding of what it will take to clean the air in the OTR. Weather is always changing, so every ozone episode is unique in its specific details. The relative influences of the transport pathways and local emissions vary by hour and day during the course of an ozone episode and between episodes. The smaller scale weather patterns that affect pollution accumulation and its transport underscore the importance of local (in-state) controls for emissions of nitrogen oxides (NO_X) and volatile organic compounds (VOCs), the main precursors of ozone formation in the atmosphere. Larger synoptic scale weather patterns, and pollution patterns associated with them, support the need for NO_X controls across the broader eastern United States. Studies and characterizations of nocturnal low level jets also support the need for local and regional controls on NO_X and VOC sources as locally generated and transported pollution can both be entrained in nocturnal low level jets

formed during nighttime hours. The presence of land, sea, mountain, and valley breezes indicate that there are unique aspects of pollution accumulation and transport that are area-specific and will warrant policy responses at the local and regional levels beyond a one-size-fits-all approach.

The mix of emission controls is also important. Regional ozone formation is primarily due to NO_X, but VOCs are also important because they influence how efficiently ozone is produced by NO_X, particularly within urban centers. While reductions in anthropogenic VOCs will typically have less of an impact on the long-range transport of ozone, they can be effective in reducing ozone in urban areas where ozone production may be limited by the availability of VOCs. Therefore, a combination of localized VOC reductions in urban centers with additional NO_X reductions across a larger region will help to reduce ozone and precursors in nonattainment areas as well as downwind transport across the entire region.

The recognition that ground-level ozone in the eastern United States is a regional problem requiring a regional solution marks one of the greatest advances in air quality management in the United States. During the 1990s, air quality planners began developing and implementing coordinated regional and local control strategies for NO_X and VOC emissions that went beyond the previous emphasis on urban-only measures. These measures have resulted in significant improvements in air quality across the OTR. Measured NO_X emissions and ambient concentrations have dropped between 1997 and 2005, and the frequency and magnitude of ozone exceedances have declined within the OTR. To maintain the current momentum for improving air quality so that the OTR states can meet their attainment deadlines, there continues to be a need for more regional NO_X reductions coupled with appropriate local NO_X and VOC controls.

1. INTRODUCTION

1.1. Background

Ground-level ozone is a persistent public health problem in the Ozone Transport Region (OTR), a large geographical area that is home to over 62 million people living in Connecticut, Delaware, the District of Columbia, Maine, Maryland, Massachusetts, New Hampshire, New Jersey, New York, Pennsylvania, Rhode Island, Vermont, and northern Virginia. Breathing ozone in the air harms lung tissue, and creates the risk of permanently damaging the lungs. It reduces lung function, making breathing more difficult and causing shortness of breath. It aggravates existing asthmatic conditions, thus potentially triggering asthma attacks that send children and others suffering from the disease to hospital emergency rooms. Ozone places at particular risk those with preexisting respiratory illnesses, such as emphysema and bronchitis, and it may reduce the body's ability to fight off bacterial infections in the respiratory system. Ground-level ozone also affects otherwise healthy children and adults who are very active, either at work or at play, during times of high ozone levels (USEPA, 1999). In addition, recent evidence suggests that short-term ozone exposure has potential cardiovascular effects that may increase the risk of heart attack, stroke, or even death (USEPA, 2006).

The Clean Air Act requires states that have areas designated "nonattainment" of the ozone National Ambient Air Quality Standard (NAAQS) to submit State Implementation Plans (SIPs) demonstrating how they plan to attain the ozone NAAQS. The SIPs must also include regulations that will yield the necessary emission reductions to attain the national ozone health standard. As part of the SIP process, the U.S. Environmental Protection Agency (USEPA) urges states to include a conceptual description of the pollution problem in their nonattainment areas. The USEPA has provided guidance on developing a conceptual description, which is contained in Chapter 8 of the document "Guidance on the Use of Models and Other Analyses in Attainment Demonstrations for the 8-hour Ozone NAAQS" (EPA-454/R-05-002, October 2005) (Appendix A of this report reproduces Chapter 8 of the USEPA guidance document).[a] This document provides the conceptual description of the ozone problem in the OTR states, consistent with the USEPA's guidance. In the guidance, the USEPA recommends addressing three questions to help define the ozone problem in a nonattainment area: (1) Is regional transport an important factor? (2) What types of meteorological episodes lead to high ozone? (3) Is ozone limited by availability of volatile organic compounds, nitrogen oxides, or combinations of the two, and therefore which source categories may be most important to control? This report addresses these

[a] At the time of this writing, the USEPA was incorporating Section 8 of the 8-hour ozone guidance into a new USEPA guidance document covering ozone, $PM_{2.5}$, and regional haze. The new guidance is in Section 11 of Draft 3.2 "Guidance on the Use of Models and other Analyses for Demonstrating Attainment of Air Quality Goals for Ozone, $PM_{2.5}$, and Regional Haze," U.S. EPA, (Draft 3.2 – September 2006), available at http://www.epa.gov/ttn/scram/guidance_sip.htm#pm2.5 (accessed Oct. 5, 2006). The newer guidance, when finalized, may differ in some respects from the text given in Section 8 of the earlier ozone guidance.

questions, as well as provides some in-depth data and analyses that can assist states in developing conceptual descriptions tailored to their specific areas, where appropriate.

1.2. Ozone formation

Ground-level ozone is formed in the atmosphere through a series of complex chemical reactions involving sunlight, warm temperatures, nitrogen oxides (NO_X) and volatile organic compounds (VOCs). Figure 1-1 is a conceptual picture of the emission sources and conditions contributing to ozone formation in the atmosphere. There are natural (biogenic) sources of NO_X, such as formation by soil microbes, lightening, and forest fires, but the dominant NO_X sources in the eastern United States arise from human activities, particularly the burning of fossil fuels in cars, trucks, power plants, and other combustion sources (MARAMA, 2005).

In contrast to NO_X sources, there are significant biogenic sources of VOCs in the eastern United States that can play an important contributing role in ozone formation. Isoprene, a highly reactive natural VOC emitted typically by deciduous trees such as oak, is an important ozone precursor across large parts of the East. Isoprene emissions typically increase with temperature up to a point before high temperatures tend to shut off emissions as leaf stomata (pores) close to reduce water loss. The tendency for increasing isoprene emissions with increasing temperatures (up to a point) coincides with the temperature and sunlight conditions favorable for increased ozone production (MARAMA, 2005).

Human-caused (anthropogenic) VOC emissions are important and may dominate the VOC emissions by mass (weight) in an urban area, even though natural sources dominate in the overall region. Some anthropogenic VOCs, such as benzene, are toxic, and may increase risks of cancer or lead to other adverse health effects in addition to helping form ozone (MARAMA, 2005).

Figure 1-1. Conceptual picture of ozone formation in the atmosphere

Picture provided by the Maryland Department of the Environment.

The relationship between the relative importance of NO_X and VOC emissions in producing ozone is complex. The relative ratio of NO_X and VOC levels in the local atmosphere can affect the efficiency of local urban ozone production, and this can vary by time (hour or day) at the same urban location, as well as across locations within the same urban area. High NO_X concentrations relative to VOC levels may hinder ozone production through the destruction of ozone by NO_X (sometimes called "NO_X scavenging"). The same NO_X, however, when diluted relative to VOCs through the downwind transport and dispersal of a pollution plume, will promote ozone formation elsewhere.

1.3. Spatial pattern of ozone episodes in the OTR

The day-to-day pattern of ground-level ozone varies according to meteorological variables that include, but are not limited to, sunlight, air temperature, wind speed, and wind direction. Generally within the OTR, one would expect elevated ozone to occur more frequently in southernmost areas, where solar elevation angles are greater and cold frontal passages are fewer. A glance at monthly composite maps (for example, July-August 2002) at the USEPA AIRNOW website seems to confirm this (http://www.epa.gov/airnow/nemapselect.html). On some days, however, one notes that the highest ozone levels shift northward to mainly affect the northern part of the OTR. Other shifts are apparent between coastal and interior areas.

This variability of the daily ozone pattern is tied to variations in the atmosphere's circulations over a range of scales, and how geographic features influence these

circulations. These features can include boundaries between land and sea, and the influence of the Appalachian Mountains on winds to their east over the Atlantic Coastal Plain.

For the OTR, Stoeckenius and Kemball-Cook (2005) have identified five general ozone patterns: (1) high ozone throughout the OTR; (2) high ozone confined to the extreme southeastern OTR; (3) high ozone along the I-95 corridor and northern New England; (4) high ozone in the western OTR; and (5) generally low ozone throughout the OTR. However, not all ozone episodes necessarily neatly fit into one of the five general patterns as daily conditions will vary and a given ozone episode may have characteristics that fall across several class types. These five general patterns, however, are a useful classification scheme for characterizing how representative an historical ozone episode is for possible use in air quality planning efforts. Appendix B presents the descriptions of the five general ozone patterns and their meteorological attributes as developed by Stoeckenius and Kemball-Cook (2005).

1.4. The regional extent of the ozone problem in the OTR

Air monitoring demonstrates that areas with ozone problems in the OTR do not exist in isolation. The map of Figure 1-2 shows an extensive pattern of closely adjacent ozone nonattainment in areas throughout the OTR. The 8-hour ozone baseline design values (defined in the figure caption) at the monitoring sites shown in the figure indicate extensive areas throughout the OTR with many monitors having values above the 8-hour ozone NAAQS of 0.08 ppm. In practice, this corresponds to levels equal to or greater than 0.085 ppm (equivalent to 85 ppb). The map also shows that many monitors outside the designated nonattainment areas of the OTR also record elevated ozone concentrations approaching the 8-hour ozone NAAQS (i.e., 75-84.9 ppb), even if not violating it. The many monitoring locations across that OTR measuring elevated ozone levels that approach or exceed the 8-hour ozone NAAQS give a strong indication of the regional nature of the OTR’s ozone problem.

Figure 1-2. Map of 8-hour ozone baseline design values in the OTR

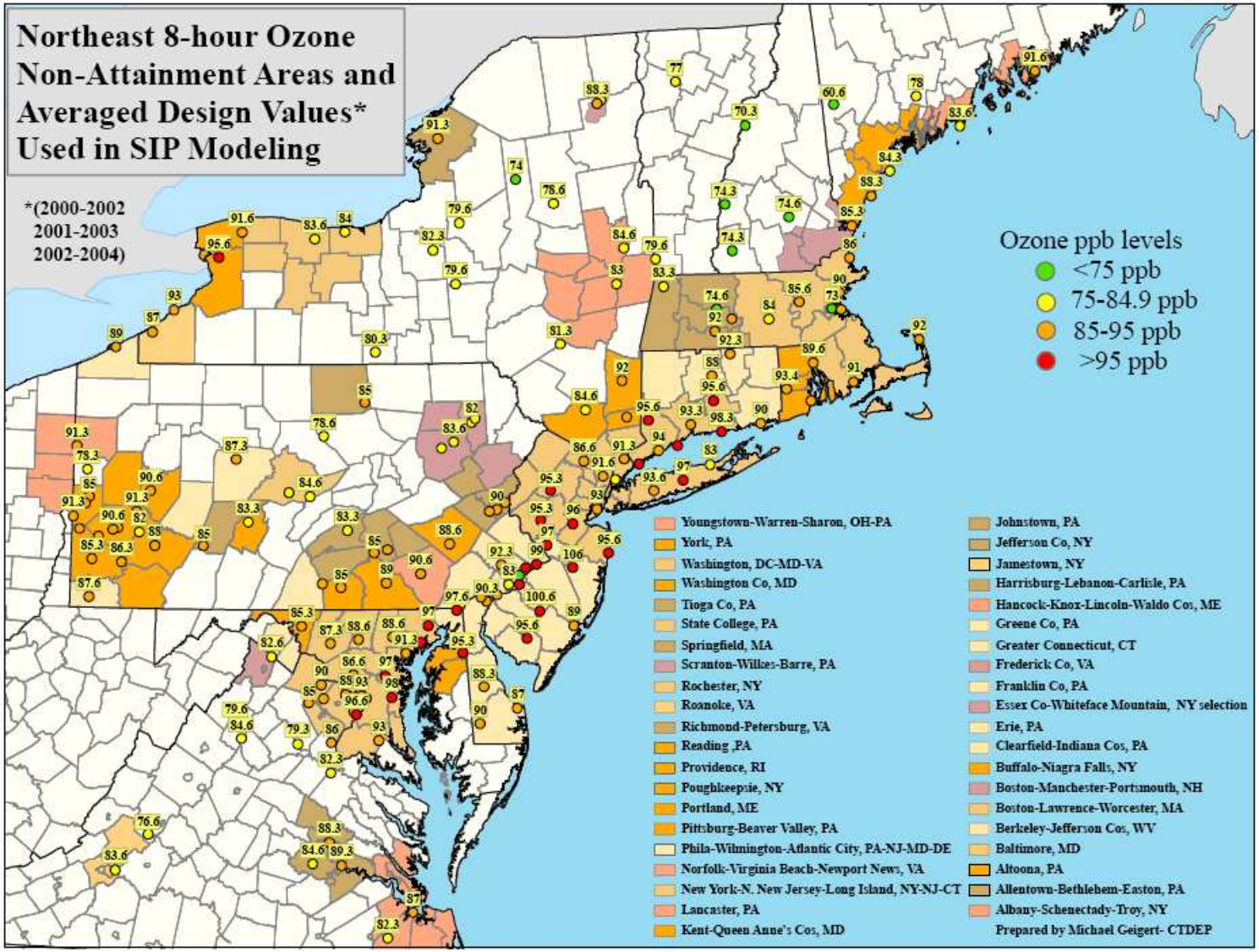

Note: A monitor's baseline design value is the average of the three design values (3-year averages of the 4th maximum 8-hour ozone level) for the set of years 2000-2002, 2001-2003, and 2002-2004. The figure shows the regional nature of ozone levels in the OTR, with a number of closely adjacent nonattainment areas (baseline design values ≥ 85 ppb) along with a broader region of elevated regional ozone (e.g., baseline design values ≥ 75 ppb) (figure by Michael Geigert, Connecticut Department of Environmental Protection).

1.5. Ozone trends in the OTR

The number of 8-hour ozone exceedance days vary year-to-year in the OTR, which is largely driven by variations in meteorology. During warmer summers conducive for ozone formation, the number of exceedance days at individual monitors in nonattainment areas of the OTR has been frequent, typically with 10 or more days above the 8-hour ozone NAAQS during the course of the summer. Figure 1-3 displays the variation in exceedance days when collectively considering all monitoring sites across the OTR since 1997. The figure also includes a line indicating the trend in the maximum 8-hour ozone concentrations observed in the OTR each year. The variation in exceedance days from year-to-year makes it difficult to discern a clear trend, although there is some hint that the number of exceedance days may be declining in recent years. There appears to be a stronger indication of a declining maximum 8-hour ozone concentration in the OTR since 1997, although the maximum concentration remains well above the 8-hour ozone NAAQS. This reflects the impact of numerous control strategies implemented locally, regionally, and nationally to reduce emissions of the precursor pollutants that contribute to ozone formation in the atmosphere.

Figure 1-3. Trends in 8-hour ozone in the OTR 1997-2005

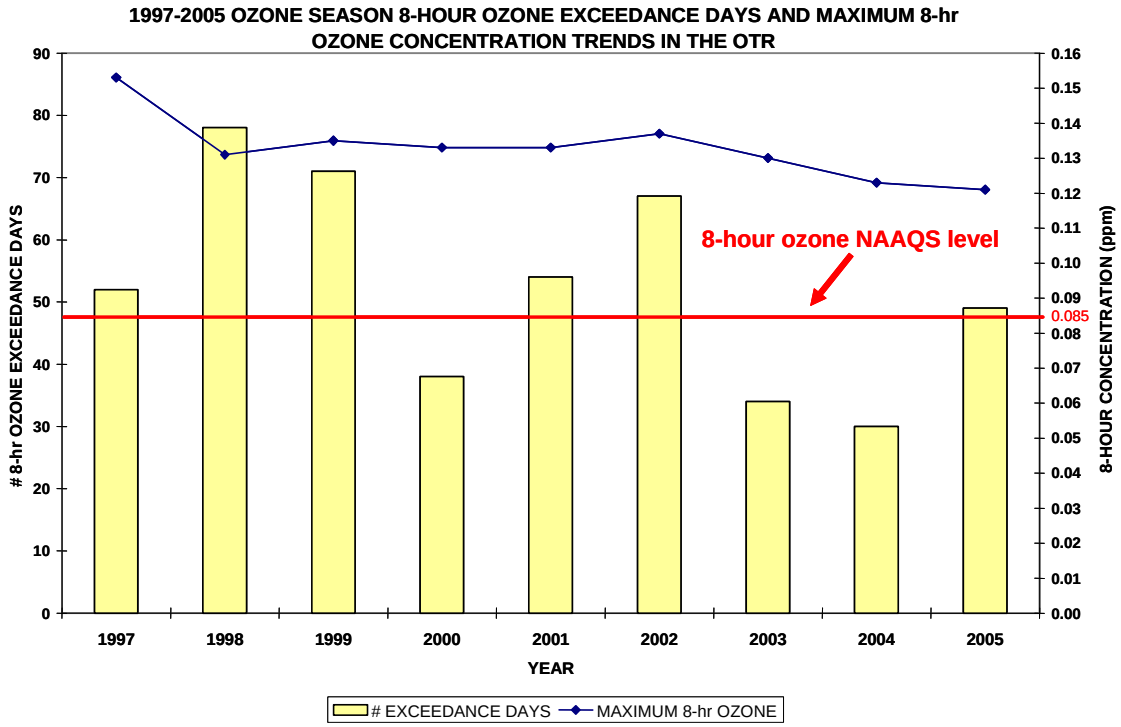

Note: The bars correspond to the number of 8-hour ozone exceedance days per year. The upper blue line indicates the trend in maximum 8-hour ozone concentrations in the OTR during 1997-2005. The lower red horizontal line indicates the level of the 8-hour ozone NAAQS (functionally 0.085 ppm). (Figure created by Tom Downs, Maine Dept. of Environmental Protection.)

The tables in Appendix C contain the frequency of ozone exceedance days for individual monitors in the OTR states from 1997 to 2005. Appendix D contains tables for the 8-hour ozone design values recorded at ozone monitors in the OTR during 1997-

2005. These tables give an indication of the number of monitors in the OTR since 1997 that have exceeded the 8-hour NAAQS of 85 ppb (equal to 0.085 ppm in the tables of Appendix D) at some point in time.

1.6. History of ozone transport science

1.6.1. From the 1970s to the National Research Council report, 1991

Research studies conducted in the 1970s gave some of the earliest indications that pollution transport plays an important role in contributing to air pollution problems in the OTR. An aircraft study in the summer of 1979 tracked a mass of ozone-laden air and its precursors leaving central Ohio, crossing the length of Pennsylvania, and entering the Northeast Corridor where it contributed upwards of 90 ppb to early morning ozone concentrations in the OTR prior to local ozone formation from local emissions (Clarke & Ching, 1983). Wolff and Lioy (1980) described a "river of ozone" extending from the Gulf Coast through the Midwest and into New England. A number of early studies also documented the role of large coal-fired power plants in forming significant amounts of ozone pollution that traveled far downwind from the power plant source and contributed to a large elevated background of regional ozone (Davis *et al.*, 1974; Miller *et al.*, 1978; Gillani & Wilson, 1980; Gillani *et al.*, 1981; White *et al.*, 1983). Section 2 below describes in more depth the observed meteorological processes identified as the ozone transport mechanisms important for the OTR.

On a regional scale, NO_X emissions within areas of high VOC emissions, such as forested regions rich in isoprene, will produce elevated levels of ozone. A number of studies have now established that regional ozone formation over the eastern United States is limited primarily by the supply of anthropogenic NO_X, with anthropogenic VOCs having less regional influence compared to their potential urban influence. This is due to the presence of significant amounts of natural VOCs across broad areas of the eastern United States (Trainer *et al.*, 1987; Chameides *et al.*, 1988; Sillman *et al.*, 1990; McKeen *et al.*, 1991; Chameides *et al.*, 1992; Trainer *et al.*, 1993; Jacob *et al.*, 1993).

The presence of dispersed NO_X emissions sources, such as coal-fired power plants, in rural regions rich in isoprene and other natural VOC emissions from trees and other vegetation often leads to elevated regional ozone during the summer months. This ozone can then be transported into urban areas where it contributes to high background concentrations during the early morning hours before local production of ozone occurs from local precursor emissions (both NO_X and VOCs).

In 1991, a National Research Council (NRC) committee, synthesizing the best available information at the time on ozone formation and transport in the eastern United States, reported (NRC, 1991):

> High ozone episodes last from 3-4 days on average, occur as many as 7-10 times a year, and are of large spatial scale: >600,000 km^2. Maximum values of non-urban ozone commonly exceed 90 ppb during these episodes, compared with average daily maximum values of 60 ppb in summer. An urban area need contribute an increment of only 30 ppb over the regional background during a high ozone episode to cause a violation of the National Ambient Air Quality Standard (NAAQS) in a downwind area. … Given the regional nature of the ozone problem in the eastern United States, a regional model is needed to develop control strategies for individual urban areas.

> [Note: The NRC discussion was in the context of the ozone NAAQS at the time of the NRC report, which was 0.12 ppm (120 ppb) averaged over one hour.]

The observed ozone spatial scale of >600,000 km^2 (>200,000 square miles) is comparable to the combined size of Kentucky, Ohio, West Virginia, Pennsylvania, Maryland, New York, and New Jersey. Additional field studies and modeling efforts since the NRC report (described below) have reinforced its basic findings and provide a consistent and coherent body of evidence for transport throughout the eastern United States.

1.6.2. Ozone Transport Assessment Group (OTAG) 1995-1997

The increasing regulatory focus on broader regional approaches to ozone control beyond the OTR began with the Ozone Transport Assessment Group (OTAG) in 1995. OTAG was a partnership between the USEPA, the Environmental Council of the States (ECOS), state and federal government officials, industry organizations, and environmental groups. OTAG's goal was "to develop an assessment of and consensus agreement for strategies to reduce ground-level ozone and its precursors in the eastern United States" (OTAG, 1997a). The effort assessed transport of ground-level ozone across state boundaries in the 37-state OTAG region and developed a set of recommendations to the USEPA. OTAG completed its work in 1997.

OTAG supported a significant modeling effort of four regional ozone episodes across the eastern United States. OTAG's Regional and Urban Scale Modeling Workgroup found that on a regional scale, modeled NO_X reductions produced widespread ozone decreases across the eastern United States with limited ozone increases generally confined to some urban areas. Also on a regional scale, VOC reductions resulted in limited ozone decreases generally confined to urban areas (OTAG, 1997b).

The OTAG Air Quality Analysis Workgroup provided additional observational and other analytical results to inform model interpretation and the development of OTAG recommendations. Among its many finding, this Workgroup observed:

> Low wind speeds (< 3 m/sec) enable the accumulation of ozone near local source areas. High winds (> 6 m/sec) reduce the concentrations but contribute to the long-range transport of ozone. The average range of ozone transport implied from an array of diverse methods is between 150 miles and 500 miles. However, the perceived range depends on whether one considers the average concentrations (300–500 miles) or peak concentrations (tens of miles at 120 ppb). The relative importance of ozone transport for the attainment of the new 80 ppb 8-hour standard is likely to be higher due to the closer proximity of nonattainment areas. (OTAG, 1997c)

Based on the variety of technical work performed by multiple stakeholders during the process, OTAG reached a number of major conclusions (OTAG, 1997d), including:

- Regional NO_X reductions are effective in producing ozone benefits; the more NO_X reduced, the greater the benefit.
- Ozone benefits are greatest in the subregions where emissions reductions are made; the benefits decrease with distance.
- Both elevated (from tall stacks) and low-level NO_X reductions are effective.
- VOC controls are effective in reducing ozone locally and are most advantageous to urban nonattainment areas.

- Air quality data indicate that ozone is pervasive, that ozone is transported, and that ozone aloft is carried over and transported from one day to the next.

The technical findings of OTAG workgroups were consistent with the modeling and observational studies of regional ozone in the eastern United States already appearing in the scientific literature at that time.

Through its work, OTAG engaged a broad group outside of the scientific community in the discussion of ozone transport. This brought a greater understanding of the role of ozone transport across the eastern United States that was then translated into air quality policy with the creation of a regional ozone control strategy focusing on the reduction of NO_X emissions from power plants.

1.6.3. Northeast Oxidant and Particle Study (NE-OPS) 1998-2002

The Northeast Oxidant and Particle Study (NE-OPS) began in 1998 as a USEPA sponsored project to study air quality issues in the Northeast. The study undertook four major field programs at a field site in northeastern Philadelphia during the summers of 1998, 1999, 2001, and 2002. It involved a collaborative effort among research groups from a number of universities, government laboratories, and representatives of the electric power industry in an investigation of the interplay between the meteorological and chemical processes that lead to air pollution events in the Northeast. A suite of measurement techniques at and above the earth's surface gave a three-dimensional regional scale picture of the atmosphere. The studies found that horizontal transport aloft and vertical mixing to the surface are key factors in controlling the evolution and severity of air pollution episodes in the Northeast (Philbrick *et al.*, 2003a).

At the conclusion of the 2002 summer field study, the NE-OPS researchers were able to draw several conclusions about air pollution episodes in Philadelphia and draw inferences from this to the conditions in the broader region. These include (Philbrick *et al.*, 2003b):

- Transported air pollution from distant sources was a major contributor to all of the major summer air pollution episodes observed in the Philadelphia area.
- Regional scale meteorology is the major factor controlling the magnitude and timing of air pollution episodes.
- Knowledge of how the planetary boundary layer evolves over the course of a day is a critical input for modeling air pollutant concentrations because it establishes the mixing volume.
- Remote sensing and vertical profiling techniques are critical for understanding the processes governing air pollution episodes.
- Ground-based sensors do not detect high levels of ozone that are frequently trapped and transported in layers above the surface.
- Horizontal and vertical nighttime transport processes, such as the nocturnal low level jets and "dynamical bursting"[b] events, are frequent contributors of pollutants during the major episodes.
- Specific meteorological conditions are important in catalyzing the region for development of major air pollution episodes.
- Tethered balloon and lidar measurements suggest a very rapid down mixing of species from the residual boundary layer during the early morning hours that is too large to be accounted for on the basis of NO_X reactions alone.

[b] "Dynamical bursting" events occur in the early morning hours due to instabilities in the lower atmosphere caused by differences in wind speeds at different altitudes below the layer of maximum winds. Bursting events can vertically mix air downwards to the surface (see Philbrick *et al.*, 2003b at p. 36).

- Summer organic aerosols in Philadelphia consist of a relatively constant level of primary organic particulate matter, punctuated by extreme episodes with high levels of secondary organic aerosol during ozone events. Primary organic particulate matter is both biogenic and anthropogenic in nature, with the relative importance fluctuating from day to day, and possibly associated more strongly with northwest winds. Secondary aerosol formation events may be responsible for dramatic increases in particulate organic carbon, while the relatively constant contribution of primary sources could make a greater contribution to annual average particulate levels. More research is needed to sort out the relative contributions of anthropogenic and biogenic sources.

The findings on nocturnal low level jets occurring in concert with ozone pollution episodes are particularly salient for air quality planning for the OTR. In 19 of 21 cases where researchers observed nocturnal low level jets during the NE-OPS 2002 summer campaign in the Philadelphia area, they also saw peak 1-hour ozone levels exceeding 100 ppbv. The nocturnal low level jets were capable of transporting pollutants in air parcels over distances of 200 to 400 km. The field measurements indicating that these jets often occur during periods of large scale stagnation in the region demonstrate the important role nocturnal low level jets can play in effectively transporting air pollutants during air pollution episodes (Philbrick *et al.*, 2003b).

The upper air observations using tethered balloons and lidar indicated the presence of high pollutant concentrations trapped in a residual layer above the surface, thus preserving the pollutants from destruction closer to the surface. Ozone, for example, when trapped in an upper layer during nighttime hours is not subject to destruction by NO_X scavenging from low-level emission sources (i.e., cars and trucks) or deposition to surfaces like vegetation, hence it is available for horizontal transport by nocturnal low level jets. The following day, it can vertically transport back down to the surface through "bursting events" and daytime convection. When involving an upper layer of ozone-laden air horizontally transported overnight by a nocturnal low level jet, downward mixing can increase surface ozone concentrations in the morning that is not the result of local ozone production (Philbrick *et al.*, 2003b).

1.6.4. NARSTO 2000

NARSTO (formerly known as the North American Research Strategy for Tropospheric Ozone) produced "An Assessment of Tropospheric Ozone Pollution – A North American Perspective" in 2000 to provide a policy-relevant research assessment of ozone issues in North America (NARSTO, 2000). While the NARSTO Assessment is continental in scope, it encompasses issues relevant to the OTR, including results from a NARSTO-Northeast (NARSTO-NE) field campaign.

Several policy-relevant findings from the NARSTO Assessment are of relevance to the OTR (NARSTO, 2000):

- Available information indicates that ozone accumulation is strongly influenced by extended periods of limited mixing, recirculation of polluted air between the ground and aloft, and the long-range transport of ozone and its precursors. As a result, air quality management strategies require accounting for emissions from distant as well as local sources.
- Local VOC emission reductions may be effective in reducing ozone in urban centers, while NO_X emission reductions become more effective at distances removed from urban centers and other major precursor emissions.
- The presence of biogenic emissions complicates the management of controllable precursor emissions and influences the relative importance of VOC and NO_X controls.

- The effectiveness of VOC and NO_X control strategies is not uniquely defined by the location or nature of emissions. It is now recognized that the relative effectiveness of VOC and NO_X controls may change from one location to another and even from episode to episode at the same location.

The NARSTO Assessment identified the stagnation of synoptic scale (>1000 km^2) high pressure systems as a commonly occurring weather event leading to ozone pollution episodes. These systems are warm air masses associated with weak winds, subsiding air from above, and strong inversions capping the planetary boundary level in the central region of the high. The warm air mass can settle into place for days to more than a week, and in the eastern U.S. tend to slowly track from west to east during the summer. These conditions result in the build up of pollution from local sources with reduced dispersion out of the region. In terms of air quality, the overall appearance of such systems is the presence of numerous local or urban-scale ozone pollution episodes embedded within a broader regional background of elevated ozone concentrations (NARSTO, 2000 at p. 3-34).

While stagnation implies little movement, the NARSTO Assessment found that a variety of processes can lead to long-range transport of air pollutants that initially accumulated in these large-scale stagnation events. Over time, pollution plumes meander, merge, and circulate within the high pressure system. Because of the difference in pressures, pollutant plumes that eventually migrate to the edges of a high pressure system get caught in increasing winds at the edge regions, creating more homogeneous regional pollution patterns. Stronger winds aloft capture the regional pollutant load, and can transport it for hundreds of kilometers downwind of the stagnated air mass's center (NARSTO, 2000 at p. 3-34). For example, air flow from west to east over the Appalachian Mountains can move air pollution originating within the Ohio River Valley into the OTR.

Studies undertaken by the NARSTO-NE field program also observed several regional scale meteorological features arising from geographical features in the eastern U.S. that affect pollutant transport. One important feature is the channeled flow of a nocturnal low level jet moving air pollution from the southwest to the northeast along the Northeast Corridor during overnight hours. The NARSTO-NE field program observed nocturnal low level jets on most nights preceding regional ozone episodes in the OTR, consistent with the observations of the NE-OPS campaign.

Another important smaller scale transport mechanism is the coastal sea breeze that can sweep ashore pollutants originally transported over the ocean parallel to the coastline. An example of this is the high ozone levels seen at times along coastal Maine that move in from the Gulf of Maine after having been transported in pollution plumes from Boston, New York City, and other Northeast Corridor locations (NARSTO, 2000 at pp. 3-34 through 3-37).

As a result of the NARSTO-NE field program, a conceptual picture of pollution transport into and within the OTR is possible. It consists of a combination of large-scale synoptic flow from the Midwest interacting with various regional and smaller-scale transport and meteorological features within the OTR, as illustrated in Figure 1-4. Synoptic-scale transport from west to east across the Appalachian Mountains occurs with the slow-moving stagnant high pressure systems that foster large regional ozone episodes across eastern U.S. Regional-scale channeled flows, specifically nocturnal low level jets

from the southwest to the northeast along the Atlantic Coastal Plain, can occur within the synoptic system. In addition, daytime sea breezes can significantly affect bay and coast line air pollution levels within the OTR (NARSTO, 2000 at 3-36 and 3-37, citing Blumenthal *et al.*, 1997).

Figure 1-4. Conceptual picture of different transport regimes contributing to ozone episodes in the OTR

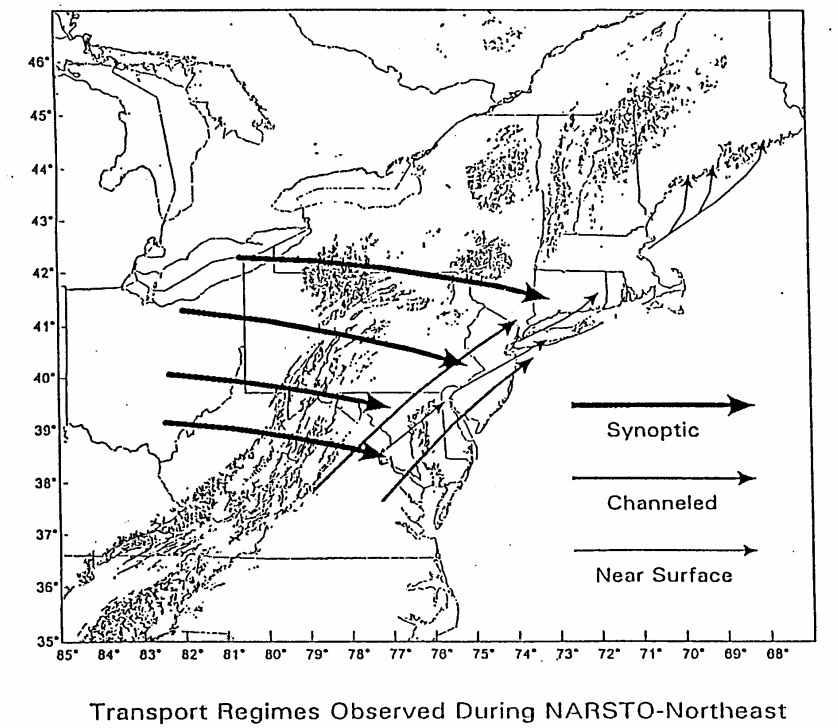

Long-range (synoptic scale) transport occurs from west to east across the Appalachian Mountains. Regional scale transport in channeled flows also occurs from west to east through gaps in the Appalachian Mountains and in nocturnal low level jets from southwest to northeast over the Northeast Corridor. Daytime sea breezes can affect local coastal areas by bringing in air pollution originally transported near the surface across water parallel to the coast (e.g., along the Maine coastline). Figure from NARSTO, 2000, citing Blumenthal *et al.*, 1997.

1.6.5. New England Air Quality Study (NEAQS) 2002-2004

The New England Air Quality Study (NEAQS) has to date conducted field campaigns during the summers of 2002 and 2004 to investigate air quality on the Eastern Seaboard and transport of North American emissions into the North Atlantic (NEAQS, 2002). Transport of air pollution into the Gulf of Maine and subsequently into coastal areas of northern New England received extensive attention.

High ozone levels in northern New England occur with light to moderate winds from source regions in the Northeast urban corridor, rather than under locally stagnant conditions. The most important transport pathways leading to high ozone in coastal New Hampshire and Maine are over water rather than over land. Transport over water is particularly important in this northern region of the OTR for several reasons. First, there is a persistent pool of cooler water in the northern and eastern Gulf of Maine and Bay of

Fundy. This creates a smoother transport surface for air pollutants relative to land transport, with a decrease in convective (vertical) mixing. Second, deposition of pollutants to the water surface is very small compared to the more rapid deposition occurring on land. Third, the lack of convective mixing allows pollution to be transported in different directions in layers at different heights in the atmosphere (Angevine *et al.*, 2004).

During the summer of 2002, researchers observed two transport events into coastal northern New England. The first occurring on July 22 through July 23 involved large-scale synoptic transport in a 400-600 m layer over the Gulf of Maine that was in contact with the water's surface. The southwesterly flow brought ozone pollution up from the New York City, Boston and other northeastern urban locations into coastal northern New England. Ozone monitors on Maine's coast extending from the New Hampshire border to Acadia National Park recorded elevated 1-hour average ozone levels between 88 and 120 ppb during this period. In a later episode during August 11-14, ozone and wind observations indicated the role of local-scale transport via a sea breeze (southeasterly flow) bringing higher ozone levels into coastal New Hampshire from a polluted layer originally transported off shore in the Gulf of Maine in a southwesterly flow arising out of the Northeast urban corridor. Transport in an elevated layer also occurred with higher ozone recorded at a monitor on Cadillac Mountain in Acadia National Park relative to two monitors located at lower elevations in the park (Angevine *et al.*, 2004).

The results of NEAQS indicate the important conditions contributing to ozone transport along the northern New England coast. The cool waters of the Gulf of Maine allow for transport of air pollutants over distances of 20-200 km in stable layers at the water's surface with little pollutant deposition or dilution. Sea breezes can modify large-scale synoptic transport over the ocean and bring high ozone levels into particular sites located on the coast. Transport within higher layers above the Gulf of Maine can carry pollutants over much greater distances, 200-2000 km (Angevine *et al.*, 2004).

1.6.6. Regional Atmospheric Measurement, Modeling, and Prediction Program (RAMMPP) 2003

The Regional Atmospheric Measurement, Modeling, and Prediction Program (RAMMPP) is a program led by researchers at the University of Maryland. Its focus is developing a state-of-the-art scientific research tool to improve understanding of air quality in the mid-Atlantic region of the United States. It has a number of facets, including ozone and $PM_{2.5}$ pollutant level forecasting, aircraft, and surface measurements, real-time weather forecasting, and chemical transport modeling.

During the August 2003 electrical blackout in the eastern United States, one of the largest in North American history, scientists with RAMMPP were able to obtain airborne measurements that directly recorded changes in air pollution due to the virtual shutdown of numerous coal-fired power plants across a large part of this region (Marufu *et al.*, 2004). Initially, aircraft measurements were collected early in the day on August 15, 2003 above western Maryland, which was outside the blackout region. These measurements were compared with aircraft measurements taken later that day over central Pennsylvania, about 24 hours into the blackout. The comparison indicated a decrease in ozone

concentrations of ~50 percent within the blackout region (as well as >90 percent decrease in SO_2 and ~70 percent reduction in light scattered by particles). These reductions were also consistent with comparisons to measurements obtained over central Pennsylvania the previous year during a period of similar synoptic patterns as occurred during the blackout. Forward trajectories indicated that the decrease in air pollution during the blackout benefited much of the eastern United States. The decrease in ozone was greater than expected based on estimates of the relative contribution of power plant NO_X emissions to ozone formation in the region. The researchers suggested that this could be due to underestimation of power plant emissions, poor representation of power plant plumes in emission models, or an incomplete set of atmospheric chemical reactions in photochemical models. This accidental "real world" experiment indicates that ozone formation across a large part of the eastern United States is sensitive to power plant NO_X emissions, and may be even more sensitive to NO_X reductions from these sources than currently predicted by air quality modeling.

1.7. Summary

The chemistry of ozone formation in the atmosphere involves reactions of NO_X and VOC emissions from numerous sources during periods of warm temperatures and abundant sunshine. The day-to-day pattern of ground-level ozone in the OTR varies according to a number of meteorological variables, such as sunlight, temperature, wind speed, and wind direction. High levels of ozone within the OTR do not occur in isolation, indicating a broad regional air quality problem. Trends in 8-hour ozone levels since 1997 indicate improvement in air quality, a reflection of numerous control strategies implemented locally, regionally, and nationally to reduce emissions of the pollutants that contribute to ozone formation.

The scientific literature prior to 1985 contains a number of peer reviewed papers describing observed episodes of ozone and precursor pollutant transport. In 1991, a National Research Council report summarized the state-of-the-science, which further highlighted the broad regional nature of the ozone problem in the eastern U.S. Since then, multiple collaborative efforts and field campaigns have further investigated specific aspects of the regional ozone problem affecting the OTR, and these provide a significant foundational basis for informed policy decisions to improve air quality.

References

Angevine, W.M., C.J. Senff, A.B. White, E.J. Williams, J. Koermer, S.T.K. Miller, R. Talbot, P.E. Johnston, S.A. McKeen, and T. Downs. "Coastal boundary layer influence on pollutant transport in New England." *J. Applied Meteor.* **43**, 1425-1437, 2004.

Blumenthal, D.L., F. Lurmann, N. Kumar., T. Dye, S. Ray, M. Korc, R. Londergan, and G. Moore. *Transport and mixing phenomena related to ozone exceedances in the northeast U.S.* EPRI Report TR-109523, Electric Power Research Institute, Palo Alto, CA, 1997.

Chameides, W.L., R.W. Lindsay, J. Richardson, and C.S. Kiang. "The role of biogenic hydrocarbons in urban photochemical smog: Atlanta as a case study." *Science* **241**, 1473-1475, 1988.

Chameides, W.L., F. Fehsenfeld, M.O. Rodgers, C. Cardelino, J. Martinez, D. Parrish, W. Lonneman, D.R. Lawson, R.A. Rasmussen, P. Zimmerman, J. Greenberg, P. Middleton, and T. Wang. "Ozone precursor relationships in the ambient atmosphere." *J. Geophys. Res.* **97**, 6037-6055, 1992.

Clarke, J.F., and J.K.S. Ching. "Aircraft observations of regional transport of ozone in the northeastern United States." *Atmos. Envt.* **17**, 1703-1712, 1983.

Davis, D.D., G. Smith, and G. Klauber. "Trace gas analysis of power plant plumes via aircraft measurement: O_3, NO_X, and SO_2 chemistry." *Science* **186**, 733-736, 1974.

Gillani, N.V., and W.E. Wilson. "Formation and transport of ozone and aerosols in power plant plumes." *Annals N.Y. Acad. Sciences* **338**, 276-296, 1980.

Gillani, N.V., S. Kohli, and W.E. Wilson. "Gas-to-particle conversion of sulfur in power plant plumes – I. Parameterization of the conversion rate for dry, moderately polluted ambient conditions." *Atmos. Envt.* **15**, 2293-2313, 1981.

Jacob, D.J., J.A. Logan, G.M. Gardner, R.M. Yevich, C.M. Spivakovsky, S.C. Wofsy, S. Sillman, and M.J. Prather. "Factors regulating ozone over the United States and its export to the global atmosphere." *J. Geophys. Res.* **98**, 14,817-14,826, 1993.

MARAMA (Mid-Atlantic Regional Air Management Association). *A guide to mid-Atlantic regional air quality.* MARAMA. Baltimore, MD, pp. 2-3, 2005 (available on-line at www.marama.org/reports).

Marufu, L.T., B.F. Taubman, B. Bloomer, C.A. Piety, B.C. Doddridge, J.W. Stehr, and R.R. Dickerson. "The 2003 North American electrical blackout: An accidental experiment in atmospheric chemistry." *Geophys. Res. Lett.* **31**, L13106, doi:10.1029/2004GL019771, 2004.

McKeen, S.A., E.-Y. Hsie, and S.C. Liu. "A study of the dependence of rural ozone on ozone precursors in the eastern United States." *J. Geophys. Res.* **96**, 15,377-15,394, 1991.

Miller, D.F., A.J. Alkezweeny, J.M. Hales, and R.N. Lee. "Ozone formation related to power plant emissions." *Science* **202**, 1186-1188, 1978

NARSTO. *An Assessment of Tropospheric Ozone Pollution*. NARSTO, July 2000.

NEAQS (New England Air Quality Study) 2002, http://www.al.noaa.gov/NEAQS/ (accessed June 20, 2006).

NRC (National Research Council). *Rethinking the ozone problem in urban and regional air pollution*. National Academy Press. Washington, DC, pp. 105-106, 1991.

OTAG (Ozone Transport Assessment Group). *OTAG Technical Supporting Document*, Appendix K – Summary of Ozone Transport Assessment Group recommendations to the U.S. Environmental Protection Agency as of June 20, 1997a. Available at http://www.epa.gov/ttn/naaqs/ozone/rto/otag/finalrpt/chp1/toc.htm.

OTAG (Ozone Transport Assessment Group). *OTAG Technical Supporting Document*. Chapter 2 – Regional and Urban Scale Modeling Workgroup. 1997b. Available at http://www.epa.gov/ttn/naaqs/ozone/rto/otag/finalrpt/chp2_new/toc.htm.

OTAG (Ozone Transport Assessment Group). *OTAG Technical Supporting Document*. Chapter 4 – Air Quality Analysis Workgroup. 1997c. Available at http://www.epa.gov/ttn/naaqs/ozone/rto/otag/finalrpt/chp4/toc.htm.

OTAG (Ozone Transport Assessment Group). *OTAG Technical Supporting Document*. Chapter 1 – Overview. 1997d. Available at http://www.epa.gov/ttn/naaqs/ozone/rto/otag/finalrpt/.

Philbrick, C.R., W.F. Ryan, R.D. Clark, B.G. Doddridge, P. Hopke, and S.R. McDow. "Advances in understanding urban air pollution from the NARSTO-NEOPS program." 83rd American Meteorological Society 5th Conference on Atmospheric Chemistry, Long Beach, CA, Feb. 8-12, 2003a.

Philbrick, C.S., W. Ryan, R. Clark, P. Hopke, and S. McDow. *Processes controlling urban air pollution in the Northeast: Summer 2002*. Final Report for the Pennsylvania Department of Environmental Protection, July 25, 2003b. Available at http://lidar1.ee.psu.edu/neopsWeb/publicSite/neopsdep/Final%20Rep-Part%201-7.pdf.

Sillman, S., J.A. Logan, and S.C. Wofsy. "The sensitivity of ozone to nitrogen oxides and hydrocarbons in regional ozone episodes." *J. Geophys. Res.* **95**, 1837-1851, 1990.

Stoeckenius, T. and Kemball-Cook, S. "Determination of representativeness of 2002 ozone season for ozone transport region SIP modeling." Final Report prepared for the Ozone Transport Commission, 2005.

Trainer, M., E.J. Williams, D.D. Parrish, M.P. Buhr, E.J. Allwine, H.H. Westberg, F.C. Fehsenfeld, and S.C. Liu. "Models and observations of the impact of natural hydrocarbons on rural ozone." *Nature* **329**, 705-707, 1987.

Trainer, M., D.D. Parrish, M.P. Buhr, R.B. Norton, F.C. Fehsenfeld, K.G. Anlauf, J.W. Bottenheim, Y.Z. Tang, H.A. Wiebe, J.M. Roberts, R.L. Tanner, L. Newman, V.C. Bowersox, J.F. Meagher, K.J. Olszyna, M.O. Rodgers, T. Wang, H. Berresheim, K.L. Demerjian, and U.K. Roychowdhury. "Correlation of ozone with NOy in photochemically aged air." *J. Geophys. Res.* **98**, 2917-2925, 1993.

USEPA. *Ozone and your Health*, EPA-452/F-99-003, September 1999 (available at http://www.airnow.gov/index.cfm?action=static.brochure).

USEPA. *Technical Support Document for the Final Clean Air Interstate Rule: Air Quality Modeling*. USEPA OAQPS, March 2005. Available at http://www.epa.gov/cleanairinterstaterule/pdfs/finaltech02.pdf.

USEPA. *Air Quality Criteria for Ozone and Related Photochemical Oxidants: Volume 1*. USEPA, EPA-600/R-05/004aF, February 2006.

White, W.H., D.E. Patterson, and W.E. Wilson, Jr. "Urban exports to the nonurban troposphere: Results from Project MISTT." *J. Geophys. Res.* **88**, 10,745-10,752, 1983.

Wolff, G.T., and P.J. Lioy. "Development of an ozone river associated with synoptic scale episodes in the eastern United States." *Envtl. Sci. & Technol.* **14,** 1257-1260, 1980.

2. METEOROLOGY AND EVOLUTION OF OZONE EPISODES IN THE OZONE TRANSPORT REGION

The following sections describe current knowledge of the factors contributing to ozone episodes in the OTR. The general description of weather patterns comes mainly from the work of Ryan and Dickerson (2000) done for the Maryland Department of the Environment. Further information is drawn from work by Hudson (2005) done for the Ozone Transport Commission and from a mid-Atlantic regional air quality guide by MARAMA (2005). The regional nature of the observed ozone episodes in the OTR is reinforced in modeling studies by the USEPA for the Clean Air Interstate Rule.

2.1. Large-scale weather patterns

Ryan and Dickerson (2000) have described the general meteorological features conducive to ozone formation and transport that are pertinent to the OTR. On the local scale, meteorological factors on which ozone concentrations depend are the amount of available sunlight (ultraviolet range), temperature, and the amount of space (volume) in which precursor emissions mix. Sunlight drives the key photochemical reactions for ozone and its key precursors and the emissions rates of many precursors (isoprene for example) are temperature dependent. Emissions confined within a smaller volume result in higher concentrations of ozone. Winds in the lowest 2 km of the atmosphere cause horizontal mixing while vertical temperature and moisture profiles drive vertical mixing. High ozone is typically associated with weather conditions of few clouds, strong temperature inversions, and light winds.

The large-scale weather pattern that combines meteorological factors conducive to high ozone is the presence of a region of upper air high pressure (an upper air ridge) with its central axis located west of the OTR. The OTR east of the axis of the high-pressure ridge is characterized by subsiding (downward moving) air. This reduces upward motion necessary for cloud formation, increases temperature, and supports a stronger lower level inversion. While the upper air ridge is located west of the OTR, surface high pressure is typically quite diffuse across the region. This pattern occurs throughout the year but is most common and longer lived in the summer months (Ryan and Dickerson, 2000).

The large, or synoptic, scale, weather pattern sketched above has important implications for transport into and within the OTR. First, the persistence of an upper air ridge west of the OTR drives generally west to northwest winds that can carry ozone generated outside the OTR into the OTR. A key point from this wind-driven transport mode is that stagnant air is not always a factor for high ozone episodes in the OTR. Second, the region in the vicinity of the ridge axis, being generally cloud free, will experience significant radiational cooling after sunset and therefore a strong nocturnal inversion will form. This inversion, typically only a few hundred meters deep, prevents ozone and its precursors from mixing downward overnight. Above the inversion layer, there is no opportunity for destruction of the pollutants by surface deposition, thus increasing the pollutants' lifetimes aloft and consequently their transport distances. Third, with diffuse surface high pressure, smaller scale effects can become dominant in the

lowest layers of the atmosphere. These include bay and land breezes, the Appalachian lee side trough, and the development of the nocturnal low level jet. Nocturnal low-level jets are commonly observed during high ozone events in the OTR (Ryan and Dickerson, 2000).

As previously mentioned in Section 1, Stoeckenius and Kemball-Cook (2005) have identified five ozone patterns in the OTR as a guide to an historical ozone episode's representativeness for air quality planning purposes. They also described the meteorological conditions that are generally associated with each of these patterns. Appendix B presents the five types with the additional meteorological detail.

2.2. Meteorological mixing processes

An important element in the production of severe ozone events is the ability of the atmosphere through temperature inversions to inhibit the mixing processes that under normal conditions would lead to dilution of the emitted pollutants. For the purposes of this discussion, we focus on two major classes of temperature inversions, (1) nocturnal (radiative) and (2) subsidence.

Figure 2-1 shows an example of nocturnal and subsidence inversions in a temperature profile taken over Albany, NY, on September 1, 2006 at 7 a.m. eastern standard time. The figure shows two distinct temperature inversions – the ground-based nocturnal inversion and an inversion at about 1600 meters caused by the sinking motion (subsidence) of the atmosphere in a high pressure system.

Figure 2-1. Temperature profile taken over Albany, NY, on September 1, 2006 at 7 a.m. eastern standard time

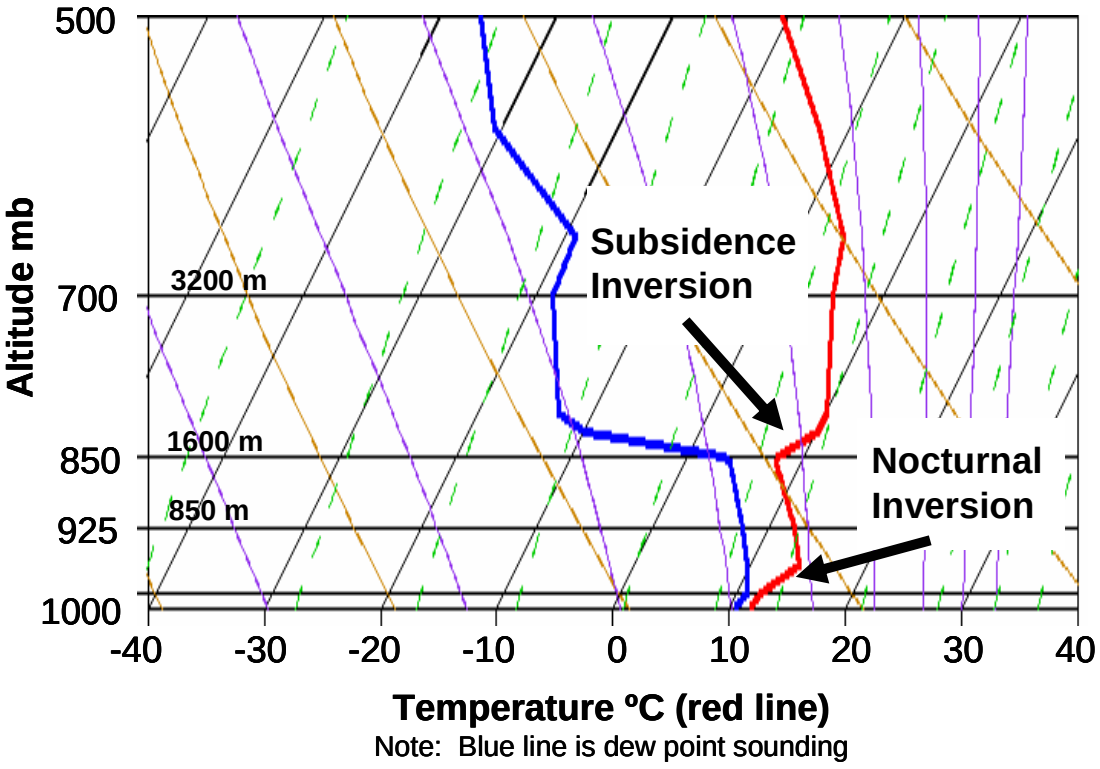

2.2.1. Nocturnal inversions

Land surfaces are far more efficient at radiating heat than the atmosphere above, hence at night, the Earth's surface cools more rapidly than the air. That temperature drop is then conveyed to the lowest hundred meters of the atmosphere. The air above this layer cools more slowly, and a temperature inversion forms. The inversion divides the atmosphere into two layers that do not mix. Below the nocturnal surface inversion, the surface winds are weak and any pollutants emitted overnight accumulate. Above the inversion, winds continue through the night and can even become stronger as the inversion isolates the winds from the friction of the rough surface.

In the morning, the sun warms the Earth's surface, and conduction and convection transfer heat upward to warm the air near the surface. By about 10:00 – 11:00 a.m., the temperature of the surface has risen sufficiently to remove the inversion. Air from above and below the inversion can then mix freely. Depending on whether the air above the inversion is cleaner or more polluted than the air at the surface, this mixing can either lower or increase air pollution levels.

2.2.2. Subsidence inversions

Severe ozone events are usually associated with high pressure systems. In the upper atmosphere, the winds around a high pressure system move in a clockwise direction. At the ground, friction between the ground and the winds turns the winds away from the center of the system and "divergence" occurs, meaning that air at the surface moves away from the center. With the movement of air horizontally away from the center of the high at the surface, air aloft moves vertically downward (or "subsides") to replace the air that left. Thus, the divergence away from the high pressure system gives rise to subsidence of the atmosphere above the high. The subsiding motion causes the air to warm as it moves downward and is compressed. As the warmer air meets the colder air below, it forms an inversion. A subsidence inversion is particularly strong because it is associated with this large scale downward motion of the atmosphere. The subsidence inversion caps pollution at a higher altitude in the atmosphere (typically from 1200 to 2000 meters), and it is far more difficult to break down than the nocturnal inversion. Hence the subsidence inversion limits vertical mixing in the middle of the day during an air pollution episode, keeping pollutants trapped closer to the ground.

2.3. Meteorological transport processes

2.3.1. Introduction

Figure 2-2 shows the classic synoptic weather pattern at the Earth's surface associated with severe ozone episodes within the OTR. A quasi-stationary high pressure system (the Bermuda high) extends from the Atlantic Ocean westward into interior southeastern U.S., where a second weaker high is located. Surface winds, circulating clockwise around the high, are especially light in the vicinity of the secondary high. Farther north, a southwesterly flow strengthens toward New York and southern New England. This situation illustrates two circulation regimes often existing in OTR ozone episodes: more stagnant conditions in southern areas and a moderate transport flow in the OTR from southwest to northeast. In addition, as discussed previously, high pressure

systems exhibit subsidence, which results in temperature inversions aloft, and cloud free skies.

Closer to the surface, the Appalachian Mountains induce changes in the wind field that also play important roles in the formation and transport of ozone in the OTR. The mountains act as a physical barrier confining, to some degree, pollution to the coastal plain. They also induce local effects such as mountain and valley breezes, which, in the case of down-slope winds, can raise surface temperatures thereby increasing chemical reactivity. In addition, mountains create a lee side trough, which helps to channel a more concentrated ozone plume, and contribute to the formation of nocturnal low level jets, the engine of rapid nighttime transport.

The Atlantic Ocean also plays a strong role during ozone episodes where sea breezes can draw either heavily ozone-laden or clean marine air into coastal areas.

Figure 2-2. Schematic of a typical weather pattern associated with severe ozone episodes in the OTR

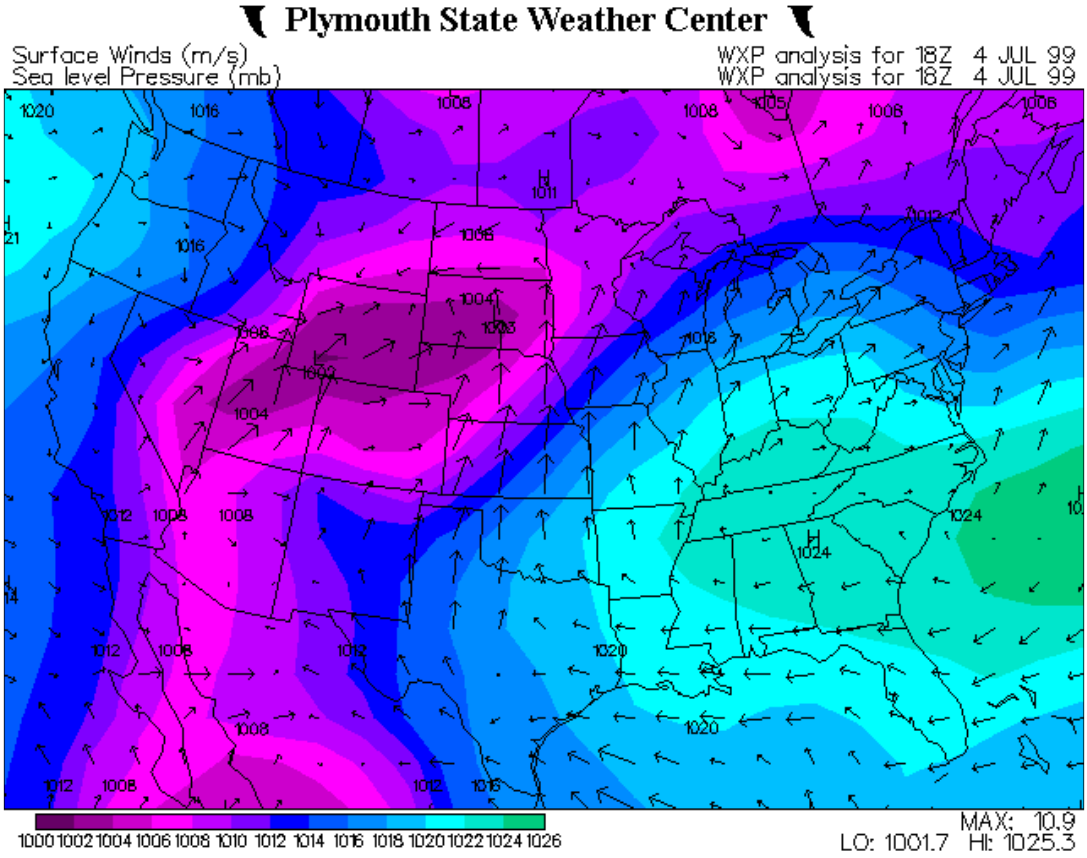

Meteorological processes that transport ozone and its precursors into and within the OTR can roughly be broken down into three levels: ground, mid and upper. The following sections discuss the three wind levels associated with meteorological transport processes in more detail.

2.3.2. Ground level winds

Land, sea, mountain, and valley breezes

In the OTR, land and sea breezes, and mountain and valley breezes can have an important influence on local air quality. These local winds are driven by a difference in temperature that produces a difference in pressure. Figure 2-3 shows a schematic of the formation of a sea breeze. The sea breeze forms in the afternoon when the land is considerably hotter than the ocean or bay. Air then flows from the high pressure over the ocean toward the low pressure over land. At night, the opposite may happen as the land cools to below the ocean's temperature, and a land breeze blows out to sea. Because the nighttime land and water temperature differences are usually much smaller than in the day, the land breeze is weaker than the sea breeze. Sea breezes typically only penetrate a few kilometers inland because they are driven by temperature contrasts that disappear inland.

Figure 2-3. Illustration of a sea breeze and a land breeze

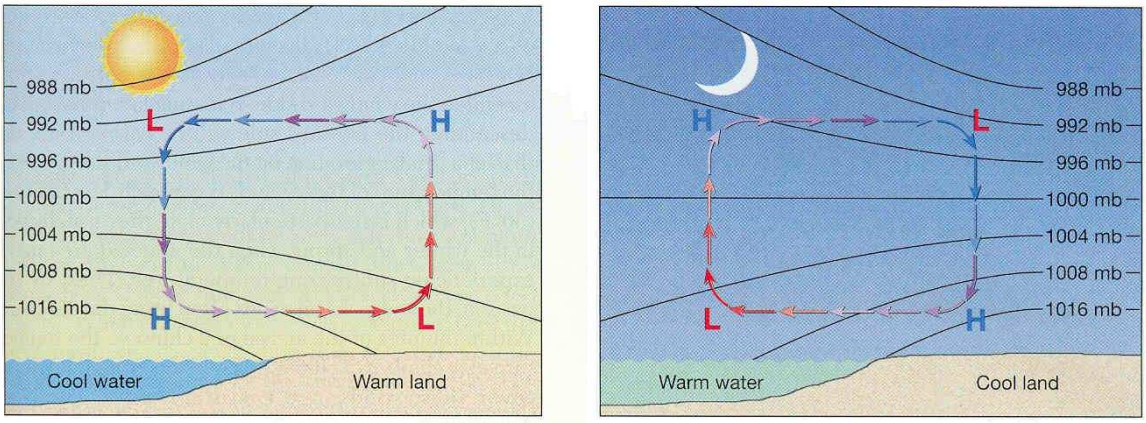

a) Sea Breeze **b) Land Breeze**

Figure from *Lutgens & Tarbuck*, 2001.

Along coastlines, such as coastal New England, sea breezes bring in air pollution transported near the surface over water from urban locations located to the southwest. Figure 2-4 shows the average 2000-2002 wind direction frequency for elevated 1-hour ozone in the vicinity of the Kennebec and Penobscot Rivers in Maine. There is a clear maximum of pollution in the direction of the sea breeze. These sites are located many miles upriver from the coast, and receive ozone transported over water from the sea up through the coastal bays and rivers.

In other cases, sea breezes can affect air quality in coastal cities because, under stagnant synoptic-scale winds, a city's emissions may be recirculated or pushed back over land after having drifted out over the sea earlier. Before sea breeze circulation begins, air pollution from a coastal city can move out over the water. In the absence of a shift in winds due to a sea breeze, the city's air pollution will be blown away. When a sea breeze circulation sets up, however, the polluted air is pushed back toward the city. The sea breeze only pushes a few miles inland, which is where the barrier to mixing lies. Later in the day, the air may be quite clean on the ocean side of the city, but the air is

usually quite dirty on the inland side. The city suffers from its own recirculated pollution, and also from the sea breeze that does not allow pollution from the city to flow away from it. Appendix E presents more detailed information on sea breezes and flow over the ocean that contribute to ozone transport in parts of the OTR.

Figure 2-4. Average 2000 – 2002 wind direction frequency associated with elevated one-hour ozone levels in coastal Maine

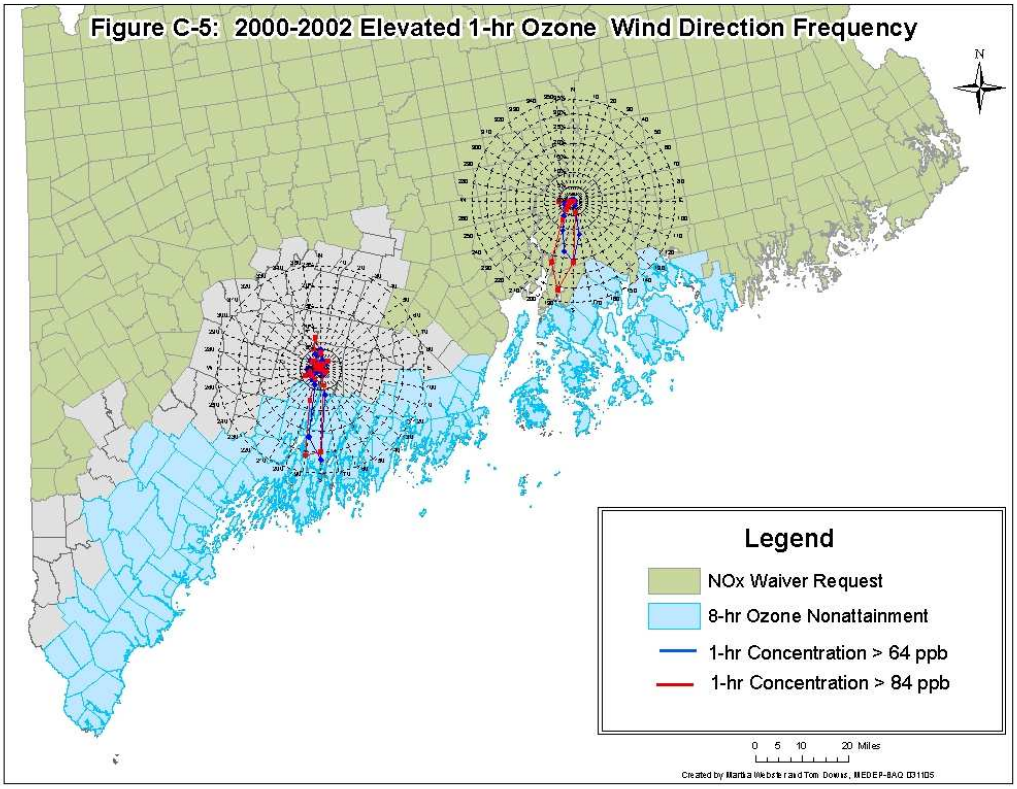

The bay breeze is a shallow circulation over large inland bays, and may only extend a couple hundred meters above the surface. For example, bay breezes from the Chesapeake Bay often make Baltimore's summertime air quality particularly poor. Air from the city cannot escape directly across the Bay. On the other hand, a few miles closer to the Bay, conditions are often considerably cleaner, since no fresh emissions have gotten into the air there since earlier that morning. Polluted air from the west side of the Bay can still mix upward, where it meets the stronger winds aloft, pass over the Bay breeze circulation and come back down on the east side of the Bay.

Mountain and valley breezes are also driven by a temperature contrast. In the daytime, the side of the mountain will heat up more quickly than the valley, and hence a flow from the valley to the mountain results. At night this flow is reversed as the mountain side cools more quickly than the valley. As a result of these differences in cooling and heating, during the day, warm winds blow up toward the peaks from the valley below, while at night, cool air sinks and flows down the valley, settling in the lowest points. Local topography is very important in generating this phenomenon, making the breeze unique to a particular area.

Mountains and valleys also serve to isolate air in the valleys, while air at the mountaintops may be coming from very far away. Mountain winds, inversions, and mixing are quite complex. On a quiet night, the mountaintop may be in the free troposphere, open to long-range transport, while the valley below is usually capped by a nocturnal inversion, isolating pollution in the valley. Air quality measurements taken during plane flights in the Shenandoah River Valley have shown that the air pollutants in the valley may be rather different from the air at the nearby peaks. Cities on the western side of the mountains will find that the Appalachians are capable of damming pollution up against them (MARAMA, 2005 at pp. 42-43).

Appalachian lee side trough

The Appalachian lee side trough forms on the leeward (downwind) side of the Appalachian Mountains. In a sense, it is the daytime companion to the nocturnal low level jet, discussed below, because it forms under similar stagnant conditions; however, the mechanism for its formation is different. In the OTR, a lee side trough forms when winds blow over the Appalachian Mountains and down the lee side of the mountain range to the coastal plain. As the column descends down the lee side, it stretches vertically and spins faster, pulling up air and creating low pressure, thus rotating the winds to the southwest. Because the air is typically rather dry, and the trough itself is rather weak, it does not usually lead to showers and thunderstorms the way a trough associated with other weather systems would. It does cause winds to shift their direction, so a wind that comes over the mountains from the west will turn and blow from the southwest along the coastal plain. Therefore, when surface winds on the coastal plain are from the southwest, if the Appalachian lee side trough is in place, it may be that the air actually came from the west, descended, and turned. The implication for air quality policy is straightforward. Pollution making its way over the mountains from the west will turn once it reaches the coastal plain and come from the southwest. Because surface winds are then from the southwest, when the Appalachian lee side trough is in place, the limits of a nonattainment area's airshed will be expanded farther south and west than they might otherwise be (MARAMA, 2005 at pp. 41-42). Studies have observed high ozone levels in the OTR associated with a lee side trough east of the Appalachian Mountains and aligned with the Northeast Corridor (Gaza, 1998; Kleinman *et al.*, 2004).

2.3.3. Mid-level winds: Nocturnal low level jets

The nocturnal low level[c] jet is a localized region of rapid winds in the lower atmosphere (typically 500-1500 m above the ground level) that form at night under the same calm conditions often present in a pollution episode. Forming just above the nighttime temperature inversion mentioned previously, the nocturnal low level jet depends on the isolation from the surface provided by the inversion. It is primarily a nocturnal phenomenon that occurs more frequently during the spring and summer seasons.

[c] "Low level" in this instance is relative to upper level jets occurring in the upper troposphere to lower stratosphere at heights of 10-15 km above the ground level. It is not a "ground level" phenomenon of the types described in the previous section.

A nocturnal low level jet is generally found where a range of mountains meets a flat plain. There is a particularly strong nocturnal low level jet in the Great Plains of the central United States on the eastern side of the Rocky Mountains. On the Eastern Seaboard, nocturnal low level jets develop along the Atlantic Coastal Plain located to the east of the Appalachian Mountains and to the west of the Atlantic Ocean. While the typical wind speed minimum of a nocturnal low level jet is often defined as more than 12 meters per second (m s^{-1}), Ryan (2004) has proposed a weaker minimum speed criterion of 8 m s^{-1} in the East because of the expected weaker terrain-induced forcing in this region. The mid-Atlantic nocturnal low level jet has a width of 300-400 km (to its half peak value) and a length scale of more than 1500 km, following closely the orientation of the Appalachian Mountains.

The nocturnal low level jet forms when fronts and storm systems are far away. Surface winds are parallel to the terrain, which in the case of the OTR is southwest running over the Atlantic Coastal Plain in front of the Appalachian Mountains. The nocturnal low level jet forms because land cools quicker than the air above it at night. The quickly cooling land results in the air closest to the surface cooling quicker than the air higher above. This creates a temperature inversion that separates the atmosphere into layers. The warmer air above the inversion layer (~200-800 m above ground) loses the frictional effect of the surface and increases in speed. In the eastern United States, the nocturnal low level jet has been observed in Georgia, the Carolinas and Virginia (Weisman, 1990; Sjostedt *et al.*, 1990) in addition to the OTR (NARSTO, 2000). Appendix F describes a specific example of an observed nocturnal low level jet occurring over the length of the OTR during a period of high ozone in July 2002.

Upper air studies have observed ozone being transported overnight in nocturnal low level jets in the OTR (Woodman *et al.*, 2006). The Maryland Department of the Environment (MDE) operates an upper air profiler at the Howard University (HU) site located in Beltsville, Maryland. On August 5, 2005, two helium-filled balloons carrying ozone sensors (called "ozonesondes") were launched at the HU – Beltsville site in the early morning hours. Using the upper air profiler, a nocturnal low level jet of 15 m s^{-1} was observed between approximately midnight and 7:30 a.m. One ozonesonde was launched at 3:30 a.m. and measured an ozone concentration of approximately 95 ppb at about 600 meters, which is within the nocturnal low level jet. Another ozonesonde was launched at 7:30 a.m. and measured an ozone concentration of approximately 90 ppb at about 1,000 meters (Figure 2-5). Each of the ozone concentrations was observed at approximately the same height as the nocturnal temperature inversion as indicated by the kink in the temperature profile. The observations indicated that elevated ozone concentrations are within the nocturnal low level jet.

Figure 2-5. Ozonesonde measurements on August 5, 2005 of elevated ozone concentrations in a nocturnal low level jet above Beltsville, MD

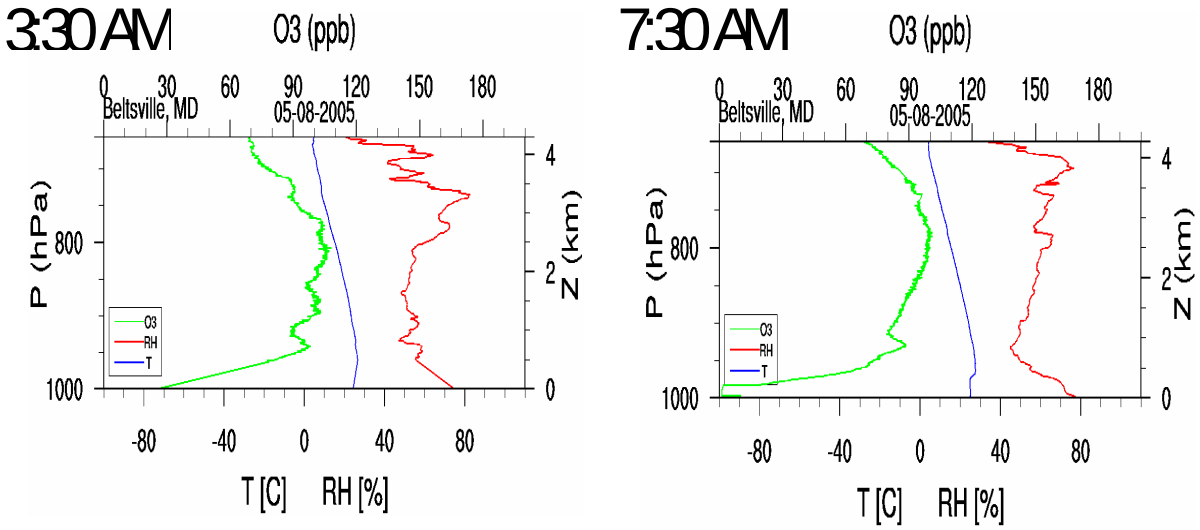

2.3.4. Upper level winds: Ozone and precursors aloft

Theoretical and numerical model simulations have suggested for some time that there is a strong regional component to urban air quality in the northeastern United States (Liu *et al*., 1987; Sillman *et al*., 1990; McKeen *et al*., 1990). Since 1992, over 300 aircraft flights have been made to measure vertical profiles of ozone, the nitrogen oxides, carbon dioxide, sulfur dioxide, and more recently aerosol particles during high ozone episodes.[d] Figure 2-6 shows the results of profiles taken over central Virginia on July 15, 1995, at about 9:00 am on the last day of a four day severe ozone episode. During this episode, winds measured at Sterling, Virginia (IAD) in the 500-3000 m layer, where ozone was at a maximum, were consistently from the west to the north. This was particularly true on July 15. There were no periods of stagnation or reversal of wind direction during this period. Figure 2-6 shows that the ozone mixing ratio above the boundary layer is much larger than that at the ground, peaking at about 1200 meters.

An examination of the various pollutant data in Figure 2-6 helps to identify possible sources of the elevated ozone. It should be noted that while both automobiles and power plants emit NO_X, automobiles emit carbon monoxide (CO) but not sulfur dioxide (SO_2), while power plants emit SO_2 but not CO. The CO profile is not correlated well with the ozone data, indicating that the source of the ozone is not from local sources, i.e., automobiles. The peak in the NO_Y[e] profile at around 800 meters is an indication of "aged air" (hence transport) as a number of studies have found a strong relationship between increasing ozone and NO_Y in photochemically aged air masses (Trainer *et al.*,

[d] These measurements were made as part of the University of Maryland's RAMMPP (Regional Atmospheric Measurement, Modeling, and Prediction Program) under the sponsorship of ARMA, MARAMA (Mid-Atlantic Regional Air Management Association), VADEQ (Virginia Department of Environmental Quality), and NCDEQ (North Carolina Department of Environmental Quality).

[e] NO_Y = NO + NO_2 + all other oxidized nitrogen products of NO_X, excluding N_2O.

1993; Kleinman *et al.*, 1994; Olszyna *et al.*, 1994). Finally, the peak in the SO_2 profile, which occurs above the nocturnal inversion, is unlikely to come from local sources. Indeed the presence of the SO_2 leads to the conclusion that the air is coming from power plants west of the Appalachian Mountains.

Figure 2-6. Altitude profiles for ozone, carbon monoxide, NO_Y, and SO_2 taken on July 15, 1995

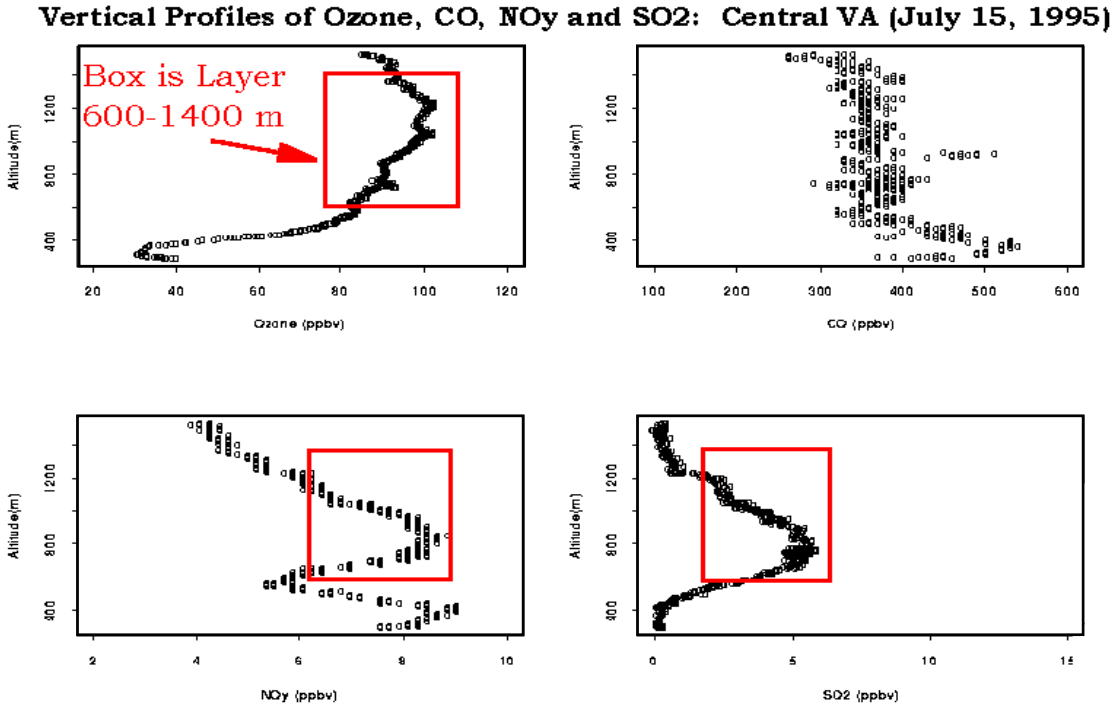

During the same July 1995 period, measurements aloft in other parts of the OTR also recorded high ozone overnight in layers 500 m or higher above the surface. Ozone aloft concentrations above Poughkeepsie, NY and New Haven, CT approached levels of 120 ppb or greater on the night of July 14 (Zhang & Rao, 1999). Figure 2-7 displays the aircraft measurements above Poughkeepsie, NY around 4 a.m. EST.

Figure 2-7. Observed vertical ozone profile measured above Poughkeepsie, NY at about 4 a.m. EST on July 14, 1995

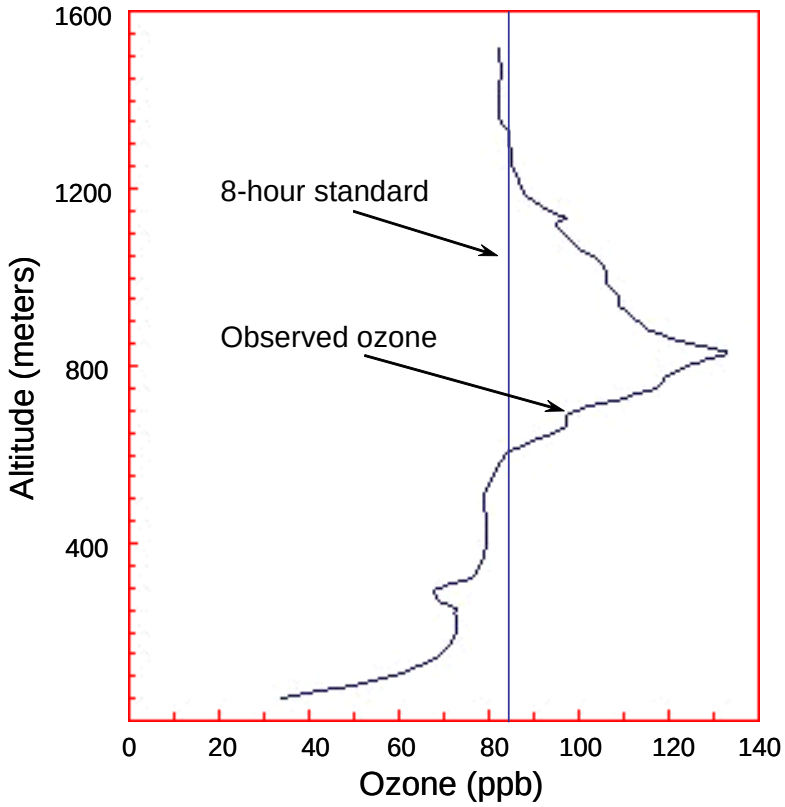

Note: The figure includes a vertical line at 85 ppb for comparing aloft measurements with the 8-hour ozone NAAQS (observed ozone data from Zhang & Rao, 1999).

The aircraft measurements since 1992 reinforce the previously mentioned observations by Clarke and Ching (1983) during the summer of 1979, in which aircraft measurements recorded aloft ozone concentrations of about 90 ppb transported overnight from eastern Ohio and entering into the Northeast Corridor over a region stretching from the lower Hudson River Valley north of New York City down across eastern Pennsylvania and into Maryland just west of Baltimore. The measurements also observed NO_X aloft during the overnight hours that could contribute to additional ozone formation in the OTR as it mixed down to the surface in the morning.

The presence of high levels of ozone and precursors aloft across a large spatial region gives rise to the concept of an "ozone reservoir" existing at night just above the nocturnal inversion boundary. The pollutants in this reservoir are not subject to destruction at the surface, and can be transported long distances in the wind flows created by the synoptic scale weather patterns conducive to ozone formation and transport.

2.4. Atmospheric modeling of regional ozone transport

Modeling results by the USEPA for the Clean Air Interstate Rule (CAIR) further underscore the regional nature of ozone transport into and within the OTR through the

various pathways described in the above sections. Based on ozone air quality modeling results, the USEPA tabulated the percent contribution to 8-hour ozone nonattainment in a number of OTR counties. The USEPA modeled the contributions for the base year 2010, which included implementation of the NO_X SIP Call and other existing and promulgated control programs. Table 2-1 shows the CAIR results for the OTR counties (USEPA, 2005, from Table VI-2).

Table 2-1. USEPA CAIR modeling results of percent contribution to 8-hour ozone nonattainment in OTR counties in 2010 due to transport from upwind states

2010 Base Nonattainment Counties	2010 Base 8-Hour Ozone (ppb)	Percent of 8-Hour Ozone due to Transport
Fairfield CT	92	80 %
Middlesex CT	90	93 %
New Haven CT	91	95 %
Washington DC	85	38 %
Newcastle DE	85	37 %
Anne Arundel MD	88	45 %
Cecil MD	89	35 %
Harford MD	93	31 %
Kent MD	86	47 %
Bergen NJ	86	38 %
Camden NJ	91	57 %
Gloucester NJ	91	62 %
Hunterdon NJ	89	26 %
Mercer NJ	95	36 %
Middlesex NJ	92	62 %
Monmouth NJ	86	65 %
Morris NJ	86	63 %
Ocean NJ	100	82 %
Erie NY	87	37 %
Richmond NY	87	55 %
Suffolk NY	91	52 %
Westchester NY	85	56 %
Bucks PA	94	35 %
Chester PA	85	39 %
Montgomery PA	88	47 %
Philadelphia PA	90	55 %
Kent RI	86	88 %
Arlington VA	86	39 %
Fairfax VA	85	33 %

From USEPA, 2005 (Table VI-2)

The CAIR modeling by the USEPA also provides information on the upwind areas (by state) contributing to downwind nonattainment in the OTR counties. Table 2-2 presents the upwind states significantly contributing to 8-hour ozone nonattainment in counties within the OTR, according to significance criteria used by the USEPA (USEPA, 2005, from Table VI-5). The states listed in the table as significantly contributing to

downwind ozone nonattainment in the OTR counties include states outside of the OTR, indicating the broad regional scale of the ozone transport problem.

Table 2-2. USEPA CAIR modeling results of upwind states that make a significant contribution to 8-hour ozone in downwind OTR nonattainment counties

Downwind State/County		Upwind States									
CT	Middlesex	MA	NJ	NY	OH	PA	VA				
CT	New Haven	MD/DC	NJ	NY	OH	PA	VA	WV			
CT	Fairfield	MD/DC	NJ	NY	OH	PA	VA	WV			
District of Columbia		MD/DC	OH	PA	VA						
DE	New Castle	MD/DC	MI	NC	OH	PA	VA	WV			
MD	Harford	NC	OH	PA	VA	WV					
MD	Kent	MI	NC	OH	PA	VA	WV				
MD	Cecil	MI	OH	PA	VA	WV					
MD	Anne Arundel	MI	NC	OH	PA	VA	WV				
NJ	Ocean	DE	MD/DC	MI	NY	OH	PA	VA	WV		
NJ	Bergen	MD/DC	MI	OH	PA	VA	WV				
NJ	Gloucester	DE	MD/DC	MI	OH	PA	VA	WV			
NJ	Morris	DE	MD/DC	MI	NY	OH	PA	VA	WV		
NJ	Middlesex	DE	MD/DC	MI	NY	OH	PA	VA	WV		
NJ	Hunterdon	DE	MD/DC	OH	PA	VA	WV				
NJ	Camden	DE	MD/DC	MI	OH	PA	VA	WV			
NJ	Mercer	DE	MD/DC	MI	NY	OH	PA	VA	WV		
NJ	Monmouth	DE	MD/DC	MI	NY	OH	PA	VA	WV		
NY	Erie	MD/DC	MI	NJ	PA	VA	WI				
NY	Westchester	MD/DC	NJ	OH	PA	VA	WV				
NY	Richmond	MD/DC	MI	NJ	PA	VA	WV				
NY	Suffolk	CT	DE	MD/DC	MI	NC	NJ	OH	PA	VA	WV
PA	Montgomery	DE	MD/DC	NJ	OH	WV					
PA	Philadelphia	DE	MD/DC	MI	NJ	OH	VA	WV			
PA	Chester	DE	MD/DC	MI	NJ	OH	VA	WV			
PA	Bucks	DE	MD/DC	MI	NJ	OH	VA	WV			
RI	Kent	CT	MA	NJ	NY	OH	PA	VA			
VA	Arlington	MD/DC	OH	PA							
VA	Fairfax	MD/DC	OH	PA	WV						

From USEPA, 2005 (Table VI-5). States are listed alphabetically and not according to order of influence.

While the USEPA modeled 40 eastern U.S. counties as in nonattainment of the 8-hour ozone NAAQS in the 2010 base year (including counties not in the OTR), it projected that only three of those 40 counties would come into attainment by 2010 with the additional NO_X reductions of CAIR (USEPA, 2005, p. 58). The USEPA modeling does predict that ozone will be lower in the remaining nonattainment counties by 2010 due to CAIR, with additional counties coming into attainment by 2015. The CAIR reductions, therefore, will bring the OTR nonattainment counties closer to attainment by 2010, but will not result in attainment for a large majority of OTR counties predicted to be in nonattainment in 2010 prior to implementation of CAIR.

2.5. Summary

This section has summarized current knowledge of the meteorological processes that affect local ozone levels within the OTR. A conceptual description of transport within the OTR can be divided into three principle components: ground level transport at the surface, transport by the nocturnal low level jet, and transport aloft. All three modes of transport depend on the location of the high pressure system. Ground level transport is the result of interaction between the synoptic flow and local effects, such as the sea breeze and the Appalachian lee side trough. Transport within the OTR can occur by the nocturnal low level jet that forms late at night or in the very early morning hours. This phenomenon is a result of the differential heating of the air between the Appalachian Mountains and the Atlantic Ocean. It has been observed throughout the Eastern Seaboard from Georgia to Maine. The nocturnal low level jet can transport ozone that formed within the OTR or was transported into the OTR from outside the region. Transport aloft is dominated by the anti-cyclonic flow around a high pressure system, which can lead to transport of an ozone reservoir into the OTR created by emissions in areas that lie outside the OTR. Local emissions within the OTR add to the polluted air mixing down from above that arrived from more distant locations.

Atmospheric modeling by the USEPA underscores the observations that the OTR's ozone problem has contributions from outside and upwind of the region. Pollution sources in the Ohio River Valley and the Southeast significantly contribute to ozone nonattainment problems in various portions of the OTR.

References

Clarke, J.F., and J.K.S. Ching. "Aircraft observations of regional transport of ozone in the northeastern United States." *Atmos. Envt.* **17**, 1703-1712, 1983.

Gaza, R.S. "Mesoscale meteorology and high ozone in the northeast United States." *J. Applied Meteor*. **37**, 961-977, 1998.

Hudson, R. "A Conceptual Model for Ozone Transport." University of Maryland, Dept. of Atmospheric and Oceanic Science. Prepared for the Ozone Transport Commission. Draft Nov. 29, 2005.

Kleinman, L., Y.N. Lee, S. Springston, L. Nunnermacker, X. Zhou, R. Brown, K. Hallock, P. Klotz, D. Leahy, J. Lee, and L. Newman. "Ozone Formation at a Rural Site in the Southeastern United States." *J. Geophys. Res*. **99**, 3469-3482, 1994.

Kleinman, L., W.F. Ryan, P.H. Daum, S.R. Springston, Y.-N. Lee, L.J. Nunnermacker, and J. Weinstein-Lloyd. "An ozone episode in the Philadelphia metropolitan area." *J. Geophys. Res.* **109**, D20302, doi:10.1029/2004JD004563, 2004.

Liu, S. C., M. Trainer, F. C. Fehsenfeld, D. D. Parrish, E. J. Williams, D. W. Fahey, G. Hubler, and P. C. Murphy. "Ozone production in the rural troposphere and the implications for regional and global ozone distributions." *J. Geophys. Res*. **92**, 4191–4207, 1987.

Lutgens, F., and E. Tarbuck. *The Atmosphere: An Introduction to Meteorology*, 8th ed., 512 pp., Prentice Hall, Upper Saddle River, New Jersey, 2001.

MARAMA (Mid-Atlantic Regional Air Management Association). *A guide to mid-Atlantic regional air quality.* MARAMA. Baltimore, MD, pp. 2-3, 2005 (available on-line at www.marama.org/reports).

McKeen, S. A., M. Trainer, E. Y. Hsie, R. K. Tallamraju, and S. C. Liu. "On the indirect determination of atmospheric OH radical concentrations from reactive hydrocarbon measurements." *J. Geophys. Res*. **95**, 7493–7500, 1990.

NARSTO. *An Assessment of Tropospheric Ozone Pollution*. NARSTO, July 2000.

Olszyna, K.J., E.M. Bailey, R. Simonaitis and J.F. Meagher. "O_3 and NO_y Relationships at a Rural Site." *J. Geophys. Res*. **99**, 14,557-14,563, 1994.

Ryan, W.F. and R.R. Dickerson. "Regional transport of pollutants and implications for 8-hour ozone non-attainment areas in Maryland." Report prepared for the Maryland Department of the Environment, Final version 2.2, 2000.

Ryan, W.F. “The low level jet in Maryland: Profiler observations and preliminary climatology.” Report prepared for the Maryland Department of the Environment, Air and Radiation Administration, 2004.

Sillman, S., J. A. Logan, and S. C. Wofsy. “A regional scale model for ozone in the United States with subgrid representation of urban and power plant plumes.” *J. Geophys. Res*. **95**, 5731–5748, 1990.

Sjostedt, D.W., J.T. Sigmon, and S.J. Colucci. “The Carolina nocturnal low-level jet: Synoptic climatology and a case study.” *Weather and Forecasting*. **5**, 404-415, 1990.

Stoeckenius, T. and Kemball-Cook, S. “Determination of representativeness of 2002 ozone season for ozone transport region SIP modeling.” Final Report prepared for the Ozone Transport Commission, 2005.

Trainer, M., D.D. Parrish, M.P. Buhr, R.B. Norton, F.C. Fehsenfeld, K.G. Anlauf, J.W. Bottenheim, Y.Z. Tang, H.A. Wiebe, J.M. Roberts, R.L. Tanner, L. Newman, V.C. Bowersox, J.F. Meagher, K.J. Olszyna, M.O. Rodgers, T. Wang, H. Berresheim, K.L. Demerjian, and U.K. Roychowdhury. “Correlation of Ozone with NO_y in Photochemically Aged Air.” *J. Geophys. Res*. **98**, 2917-2925, 1993.

Weisman, R.A. “An observational study of warm season southern Appalachian lee troughs. Part I: Boundary layer circulation.” *Monthly Weather Review*. **118**, 950-962, 1990.

Woodman, M.F., D.T. Nguyen, D.J. Krask, E. Joseph, V. Davis, R. Hoff, R. Rogers, M.G. Seybold. “Maryland Ozonesonde Campaign 2005.” Poster at EPA National Air Quality Conference, San Antonio, TX, 2006.

Zhang J. and S.T. Rao. “The role of vertical mixing in the temporal evolution of ground-level ozone concentrations.” *J. Applied Meteor.* **38**, 1674-1691, 1999.

3. OZONE-FORMING POLLUTANT EMISSIONS

The pollutants that affect ozone formation are volatile organic compounds (VOCs) and nitrogen oxides (NO_X). The emissions dataset presented for the OTR in the first section below is from the 2002 MANE-VU (Mid-Atlantic/Northeast Visibility Union) Version 2 regional haze emissions inventory. MANE-VU is the regional planning organization (RPO) for the mid-Atlantic and Northeast states coordinating regional haze planning activities for the region. While the context of the MANE-VU inventory is regional haze, it includes inventories of NO_X and VOCs that also inform air quality planners on sources important to ozone formation.[f] To provide a fuller context of precursor emissions contributing to regional ozone affecting the OTR, the section following the MANE-VU information presents NO_X and VOC emissions information from the 2002 National Emissions Inventory (NEI) for states in adjacent RPOs.

3.1. Emissions inventory characteristics in the OTR

3.1.1. Volatile organic compounds (VOCs)

Existing emission inventories generally refer to VOCs as hydrocarbons whose volatility in the atmosphere makes them particularly important in enhancing ozone formation in the presence of NO_X.

As shown in Figure 3-1, the VOC inventory for the OTR is dominated by mobile and area sources. Most VOC emissions in the OTR, however, come from natural sources, which are not shown in the figure. Among the human-caused VOC emissions, on-road mobile sources of VOCs include exhaust emissions from gasoline passenger vehicles and diesel-powered heavy-duty vehicles as well as evaporative emissions from transportation fuels. VOC emissions may also originate from a variety of area sources (including solvents, architectural coatings, and dry cleaners) as well as from some point sources (e.g., industrial facilities and petroleum refineries).

Naturally occurring (biogenic) VOC emissions are caused by the release of natural organic compounds from plants in warm weather. Many natural VOCs that contribute to ozone formation are highly reactive. Isoprene, for example, is a highly reactive five-carbon natural VOC emitted from mostly deciduous trees (e.g., oaks) that plays an important role in enhancing regional ozone formation across the eastern U.S. (Trainer *et al.*, 1987; Chameides *et al.*, 1988). Because biogenic VOC emissions are large and reactive, they are the most important part of the VOC inventory for understanding and predicting ozone formation. Biogenic VOCs are not included in Figure 3-1, but nationally, they represent roughly two-thirds of all annual VOC emissions (USEPA, 2006a). Modeling biogenic emissions can be difficult as it requires simulating biological responses to a range of environmental conditions, such as leaf temperature and the amount of sunlight reaching a leaf surface.

[f] The description of OTR state inventories discussed in the first section does not include the portion of Virginia in the Washington, DC metropolitan area. Information for Virginia is in the following section and comes from the 2002 National Emissions Inventory.

Figure 3-1. 2002 MANE-VU state VOC inventories in the OTR

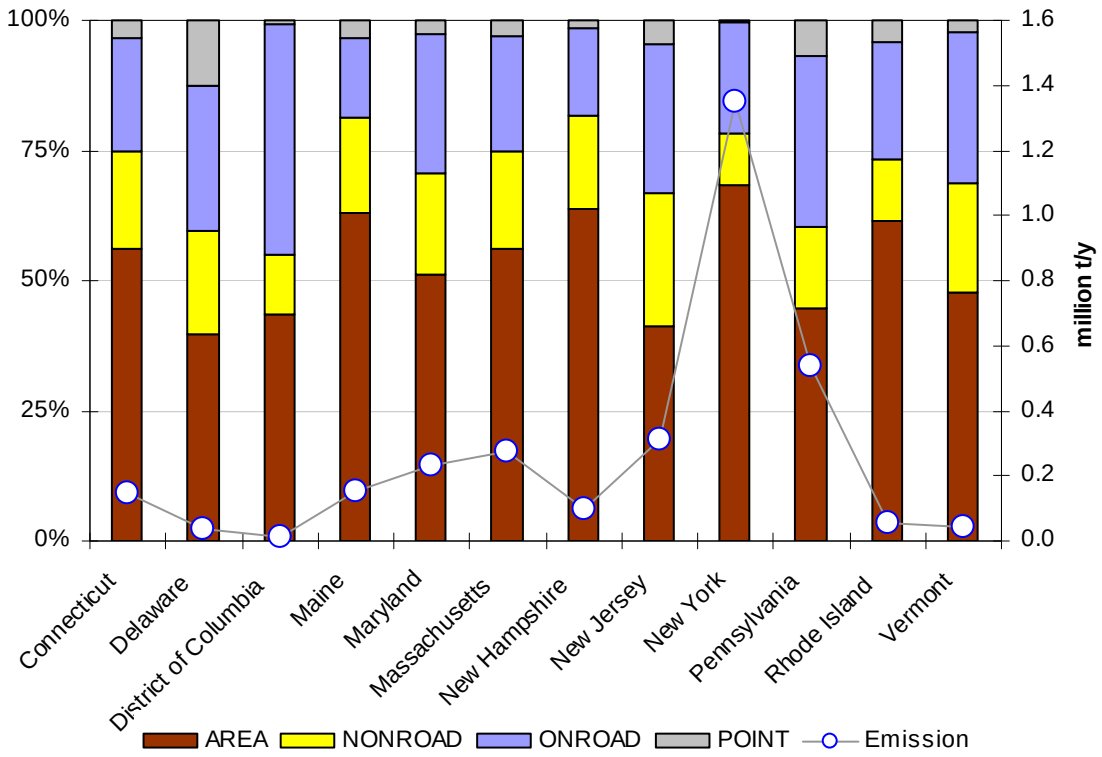

Figure key: Bars = Percentage fractions of four source categories; Circles = Annual emissions amount in 10^6 tons per year. The Virginia portion of the Washington, DC metropolitan area is not shown in the figure.

3.1.2. Oxides of nitrogen (NO_X)

NO_X emissions are a fundamental necessity for the atmospheric formation of ozone. Without NO_X, ozone formation during warm summer days would virtually cease, regardless of the amount of reactive VOCs present. By contrast, without VOCs, NO_X would still produce ozone in the presence of sunlight, albeit at a much diminished efficiency.

Figure 3-2 shows NO_X emissions in the OTR at the state level. Since 1980, nationwide emissions of NO_X from all sources have shown little change. In fact, emissions increased by 2 percent between 1989 and 1998 (USEPA, 2000). This increase is most likely due to industrial sources and the transportation sector, as power plant combustion sources have implemented modest emissions reductions during the same time period. Most states in the OTR experienced declining NO_X emissions from 1996 through 2002, except Massachusetts, Maryland, New York, and Rhode Island, which show an increase in NO_X emissions in 1999 before declining to levels below 1996 emissions in 2002.

Figure 3-2. State level nitrogen oxides emissions

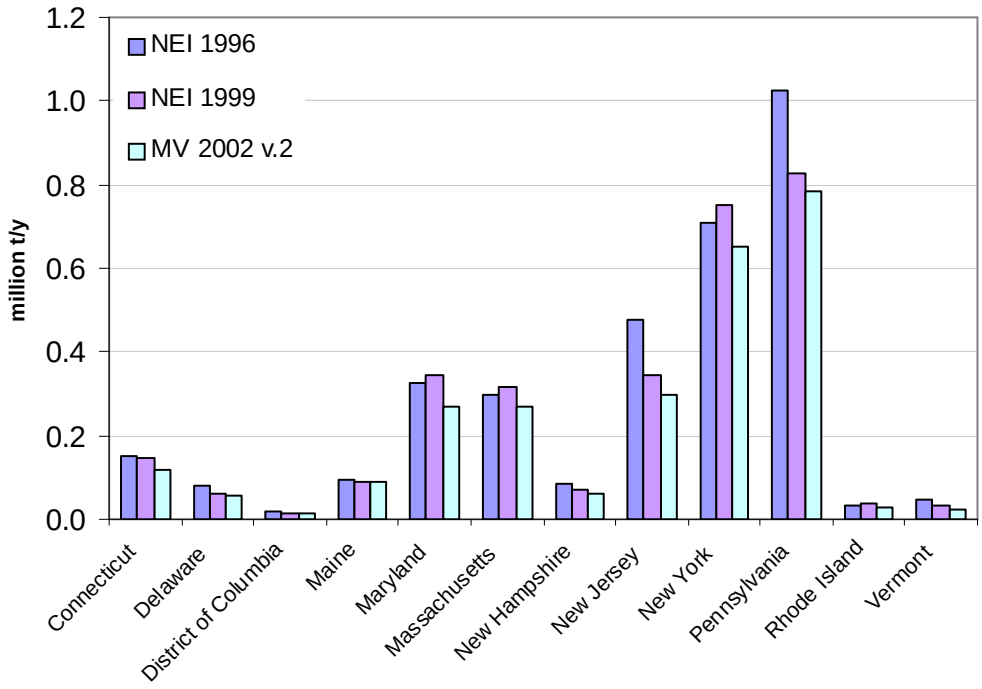

Monitored ambient NO_X trends during the summer from 1997 to 2005 corroborate the downward trend in NO_X emissions seen in the emissions inventories for the OTR. As seen in Figure 3-3, the 24-hour (lower trend lines) and 6 a.m.-8 a.m. (upper trend lines) NO_X concentrations indicate decreases in NO_X over this time period in the OTR. The NO_X reductions likely come from decreasing vehicle NO_X emissions due to more stringent motor vehicle standards as well as NO_X reductions from the OTR NO_X Budget Program and the NO_X SIP Call (mainly power plants).

Figure 3-3. Plot of monitored NO_X trends in OTR during 1997-2005

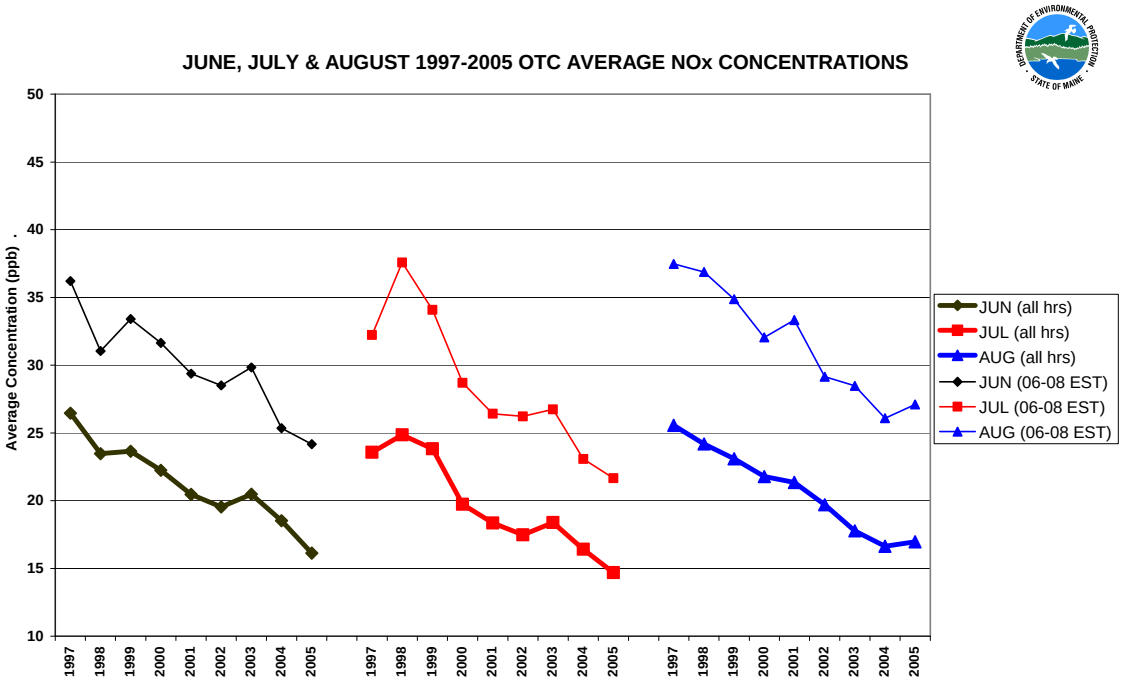

Note: Upper trend lines correspond to ambient NO_X measured from 0600-0800 EST in the morning. Lower trend lines correspond to NO_X measured over entire day (created by Tom Downs, Maine Department of Environmental Protection).

Power plants and mobile sources generally dominate state and national NO_X emissions inventories. Nationally, power plants account for more than one-quarter of all NO_X emissions, amounting to over six million tons. The electric sector plays an even larger role, however, in parts of the industrial Midwest where high NO_X emissions have a particularly significant power plant contribution. By contrast, mobile sources dominate the NO_X inventories for more urbanized mid-Atlantic and New England states to a far greater extent, as shown in Figure 3-4. In these states, on-road mobile sources — a category that mainly includes highway vehicles — represent the most significant NO_X source category. Emissions from non-road (i.e., off-highway) mobile sources, primarily diesel-fired engines, also represent a substantial fraction of the inventory.

Figure 3-4. 2002 MANE-VU state NO_X inventories in the OTR

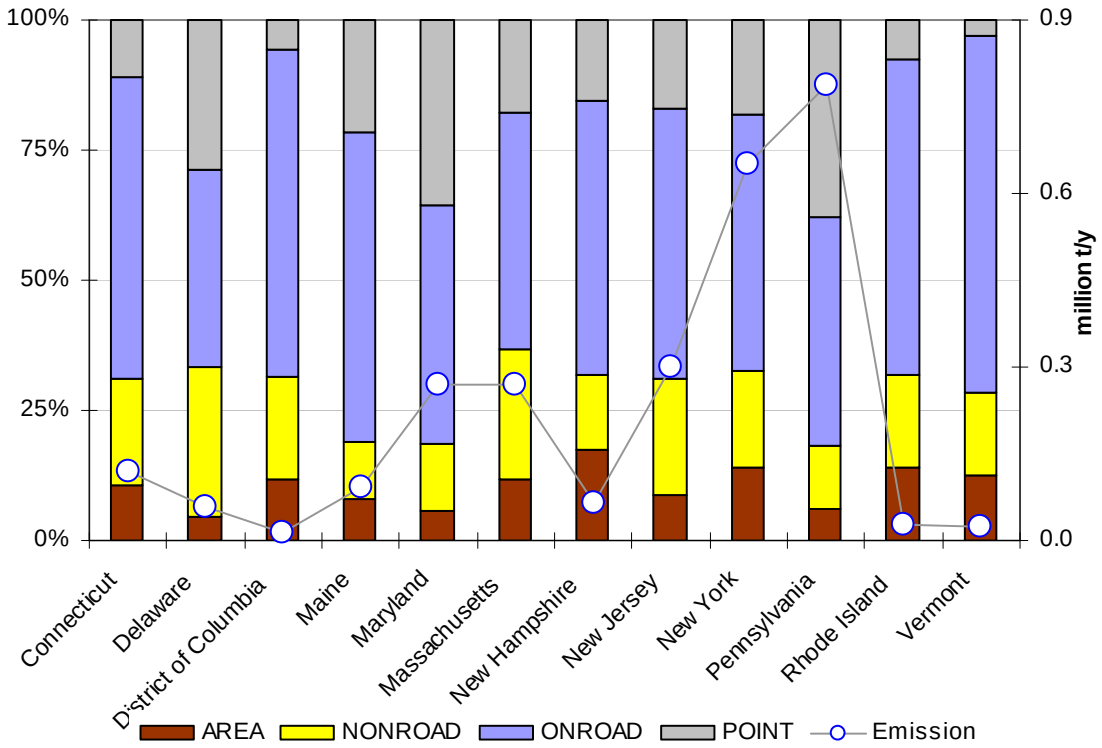

Figure key: Bars = Percentage fractions of four source categories; Circles = Annual emissions amount in 10^6 tons per year. The Virginia portion of the Washington, DC metropolitan area is not shown in the figure.

3.2. Emissions inventory characteristics outside the OTR

NO_X and VOC emissions in the OTR are only one component of the emissions contributing to ozone affecting the OTR. As regional modeling for the NO_X SIP Call and CAIR have shown, emission sources, primarily of NO_X, located outside the OTR can significantly contribute to ozone transported into the OTR. Here we present regional emissions information grouped by the three eastern RPOs – MANE-VU, VISTAS (Visibility Improvement State and Tribal Association of the Southeast), and the MWRPO (Midwest RPO). Table 3-1 lists the states in each RPO.

The inventory information is extracted from the USEPA final 2002 National Emissions Inventory (NEI). For consistency, the MANE-VU information here also comes from the 2002 NEI rather than from the MANE-VU Version 2 regional haze emissions inventory described above. The differences between the inventories are not great, as the NEI and the MANE-VU Version 2 inventory are both based on the same inventory information provided by the states.

Table 3-1. Eastern U.S. RPOs and their state members

RPO	State
MWRPO	Illinois
MWRPO	Indiana
MWRPO	Michigan
MWRPO	Ohio
MWRPO	Wisconsin
MANE-VU	Connecticut
MANE-VU	Delaware
MANE-VU	District of Columbia
MANE-VU	Maine
MANE-VU	Maryland
MANE-VU	Massachusetts
MANE-VU	New Hampshire
MANE-VU	New Jersey
MANE-VU	New York
MANE-VU	Pennsylvania
MANE-VU	Rhode Island
MANE-VU	Vermont
VISTAS	Alabama
VISTAS	Florida
VISTAS	Georgia
VISTAS	Kentucky
VISTAS	Mississippi
VISTAS	North Carolina
VISTAS	South Carolina
VISTAS	Tennessee
VISTAS	Virginia
VISTAS	West Virginia

Table 3-2 presents VOC emissions by source sector and RPO for the eastern United States. The NO_X emissions by source sector and RPO are presented in Table 3-3. Regionally, NO_X emissions are more important with respect to regional ozone formation and transport. NO_X emissions in combination with abundant naturally occurring VOC emissions from oaks and other vegetation have been shown to be important sources of regional ozone in the eastern U.S. (Trainer et al. 1987; Chameides et al. 1988).

Table 3-2. VOC emissions in eastern RPOs

RPO	Point	Area	On-road	Non-road	Total
MWRPO	234,938	1,182,186	660,010	492,027	2,569,160
MANE-VU	93,691	1,798,158	793,541	494,115	3,179,504
VISTAS	458,740	2,047,359	1,314,979	609,539	4,430,617

Table 3-3. NO_X emissions in eastern RPOs

RPO	Point	Area	On-road	Non-road	Total
MWRPO	1,437,284	184,790	1,290,178	723,844	3,636,096
MANE-VU	680,975	268,997	1,297,357	534,454	2,781,783
VISTAS	2,094,228	266,848	2,160,601	812,615	5,334,293

3.3. Are NO_X or VOC control strategies most effective at reducing ozone?

The effectiveness of a NO_X-focused or VOC-focused control strategy to reduce ozone is not constant by location or emissions; rather it is a changing chemical characteristic of an air parcel affecting a particular location. As a result, the effectiveness of a NO_X or VOC-focused control strategy can vary within an air parcel as it dynamically evolves over time with transport, dispersion, and photochemical aging (NARSTO, 2000).

On a regional basis, OTAG, CAIR and other modeling studies have consistently shown that NO_X reductions have the greatest impact on regional ozone concentrations, while VOC reductions have more local impacts. This is largely a result of significant naturally occurring VOC emissions (especially isoprene) in large forested regions of the eastern U.S. Real-world results from regional NO_X reductions at power plants (i.e., the NO_X SIP Call) are now indicating that significant ozone reductions are occurring on a regional basis as a result of regional NO_X strategies. A recent USEPA report finds a strong association between areas with the greatest NO_X emission reductions due to the NO_X SIP Call and downwind sites exhibiting the greatest improvement in ozone in 2005 (USEPA, 2006b).

As a general rule, VOC reductions may be effective at reducing urban-scale ozone pollution in lieu of or in combination with local NO_X reductions, while regional NO_X controls are most effective at reducing regional ozone. While a general rule can be outlined in evaluating the potential effectiveness of NO_X and VOC-focused control strategies, the optimal strategy for a specific location will depend on the particular circumstances of that location. Exceptions to a VOC-only strategy for an urban area can occur when the urban area has large natural VOC emissions, ozone is transported from upwind, or there is recirculation of aged local pollution (e.g., sea breeze effect). Furthermore, because the conditions causing individual ozone episodes can vary, a given urban area may change in sensitivity between a NO_X and VOC-focused strategy depending on a particular episode's conditions (NARSTO, 2000). Therefore, the appropriate combination of VOC and NO_X controls at the local level depends on local circumstances with the realization that a single approach focusing on NO_X or VOC-only controls is not necessarily effective for all episode types. It is clear, however, that regional NO_X reductions provide regional ozone reductions, and this will influence ozone levels being transported into local urban areas.

3.4. Summary

There are large emissions of VOCs and NO_X within and outside the OTR that contribute to local and regional ozone problems. Naturally occurring VOC emissions play an important role in combination with human-caused NO_X emissions in forming regional ozone across large sections of the eastern U.S. Regional NO_X control strategies are demonstrating success in reducing regional ozone. On a more local scale, some combination of VOC and NO_X controls may be needed, with the specific combination dependent upon local circumstances.

References

Chameides, W.L., R.W. Lindsay, J. Richardson, and C.S. Kiang. "The role of biogenic hydrocarbons in urban photochemical smog: Atlanta as a case study." *Science* **241**, 1473-1475, 1988.

NARSTO. *An Assessment of Tropospheric Ozone Pollution*. NARSTO, July 2000.

Trainer, M., E.J. Williams, D.D. Parrish, M.P. Buhr, E.J. Allwine, H.H. Westberg, F.C. Fehsenfeld, and S.C. Liu. "Models and observations of the impact of natural hydrocarbons on rural ozone." *Nature* **329**, 705-707, 1987.

USEPA. *National Air Quality and Emission Trends Report, 1998*, EPA 454/R-00-003, available online: http://www.epa.gov/oar/aqtrnd98/, 2000.

USEPA. *2002 Final National Emissions Inventory (NEI)*, available online: ftp://ftp.epa.gov/EmisInventory/2002finalnei/, 2006a (accessed October 10, 2006) [The 2002 NEI reports national annual emissions for total anthropogenic VOC emissions as 16.8 million tons, and total biogenic VOC emissions as 41.8 million tons].

USEPA. *NO_X Budget Trading Program 2005 Compliance and Environmental Results*, EPA430-R-06-013, available online: http://www.epa.gov/airmarkets/fednox/, 2006b.

4. WHAT WILL IT TAKE TO CLEAN THE AIR? – LINKING THE SCIENCE TO POLICY

4.1. The three phases of a bad ozone day and the ozone reservoir

With the atmospheric chemistry, meteorology, and air emission inventory elements presented in the previous sections, a conceptual description emerges of ozone problem in the OTR. Consider a typical "day," defined as starting at sunset, for a severe ozone event associated with a high pressure system. Conceptually, a bad ozone day can be considered as occurring in three phases. During phase one, a nocturnal inversion forms as the temperature of the earth drops following sunset, isolating the surface from stronger winds only a few hundred feet overhead. Ozone near the surface cannot mix with ozone above and is destroyed as it reacts with the Earth's surface. In a city, fresh NO_X emissions react with ozone, further reducing its concentration, so that by morning, very little ozone is left below the nocturnal inversion. At this time, the nocturnal inversion is at its strongest, and winds at the surface are typically calm.

Above the nocturnal inversion, the situation is quite different. Ozone and its precursors, both from the previous day's local emissions and from transport, remain largely intact. There are no surfaces to react with the ozone and a large reservoir of ozone remains above the inversion. During phase two of a bad ozone day, the nocturnal inversion breaks down at mid-morning, with the result that the ozone and precursors above the inversion can now mix with the air near the surface. The result of this mixing is a sudden change in ozone. Figure 4-1 shows median ozone profiles for morning and afternoon aircraft flights from 1996 – 2003. One can clearly see the breakdown of the nocturnal inversion throughout the day (Hudson, 2005).

Figure 4-1. Median ozone profiles for morning and afternoon flights from 1996 – 2003

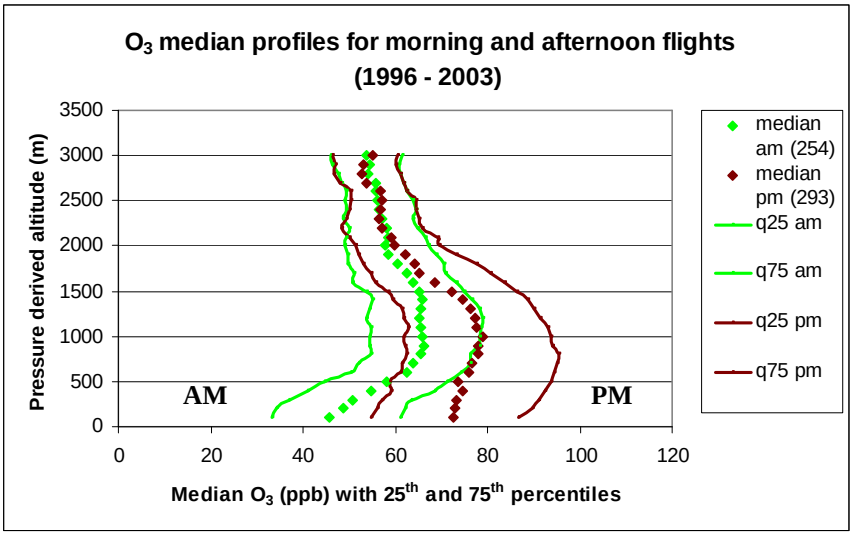

In phase three of a bad ozone day, ozone concentrations reach their highest levels in the afternoon through the combined accumulation of local pollution produced that day mixed with the transported regional pollution load brought in overnight from the ozone reservoir. Figure 4-2 shows this graphically for the southern OTR. The ozone monitor at Methodist Hill, PA is a high elevation site located at 1900 ft in altitude in south central Pennsylvania, and is above the nocturnal inversion. In the early morning hours of August 12, 2002 (e.g., 5 a.m.), it recorded ozone concentrations above 80 ppb, which was much higher than what other lower elevation monitors in the region were recording (e.g., Little Buffalo State Park, PA, South Carroll County, MD, Frederick, MD, Ashburn, VA, Long Park, VA). Due to the lack of sunlight necessary to produce ozone photochemically during nighttime hours, the high ozone levels seen at Methodist Hill, PA indicate the presence of a significant ozone reservoir above the nocturnal inversion layer produced during daylight hours at some earlier point in time and transported into the region. With the break up of the nocturnal inversion after sunrise (e.g., starting about 7 a.m.), ozone concentrations at the lower elevation monitors show a rapid increase. This reflects the mixing down of the ozone reservoir from higher altitude to the surface in combination with local ozone production near the surface now that the sun has begun inducing its photochemical production.

Figure 4-2. Hourly ozone profiles in the southern OTR, August 12, 2002

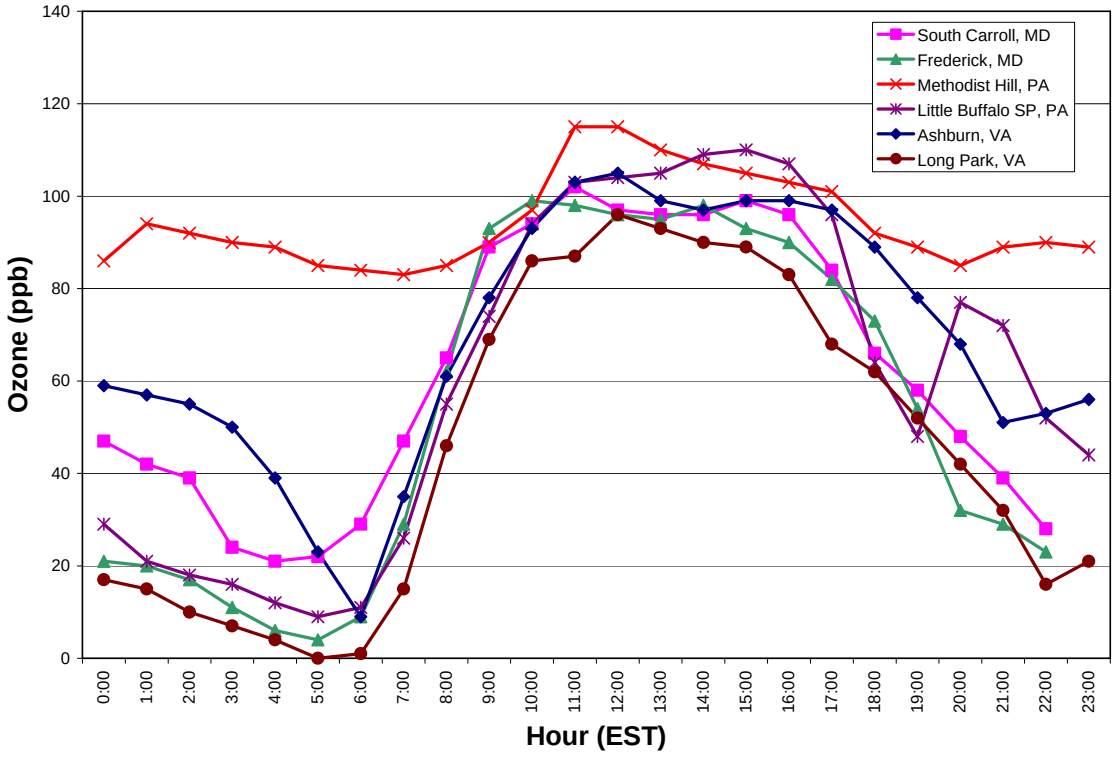

The ozone reservoir extends across the OTR, as seen on the same night in high elevation ozone monitoring sites in the northern OTR. Figure 4-3 shows the hourly ozone concentrations measured on August 12, 2002 at Mohawk Mountain, CT, Cadillac Mountain, ME, Mt. Greylock, MA, Mt. Monadanock, NH, Mt. Washington, NH, and

Whiteface Mountain, NY. As with Methodist Hill, PA on this day, these sites show elevated ozone concentrations during nighttime hours, as compared to lower elevation sites below the nocturnal inversion (e.g., Danbury, CT). By mid-day, however, the nocturnal boundary layer has broken down, mixing the transported ozone from the reservoir above into the locally produced ozone below. Appendix G provides more detail on contributions to the ozone reservoir within and outside the OTR.

Figure 4-3. Hourly ozone profiles in the northern OTR, August 12, 2002

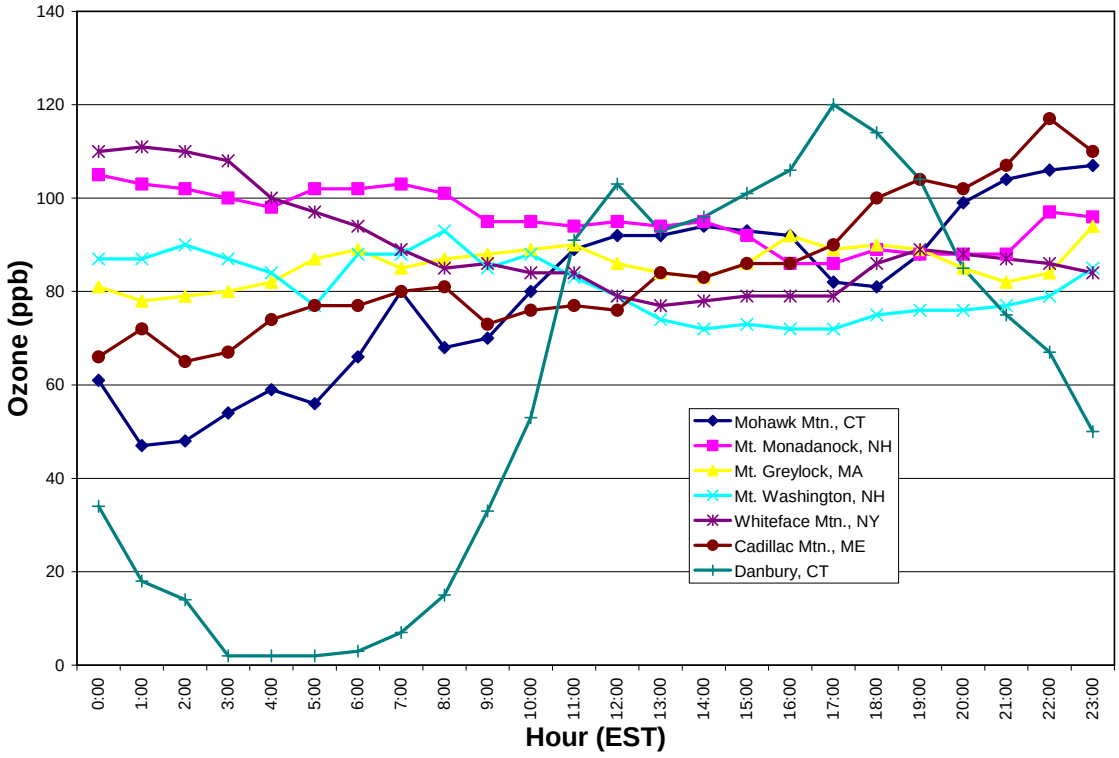

Data provided by Tom Downs, Maine Department of Environmental Protection.

4.2. Chronology of an ozone episode – August 2002

The chronology of an historical ozone episode occurring in the OTR from August 8 to August 16, 2002 provides a real-world example that pieces together the elements of the ozone conceptual description given in this document. Surface maps from the period provide a synoptic overview of major weather systems that were influencing air quality across the OTR during that time. Meteorological insights combined with ozone concentration information provide a picture of the evolving ozone episode on a day-by-day basis. Figure 4-4, Figure 4-5, and Figure 4-6, respectively, show eight-panel displays of surface weather maps, back trajectories, and 8-hour maximum ozone concentrations from each day. The daily progression shows the formation of high ozone that shifts from west to east, and ultimately northward, during successive days of the episode according to local ozone formation and transport shaped by wind patterns within and outside of the OTR.

The August 2002 episode began with a slow-moving high pressure system centered over the Great Lakes initiating a northerly flow over the OTR on August 8. Over

the next several days, the high drifted southeastward and became extended across a large part of the eastern U.S., bringing high temperatures to the region. Calm conditions west of the OTR on August 10 were pivotal for the formation of ozone, which first began building in the Ohio River Valley. Over the next four days, 8-hour ozone concentrations climbed well above the 85 ppb (0.08 ppm) NAAQS over a wide area of the OTR. Large parts of the heavily populated Northeast Corridor experienced 8-hour ozone levels above 100 ppb during the height of the episode, which far exceeded the 85 ppb NAAQS.

The following chronology provides a day-by-day evolution of the August 2002 ozone episode. Parts of this description are taken from Ryan (2003).

August 8: A high pressure system over the Great Lakes produces NW-N prevailing surface winds (~4-8 mph) throughout the region. Maximum daily temperatures approach or exceed 80º F.

August 9: Wind speeds fall off but the direction remains NW-N as the high moves into the Pennsylvania-New York region. Temperatures rise as cloud cover declines. Background ozone levels begin to build in the Ohio River Valley with 8-hour maximum concentrations reaching the 60-80 ppb range.

August 10: High pressure is directly over the mid-Atlantic. With dew points still in the mid-50º's F, the skies are extraordinarily clear throughout the day. Temperatures (except in northern-most areas) approach 90º F while surface-level winds turn to more southerly directions. With high pressure overhead, the back trajectories suggest very light winds and recirculation. Calm conditions through the morning hours in the lower Ohio River Valley promote increasingly higher levels of ozone noted in surface observations – now reaching above the 85 ppb 8-hour ozone NAAQS over much of Indiana, Ohio, and other states along the Ohio River, as well as states around Lake Michigan and large portions of the southeastern U.S. Ozone levels above the 8-hour NAAQS now begin appearing for the first time in the western and southern parts of the OTR.

August 11: Surface high pressure drops slowly southeastward across the mid-Atlantic with the center in western North Carolina drifting to coastal South Carolina during the day. The upper level ridge has also moved east and is located over the mid-Atlantic. Circulation around the high becomes well established. A surface-level trough descends from north of the Great Lakes during the day, passes eastward through the Ohio River Valley and stalls over the Allegheny Mountains and southward. Peak temperatures are in the low to mid-90º's F. Morning winds are low-to-calm in the area east of the Mississippi – the area of ozone now reaches from eastern Wisconsin to Tennessee and eastward to Georgia up through the Carolinas into the OTR, covering most of Pennsylvania, New York, New Jersey, Connecticut, Rhode Island and Massachusetts. Winds are generally south to southwest as is reflected in the boundary layer back trajectories. The key factor driving local ozone production appears to be a very stable boundary layer. The 8 a.m. sounding at the Washington-Dulles airport shows a very strong low-level inversion from 950-900 mb with a deep residual layer beneath a continuing strong subsidence inversion – now based at 760 mb.

August 12: The upper level ridge remains quasi-stationary with its axis over the mid-Atlantic. The center of high pressure at 850 mb is over North Carolina and Georgia. At the surface, the characteristic Appalachian lee side trough forms. Temperatures exceed

90º F throughout the OTR except in coastal Maine. Winds are fairly strong from the northwest. This is reflected in the back trajectories that show a shift to westerly transport. Elevated upwind ozone concentrations at 11 a.m. on August 11 occur in the vicinity of the origin of the back trajectories, on the order of 78-86 ppb. Ozone concentrations fall this day west of the Appalachians but increase markedly across the mid-Atlantic. The area of highest ozone has pushed eastward and now extends from southern Maine across central Pennsylvania down through Maryland into the Carolinas, Georgia, and eastern Tennessee. Ozone builds throughout the day as circulation forces it to channel northeast between the stalled trough and a cold front approaching from the Midwest. Some of the highest 8-hour concentrations occur through the central to southern OTR on this day.

August 13: Calm conditions prevail as the trough reaches coastal New Jersey by 8 a.m. Generally clear skies allow temperatures to reach the mid-90º's F everywhere except in coastal Maine. Dew points, which had been rising since August 8, reach the upper 60º's F. A morning sounding at the Washington-Dulles airport showed a continuing strong low level inversion with a residual mixed layer to 850 mb ending just beneath a weak secondary inversion. The cap aloft has lifted to ~ 630 mb and the sounding is more unstable compared to previous day's between the two inversion layers. The Appalachian lee side trough continues in place from late on August 12. As is typically the case, the highest ozone concentrations are found in proximity to this boundary. The highest 8-hour ozone concentrations are along the eastern portions of the OTR from northeastern Virginia through New Jersey, Long Island, Connecticut, and into eastern Massachusetts. By 8 p.m., showers associated with the approaching cold front have reached into Ohio.

August 14: By 8 a.m., the trough has dissipated and the high is moving offshore, resulting in an increasing southerly wind component, which pushes maritime air northward. Dew points remain in the upper 60º's F and peak temperatures reach into the 90º's F everywhere and top 100º F in several locations. Ozone concentrations build again, with the highest levels concentrated in the central OTR from eastern Pennsylvania across to Massachusetts. A "hotspot" of ozone appears in upstate New York at the eastern end of Lake Ontario, and may be the result of transport from the west across the lake. Ozone concentrations decrease south and west of Baltimore and along coastal New Jersey as cleaner maritime air pushes in from the south.

August 15: This episode ends in a very different manner than the standard high ozone episode. Instead of the passage of a sharp cold front, this episode ends gradually as cleaner air sweeps north, winds increase, and the atmosphere steadily destabilizes. Ozone concentrations fall across the middle and lower OTR as low level flow becomes more southeast and the Bermuda high fills in westward. The highest levels, still exceeding the 8-hour ozone NAAQS, now occur in the northern reaches of the OTR in upstate New York, Vermont, New Hampshire, and Maine.

August 16: Cloud cover spreads over the region with ozone falling further. The new high building into the upper Midwest pushes the remains of the showers out of the Northeast. A spot of high ozone persists in central New Jersey. This is the last exceedance day in a string of seven exceedance days within the OTR during this extended episode.

Figure 4-4. Surface weather maps for August 9-16, 2002

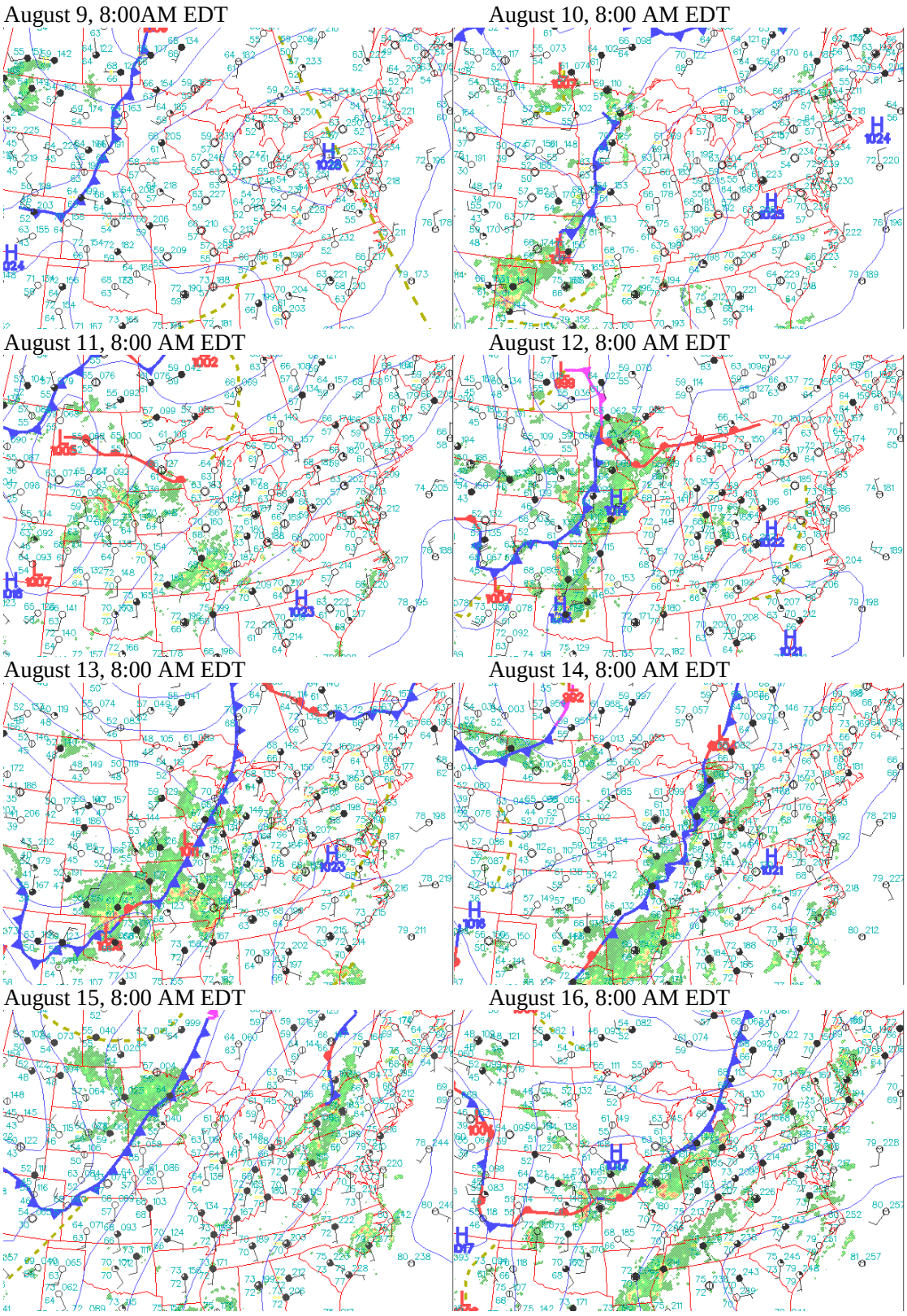

Figure 4-5. HYSPLIT 72-hour back trajectories for August 9-16, 2002

Aug 9, 2002 8 am EDT

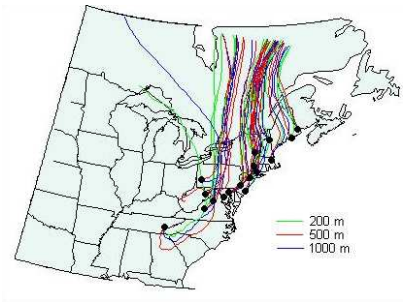

Aug 10, 2002 8 am EDT

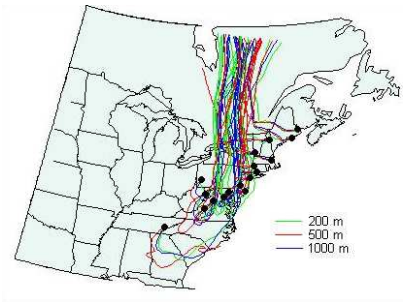

Aug 11, 2002 8 am EDT

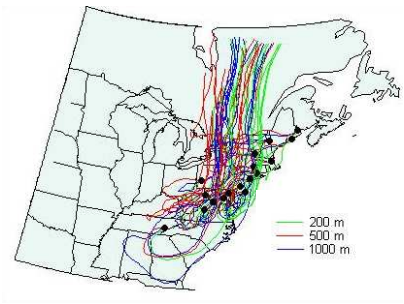

Aug 12, 2002 8 am EDT

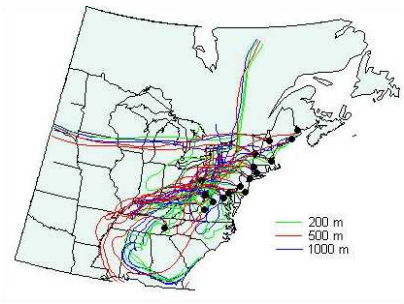

Aug 13, 2002 8 am EDT

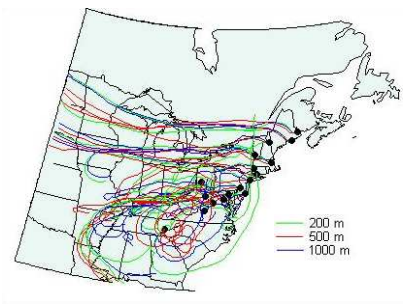

Aug 14, 2002 8 am EDT

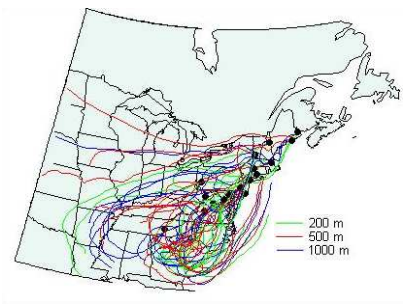

Aug 15, 2002 8 am EDT

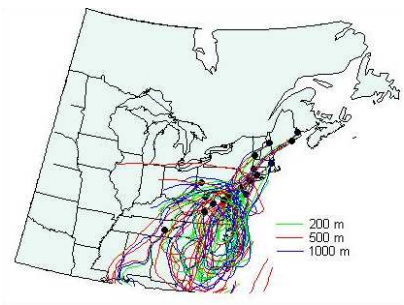

Aug 16, 2002 8 am EDT

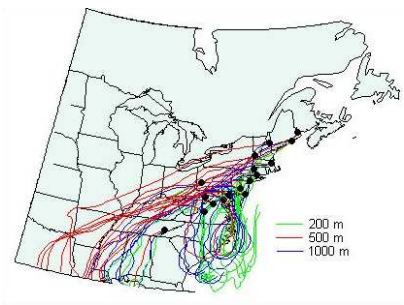

Figure 4-6. Spatially interpolated maps of maximum 8-hour surface ozone concentrations August 9 – 16, 2002

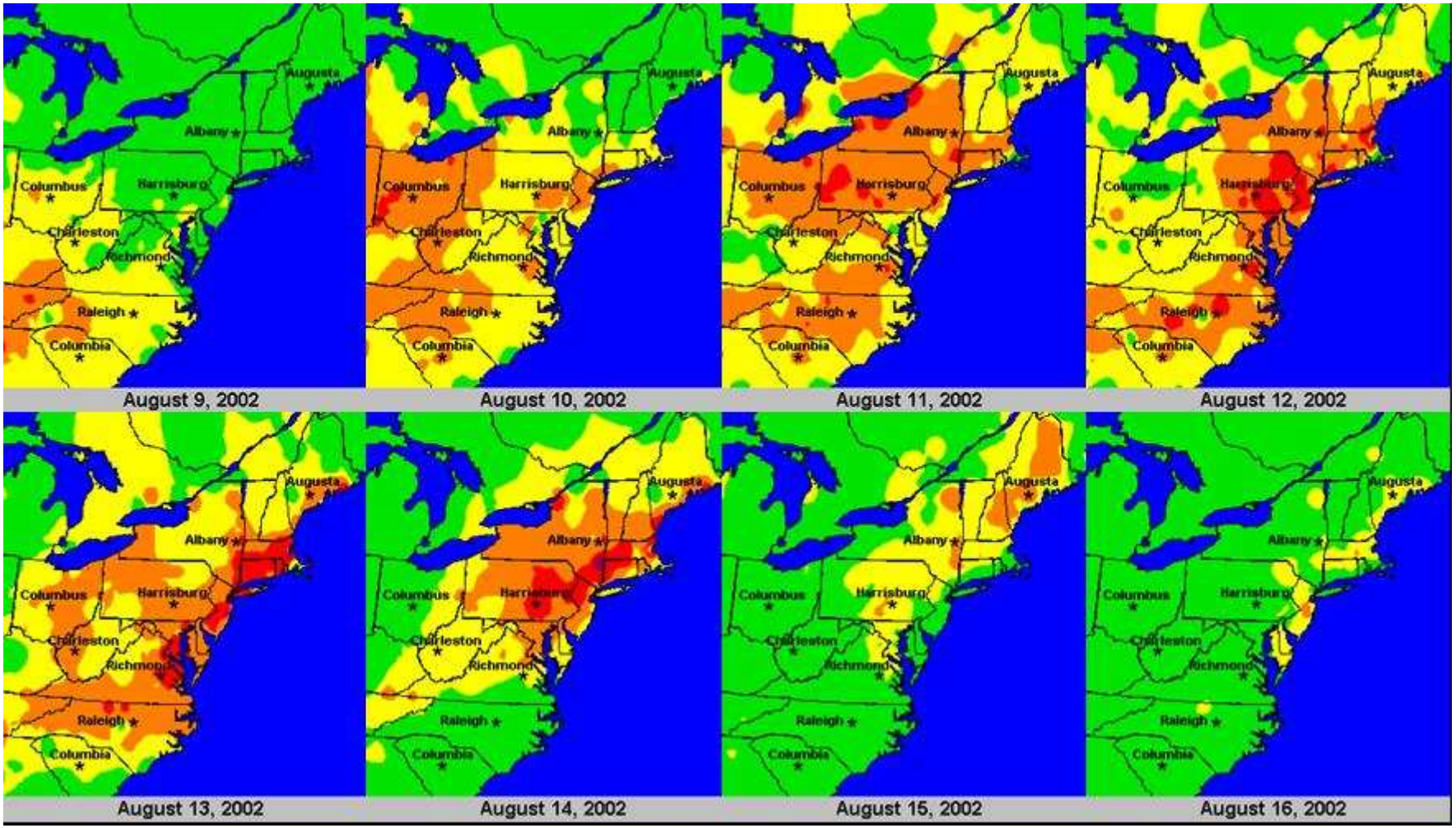

4.3. Clean Air Act provisions

As is evident from the myriad source regions and transport pathways affecting the OTR, the regional ozone nonattainment problem presents a significant challenge to air quality planners. To improve air quality, emission reductions of the appropriate pollutants must occur at the appropriate levels (i.e., stringency of controls) and over the appropriate geographic extent. States have primary responsibility for achieving the goals of the Clean Air Act, as they are responsible for developing State Implementation Plans and implementing and enforcing emission reduction programs to meet the health-protective National Ambient Air Quality Standards (NAAQS).

When Congress passed the Clean Air Act Amendments of 1990, it recognized that air pollution transcends political boundaries and that tools for addressing transport must be made available to state and federal governments. Accordingly, several Clean Air Act provisions deal with transported pollution, including: (1) prohibiting the USEPA from approving State Implementation Plans that interfere with another state's ability to attain or maintain a NAAQS; (2) requiring the USEPA to work with states to prevent emissions that contribute to air pollution in a foreign country; (3) allowing states to form ozone transport regions; (4) requiring states in ozone transport regions to adopt a prescribed set of controls in order to achieve a minimum level of regional emission reductions; and (5) allowing states to petition the USEPA for timely relief from stationary source emissions that interfere with attainment or maintenance of a NAAQS, and requiring the USEPA to act on such petitions within a very short, prescribed timeframe. Taken together, these provisions provide a framework for air quality planning. Its inherent principles are:

- Timely action is critical in order to protect public health;
- States must act locally to address air pollution;
- While acting locally, states must also consider their impacts downwind in addition to in-state impacts when developing state implementation plans (SIPs), and ameliorate such impacts through SIPs;
- Regional actions have been and can continue to be effective;
- To be effective on a regional level, states working together must work off of a level playing field.

What the science tells us of the nature of the ozone problem in the OTR supports this framework. The smaller scale weather patterns that affect pollution accumulation and transport underscore the importance of local (in-state) controls for NO_X and VOC emissions. Larger synoptic scale weather patterns, and pollution patterns associated with them, support the need for NO_X controls across the eastern United States. Studies and characterizations of nocturnal low level jets (i.e., channeled transport) also support the need for local and regional controls on NO_X and VOC sources as local and transported pollution from outside the OTR can be entrained in nocturnal low level jets formed during nighttime hours within the OTR. Land, sea, mountain, and valley breezes indicate that there are unique aspects of pollution accumulation and transport that are area-specific and will warrant policy responses at the local and regional levels beyond a one-size-fits-all approach.

The mix of emission controls is also important for states to consider. While long-range transport of ozone is primarily due to NO_X, VOCs are important because they contribute to ozone formation by influencing how efficiently ozone is produced by NO_X, particularly within urban centers. While reductions in anthropogenic VOCs will typically have less of an impact on the long-range transport of ozone, they can be effective in reducing ozone in those urban areas where ozone production may be limited by the availability of VOCs. Therefore, a combination of localized VOC reductions in urban centers with additional NO_X reductions (from both mobile and point sources) across a larger region will help to reduce ozone and precursors in nonattainment areas as well as their downwind transport across the entire region (NESCAUM, 1997).

4.4. Past regional efforts

While states are somewhat limited in their ability to directly affect emissions reductions beyond their own geo-political boundaries, over the past 15-20 years, the Northeast states have acted regionally with tremendous success. Such efforts have included:

- In 1989, regional low volatility gasoline (i.e., Reid Vapor Pressure pf 9.0 psi) was introduced into the NESCAUM region, resulting in significant VOC reductions;
- In 1994, the California Low Emission Vehicle (LEV) program commenced in the Northeast Corridor as regulations were adopted by Maine, Massachusetts, New York, and Vermont. To date, four additional states have joined the program, which continues to yield reductions in NO_X, VOC, CO, and air toxics.
- In 1994, the states of the Ozone Transport Commission agreed to promulgate regional NO_X RACT controls and a NO_X cap-and-trade program. The adopted regional RACT deadline was 1995. By 1999, the NO_X Budget Program was implemented over the 12-state region from Maine to Washington, DC. In 2002, the USEPA reported that the NO_X Budget sources "emitted at a level approximately 12 percent below 2001 allocations" (USEPA, 2002). Progress continues with a more stringent cap taking effect in 2003.
- In 1997, eight OTR states petitioned the USEPA under section 126 of the Clean Air Act, requesting NO_X emissions reductions on certain stationary sources in the Eastern U.S. In 1999, four more OTR members filed section 126 petitions. The USEPA granted four of the initial eight state petitions in 2000.[g]
- In 2001, the states of the Ozone Transport Commission agreed to support a suite of model rules for inclusion in SIPs as appropriate to address 1-hour ozone problems. The model rules included controls for: (1) architectural and industrial maintenance coatings; (2) portable fuel containers; (3) consumer products; (4) solvent cleaning; (5) mobile equipment repair and refinishing; and (5) additional

[g] The initial eight section 126 OTR states were Connecticut, Maine, Massachusetts, New Hampshire, New York, Pennsylvania, Rhode Island, and Vermont. The additional four OTR members filing section 126 petitions were Delaware, the District of Columbia, Maryland, and New Jersey. The four granted petitions were from Connecticut, Massachusetts, New York, and Pennsylvania.

NO_X controls for industrial boilers, cement kilns, stationary reciprocating engines, and stationary combustion engines.

These regional efforts have led the way for similar broader regional and national programs. For mobile sources, the USEPA promulgated its federal Reformulated Gasoline Program in 1995 and the National LEV program in 1998. For stationary sources, the USEPA announced in 1997 that it would expand the OTR NO_X Budget Program through the NO_X SIP Call, which included 22 states and NO_X caps in place by 2003. The NO_X SIP Call also served as a response to the states' Section 126 petitions under the Clean Air Act.

In 2005, the USEPA took a further step to address the regional ozone problem by issuing the Clean Air Interstate Rule (CAIR), which requires additional NO_X reductions in 25 eastern states and the District of Columbia. The USEPA projects that CAIR will achieve NO_X reductions of 2 million tons in 2015, a 61% decrease from 2003 levels. This will be a significant step forward in improving air quality, but the time allowed to achieve these reductions is later than the deadline many eastern states are facing to meet the current 8-hour ozone NAAQS. This, therefore, only partially provides the OTR with a regional measure that helps achieve the Clean Air Act's goal of attaining the ozone air quality health standard within the Act's mandatory deadlines.

4.5. Summary: Building upon success

A conceptual understanding of ozone as a regional problem in the OTR and throughout the eastern U.S. is now well established. With this evolution in understanding, regional approaches to the ozone problem are now underway, starting with the 1990 Clean Air Act Amendments that created the Ozone Transport Region. This initial regional approach, however, did not include large source regions outside of the OTR containing many large coal-fired power plants and other pollution sources contributing to the long-range transport of ozone into the OTR.

In 1998, the USEPA took another step in addressing the regional problem by finalizing the NO_X SIP Call, which covered emissions of NO_X, the main precursor of regional ozone, in additional parts of the East. Even with these reductions, air quality modeling has projected continuing significant contributions from upwind sources in out-of-state regions. As a result, the USEPA promulgated a further round of regional NO_X reductions in the East with the adoption of CAIR in 2005. With the modeling foundation for CAIR, the USEPA has presented a compelling technical case on the need for additional regional NO_X reductions in the eastern U.S. to reduce ozone levels and protect public health. While states in the Northeast disagree with the extent of NO_X reductions and the timeline for those reductions to occur, the program is an excellent next step toward reducing ozone in the OTR.

There is a tendency to characterize the nonattainment problems persisting after implementation of the USEPA's Clean Air Interstate Rule and other federal programs as "residual," but care must be taken in assessing these continuing nonattainment problems. A "residual" ozone problem is better characterized as a persistent nonattainment problem that still requires broad regional responses coupled with local controls. As this conceptual description points out, one of the great lessons and successes seen in the history of air

quality policy was the shift from urban-only air pollution control strategies to broader regional approaches in the East at the end of the 1990s (e.g., NO_X SIP Call). The danger exists, however, that the perception of a "residual" ozone problem as being only a local issue will ignore the lessons learned from effective regional approaches.

The current suite of local and regional controls have a proven track record of success, and have helped to significantly lower NO_X, VOC, and ozone levels across the eastern U.S. As described earlier in this report, monitored NO_X emissions and ambient concentrations have dropped between 1997 and 2005, and the frequency and magnitude of ozone exceedances have declined within the OTR. To maintain the current momentum for improving air quality so that the OTR states can meet their attainment deadlines, there continues to be a need for more regional NO_X reductions coupled with appropriate local NO_X controls and regional and local VOC controls.

References

Hudson, R. "A Conceptual Model for Ozone Transport." University of Maryland, Dept. of Atmospheric and Oceanic Science. Prepared for the Ozone Transport Commission. Draft Nov. 29, 2005.

NESCAUM. *The Long Range Transport of Ozone and Its Precursors in the Eastern United States*. NESCAUM, Boston, MA, p.6, 1997.

Ryan, W.F. *Air Quality Forecast Report Philadelphia Forecast Area 2002*. The Pennsylvania State University, Department of Meteorology, University Park, PA, March 2003 (available on-line at http://www.meteo.psu.edu/~wfryan/phl_2002_final_report.htm).

USEPA. *OTC NO_X Budget Program Compliance Report 2001*. U.S. Environmental Protection Agency, Washington, DC, p. 1, 2002.

Appendix A: USEPA Guidance on Ozone Conceptual Description

From "Guidance on the Use of Models and Other Analyses in Attainment Demonstrations for the 8-hour Ozone NAAQS," U.S. Environmental Protection Agency, EPA-454/R-05-002, Section 8, October 2005.

Note: At the time of this writing, the USEPA was incorporating Section 8 of the 8-hour ozone guidance into a new USEPA guidance document covering ozone, $PM_{2.5}$, and regional haze. The new draft guidance is in Section 11 of Draft 3.2 "Guidance on the Use of Models and other Analyses for Demonstrating Attainment of Air Quality Goals for Ozone, $PM_{2.5}$, and Regional Haze," U.S. EPA, (Draft 3.2 – September 2006), available at http://www.epa.gov/ttn/scram/guidance_sip.htm#pm2.5 (accessed Oct. 5, 2006). The newer guidance, when finalized, may differ in some respects from the text given in Section 8 of the earlier ozone guidance.

Excerpt of Section 8 from EPA 8-hour ozone NAAQS guidance document:

8.0 How Do I Get Started? – A "Conceptual Description"
- 8.1 What Is A "Conceptual Description"?
- 8.2 What Types Of Analyses Might Be Useful For Developing And Refining A Conceptual Description?
  - 8.2.1. Is regional transport an important factor affecting the nonattainment area?
  - 8.2.2. What types of meteorological episodes lead to high ozone?
  - 8.2.3. Is ozone limited by availability of VOC, NO_X or combinations of the two? Which source categories may be most important?

Appendix A: USEPA Guidance on Ozone Conceptual Description

8.0 How Do I Get Started? - A "Conceptual Description"

A State/Tribe should start developing information to support a modeled attainment demonstration by assembling and reviewing available air quality, emissions and meteorological data. Baseline design values should be calculated at each ozone monitoring site, as described in Section 3. If past modeling has been performed, the emission scenarios examined and air quality predictions may also be useful. Readily available information should be used by a State/Tribe to develop an initial conceptual description of the nonattainment problem in the area which is the focus of a modeled attainment demonstration. A conceptual description is instrumental for identifying potential stakeholders and for developing a modeling/analysis protocol. It may also influence a State's choice of air quality model, modeling domain, grid cell size, priorities for quality assuring and refining emissions estimates, and the choice of initial diagnostic tests to identify potentially effective control strategies. In general, a conceptual description is useful for helping a State/Tribe identify priorities and allocate resources in performing a modeled attainment demonstration.

In this Section, we identify key parts of a conceptual description. We then present examples of analyses which could be used to describe each of these parts. We note that initial analyses may be complemented later by additional efforts performed by those implementing the protocol.

8.1 What Is A "Conceptual Description"?

A "conceptual description" is a qualitative way of characterizing the nature of an area's nonattainment problem. It is best described by identifying key components of a description. Examples are listed below. The examples are not necessarily comprehensive. There could be other features of an area's problem which are important in particular cases. For purposes of illustration later in the discussion, we have answered each of the questions posed below. Our responses appear in parentheses.

1. Is the nonattainment problem primarily a local one, or are regional factors important?

(Surface measurements suggest transport of ozone close to 84 ppb is likely. There are some other nonattainment areas not too far distant.)

2. Are ozone and/or precursor concentrations aloft also high?

(There are no such measurements.)

3. Do violations of the NAAQS occur at several monitoring sites throughout the nonattainment area, or are they confined to one or a small number of sites in proximity to one another?

(Violations occur at a limited number of sites, located throughout the area.)

4. Do observed 8-hour daily maximum ozone concentrations exceed 84 ppb frequently or just on a few occasions?

(This varies among the monitors from 4 times up to 12 times per year.)

5. When 8-hour daily maxima in excess of 84 ppb occur, is there an accompanying characteristic spatial pattern, or is there a variety of spatial patterns?

(A variety of patterns is seen.)

6. Do monitored violations occur at locations subject to mesoscale wind patterns (e.g., at a coastline) which may differ from the general wind flow?

(No.)

7. Have there been any recent major changes in emissions of VOC or NO_X in or near the nonattainment area? If so, what changes have occurred?

(Yes, several local measures [include a list] believed to result in major reductions in VOC [quantify in tons per summer day] have been implemented in the last five years. Additionally, the area is expected to benefit from the regional NO_X reductions from the NO_X SIP call.)

8. Are there discernible trends in design values or other air quality indicators which have accompanied a change in emissions?

(Yes, design values have decreased by about 10% at four sites over the past [x] years. Smaller or no reductions are seen at three other sites.)

9. Is there any apparent spatial pattern to the trends in design values?

(No.)

10. Have ambient precursor concentrations or measured VOC species profiles changed?

(There are no measurements.)

11. What past modeling has been performed and what do the results suggest?

(A regional modeling analysis has been performed. Two emission scenarios were modeled: current emissions and a substantial reduction in NO_X emissions throughout the regional domain. Reduced NO_X emissions led to substantial predicted reductions in 8-hour daily maximum ozone in most locations, but changes near the most populated area in the nonattainment area in question were small or nonexistent.)

12. Are there any distinctive meteorological measurements at the surface or aloft which appear to coincide with occasions with 8-hour daily maxima greater than 84 ppb?

(Other than routine soundings taken twice per day, there are no measurements aloft. There is no obvious correspondence with meteorological measurements other than daily maximum temperatures are always > 85 F on these days.)

Using responses to the preceding questions in this example, it is possible to construct an initial conceptual description of the nonattainment area's ozone problem. First, responses to questions 1 and 11 suggest there is a significant regional component to the area's nonattainment problem. Second, responses to questions 3, 4, 7, 8, and 11 indicate there is an important local component to the area's nonattainment problem. The responses to questions 4, 5 and 12 indicate that high ozone concentrations may be observed under several sets of meteorological conditions. The responses to questions 7, 8, and 11 suggest that ozone in and near the nonattainment area may be responsive to both VOC and NO_X controls and that the extent of this response may vary spatially. The response to question 6 suggests that it may be appropriate to develop a strategy using a model with 12 km grid cells.

The preceding conceptual description implies that the State/Tribe containing the nonattainment area in this example will need to involve stakeholders from other, nearby States/Tribes to develop and implement a modeling/analysis protocol. It also suggests that a nested regional modeling analysis will be needed to address the problem. Further, it may be necessary to model at least several distinctive types of episodes and additional analyses will be needed to select episodes. Finally, sensitivity (i.e., diagnostic) tests, or other modeling probing tools, will be needed to assess the effects of reducing VOC and NO_X emissions separately and at the same time.

It should be clear from the preceding example that the initial conceptual description of an area's nonattainment problem may draw on readily available information and need not be detailed. It is intended to help launch development and implementation of a modeling/analysis protocol in a productive direction. It will likely be supplemented by subsequent, more extensive modeling and ambient analyses performed by or for those implementing the modeling/analysis protocol discussed in Section 9.

8.2 What Types Of Analyses Might Be Useful For Developing And Refining A Conceptual Description?

Questions like those posed in Section 8.1 can be addressed using a variety of analyses ranging in complexity from an inspection of air quality data to sophisticated mathematical analyses. We anticipate the simpler analyses will often be used to develop the initial conceptual description. These will be followed by more complex approaches or by approaches requiring more extensive data bases as the need later becomes apparent. In the following paragraphs, we revisit key parts of the conceptual description identified in Section 8.1. We note analyses which may help to develop a description of each part. The list serves as an illustration. It is not necessarily exhaustive.

8.2.1. Is regional transport an important factor affecting the nonattainment area?

- Are there other nonattainment areas within a day's transport of the nonattainment area?

- Do "upwind" 8-hour daily maximum ozone concentrations approach or exceed 84 ppb on some or all of the days with observed 8-hour daily maxima > 84 ppb in the nonattainment area?
- Are there major sources of emissions upwind?
- What is the size of the downwind/upwind gradient in 8-hour daily maximum ozone concentrations compared to the upwind values?
- Do ozone concentrations aloft but within the planetary boundary layer approach or exceed 84 ppb at night or in the morning hours prior to breakup of the nocturnal surface inversion?
- Is there a significant positive correlation between observed 8-hour daily maximum ozone concentrations at most monitoring sites within or near the nonattainment area?
- Is the timing of high observed ozone consistent with impacts estimated from upwind areas using trajectory models?
- Do available regional modeling simulations suggest that 8-hour daily maximum ozone concentrations within the nonattainment area respond to regional control measures?
- Does source apportionment modeling indicate significant contributions to local ozone from upwind emissions?

8.2.2. What types of meteorological episodes lead to high ozone?

- Examine the spatial patterns of 8-hour daily maxima occurring on days where the ozone is > 84 ppb and try to identify a limited number of distinctive patterns.
- Review synoptic weather charts for days having observed concentrations > 84 ppb to identify classes of synoptic scale features corresponding to high observed ozone.
- Perform statistical analyses between 8-hour daily maximum ozone and meteorological measurements at the surface and aloft to identify distinctive classes of days corresponding with observed daily maxima > 84 ppb.

8.2.3. Is ozone limited by availability of VOC, NO_X or combinations of the two? Which source categories may be most important?

- What are the major source categories of VOC and NO_X and what is their relative importance in the most recent inventory?
- Review results from past modeling analyses to assess the likelihood that ozone in the nonattainment area will be more responsive to VOC or NO_X controls. Do conclusions vary for different locations?
- Apply modeling probing tools (e.g., source apportionment modeling) to determine which source sectors appear to contribute most to local ozone formation.
- Apply indicator species methods such as those described by Sillman (1998, 2002) and Blanchard (1999, 2000, 2001) at sites with appropriate measurements on days with 8-hour daily maximum ozone exceedances. Identify classes of days where further ozone formation appears limited by available NO_X versus classes of days where further ozone formation appears limited by available VOC. Do the conclusions differ for different days? Do the results differ on weekdays versus weekends?
- Apply receptor modeling approaches such as those described by Watson (1997, 2001), Henry (1994) and Henry (1997a, 1997b, 1997c) to identify source categories contributing to ambient VOC on days with high observed ozone. Do the conclusions differ on days when measured ozone is not high?

Additional analyses may be identified as issues arise in implementing a modeling/analysis protocol. These analyses are intended to channel resources available to support modeled attainment demonstrations onto the most productive paths possible. They will also provide other pieces of information which can be used to reinforce conclusions reached with an air quality model, or cause a reassessment of assumptions made previously in applying the model. As noted in Section 4, corroboratory analyses should be used to help assess whether a simulated control strategy is sufficient to meet the NAAQS.

References

Blanchard, C.L., F.W. Lurmann, P.M. Roth, H.E. Jeffries and M. Korc. "The use of ambient data to corroborate analyses of ozone control strategies." *Atmos. Envt.* **33**, 369-381, 1999.

Blanchard, C. L. "Ozone process insights from field experiments – Part III: Extent of reaction and ozone formation." *Atmos. Envt.* **34**, 2035-2043, 2000.

Blanchard, C. L., and T. Stoeckenius. "Ozone response to precursor controls: comparison of data analysis methods with the predictions of photochemical air quality simulation models." *Atmos. Envt.* **35**, 1203-1216, 2001.

Henry, R.C., C.W. Lewis, and J.F. Collins. "Vehicle-related hydrocarbon source compositions from ambient data: The GRACE/SAFER Method." *Envtl. Sci. & Technol.* **28**, 823-832, 1994.

Henry, R.C. "Receptor Model Applied to Patterns in Space (RMAPS) Part I. Model description." *J. Air & Waste Mgmt. Assoc.* **47**, 216-219, 1997a.

Henry, R.C. "Receptor Model Applied to Patterns in Space (RMAPS) Part II. Apportionment of airborne particulate sulfur from Project MOHAVE." *J. Air & Waste Mgmt. Assoc.* **47**, 220-225, 1997b.

Henry, R.C. "Receptor Modeling Applied to Patterns in Space (RMAPS) Part III. Apportionment of airborne particulate sulfur in western Washington State." *J. Air & Waste Mgmt. Assoc.* **47**, 226-230, 1997c.

Sillman, S. "Evaluating the Relation between Ozone, NO_X and Hydrocarbons: The Method of Photochemical Indicators." EPA/600R-98/022, http://www-personal.engin.umich.edu/~sillman/publications.htm, 1998.

Sillman, S., and D. He. "Some theoretical results concerning O_3-NO_X-VOC chemistry and NO_X-VOC indicators." *J. Geophys. Res.* **107**, 4659-4673, 2002.

Watson, J.G. "Observational Models: The Use of Chemical Mass Balance Methods." Prepared for the U.S. EPA Source Attribution Workshop, Research Triangle Park, NC, July 16-18, 1997, available at http://www.epa.gov/ttn/faca/stissu.html, Source Attribution Workshop Materials, 1997.

Watson, J.G., J.C. Chow, and E.M. Fujita. "Review of volatile organic compound source apportionment by chemical mass balance." *Atmos. Envt.* **35**, 1567-1584, 2001.

Appendix B: Ozone pattern classifications in the OTR

Appendix B: Ozone pattern classifications in the OTR

The following five types of ozone patterns in the OTR are taken from: Stoeckenius, T. and Kemball-Cook, S. "Determination of representativeness of 2002 ozone season for ozone transport region SIP modeling." Final Report prepared for the Ozone Transport Commission, 2005. Figure B-1 shows the 850 mb height and wind fields and Figure B-2 shows the surface temperatures and 10 meter wind fields for the five patterns (reproduced from Figures 3-2 and 3-5 of Stoeckenius & Kemball-Cook, 2005).

"Type A" – High ozone throughout the OTR. This pattern is characterized by strong high pressure over the southeastern states extending from the surface to 500 mb with high temperatures extending into New England and southwest surface winds throughout the OTR. The 850 mb temperatures and heights, and surface temperatures are above average at all locations except Washington DC; winds are southwest to west throughout the OTR except more variable at LaGuardia and magnitudes of resultant wind vectors are higher than average (indicative of a fairly steady, well defined flow regime), east-west surface pressure gradients are near neutral but southwest-northeast gradients along the I-95 corridor and in the west (Pittsburgh to Buffalo) are positive, which is consistent with the southwest flow. The stable air mass and high temperatures promote ozone formation throughout the OTR under these conditions.

"Type B" – High ozone confined to the extreme southeastern OTR. This pattern is characterized by an upper-level trough offshore of the OTR and a surface high centered over Kentucky. This results in cooler air advection over nearly all of the OTR with northwest flow aloft and a more westerly flow at the surface. The 850 mb heights are lower than average (especially in New England) and surface winds are more frequently from the northwest along the I-95 corridor than under Type A. Temperatures at 850 mb along the I-95 corridor are only slightly cooler than under Type A but inland temperatures, especially in the north, are much cooler (e.g., at Buffalo); similarly, surface temperatures along the I-95 corridor are about the same as under Type A but temperatures are cooler in Buffalo and Albany. Type B events have the strongest positive west-east surface pressure gradients of any category, consistent with the northwest winds but gradients from Washington to New York and Boston are positive. The cooler air over the western OTR and westerly to northwesterly flow result in the higher ozone levels being confined to just the extreme southern portion of the OTR under this pattern.

"Type C" – High ozone along the I-95 corridor and northern New England. This pattern is characterized by an extension of the semi-permanent Bermuda high into the southeastern U.S. and an area of high surface and 850 mb temperatures extending from Maryland to Maine; the 500 mb pattern is nearly zonal (east-west flow) while flow at the surface is generally from the southwest. The 850 mb heights are intermediate between Type A and Type B but 850 mb temperatures are very high along the I-95 corridor and slightly cooler further inland. Winds are more consistently south - southwest at all sites than under other episode types and almost no northwest-north-northeast winds are seen at LaGuardia in contrast to other types. Resultant wind vector magnitudes are much higher

than average, consistent with the steady southwest flow. Southwest – northeast pressure gradients along the I-95 corridor and from Pittsburgh to Buffalo are positive, consistent with the southwest flow. Average east-west pressure gradients are near zero. These conditions result in above average ozone levels all along the I-95 corridor with advection north into coastal and interior New England. Ozone levels are slightly below average in the extreme southeastern and western OTR.

"Type D" – High ozone in the western OTR. This pattern is characterized by an area of mean upper level divergence with associated cut-off low at 850 mb off the Outer Banks of North Carolina. A relatively vigorous mean low pressure center can be seen at the surface. An east-west temperature gradient across the OTR is evident at 850 mb. Surface temperatures along the I-95 corridor and in Albany are below average but surface temperature is above average at Buffalo. The 850 mb heights are the highest of any episode type due to a strong ridge over New England. Surface winds are mostly east-northeast along the I-95 corridor from DC to New York but more variable further north. In contrast to episode types A, B, or C, the southwest-northeast pressure gradients along the I-95 corridor are negative, consistent with the northeast surface winds. West-east pressure gradients are flat. These conditions result in below average ozone in the eastern OTR due to the on-shore flow in the north and cyclonic conditions in the south but above average ozone levels in the western OTR due to stable, warm conditions with light winds.

"Type E" – Generally low ozone throughout the OTR. This category includes days with moderately low to lowest average ozone readings of all OTR exceedance days used in the characterization scheme. The Bermuda high is shifted east relative to the other types and flow over the southeastern U.S. is only weakly anti-cyclonic with a nearly zonal flow pattern at the 850 and 500 mb levels over the OTR. Temperatures at the surface and aloft are the coolest of any episode type. While winds aloft are nearly westerly, surface winds are generally south-southeast over most of the OTR. The southwest-northeast pressure gradients are negative along the I-95 corridor and east-west gradients are positive, consistent with the southeast flow. These conditions result in below average ozone throughout the OTR due to the relatively low temperatures and southeasterly onshore flow at coastal locations.

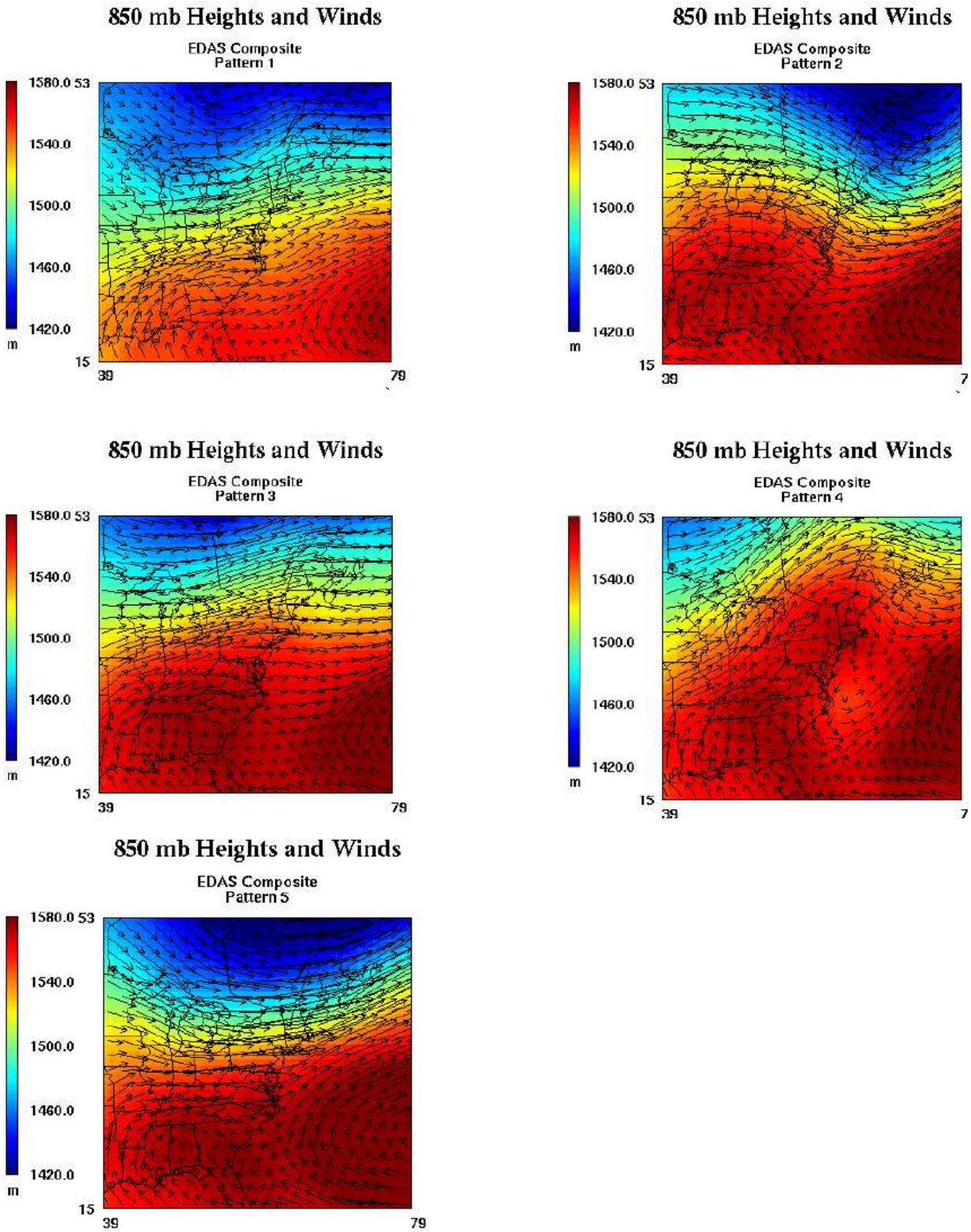

Figure B-1. Average 850 mb height and wind fields for each episode (pattern) type identified by Stoeckenius and Kemball-Cook (pattern numbers refer to the episode types listed in text): Pattern 1 = Episode Type E, 2 = B, 3 = A, 4 = D, 5 = C) (Figure 3-2 of Stoeckenius & Kemball-Cook (2005)).

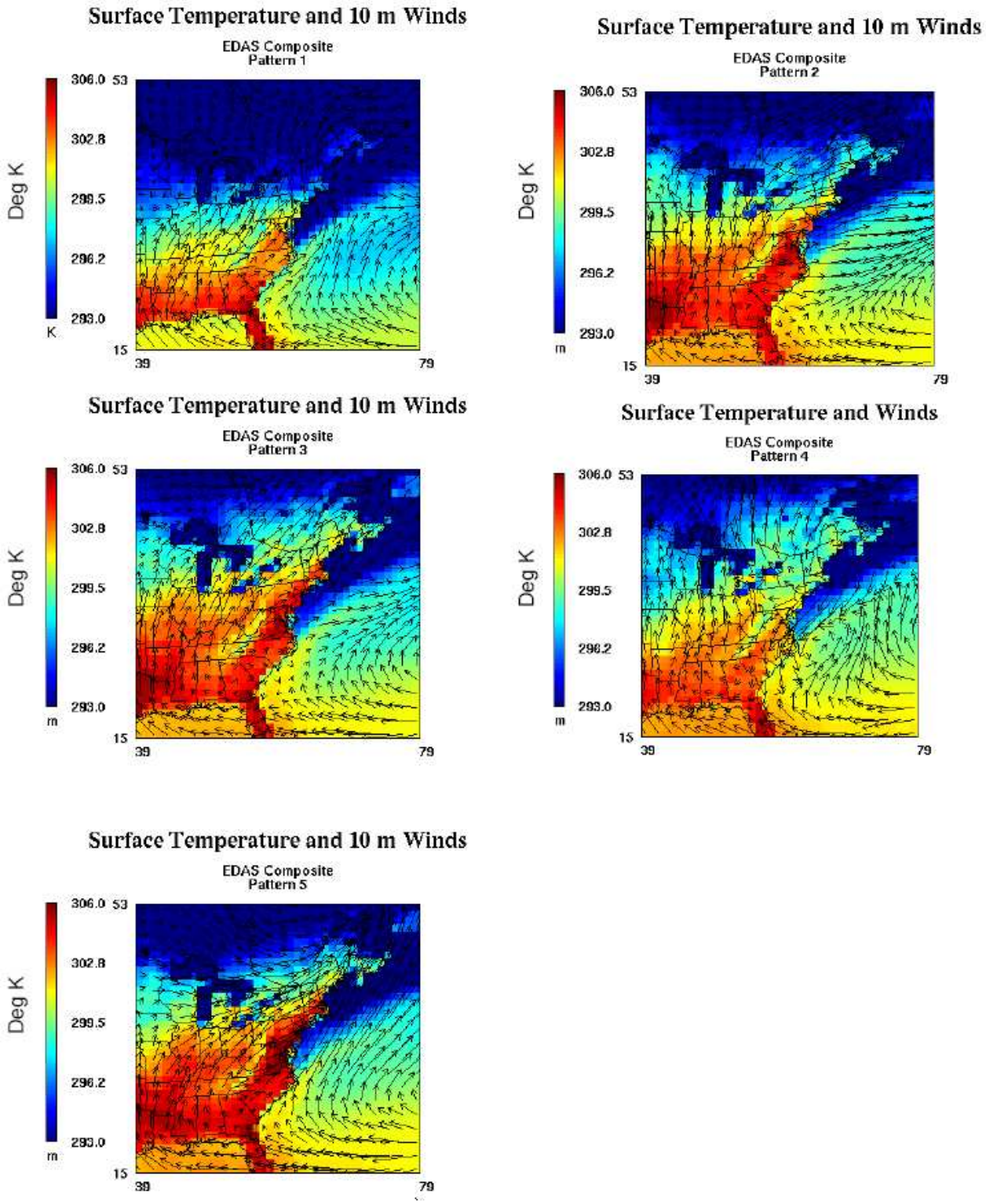

Figure B-2. Average surface temperature and 10 m wind fields for each episode (pattern) type identified by Stoeckenius and Kemball-Cook (pattern numbers refer to the episode types listed in text): Pattern 1 = Episode Type E, 2 = B, 3 = A, 4 = D, 5 = C) (Figure 3-5 of Stoeckenius & Kemball-Cook (2005)).

Appendix C: Exceedance days by monitor in the OTR

Appendix C: Exceedance days by monitor in the OTR

Tables of the number of 8-hour ozone NAAQS exceedance days recorded at individual monitors in the OTR nonattainment/attainment areas for the 1997-2005 ozone seasons. Hourly data were downloaded in January 2006 from the USEPA Air Quality System (AQS) database. The number of 8-hour ozone exceedance days were calculated using procedures specified in USEPA's "Guideline on Data Handling Conventions for the 8-hour Ozone NAAQS" (OAQPS, EPA-454/R-98-017, Dec. 1998) with flagged data (due to a regional forest fire smoke event) eliminated from the analysis. While these tables are derived from the publicly available data in the USEPA AQS database, states may have monitoring data that differ from these. For example, the tables contain state-specific data provided by the Maryland Department of the Environment and the New Jersey Department of Environmental Protection that differ from the USEPA AQS database at the time the data were downloaded in January 2006. "***" indicates years during which a monitor was not in operation or had less than 75 percent data collection during the ozone season.

Philadelphia-Wilmington-Atlantic City, PA-NJ-MD-DE (Classification: MODERATE)

AQS MONITOR ID	COUNTY	MONITOR NAME	ST	**8-hr Ozone exceedance days**								
				1997	1998	1999	2000	2001	2002	2003	2004	2005
100010002	Kent	Killens Pond	DE	14	17	13	5	8	10	3	0	2
100031003	New Castle	Bellefonte	DE	6	8	10	5	5	11	***	***	***
100031007	New Castle	Lums Pond	DE	15	12	12	5	9	9	4	0	6
100031010	New Castle	Brandywine Creek	DE	17	17	16	7	15	18	3	3	3
100031013	New Castle	Wilmington (Bellefonte2)	DE	***	***	***	***	***	8	3	1	4
100051002	Sussex	Seaford	DE	14	16	17	5	4	10	4	0	3
100051003	Sussex	Lewes	DE	***	17	17	6	10	14	4	2	7
240150003	Cecil	Fairhill	MD	19	20	20	18	16	17	6	3	9
340010005	Atlantic	Nacote Creek	NJ	18	24	14	4	9	11	4	0	3
340070003	Camden	Camden Lab	NJ	12	15	16	6	19	19	4	3	5
340071001	Camden	Ancora	NJ	23	29	25	10	17	27	9	6	12
340110007	Cumberland	Millville	NJ	14	17	17	6	14	20	6	2	4
340150002	Gloucester	Clarksboro	NJ	19	22	21	8	17	24	6	4	6
340210005	Mercer	Rider Univ.	NJ	16	17	24	11	15	26	7	1	7
340290006	Ocean	Colliers Mills	NJ	21	28	23	11	21	30	9	8	14
420170012	Bucks	Bristol	PA	14	17	24	14	16	17	9	2	7

Philadelphia-Wilmington-Atlantic City, PA-NJ-MD-DE (Classification: MODERATE)

AQS MONITOR ID	COUNTY	MONITOR NAME	ST	8-hr Ozone exceedance days								
				1997	1998	1999	2000	2001	2002	2003	2004	2005
420290050	Chester	West Chester	PA	***	***	***	***	20	19	4	***	***
420290100	Chester	New Garden	PA	***	***	***	***	17	23	4	5	8
420450002	Delaware	Chester	PA	19	17	19	7	12	16	3	2	4
420910013	Montgomery	Norristown	PA	19	17	20	11	18	12	4	1	8
421010004	Philadelphia	Philadelphia - Downtown	PA	0	1	2	1	0	0	2	0	0
421010014	Philadelphia	Philadelphia - Roxborough	PA	10	7	***	4	10	13	2	0	3
421010024	Philadelphia	Philadelphia - NE Airport	PA	17	15	***	5	13	22	4	6	8
421010136	Philadelphia	Philadelphia - Elmwood	PA	0	4	12	3	5	13	2	0	***

Baltimore, MD (Classification: MODERATE)

AQS MONITOR ID	COUNTY	MONITOR NAME	ST	8-hr Ozone exceedance days								
				1997	1998	1999	2000	2001	2002	2003	2004	2005
240030014	Anne Arundel	Davidsonville	MD	20	42	31	7	14	25	5	4	9
240030019	Anne Arundel	Fort Meade	MD	24	25	27	10	19	20	3	5	***
240051007	Baltimore	Padonia	MD	10	7	14	3	9	19	2	1	2
240053001	Baltimore	Essex	MD	10	11	11	3	10	14	3	2	6
240130001	Carroll	South Carroll	MD	9	18	16	5	10	10	2	1	5
240251001	Harford	Edgewood	MD	18	17	17	11	20	25	7	6	11
240259001	Harford	Aldino	MD	20	12	17	8	18	22	4	3	10
245100053	Baltimore (City)	Baltimore-Ponca St	MD	***	***	***	***	***	8	***	***	***
245100050	Baltimore (City)	Baltimore-0050	MD	16	***	***	***	***	***	***	***	***
245100051	Baltimore (City)	Baltimore-0051	MD	9	5	7	***	***	***	***	***	***

New York-N. New Jersey-Long Island, NY-NJ-CT (Classification: MODERATE)

AQS MONITOR ID	COUNTY	MONITOR NAME	ST	8-hr Ozone exceedance days								
				1997	1998	1999	2000	2001	2002	2003	2004	2005
90010017	Fairfield	Greenwich	CT	13	8	14	3	13	18	7	1	8
90011123	Fairfield	Danbury	CT	14	9	17	7	9	17	4	4	11

New York-N. New Jersey-Long Island, NY-NJ-CT (Classification: MODERATE)

AQS MONITOR ID	COUNTY	MONITOR NAME	ST	**8-hr Ozone exceedance days**								
				1997	1998	1999	2000	2001	2002	2003	2004	2005
90013007	Fairfield	Stratford	CT	17	11	9	4	10	20	8	2	8
90019003	Fairfield	Westport	CT	15	13	13	3	15	19	6	2	10
90010113	Fairfield	Bridgeport	CT	6	***	***	***	***	***	***	***	***
90070007	Middlesex	Middletown	CT	12	5	15	6	11	16	7	1	7
90091123 & 90090027	New Haven	New Haven	CT	7	3	5	***	***	***	***	1	2
90093002	New Haven	Madison	CT	19	9	16	6	11	19	9	2	8
90099005	New Haven	Hamden	CT	***	***	11	2	9	14	7	***	***
340030005	Bergen	Teaneck	NJ	***	***	***	2	10	18	4	2	8
340030001	Bergen	Cliffside Park	NJ	5	***	***	***	***	***	***	***	***
340130011 & 340130016	Essex	Newark Lab	NJ	6	5	6	***	***	6	***	***	***
340170006	Hudson	Bayonne	NJ	9	7	17	3	6	6	2	1	6
340190001	Hunterdon	Flemington	NJ	18	21	23	9	12	19	7	6	13
340230011	Middlesex	Rutgers Univ.	NJ	16	15	23	10	17	26	5	2	10
340250005	Monmouth	Monmouth Univ.	NJ	12	20	12	5	8	17	10	2	8
340273001	Morris	Chester	NJ	13	22	21	6	15	27	5	0	3
340315001	Passaic	Ramapo	NJ	***	8	16	1	9	13	2	2	8
340390008	Union	Plainfield	NJ	5	***	***	***	***	***	***	***	***
360050080	Bronx	NYC-Morrisania Center	NY	5	1	5	***	***	***	***	***	***
360050083	Bronx	NYC-200th St & Southern Blvd	NY	5	0	8	1	1	6	2	1	0
360050110	Bronx	NYC-IS52	NY	***	***	***	1	***	6	2	0	1
360610010	New York	NYC-Mabel Dean HS	NY	***	2	3	0	***	***	***	***	***
360610063	New York	NYC-Roof WTC	NY	16	22	18	5	12	***	***	***	***
360810004	Queens	NYC-Queens College	NY	10	***	***	***	***	***	***	***	***
360810097	Queens	NYC-QBORO	NY	***	***	10	3	3	***	***	***	***
360810098	Queens	NYC-College Pt	NY	***	***	***	1	1	1	1	0	0
360810124	Queens	NYC-Queens	NY	***	***	***	***	***	7	4	0	4
360850067	Richmond	NYC-Susan Wagner HS	NY	21	12	17	11	10	19	5	2	8

New York-N. New Jersey-Long Island, NY-NJ-CT (Classification: MODERATE)

AQS MONITOR ID	COUNTY	MONITOR NAME	ST	8-hr Ozone exceedance days								
				1997	1998	1999	2000	2001	2002	2003	2004	2005
361030002	Suffolk	Babylon	NY	8	10	11	4	2	9	6	2	6
361030004	Suffolk	Riverhead	NY	11	9	16	4	3	6	3	***	6
361030009	Suffolk	Holtsville	NY	***	***	***	4	8	18	6	2	***
361192004	Westchester	White Plains	NY	11	6	12	2	8	15	4	0	9

Washington, DC-MD-VA (Classification: MODERATE)

AQS MONITOR ID	COUNTY	MONITOR NAME	ST	8-hr Ozone exceedance days								
				1997	1998	1999	2000	2001	2002	2003	2004	2005
110010025	District of Columbia (all)	Takoma	DC	11	18	15	5	7	13	3	2	1
110010041	District of Columbia (all)	River Terrace	DC	12	11	16	2	7	12	2	0	1
110010043	District of Columbia (all)	McMillian Reservoir	DC	18	20	22	2	12	21	3	3	5
240090010 & 240090011	Calvert	Calvert	MD	4	10	10	5	5	***	***	***	2
240170010	Charles	S. Maryland	MD	17	30	31	5	9	15	6	1	6
240210037	Frederick	Frederick Municipal Airport	MD	***	***	19	4	14	13	3	1	1
240313001	Montgomery	Rockville	MD	13	22	16	2	11	11	3	2	3
240330002	Prince George's	Greenbelt	MD	24	24	23	7	19	15	3	***	***
240338001	Prince George's	Suitland	MD	14	25	18	3	14	***	***	***	***
240338003	Prince George's	Equestrian Center	MD	***	***	***	***	***	15	4	5	5
510130020	Arlington Co	Aurora Hills	VA	17	10	21	3	12	18	4	4	5
510590005	Fairfax	Chantilly (Cub Run)	VA	2	16	6	2	9	12	2	3	0
510590018	Fairfax	Mount Vernon	VA	***	17	16	4	10	16	5	6	8
510590030	Fairfax	Franconia	VA	***	***	19	0	14	18	5	5	6
510591004 & 510591005	Fairfax	Seven Corners & Annandale	VA	10	17	9	2	***	20	3	4	4
510595001	Fairfax	McLean – Lewinsville	VA	3	7	6	2	8	7	3	3	2
511071005	Loudoun	Ashburn	VA	***	17	7	1	9	23	3	2	***
511530009	Prince William	James S. Long Park	VA	4	13	9	2	6	7	4	1	0
515100009	Alexandria (City)	Alexandria	VA	5	10	10	2	6	10	3	3	2

Jefferson Co., NY (Classification: MODERATE)

AQS MONITOR ID	COUNTY	MONITOR NAME	ST	8-hr Ozone exceedance days								
				1997	1998	1999	2000	2001	2002	2003	2004	2005
360450002	Jefferson	Perch River	NY	8	4	6	1	17	13	9	2	3

Greater Connecticut, CT (Classification: MODERATE)

AQS MONITOR ID	COUNTY	MONITOR NAME	ST	8-hr Ozone exceedance days								
				1997	1998	1999	2000	2001	2002	2003	2004	2005
90031003	Hartford	East Hartford	CT	7	2	11	2	8	10	0	1	5
90050005	Litchfield	Cornwall (Mohawk Mt)	CT	***	***	***	***	***	13	4	2	8
90050006	Litchfield	Torrington	CT	9	10	12	4	***	***	***	***	***
90110008	New London	Groton	CT	17	3	11	3	7	7	5	1	4
90131001	Tolland	Stafford	CT	10	8	12	1	10	13	1	2	8

Boston-Lawrence-Worcester (E. MA), MA (Classification: MODERATE)

AQS MONITOR ID	COUNTY	MONITOR NAME	ST	8-hr Ozone exceedance days								
				1997	1998	1999	2000	2001	2002	2003	2004	2005
250010002	Barnstable	Truro	MA	17	2	12	3	13	9	8	3	7
250051002	Bristol	Fairhaven	MA	12	2	8	3	8	5	8	1	1
250051005	Bristol	Easton	MA	7	7	3	0	14	***	***	***	***
250070001	Dukes	Wampanoag Laboratory – Martha's Vineyard	MA	***	***	***	***	***	***	***	0	4
250095005	Essex	Lawrence-Haverhill	MA	2	1	1	0	0	6	***	***	0
250092006	Essex	Lynn	MA	6	7	6	1	11	13	3	2	6
250094004	Essex	Newbury	MA	6	6	6	0	8	9	2	1	0
250170009	Middlesex	USEPA Region 1 Lab – Chelmsford	MA	***	***	***	***	***	***	***	***	2
250171102	Middlesex	Stow	MA	***	5	8	1	12	8	0	1	2
250171801	Middlesex	Sudbury	MA	6	4	***	***	***	***	***	***	***
250174003	Middlesex	Waltham	MA	6	7	5	***	***	***	***	***	***
250213003	Norfolk	E Milton (Blue Hill)	MA	***	***	***	***	***	17	5	2	4

Boston-Lawrence-Worcester (E. MA), MA (Classification: MODERATE)

AQS MONITOR ID	COUNTY	MONITOR NAME	ST	8-hr Ozone exceedance days								
				1997	1998	1999	2000	2001	2002	2003	2004	2005
250250041	Suffolk	Boston-Long Island	MA	***	***	4	0	9	10	1	1	5
250250042	Suffolk	Boston-Roxbury	MA	***	***	0	0	2	2	1	1	1
250251003	Suffolk	Chelsea	MA	2	4	3	***	***	***	***	***	***
250270015	Worcester	Worcester	MA	5	6	8	1	6	***	1	0	5

Providence (All RI), RI (Classification: MODERATE)

AQS MONITOR ID	COUNTY	MONITOR NAME	ST	8-hr Ozone exceedance days								
				1997	1998	1999	2000	2001	2002	2003	2004	2005
440030002	Kent	W Greenwich	RI	10	4	7	5	13	12	1	2	5
440071010	Providence	E Providence	RI	3	2	2	2	10	9	4	2	4
440090007	Washington	Narragansett	RI	***	1	11	4	11	8	8	4	5

Springfield (Western MA), MA (Classification: MODERATE)

AQS MONITOR ID	COUNTY	MONITOR NAME	ST	8-hr Ozone exceedance days								
				1997	1998	1999	2000	2001	2002	2003	2004	2005
250034002	Berkshire	Adams	MA	***	***	1	***	16	4	2	1	6
230130003	Hampden	Agawam	MA	9	1	1	1	2	6	***	***	***
250130008	Hampden	Chicopee	MA	7	5	7	1	9	10	3	1	8
250150103	Hampshire	South Hadley (Amherst)	MA	2	2	3	1	3	4	0	1	1
250154002	Hampshire	Ware	MA	9	6	9	2	12	10	0	3	8

Poughkeepsie, NY (Classification: MODERATE)

AQS MONITOR ID	COUNTY	MONITOR NAME	ST	8-hr Ozone exceedance days								
				1997	1998	1999	2000	2001	2002	2003	2004	2005
360270007	Dutchess	Millbrook	NY	7	8	8	2	8	8	0	1	3
360715001	Orange	Valley Central	NY	6	6	8	1	12	4	4	2	7
360790005	Putnam	Mt Ninham	NY	7	8	15	1	10	19	2	1	7

Boston-Manchester-Portsmouth (SE), NH (Classification: MODERATE)

AQS MONITOR ID	COUNTY	MONITOR NAME	ST	8-hr Ozone exceedance days								
				1997	1998	1999	2000	2001	2002	2003	2004	2005
330110016 & 330110019 & 330110020	Hillsborough	Manchester	NH	3	0	***	0	***	4	0	1	0
330111010 & 330111011	Hillsborough	Nashua	NH	4	3	8	1	7	5	1	2	1
330150009 & 330150015 & 330150014	Rockingham	Portsmouth	NH	5	3	5	0	***	8	0	1	0
330150013	Rockingham	Brentwood	NH	***	0	1	0	4	10	***	***	***
330150012 & 330150016	Rockingham	Rye	NH	9	4	3	0	7	7	0	1	0
330173002	Strafford	Rochester	NH	1	0	2	0	1	6	0	***	***

Kent and Queen Anne's Cos., MD (Classification: MARGINAL)

AQS MONITOR ID	COUNTY	MONITOR NAME	ST	8-hr Ozone exceedance days								
				1997	1998	1999	2000	2001	2002	2003	2004	2005
240290002	Kent	Millington	MD	19	16	22	6	13	17	4	1	3

Lancaster, PA (Classification: MARGINAL)

AQS MONITOR ID	COUNTY	MONITOR NAME	ST	8-hr Ozone exceedance days								
				1997	1998	1999	2000	2001	2002	2003	2004	2005
420710007	Lancaster	Lancaster	PA	21	27	18	5	15	18	3	1	6

Portland, ME (Classification: MARGINAL)

AQS MONITOR ID	COUNTY	MONITOR NAME	ST	8-hr Ozone exceedance days								
				1997	1998	1999	2000	2001	2002	2003	2004	2005
230050027	Cumberland	Portland	ME	***	***	***	***	***	***	***	0	0
230052003	Cumberland	Cape Elizabeth	ME	6	5	2	0	8	5	0	0	0
230230003 & 230230004	Sagadahoc	Phippsburg/Georgetown (Reid State Park)	ME	7	4	4	1	***	5	1	0	0
230313002	York	Kittery	ME	7	4	4	0	4	12	2	1	0
230312002	York	Kennebunkport	ME	5	5	5	1	8	10	2	1	0
230310037 & 230310038	York	Hollis	ME	2	0	1	0	***	3	0	0	0

Buffalo-Niagara Falls, NY (Classification: SUBPART 1)

AQS MONITOR ID	COUNTY	MONITOR NAME	ST	8-hr Ozone exceedance days								
				1997	1998	1999	2000	2001	2002	2003	2004	2005
360290002	Erie	Amherst	NY	0	13	6	4	10	21	7	0	5
360631006	Niagara	Middleport	NY	1	6	7	3	10	16	6	0	4

Youngstown-Warren-Sharon, OH-PA (Classification: SUBPART 1)

AQS MONITOR ID	COUNTY	MONITOR NAME	ST	8-hr Ozone exceedance days								
				1997	1998	1999	2000	2001	2002	2003	2004	2005
390990009 & 390990013	Mahoning	Youngstown - Oakhill	OH	3	15	7	1	5	14	4	1	2
391550008 & 391550011	Trumbull	Warren-Trumbull County	OH	8	19	10	2	12	24	5	2	5
391550009	Trumbull	Kinsman	OH	7	15	10	2	5	16	4	0	2
420850100	Mercer	Farrell	PA	9	24	8	2	15	20	6	1	4

Pittsburgh-Beaver Valley, PA (Classification: SUBPART 1)

AQS MONITOR ID	COUNTY	MONITOR NAME	ST	8-hr Ozone exceedance days								
				1997	1998	1999	2000	2001	2002	2003	2004	2005
420030008	Allegheny	Lawrenceville	PA	7	14	10	3	4	16	5	0	1
420030010	Allegheny	Pittsburg	PA	***	6	16	4	9	25	5	0	4
420030067	Allegheny	South Fayette	PA	8	24	15	4	7	17	4	1	4
420030088	Allegheny	Penn Hills	PA	5	16	11	4	***	***	***	***	***
420031005	Allegheny	Harrison Township	PA	12	18	14	4	8	14	2	0	6
420050001	Armstrong	Kittanning	PA	***	21	18	2	16	15	5	1	4
420070002	Beaver	Hookstown	PA	4	11	9	1	9	19	6	0	5
420070005	Beaver	Brighton Township	PA	3	15	11	1	8	23	3	0	4
420070014	Beaver	Beaver Falls	PA	5	10	6	3	4	9	3	0	2
421250005	Washington	Charleroi	PA	14	34	11	3	7	14	4	0	2
421250200	Washington	Washington	PA	6	15	11	3	6	9	5	0	4
421255001	Washington	Florence	PA	4	11	9	2	7	17	3	0	4
421290006	Westmoreland	Murrysville	PA	4	3	5	2	1	9	2	0	4
421290008	Westmoreland	Greensburg	PA	***	***	16	3	3	10	4	0	2

Jamestown, NY (Classification: SUBPART 1)

AQS MONITOR ID	COUNTY	MONITOR NAME	ST	8-hr Ozone exceedance days								
				1997	1998	1999	2000	2001	2002	2003	2004	2005
360130006	Chautauqua	Dunkirk	NY	***	***	12	5	11	23	7	4	6
360130011	Chautauqua	Westfield	NY	4	11	8	3	4	18	4	0	2

Hancock, Knox, Lincoln & Waldo Cos., ME (Classification: SUBPART 1)

AQS MONITOR ID	COUNTY	MONITOR NAME	ST	8-hr Ozone exceedance days								
				1997	1998	1999	2000	2001	2002	2003	2004	2005
230130004	Knox	Port Clyde	ME	6	3	2	0	6	5	3	0	1
230090401	Hancock	Schoodic Point	ME	***	***	***	***	***	***	1	0	***
230090001	Hancock	Seawall	ME	***	***	***	0	4	***	***	***	***
230090101 & 230090103	Hancock	Acadia National Park – McFarland Hill	ME	1	4	5	0	9	6	2	0	0
230090102	Hancock	Acadia National Park – Cadillac Mtn.	ME	5	8	4	3	9	8	3	0	3

Franklin Co., PA (Classification: SUBPART 1)

AQS MONITOR ID	COUNTY	MONITOR NAME	ST	8-hr Ozone exceedance days								
				1997	1998	1999	2000	2001	2002	2003	2004	2005
420550001	Franklin	Methodist Hill	PA	7	22	20	4	15	27	3	0	0

Erie, PA (Classification: SUBPART 1)

AQS MONITOR ID	COUNTY	MONITOR NAME	ST	8-hr Ozone exceedance days								
				1997	1998	1999	2000	2001	2002	2003	2004	2005
420490003	Erie	Erie	PA	6	12	13	2	4	17	4	0	4

Essex Co. (Whiteface Mtn.), NY (Classification: SUBPART 1)

AQS MONITOR ID	COUNTY	MONITOR NAME	ST	8-hr Ozone exceedance days								
				1997	1998	1999	2000	2001	2002	2003	2004	2005
360310002	Essex (Whiteface Mountain above 1,900 foot elevation)	Whiteface Mountain Summit	NY	2	1	3	2	5	12	7	0	***
360310003		Whiteface Mtn. Base	NY	1	2	3	0	3	11	5	0	1

Allentown-Bethlehem-Easton, PA (Classification: SUBPART 1)

AQS MONITOR ID	COUNTY	MONITOR NAME	ST	**8-hr Ozone exceedance days**								
				1997	1998	1999	2000	2001	2002	2003	2004	2005
420770004	Lehigh	Allentown	PA	12	18	19	5	9	16	4	3	6
420950025	Northampton	Freemansburg	PA	0	5	22	6	14	12	4	6	5
420950100 & 420958000	Northampton	Easton	PA	11	8	12	2	11	13	3	1	1

Reading, PA (Classification: SUBPART 1)

AQS MONITOR ID	COUNTY	MONITOR NAME	ST	**8-hr Ozone exceedance days**								
				1997	1998	1999	2000	2001	2002	2003	2004	2005
420110001	Berks	Kutztown	PA	6	14	12	2	7	11	1	***	***
420110009 & 420110010	Berks	Reading	PA	10	16	14	3	8	13	3	1	4

Clearfield and Indiana Cos., PA (Classification: SUBPART 1)

AQS MONITOR ID	COUNTY	MONITOR NAME	ST	**8-hr Ozone exceedance days**								
				1997	1998	1999	2000	2001	2002	2003	2004	2005
420630004	Indiana	Strongstown	PA	***	***	***	***	***	***	***	***	5
420334000	Clearfield	Moshannon	PA	12	16	1	2	8	13	4	0	4

Greene Co., PA (Classification: SUBPART 1)

AQS MONITOR ID	COUNTY	MONITOR NAME	ST	**8-hr Ozone exceedance days**								
				1997	1998	1999	2000	2001	2002	2003	2004	2005
420590002	Greene	Holbrook	PA	***	***	21	6	12	9	3	0	5

York, PA (Classification: SUBPART 1)

AQS MONITOR ID	COUNTY	MONITOR NAME	ST	**8-hr Ozone exceedance days**								
				1997	1998	1999	2000	2001	2002	2003	2004	2005
420010002	Adams	Biglerville	PA	***	***	***	***	***	7	2	0	1
421330008	York	York	PA	13	18	10	6	8	12	3	1	6

Rochester, NY (Classification: SUBPART 1)

AQS MONITOR ID	COUNTY	MONITOR NAME	ST	**8-hr Ozone exceedance days**								
				1997	1998	1999	2000	2001	2002	2003	2004	2005
360551004 & 360551007	Monroe	Rochester	NY	4	1	***	1	3	12	3	0	0
361173001	Wayne	Williamson	NY	4	4	7	1	5	10	2	0	0

Albany-Schenectady-Troy, NY (Classification: SUBPART 1)

AQS MONITOR ID	COUNTY	MONITOR NAME	ST	**8-hr Ozone exceedance days**								
				1997	1998	1999	2000	2001	2002	2003	2004	2005
360010012	Albany	Albany – Loudonville	NY	2	1	3	1	6	6	2	2	3
360830004	Rensselaer	Grafton State Park	NY	***	***	***	***	***	16	2	2	2
360910004	Saratoga	Stillwater	NY	3	2	6	1	7	6	5	2	3
360930003 & 360930093	Schenectady	Schenectady	NY	1	0	2	1	1	3	2	0	0

Harrisburg-Lebanon-Carlisle, PA (Classification: SUBPART 1)

AQS MONITOR ID	COUNTY	MONITOR NAME	ST	**8-hr Ozone exceedance days**								
				1997	1998	1999	2000	2001	2002	2003	2004	2005
420430401	Dauphin	Harrisburg	PA	3	22	15	3	7	11	2	1	3
420431100	Dauphin	Hershey	PA	9	9	15	5	12	13	2	0	4
420990301	Perry	Little Buffalo State Park	PA	7	8	13	2	10	7	3	0	1

Johnstown, PA (Classification: SUBPART 1)

AQS MONITOR ID	COUNTY	MONITOR NAME	ST	8-hr Ozone exceedance days								
				1997	1998	1999	2000	2001	2002	2003	2004	2005
420210011	Cambria	Johnstown	PA	7	13	11	5	5	6	2	0	1

Scranton-Wilkes-Barre, PA (Classification: SUBPART 1)

AQS MONITOR ID	COUNTY	MONITOR NAME	ST	8-hr Ozone exceedance days								
				1997	1998	1999	2000	2001	2002	2003	2004	2005
420690101	Lackawanna	Peckville	PA	6	5	11	1	5	14	2	0	2
420692006	Lackawanna	Scranton	PA	4	5	11	1	5	8	2	0	1
420791100	Luzerne	Nanticoke	PA	0	2	4	1	5	6	3	0	0
420791101	Luzerne	Wilkes-Barre	PA	8	7	9	1	7	7	2	0	1

State College, PA (Classification: SUBPART 1)

AQS MONITOR ID	COUNTY	MONITOR NAME	ST	8-hr Ozone exceedance days								
				1997	1998	1999	2000	2001	2002	2003	2004	2005
420270100	Centre	State College	PA	***	***	***	2	5	8	3	0	1
420274000	Centre	Penn Nursery	PA	7	8	4	2	1	12	4	0	***

Tioga Co., PA (Classification: SUBPART 1)

AQS MONITOR ID	COUNTY	MONITOR NAME	ST	8-hr Ozone exceedance days								
				1997	1998	1999	2000	2001	2002	2003	2004	2005
421174000	Tioga	Tioga	PA	***	***	***	2	3	8	3	0	0

Altoona, PA (Classification: SUBPART 1)

AQS MONITOR ID	COUNTY	MONITOR NAME	ST	8-hr Ozone exceedance days								
				1997	1998	1999	2000	2001	2002	2003	2004	2005
420130801	Blair	Altoona	PA	7	17	6	2	3	9	3	0	1

Washington Co. (Hagerstown), MD (Classification: SUBPART 1 EARLY ACTION COMPACT)

AQS MONITOR ID	COUNTY	MONITOR NAME	ST	8-hr Ozone exceedance days								
				1997	1998	1999	2000	2001	2002	2003	2004	2005
240430009	Washington	Hagerstown	MD	***	***	11	2	5	17	3	1	2

New York (Classification: ATTAINMENT)

AQS MONITOR ID	COUNTY	MONITOR NAME	ST	8-hr Ozone exceedance days								
				1997	1998	1999	2000	2001	2002	2003	2004	2005
360150003	Gloucester	Elmira	NY	0	2	2	1	2	4	1	0	0
360410005	Hamilton	Piseco Lake	NY	1	1	1	1	2	4	2	0	1
360430005	Herkimer	Nicks Lake	NY	0	0	0	1	0	1	2	0	0
360530006	Madison	Camp Georgetown	NY	0	2	1	1	2	5	2	0	0
360650004	Oneida	Camden	NY	0	1	1	1	3	5	2	0	0
360671015	Onondaga	East Syracuse	NY	2	3	4	1	4	9	2	0	2
360750003	Oswego	Fulton	NY	***	***	***	***	***	***	5	0	2
361111005	Ulster	Belleayre Mountain	NY	4	1	3	1	3	1	3	0	0

Maine (Classification: ATTAINMENT)

AQS MONITOR ID	COUNTY	MONITOR NAME	ST	8-hr Ozone exceedance days								
				1997	1998	1999	2000	2001	2002	2003	2004	2005
230112005	Kennebec	Gardiner	ME	2	3	1	0	3	4	1	0	0
230090301	Hancock	Castine	ME	***	***	***	***	***	3	1	0	0
230210003	Piscataquis	Dover-Foxcroft	ME	***	0	1	0	0	***	***	***	***
230194008	Penobscot	Holden	ME	0	2	0	***	6	4	1	0	0
230173001	Oxford	North Lovell	ME	0	0	0	0	0	1	0	0	0
CC0040002	NB CAN	Roosevelt-Campobello IP	NB	0	1	0	0	0	0	0	0	0
230194007	Penobscot	Howland	ME	0	0	1	0	0	1	0	0	0
230038001	Aroostook	Ashland	ME	0	0	0	0	0	1	0	0	0

Pennsylvania (Classification: ATTAINMENT)

AQS MONITOR ID	COUNTY	MONITOR NAME	ST	8-hr Ozone exceedance days								
				1997	1998	1999	2000	2001	2002	2003	2004	2005
420730015	Lawrence	New Castle	PA	4	2	5	0	1	6	2	0	1
420810100	Lycoming	Montoursville	PA	***	***	***	***	***	7	3	0	3
420810403	Lycoming	Williamsport	PA	0	1	0	1	1	***	***	***	***
420814000	Lycoming	Tiadaghton	PA	0	3	0	1	1	3	2	0	***

Vermont (Classification: ATTAINMENT)

AQS MONITOR ID	COUNTY	MONITOR NAME	ST	8-hr Ozone exceedance days								
				1997	1998	1999	2000	2001	2002	2003	2004	2005
500030004	Bennington	Bennington	VT	2	0	3	1	2	4	0	2	0
500070007	Chittenden	Underhill	VT	0	0	1	0	0	3	0	0	0

New Hampshire (Classification: ATTAINMENT)

AQS MONITOR ID	COUNTY	MONITOR NAME	ST	8-hr Ozone exceedance days								
				1997	1998	1999	2000	2001	2002	2003	2004	2005
330012003 & 330012004	Belknap	Laconia	NH	1	0	0	***	2	3	0	0	0
330031002	Carroll	Conway	NH	0	0	0	0	0	1	***	***	***
330050007	Cheshire	Keene	NH	1	1	1	1	1	1	0	0	0
330074002	Coos	Mt Washington Base	NH	***	***	***	***	***	0	0	1	0
330074003	Coos	Pittsburg	NH	***	***	***	***	***	***	0	0	0
330090008 & 330092005	Grafton	Haverhill-Lebanon	NH	0	0	0	0	0	1	0	0	0
330115001	Hillsborough	Peterborough (Miller State Park)	NH	***	***	***	***	***	***	0	1	3
330170007 & 330171007	Strafford	Concord	NH	1	0	0	0	1	4	0	1	0
330190003	Sullivan	Claremont	NH	1	0	0	1	0	3	0	1	0

Appendix D: 8-hour ozone design values in the OTR, 1997-2005

Appendix D: 8-hour ozone design values in the OTR, 1997-2005

Tables of the valid 8-hour ozone design values (3-year averages of the ozone season 4th maximum 8-hour ozone concentrations) recorded at individual monitors in OTR nonattainment/attainment areas for the 1997-2005 ozone seasons. Hourly data were downloaded from the USEPA Air Quality System (AQS) database in January 2006. The 8-hour averages and design values were calculated using procedures specified in EPA's "Guideline on Data Handling Conventions for the 8-hour Ozone NAAQS" (OAQPS, EPA-454/R-98-017, Dec. 1998) with flagged data (due to a regional forest fire smoke event) eliminated from the analysis. "***" indicates years during which a monitor was not in operation or had less than 90 percent data collection (with a design value less than 85 ppb) for the respective 3-year period. Red shading indicates averages ≥ 85 ppb (violating the 8-hr ozone NAAQS), orange shading indicates averages between 80 and 84 ppb, yellow shading indicates average between 75 and 79 ppb and green shading indicates averages < 75 ppb. While these tables are derived from the publicly available data downloaded in January 2006 from the USEPA AQS database, states may have monitoring data that differ from these. For example, design values for New Jersey were provided by the New Jersey Department of Environmental Protection and differ in some instances from the derived values based on the USEPA AQS database.

Philadelphia-Wilmington-Atlantic City, PA-NJ-MD-DE (Classification: MODERATE) 8-hr Ozone DESIGN VALUE (ppb)

AQS MONITOR ID	COUNTY	MONITOR NAME	ST	1997-1999	1998-2000	1999-2001	2000-2002	2001-2003	2002-2004	2003-2005
100010002	Kent	Killens Pond	DE	99	97	93	92	89	84	80
100031003	New Castle	Bellefonte	DE	90	91	91	92	***	***	***
100031007	New Castle	Lums Pond	DE	100	97	97	96	93	84	80
100031010	New Castle	Brandywine Creek	DE	99	96	95	96	93	89	82
100031013	New Castle	Wilmington (Bellefonte2)	DE	***	***	***	***	90	85	82
100051002	Sussex	Seaford	DE	99	98	95	94	91	85	82
100051003	Sussex	Lewes	DE	***	95	90	87	88	85	84
240150003	Cecil	Fairhill	MD	110	106	106	104	98	91	89
340010005	Atlantic	Nacote Creek	NJ	101	94	95	91	91	85	82
340070003	Camden	Camden Lab	NJ	104	101	104	101	102	93	85
340071001	Camden	Ancora	NJ	111	106	108	104	102	96	92
340110007	Cumberland	Millville	NJ	104	101	102	98	98	91	86
340150002	Gloucester	Clarksboro	NJ	106	105	105	104	100	94	88
340210005	Mercer	Rider Univ.	NJ	112	109	112	102	99	91	85

Philadelphia-Wilmington-Atlantic City, PA-NJ-MD-DE (Classification: MODERATE) 8-hr Ozone DESIGN VALUE (ppb)

AQS MONITOR ID	COUNTY	MONITOR NAME	ST	1997-1999	1998-2000	1999-2001	2000-2002	2001-2003	2002-2004	2003-2005
340290006	Ocean	Colliers Mills	NJ	113	114	115	113	109	99	94
420170012	Bucks	Bristol	PA	103	102	105	104	100	93	86
420290050	Chester	West Chester	PA	***	***	***	***	95	***	***
420290100	Chester	New Garden	PA	***	***	***	95	98	91	87
420450002	Delaware	Chester	PA	100	96	94	95	92	88	82
420910013	Montgomery	Norristown	PA	104	102	100	97	92	88	86
421010004	Philadelphia	Philadelphia – Downtown	PA	72	72	71	74	75	68	63
421010014	Philadelphia	Philadelphia – Roxborough	PA	90	87	88	93	93	86	81
421010024	Philadelphia	Philadelphia – NE Airport	PA	***	***	***	98	97	95	90
421010136	Philadelphia	Philadelphia – Elmwood	PA	86	89	88	87	84	80	***

Baltimore, MD (Classification: MODERATE) 8-hr Ozone DESIGN VALUE (ppb) 8-hr Ozone DESIGN VALUE (ppb)

AQS MONITOR ID	COUNTY	MONITOR NAME	ST	1997-1999	1998-2000	1999-2001	2000-2002	2001-2003	2002-2004	2003-2005
240030014	Anne Arundel	Davidsonville	MD	109	107	103	102	98	94	89
240030019	Anne Arundel	Fort Meade	MD	107	100	100	101	97	93	***
240051007	Baltimore	Padonia	MD	95	92	93	92	89	85	77
240053001	Baltimore	Essex	MD	99	93	93	93	93	88	83
240130001	Carroll	South Carroll	MD	95	94	93	92	89	85	82
240251001	Harford	Edgewood	MD	105	100	104	104	103	94	91
240259001	Harford	Aldino	MD	106	97	98	100	98	93	86
245100053	Baltimore (City)	Baltimore-Ponca St	MD	***	***	***	***	***	***	***
245100050	Baltimore (City)	Baltimore-0050	MD	***	***	***	***	***	***	***
245100051	Baltimore (City)	Baltimore-0051	MD	90	***	***	***	***	***	***

New York-N. New Jersey-Long Island, NY-NJ-CT (Classification: MODERATE) 8-hr Ozone DESIGN VALUE (ppb)

AQS MONITOR ID	COUNTY	MONITOR NAME	ST	1997-1999	1998-2000	1999-2001	2000-2002	2001-2003	2002-2004	2003-2005
90010017	Fairfield	Greenwich	CT	99	93	96	95	100	92	87
90011123	Fairfield	Danbury	CT	101	96	97	98	96	93	91

New York-N. New Jersey-Long Island, NY-NJ-CT (Classification: MODERATE) 8-hr Ozone DESIGN VALUE (ppb)

AQS MONITOR ID	COUNTY	MONITOR NAME	ST	1997-1999	1998-2000	1999-2001	2000-2002	2001-2003	2002-2004	2003-2005
90013007	Fairfield	Stratford	CT	98	94	96	98	102	95	90
90019003	Fairfield	Westport	CT	103	94	97	93	97	92	89
90010113	Fairfield	Bridgeport	CT	***	***	***	***	***	***	***
90070007	Middlesex	Middletown	CT	99	95	99	97	98	92	90
90091123 & 90090027	New Haven	New Haven	CT	86	***	***	***	***	***	***
90093002	New Haven	Madison	CT	103	96	97	98	102	95	90
90099005	New Haven	Hamden	CT	***	***	95	94	98	***	***
340030005	Bergen	Teaneck	NJ	***	***	***	92	95	89	86
340030001	Bergen	Cliffside Park	NJ	***	***	***	***	***	***	***
340130011 & 340130016	Essex	Newark Lab	NJ	93	***	***	***	***	***	***
340170006	Hudson	Bayonne	NJ	107	99	100	86	87	82	84
340190001	Hunterdon	Flemington	NJ	106	103	104	97	97	92	90
340230011	Middlesex	Rutgers Univ.	NJ	113	109	111	101	98	89	86
340250005	Monmouth	Monmouth Univ.	NJ	100	102	101	97	97	93	89
340273001	Morris	Chester	NJ	102	100	101	98	98	90	82
340315001	Passaic	Ramapo	NJ	***	89	94	88	88	84	81
340390008	Union	Plainfield	NJ	***	***	***	***	***	***	***
360050080	Bronx	NYC-Morrisania Center	NY	84	***	***	***	***	***	***
360050083	Bronx	NYC-200th St & Southern Blvd	NY	88	80	83	81	84	83	75
360050110	Bronx	NYC-IS52	NY	***	***	***	***	***	80	76
360610010	New York	NYC-Mabel Dean HS	NY	***	69	***	***	***	***	***
360610063	New York	NYC-Roof WTC	NY	106	98	98	***	***	***	***
360810004	Queens	NYC-Queens College	NY	***	***	***	***	***	***	***
360810097	Queens	NYC-QBORO	NY	***	88	86	***	***	***	***
360810098	Queens	NYC-College Pt	NY	***	***	68	74	75	72	69
360810124	Queens	NYC-Queens	NY	***	***	***	***	***	***	***
360850067	Richmond	NYC-Susan Wagner HS	NY	105	96	98	96	94	89	87
361030002	Suffolk	Babylon	NY	97	91	87	92	95	94	91

New York-N. New Jersey-Long Island, NY-NJ-CT (Classification: MODERATE) 8-hr Ozone DESIGN VALUE (ppb)

AQS MONITOR ID	COUNTY	MONITOR NAME	ST	1997-1999	1998-2000	1999-2001	2000-2002	2001-2003	2002-2004	2003-2005
361030004	Suffolk	Riverhead	NY	98	94	91	85	***	***	***
361030009	Suffolk	Holtsville	NY	***	***	***	97	100	94	***
361192004	Westchester	White Plains	NY	98	92	92	90	94	90	88

Washington, DC-MD-VA (Classification: MODERATE) 8-hr Ozone DESIGN VALUE (ppb)

AQS MONITOR ID	COUNTY	MONITOR NAME	ST	1997-1999	1998-2000	1999-2001	2000-2002	2001-2003	2002-2004	2003-2005
110010025	District of Columbia (all)	Takoma	DC	95	96	93	93	88	85	78
110010041	District of Columbia (all)	River Terrace	DC	91	88	88	91	92	84	77
110010043	District of Columbia (all)	McMillian Reservoir	DC	100	96	94	95	94	89	82
240090010 & 240090011	Calvert	Calvert	MD	90	91	89	***	***	***	***
240170010	Charles	S. Maryland	MD	104	101	96	94	94	91	88
240210037	Frederick	Frederick Municipal Airport	MD	***	92	91	91	88	83	78
240313001	Montgomery	Rockville	MD	95	90	89	89	88	83	80
240330002	Prince George's	Greenbelt	MD	106	99	97	95	93	***	***
240338001	Prince George's	Suitland	MD	99	94	93	***	***	***	***
240338003	Prince George's	Equestrian Center	MD	***	***	***	***	***	94	91
510130020	Arlington Co	Aurora Hills	VA	97	92	92	96	99	95	87
510590005	Fairfax	Chantilly (Cub Run)	VA	91	91	88	88	89	84	79
510590018	Fairfax	Mount Vernon	VA	96	97	95	97	97	96	91
510590030	Fairfax	Franconia	VA	***	90	89	92	97	96	89
510591004 & 510591005	Fairfax	Seven Corners & Annandale	VA	95	90	***	***	***	94	86
510595001	Fairfax	McLean – Lewinsville	VA	86	86	86	90	88	86	79
511071005	Loudoun	Ashburn	VA	***	89	86	90	92	88	***
511530009	Prince William	James S. Long PARK	VA	91	88	85	85	87	83	79
515100009	Alexandria (City)	Alexandria	VA	91	89	88	90	92	88	81

Jefferson Co., NY (Classification: MODERATE) 8-hr Ozone DESIGN VALUE (ppb)

AQS MONITOR ID	COUNTY	MONITOR NAME	ST	1997-1999	1998-2000	1999-2001	2000-2002	2001-2003	2002-2004	2003-2005
360450002	Jefferson	Perch River	NY	90	82	87	91	97	86	81

Greater Connecticut, CT (Classification: MODERATE) 8-hr Ozone DESIGN VALUE (ppb)

AQS MONITOR ID	COUNTY	MONITOR NAME	ST	1997-1999	1998-2000	1999-2001	2000-2002	2001-2003	2002-2004	2003-2005
90031003	Hartford	East Hartford	CT	91	84	88	90	90	84	80
90050005	Litchfield	Cornwall (Mohawk Mt)	CT	***	***	***	***	***	89	87
90050006	Litchfield	Torrington	CT	97	93	***	***	***	***	***
90110008	New London	Groton	CT	94	87	90	89	93	88	85
90131001	Tolland	Stafford	CT	95	89	90	94	95	88	86

Boston-Lawrence-Worcester (E. MA), MA (Classification: MODERATE) 8-hr Ozone DESIGN VALUE (ppb)

AQS MONITOR ID	COUNTY	MONITOR NAME	ST	1997-1999	1998-2000	1999-2001	2000-2002	2001-2003	2002-2004	2003-2005
250010002	Barnstable	Truro	MA	95	89	96	93	95	88	86
250051002	Bristol	Fairhaven	MA	91	87	93	90	95	88	86
250051005	Bristol	Easton	MA	88	81	84	***	***	***	***
250070001	Dukes	Wampanoag Laboratory – Martha's Vineyard	MA	***	***	***	***	***	***	***
250095005	Essex	Lawrence-Haverhill	MA	74	68	63	70	***	***	***
250092006	Essex	Lynn	MA	93	86	86	90	93	87	83
250094004	Essex	Newbury	MA	87	82	83	86	89	83	78
250170009	Middlesex	USEPA Region 1 Lab – Chelmsford	MA	***	***	***	***	***	***	***
250171102	Middlesex	Stow	MA	***	86	88	89	89	79	75
250171801	Middlesex	Sudbury	MA	***	***	***	***	***	***	***
250174003	Middlesex	Waltham	MA	93	***	***	***	***	***	***
250213003	Norfolk	E Milton (Blue Hill)	MA	***	***	***	***	***	91	85
250250041	Suffolk	Boston-Long Island	MA	***	***	84	89	91	86	81
250250042	Suffolk	Boston-Roxbury	MA	***	***	66	72	76	71	68
250251003	Suffolk	Chelsea	MA	82	***	***	***	***	***	***
250270015	Worcester	Worcester	MA	94	88	85	85	86	***	79

Providence (All RI), RI (Classification: MODERATE) 8-hr Ozone DESIGN VALUE (ppb)

AQS MONITOR ID	COUNTY	MONITOR NAME	ST	1997-1999	1998-2000	1999-2001	2000-2002	2001-2003	2002-2004	2003-2005
440030002	Kent	W Greenwich	RI	92	88	94	97	95	87	84
440071010	Providence	E Providence	RI	***	***	87	91	93	***	82
440090007	Washington	Narragansett	RI	***	85	92	93	95	90	89

Springfield (Western MA), MA (Classification: MODERATE) 8-hr Ozone DESIGN VALUE (ppb)

AQS MONITOR ID	COUNTY	MONITOR NAME	ST	1997-1999	1998-2000	1999-2001	2000-2002	2001-2003	2002-2004	2003-2005
250034002	Berkshire	Adams	MA	***	***	***	***	87	***	***
230130003	Hampden	Agawam	MA	84	77	77	83	***	***	***
250130008	Hampden	Chicopee	MA	91	86	85	92	94	90	84
250150103	Hampshire	South Hadley (Amherst)	MA	82	76	77	78	77	69	67
250154002	Hampshire	Ware	MA	99	89	89	89	87	84	82

Poughkeepsie, NY (Classification: MODERATE) 8-hr Ozone DESIGN VALUE (ppb)

AQS MONITOR ID	COUNTY	MONITOR NAME	ST	1997-1999	1998-2000	1999-2001	2000-2002	2001-2003	2002-2004	2003-2005
360270007	Dutchess	Millbrook	NY	90	87	87	93	94	89	79
360715001	Orange	Valley Central	NY	90	86	87	84	87	83	84
360790005	Putnam	Mt Ninham	NY	94	89	89	92	93	89	86

Boston-Manchester-Portsmouth (SE), NH (Classification: MODERATE) 8-hr Ozone DESIGN VALUE (ppb)

AQS MONITOR ID	COUNTY	MONITOR NAME	ST	1997-1999	1998-2000	1999-2001	2000-2002	2001-2003	2002-2004	2003-2005
330110016 & 330110019 & 330110020	Hillsborough	Manchester	NH	***	***	***	***	***	75	70
330111010 & 330111011	Hillsborough	Nashua	NH	89	81	83	85	87	84	80

Boston-Manchester-Portsmouth (SE), NH (Classification: MODERATE) 8-hr Ozone DESIGN VALUE (ppb)

AQS MONITOR ID	COUNTY	MONITOR NAME	ST	1997-1999	1998-2000	1999-2001	2000-2002	2001-2003	2002-2004	2003-2005
330150009 & 330150015 & 330150014	Rockingham	Portsmouth	NH	87	80	***	***	***	80	75
330150013	Rockingham	Brentwood	NH	***	69	76	80	***	***	***
330150012 & 330150016	Rockingham	Rye	NH	90	79	81	83	84	78	73
330173002	Strafford	Rochester	NH	81	76	75	77	80	***	***

Kent and Queen Anne's Cos., MD (Classification: MARGINAL) 8-hr Ozone DESIGN VALUE (ppb)

AQS MONITOR ID	COUNTY	MONITOR NAME	ST	1997-1999	1998-2000	1999-2001	2000-2002	2001-2003	2002-2004	2003-2005
240290002	Kent	Millington	MD	100	101	100	102	95	89	82

Lancaster, PA (Classification: MARGINAL) 8-hr Ozone DESIGN VALUE (ppb)

AQS MONITOR ID	COUNTY	MONITOR NAME	ST	1997-1999	1998-2000	1999-2001	2000-2002	2001-2003	2002-2004	2003-2005
420710007	Lancaster	Lancaster	PA	101	97	96	94	92	86	83

Portland, ME (Classification: MARGINAL) 8-hr Ozone DESIGN VALUE (ppb)

AQS MONITOR ID	COUNTY	MONITOR NAME	ST	1997-1999	1998-2000	1999-2001	2000-2002	2001-2003	2002-2004	2003-2005
230050027	Cumberland	Portland	ME	***	***	***	***	***	***	***
230052003	Cumberland	Cape Elizabeth	ME	89	77	80	86	88	79	71
230230003 & 230230004	Sagadahoc	Phippsburg/Georgetown (Reid State Park)	ME	92	84	***	***	***	79	70
230313002	York	Kittery	ME	88	81	81	84	88	84	77
230312002	York	Kennebunkport	ME	92	82	86	90	91	84	74
230310037 & 230310038	York	Hollis	ME	76	72	***	***	***	75	73

Buffalo-Niagara Falls, NY (Classification: SUBPART 1) 8-hr Ozone DESIGN VALUE (ppb)

AQS MONITOR ID	COUNTY	MONITOR NAME	ST	1997-1999	1998-2000	1999-2001	2000-2002	2001-2003	2002-2004	2003-2005
360290002	Erie	Amherst	NY	85	89	92	97	99	91	86
360631006	Niagara	Middleport	NY	86	85	87	91	95	89	86

Youngstown-Warren-Sharon, OH-PA (Classification: SUBPART 1) 8-hr Ozone DESIGN VALUE (ppb)

AQS MONITOR ID	COUNTY	MONITOR NAME	ST	1997-1999	1998-2000	1999-2001	2000-2002	2001-2003	2002-2004	2003-2005
390990009 & 390990013	Mahoning	Youngstown - Oakhill	OH	91	89	86	87	89	85	80
391550008 & 391550011	Trumbull	Warren-Trumbull County	OH	95	91	88	90	95	91	86
391550009	Trumbull	Kinsman	OH	95	91	87	87	90	87	83
420850100	Mercer	Farrell	PA	96	92	88	92	94	88	83

Pittsburgh-Beaver Valley, PA (Classification: SUBPART 1) 8-hr Ozone DESIGN VALUE (ppb)

AQS MONITOR ID	COUNTY	MONITOR NAME	ST	1997-1999	1998-2000	1999-2001	2000-2002	2001-2003	2002-2004	2003-2005
420030008	Allegheny	Lawrenceville	PA	91	88	85	89	92	87	81
420030010	Allegheny	Pittsburg	PA	***	91	92	93	93	86	84
420030067	Allegheny	South Fayette	PA	99	96	90	90	91	87	82
420030088	Allegheny	Penn Hills	PA	92	91	88	***	***	***	***
420031005	Allegheny	Harrison Township	PA	101	94	92	95	92	87	81
420050001	Armstrong	Kittanning	PA	86	93	92	91	93	88	84
420070002	Beaver	Hookstown	PA	92	89	88	90	94	90	84
420070005	Beaver	Brighton Township	PA	91	90	89	90	92	87	81
420070014	Beaver	Beaver Falls	PA	90	89	85	88	86	81	75
421250005	Washington	Charleroi	PA	101	94	87	86	89	84	80
421250200	Washington	Washington	PA	91	88	86	86	88	82	81
421255001	Washington	Florence	PA	91	90	88	88	87	82	78
421290006	Westmoreland	Murrysville	PA	85	81	80	81	84	81	80
421290008	Westmoreland	Greensburg	PA	***	***	86	86	91	87	82

Jamestown, NY (Classification: SUBPART 1) 8-hr Ozone DESIGN VALUE (ppb)

AQS MONITOR ID	COUNTY	MONITOR NAME	ST	1997-1999	1998-2000	1999-2001	2000-2002	2001-2003	2002-2004	2003-2005
360130006	Chautauqua	Dunkirk	NY	***	***	89	92	94	93	89
360130011	Chautauqua	Westfield	NY	89	88	85	87	89	85	79

Hancock, Knox, Lincoln & Waldo Cos., ME (Classification: SUBPART 1)

AQS MONITOR ID	COUNTY	MONITOR NAME	ST	1997-1999	1998-2000	1999-2001	2000-2002	2001-2003	2002-2004	2003-2005
230130004	Knox	Port Clyde	ME	82	76	80	83	87	81	77
230090401	Hancock	Schoodic Point	ME	***	***	***	***	***	***	***
230090001	Hancock	Seawall	ME	***	***	***	***	***	***	***
230090101 & 230090103	Hancock	Acadia National Park - McFarland Hill	ME	85	83	85	84	87	80	75
230090102	Hancock	Acadia National Park - Cadillac Mtn.	ME	89	87	89	93	94	88	82

Franklin Co., PA (Classification: SUBPART 1) 8-hr Ozone DESIGN VALUE (ppb)

AQS MONITOR ID	COUNTY	MONITOR NAME	ST	1997-1999	1998-2000	1999-2001	2000-2002	2001-2003	2002-2004	2003-2005
420550001	Franklin	Methodist Hill	PA	97	95	92	94	93	85	75

Erie, PA (Classification: SUBPART 1) 8-hr Ozone DESIGN VALUE (ppb)

AQS MONITOR ID	COUNTY	MONITOR NAME	ST	1997-1999	1998-2000	1999-2001	2000-2002	2001-2003	2002-2004	2003-2005
420490003	Erie	Erie	PA	93	90	87	88	92	87	83

Essex Co. (Whiteface Mtn.), NY (Classification: SUBPART 1) 8-hr Ozone DESIGN VALUE (ppb)

AQS MONITOR ID	COUNTY	MONITOR NAME	ST	1997-1999	1998-2000	1999-2001	2000-2002	2001-2003	2002-2004	2003-2005
360310002	Essex (Whiteface Mountain above 1,900 foot elevation)	Whiteface Mountain Summit	NY	80	***	***	87	91	89	***
360310003		Whiteface Mtn. Base	NY	79	76	78	82	88	83	77

Allentown-Bethlehem-Easton, PA (Classification: SUBPART 1) 8-hr Ozone DESIGN VALUE (ppb)

AQS MONITOR ID	COUNTY	MONITOR NAME	ST	1997-1999	1998-2000	1999-2001	2000-2002	2001-2003	2002-2004	2003-2005
420770004	Lehigh	Allentown	PA	100	97	96	93	91	88	85
420950025	Northampton	Freemansburg	PA	87	95	97	92	90	88	87
420950100 & 420958000	Northampton	Easton	PA	93	90	91	89	89	86	82

Reading, PA (Classification: SUBPART 1) 8-hr Ozone DESIGN VALUE (ppb)

AQS MONITOR ID	COUNTY	MONITOR NAME	ST	1997-1999	1998-2000	1999-2001	2000-2002	2001-2003	2002-2004	2003-2005
420110001	Berks	Kutztown	PA	92	89	90	87	84	***	***
420110009 & 420110010	Berks	Reading	PA	96	92	95	92	91	83	80

Clearfield and Indiana Cos., PA (Classification: SUBPART 1) 8-hr Ozone DESIGN VALUE (ppb)

AQS MONITOR ID	COUNTY	MONITOR NAME	ST	1997-1999	1998-2000	1999-2001	2000-2002	2001-2003	2002-2004	2003-2005
420630004	Indiana	Strongstown	PA	***	***	***	***	***	***	***
420334000	Clearfield	Moshannon	PA	93	87	83	87	90	85	82

Greene Co., PA (Classification: SUBPART 1) 8-hr Ozone DESIGN VALUE (ppb)

AQS MONITOR ID	COUNTY	MONITOR NAME	ST	1997-1999	1998-2000	1999-2001	2000-2002	2001-2003	2002-2004	2003-2005
420590002	Greene	Holbrook	PA	97	96	92	90	89	84	81

York, PA (Classification: SUBPART 1) 8-hr Ozone DESIGN VALUE (ppb)

AQS MONITOR ID	COUNTY	MONITOR NAME	ST	1997-1999	1998-2000	1999-2001	2000-2002	2001-2003	2002-2004	2003-2005
420010002	Adams	Biglerville	PA	***	***	***	***	***	80	76
421330008	York	York	PA	94	93	90	92	89	86	82

Rochester, NY (Classification: SUBPART 1) 8-hr Ozone DESIGN VALUE (ppb)

AQS MONITOR ID	COUNTY	MONITOR NAME	ST	1997-1999	1998-2000	1999-2001	2000-2002	2001-2003	2002-2004	2003-2005
360551004 & 360551007	Monroe	Rochester	NY	***	***	***	85	88	79	73
361173001	Wayne	Williamson	NY	86	81	81	83	88	81	71

Albany-Schenectady-Troy, NY (Classification: SUBPART 1) 8-hr Ozone DESIGN VALUE (ppb)

AQS MONITOR ID	COUNTY	MONITOR NAME	ST	1997-1999	1998-2000	1999-2001	2000-2002	2001-2003	2002-2004	2003-2005
360010012	Albany	Albany - Loudonville	NY	80	77	80	83	86	80	76
360830004	Rensselaer	Grafton State Park	NY	***	***	***	***	***	86	80
360910004	Saratoga	Stillwater	NY	84	80	84	***	87	84	82
360930003 & 360930093	Schenectady	Schenectady	NY	75	71	75	76	81	76	74

Harrisburg-Lebanon-Carlisle, PA (Classification: SUBPART 1) 8-hr Ozone DESIGN VALUE (ppb)

AQS MONITOR ID	COUNTY	MONITOR NAME	ST	1997-1999	1998-2000	1999-2001	2000-2002	2001-2003	2002-2004	2003-2005
420430401	Dauphin	Harrisburg	PA	92	90	86	87	86	82	78
420431100	Dauphin	Hershey	PA	94	93	94	91	88	81	78
420990301	Perry	Little Buffalo State Park	PA	90	85	84	83	87	80	78

Johnstown, PA (Classification: SUBPART 1) 8-hr Ozone DESIGN VALUE (ppb)

AQS MONITOR ID	COUNTY	MONITOR NAME	ST	1997-1999	1998-2000	1999-2001	2000-2002	2001-2003	2002-2004	2003-2005
420210011	Cambria	Johnstown	PA	93	91	88	88	87	80	77

Scranton-Wilkes-Barre, PA (Classification: SUBPART 1) 8-hr Ozone DESIGN VALUE (ppb)

AQS MONITOR ID	COUNTY	MONITOR NAME	ST	1997-1999	1998-2000	1999-2001	2000-2002	2001-2003	2002-2004	2003-2005
420690101	Lackawanna	Peckville	PA	90	87	86	85	85	80	75
420692006	Lackawanna	Scranton	PA	88	84	84	83	84	79	76
420791100	Luzerne	Nanticoke	PA	82	81	82	83	84	78	73
420791101	Luzerne	Wilkes-Barre	PA	92	84	84	84	86	81	77

State College, PA (Classification: SUBPART 1) 8-hr Ozone DESIGN VALUE (ppb)

AQS MONITOR ID	COUNTY	MONITOR NAME	ST	1997-1999	1998-2000	1999-2001	2000-2002	2001-2003	2002-2004	2003-2005
420270100	Centre	State College	PA	***	***	***	85	86	82	79
420274000	Centre	Penn Nursery	PA	90	84	80	82	88	84	***

Tioga Co., PA (Classification: SUBPART 1) 8-hr Ozone DESIGN VALUE (ppb)

AQS MONITOR ID	COUNTY	MONITOR NAME	ST	1997-1999	1998-2000	1999-2001	2000-2002	2001-2003	2002-2004	2003-2005
421174000	Tioga	Tioga	PA	***	***	***	84	86	85	81

Altoona, PA (Classification: SUBPART 1) 8-hr Ozone DESIGN VALUE (ppb)

AQS MONITOR ID	COUNTY	MONITOR NAME	ST	1997-1999	1998-2000	1999-2001	2000-2002	2001-2003	2002-2004	2003-2005
420130801	Blair	Altoona	PA	95	89	84	84	85	81	77

Washington Co. (Hagerstown), MD (Classification: SUBPART 1) 8-hr Ozone DESIGN VALUE (ppb)

AQS MONITOR ID	COUNTY	MONITOR NAME	ST	1997-1999	1998-2000	1999-2001	2000-2002	2001-2003	2002-2004	2003-2005
240430009	Washington	Hagerstown	MD	***	***	85	87	86	83	78

New York (Classification: ATTAINMENT) 8-hr Ozone DESIGN VALUE (ppb)

AQS MONITOR ID	COUNTY	MONITOR NAME	ST	1997-1999	1998-2000	1999-2001	2000-2002	2001-2003	2002-2004	2003-2005
360150003	Gloucester	Elmira	NY	79	79	79	81	83	77	70
360410005	Hamilton	Piseco Lake	NY	79	77	77	79	81	76	73
360430005	Herkimer	Nicks Lake	NY	72	70	72	74	76	72	69
360530006	Madison	Camp Georgetown	NY	79	78	78	80	82	77	73
360650004	Oneida	Camden	NY	76	73	76	78	83	78	72
360671015	Onondaga	East Syracuse	NY	82	80	81	83	85	***	74
360750003	Oswego	Fulton	NY	***	***	***	***	***	***	82
361111005	Ulster	Belleayre Mountain	NY	83	80	81	81	83	80	79

Maine (Classification: ATTAINMENT) 8-hr Ozone DESIGN VALUE (ppb)

AQS MONITOR ID	COUNTY	MONITOR NAME	ST	1997-1999	1998-2000	1999-2001	2000-2002	2001-2003	2002-2004	2003-2005
230112005	Kennebec	Gardiner	ME	77	73	75	78	80	76	70
230090301	Hancock	Castine	ME	***	***	***	***	***	75	70
230210003	Piscataquis	Dover-Foxcroft	ME	***	62	65	***	***	***	***
230194008	Penobscot	Holden	ME	75	***	76	***	83	75	68
230173001	Oxford	North Lovell	ME	59	58	61	60	62	60	61
CC0040002	NB CAN	Roosevelt-Campobello IP	NB	62	60	61	60	61	54	54
230194007	Penobscot	Howland	ME	71	68	69	68	68	64	61
230038001	Aroostook	Ashland	ME	65	62	64	65	64	63	60

Pennsylvania (Classification: ATTAINMENT) 8-hr Ozone DESIGN VALUE (ppb)

AQS MONITOR ID	COUNTY	MONITOR NAME	ST	1997-1999	1998-2000	1999-2001	2000-2002	2001-2003	2002-2004	2003-2005
420730015	Lawrence	New Castle	PA	83	78	78	78	80	77	73
420810100	Lycoming	Montoursville	PA	***	***	***	***	***	82	79
420810403	Lycoming	Williamsport	PA	74	71	71	***	***	***	***
420814000	Lycoming	Tiadaghton	PA	***	77	76	79	80	77	***

Vermont (Classification: ATTAINMENT) 8-hr Ozone DESIGN VALUE (ppb)

AQS MONITOR ID	COUNTY	MONITOR NAME	ST	1997-1999	1998-2000	1999-2001	2000-2002	2001-2003	2002-2004	2003-2005
500030004	Bennington	Bennington	VT	80	76	79	80	80	78	73
500070007	Chittenden	Underhill	VT	74	74	75	77	78	76	71

New Hampshire (Classification: ATTAINMENT) 8-hr Ozone DESIGN VALUE (ppb)

AQS MONITOR ID	COUNTY	MONITOR NAME	ST	1997-1999	1998-2000	1999-2001	2000-2002	2001-2003	2002-2004	2003-2005
330012003 & 330012004	Belknap	Laconia	NH	68	***	***	***	78	75	73
330031002	Carroll	Conway	NH	67	64	66	67	***	***	***
330050007	Cheshire	Keene	NH	75	71	72	73	76	74	71
330074002	Coos	Mt Washington Base	NH	***	***	***	***	***	***	67
330074003	Coos	Pittsburg	NH	***	***	***	***	***	***	60
330090008 & 330092005	Grafton	Haverhill-Lebanon	NH	70	70	69	68	72	72	71
330115001	Hillsborough	Peterborough (Miller State Park)	NH	***	***	***	***	***	***	77
330170007 & 330171007	Strafford	Concord	NH	74	71	70	74	75	75	71
330190003	Sullivan	Claremont	NH	73	70	72	73	75	77	72

Appendix E: The sea breeze and flow over the ocean in-depth

Appendix E: The sea breeze and flow over the ocean in-depth

Figure E-1 displays a general description of ozone transport in coastal New England. This figure shows 90th percentile ozone concentration wind direction plots at four sites along the coast. For the first site, Lynn, MA, high ozone days are affected mainly by winds from the southwest bringing ozone up the coast to the site. At the second site, Newbury, MA, winds arrive to the site from two directions, up the coast, in a similar pattern seen at Lynn, but also from the ocean. The high ozone days therefore can result from ozone and its precursors coming from inland or from the ocean in the sea breeze. At the two northern sites in Maine, Cape Elizabeth and Acadia National Park, winds on high ozone days come mostly off the ocean. This is mainly due to the orientation of the Maine coastline, as summertime winds generally come from the southwest, therefore traveling over the ocean before arriving to these sites.

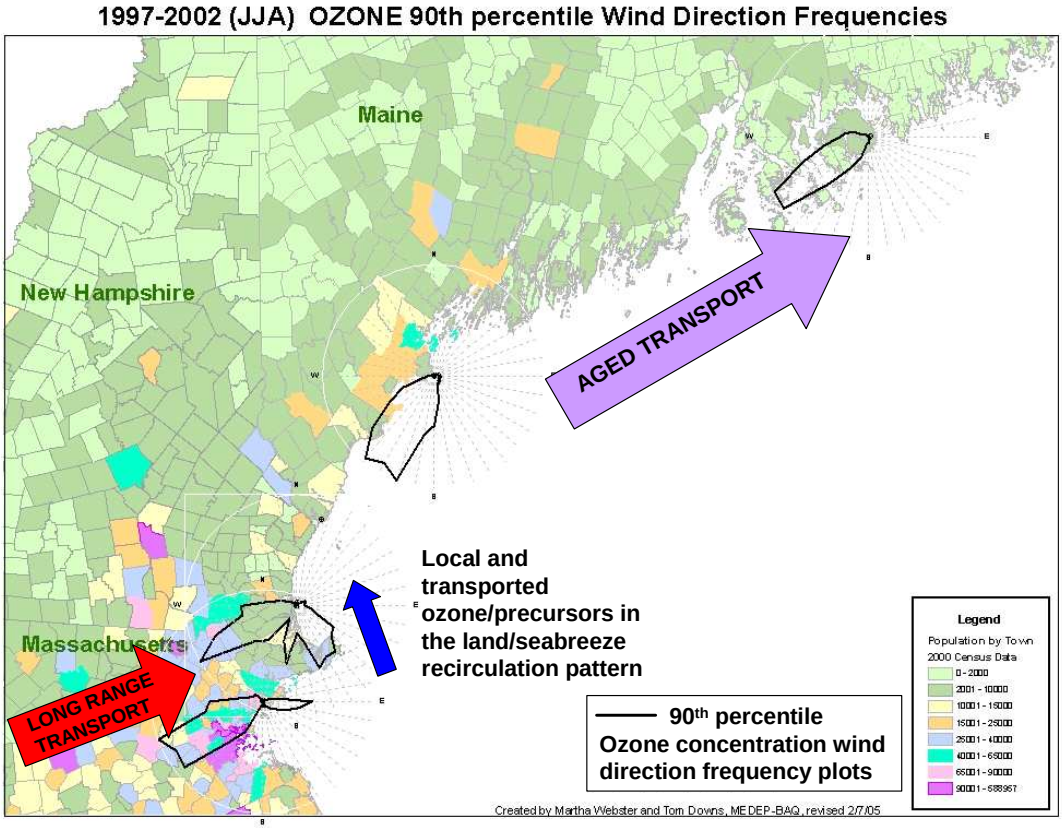

Figure E-1. 90th percentile ozone concentration wind direction frequency plots at four coastal sites in northern New England (figure provided by Tom Downs, Maine Department of Environmental Protection).

Figure E-2 displays wind directions at Newbury, MA on June 29, 1997 where hourly ozone concentrations ranged from 88 ppb to 107 ppb during the afternoon hours and a sea breeze can be identified. The forward trajectory starting in Boston at 6 a.m. shows winds pushing air from the Boston metro area out into the harbor throughout the day. The hourly ozone wind rose at Newbury, MA shows the afternoon wind shift that

occurred on this day where vector direction indicates wind direction and magnitude indicates ozone concentrations. Morning winds came from a west/northwesterly direction when hourly ozone concentrations at the site ranged from 47 to 68 ppb. At 1 p.m., the wind shifted direction, now coming off the ocean from the southeast, accompanied by a 20 ppb increase in hourly ozone. Hourly ozone levels then continued to increase in the early afternoon, peaking at 107 ppb at 3 p.m. This increase in ozone levels accompanying a shift in winds pushing air masses from the ocean to a coastal site illustrates how the sea breeze can contribute to poor air quality along the coast. The poor air quality could be a result of polluted air from Boston being pushed back to the site in the sea breeze. Sea breezes, however, are not always associated with worsening air quality as the afternoon sea breeze doesn't always bring in polluted air.

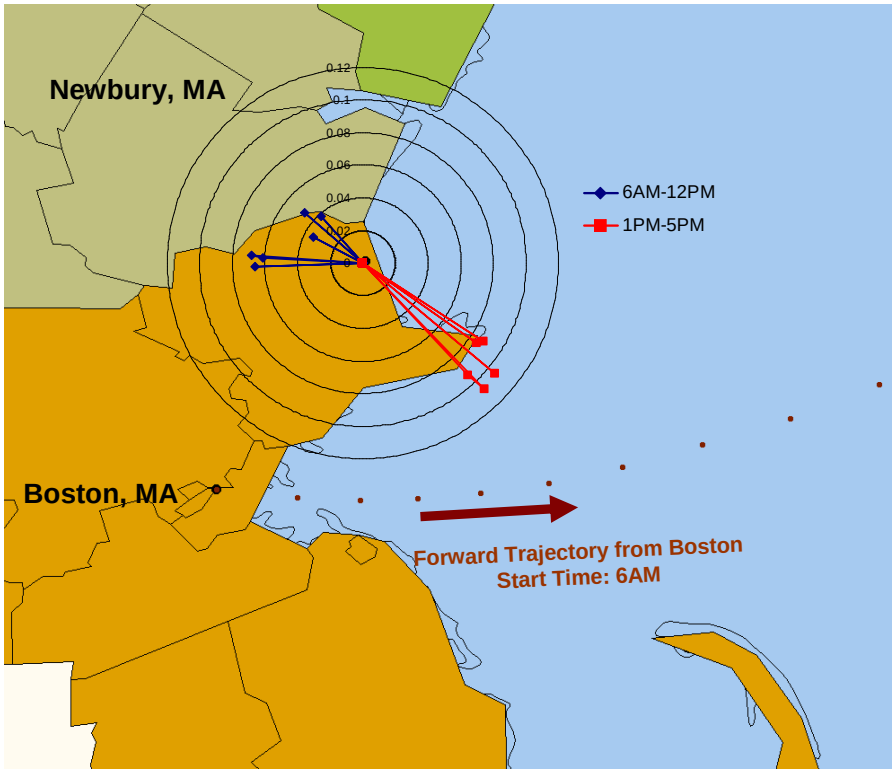

Figure E-2. Example of a sea breeze effect occurring in Newbury, MA on June 29, 1997 (figure data provided by Tom Downs, Maine Department of Environmental Protection).

At sites further north in Maine, the sea breeze effect is less dramatic due to the orientation of the Maine coastline. Figure E-3 shows a similar ozone wind rose plot for Cape Elizabeth, ME on the same day illustrated in Figure E-2. With the exception of the winds at 6 a.m. that came from the northwest, the winds arrived to the site from the southwest direction. There are some slight shifts in wind direction, particularly a shift after 5 p.m. that began to bring winds from the inland side of the coast, but it is difficult to determine whether these shifts are due to a sea breeze effect or if the evening shift is due to the weakened sea breeze. Winds are generally moving up the coast, over water, and winds in the same direction of the sea breeze can bring poor air quality. On this day, ozone concentrations ranged between 89 and 102 ppb between 3 p.m. and 7 p.m.

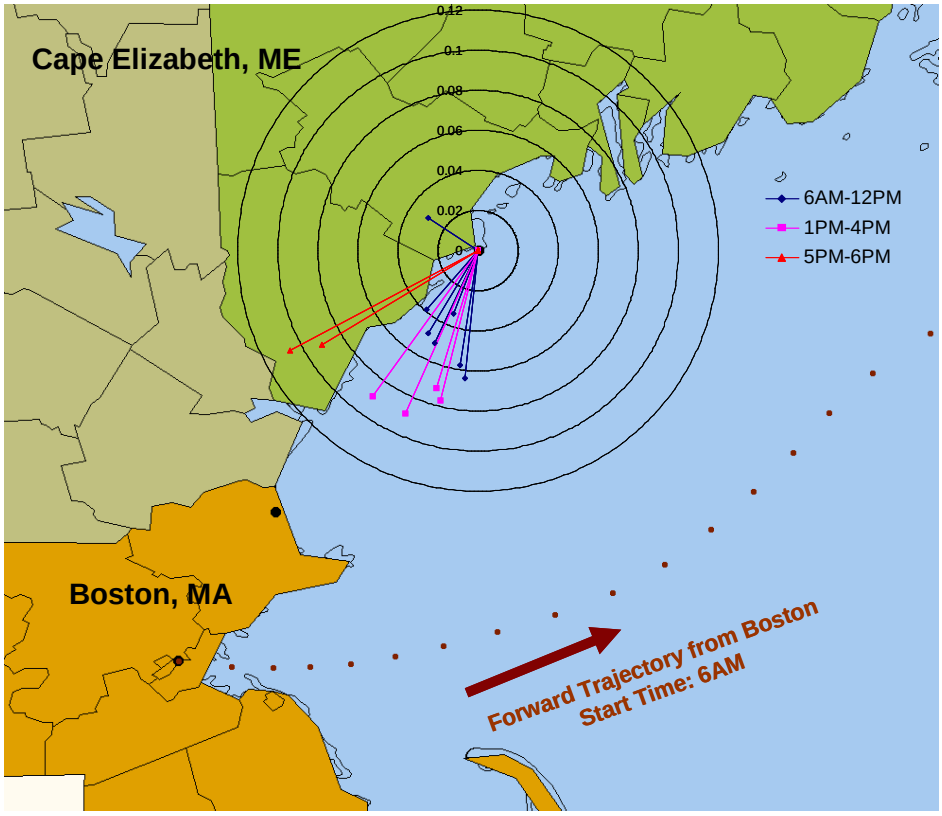

Figure E-3. Wind directions and ozone concentrations at Cape Elizabeth, ME on June 29, 1997 (figure data provided by Tom Downs, Maine Department of Environmental Protection).

Transport over the ocean is commonly observed downwind of the New York City metropolitan area during the summer months due its proximity to the Atlantic Ocean and the Long Island Sound. The four pollution rose plots presented in Figure E-4 represent the frequency of wind direction on the highest 10 percentile ozone concentration days from April 1 to October 31 during the years 1997 to 2005. The winds on the highest ozone days point at the New York City metropolitan area at all locations along the Connecticut shoreline. Going along the Connecticut shoreline to the east (towards Groton), the predominant wind frequency direction shifts increasingly to the west, tracking the upwind location of the New York City metropolitan area.

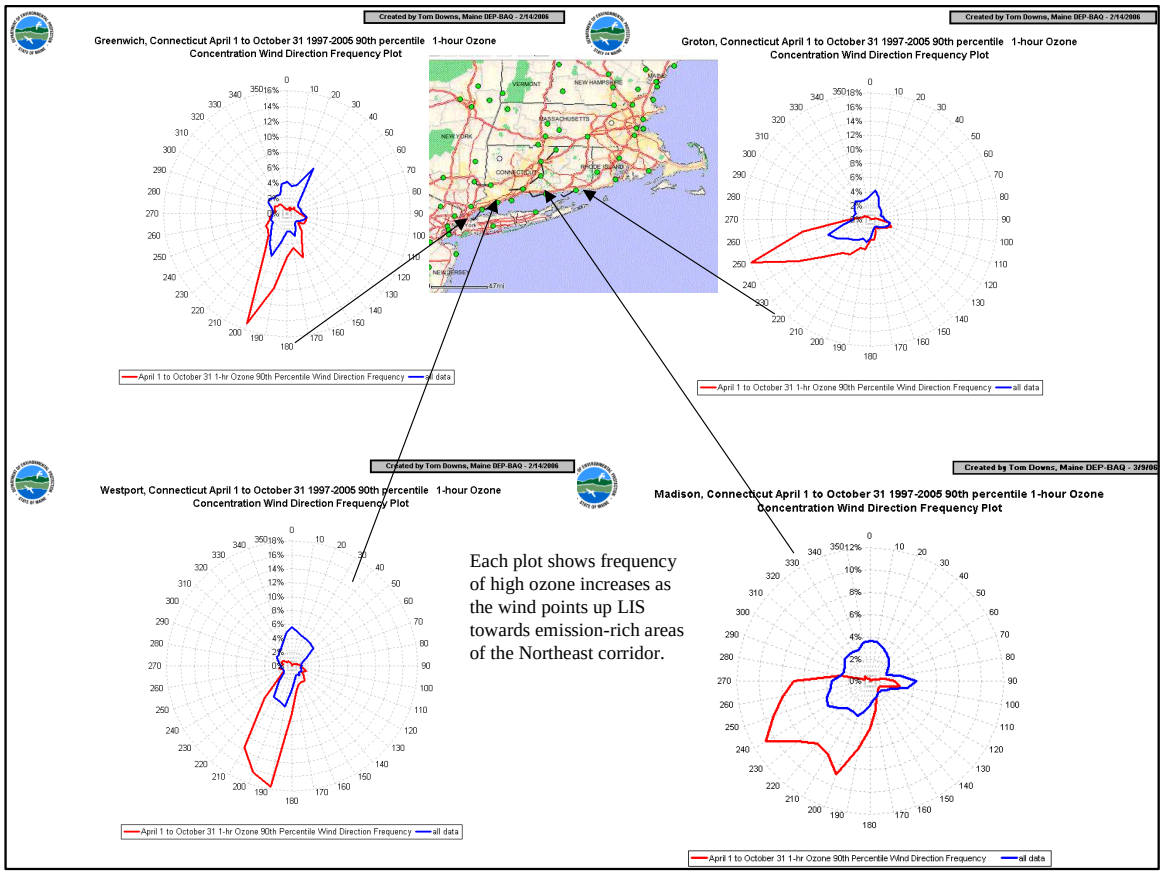

Figure E-4. Wind rose plots along Connecticut shoreline for the time period April 1 to October 31 during the years 1997 through 2005. The elongated red outlines pointing to the southwest to west are wind directions on the highest 10 percentile ozone concentration days at four Connecticut coastal locations. For comparison, the blue outlines are the wind rose plots for all days over the same period. The high ozone day wind rose plots indicate pollution flow over Long Island Sound that tracks the upwind location of the New York City metropolitan area (figure from Tom Downs, Maine Department of the Environment).

Appendix F: Observed nocturnal low level jet across the OTR, July 2002

Appendix F: Observed nocturnal low level jet across the OTR, July 2002

An example of the nocturnal low level jet across the OTR can be seen on the nights of July 22 through July 24, 2002, as night time winds at altitudes between 450 m and 1500 m were observed at several coastal sites. Figure F-1 shows wind profiler data on the night of July 22-July 23, 2002 for five sites along the east coast: Fort Meade, MD (FME), Orange, MA (ORE), Stow, MA (STW), Appledore Island, ME (ADI), and Pease Air Force Base, NH (PSE). These wind "barb" plots show wind direction (direction of arrow indicating where wind is coming from), wind speed (wind barb color), time of day (UTC time, x-axis), and altitude (meters, y-axis). The location of the nocturnal low level jet appears within the circle in each wind barb plot of Figure F-1. The figure shows a weak nocturnal low level jet at the southernmost site, Fort Meade, with wind speeds of 15 to 25 knots between 300 m and 500 m in the early part of the night. Further north, the nocturnal low level jet is more pronounced with wind speeds between 500 m and 1500 m above ground reaching 40 knots. Figure F-1 shows on this day the nocturnal low level jet extending from Maryland up through southern Maine. In addition, the wind barb plots show the northeasterly direction of the nocturnal low level jet. Above this jet, we see slower winds coming from the west to all the sites.

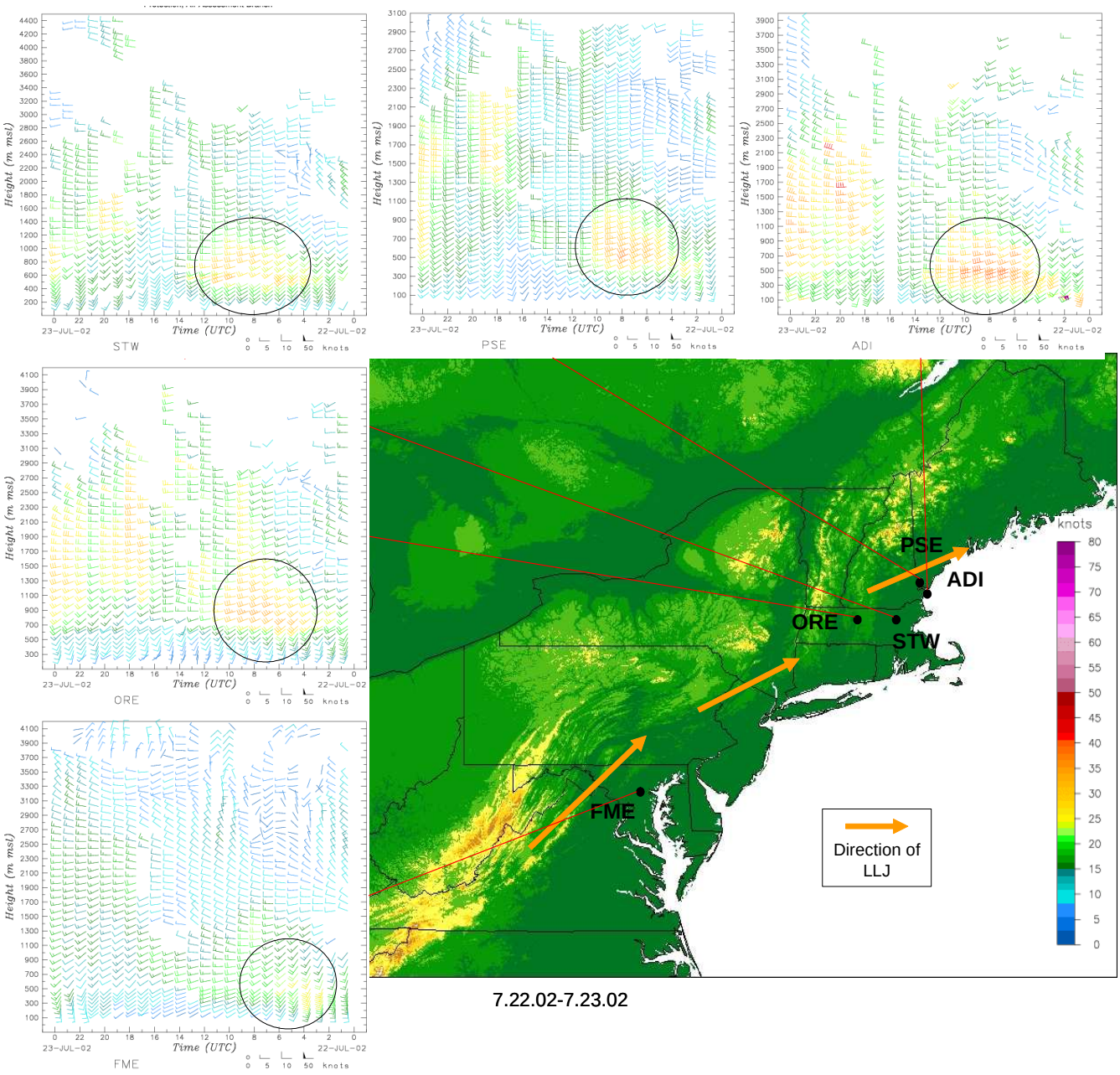

Figure F-1. Nocturnal low level jet on July 22 – 23, 2002. Note: Circles in the wind barb plots indicate the location of the nocturnal low level jet.

Figure F-1 shows that throughout the night, the nocturnal low level jet travels in a northeasterly direction along the east coast. The pollution implications of this nocturnal low level jet episode can be seen in Figure F-2. The Cadillac Mountain ozone monitor is located on the coast of Maine at an elevation of 466 m. At this elevated position, we can see how the nocturnal low level jet affects overnight and early morning ozone levels. Between midnight and 4 a.m. during the northeasterly nocturnal low level jet, hourly ozone concentrations at Cadillac Mountain are between 70 ppb and 80 ppb. Ozone levels

had begun to increase early in the evening on July 22 and continued to increase throughout the night and peak at 3 a.m. This increasing nighttime ozone at an elevated position corresponds to the nocturnal low level jet channeling air up the coast during the night. Conversely, at Cape Elizabeth, a ground level site relatively close to Cadillac Mountain, night time ozone levels are much lower than on top of Cadillac Mountain. This difference in ozone at upper and lower levels shows how the nocturnal inversion can isolate air masses above and below the inversion.

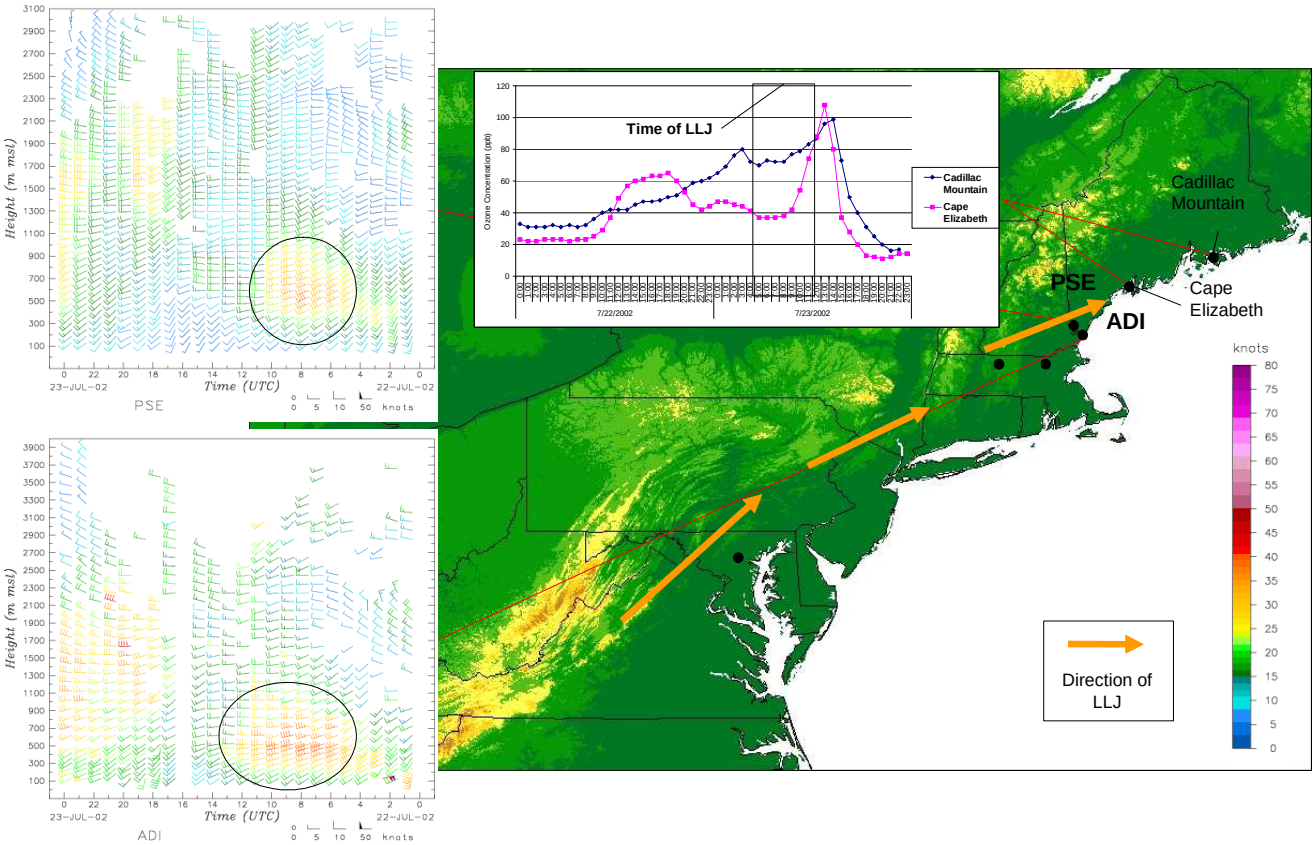

Figure F-2. Nocturnal low level jet with hourly ozone concentrations at Cadillac Mountain, ME and Cape Elizabeth, ME on July 22 – 23, 2002. Note: Circles in the wind barb plots indicate the location of the nocturnal low level jet.

The air mass affecting early morning ozone concentrations in Figure F-2 can be roughly tracked using wind speed and wind direction information from Cadillac Mountain, Pease, Appledore Island, and Orange. Assuming the nocturnal low level jet occurs for five hours that night (based on neighboring wind barb plots), the air mass arriving at Cadillac Mountain at 3 a.m. during peak ozone conditions was over central Massachusetts around 11 p.m. on July 22 when the nocturnal low level jet began to form. Tracking this farther back shows that the air mass affecting Cadillac Mountain was over western Connecticut around 6 p.m. on July 22. Looking at ozone levels in Cornwall, CT, we see that high ozone conditions existed in this region during the afternoon of July 22 with the average hourly ozone at 112 ppb between 4 p.m. and 7 p.m. Elevated ozone from this region first slowly traveled up the coast in the evening. When the nocturnal low level

jet formed, it quickly pushed ozone up the coast affecting ozone levels at Cadillac Mountain, an elevated site in the jet, in the early morning hours (~3 a.m.).

Figure F-3 shows wind profiler information for the next day, July 24, 2002. In this case we see a stronger nocturnal low level jet between midnight and 8am that originates further to the south. The Fort Meade and Rutgers (RUT) sites show the nocturnal low level jet in the early part of the evening with flow in the northeasterly direction. At higher altitudes slower winds from the west pass over the nocturnal low level jet. Further north, a strong nocturnal low level jet can be seen at Stow, Appledore Island, and Pease. It is difficult to determine if a nocturnal low level jet exists at Orange as high winds continue at the upper altitudes and data are missing for the highest altitudes. Figure F-3 demonstrates an example of the nocturnal low level jet passing along the east coast as far south as Maryland and as far north as southern Maine.

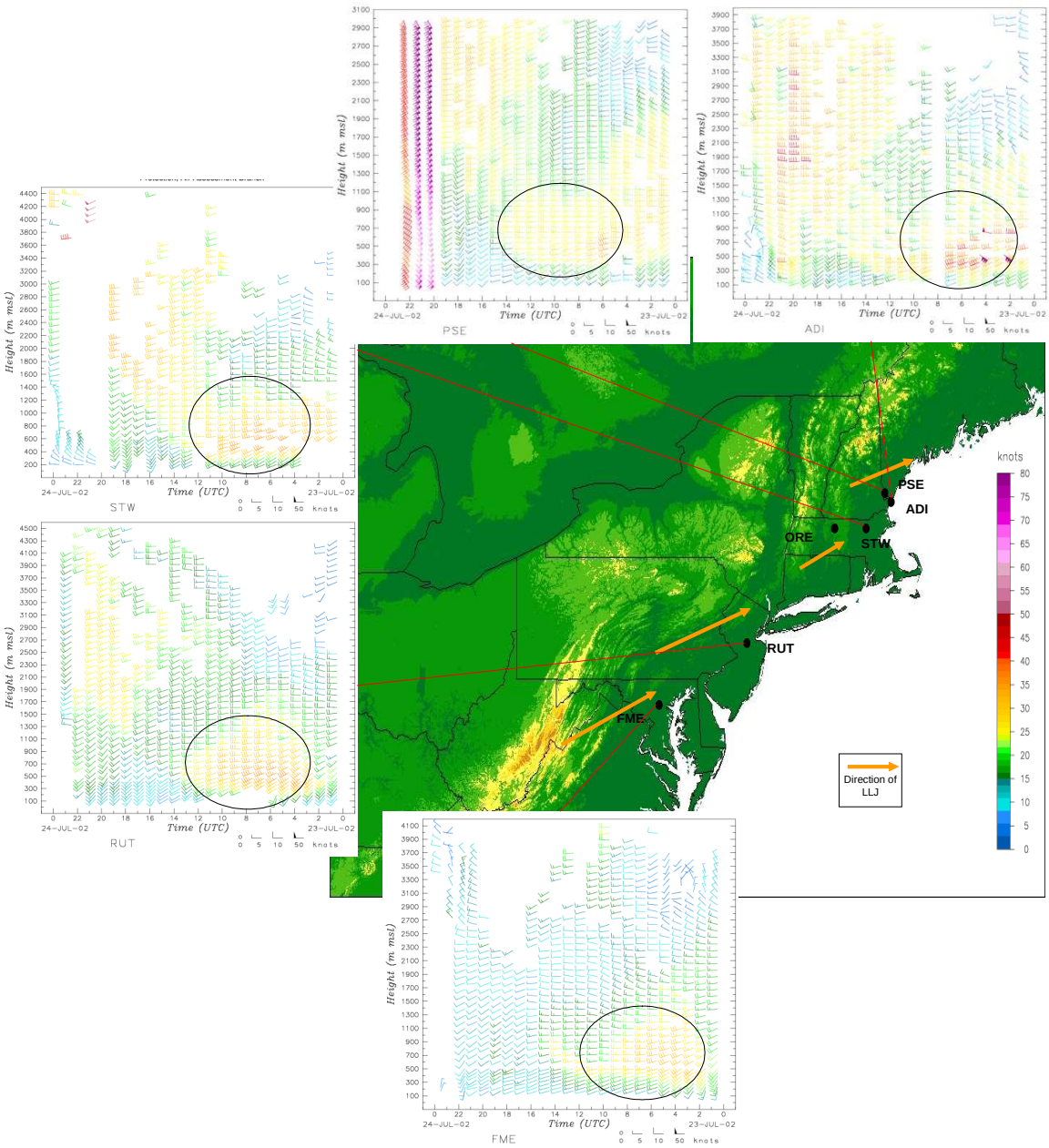

Figure F-3. Nocturnal low level jet on July 23 – 24, 2002. Note: Circles in the wind barb plots indicate the location of the nocturnal low level jet. Data are inconclusive for identifying a nocturnal low level jet at Orange, MA.

Figure F-3 shows that the nocturnal low level jet occurred on the night of July 23-24 as it did on the previous night. Figure F-4 shows ozone levels overnight on the July 23-24 at Cadillac Mountain and Cape Elizabeth. In this case, we see that low ozone is occurring at both sites during the early hours of July 24. Applying the same methods utilized earlier, wind speed and wind direction information from Cadillac Mountain indicate that the air arriving at Cadillac Mountain was also roughly over central Massachusetts at 10 p.m. on July 23 (same wind direction and wind speed as previous day). Wind profiler data show that winds moved this air mass from eastern New York and western Connecticut in the late afternoon. Average ozone levels between 4 p.m. and 7 p.m. were 53 ppb at Cornwall, CT. Therefore, much like on the previous day, air masses were tracked back to the western Connecticut area upwind. In this case, however, low levels of ozone existed in the air mass.

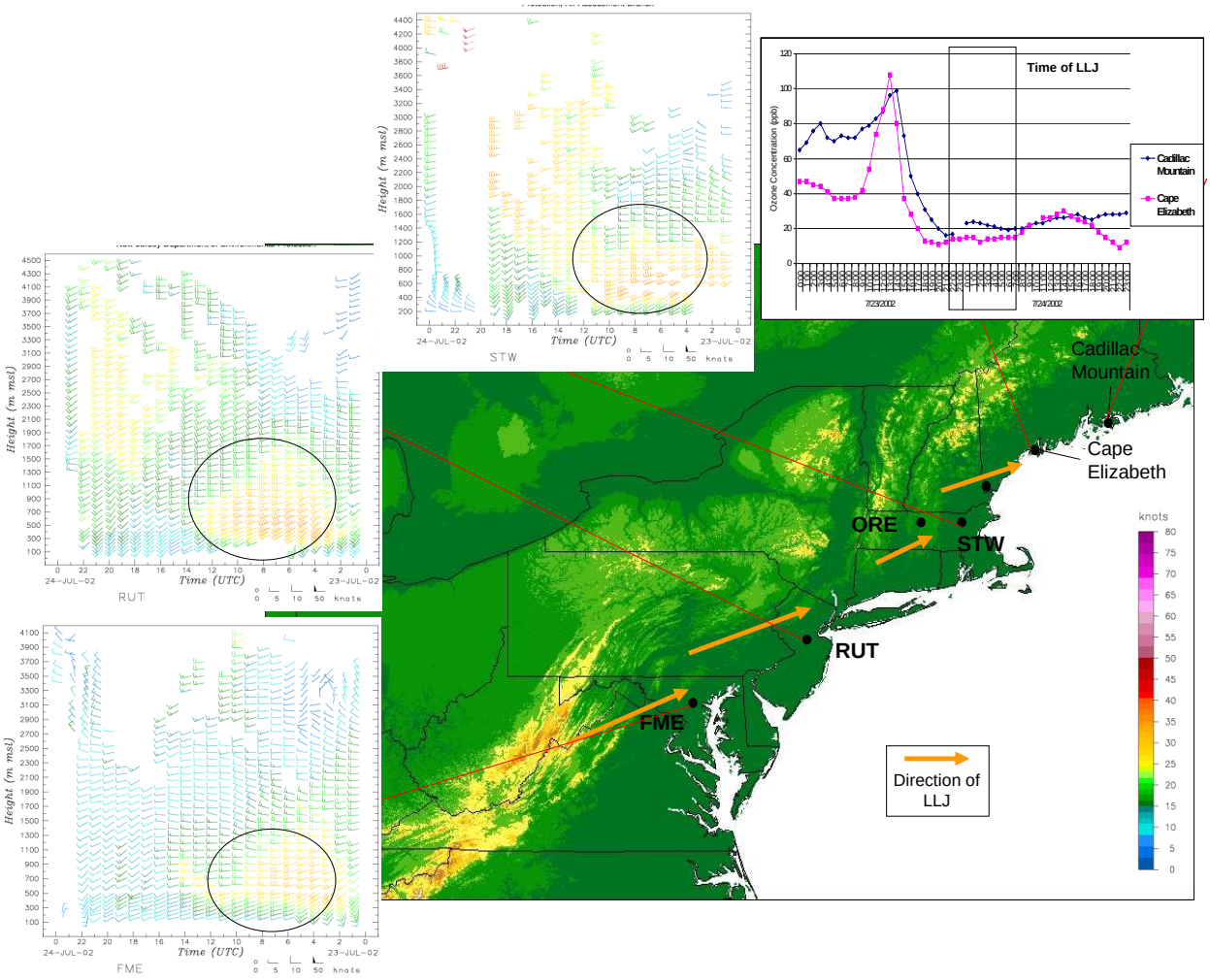

Figure F-4. Nocturnal low level jet with hourly ozone concentrations at Cadillac Mountain, ME and Cape Elizabeth, ME on July 23 – 24, 2002. Note: Circles in the wind barb plots indicate the location of the nocturnal low level jet. Data are inconclusive for identifying a nocturnal low level jet at Orange, MA.

Examining the wind profiler data from 4 p.m. to midnight on July 23 (Figure F-1 and Figure F-3), we see high winds at all altitudes developing throughout the region. Figure F-5 shows that these high winds are part of a weather front that passed through the region in the afternoon of July 23. This corresponds with the sharp drop in ozone levels at Cornwall, CT, Cadillac Mountain, ME, and Cape Elizabeth, ME (Figure F-6) as the front pushed ozone out of the region. This explains the low levels of ozone seen at Cadillac Mountain during the nocturnal low level jet in the early hours of July 24. This example demonstrates that not all nocturnal low level jets are associated with high ozone levels at elevated sites. A necessary condition for the transport of ozone in a nocturnal low level jet is the presence of upwind elevated ozone levels. The front that pushed through the region on the previous day resulted in “clean” air being transported in the nocturnal low level jet.

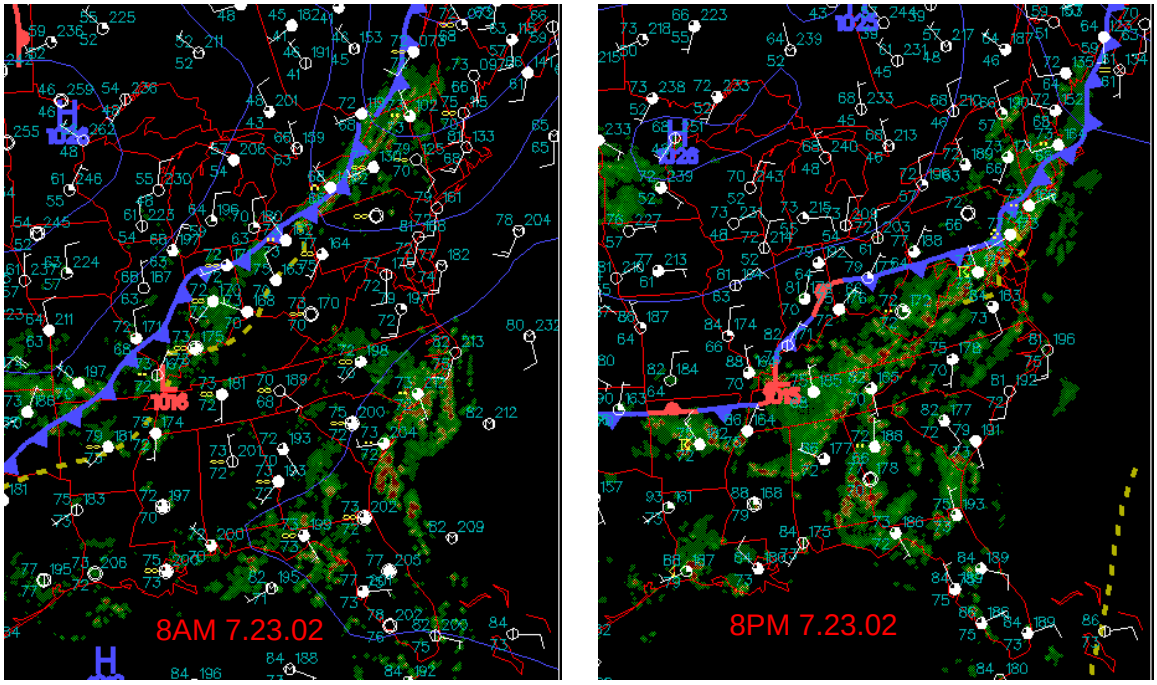

Figure F-5. Weather map displaying a front passing through the East on July 23, 2002.

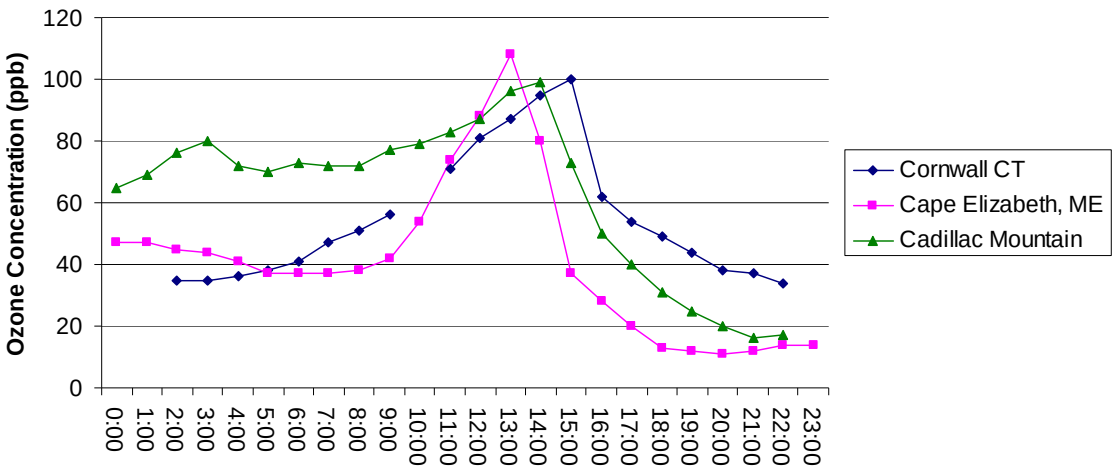

Figure F-6. Hourly ozone concentrations on July 23, 2002 at three sites.

Appendix G: Contributions to the ozone reservoir

Appendix G: Contributions to the ozone reservoir

Contributions to the ozone reservoir can come from two sources. The first is from the residual local ozone and precursors in the atmosphere at sunset. The second is from transport of ozone and precursors from outside of the local region. To identify these outside sources, Taubman *et al*. (2006) have made an analysis of the complete set of aircraft flights undertaken by RAMMPP between 1992 and 2003. Initially, the data were divided into morning and afternoon profiles to identify diurnal patterns. Little diurnal variation was observed in the carbon monoxide and sulfur dioxide profiles. The ozone values were greater in the afternoon than the morning, while ozone in the lower free troposphere (i.e., above the boundary level), where long range transport is possible, was consistently ~55 ppb. Transport patterns and source regions during summertime haze and ozone episodes were analyzed with a cluster analysis of back trajectory data. Eight clusters were identified, which were then divided into morning and afternoon profiles. Table G-1 lists the characteristics of each cluster, and Figure G-1 shows the back trajectories calculated for each profile divided by cluster at an altitude of 2000 meters. The median profile values were calculated and statistical differences were determined using a nonparametric procedure. When the greatest trajectory density lay over the northern Ohio River Valley, which has large NO_X and sulfur dioxide sources, the results were large ozone values, a large SO_2/CO ratio, large scattering particles, and high aerosol optical depth over the mid-Atlantic U.S. In contrast, relatively clean conditions over the mid-Atlantic occurred when the greatest trajectory density lay over the southern Ohio River Valley and nearly missed many large NO_X and SO_2 sources. The greatest afternoon ozone values occurred during periods of stagnation that were most conducive to photochemical production. The least pollution occurred when flow from the north-northwest was too fast for pollution to accumulate and when flow was from the north, where there are few urban or industrial sources.

Figure G-1: Maps of the 2 km, 48 hr HY-SPLIT back trajectory clusters for mid-Atlantic region

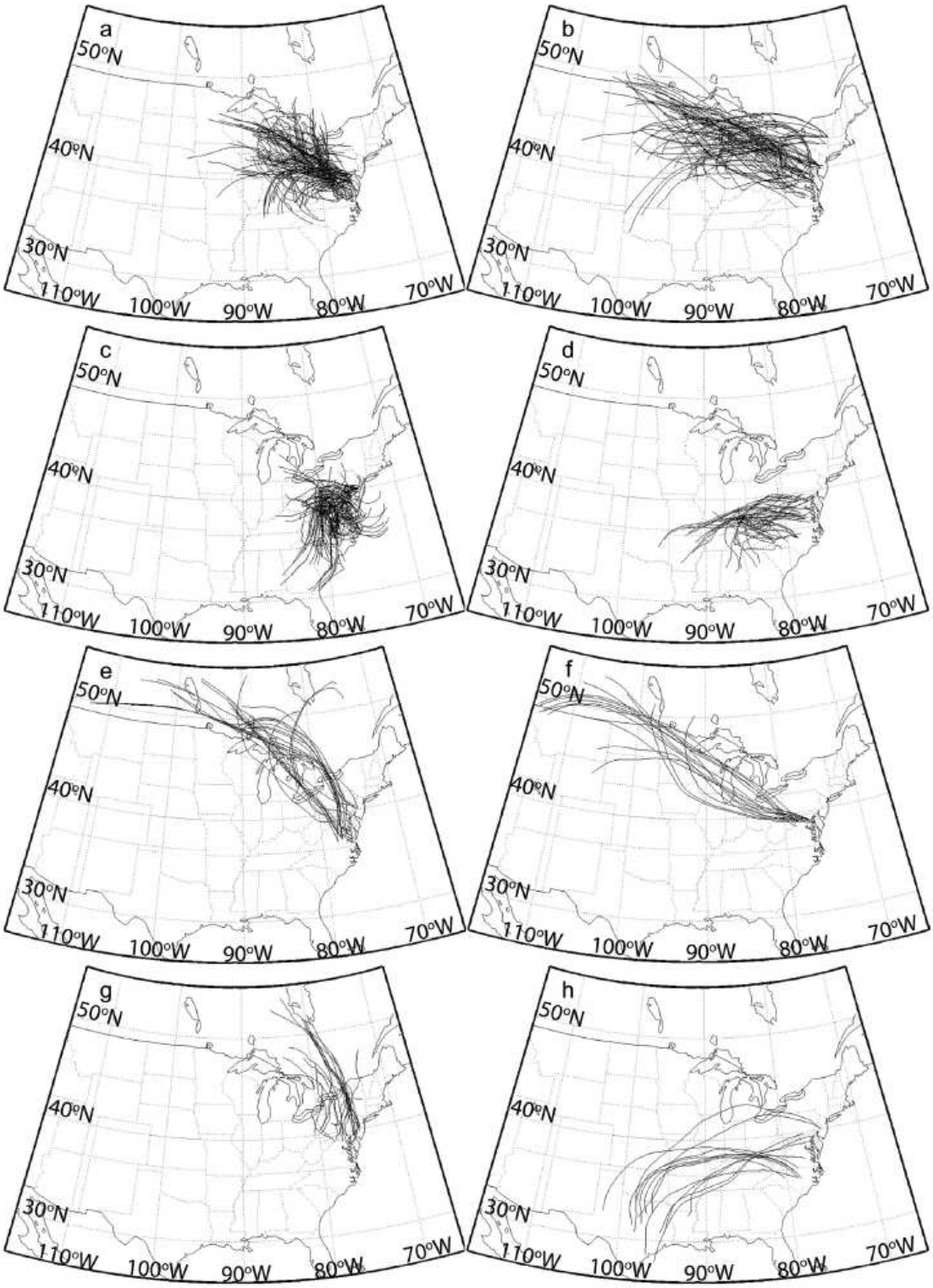

Note: Cluster groupings are a) cluster 1, b) cluster 2, c) cluster 3, d) cluster 4, e) cluster 5, f) cluster 6, g) cluster 7, and h) cluster 8. Figure from Taubman *et al.*, 2006.

Ozone transport over several hundred kilometers into the mid-Atlantic U.S. was estimated by calculating the ratio of the residual layer ozone between 500 m and 2 km in the upwind morning profiles to the downwind afternoon boundary layer values between 100 m and 2 km. The greatest level of transported ozone (69-82 percent) occurred when the maximum trajectory density lay over the southern and northern Ohio River Valley (clusters 1, 2, 4, and 6); ~59 percent of the total profiles). The least amount of transported ozone (55-58 percent) was associated with fast southwesterly flow (cluster 8; ~3 percent of the total profiles), fast north-northwesterly flow or clean northerly flow from regions with relatively few urban or industrial pollution sources (clusters 5 and 7; ~6 percent of the total profiles), and stagnant conditions within the mid-Atlantic conducive to greater local ozone production (cluster 3; ~27 percent of the total profiles). The average amount of ozone transported into the Baltimore-Washington urban corridor is 64 percent of the total observed ozone in the afternoon boundary layer. If the background ozone is removed, then this value is lowered to 55 percent.

When trajectory density plots were overlaid on maps with the largest annual NO_X and SO_2 emitters, specific source regions were identified. The results indicate that the areas of maximum trajectory density together with wind speed are effective predictors of regional pollution and loadings. Additionally, due to the Lagrangian nature of the dataset, the regionally transported contribution to the total afternoon boundary layer column ozone content in each cluster could be quantified.

Table G-1. Cluster groups for air mass trajectories into mid-Atlantic Region

Cluster	Description	Upwind Region
1	Large ozone values, large SO_2/CO ratio, large highly scattering particles. Moderate northwesterly flow – aged point source air.	Northern Ohio River Valley
2	Small ozone values, large SO_2/CO ratio. Northwesterly flow at higher wind speeds than Cluster 1 – aged point source air.	Northern Ohio River Valley, extending into the Great Lakes region
3	Large ozone values, small SO_2/CO ratio. Stagnant conditions with light southerly flow.	Central mid-Atlantic region
4	Small ozone values, small SO_2/CO ratio. Moderate southwesterly flow, small pollution loading – fewer point sources.	Southern Ohio River Valley
5	Fairly fast north-northwesterly flow. Flow too fast for pollution to accumulate from source region.	Northern Great Lakes
6	Moderately large ozone values, SO_2/CO ratio very large, smaller less scattering particles. Northwesterly flow, but faster wind speeds than Clusters 1 and 2. Crosses several large SO_2 and NO_X sources.	Northern Ohio River Valley
7	Least pollution of any of the clusters. Flow is out of the north. Relatively cool, dry continental air.	Eastern Ontario, western Quebec
8	Small ozone values, small SO_2/CO ratio. Fast southwest flow. Very few trajectories.	Vicinity of Texas

Reference

Taubman, B.F., J.C. Hains, A.M. Thompson, L.T. Marufu, B.G. Doddridge, J.W. Stehr, C.A. Peity, and R.R. Dickerson. "Aircraft vertical profiles of trace gas and aerosol pollution over the mid-Atlantic United States: Statistics and meteorological cluster analysis." *J. Geophys. Res.* **111**, D10S07, doi:10.1029/2005JD006196, 2006.

Appendix F-3

Episode Selection Documentation

FINAL REPORT

DETERMINATION OF REPRESENTATIVENESS OF 2002 OZONE SEASON FOR OZONE TRANSPORT REGION SIP MODELING

Prepared for

Tom Frankiewicz
Ozone Transport Commission
444 North Capitol St., NW, Suite 638
Washington, DC 20001

Prepared by

Till Stoeckenius
Sue Kemball-Cook
ENVIRON International Corporation
101 Rowland Way, Suite 220
Novato, CA 94945

June 3, 2005

TABLE OF CONTENTS

APPENDICES

TABLES

FIGURES

1. INTRODUCTION

The Ozone Transport Commission is coordinating a photochemical modeling study of the Ozone Transport Region (OTR) in support of State Implementation Plan development for certain areas recently designated by the United States Environmental Protection Agency (U.S. EPA) as being in nonattainment of the 8-hour ozone National Ambient Air Quality Standard (NAAQS). The OTR is comprised of 12 states (DC, CT, DE, ME, MD, MA, NH, NJ, NY, PA, RI, VT) and that portion of Virginia contained within the Washington DC Consolidated Metropolitan Statistical Area (see Figure 1-1). Areas within the OTR designated nonattainment for the 8-hour ozone NAAQS are shown in Figure 1-2; detailed attainment demonstrations are required for the nonattainment areas within the OTR classified as "moderate".

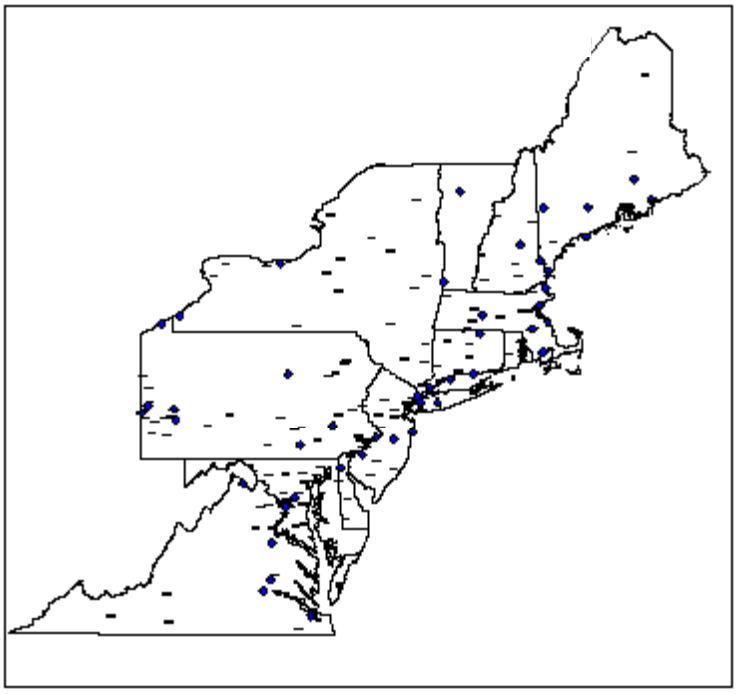

Figure 1-1. Ozone monitoring sites in the Ozone Transport Region which is comprised of DC, CT, DE, ME, MD, MA, NH, NJ, NY, PA, RI, VT, and that portion of Virginia contained within the DC Consolidated Metropolitan Statistical Area.

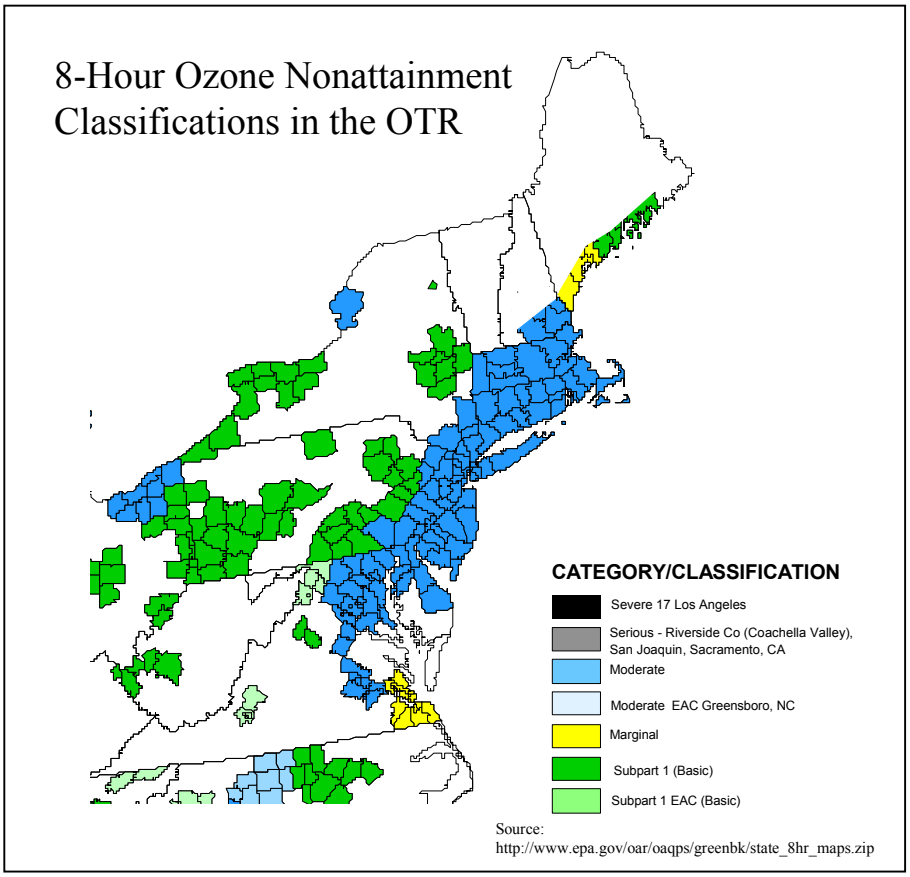

Figure 1-2. 8-hour ozone nonattainment classifications in the OTR and adjacent areas.

Development of effective 8-hour ozone attainment strategies requires application of photochemical models to a set of episodes that adequately represent the range of meteorological conditions associated with violations of the ambient standard. EPA's 8-hour ozone NAAQS modeling guidance (EPA, 1999) lists four criteria for episode selection:

1. Select episodes that both represent a variety of meteorological conditions and frequently correspond to exceedances of the 8-hour ozone standard.
2. Select episodes during which the daily maximum 8-hour ozone averages are close to the 8-hour ozone design value, i.e., the average annual 4th highest daily maximum 8-hour ozone average.
3. Select episodes for which extensive meteorological and air quality data sets are available.
4. Select a sufficient number of episode days for modeling so that the modeled attainment test specified in EPA's guidance is based on several days.

In practice, it is difficult, if not impossible, to meet all of these criteria simultaneously. In general, it is important to include episodes that represent as completely as possible the full range of meteorological conditions associated with exceedances of the ozone standard. Differences among episode types are important in so far as they influence the predicted effectiveness of alternative emission control strategies.

Because the OTR is a large region that experiences a wide variety of weather patterns associated with 8-hour ozone NAAQS exceedances, the OTC has decided to perform ozone SIP modeling of the full 2002 ozone season, May 15 - September 15, to incorporate a fairly large number of episode days in different portions of the OTR. Thus, there should be a good chance that all of the important episode types are covered within this period. However, the 2002 season includes some of the most prolonged and severe ozone episodes in recent years, raising the possibility that one or more episode types of interest are not adequately represented within the 2002 season. The goal of this study, therefore, is to assess the representativeness of conditions during the 2002 season with respect to exceedance events that have occurred in other years and determine if there are any types of episodes that are not adequately represented within the 2002 season.

EPA's 1999 draft guidance recommends joint use of subjective and statistical methods for characterizing and classifying 8-hr ozone episodes. Subjective methods include "typing" of episode meteorological conditions in which episodes are classified via inspection on the basis of similarities in meso- and synoptic-scale weather patterns. In contrast, statistical methods can produce objective classifications either by use of tree models[1] or and various forms of cluster analysis (often in conjunction with a principal components analysis). A predictive classification procedure such as a classification tree model (which can be viewed as a non-parametric form of least-squares regression) does not actually classify episodes, although it can be used to identify potential episodes with common meteorological features. This information can then be used to inform the episode selection process. A cluster analysis, on the other hand, is designed to identify natural groupings of conditions within the set of candidate episodes. In either case, considerable expert judgment is required in variable selection, selection of different modeling methods, and interpretation of results so even the statistical methods are not wholly objective. Nevertheless, these approaches are well suited to the development of valid, defensible episode classification schemes that are sufficiently robust to explain the major characteristics of ozone episode types.

In this study, we apply a combination of exploratory statistical techniques, cluster analyses, and classification tree building algorithms to ozone and meteorological data from the OTR to assess the representativeness of 8-hour ozone episodes occurring during the 2002 season. Data sources and preliminary analyses are described in Section 2. Procedures and results used to identify the major Northeastern U.S. ozone episode types and their key characteristics are presented in Section 3 along with a comparison of the frequency of occurrence and features of each episode type in 2002 versus those in other recent years. Our conclusions regarding the representativeness of the 2002 season are detailed in Section 4.

[1] A commonly used tree modeling approach is based on the CART methodology (Breiman et al., 1984).

2. DATA GATHERING AND INITIAL ANALYSIS

DATA

Daily ozone and meteorological data required for the episode representativeness analysis were obtained from a variety of sources. To capture the full range of OTR episode characteristics and insure statistical significance, a seven year period (1997 – 2003) was chosen for analysis. Data prior to 1997 were not used to avoid any confounding influences of long-term air quality trends. For purposes of this study, data from the warm season months (May – September) were used to capture most if not all high ozone events during the year.

Ozone and meteorological data were separated into two groups: data from 1997 – 2001 and 2003 were treated as the "historical" period and were used to define the types of ozone episode conditions occurring in the OTR. Data from 2002 were treated as an independent data set with data in this year to be compared against the types of conditions found in the historical period.

Hourly ozone concentrations at monitoring sites throughout the OTR for the period 1997-2003 were provided by the New York State Department of Environmental Conservation. Stations missing more than one year of data were excluded from the study, leaving a total of 158 stations with nearly complete data. Daily maximum 8-hour averages were calculated from the hourly data using the data handling conventions specified in 40 CFR 50, Appendix I. Because the spatial pattern analysis procedure requires a complete data set, missing daily maxima were set to the station mean daily maximum (this conforms to the procedure used by Cox, 1997).

Hourly surface meteorological data (winds, temperature, etc.) from airports and other locations in the OTR were obtained from the National Center for Atmospheric Research (NCAR) as dataset ds472. Upper air data were extracted from the ETA Data Assimilation System (EDAS) files available from the National Climatic Data Center. EDAS contains 3-hourly objective analysis initialization and forecast fields from the National Center for Environmental Prediction's (NCEP) ETA model at 40 km resolution. By using the EDAS data, we were able to obtain a consistent set of surface and upper air variables covering the entire eastern half of the U.S. at high temporal resolution.

IDENTIFICATION OF OZONE MONITORING SUB-REGIONS

Monitoring sub-regions were defined within the OTR to emphasize the spatial ozone patterns associated with different types of ozone episodes and to reduce the number of variables required to describe the spatial ozone distribution under different episode patterns. Sub-regions were defined by combining results of a station clustering analysis with information on typical ozone concentration patterns provided by air quality analysts from several OTR states. A variable clustering procedure (VARCLUS) based on principal components analysis was used to group the OTR ozone monitoring sites into disjoint geographic clusters (Sarle, 1990, Harrell 1999). This procedure essentially divides the monitoring stations into groups of highly correlated sites. Station clusters are selected to explain most of the day-to-day variation in ozone levels over the OTR using a small number of station groups. VARCLUS works by performing a principal components analysis on the ozone values in each candidate cluster and seeks to find the set of

clusters that maximize the total (across clusters) of the variance explained by the first principal components.

Required input for the VARCLUS procedure is the number of clusters to be formed. As with any clustering procedure, this introduces an element of subjectivity that can be minimized by repeating the analysis several times, each time varying the number of clusters to be formed and examining the robustness of the cluster memberships as the number of requested clusters (k) changes.

Application of the clustering algorithm for various values of k showed that, for a given value of k, the VARCLUS procedure produced several spatially coherent clusters as well as other clusters which were not spatially coherent. Clusters which were not spatially coherent were always made up of just 5 or fewer member stations. For example, setting k=5 produced 2 coherent clusters (clusters 1 and 2) and 3 smaller clusters (clusters 3-5) whose members tended to be widely separated in space (see Figure 2-1). The version of VARCLUS used for our analysis assigns the lowest cluster identification numbers to the "tightest" (i.e., most easily identifiable and robust) clusters. As the results in Figure 2-1 show, these lowest numbered clusters (in this case Clusters 1 and 2) turned out to also be the most spatially coherent (note that the clustering is based on ozone correlations only – the locations of each monitoring site are not an input to the clustering algorithm). This is consistent with our expectation that sites located close to one another will be highly correlated. Clusters 1 and 2 are similar to the two northeast clusters found by Cox (1997), who used a similar analysis technique applied over the entire eastern U.S.. Successive increases in k over the range 6-10 produced additional coherent clusters which subdivided the two large clusters seen in Figure 2-1. The smaller, non-contiguous clusters remained largely unchanged for all values of k.

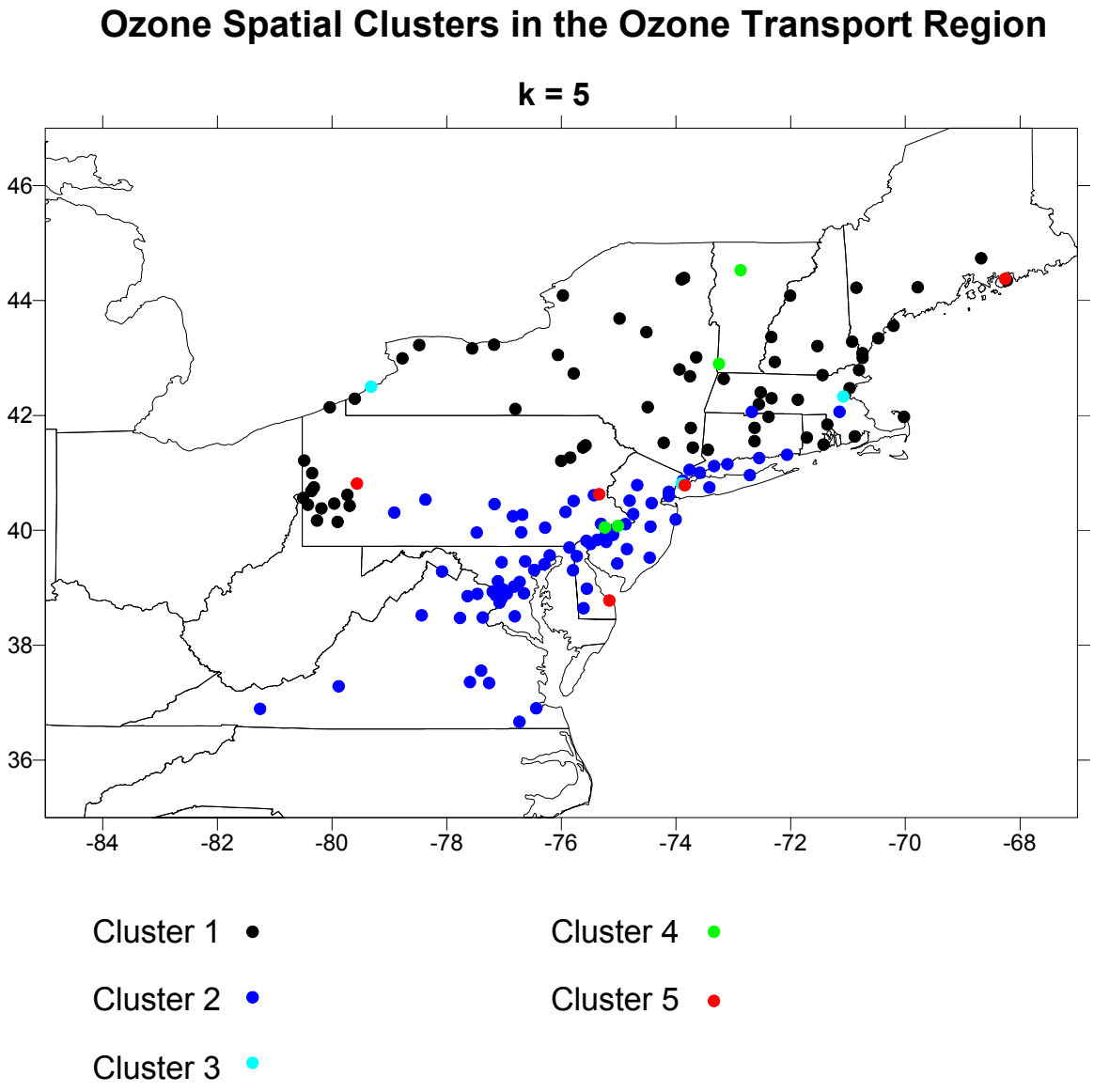

Figure 2-1. Ozone monitoring station cluster assignments for k = 5 clusters.

With k = 10, VARCLUS produced 6 spatially coherent clusters, and 4 smaller, non-coherent clusters (Figure 2-2)[2]. As in the k=5 case, the spatially coherent clusters are the lowest numbered clusters, 1-5, and the non-contiguous clusters are 6-8, and 10. The k=10 case is unusual because cluster 9 (located on the Rhode Island/Massachusetts coast) turned out to be spatially coherent, even though the lower numbered clusters 6-8 were not. We investigated the possibility that cluster 9 should be treated as a separate sub-region. After examining the way exceedances in cluster 9 vary with those in surrounding clusters, however, we concluded that this area could be adequately treated by including it in with cluster 4 (along the Washington – New York City corridor). In order to use only the clusters which seemed robust under variations in k, we therefore based the final ozone monitoring sub-regions largely on the first five clusters obtained under the k=9 scenario (which were slightly more coherent than those under the k=10 case).

[2]Ask was increased beyond 10, the coherent clusters produced were judged to be too small in spatial dimension to be useful in classifying ozone exceedance regimes.

However, the RI – MA coastal sites were associated with the New York City metropolitan area sites rather than the other MA sites based both on the k=10 result described above and input from several state air quality analysts. In addition, all stations on the ME coast were assigned to the southern New England group (Cluster 1) based on input from state air quality analysts. Stations from the other higher numbered, non-contiguous clusters were integrated into the surrounding clusters; there were no such stations for which the appropriate cluster assignment was ambiguous.

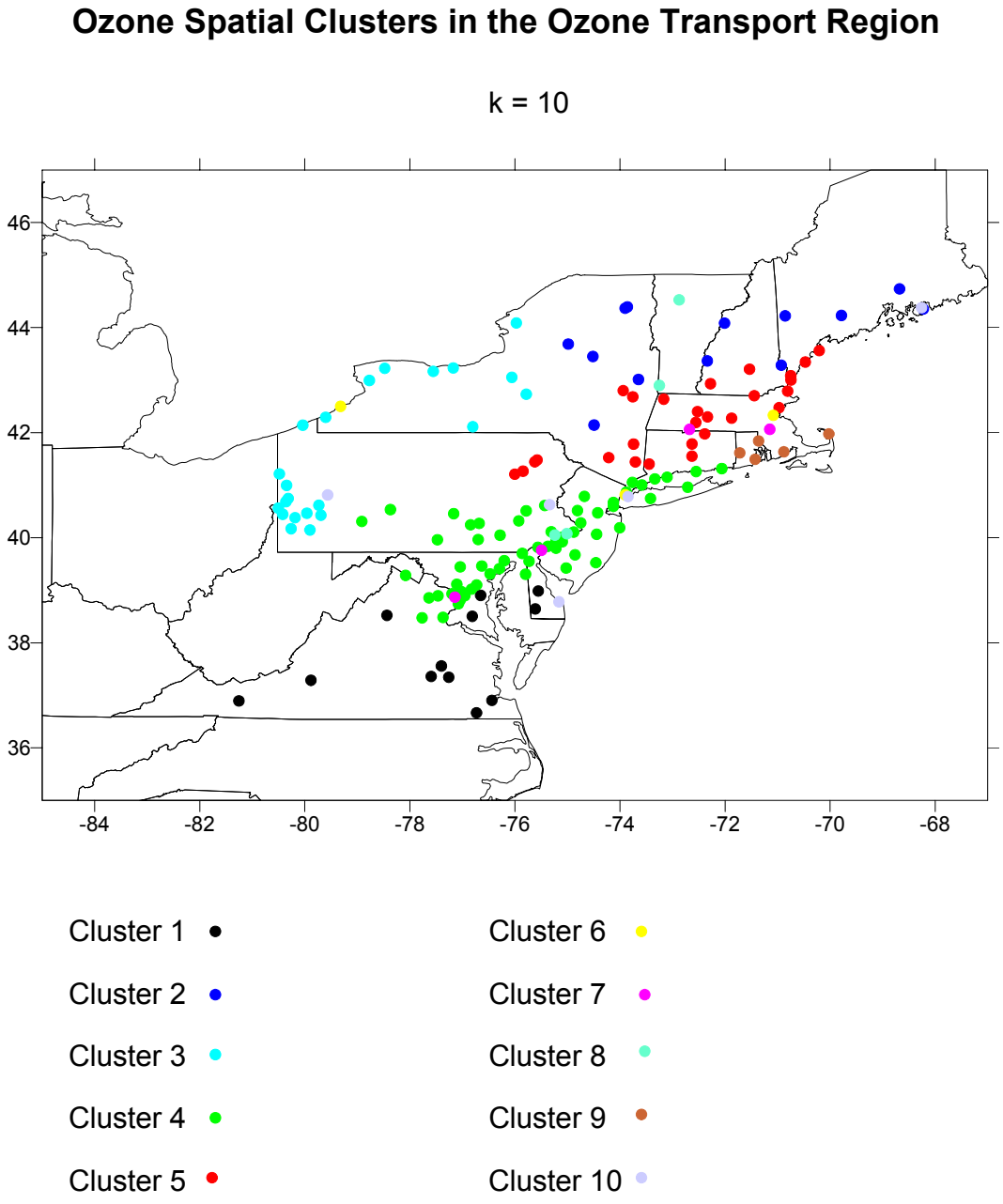

Figure 2-2. Ozone monitoring station cluster assignments for k = 10 clusters.

Another adjustment to the VARCLUS results was made along the Philadelphia – New York corridor. Figure 2-3 shows the number of 8-hour exceedances at each monitoring site during the period analyzed. Exceedance events in the Washington – Philadelphia corridor are more frequent than within and downwind (northeast) of the New York City metropolitan area. Furthermore, based on our discussions with state ozone forecasters in the OTR, we expect transport of ozone and ozone precursors along the I-95 corridor to play an important role in exceedance events. This suggests that leaving the entire Washington to New York City cluster intact might cause our final episode classification scheme to overlook events in which transport northeast from Washington-Baltimore-Philadelphia to New York is an important feature. We therefore decided to split this cluster into two parts as shown in the final ozone monitoring sub-region assignments presented in Figure 2-4. Cluster 5 extends from the Washington area through Trenton and a new cluster 6 covers the New York City-Long Island-Southern Connecticut region. A list of the monitoring sites assigned to each cluster is provided in Appendix D.

Number of 8-Hour Station Ozone Exceedances for 1997-2003 Excluding 2002

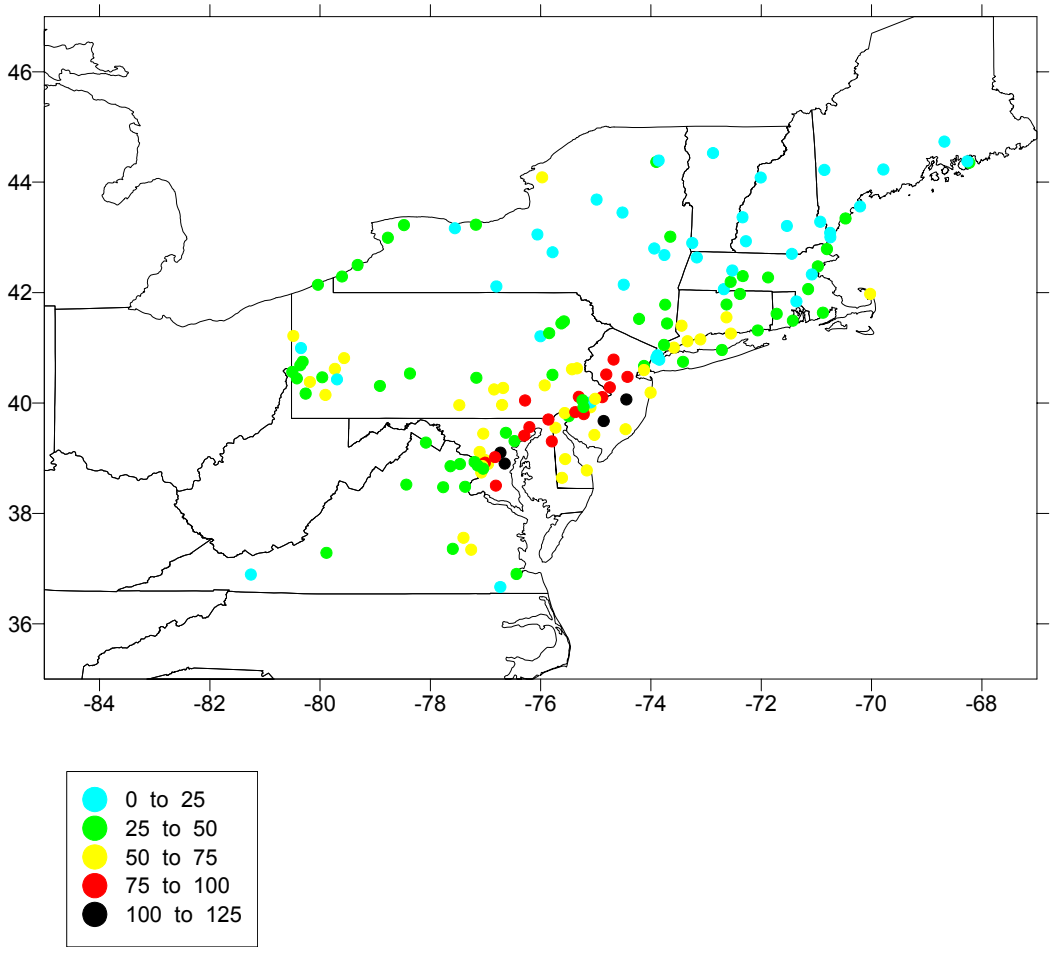

Figure 2-3. Number of 8-hour ozone NAAQS exceedance days at each monitoring site during the study period (1997 – 2001 and 2003).

Ozone Spatial Clusters in the Ozone Transport Region

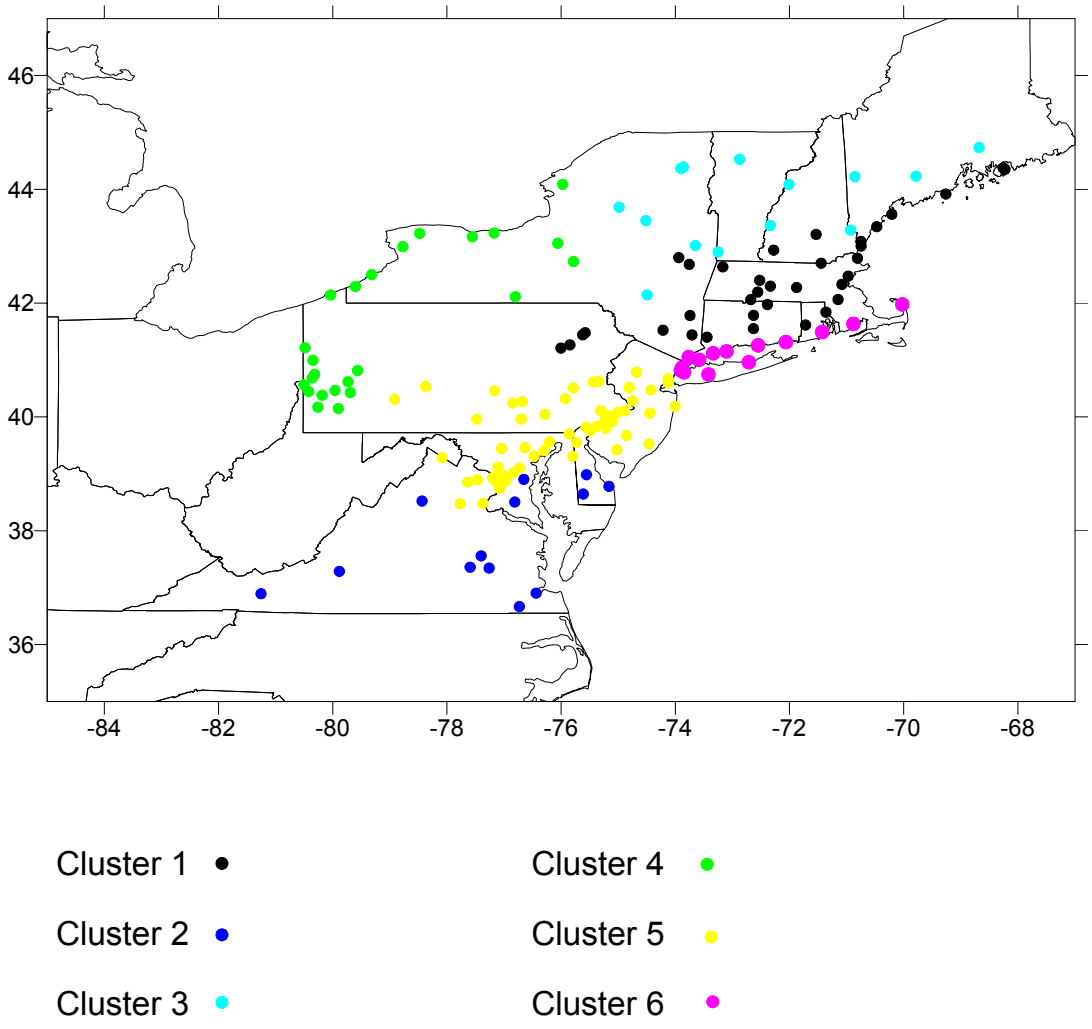

Figure 2-4. Ozone monitoring sub-regions in the OTR.

SPATIAL OZONE PATTERN ANALYSIS

An initial analysis of episode patterns was performed based on 8-hour ozone concentrations within the sub-regions (spatial clusters) described above. For each day, a cluster was determined to be in exceedance if any one monitoring site in the cluster recorded an exceedance. We then counted the number of joint exceedance events between each pair of clusters and examined exceedance patterns across all six clusters. Detailed results from this analysis were provided in a technical memorandum to the OTC (Stoeckenius and Kemball-Cook, 2004) but are not repeated here because this approach was eventually discarded in favor of an integrated analysis approach in which the daily ozone levels in each sub-region were combined with daily meteorological data to determine the key characteristics of the major types of ozone episodes occurring in the OTR.

METEOROLOGICAL VARIABLE SELECTION

The extensive amount of meteorological data collected for this study was reduced to allow processing of days into groups with similar conditions as described in Section 3. Selection of key meteorological variables that best represent conditions across the OTR on exceedance days was based on a review of previous studies (Deuel and Douglas, 1996; McHenry et al., 2004) and on discussions with state and local agency air quality personnel involved in ozone forecast programs within the OTR. Key variables focused on both surface conditions (maximum temperature, morning and afternoon average wind direction and speed, pressure) and conditions aloft (500 and 850 mb heights, temperatures, and winds). The final selected set of key daily meteorological parameters are:

Surface resultant wind speed and direction computed for both morning (05:00 – 10:00 EST) and afternoon (12:00 – 17:00 EST) hours at New York City (LaGuardia), NY; Philadelphia, PA; Boston, MA; Buffalo, NY; Albany, NY; Washington, DC; Portland, ME, Atlantic City, NJ; Islip (Long Island), NY; Hyannis (Cape Cod), MA; Worcester, MA; and Hartford, CT.[3]

Surface daily maximum temperatures at New York City (LaGuardia), NY; Philadelphia, PA; Boston, MA; Buffalo, NY; Albany, NY; Washington, DC; Portland, ME, Atlantic City, NJ; Islip (Long Island), NY; Hyannis (Cape Cod), MA; Worcester, MA; and Hartford, CT.[3]

Temperatures, heights, and winds at 850 mb pressure surface at Washington, DC; New York, NY; Boston, MA; Pittsburgh, PA; Buffalo, NY; and Portland, ME.

Surface pressure gradients across the OTR computed as pressure differences between:

Washington, DC and New York City, NY;
Washington, DC and Boston, MA;
Washington, DC and Pittsburgh, PA;
Pittsburgh, PA and Buffalo, NY;
Buffalo, NY and Boston, MA.

[3]Surface wind and temperature data from Concord, NH and New Haven, CT were also examined but these sites had a high frequency of missing data which prevented their use in this analysis.

3. EPISODE CLASSIFICATION ANALYSIS

In this section we describe a series of clustering and exploratory analyses performed on the ozone and meteorological data discussed in Section 2. Clustering was performed with data from the historical (1997 – 2001 and 2003) period to identify the major types of ozone episodes in the OTR and their key characteristics. Once the key episode types were identified, we developed a decision rule for classifying any given day into one of the identified episode types based on ozone levels and meteorological conditions. This decision rule was then used to classify days during the 2002 ozone season by episode type. The resulting distribution of episode types and the ozone and meteorological conditions occurring within each type in 2002 were subsequently compared with results from the historical period to determine the representativeness of the 2002 with respect to conditions during the historical period.

CLUSTERING ANALYSIS

Clustering was performed with data for the 329 days in the 1997-2001/2003 historical period on which an 8-hour ozone exceedance was recorded at one or more of the monitoring sites shown in Figure 2-4. As the clustering algorithms require numerical variables, wind directions were decomposed into u (east-west) and v (north-south) components. Meteorological data were prepared for clustering by first filling in missing values with exceedance day means. This step was necessary as the clustering procedures cannot process any days that have missing values for one or more variables. While the fraction of data that are missing for any individual variable is fairly small, roughly two-thirds of the 329 8-hour ozone exceedance days in our historical dataset had at least one missing value, so it was important to impute the missing values in some fashion even though the clustering results are not likely to be too sensitive to the exact method of imputation. All of the data were then standardized by computing z-scores (i.e., subtracting the mean and dividing by the standard deviation) prior to clustering so that variables with different scales of measure are given equal weight.

Ozone data were also prepared for use in the clustering analysis. Two daily ozone summary statistics, AvgEx08 and AvgEx00 were computed for each monitoring sub-region shown in Figure 2-4. AvgEx08 was defined as the average, over all sites in a given sub-region, of the amount by which the daily maximum 8-hour average exceeded 0.08 ppm (with values for sites below 0.08 ppm set equal to zero). AvgEx00 is identical to AvgEx08 but with the exceedance threshold set to 0 ppm. As with the meteorological data, z-scores were computed for the daily AvgEx08 in each sub-region for use in the clustering analysis. Preliminary clustering analyses were performed using the methods described below with first the AvgEx08 measure and then the AvgEx00 measure. Of the two, cluster results based on the AvgEx00 measure were chosen, as they were more robust and physically meaningful then results based on the AvgEx08 measure.

Initially, clustering was applied to the meteorological variables only. Both agglomerative and divisive hierarchical clustering techniques were used. Classifications of days under the resulting meteorological clusters were compared with the classification of days by ozone exceedance pattern, which had previously been reported (Stoeckenius and Kemball-Cook, 2004). These comparisons showed that, while some pairs of exceedance and meteorological patterns showed a dominant one-to-one relationship, others did not. In other words, some of the exceedance

patterns were typically associated with more than one meteorological pattern and some meteorological patterns were typically associated with more than one exceedance pattern. This result was found to be robust in the sense that it occurred under a variety of clustering approaches. We interpreted this to mean that at least some of the ozone exceedance patterns described by Stoeckenius and Kemball-Cook were not sufficiently unique from a meteorological perspective to serve as adequate archetypes of different types of ozone episodes. Given this result, we decided to examine clustering approaches based on using both the meteorological and ozone (AvgEx00) data simultaneously.

Before proceeding further, we performed a principal components analysis (PCA) on the combined ozone and meteorological data set prior to clustering to determine if it would be possible to reduce the number of variables required for the analysis. Preliminary results showed, however, that the first four components only explained 14% of the total variance. As a result, we did not pursue the PCA any further but simply retained all of the key variables in the clustering analysis.

Several different clustering procedures were applied to the data. Application of single and complete linkage hierarchical agglomerative clustering methods (Venables and Ripley, 1994) to the combined ozone and meteorological data resulted in the formation of one large cluster containing most of the days in the dataset and a large number of additional clusters containing at most a few days each. Use of Ward's method (Ward, 1963) produced a more even distribution of cluster membership at each stage of the agglomeration but with fairly evenly spaced reductions in deviance (see resulting dendrogram in Figure 3-1). In other words, these results did not provide much guidance as to what would constitute a reasonable number of clusters to use in describing the data.

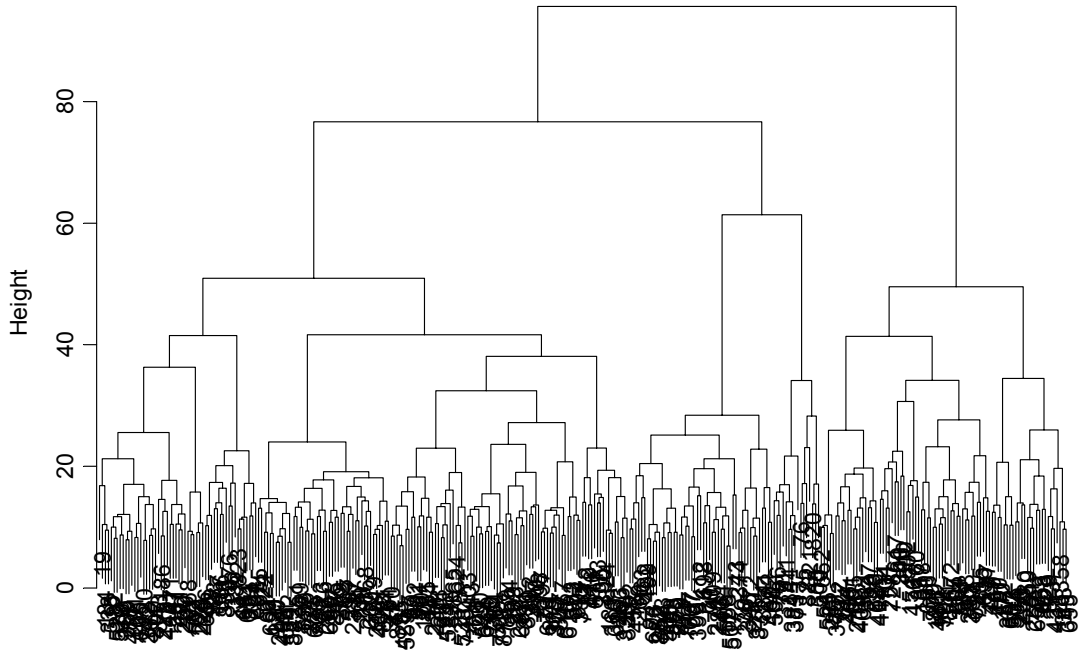

Figure 3-1. Dendrogram from application of Ward's hierarchical agglomerative clustering to the combined daily ozone and meteorological data. Each leaf at the bottom of the figure represents one day; the vertical height at which pairs of leaves (or pairs of clusters of leaves) are joined represents a measure of the distance between the leaves (or cluster centroids) in the multivariate data space.

Based on the agglomerative clustering results, we decided to apply Hartigan's k-means clustering algorithm (Hartigan, 1979) several times, specifying a different value for the number of clusters to form in each application. Under the k-means algorithm, data are arranged into a pre-specified number of clusters so as to minimize the total within-cluster sum of squares. Initial cluster centroids are determined via agglomerative hierarchical clustering. After this initial step, each day is assigned to the nearest cluster centroid where "nearest" is in this case defined as the minimum least squares distance computed over all of the standardized variables. After this initial assignment phase, the algorithm iteratively reassigns days to different clusters until the sum of the within-cluster sums of squares is minimized.[4]

Due to the large number of variables used in the clustering procedure, it is difficult to obtain a complete picture of the meteorological and air quality conditions associated with days falling in each cluster, especially when looking at several alternative cluster configurations. As one of the most important features of each cluster is the spatial ozone distribution, we tabulated the mean

[4]As finding the global minimum of this objective function is not computationally feasible, Hartigan's algorithm actually finds a local minimum such that switching any single observation from one cluster to another does not reduce the objective. As a result, the final cluster assignments may be sensitive to the selection of initial cluster centroids.

values of the ozone measure described above (AvgExc00) for each sub-region within each cluster identified by the k-means algorithm when the data are divided into between 4 and 7 clusters (see Table 3-1). We also examined similar sets of results for each key meteorological variable. Inspection of these results revealed the presence of five distinct sets of ozone and meteorological conditions that are robust in the sense that they show up consistently whether the data are divided into 4, 5, 6 or 7 clusters.

Table 3-1. Mean z-scores for the AvgEx00 ozone summary statistic within each monitoring sub-region under four different candidate sets of cluster designations. The episode pattern ID in the far right-hand column is keyed to the episode patterns described in the text.

a) 4 clusters							**Episode Pattern**
Cluster #	**Sub-Region 1**	**Sub-Region 2**	**Sub-Region 3**	**Sub-Region 4**	**Sub-Region 5**	**Sub-Region 5a**	**ID**
1	0.51	0.08	0.40	-0.08	0.26	0.56	C
2	-0.86	0.49	-0.86	-0.40	-0.15	-0.37	B
3	0.27	0.05	0.22	0.30	0.30	0.20	A
4	-0.72	-0.57	-0.45	-0.31	-0.93	-0.96	E
b) 5 clusters							
Cluster #	**Sub-Region 1**	**Sub-Region 2**	**Sub-Region 3**	**Sub-Region 4**	**Sub-Region 5**	**Sub-Region 5a**	
1	-0.74	0.07	-0.40	-0.58	-0.34	-0.78	E
2	-0.70	0.45	-0.73	-0.37	-0.06	-0.17	B
3	0.45	0.16	0.32	0.35	0.45	0.46	A
4	-0.49	-0.97	-0.35	0.22	-1.07	-0.91	D
5	0.54	-0.04	0.47	-0.10	0.17	0.42	C
c) 6 clusters							
Cluster #	**Sub-Region 1**	**Sub-Region 2**	**Sub-Region 3**	**Sub-Region 4**	**Sub-Region 5**	**Sub-Region 5a**	
1	-0.83	0.47	-0.88	-0.47	-0.17	-0.27	B
2	0.38	0.21	0.23	0.44	0.49	0.46	A
3	0.05	-1.62	0.17	0.58	-1.32	-0.86	D
4	-1.13	-0.17	-0.91	-0.52	-0.89	-1.10	E1
5	0.49	0.03	0.43	-0.10	0.21	0.48	C
6	-0.19	-0.14	0.11	-0.39	-0.17	-0.48	E2
d) 7 clusters							
Cluster #	**Sub-Region 1**	**Sub-Region 2**	**Sub-Region 3**	**Sub-Region 4**	**Sub-Region 5**	**Sub-Region 5a**	
1	0.59	-0.30	0.56	-0.39	-0.02	-0.01	C
2	0.08	0.02	0.02	0.32	0.32	0.10	D1
3	0.08	-1.77	0.21	0.65	-1.52	-1.00	D2
4	-1.17	-0.15	-0.97	-0.54	-0.88	-1.11	E1
5	0.60	0.44	0.39	0.45	0.60	1.03	A
6	-0.38	-0.12	-0.03	-0.45	-0.27	-0.58	E2
7	-0.89	0.47	-0.89	-0.47	-0.19	-0.39	B

We prepared summaries of the meteorological characteristics of each of these five episode types as follows:

1) Composite maps of surface and upper air (850 mb) meteorological variables for each cluster,

2) Side-by-side box plots comparing the distributions of selected key meteorological variables within each cluster, and

3) Tables of morning and afternoon resultant wind direction frequencies within each cluster.

Full results of items 1 – 3 above are presented in Appendix A, B, and C, respectively. By way of example, we show the 850 mb height and wind fields, 850 mb temperature, surface pressure, and surface daily maximum temperature and 10 m wind fields composited for each episode type in Figures 3-2 to 3-5, respectively. Comparing these composite fields for different episode types reveals that each episode type is characterized by a distinct meteorological pattern and these patterns are consistent with the ozone patterns noted in Table 3-1. Key characteristics of the five episode types are presented in Table 3-2. In the description of each episode type, "average" refers to averages over all OTR exceedance days used in the cluster analysis.

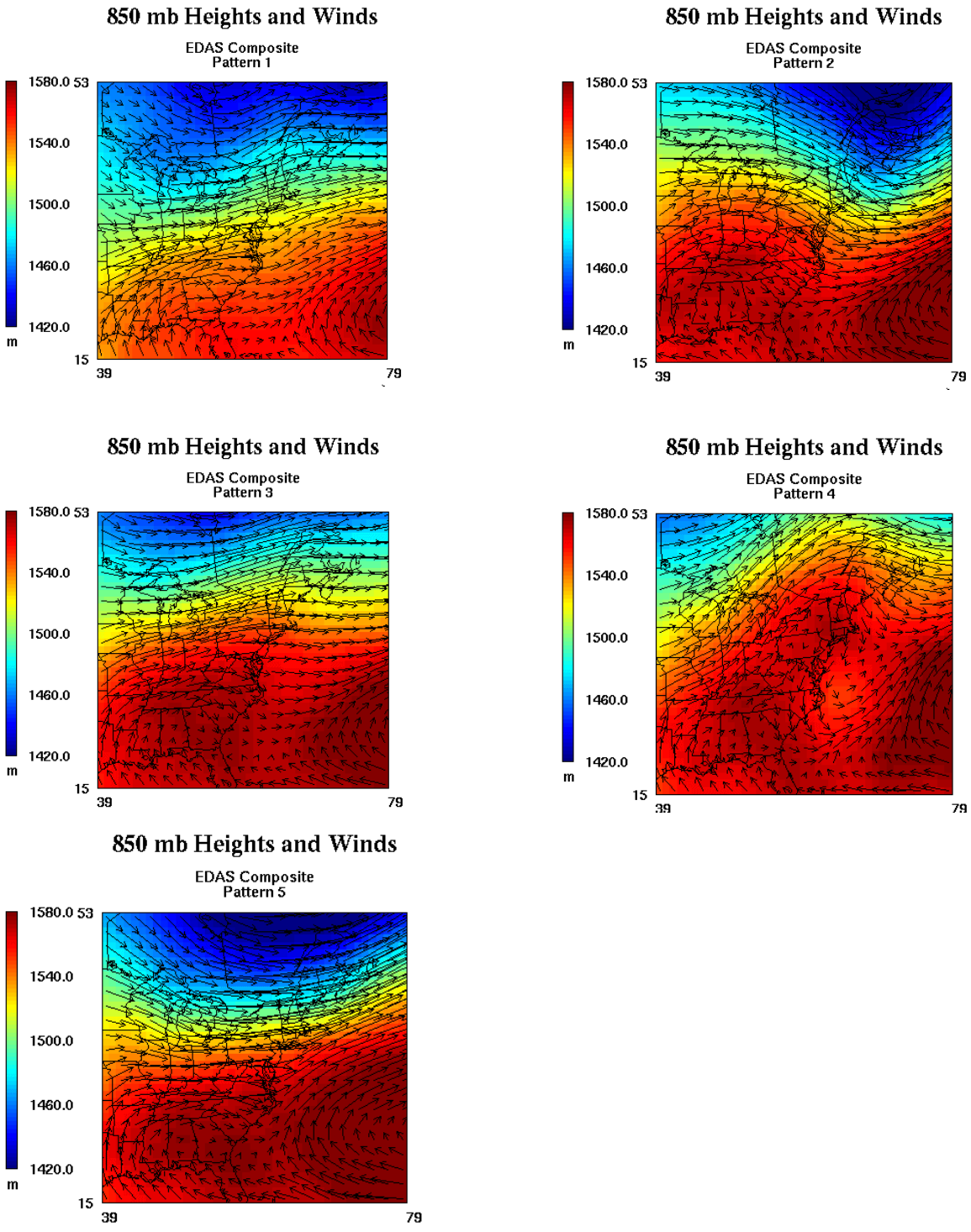

Figure 3-2. Average 850 mb height and wind fields for each episode (pattern) type (pattern numbers refer to the episode types listed in Table 3-2): Pattern 1 = Episode Type E, 2 = B, 3 = A, 4 = D, 5 = C).

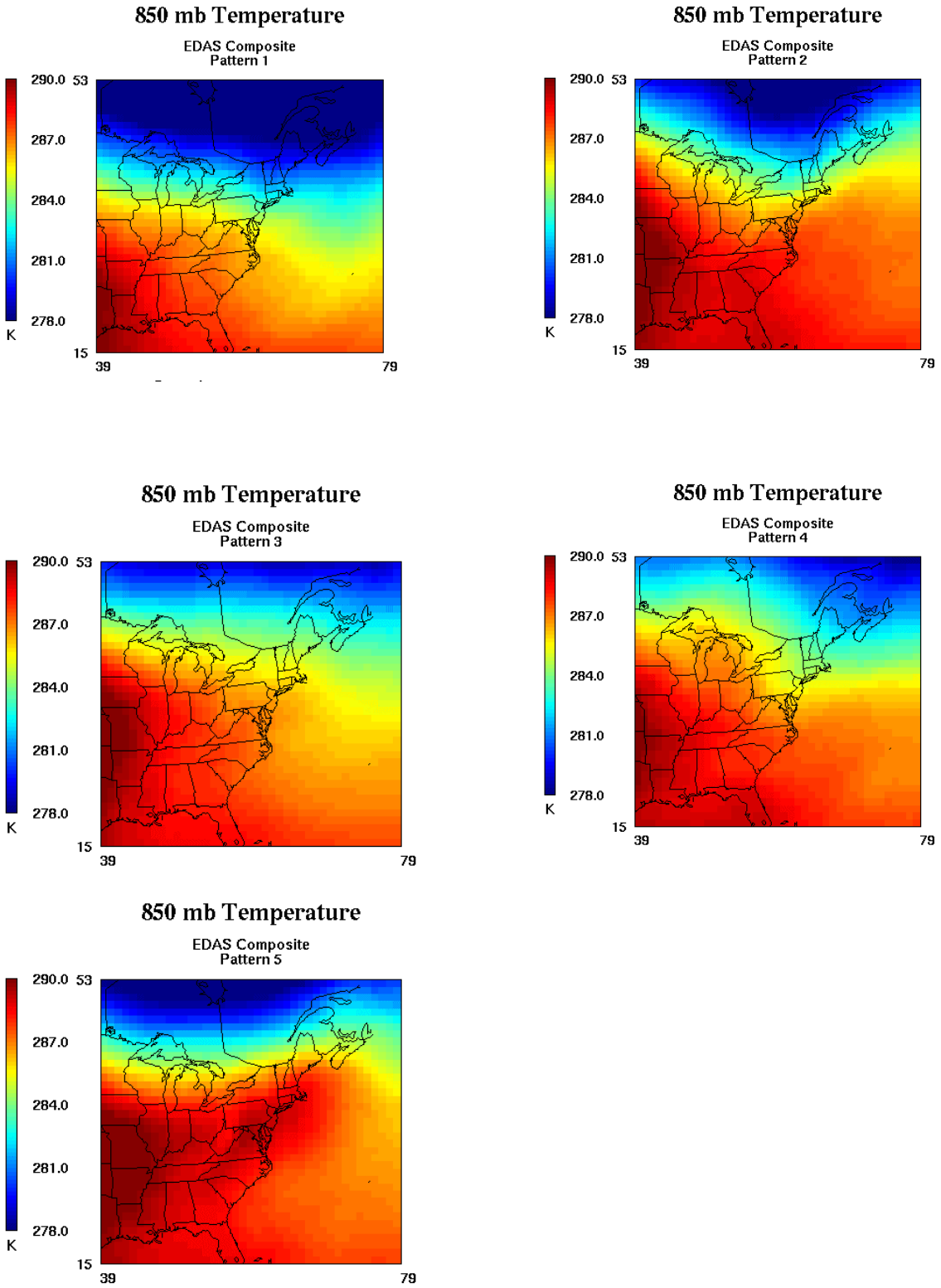

Figure 3-3. Average 850 mb temperature fields for each episode (pattern) type (pattern numbers refer to the episode types listed in Table 3-2): Pattern 1 = Episode Type E, 2 = B, 3 = A, 4 = D, 5 = C).

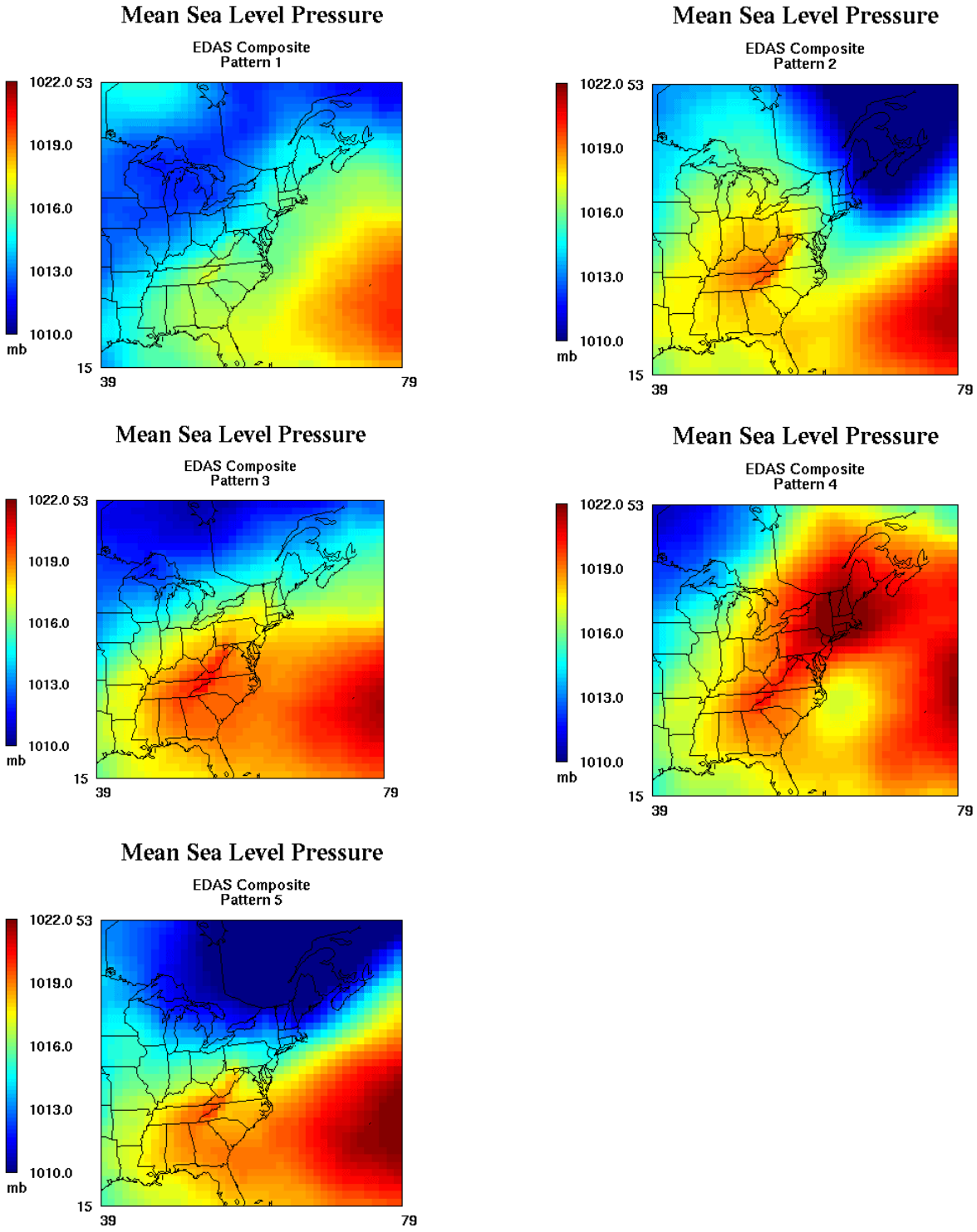

Figure 3-4. Average surface sea level pressure for each episode (pattern) type (pattern numbers refer to the episode types listed in Table 3-2). Pattern 1 = Episode Type E, 2 = B, 3 = A, 4 = D, 5 = C).

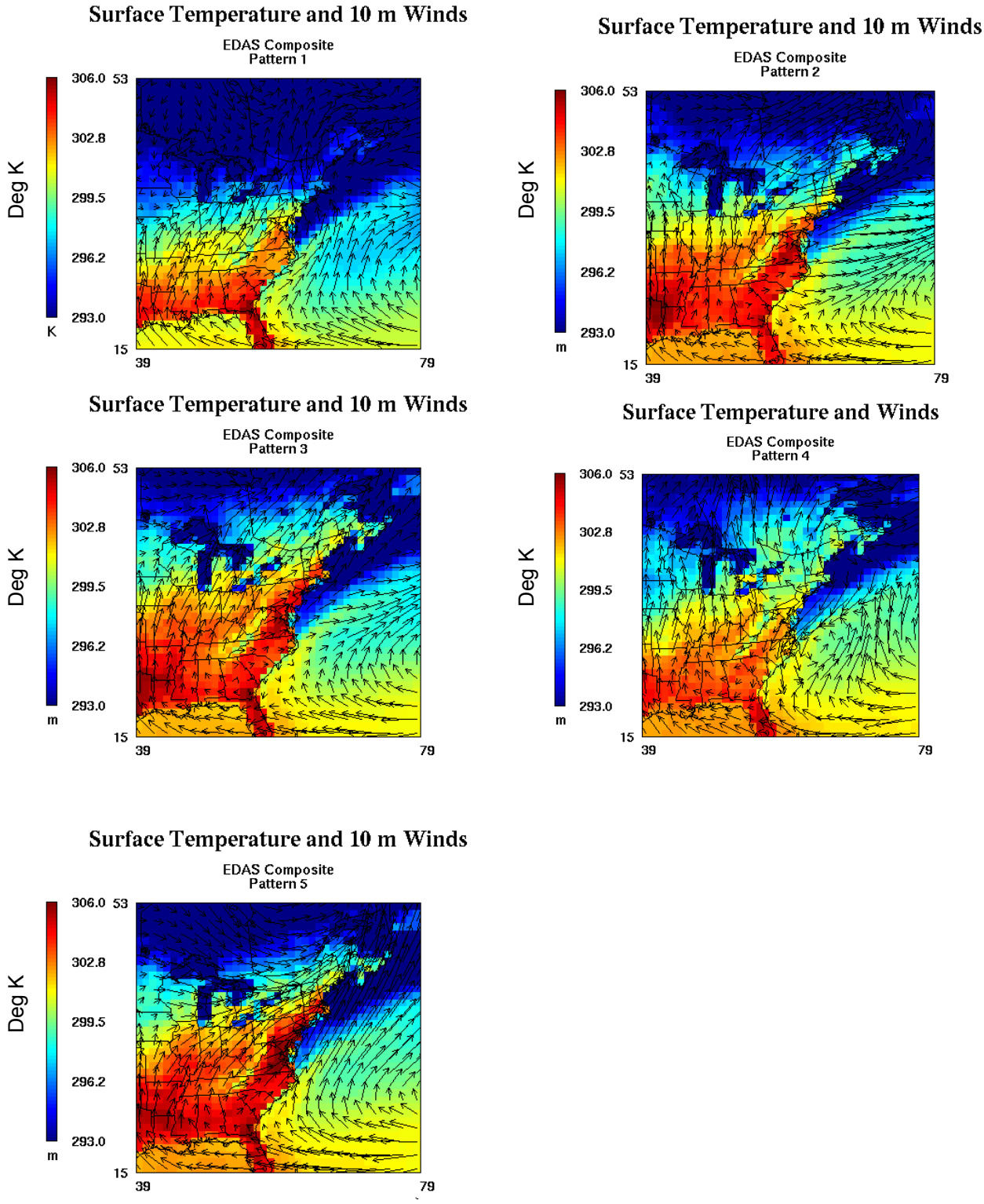

Figure 3-5. Average surface temperature and 10 m wind fields for each episode (pattern) type (pattern numbers refer to the episode types listed in Table 3-2). Pattern 1 = Episode Type E, 2 = B, 3 = A, 4 = D, 5 = C).

Table 3-2. Key characteristics of each OTR episode type.

Episode Type	Pattern No.	Description
A	3	*High ozone throughout the OTR.* This pattern is characterized by strong high pressure over the southeastern states extending from the surface to 500 mb with high temperatures extending into New England and southwest surface winds throughout the OTR. 850 mb temperatures and heights, and surface temperatures are above average at all locations except Washington DC; winds are SW to W throughout the OTR except more variable at LaGuardia and magnitudes of resultant wind vectors are higher than average (indicative of a fairly steady, well defined flow regime), E-W surface pressure gradients are near neutral but SW-NE gradients both along the I-95 corridor and in the west (Pittsburgh to Buffalo) are positive which is consistent with the SW flow. Ozone formation under these conditions is promoted throughout the OTR by the stable air mass and high temperatures.
B	2	*High ozone confined to the extreme southeastern OTR.* This pattern is characterized by an upper-level trough offshore of the OTR and a surface high centered over Kentucky. This results in cooler air advection over nearly all of the OTR with northwest flow aloft and a more westerly flow at the surface. 850 mb heights are lower than average (especially in New England) and surface winds are more frequently from NW along the I-95 corridor than under Type A. Temperatures at 850 mb along the I-95 corridor are only slightly cooler than under Type A but inland temperatures, especially in the north, are much cooler (e.g., at Buffalo); similarly, surface temperatures along the I-95 corridor are about the same as under Type A but temperatures are cooler in Buffalo and Albany. Type B events have the strongest positive W – E surface pressure gradients of any category, consistent with the NW winds but gradients from Washington to New York and Boston are positive. The cooler air over the western OTR and westerly to northwesterly flow result in the higher ozone levels being confined to just the extreme southern portion of the OTR under this pattern.
C	5	*High ozone along I-95 corridor and northern New England.* This pattern is characterized by an extension of the semi-permanent Bermuda high into the southeastern U.S. and an area of high surface and 850 mb temperatures extending from Maryland to Maine; the 500 mb pattern is nearly zonal (east – west flow) while flow at the surface is generally from the SW. 850 mb heights intermediate between Type A and Type B but 850 mb temperatures are very high along the I-95 corridor and slightly cooler further inland. Winds are more consistently S - SW at all sites than under other episode types and almost no NW-N-NE winds are seen at LaGuardia in contrast to other types. Resultant wind vector magnitudes are much higher than average, consistent with the steady SW flow. SW – NE pressure gradients along I-95 corridor and from Pittsburgh to Buffalo are positive, consistent with the SW flow. Average E-W pressure gradients are near zero. These conditions result in above average ozone levels all along the I-95 corridor with advection north into coastal and interior New England. Ozone levels are slightly below average in the extreme southeastern and western OTR (subregions 2 and 4).

Episode Type	Pattern No.	Description
D	4	*High ozone in the western OTR*. This pattern is characterized by an area of mean upper level divergence with associated cut-off low at 850 mb off the Outer Banks of North Carolina. A relatively vigorous mean low pressure center can be seen at the surface. An east-west temperature gradient across the OTR is evident at 850 mb. Surface temperatures along the I-95 corridor and in Albany are below average but surface temperature is above average at Buffalo. 850 mb heights are the highest of any episode type due to a strong ridge over New England. Surface winds are mostly E - NE along I-95 corridor from DC to NY but more variable further north. In contrast to episode types A, B, or C, SW – NE pressure gradients along the I-95 corridor are negative, consistent with the NE surface winds. W – E pressure gradients are flat. These conditions result in below average ozone in the eastern OTR (sub-regions 1, 2, 3, 5, and 6) due to the on-shore flow in the north and cyclonic conditions in the south but above average ozone levels in the western OTR (sub-region 4) due to stable, warm conditions with light winds.
E	1	*Generally low ozone throughout OTR*. This category includes days with moderately low to lowest average ozone readings of all OTR exceedance days included in the cluster analysis. The Bermuda high is shifted east relative to the other types and flow over the southeastern U.S. is only weakly anti-cyclonic with a nearly zonal flow pattern at the 850 and 500 mb levels over the OTR. Temperatures at the surface and aloft are the coolest of any episode type. While winds aloft are nearly westerly, surface winds are generally S – SE over most of the OTR. SW – NE pressure gradients are negative along the I-95 corridor and E-W gradients are positive, consistent with the SE flow. These conditions result in below average ozone throughout the OTR due to the relatively low temperatures and southeasterly onshore flow at coastal locations.

The five episode types described in Table 3-2 exhibit characteristics, which are largely consistent across the different cluster allocations noted in Table 1 (4, 5, 6 or 7 clusters). When four clusters are specified, the Type D events are subsumed into the remaining four episode types. Finer division of days into six clusters results in a split of the Type E events into two groups (denoted as E1 and E2 in Table 1) with generally very similar meteorological conditions but distinguished in part by E-W pressure gradient anomalies that are slightly greater under type E2. Further division into seven clusters appears to preserve the Type A, B, and, to a lesser extent, Type C events along with the Type E1 and E2 events found in the seven cluster result while the Type D events are split into two new categories (denoted D1 and D2 in Table 1). Both D1 and D2 events are associated with high ozone in the west (sub-region 4) under S – SW flow as is typical of Type D but differ in the surface wind pattern, and hence ozone anomalies, along the I-95 corridor.

It is important to keep in mind that there is no *a priori* expectation that all ozone exceedance events in the OTR fall into one of a finite number of distinct patterns: daily conditions differ from one another to varying degrees and some days will always have characteristics that cross over any predetermined classification boundaries. This means that an episode classification system will always have a certain degree of arbitrariness to it and division of days into bins will always result in some days that do not fit particularly well into any single bin. Nevertheless, for purposes of this study, we seek a reasonable classification system based on a handful of pattern types each of which is uniquely identifiable by a set of characteristics related to ozone formation

across the *entire* OTR.[5] Based on the clustering results described above, it appears that the episode Types A – E meet these requirements reasonably well. Frequencies of occurrence for these five types are shown in Table 3-3.

Table 3-3. Frequencies of occurrence of OTR episode types.

	Type A	Type B	Type C	Type D	Type E
No. Days	123	50	66	44	46
Pct.	37%	15%	20%	13%	14%

DEVELOPMENT OF AN OBJECTIVE CLASSIFICATION PROCEDURE

In order to complete our analysis, we needed to develop a final episode classification rule based on results of the above analysis of the 1997 – 2001 and 2003 data which can then be applied to the 2002 data to determine the classification of episodes in 2002 to the five ozone event types described above. A classification tree model was created for this purpose using the ozone and meteorological data from 1997-2001 and 2003 as predictors and the episode pattern type as the response variable. In the classification tree model, data from all exceedance days start out together in the root node of the tree and are then split into two daughter nodes based on the value of one of the predictor variables. For example, a split might consist of sending all days with resultant afternoon wind speed at Hartford, CT less than 4.8 m/s to one node and all remaining days to the other. The variable and value of that variable used to perform a split is determined by examining all possible splits and finding the one which results in the greatest reduction in deviance in the response variable (deviance is a measure of the degree of heterogeneity of the response variable in a node). The splitting process is then repeated for each resulting daughter node and so on until a stopping criterion is reached. The daughter nodes resulting from the last split along each branch of the tree are referred to as *terminal* nodes. The resulting classification tree, grown using the 1997-2001/2003 data as the *learning* dataset, can then be applied to the 2002 data for which the episode classifications are unknown by running the 2002 daily data down the tree, separating days at each node according to the previously determined splitting criteria. Each day from the 2002 data will fall into one of the terminal nodes of the tree, and the probability of that day belonging to the ith episode type is estimated from the fraction of days from the learning dataset in the terminal node belonging to the ith episode type. The *predicted* episode type for days in 2002 falling in the terminal node is taken to be the episode type with the highest probability of occurrence.

Initially, the classification tree was grown by making successive splits until only a small number of days (in this case five) ends up in each terminal node. This results in a relatively large tree with many terminal nodes, each of which will typically be very homogeneous: most of the days in any one terminal node will belong to the same episode type. This large tree represents an over fit to the data in the learning dataset. In other words, if the tree were to be validated against an independent set of days for which the episode types are known (i.e., a test dataset) the frequency of misclassification will generally be higher than the low misclassification frequency determined

[5]It is worth reiterating here that we are seeking a general classification system applicable to the whole of the OTR. More precise classification systems could be developed for individual sub-regions within the OTR but the resulting two dimensional system (consisting of a unique set of episode types for each of several sub-regions) would not only be very time-consuming to develop but would lead to results from which it would most likely be very difficult to draw any conclusions regarding the representativeness of a single season with respect to conditions over the whole of the OTR.

by applying the full tree against the learning dataset. Thus, a smaller tree (one with fewer splits and therefore fewer terminal nodes), is likely to perform at least as well against a test dataset as the initial, large tree. We therefore applied a recursive tree-pruning algorithm known as *cost-complexity pruning* to the large tree (Venables and Ripley, 1994). This results in a sequence of trees, each of which can be characterized by the number of terminal nodes and the cost-complexity parameter, which is a measure of the trade off between growth in tree size and reduction in deviance. The resulting tree sequence is shown in Figure 3-6. As this figure shows, there is a diminishing return in deviance reduction as the size of the tree increases beyond about 5 terminal nodes.

To further evaluate the relative value of different size trees, we performed a ten-fold cross-validation using the learning dataset. The ten-fold cross-validation consists of setting aside 1/10th of the days in the learning sample as a test sample, building a tree using the remaining 90% of days, and evaluating the deviance reduction using the reserved days. This process is repeated 10 times with a different set days set aside in each case. Results from the cross-validation (Figure 3-7) suggests that the residual deviance is minimized at a tree size of about five or six terminal nodes. These results, together with an examination of the misclassification rates from the learning dataset for the pruned tree sequence shows that the 6 terminal node tree is about the optimal size.

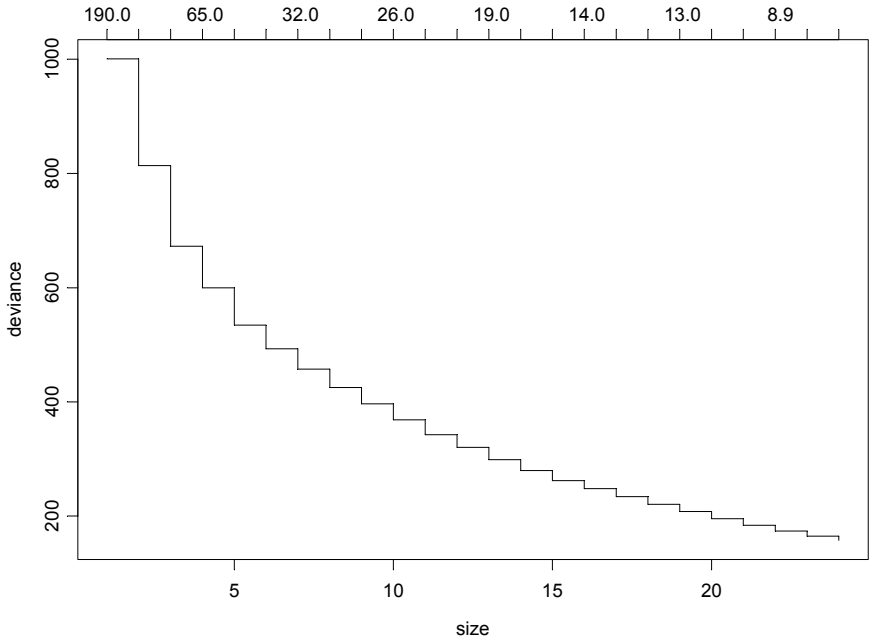

Figure 3-6. Deviance as a function of tree size (number of terminal nodes) for sequence of trees generated by the pruning algorithm.

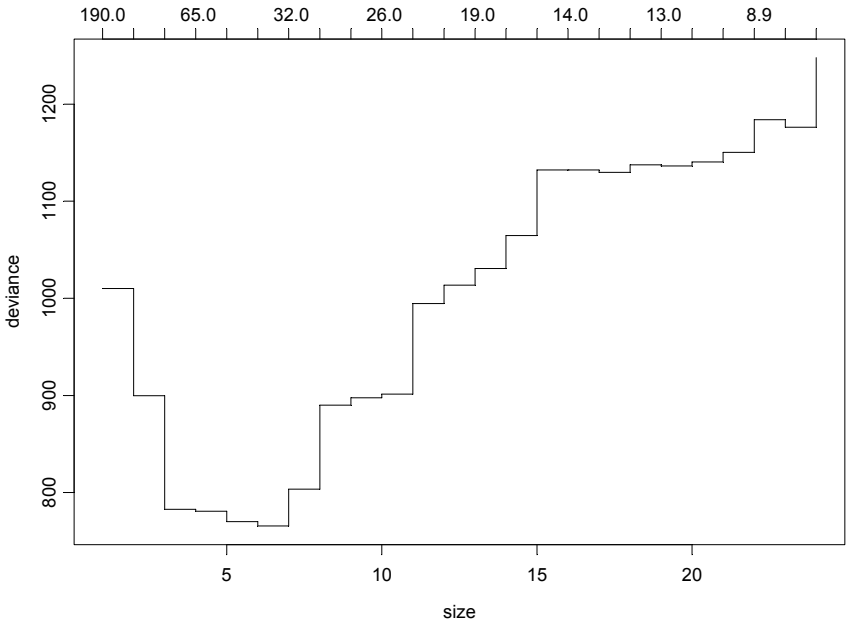

Figure 3-7. Deviance from 10-fold cross-validation as a function of tree size (number of terminal nodes) for sequence of trees generated by pruning algorithm.

The selected classification tree is shown in Figure 3-8; Table 3-4 summarizes the distribution of days by episode type in each terminal node. Two nodes are made up of predominantly Type E days, each of the rest are most representative of one of the four other episode types. Each terminal node has a dominant episode type accounting for between 64 and 81% of days assigned to the node. To use the classification tree for assigning an episode type to a previously unclassified day, we define the *predicted* episode type for all days reaching a given terminal node as the dominant episode type for the node as shown by the shaded boxes in Table 3-4. When this rule is applied to the 329 episode days during the historical period, a comparison of the predicted episode types with the episode types assigned by the cluster analysis shows an overall misclassification rate of 23%.

Table 3-4. Distribution of episode types during the 1997-2001/2003 historical period (as determined via the clustering analysis) for days in each terminal node of the classification tree shown in Figure 3-8.

	Episode Type					
Node No.	**A**	**B**	**C**	**D**	**E**	**Total**
4	6	3	0	0	16	25
5	100	16	9	1	0	126
7	5	3	53	0	5	66
8	1	25	3	0	2	31
10	5	0	0	4	19	28
11	6	3	1	39	4	53
Total	123	50	66	44	46	329

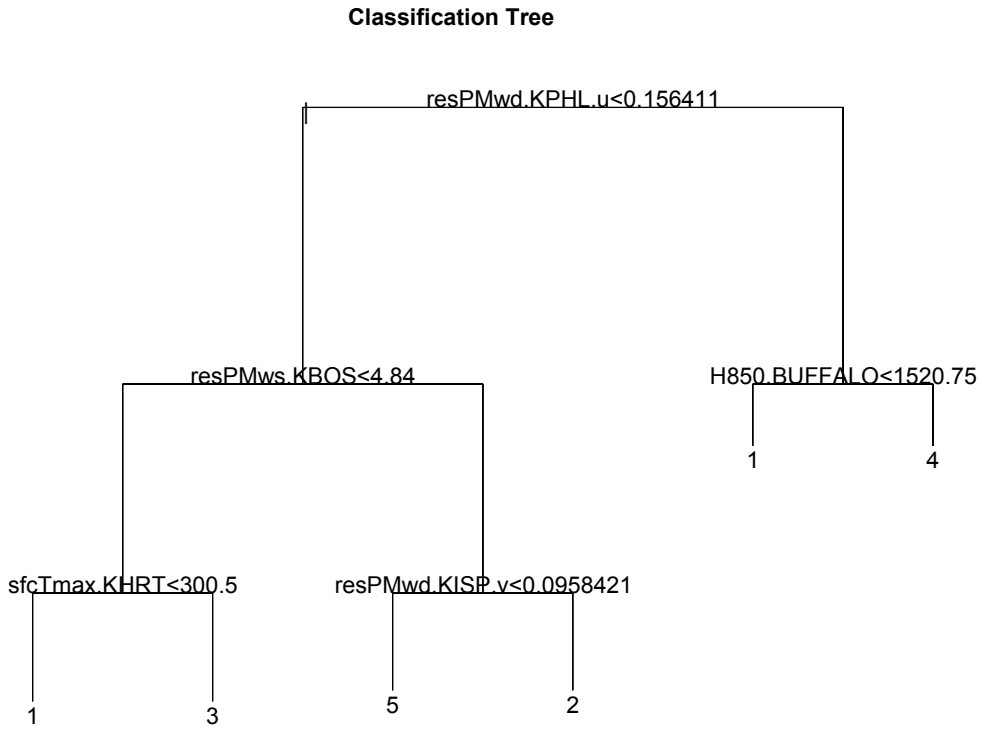

Figure 3-8. Classification tree used to group days by episode type. Variable names and values used to divide data at each splitting node are shown: days meeting the specified criterion are moved down the left branch in each case (resPMwd.KPHL.u = easterly component of the resultant afternoon wind direction at Philadelphia [m/s]; resPMws.KBOS = resultant afternoon wind speed at Boston [m/s]; H850.BUFFALO = 850 mb pressure height at Buffalo [m]; sfcTmax.KHRT = daily maximum surface temperature at Hartford, CT [K]; resPMwd.KISP.v = northerly component of afternoon wind direction at Islip, NY [m/s]). Terminal nodes are numbered 1 – 5 and are keyed to the summary in Table 3-4.

CLASSIFICATION OF 2002 OZONE EPISODES

Data from the 2002 ozone season were analyzed using the classification tree described above to yield a division of the ozone exceedance days into the five episode types. The resulting frequency distribution of episode types in 2002 was then compared with the historical episode type frequency distribution shown in Table 3-4, thereby providing an indication of the degree to which conditions during 2002 are representative of conditions observed in other years. We also compared ozone concentration distributions and composite meteorological fields by episode type in 2002 with those during the historical period as a way of further evaluating the representativeness of conditions during the 2002 ozone season.

Episode Type Classification

We applied the 6-node tree shown in Figure 3-8 to all 8-hour ozone exceedance days in 2002. Of the 71 exceedance days, 69 could be assigned to terminal nodes on the tree; missing data prevented classification of two of the days. Examination of the classification results showed that

if surrogate splits[6] were used to assign these two days to one of the terminal nodes, the number of days falling into the node would change by no more than 3 percentage points, so the two days with missing data were simply ignored. The predicted episode type for each exceedance day in 2002 was taken to be the predominant episode type in the terminal node to which it was assigned (as indicated by the shaded boxes in Table 3-4). Appendix E lists the resulting episode type associated with each exceedance day in 2002. The resulting distributions of days by episode type for the 2002 season and the 1997-2001/2003 historical period are shown in Figure 3-9.[7] For the historical days, both the episode type assignments based on the classification tree and the episode types as originally assigned in the clustering analysis are shown. The overall pattern of episode type occurrence frequencies for the historical period is similar between the classification tree and the clustering analysis, as we would expect. Frequencies of occurrence of the episode types are within two percentage points of each other except for Type D events (slightly more Type D days assigned by the classification tree) and Type B events (about a third fewer Type B days determined by the classification tree).

Comparison of the occurrence frequencies over the historical period with the 2002 data also suggest a generally similar pattern of episode types. Note that the error bars in Figure 3-9 show the 10^{th} and 90^{th} percentile range in the frequencies of occurrence of each episode type observed within individual years during the historical period: an individual year would be expected to fall within this range with 80% probability. The 2002 type frequencies generally fall within these error bars except for a somewhat higher frequency of Type C events and a lower frequency of Type E events. As Type E events are characterized by below average ozone (relative to all exceedance days) throughout all but the southernmost OTR, this difference reflects the higher frequency of exceedance days in 2002 relative to the historical period as noted above. If we ignore the Type E events and renormalize (see Figure 3-10), the occurrence frequencies in 2002 of the remaining episode types are found to be similar to those in the historical period and fall within the 10^{th} to 90^{th} percentile range in each case. Thus, each of the event types A – D appear to be well represented within the 2002 season.

[6]Surrogate splitting uses the best alternative splits (based on the non-missing variable that produces nearly the same split as the primary splitting variable).

[7]The bars in this figure are scaled to the fraction of OTR exceedance days assigned to each episode type. Thus, these comparisons are not effected by the above average number of exceedance days in 2002 noted earlier.

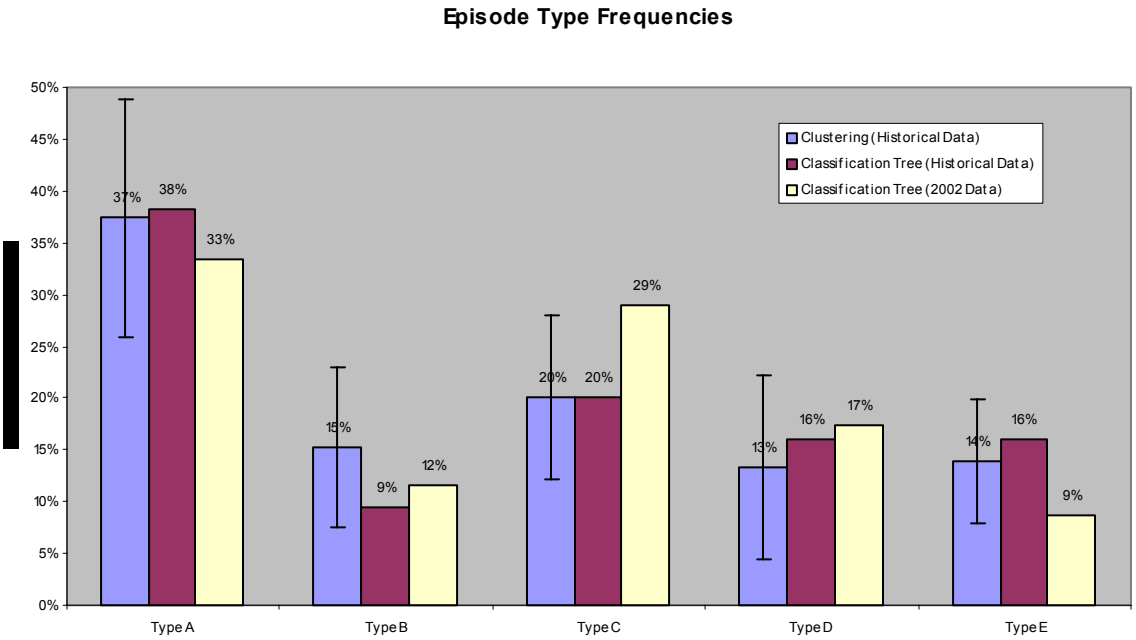

Figure 3-9. Percent of episode days by type in the 1997 – 2001/2003 historical period (as determined by the cluster analysis and by the classification tree) and in 2002; error bars show 10th and 90th percentiles of annual frequencies of occurrence during 1997-2001&2003.

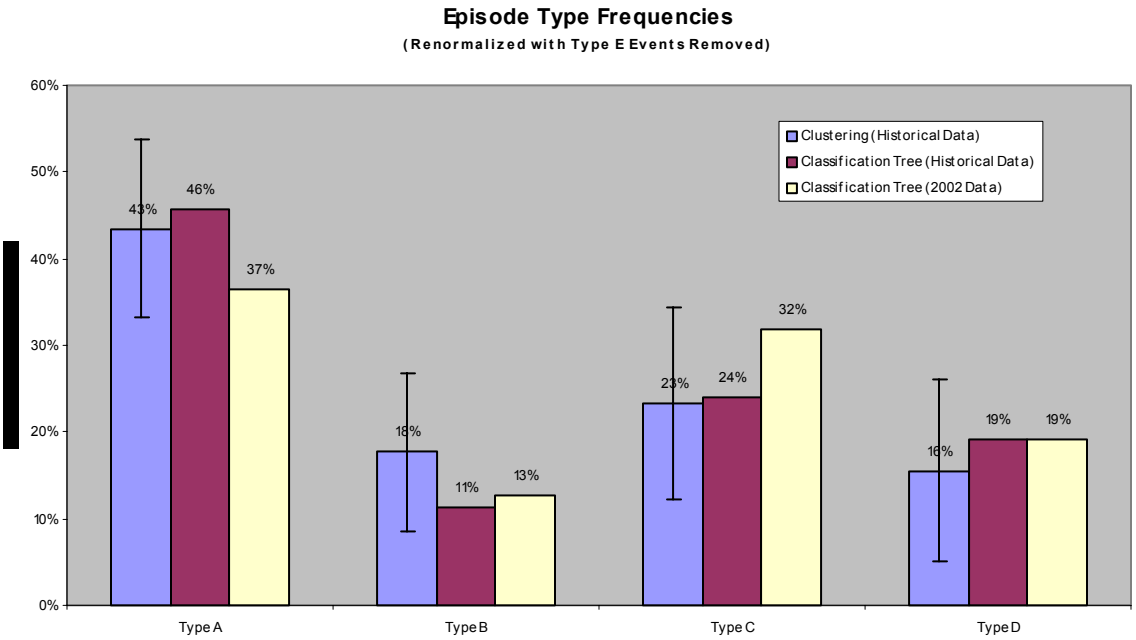

Figure 3-10. Percent of episode days by type in the 1997 – 2001/2003 historical period (as determined by the cluster analysis and by the classification tree) and in 2002 with Type E events removed and frequencies re-normalized; error bars show 10th and 90th percentiles of annual frequencies of occurrence during 1997-2001&2003.

Ozone Concentration levels

An exceedance of the 8-hour ozone standard occurred at one or more sites in the study region on 71 days during 2002, representing 46% of the 153 days during the May – September season analyzed in this study. For the 1997 – 2001/2003 historical period, the corresponding percentage was 36% so exceedances were more frequent during 2002. The greater frequency of ozone exceedance events was distributed throughout the OTR as shown by the comparison by monitoring sub-region in Table 3-5. Exceedances occurred with 20 – 50% greater frequency in 2002 in all sub-regions (100% greater in sub-region 3). This difference in the frequency of exceedances in 2002 as compared to the historical period does not necessarily mean, however, that the exceedance events themselves have characteristics that significantly differ from those seen during the historical period.

Table 3-5. Number of days during May-September with 8-hour daily maximum ozone greater than 0.08 ppm in each monitoring sub-region averaged over the 1997-2001/2003 historical period and in 2002.

	Sub-Region					
	1	2	3	4	5	6
>0.08 ppm						
1997-2001/2003	22.3	31.0	8.5	27.3	42.0	30.8
2002	34	38	17	39	58	44
Pct. Difference	52%	23%	100%	43%	38%	43%

Distributions of daily maximum 8-hour average ozone concentrations averaged over monitors in each sub-region (the AvgExc00 statistic) in 2002 and the historical period are compared for each event type in Figures 3-12(a-e), a key to the boxplot symbols used to summarize the ozone distribution is shown in Figure 3-11. Overall, the range of ozone under each event type in 2002 is similar to that under the corresponding event type in the historical period. The most notable exceptions are higher ozone levels during Type D events in 2002 along the Washington – New York City corridor (sub-regions 2, 5, and 6). This is consistent with a less pronounced low pressure center off the NC coast in the 2002 Type D events as compared to the historical period (see further discussion below). Aside from this difference, the overall ozone levels during the 2002 exceedance events were generally very consistent with those observed during the historical period, not withstanding the fact that exceedance days were more frequent during 2002.

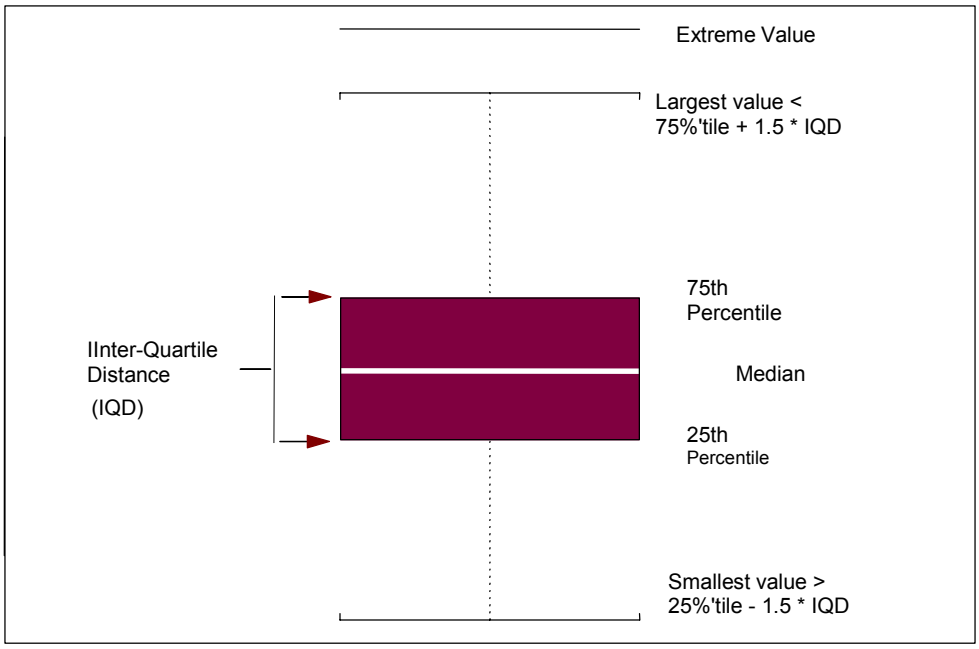

Figure 3-11. Key to boxplot symbols.

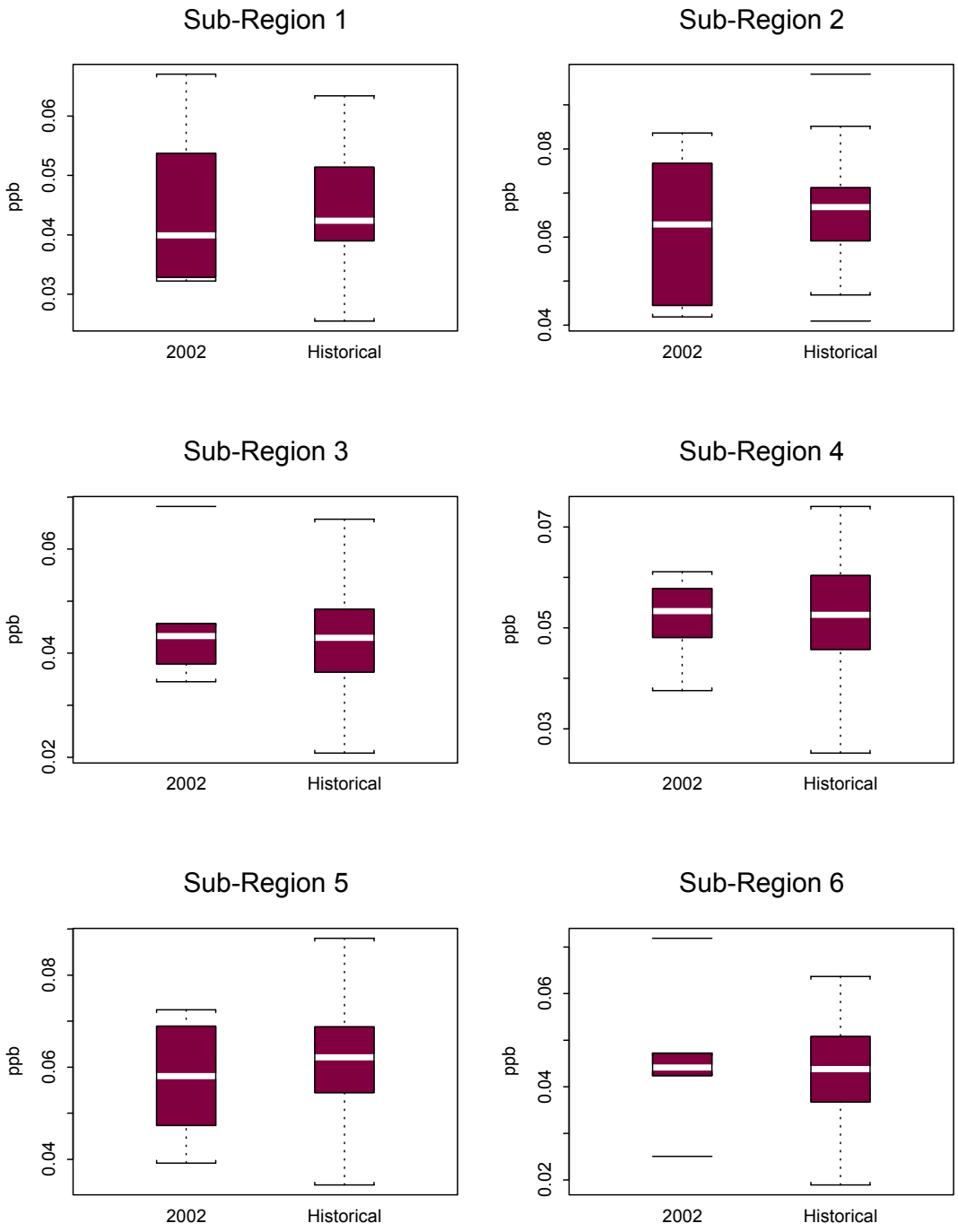

Figure 3-12a. Boxplots of average 8-hour daily maximum ozone (ppb) in each monitoring sub-region during 2002 and during the 1997-2001 and 2003 "historical" period: Type E (Pattern No. 1) events.

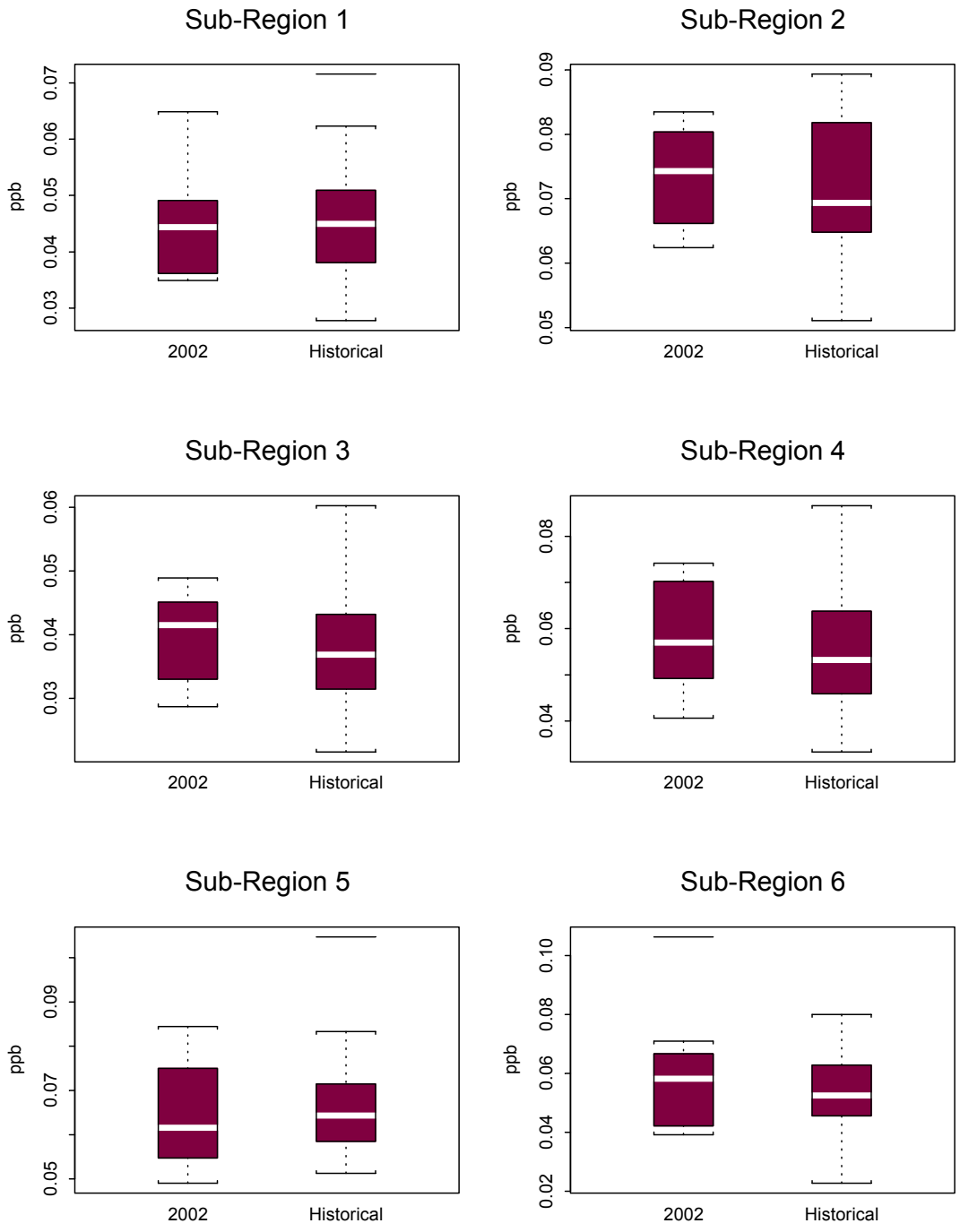

Figure 3-12b. Boxplots of average 8-hour daily maximum ozone (ppb) in each monitoring sub-region during 2002 and during the 1997-2001 and 2003 "historical" period: Type B (Pattern No. 2) events.

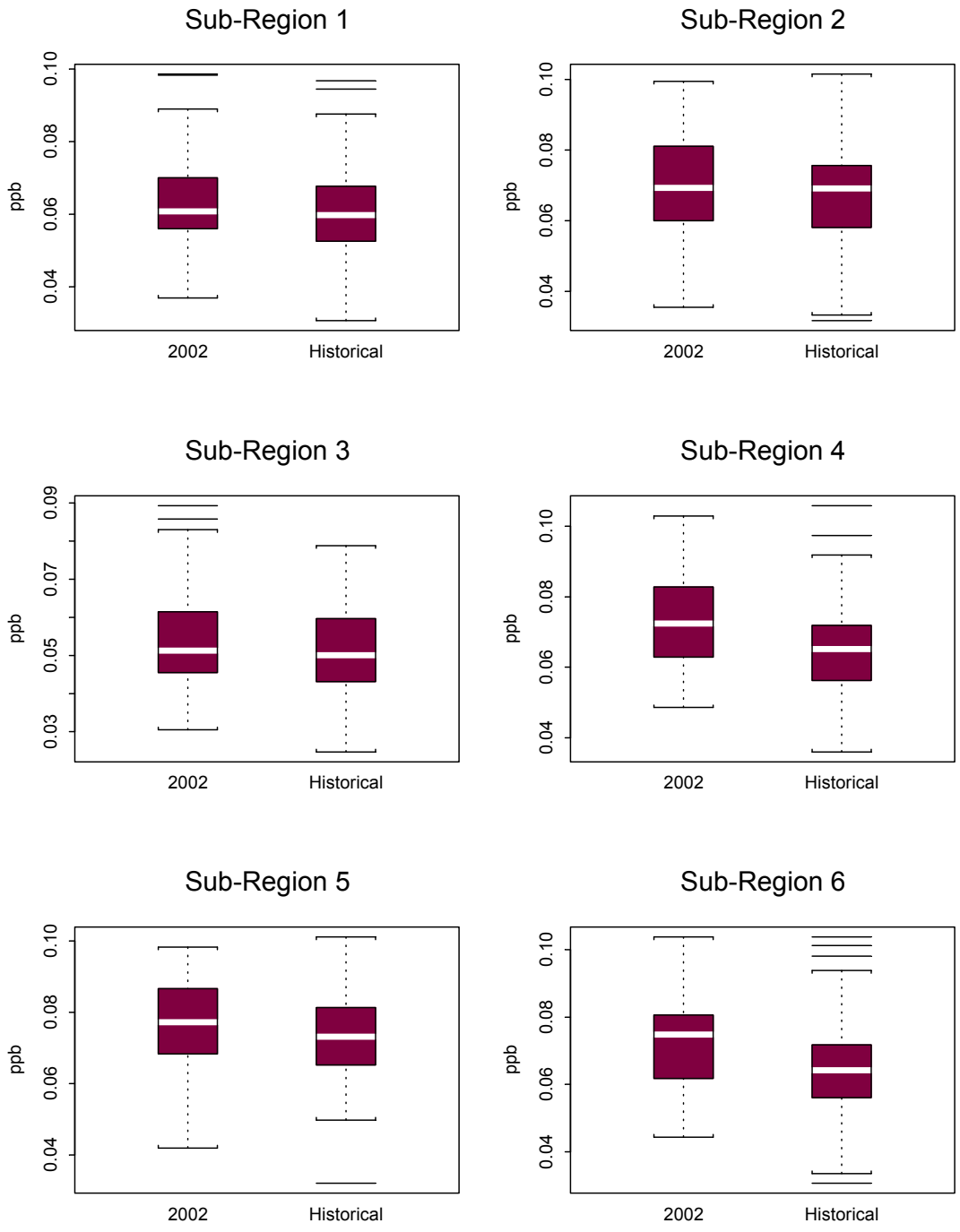

Figure 3-12c. Boxplots of average 8-hour daily maximum ozone (ppb) in each monitoring sub-region during 2002 and during the 1997-2001 and 2003 "historical" period: Type A (Pattern No. 3) events.

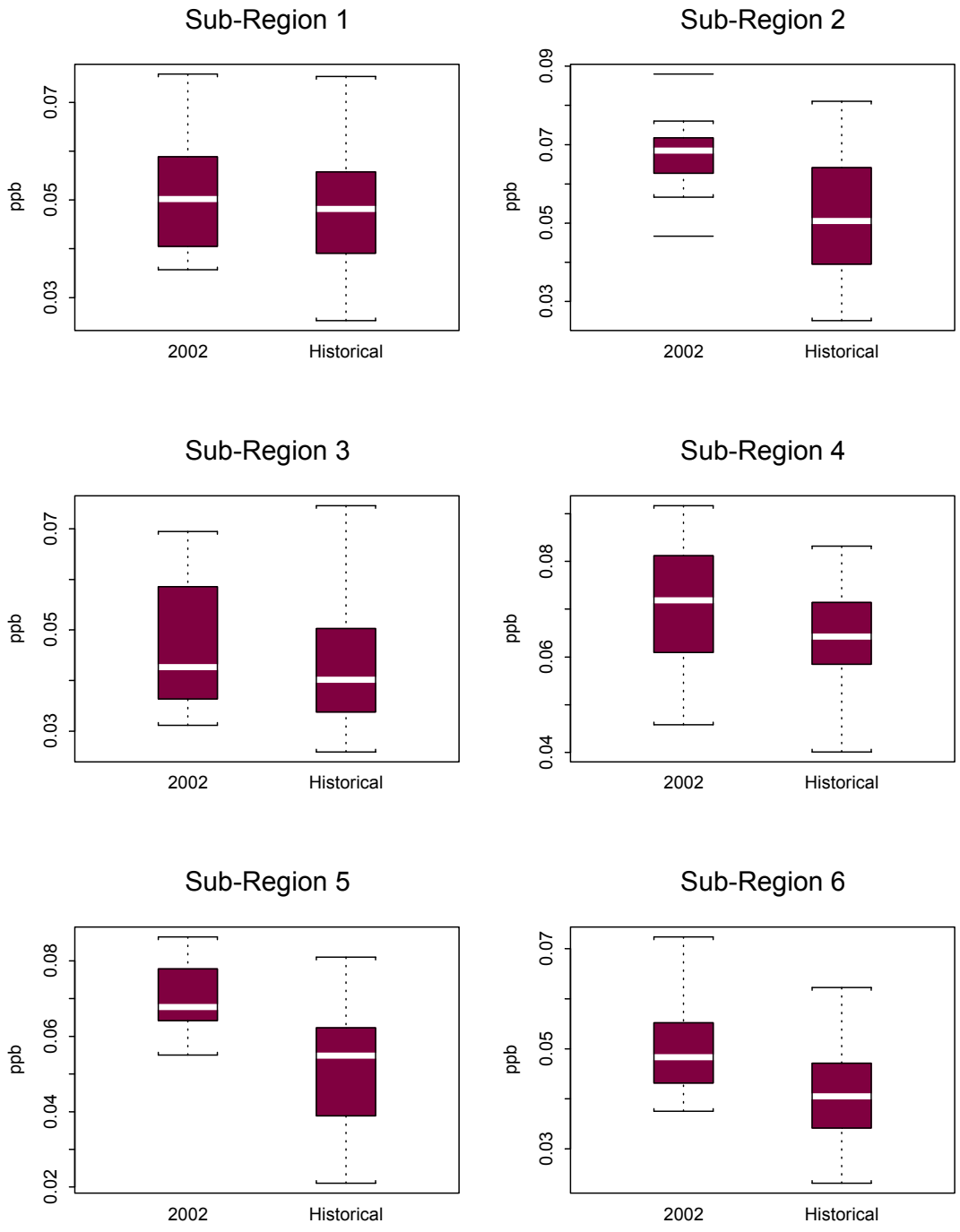

Figure 3-12d. Boxplots of average 8-hour daily maximum ozone (ppb) in each monitoring sub-region during 2002 and during the 1997-2001 and 2003 "historical" period: Type D (Pattern No. 4) events.

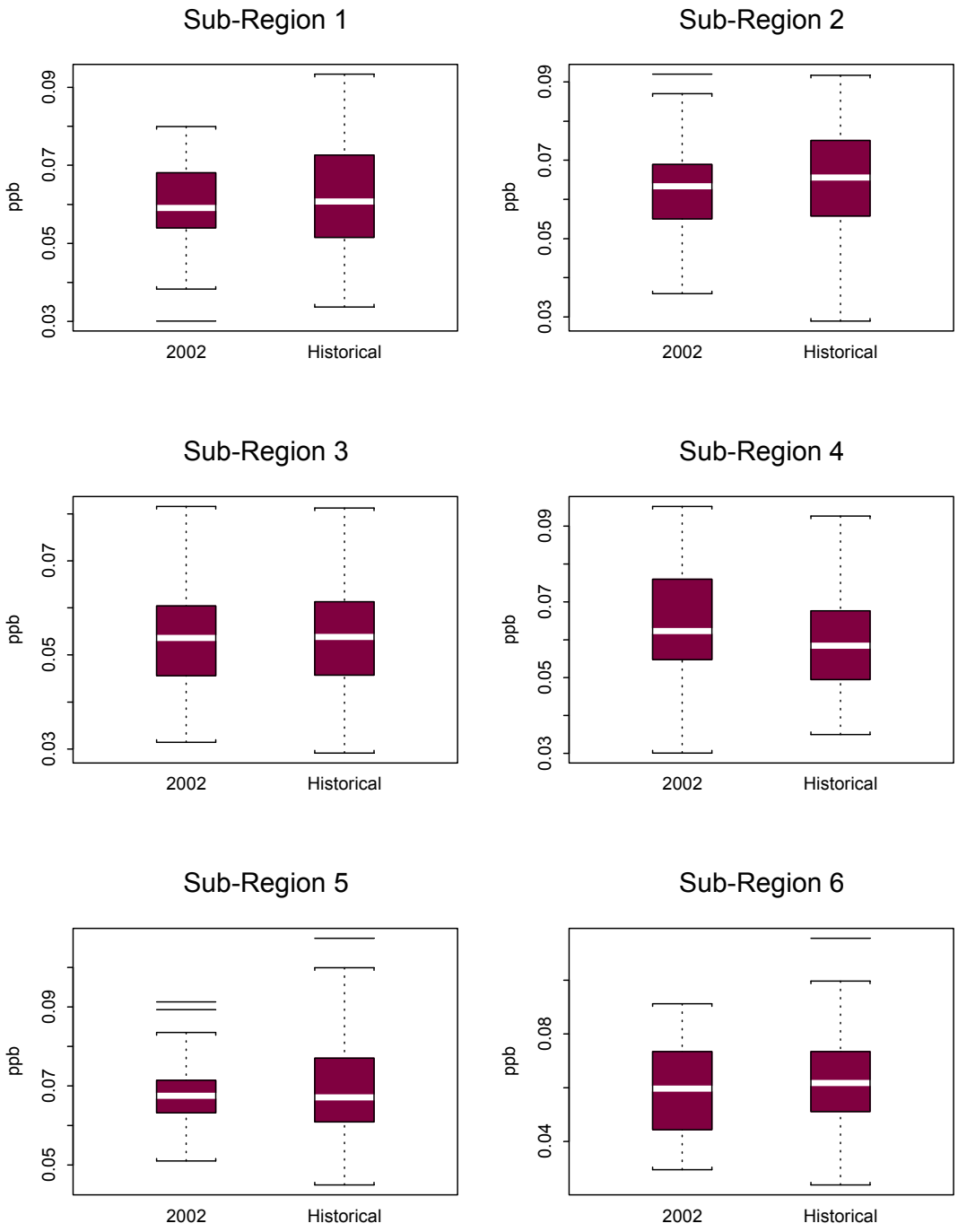

Figure 3-12e. Boxplots of average 8-hour daily maximum ozone (ppb) in each monitoring sub-region during 2002 and during the 1997-2001 and 2003 "historical" period: Type C (Pattern No. 5) events.

Meteorological Conditions

Selected composite meteorological fields for each episode type in 2002 as predicted by application of the classification tree were computed and displayed for comparison with the historical period composite fields. Results are shown in Figure 3-13 through 3-16. Comparing of these results with those for the historical period (Figures 3-2 to 3-5), we see a remarkable degree of similarity:[8] the surface and upper air meteorological patterns for a given episode type in 2002 are very similar to those for the same episode type observed in the historical period. In other words, the key characteristics of each type observed in the historical dataset are reproduced within the 2002 data. Perhaps the most significant difference is the less pronounced low pressure center off the NC coast under Type D events in 2002 which allowed for the formation of higher ozone concentrations along the Washington – New York City corridor for these event types in 2002 as compared to the historical period. Overall, however, the close match in weather patterns associated with each event type in 2002 and the historical period strongly supports the conclusion that the 2002 ozone episodes, although more numerous than in other years, are of substantially similar character.

[8] In making these comparisons, note that different color and wind vector scales had to be used in some plots of the 2002 data.

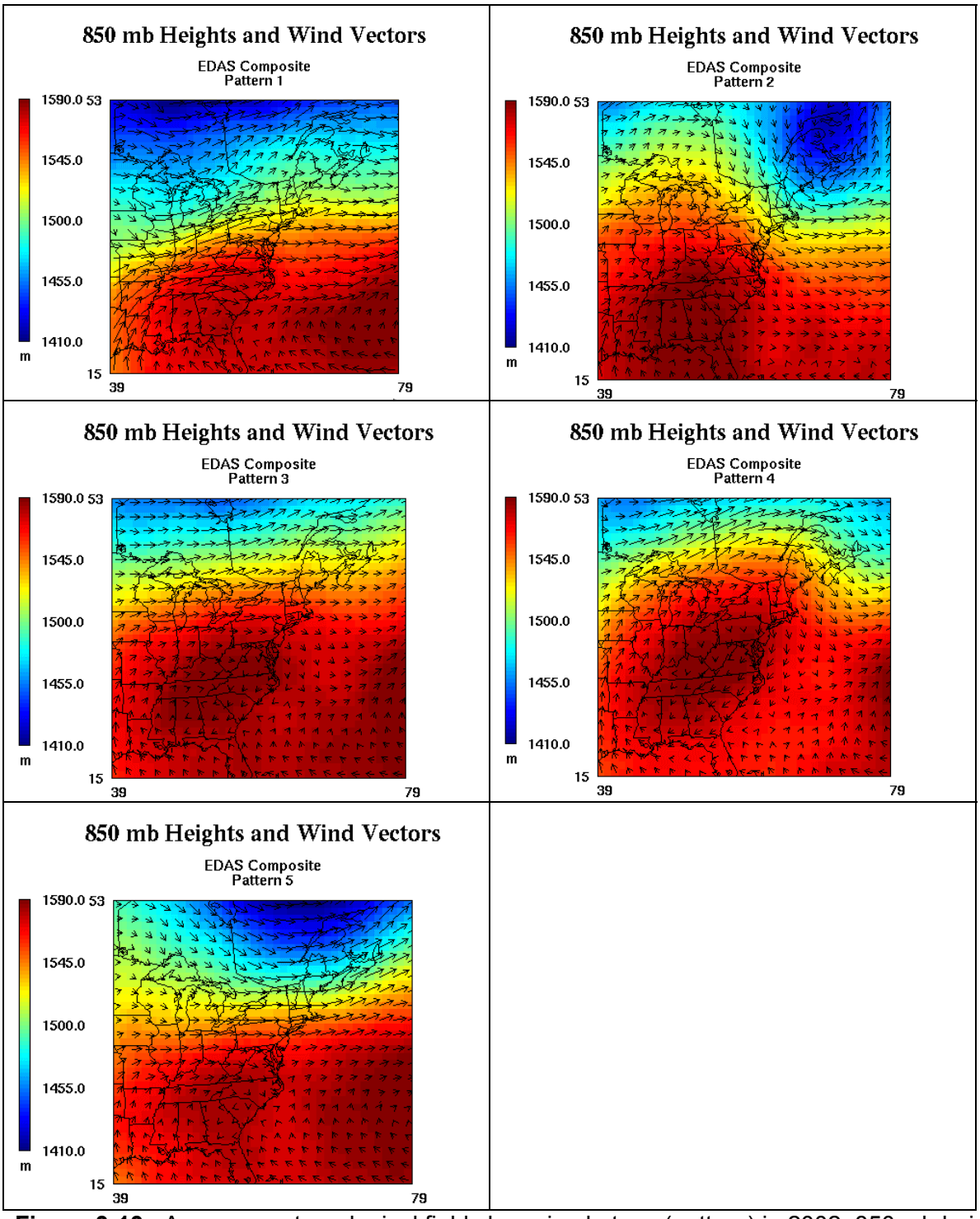

Figure 3-13. Average meteorological fields by episode type (pattern) in 2002: 850 mb heights and winds. Pattern numbers refer to the episode types listed in Table 3-2: Pattern 1 = Episode Type E, 2 = B, 3 = A, 4 = D, 5 = C).

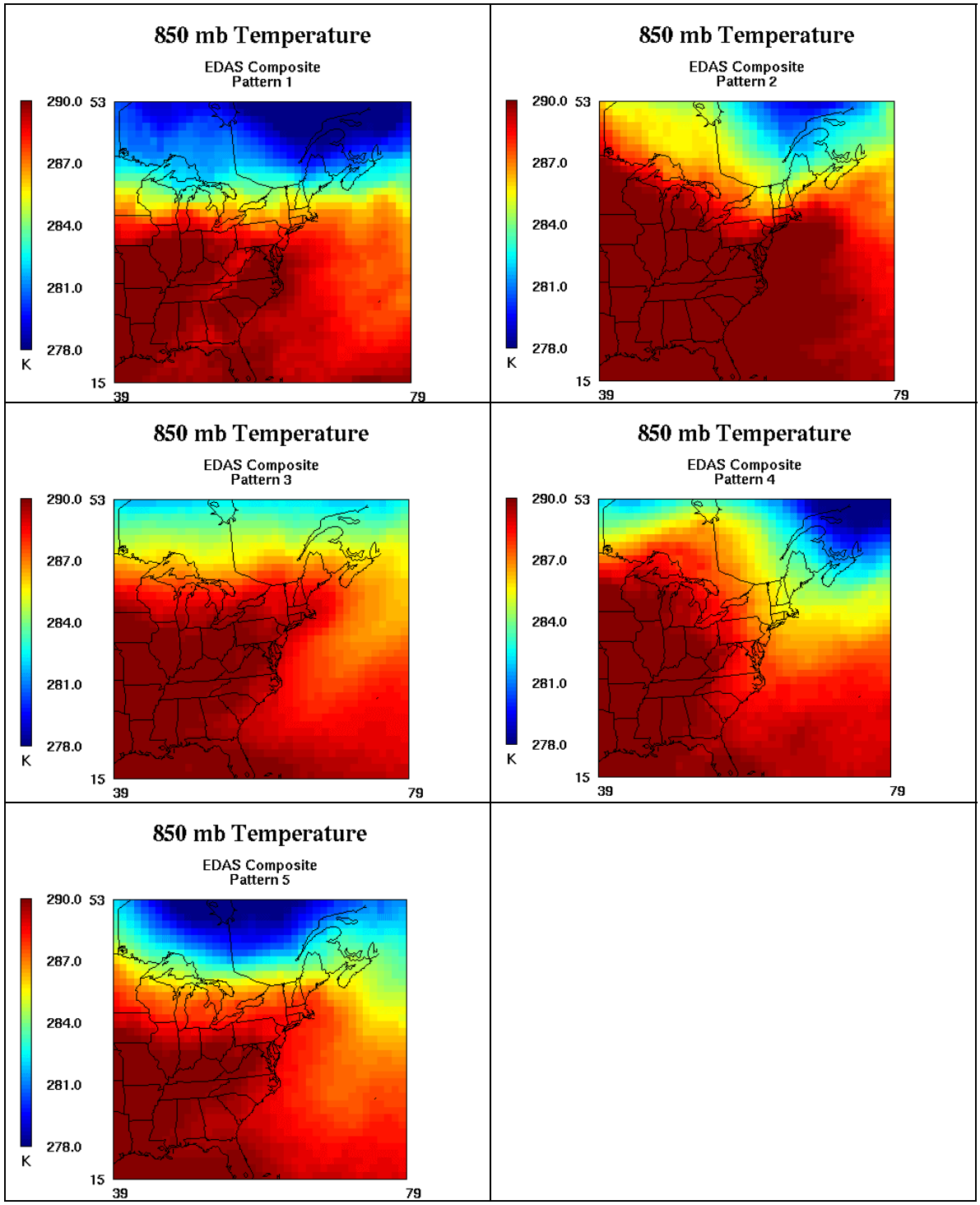

Figure 3-14. Average meteorological fields by episode type (pattern) in 2002: 850 mb temperature. Pattern numbers refer to the episode types listed in Table 3-2: Pattern 1 = Episode Type E, 2 = B, 3 = A, 4 = D, 5 = C).

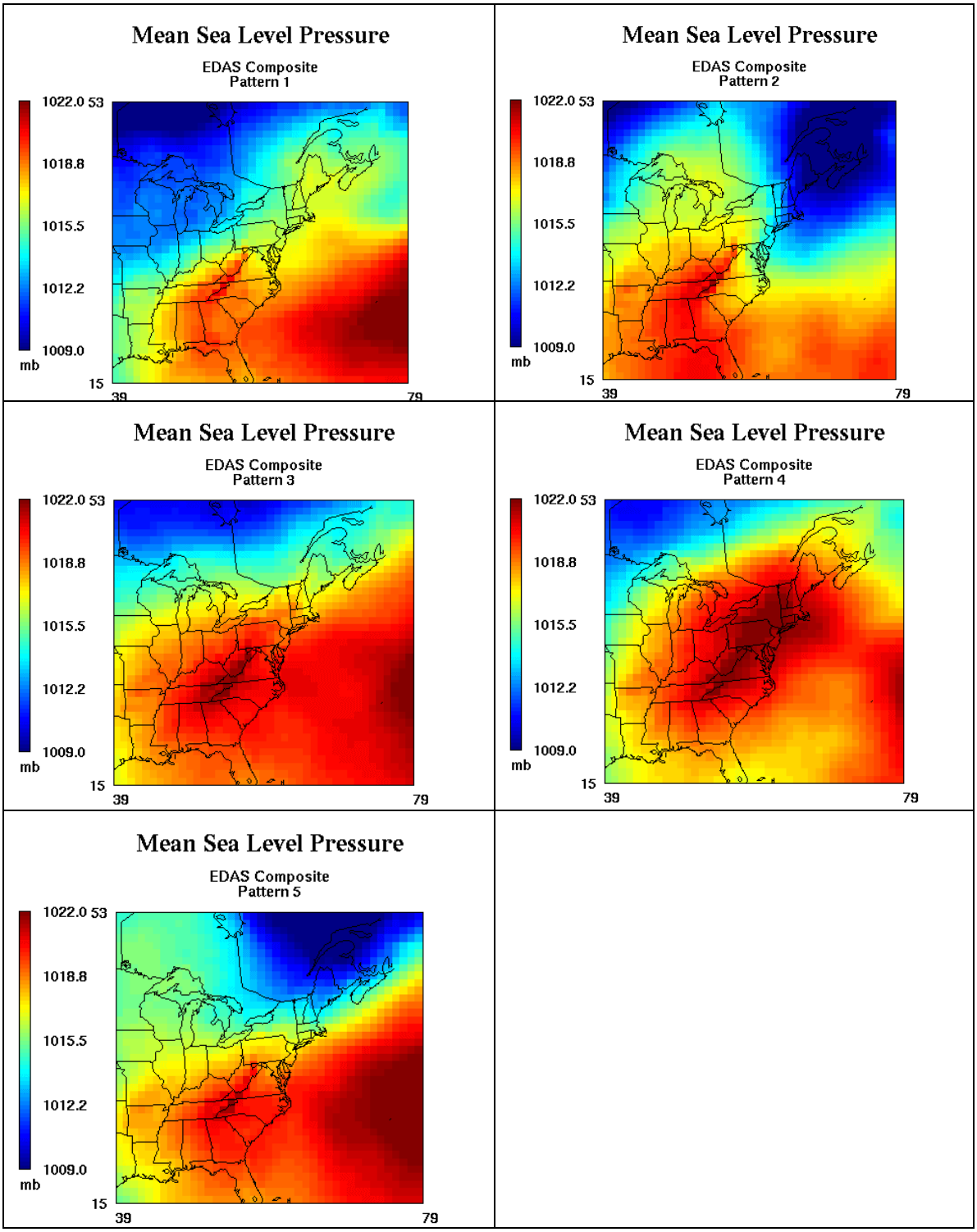

Figure 3-15. Average meteorological fields by episode type (pattern) in 2002: sea level pressure. Pattern numbers refer to the episode types listed in Table 3-2: Pattern 1 = Episode Type E, 2 = B, 3 = A, 4 = D, 5 = C).

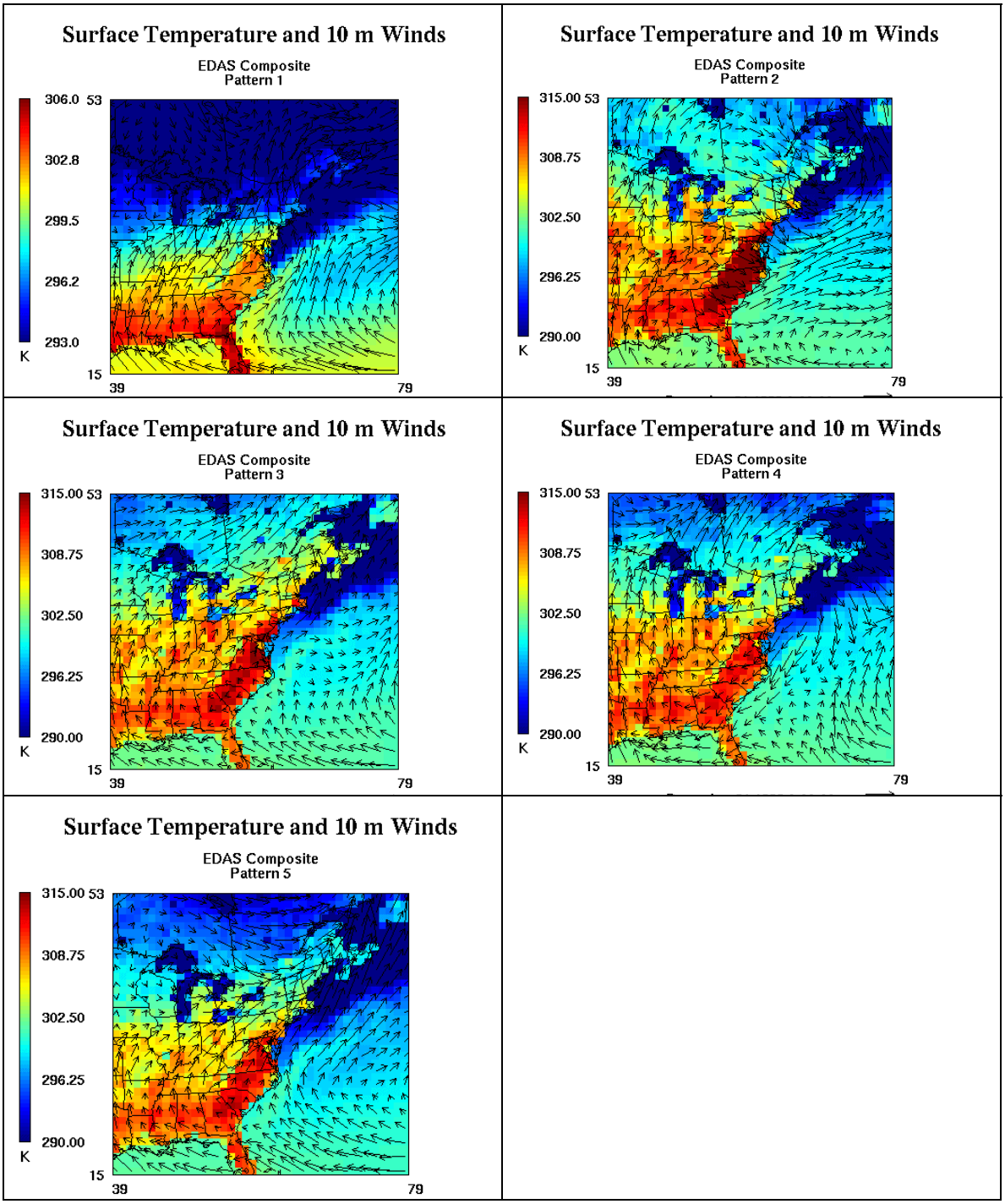

Figure 16. Average meteorological fields by episode type (pattern) in 2002: surface temperature and 10 m winds. Pattern numbers refer to the episode types listed in Table 3-2: Pattern 1 = Episode Type E, 2 = B, 3 = A, 4 = D, 5 = C).

4. CONCLUSIONS AND RECOMMENDATIONS

Results from the application of statistical clustering analyses presented in Section 3 show that regional ozone episode conditions over the OTR can be reasonably well described by a set of five different episode types. Our examination of mean ozone and meteorological conditions shows that each of these episode types is associated with a unique set of distinguishing characteristics. While we would not expect every exceedance day to exhibit all of the characteristics of one type or another, our results provide no clear evidence for the existence of any other additional sufficiently unique types that occur frequently enough to be distinguishable within the six year historical period analyzed.

Data from the 2002 ozone season were analyzed within the framework of the five identified episode types with respect to: a) frequencies of occurrence of each type and b) characteristics of the ozone and meteorological conditions within each type in 2002 as compared to the 1997 – 2001/2003 historical period.

A key feature of the 2002 season is that ozone episodes (defined as an exceedance of the 8-hour ozone NAAQS at one or more monitoring sites within the OTR) occurred more frequently than during the historical period (71 exceedance days during the May – September season in 2002 as compared to an average of 55 days per season during the historical period). Taken by itself, however, this difference does not necessarily mean that region-wide meteorological and ozone concentration patterns *during exceedance days* were significantly different in 2002 as compared to other years: the greater number of exceedance days in 2002 may just reflect a lower than average frequency of days with meteorological conditions not conducive to ozone formation in 2002. The higher than average exceedance rate in 2002 is by itself not an indication of any lack of representativeness of the 2002 exceedance events.

Our examination of conditions during exceedance days in 2002 showed that:

- Except for the Type E events during which ozone exceedances are typically confined to the extreme southeastern corner of the OTR, each of the five episode types identified in the historical period was found to occur on about as many days in 2002 as one would expect based on their rate of occurrence during the historical record. Thus the meteorological conditions on episode days in 2002 exhibit a normal range of variation and each of the five types of episodes are well represented.
- Type E events are under represented in the 2002 season. This is consistent with the higher than average frequency of exceedance days in 2002. The relative lack of Type E events in 2002 should not be of concern from a SIP modeling standpoint, however, as these events are characterized by relatively low ozone levels throughout nearly all of the OTR (except the Washington and Virginia area).
- The distribution of daily maximum 8-hour average ozone levels during each event type in 2002 is generally very similar to that within the same event type during the historical period. The only significant exception is higher ozone along the Washington – New York City corridor under Type D events in 2002 as compared to the historical average.
- Regional-scale meteorological conditions during each event type in 2002 exhibit the same key characteristics as observed for the event types during the historical period. A less

pronounced low pressure center off of the NC coast under the 2002 Type D events appears to be responsible for the higher Washington – New York City ozone levels under this event type noted in the previous bullet.

In summary, while ozone exceedances were more frequent during 2002, conditions during the 2002 exceedance events were for the most part very similar to those found to occur in other years. This leads us to conclude that the 2002 season can be considered to be representative for purposes of photochemical modeling in support of SIP development.

REFERENCES

Breiman, L., J.H. Friedman, R.A. Olshen and C.J. Stone, 1984. Classification and Regression Trees. Wadsworth, Belmont, CA

Cox, W.M., 1997. Spatial Clustering of Ambient Ozone in Eastern U.S., Draft, U.S. Environmental Protection Agency, January (available at http://www.epa.gov/ttn/naaqs/ozone/areas/misc/ozclus2a.htm)

Deuel, H.P. and S.G. Douglas, 1996. "Regional Ozone Patterns in the Eastern U.S. 1985-1995: Statistical Pattern Analysis and Classification and Regression Tree (CART) Analysis in Support of the Ozone Transport and Assessment Group (OTAG) Modeling Effort." Systems Applications Inc. San Rafael, CA October.

EPA, 1999. "Draft Guidance on the Use of Models and Other Analyses in Attainment Demonstrations for the 8-Hour Ozone NAAQS." EPA-54/R-99-004, U.S. Environmental Protection Agency, May.

Harrell, F.E., 1999. Hmisc S-PLUS function library. Programs available from lib.stat.cmu.edu.

Hartigan, J. A. and M.A. Wong, 1979. A k-means clustering algorithm. *Applied Statistics 28*, 100-108.

McHenry, J.N., W.F. Ryan, N.L. Seaman, C.J. Coats, J. Pudykiewicz, S. Arunachalam and J.M. Vukovich, 2004. A real-time Eulerian photochemical model forecast system: Overview and initial ozone forecast performance in the northeastern U.S. corridor. *Bulletin of the American Meteorological Society*, 85(4), April.

Sarle, WS: The VARCLUS Procedure. SAS/STAT User's Guide, 4th Edition, 1990. Cary NC: SAS Institute, Inc.

Stoeckenius, T.E. and S. Kemball-Cook, 2004. Ozone episode classification project: spatial ozone pattern analysis (Task 2a). Memo to T. Frankiewicz, Ozone Transport Comission, 21 September.

Venables, W.N. and B.D. Ripley, 1994. "Modern Applied Statistics with S-Plus." Springer-Verlag, New York.

Ward, J.H., 1963. Hierarchical groupings to optimize an objective function. *J. Amer. Statistical Assoc.*, 58:236-244.

Appendix A

Composites Representing Mean Meteorological Conditions During Each Ozone Episode Pattern

Composites Representing Mean Meteorological Conditions During Each Ozone Episode Pattern

Mean meteorological fields were computed over days falling into each of the five ozone episode patterns in the Ozone Transport Region defined in the text. The five episode patterns and their composite pattern identifiers are:

Composite Pattern	Episode Type
3	Type A: High ozone throughout the OTR
2	Type B: High ozone confined to extreme southeastern OTR
5	Type C: High ozone along I-95 corridor and northern New England
4	Type D: High ozone in the western OTR
1	Type E: Generally low ozone throughout the OTR

Mean fields were computed for the following parameters extracted from the EDAS data:

Parameter ID	Description
H850	850 mb height
850 mb Wind	Resultant wind vector at 850 mb
T(850 mb)	850 mb temperature (deg K)
MSLP	Mean sea level pressure (mb)
TSFC	Surface temperature (deg K)
10m Wind	Resultant wind vector at 10 m height
w_500	w (vertical) component of 500 mb wind vector
H500	500 mb heights

850 mb Heights and Winds

EDAS Composite
Pattern 1

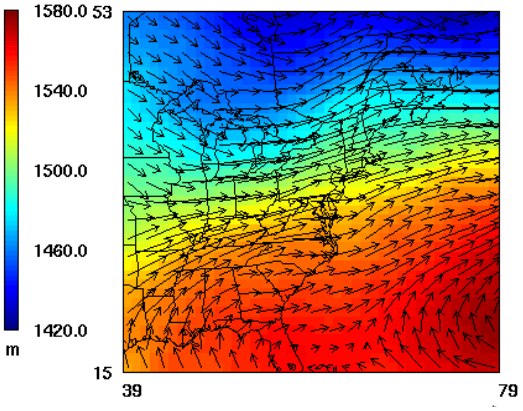

850 mb Heights and Winds

EDAS Composite
Pattern 2

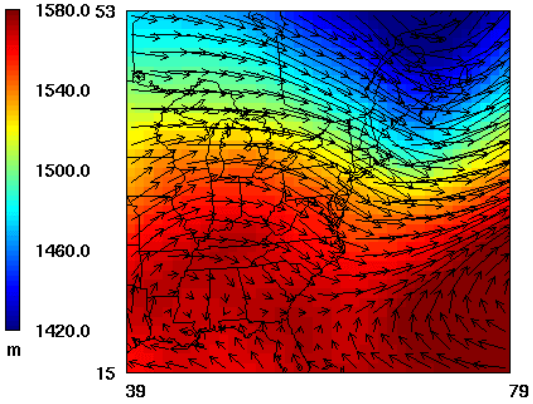

850 mb Heights and Winds

EDAS Composite
Pattern 3

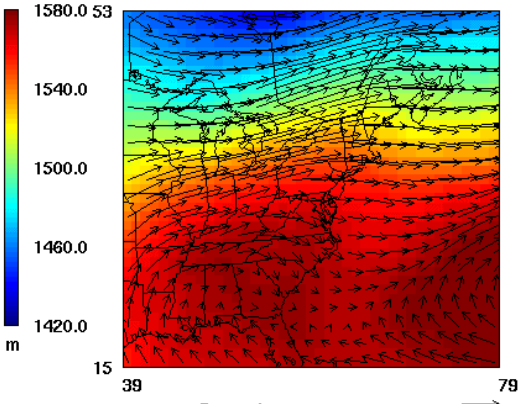

850 mb Heights and Winds

EDAS Composite
Pattern 4

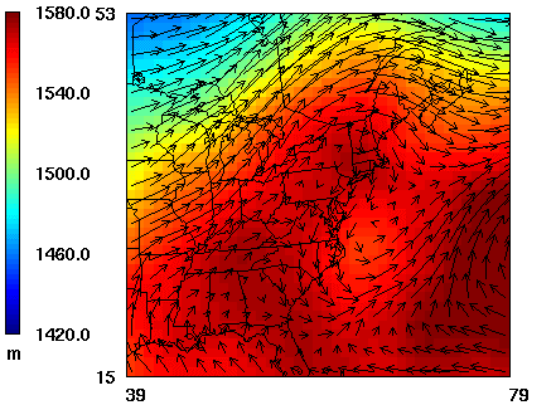

850 mb Heights and Winds

EDAS Composite
Pattern 5

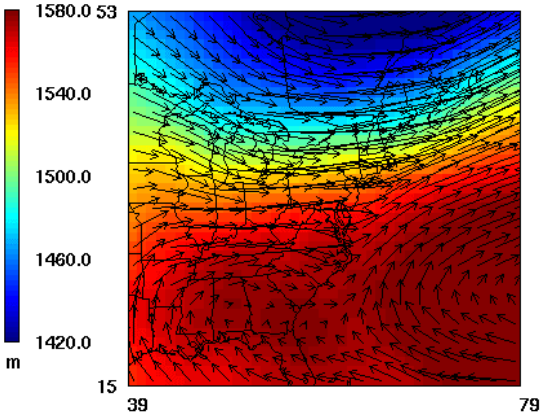

850 mb Temperature

EDAS Composite
Pattern 1

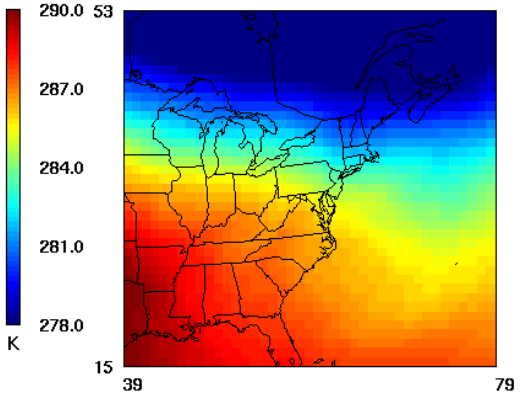

850 mb Temperature

EDAS Composite
Pattern 2

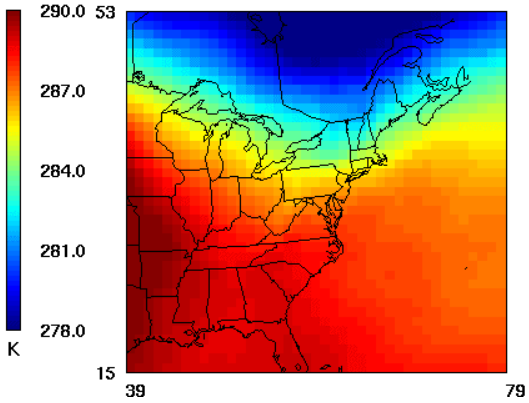

850 mb Temperature

EDAS Composite
Pattern 3

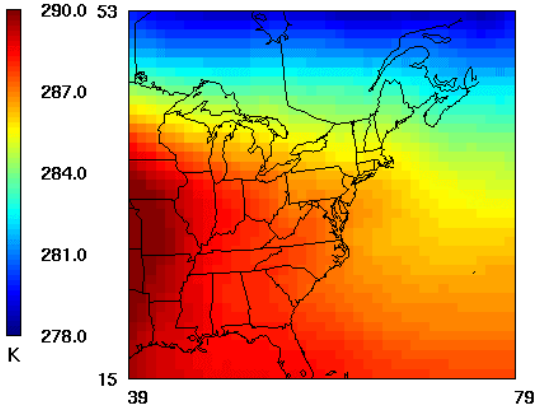

850 mb Temperature

EDAS Composite
Pattern 4

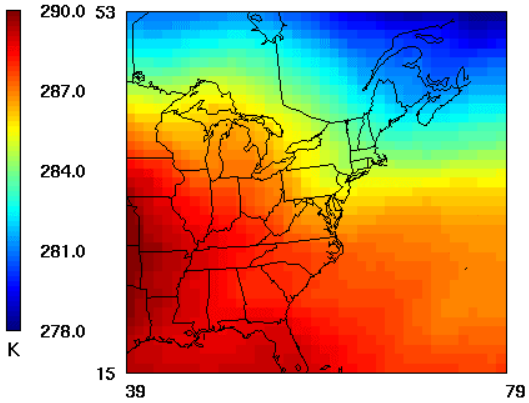

850 mb Temperature

EDAS Composite
Pattern 5

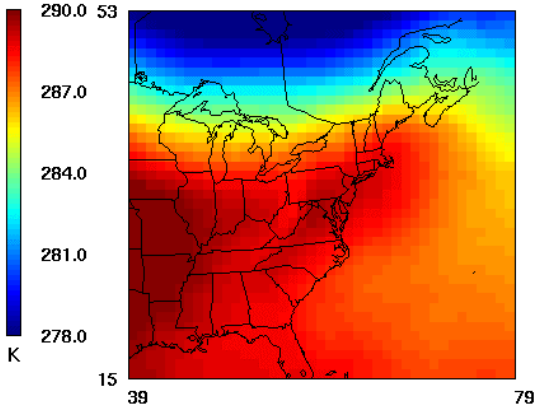

Mean Sea Level Pressure

EDAS Composite
Pattern 1

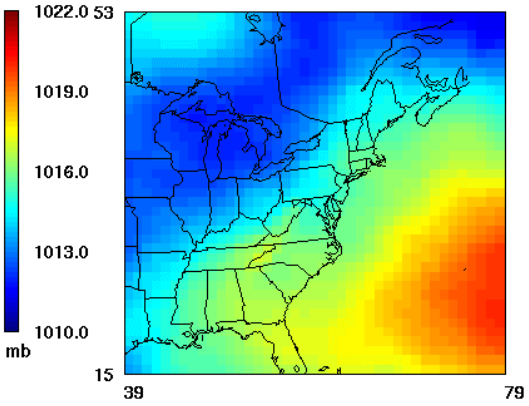

Mean Sea Level Pressure

EDAS Composite
Pattern 2

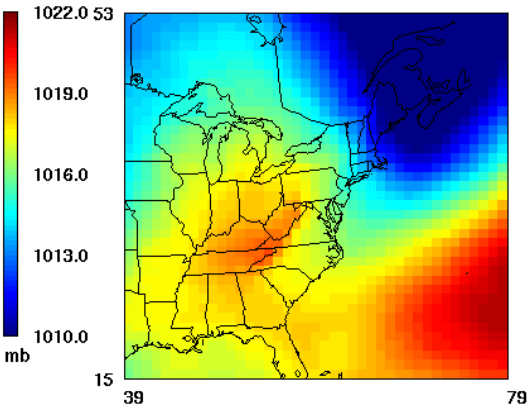

Mean Sea Level Pressure

EDAS Composite
Pattern 3

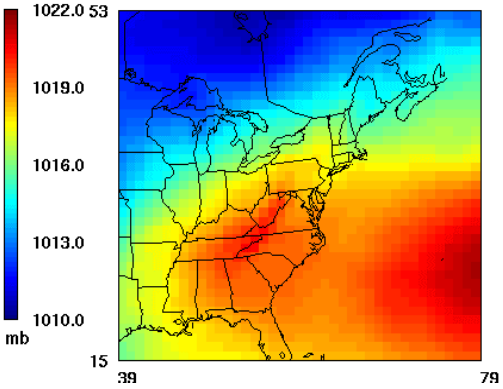

Mean Sea Level Pressure

EDAS Composite
Pattern 4

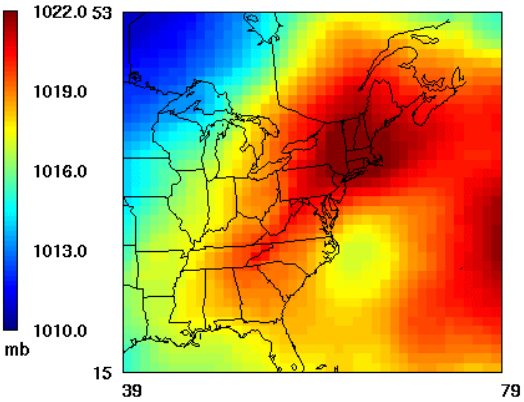

Mean Sea Level Pressure

EDAS Composite
Pattern 5

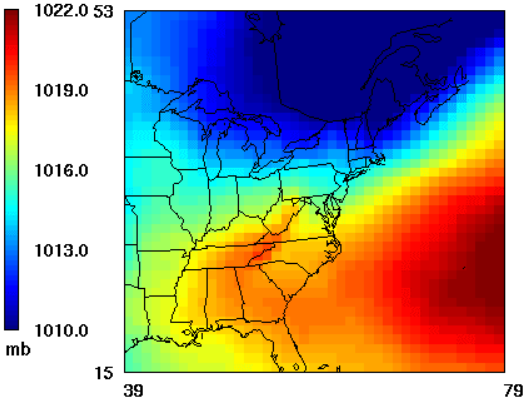

Surface Temperature and 10 m Winds

EDAS Composite
Pattern 1

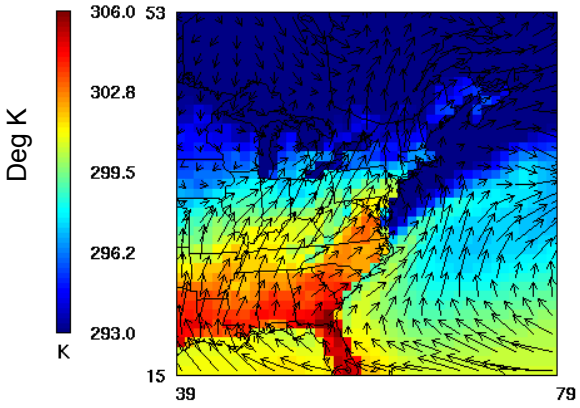

Surface Temperature and 10 m Winds

EDAS Composite
Pattern 2

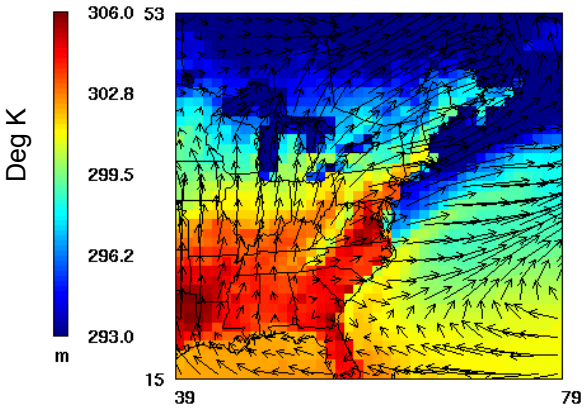

Surface Temperature and 10 m Winds

EDAS Composite
Pattern 3

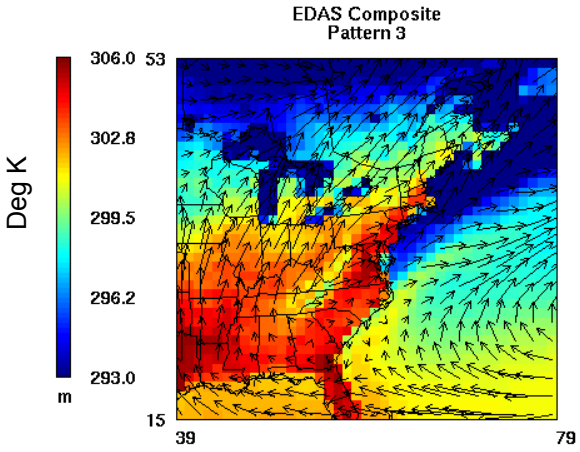

Surface Temperature and Winds

EDAS Composite
Pattern 4

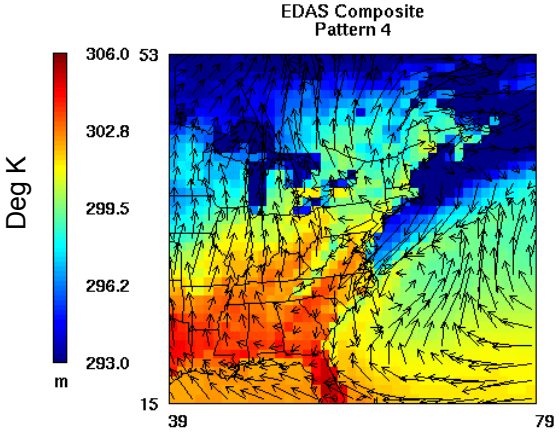

Surface Temperature and 10 m Winds

EDAS Composite
Pattern 5

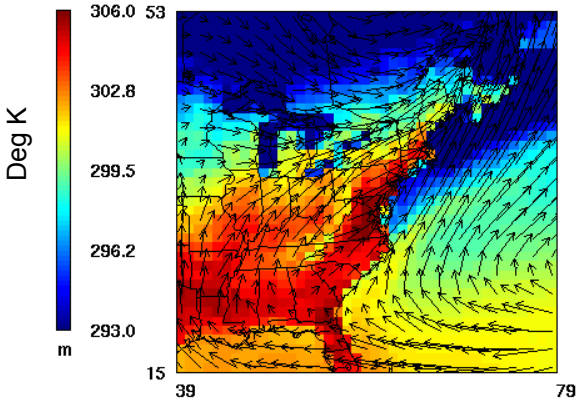

500 mb Vertical Velocity

EDAS Composite
Pattern 1

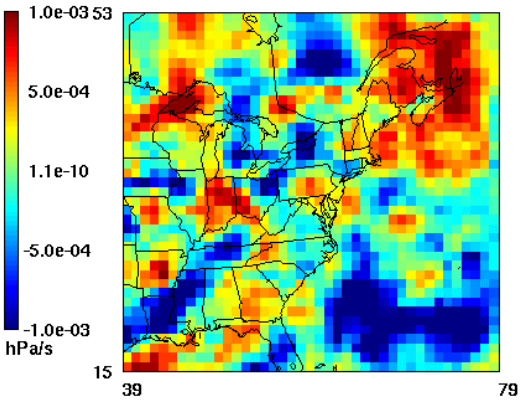

500 mb Vertical Velocity

EDAS Composite
Pattern 2

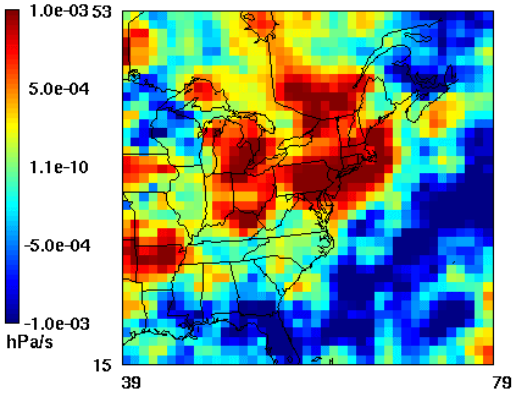

500 mb Vertical Velocity

EDAS Composite
Pattern 3

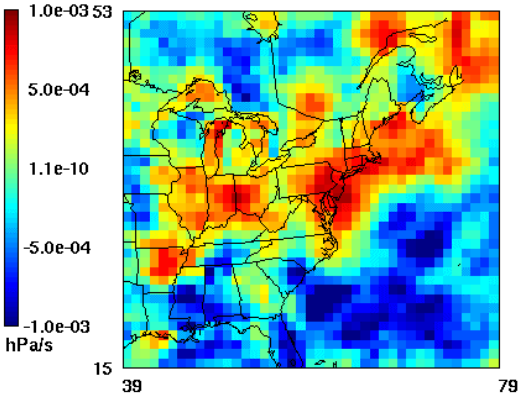

500 mb Vertical Velocity

EDAS Composite
Pattern 4

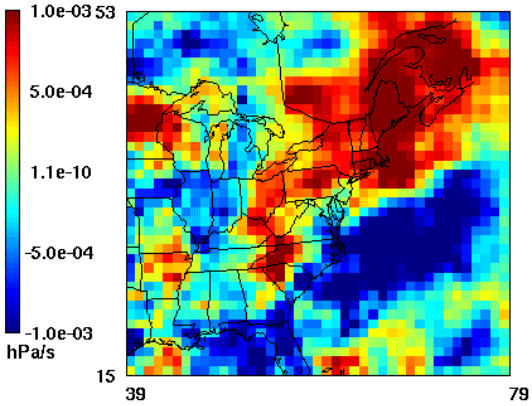

500 mb Vertical Velocity

EDAS Composite
Pattern 5

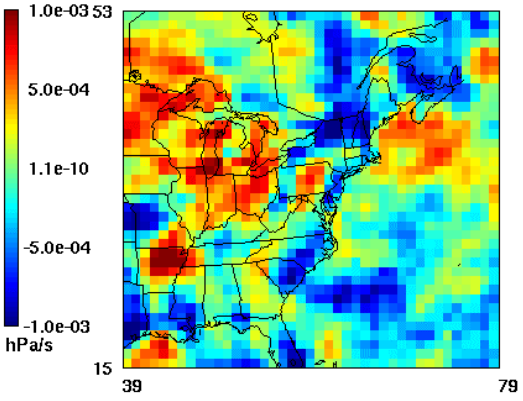

500 mb Heights

EDAS Composite
Pattern 1

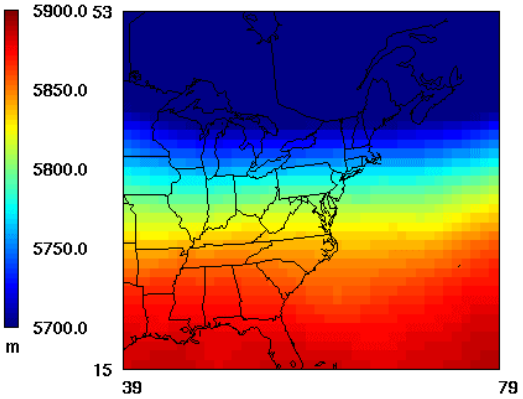

500 mb Heights

EDAS Composite
Pattern 2

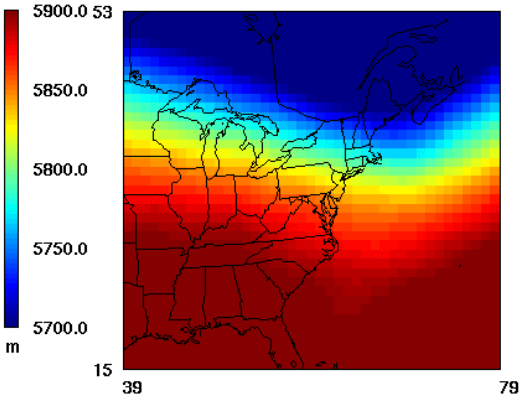

500 mb Heights

EDAS Composite
Pattern 3

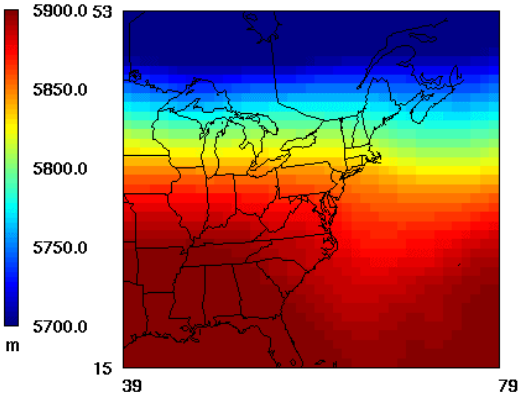

500 mb Heights

EDAS Composite
Pattern 4

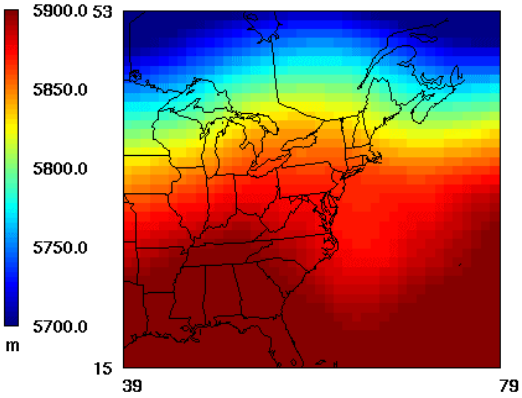

500 mb Heights

EDAS Composite
Pattern 5

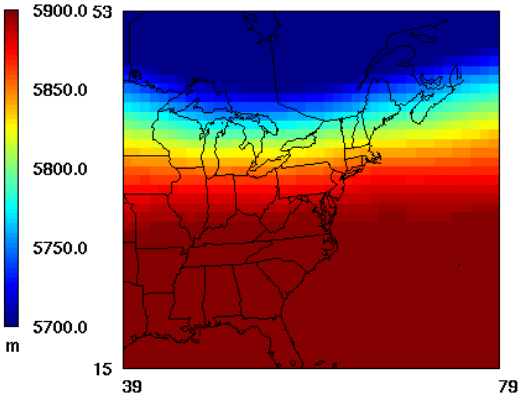

Appendix B

Boxplots of Key Meteorological Variables

Boxplots Of Key Meteorological Variables

Boxplots in this Appendix summarize distributions of the sub-regional ozone summary statistic, AvgEx00, described in the text along with selected key daily meteorological variables by episode pattern membership for the five cluster case. Pattern membership identifiers ("Met Cluster") used in these plots correspond to the episode types described in the text as follows:

Met Cluster	Episode Type
1	Type E
2	Type B
3	Type A
4	Type D
5	Type C

Ozone and meteorological variables are:

Variable	Description
clnx	AvgEx00 ozone summary statistic for ozone monitoring cluster x (x = 1,2…6; see Figure 1 in text)
DelPsfc.edas.DCtoNYC	Surface pressure gradient: Washington DC – New York City
DelPsfc.edas.DCtoBOSTON	Surface pressure gradient: Washington DC to Boston
DelPsfc.edas.DCtoPITTSBURGH	Surface pressure gradient: Washington DC to Pittsburgh
DelPsfc.edas.BUFFALOtoBOSTON	Surface pressure gradient: Buffalo to Boston
DelPsfc.edas.PITTSBURGHtoBUFFALO	Surface pressure gradient: Pittsburgh to Buffalo
H850.DC	850 mb height: Washington DC
H850.BOSTON	850 mb height: Boston
H850.PITTSBURGH	850 mb height: Pittsburgh
H850.BUFFALO	850 mb height: Buffalo
H850.PORTLAND	850 mb height: Portland, ME
H850.NYC	850 mb height: New York City
T850.DC	850 mb temperature: Washington DC
T850.BOSTON	850 mb temperature: Boston
T850.PITTSBURGH	850 mb temperature: Pittsburgh
T850.BUFFALO	850 mb temperature: Buffalo
T850.PORTLAND	850 mb temperature: Portland, ME
T850.NYC	850 mb temperature: New York City
sfcTmax.KLGA	Daily max surface temperature: La Guardia
sfcTmax.KPHL	Daily max surface temperature: Philadelphia
sfcTmax.KBOS	Daily max surface temperature: Boston
sfcTmax.KBUF	Daily max surface temperature: Buffalo
sfcTmax.KALB	Daily max surface temperature: Albany
sfcTmax.KDCA	Daily max surface temperature: Washington DC

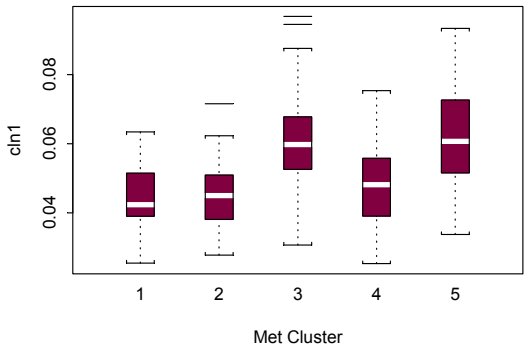
cln1
0.04
0.06
0.08
1
2
3
4
5
Met Cluster

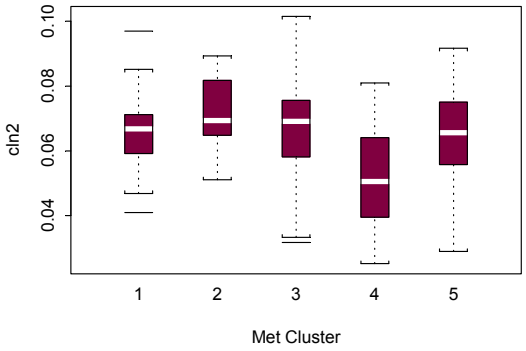
cln2
0.04
0.06
0.08
0.10
1
2
3
4
5
Met Cluster

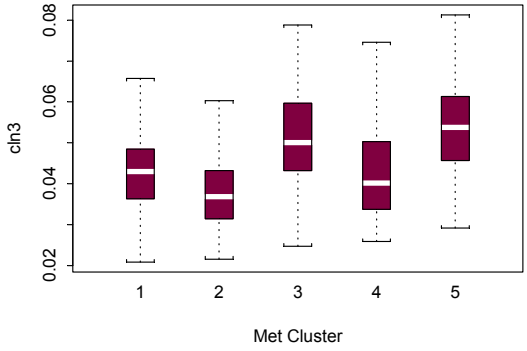
cln3
0.02
0.04
0.06
0.08
1
2
3
4
5
Met Cluster

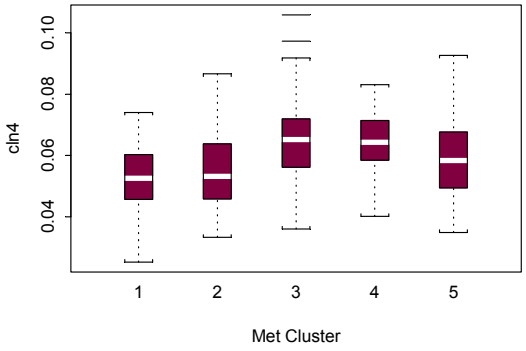
cln4
0.04
0.06
0.08
0.10
1
2
3
4
5
Met Cluster

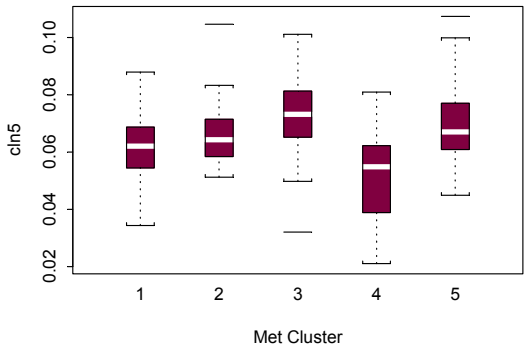
cln5
0.02
0.04
0.06
0.08
0.10
1
2
3
4
5
Met Cluster

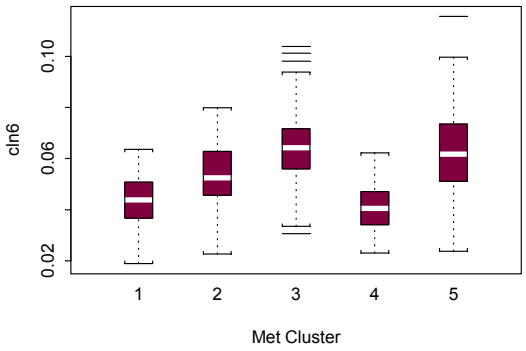
cln6
0.02
0.06
0.10
1
2
3
4
5
Met Cluster

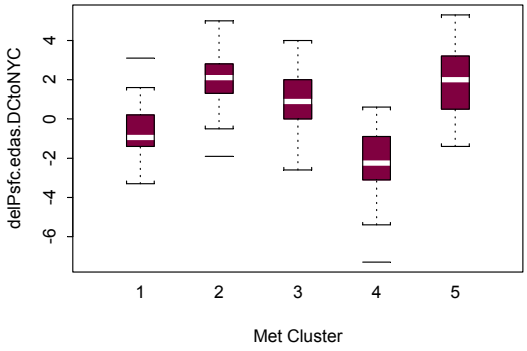
delPsfc.edas.DCtoNYC
-6
-4
-2
0
2
4
1
2
3
4
5
Met Cluster

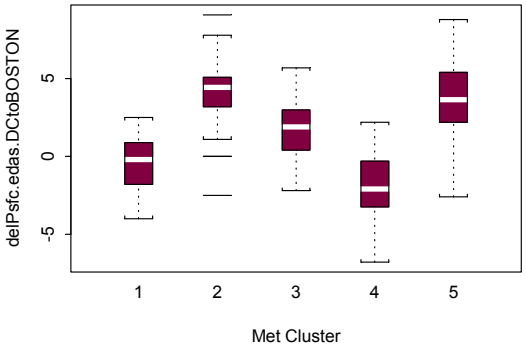
delPsfc.edas.DCtoBOSTON
-5
0
5
1
2
3
4
5
Met Cluster

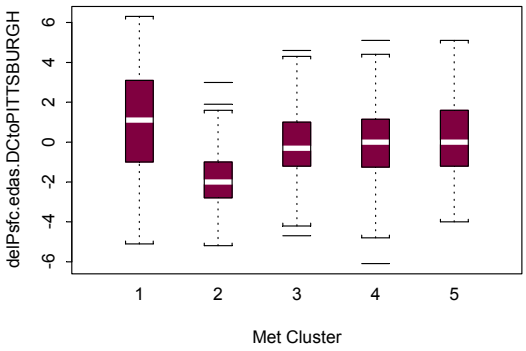
delPsfc.edas.DCtoPITTSBURGH
6
4
2
0
-2
-4
-6
1
2
3
4
5
Met Cluster

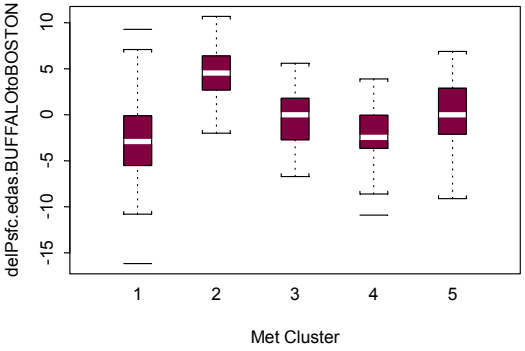
delPsfc.edas.BUFFALOtoBOSTON
10
5
0
-5
-10
-15
1
2
3
4
5
Met Cluster

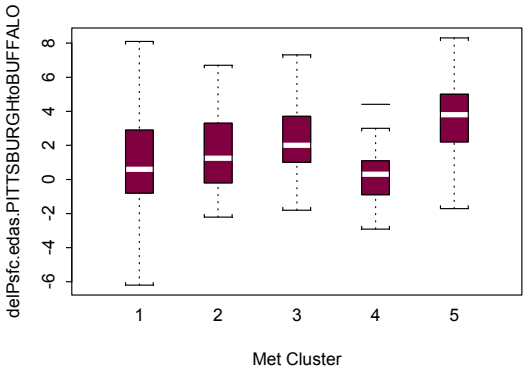
delPsfc.edas.PITTSBURGHtoBUFFALO
8
6
4
2
0
-2
-4
-6
1
2
3
4
5
Met Cluster

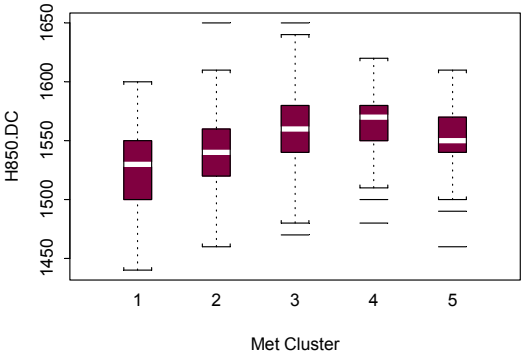
H850.DC
1650
1600
1550
1500
1450
1
2
3
4
5
Met Cluster

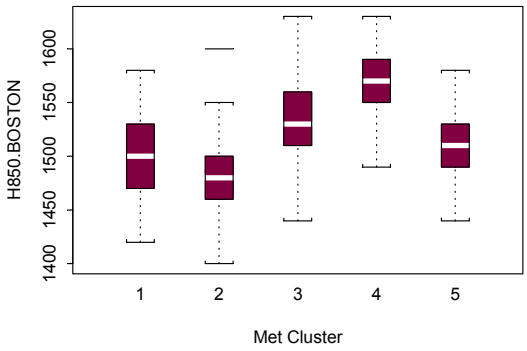
H850.BOSTON
1400
1450
1500
1550
1600
1
2
3
4
5
Met Cluster

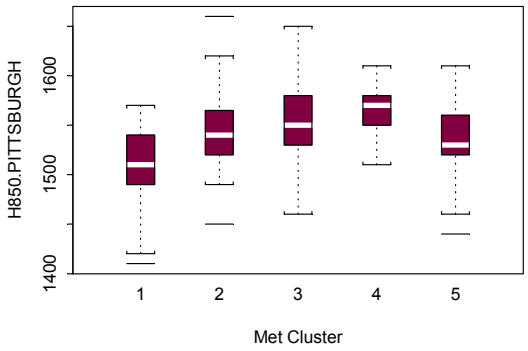
H850.PITTSBURGH
1400
1500
1600
1
2
3
4
5
Met Cluster

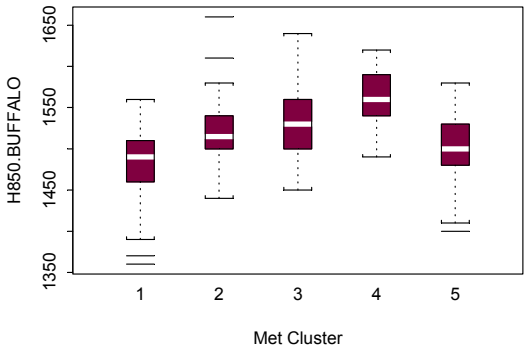
H850.BUFFALO
1350
1450
1550
1650
1
2
3
4
5
Met Cluster

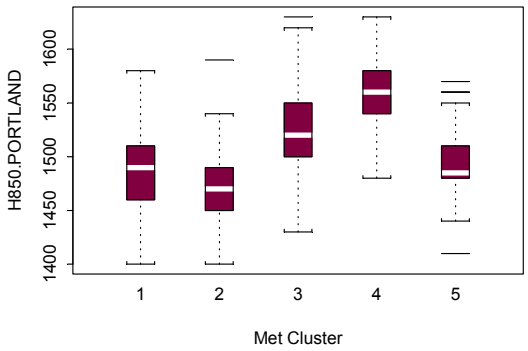
H850.PORTLAND
1400
1450
1500
1550
1600
1
2
3
4
5
Met Cluster

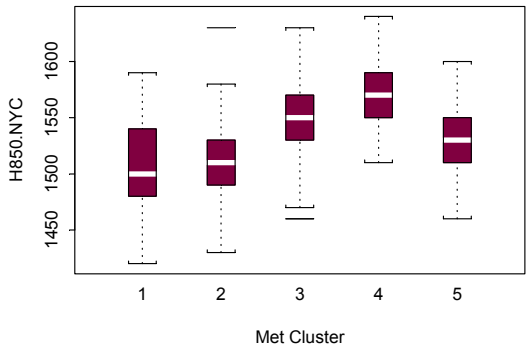
H850.NYC
1450
1500
1550
1600
1
2
3
4
5
Met Cluster

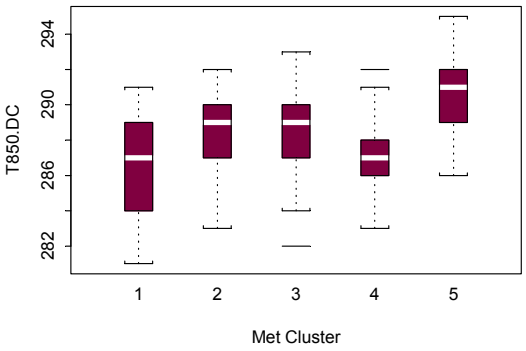
T850.DC
282
286
290
294
1
2
3
4
5
Met Cluster

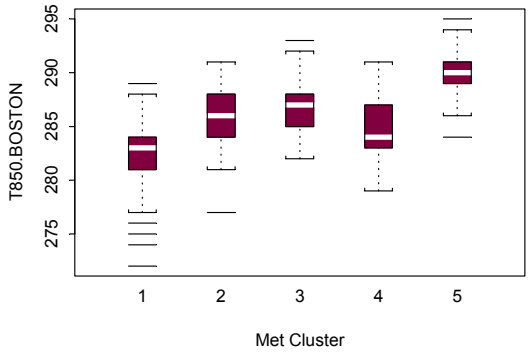
T850.BOSTON
275
280
285
290
295
1
2
3
4
5
Met Cluster

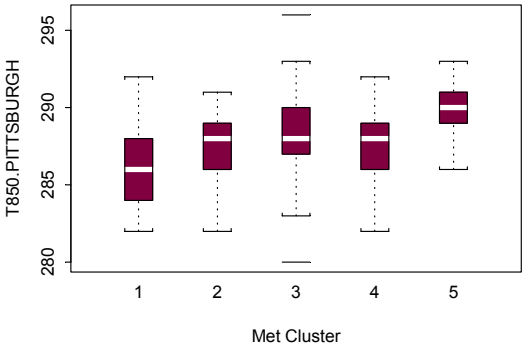
T850.PITTSBURGH
280
285
290
295
1
2
3
4
5
Met Cluster

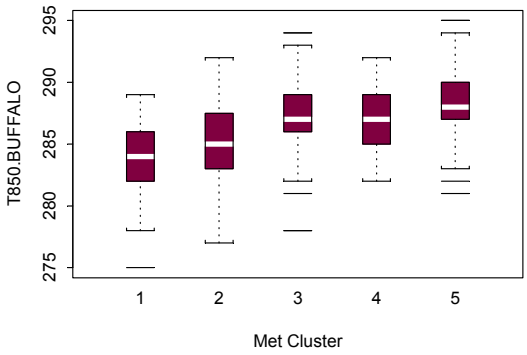
T850.BUFFALO
275
280
285
290
295
1
2
3
4
5
Met Cluster

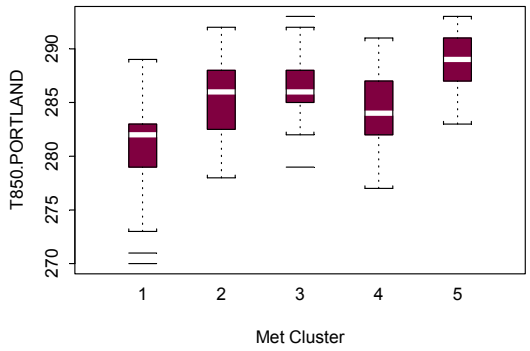
T850.PORTLAND
270
275
280
285
290
1
2
3
4
5
Met Cluster

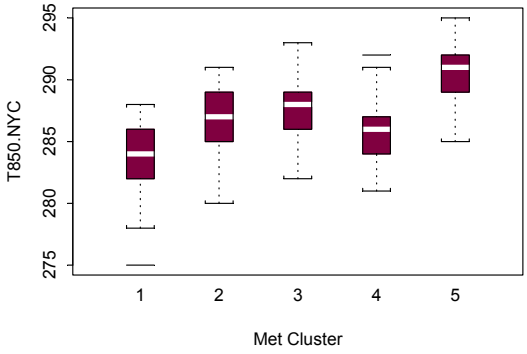
T850.NYC
275
280
285
290
295
1
2
3
4
5
Met Cluster

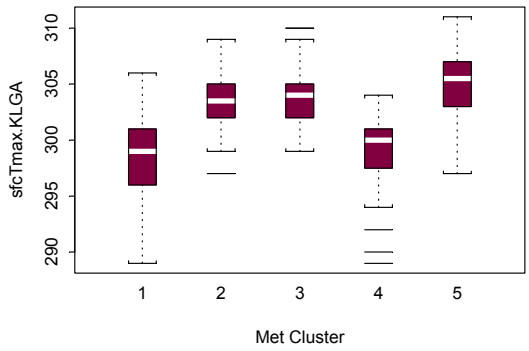
sfcTmax.KLGA
290
295
300
305
310
1
2
3
4
5
Met Cluster

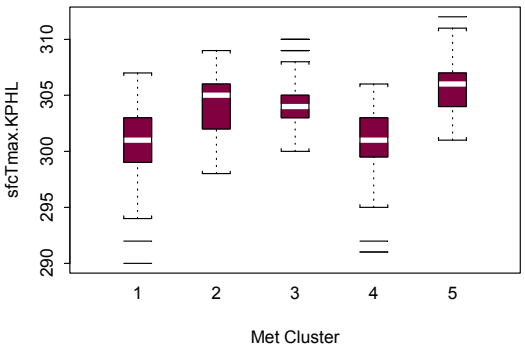
sfcTmax.KPHL
290
295
300
305
310
1
2
3
4
5
Met Cluster

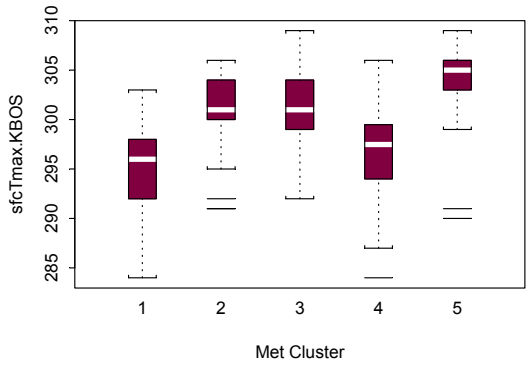
sfcTmax.KBOS
285
290
295
300
305
310
1
2
3
4
5
Met Cluster

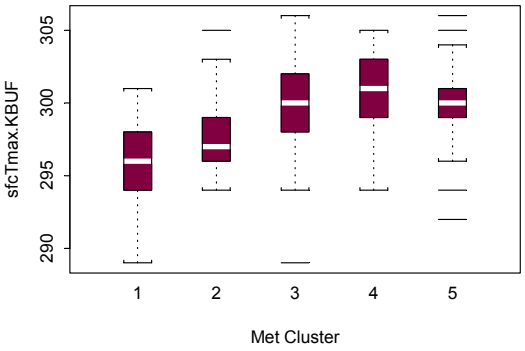
sfcTmax.KBUF
290
295
300
305
1
2
3
4
5
Met Cluster

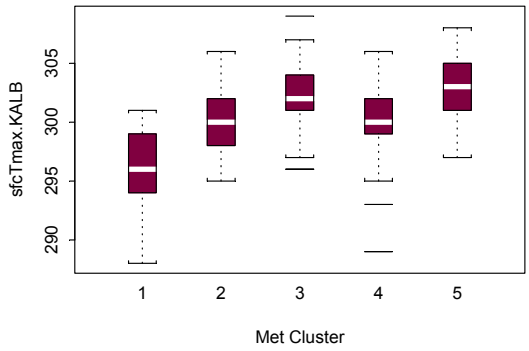
sfcTmax.KALB
290
295
300
305
1
2
3
4
5
Met Cluster

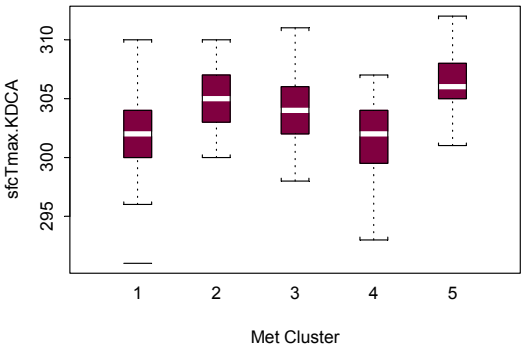
sfcTmax.KDCA
295
300
305
310
1
2
3
4
5
Met Cluster

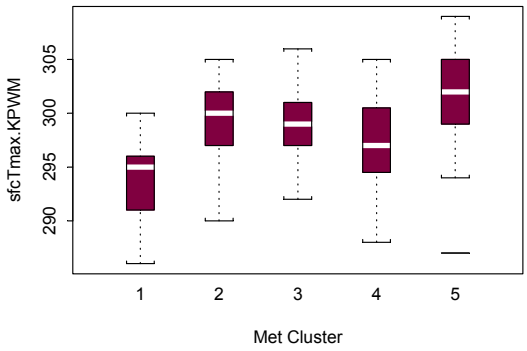
sfcTmax.KPWM
290
295
300
305
1
2
3
4
5
Met Cluster

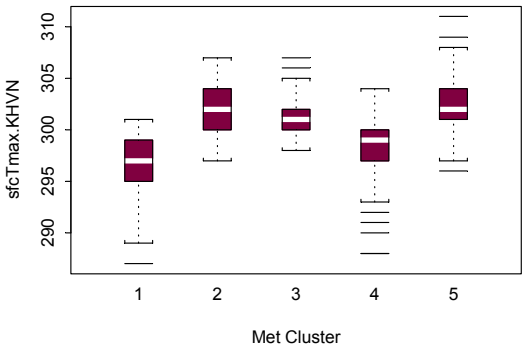
sfcTmax.KHVN
290
295
300
305
310
1
2
3
4
5
Met Cluster

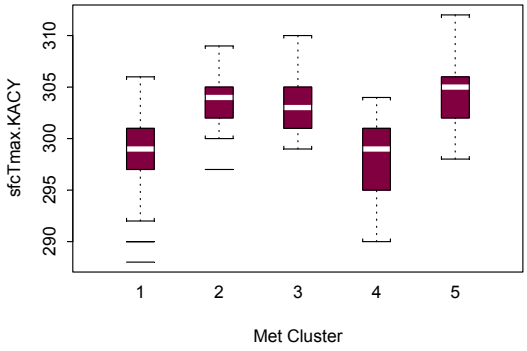
sfcTmax.KACY
290
295
300
305
310
1
2
3
4
5
Met Cluster

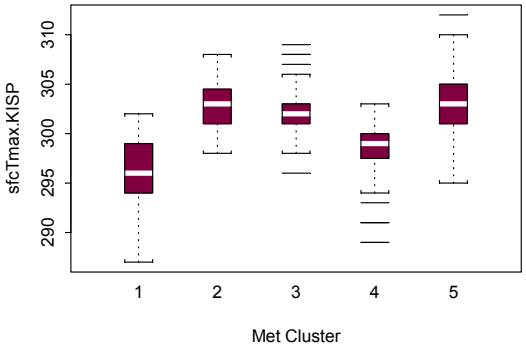
sfcTmax.KISP
290
295
300
305
310
1
2
3
4
5
Met Cluster

Appendix C

Wind Direction Frequency Tables

Wind Direction Frequency Tables

Contingency tables showing resultant surface wind direction frequencies were prepared for the five cluster membership cases. These results show relative frequency of days with the indicated wind direction in each cluster, i.e., the values for each cluster (column) sum to 100%. Tabulations are shown for both morning (AM) and afternoon (PM) resultant wind direction. Site location codes referenced in these tables are shown below.

Site Code	Location
KLGA	LaGuardia airport, New York, NY
KPHL	Philadelphia, PA
KBOS	Boston, MA
KBUF	Buffalo, NY
KALB	Albany, NY
KDCA	Washington, DC
KPWM	Portland, ME
KHVN	New Haven, CT
KACY	Atlantic City, NJ
KISP	Islip, Long Island, NY
KHYA	Hayannis, Cape Cod, MA
KWOR	Worcester, MA (KORH)
KHRT	Hartford, CT (KHFD)

Table B-1. Morning and afternoon daily resultant wind direction frequencies (%) by cluster membership for the five cluster case (columns sum to 100%). Header row for each table indicates AM or PM and four letter site ID as described in text (e.g., KLGA = LaGuardia, NY). Cluster identifier (A, B, C, D, E) is shown in first row of each table.

a) Morning wind directions

$resAMwd.KLGA:

	E	B	A	D	C
E	2	2	5	47	3
N	4	4	1	0	0
NE	27	4	7	35	0
NW	7	42	10	0	0
S	33	6	12	5	6
SE	11	0	7	7	2
SW	16	10	34	2	76
W	0	32	23	5	14

$resAMwd.KPHL:

	E	B	A	D	C
E	9	0	2	32	2
N	4	4	1	2	0
NE	7	0	0	34	0
NW	4	28	4	5	0
S	24	4	17	9	29
SE	20	0	4	7	2
SW	26	34	55	9	64
W	7	30	17	2	5

$resAMwd.KBOS:

	E	B	A	D	C
E	2	0	4	9	2
N	2	0	1	0	0
NE	9	4	1	14	0
NW	9	22	13	20	0
S	17	8	11	16	11
SE	15	2	2	7	3
SW	22	26	43	20	77
W	24	38	25	14	8

$resAMwd.KBUF:

	E	B	A	D	C
E	16	2	3	16	0
N	0	0	1	0	0
NE	13	0	0	5	3
NW	0	10	0	0	5
S	31	29	44	16	17
SE	24	0	24	57	6
SW	16	40	25	7	59
W	0	19	2	0	11

$resAMwd.KALB:

	E	B	A	D	C
E	2	0	8	6	0
N	10	7	5	20	2
NE	2	0	1	3	0
NW	10	20	4	3	0
S	34	20	55	49	87
SE	15	0	9	6	3
SW	20	26	12	9	8
W	7	28	5	6	0

$resAMwd.KDCA:

	E	B	A	D	C
E	4	0	0	26	0
N	2	14	2	2	0
NE	7	0	1	28	0
NW	9	24	5	5	0
S	46	24	38	16	68
SE	4	0	5	16	2
SW	22	28	45	2	29
W	7	10	5	5	2

$resAMwd.KPWM:

	E	B	A	D	C
E	10	8	3	2	3
N	2	0	1	7	0
NE	7	2	0	0	2
NW	12	17	14	17	2
S	12	8	11	5	27
SE	2	4	7	2	5
SW	15	8	16	29	50
W	39	52	49	38	12

$resAMwd.KACY:

	E	B	A	D	C
E	7	0	1	26	0
N	2	2	2	10	0
NE	5	0	1	23	0
NW	5	22	7	10	0
S	29	0	17	10	41
SE	12	2	6	8	3
SW	22	29	45	8	52
W	17	45	22	5	5

$resAMwd.KISP:

	E	B	A	D	C
E	9	0	5	14	0
N	9	9	6	19	0
NE	9	0	7	36	0
NW	0	34	10	5	0
S	32	2	8	2	11
SE	14	0	3	14	2
SW	11	21	44	7	80
W	16	34	18	2	8

$resAMwd.KHYA:

	E	B	A	D	C
E	6	0	0	8	0
N	3	13	3	14	0
NE	11	2	1	43	0
NW	6	20	6	0	0
S	14	7	6	11	3
SE	8	4	6	3	0
SW	31	22	41	19	60
W	22	33	38	3	37

$resAMwd.KWOR:

	E	B	A	D	C
E	5	2	0	7	0
N	0	4	3	10	0
NE	10	0	1	15	2
NW	5	23	10	17	0
S	5	2	0	5	2
SE	5	0	2	7	0
SW	33	4	19	12	62
W	38	65	65	27	35

$resAMwd.KHRT:

	E	B	A	D	C
E	5	5	5	19	0
N	5	2	2	6	0
NE	8	2	2	9	0
NW	3	7	0	0	0
S	51	36	71	41	94
SE	5	12	13	16	3
SW	19	19	2	6	3
W	3	17	5	3	0

Table B-1 (concl).

b) Afternoon wind directions

$resPMwd.KLGA:

	E	B	A	D	C
E	9	0	7	20	0
N	0	6	1	0	0
NE	30	0	15	68	0
NW	4	68	26	0	8
S	30	6	12	2	8
SE	13	2	8	7	0
SW	11	6	17	0	48
W	2	12	14	2	36

$resPMwd.KPHL:

	E	B	A	D	C
E	13	2	4	57	0
N	0	8	2	0	0
NE	4	0	0	32	0
NW	2	40	5	0	2
S	22	0	20	2	8
SE	26	4	3	9	2
SW	30	22	50	0	73
W	2	24	16	0	17

$resPMwd.KBOS:

	E	B	A	D	C
E	20	2	13	34	5
NE	9	2	2	9	0
NW	4	30	2	0	0
S	17	4	23	18	8
SE	15	2	20	25	0
SW	26	10	24	7	65
W	9	50	16	7	23

$resPMwd.KBUF:

	E	B	A	D	C
E	7	2	3	19	0
N	0	2	0	0	0
NE	11	4	1	5	5
NW	2	6	6	0	8
S	28	12	20	33	3
SE	11	6	2	16	0
SW	37	51	61	28	68
W	4	16	7	0	17

$resPMwd.KALB:

	E	B	A	D	C
E	2	0	3	8	0
N	2	2	2	11	0
NE	4	2	2	3	0
NW	7	41	6	0	2
S	59	2	45	50	58
SE	15	2	5	18	2
SW	7	20	17	8	24
W	4	31	20	3	15

$resPMwd.KDCA:

	E	B	A	D	C
E	7	4	5	23	0
N	0	4	2	2	0
NE	9	6	2	48	0
NW	2	34	4	0	5
S	57	14	53	9	59
SE	11	6	9	11	3
SW	11	6	17	2	21
W	4	26	8	5	12

$resPMwd.KPWM:

	E	B	A	D	C
E	11	8	17	20	5
N	0	4	2	0	0
NE	13	2	2	7	2
NW	11	42	11	0	2
S	20	6	24	27	29
SE	20	4	16	25	6
SW	16	14	15	14	33
W	9	20	13	7	24

$resPMwd.KACY:

	E	B	A	D	C
E	15	2	3	42	0
N	0	6	1	2	0
NE	7	4	1	47	0
NW	2	48	11	0	0
S	33	4	21	0	23
SE	24	0	10	9	0
SW	13	8	26	0	55
W	7	28	27	0	22

$resPMwd.KISP:

	E	B	A	D	C
E	11	0	6	36	0
N	2	10	5	2	0
NE	11	0	3	36	0
NW	2	52	11	2	3
S	38	0	17	2	14
SE	20	0	8	18	0
SW	11	8	39	2	68
W	4	29	13	0	15

$resPMwd.KHYA:

	E	B	A	D	C
E	16	11	7	9	0
N	0	9	2	7	0
NE	9	4	5	27	0
NW	0	11	6	0	0
S	13	9	12	20	5
SE	18	6	8	20	0
SW	38	21	48	16	75
W	7	30	11	0	20

$resPMwd.KWOR:

	E	B	A	D	C
E	14	4	3	17	2
N	5	4	1	2	0
NE	14	4	4	22	0
NW	9	35	9	2	0
S	9	0	7	22	5
SE	5	0	3	10	0
SW	37	4	28	7	54
W	7	49	44	17	40

$resPMwd.KHRT:

	E	B	A	D	C
E	11	2	16	16	0
N	4	9	3	3	0
NE	0	4	7	22	0
NW	2	22	1	0	0
S	56	13	43	22	52
SE	13	11	18	24	2
SW	11	11	9	11	35
W	2	28	4	3	11

Appendix D

Ozone Monitoring Stations by Sub-Region

Cluster	Site ID	State	City	Location
6	90010017	Connecticut	GREENWICH	GREENWICH POINT PARK
1	90011123	Connecticut	DANBURY	TRAILER, W. CONNECTICUT STATE UNIVERSITY
6	90013007	Connecticut	STRATFORD	USCG LIGHTHOUSE, PROSPECT STREET
6	90019003	Connecticut	WESTPORT	SHERWOOD ISLAND STATE PARK
1	90031003	Connecticut	EAST HARTFORD	MCAULIFFEE PARK
1	90070007	Connecticut	MIDDLETOWN	CONN. VALLEY HOSP., SHEW HALL, EASTERN D
6	90093002	Connecticut	MADISON	HAMMONASSET STATE PARK
6	90110008	Connecticut	GROTON	UNIVERSITY OF CONNECTICUT, AVERY POINT
1	90131001	Connecticut	STAFFORD	ROUTE 190, SHENIPSIT STATE FOREST
2	100010002	Delaware	NOT IN A CITY	STATE ROAD 384
5	100031003	Delaware	NOT IN A CITY	RIVER ROAD PARK, BELLEFONTE
5	100031007	Delaware	NOT IN A CITY	LUMS POND STATE PARK
5	100031010	Delaware	NOT IN A CITY	BRANDYWINE CREEK STATE PARK
2	100051002	Delaware	SEAFORD	350 VIRGINIA AVE SEAFORD
2	100051003	Delaware	LEWES	UNIV. OF DE COLLEGE OF MARINE STUDIES
5	110010025	Washington DC	NOT IN A CITY	TAKOMA SC. PINEY BRANCH RD & DAHLIA ST N
5	110010041	Washington DC	NOT IN A CITY	34TH. AND DIX STREETS, N.E.
5	110010043	Washington DC	NOT IN A CITY	S.E. END MCMILLIAN RESERVOIR, WASH. DC.
1	230052003	Maine	CAPE ELIZABETH	TWO LIGHTS STATE PARK
1	230090102	Maine	BAR HARBOR	TOP OF CADILLAC MOUNTAIN
1	230090103	Maine	BAR HARBOR	MCFARLAND HILL-DISPRO SITE
3	230112005	Maine	GARDINER	PRAY STREET SCHOOL
1	230130004	Maine	NOT IN A CITY	PORT CLYDE, MARSHALL POINT LIGHTHOUSE
3	230173001	Maine	NOT IN A CITY	ROUTE 5, NORTH LOVELL DOT
3	230194008	Maine	NOT IN A CITY	SUMMIT OF RIDER BLUFF (WLBZ TRANSMITTER)
1	230312002	Maine	NOT IN A CITY	OCEAN AVE/PARSONS WAY, KENNEBUNKPORT
1	230313002	Maine	KITTERY	FRISBEE SCHOOL, GOODSOE ROAD
2	240030014	Maryland	NOT IN A CITY	QUEEN ANNE AND WAYSON ROADS
5	240030019	Maryland	FORT MEADE	9001 'Y'STREET, FT. MEADE, ANNE ARUNDEL MD
5	240051007	Maryland	COCKEYSVILLE	GREENSIDE DRIVE, COCKEYSVILLE MD
5	240053001	Maryland	ESSEX	WOODWARD & DORSEY RDS, ESSEX MD
5	240130001	Maryland	NOT IN A CITY	1300 W. OLD LIBERTY ROAD, WINFIELD, MD
5	240150003	Maryland	NOT IN A CITY	RTE.273, FAIR HILL, CEIL CO., MARYLAND
2	240170010	Maryland	NOT IN A CITY	SO MD CORRECTIONAL CAMP, HUGHESVILLE MD
5	240251001	Maryland	EDGEWOOD	EDGEWOOD ARMY CHEM CENTER EDGEWOOD MD
5	240259001	Maryland	NOT IN A CITY	3538 ALDINO ROAD, HARFORD COUNTY MARYLAND
5	240290002	Maryland	NOT IN A CITY	KENT COUNTY; MILLINGTON
5	240313001	Maryland	ROCKVILLE	LOTHROP E SMITH ENV.ED CENTER ROCKVILLE
5	240330002	Maryland	GREENBELT	GODDARD SPACE FLIGHT CENTER
6	250010002	Massachusetts	TRURO	FOX BOTTOM AREA-CAPE COD NAT'L SEASHORE
1	250034002	Massachusetts	ADAMS	MT. GREYLOCK SUMMIT
6	250051002	Massachusetts	FAIRHAVEN	LEROY WOOD SCHOOL
1	250051005	Massachusetts	EASTON	1 BORDERLAND ST.
1	250092006	Massachusetts	LYNN	390 PARKLAND AVE. (LYNN WATER TREATMENT)
1	250094004	Massachusetts	NEWBURY	SUNSET BOULEVARD
1	250130003	Massachusetts	AGAWAM	152 SOUTH WESTFIELD STREET, FEEDING HILL

Cluster	Site ID	State	City	Location
1	250130008	Massachusetts	CHICOPEE	ANDERSON ROAD AIR FORCE BASE
1	250150103	Massachusetts	AMHERST	NORTH PLEASANT ST. U. MASS PATHOLOGY DEPT
1	250154002	Massachusetts	WARE	QUABBIN SUMMIT
1	250250042	Massachusetts	BOSTON	HARRISON AVENUE
1	250270015	Massachusetts	WORCESTER	WORCESTER AIRPORT
1	330050007	New Hampshire	KEENE	RAILROAD STREET
3	330090008	New Hampshire	HAVERHILL	HAVERHILL ARMORY, RT 116, HAVERHILL, NH
1	330111010	New Hampshire	NASHUA	SANDERS ASSOCIATES, PARKING LOT D
1	330130007	New Hampshire	CONCORD	STORRS STREET
1	330150012	New Hampshire	RYE	RYE HARBOR STATE PARK OCEAN BLVD, RTE. 1A
3	330173002	New Hampshire	ROCHESTER	ROCHESTER HILL ROAD, ROCHESTER
3	330190003	New Hampshire	CLAREMONT	SOUTH STREET
5	340010005	New Jersey	NOT IN A CITY	BRIGANTINE WILDLIFE REFUGE, NACOTE CREEK
5	340070003	New Jersey	NOT IN A CITY	COPEWOOD E. DAVIS STS; TRAILER
5	340071001	New Jersey	NOT IN A CITY	ANCORA STATE HOSPITAL, ANCORA
5	340110007	New Jersey	NOT IN A CITY	LINCOLN AVE.&HIGHWAY 55,NE OF MILLVILLE
5	340150002	New Jersey	NOT IN A CITY	CLARKSBORO, SHADY LANE REST HOME
5	340170006	New Jersey	BAYONNE	VETERANS PARK ON NEWARK BAY
5	340190001	New Jersey	FLEMINGTON	RARITAN STP, RTE.613S, THREE BRIDGES
5	340210005	New Jersey	NOT IN A CITY	RIDER COLLEGE; LAWRENCE TOWNSHIP
5	340230011	New Jersey	NOT IN A CITY	R.U. VEG RESEARCH FARM 3,RYDERS LN, NEWB
5	340250005	New Jersey	WEST LONG BRANC	MONMOUTH COLLEGE, WEST LONG BRANCH
5	340273001	New Jersey	NOT IN A CITY	BLDG.#1, BELL LABS, OFF ROUTE 513
5	340290006	New Jersey	NOT IN A CITY	COLLIERS MILLS, JACKSON TOWNSHIP
1	360010012	New York	ALBANY	LOUDONVILLE RESERVOIR
6	360050083	New York	NEW YORK CITY	200TH STREET AND SOUTHERN BLVD
6	360050110	New York	NEW YORK CITY	E 156TH ST BET DAWSON AND KELLY
4	360130006	New York	DUNKIRK	STP LAKESIDE BLD DUNKIRK
4	360130011	New York	NOT IN A CITY	TOWN OF WESTFIELD
4	360150003	New York	ELMIRA	SULLIVAN ST., WATER TR. PL.
1	360270007	New York	NOT IN A CITY	VILLAGE OF MILLBROOK
4	360290002	New York	AMHERST	AUDUBON GOLF COURSE, MAPLE ROAD
3	360310002	New York	NOT IN A CITY	SUMMIT, WHITEFACE MTN, WEATHER STATION
3	360310003	New York	NOT IN A CITY	BASE WHITEFACE MTN, ASRC, SUNY
3	360410005	New York	NOT IN A CITY	PISECO LAKE AIRPORT
3	360430005	New York	NOT IN A CITY	NICKS LAKE CAMPGROUND
4	360450002	New York	NOT IN A CITY	VADAI ROAD, PERCH RIVER, BROWNVILLE
4	360530006	New York	NOT IN A CITY	TOWN OF GEORGETOWN
4	360551004	New York	NOT IN A CITY	TRAILER, WEST END OF FARMINGTON ROAD
4	360631006	New York	NOT IN A CITY	MIDDLEPORT STP, NORTH HARTLAND RD
4	360671015	New York	NOT IN A CITY	5895 ENTERPRISE PARKWAY,
1	360715001	New York	NOT IN A CITY	1175 ROUTE 17K, MONTGOMERY
1	360790005	New York	NOT IN A CITY	NYSDEC FIELD HQTRS GYPSY TRAIL ROAD
6	360810098	New York	NEW YORK CITY	120-07 15TH AVE
5	360850067	New York	NEW YORK CITY	SUSAN WAGNER HS, BRIELLE AVE.& MANOR RD,
3	360910004	New York	NOT IN A CITY	SARATOGA NATIONAL HISTORICAL PARK
1	360930003	New York	SCHENECTADY	MT.PLEASANT HS, NORWOOD AVE.& FOREST RD.

Cluster	Site ID	State	City	Location
6	361030002	New York	BABYLON	EAST FARMINGDALE WATER DIST., GAZZA BLVD.
6	361030004	New York	RIVERHEAD	39 SOUND AVENUE, RIVERHEAD
3	361111005	New York	NOT IN A CITY	BELLEAYRE MOUNTAIN
4	361173001	New York	NOT IN A CITY	WAYNE EDUCATIONAL CENTER, WILLIAMSON
6	361192004	New York	WHITE PLAINS	WHITE PLAINS PUMP STATION, ORCHARD STREET
4	420030008	Pennsylvania	PITTSBURGH	BAPC 301 39TH STREET BLDG #7
4	420030067	Pennsylvania	NOT IN A CITY	OLD OAKDALE ROAD SOUTH FAYETTE
4	420031005	Pennsylvania	NOT IN A CITY	CALIFORNIA & 11TH, HARRISON TWP
4	420050001	Pennsylvania	KITTANNING	GLADE DR. & NOLTE RD. KITTANNING
4	420070002	Pennsylvania	NOT IN A CITY	ROUTE 168 & TOMLINSON ROAD
4	420070005	Pennsylvania	NOT IN A CITY	1015 SEBRING ROAD
4	420070014	Pennsylvania	BEAVER FALLS	EIGHT STREET AND RIVER ALLEY
5	420110001	Pennsylvania	KUTZTOWN	KUTZTOWN UNIVERSITY - GRIM SCIENCE BLDG
5	420110009	Pennsylvania	READING	UGI CO MONGANTOWN RD AND PROSPECT ST
5	420130801	Pennsylvania	ALTOONA	2ND AVE & 7TH ST
5	420170012	Pennsylvania	BRISTOL (BOROUG	ROCKVIEW LANE
5	420210011	Pennsylvania	NOT IN A CITY	MILLER AUTO SHOP 1 MESSENGER ST
5	420430401	Pennsylvania	HARRISBURG	1833 UPS DRIVE HARRISBURG PA
5	420431100	Pennsylvania	HERSHEY	SIPE AVE & MAE STREET
5	420450002	Pennsylvania	CHESTER	FRONT ST & NORRIS ST
4	420490003	Pennsylvania	NOT IN A CITY	10TH AND MARNE STREETS
5	420550001	Pennsylvania	NOT IN A CITY	FOREST ROAD - METHODIST HILL
1	420690101	Pennsylvania	NOT IN A CITY	WILSON FIRE CO. ERIE & PLEASANT
1	420692006	Pennsylvania	SCRANTON	GEORGE ST TROOP AND CITY OF SCRANTON
5	420710007	Pennsylvania	LANCASTER CITY	ABRAHAM LINCOLN JR HIGH GROFFTOWN RD
4	420730015	Pennsylvania	NEW CASTLE	CROTON ST & JEFFERSON ST.
5	420770004	Pennsylvania	ALLENTOWN	STATE HOSPITAL REAR 1600 HANOVER AVE
1	420791100	Pennsylvania	NANTICOKE	255 LOWER BROADWAY (NEXT TO LEON&EDDY'S)
1	420791101	Pennsylvania	WILKES-BARRE	CHILWICK & WASHINGTON STS
4	420850100	Pennsylvania	NOT IN A CITY	PA518 (NEW CASTLE ROAD) & PA418
5	420910013	Pennsylvania	NORRISTOWN	STATE ARMORY - 1046 BELVOIR RD
5	420950025	Pennsylvania	NOT IN A CITY	WASHINGTON & CAMBRIA STS. FREEMANSBURG
5	420990301	Pennsylvania	NOT IN A CITY	ROUTE 34 LITTLE BUFFALO STATE PARK
5	421010004	Pennsylvania	PHILADELPHIA	1501 E LYCOMING AVE AMS LAB
5	421010014	Pennsylvania	PHILADELPHIA	ROXY WATER PUMP STA EVA-DEARNLEY STS
5	421010024	Pennsylvania	PHILADELPHIA	GRANT-ASHTON ROADS PHILA NE AIRPORT
5	421010136	Pennsylvania	PHILADELPHIA	AMTRAK, 5917 ELMWOOD AVENUE
4	421250005	Pennsylvania	CHARLEROI	CHARLER01 WASTE TREATMENT PLANT
4	421250200	Pennsylvania	WASHINGTON	MCCARRELL AND FAYETTE STS
4	421255001	Pennsylvania	NOT IN A CITY	HILLMAN STATE PARK - KINGS CREEK ROAD
4	421290006	Pennsylvania	NOT IN A CITY	OLD WILLIAM PENN HWY & SARDIS AVE
5	421330008	Pennsylvania	YORK	HILL ST.
1	440030002	Rhode Island	NOT IN A CITY	W. ALTON JONES CAMPUS URI PARKERFIELD WE
1	440071010	Rhode Island	EAST PROVIDENCE	FRANCIS SCHOOL, 64 BOURNE AVE
6	440090007	Rhode Island	NARRAGANSETT	TARWELL ROAD, NARRAGANSETT
3	500030004	Vermont	BENNINGTON	AIRPORT RD, BENNINGTON, VERMONT
3	500070007	Vermont	UNDERHILL	PROCTOR MAPLE RESEARCH FARM

Cluster	Site ID	State	City	Location
5	510130020	Virginia	NOT IN A CITY	S 18TH AND HAYES ST
2	510360002	Virginia	NOT IN A CITY	SHIRLEY PLANTATION, ROUTE 5
2	510410004	Virginia	NOT IN A CITY	BEACH, INTERSECTION OF CO.ROADS 655 & 654
5	510590005	Virginia	NOT IN A CITY	CUBRUN LEE RD CHANT, (CUBRUN TREAT PLANT)
5	510590018	Virginia	NOT IN A CITY	MT.VERNON 2675 SHERWOOD HALL LANE
5	510591004	Virginia	SEVEN CORNERS	6100 ARLINGTON BLVD MONTG WARD
5	510595001	Virginia	MC LEAN	LEWINSVILLE 1437 BALLS HILL RD
5	510610002	Virginia	NOT IN A CITY	RT651 C PHELPS WILDLIFE MANAGEMENT AREA
5	510690010	Virginia	NOT IN A CITY	RTE 669, BUTLER MANUF. CO NEAR REST VA
2	510870014	Virginia	NOT IN A CITY	2401 HARTMAN STREET MATH & SCIENCE CTR
2	511130003	Virginia	NOT IN A CITY	SHENANDOAH NP BIG MEADOWS
5	511530009	Virginia	NOT IN A CITY	JAMES S. LONG PARK
2	511611004	Virginia	VINTON	EAST VINTON ELEMENTARY SCHOOL
5	511790001	Virginia	NOT IN A CITY	WIDEWATER ELEM. SCH., DEN RICH ROAD
2	511970002	Virginia	NOT IN A CITY	16-B RURAL RETREAT SEWAGE DISPOSAL
5	515100009	Virginia	ALEXANDRIA	517 N SAINT ASAPH ST, ALEXANDRIA HEALTH
2	518000004	Virginia	SUFFOLK	TIDEWATER COMM. COLLEGE, FREDERIC CAMPUS
2	518000005	Virginia	SUFFOLK	TIDEWATER RESEARCH STATION, HARE ROAD

Appendix E

Episode Types Associated with 8-Hour Ozone Exceedance Days in 2002

Episode Pattern	Year	Month	Day
5	2002	5	16
3	2002	5	24
1	2002	5	25
5	2002	6	1
5	2002	6	5
5	2002	6	6
5	2002	6	9
4	2002	6	10
5	2002	6	11
1	2002	6	12
4	2002	6	20
5	2002	6	21
3	2002	6	22
3	2002	6	23
2	2002	6	24
4	2002	6	25
5	2002	6	26
5	2002	6	27
5	2002	6	29
3	2002	6	30
5	2002	7	1
3	2002	7	2
3	2002	7	3
3	2002	7	4
2	2002	7	5
3	2002	7	7
3	2002	7	8
5	2002	7	9
4	2002	7	12
3	2002	7	13
3	2002	7	14
5	2002	7	15
2	2002	7	16
3	2002	7	17
2	2002	7	18
3	2002	7	19
4	2002	7	20
4	2002	7	21
5	2002	7	22
5	2002	7	23
1	2002	7	27
1	2002	7	28
2	2002	7	29
2	2002	7	30
2	2002	7	31

Episode Pattern	Year	Month	Day
3	2002	8	1
4	2002	8	2
3	2002	8	3
3	2002	8	4
5	2002	8	5
4	2002	8	9
3	2002	8	10
3	2002	8	11
3	2002	8	12
3	2002	8	13
3	2002	8	14
5	2002	8	15
3	2002	8	16
3	2002	8	17
3	2002	8	18
1	2002	8	19
4	2002	8	21
5	2002	8	22
2	2002	8	23
3	2002	9	7
4	2002	9	8
4	2002	9	9
5	2002	9	10
5	2002	9	13
1	2002	9	14
4	2002	9	18

Qualitative Episode Analysis for 2002 Ozone Season

(Ryan & Piety, 2002)

Episode of June 10-12, 2002

***June 10*:** At 0000 UTC, at cold front is analyzed in northern PA. This boundary drifts slightly south and becomes stationary along a Dover-Baltimore-Pittsburgh line by 1200 UTC. Visible images show clear skies with hints of haze at 1600 UTC with only shallow cumulus developing by 1800 UTC. Surface reports at 1800 UTC have scattered reports of haze in the Washington area and more widespread reports west of the Appalachians. The upper air pattern is conducive to the development of a high ozone period with high pressure at 850 mb centered over KY and a modest ridge west of the region at 500 mb. The forecast back trajectories are consistent with standard high ozone cases with westerly flow. Upstream ozone at 1500 UTC at the source of the back trajectories on June 9 is strongly enhanced – in the 70-80 ppb (1-hour average) range. Widespread Code Orange concentrations are found south of the frontal boundary.

June 11: The slow moving/near stationary frontal boundary has now taken the form of a retreating warm front and is well into New England at 1800 UTC with an Appalachian lee trough (ALT) analyzed from Baltimore to northern NC. A broad ridge at 850 mb stretches from AL to the Delmarva with the 500 mb ridge axis remaining just west of the mid-Atlantic. High ozone concentrations are reported right along the I-95 Corridor with scattered Code Red concentrations. The forecast back trajectories show a shift from west-northwesterly flow to along-Corridor. The 1200 UTC sounding at Dulles Airport, VA (IAD) showed continuing westerly flow through the depth of the boundary layer with a very strong cap at 660 mb. A residual mixed layer, often found in association with high ozone cases, is also seen.

June 12: Ozone concentrations fall region-wide on June 12 with strong southwest winds observed. Forecast back trajectories suggest very fast flow backing further to the southwest than the previous two days. Convection develops by afternoon across central PA with a substantial cirrus cloud shield moving into the mid-Atlantic in advance of the rain.

Episode of June 22-26:

During this episode, the mid-Atlantic is sandwiched between two systems. First, a vigorous low that crosses southern Canada on June 20-21 and, second, an upper level low that develops over the southeastern US and then drifts westward with time. A small area of high pressure is wedged between the systems and the highest ozone concentrations are found beneath this high pressure wedge.

***June 22*:** The strong system that crossed Canada earlier in the period has now weakened and moved just northeast of ME (500 mb). A sprawling area of high pressure at 850 mb is found from IN east to just south of Long Island. At the surface at 1200 UTC, high

pressure is located over WV. The frontal boundary associated with the departing Canadian system is quasi-stationary over New England and northern NY. Further south, the upper level low over the eastern Gulf of Mexico has resulted in the development of a coastal trough with sustained easterly winds reaching as far north as NC. The ozone pattern this day follows the synoptic situation closely with good air quality north of the frontal boundary and south across VA and NC where the maritime inflow is strongest. In the Washington, DC area a wide range of concentrations is found. Concentrations range from Code Green in the northwest suburbs to upper Code Orange in the near southern suburbs.

Skies are generally clear across the Washington region with some shallow cumulus developing by afternoon. The 1200 UTC IAD sounding showed light southwest winds beneath the surface based inversion with easterly flow aloft and a very strong cap at 820 mb. The air mass is relatively dry for the season (62-63 $^{\circ}$F).

***June 23*:** Areas of good air quality (Code Green) are again found in the Washington area with no 8-hour ozone violations on this day. The very clean maritime air mass associated with the coastal trough and associated upper level low is seen over VA. The forecast back trajectories show a complex transport pattern with an offshore component at 500 m. Back trajectories based on analysis field are roughly similar with a weaker maritime component. The morning IAD sounding again has a strong inversion based at 850 mb with light and variable winds beneath it.

June 24: By mid-afternoon on June 23, low pressure develops along a frontal boundary north of the Washington area. This system develops quickly so that, by 1200 UTC on June 24, a reinforced cold front has pushed to just north of New York City. By 1800 UTC, the boundary is quasi-stationary across northern NJ and central PA with scattered convection occurring across central PA. Scattered haze is reported south of this frontal boundary in the morning hours, persisting into afternoon. The 1200 UTC IAD sounding shows a residual inversion present at 800 mb though much weaker than the two previous days. An elevated mixed layer is evident just beneath the inversion. The highest ozone concentrations are organized in a west-to-east band across OH and PA into NJ and MD. Scattered Code Red concentrations are found east and northeast of Washington, DC.

***June 25*:** The frontal boundary that was driven southward on June 24 reaches as far as southern NJ by 1200 UTC before returning northward by mid-afternoon. Scattered Code Red concentrations are present in the Washington area. The most unusual aspect of the ozone field on this day is the presence of Code Red concentrations over the urban center of Washington. Haze reports are widespread and forecast back trajectories are less complex than previous days with standard west-northwest flow within the boundary layer.

***June 26*:** The episode ends on June 26 when the upper level ridge begins to flatten. This allows for increased boundary layer winds and a much more unstable atmosphere. The 1200 UTC IAD sounding is nearly dry adiabatic on June 26 in the boundary layer with

strong SW winds throughout (10-15 knots range). The unstable air mass results in convection developing along the Blue Ridges by 1900 UTC with widespread convection later in the afternoon.

Episode of July 1-3, 2002

A relatively mild ozone episode with strong local peaks on July 2, 2002. The peak 1-hour ozone concentration in the Washington area was 158 ppbv in the Washington area on July 2, 2002. Widespread one-hour exceedances on July 2, 2002 were reported near Washington, DC. Throughout the episode, the highest concentrations were found along and east of the I-95 Corridor with lower concentrations further west.

The high ozone event of June 22-26, 2002 ended with an upper level trough crossing the northeastern US. The trough exited the region fairly rapidly but the transition to a ridging pattern was complicated by a small "cut off" low left behind by the trough over New England. This low drifted only slowly eastward to near Nova Scotia by July 2, 2002. Surface winds were north to northeast on June 29, 2002 becoming southwest early on June 30, 2002.

July 1: The 1200 UTC surface analysis shows a fairly standard high ozone pattern. The center of high pressure is located in western VA with a very weak pressure gradient across the region. At 850 mb, high pressure is centered further west over western TN with a weak trough exiting New England. A similar pattern is present at 500 mb although the presence of a lingering closed low just east of Maine suggests that the pattern will remain stationary in the short term not allowing the ridge to build quickly east.

Ozone concentrations in the Washington, DC region were relatively high (86-87 ppbv 8-hour average) on the preceding day (June 30), and back trajectories suggested slow transport along and slightly west of the I-95 Corridor. Peak 1-hour ozone concentrations rose into the 87-99 ppbv range in the Washington area. The bulk of the monitors exceeding the 8-hour standard were in the 90-100 ppbv range, reflecting a rising regional ozone load.

The morning IAD sounding showed a layer of strong southwest winds and the Fort Meade, MD profiler showed steady WSW winds through the day. As reflected in the afternoon visible image, there was significant boundary layer overturning producing widespread, though shallow, cumulus beneath a subsidence inversion based at ~ 770 mb. The 0000 UTC IAD sounding for July 2 shows a residual mixed layer to ~ 800 mb corroborating that deep boundary layer mixing occurred.

***July 2*:** The most unusual aspect of this day was the abrupt decrease in visibility beginning in the late morning and continuing through the afternoon and the speed with which the haze layer moved northeastward into New England. Typically, visibility reaches its maximum with mixing and increased winds in the afternoon and then reaches a minimum just before sunrise. This occurred in the context of continuing brisk southwest winds with 10-13 knots reported by afternoon. The regional surface wind field

was complex with variable winds through the early afternoon becoming southeast.

The upper level analyses at 850 mb and 500 mb are barely distinguishable from the previous day. Of most interest is the position of high pressure at 850 mb that is slightly further north over IL at 1200 UTC. Unlike the standard mid-Atlantic pollution case, however, this continental high has not linked up with the semi-permanent Bermuda High as a lingering trough is present along the Eastern Seaboard. As a result, 850 mb winds reported at IAD were north to north-northwest early on July 2, 2002. At IAD, this flow pattern is consistent to the base of a strong capping inversion at ~ 800 mb. The IAD sounding at 0000 UTC on July 3 showed the boundary layer was further suppressed during the day with mixing only to ~ 1500 m. As a result, only shallow cumulus develops over the mid-Atlantic during the afternoon with the exception of scattered strong convective activity across western PA south into WV.

Back trajectories, and regional surface observations, suggest transport of pollutants from locations northwest of the I-95 Corridor. Upstream ozone at 1600 UTC across northwestern PA was on the order of 70-80 ppbv.

***July 3*:** Although temperatures continued very warm in the upper 90's °F, the characteristics of the air mass appear to change rapidly yet again. Ozone concentrations fell across the region with peaks reaching the Code Orange range.

Forecast back trajectories for July 3 were quite similar to the preceding day and verify well with analysis trajectories. Ozone concentrations upstream, however, ran ~ 10 ppbv lower than on the preceding day. The morning sounding for July 3 was more unstable with a much reduced cap from the previous day although only shallow cumulus formed during the afternoon hours.

The ALT, which was analyzed along the I-95 Corridor for much of July 2, slips slowly eastward and the region of highest ozone concentrations is roughly aligned with its later afternoon position.

<u>Episode of July 31-August 5</u>

***July 31*:** Scattered Code Orange reported in the southern mid-Atlantic. Generally moderate ozone is reported along the I-95 Corridor. Forecast back trajectories suggest fairly fast boundary layer flow with the air mass origination in southern Ontario. Ozone concentrations at 1600 UTC on July 30th in that region were about average (45-50 ppbv). The cold front, located near Norfolk, VA at 0000 UTC, drifts a bit further south by 1200 UTC and then dissipates by 1800 UTC.

***August 1*:** Ozone concentrations rise region-wide. Forecast back trajectories show a strong anti-cyclonic curvature from near Lake Ontario through northern NJ. Again, upstream ozone is relatively low (40-50 ppbv) in southern Canada and northern PA but emissions along the path are likely quite high as the air parcels cross the metropolitan New York area. An ALT is analyzed overnight along and east of the I-95 Corridor. By 1200 UTC, high pressure is centered over WV a climatologically favored location for

high ozone in the I-95 Corridor. A very strong low-level inversion is observed with northeast winds in the layer beneath 800 mb.

***August 2*:** Highest O3 concentrations are reported right along the I-95 Corridor with scattered Code Red observations in the Washington area. The highest ozone concentrations are found south and west of Washington DC. Forecast back trajectories show a good deal of variability. At 1200 UTC, a back door front is analyzed near NYC with surface high pressure still centered near WV. As on August 1, the sounding at IAD shows a strong low-level inversion. Early morning observations show haze along the I-95 Corridor with the most numerous observations in VA and NC. As afternoon mixing occurs, only widely scattered haze reports by afternoon.

***August 3*:** High ozone levels are concentrated along the I-95 Corridor again on August 3. The forecast back trajectories are the standard west-northwest flow although mid-day ozone across northern OH on the preceding day was not extreme (47-56 ppbv). This likely reflects difficulties in the trajectory model in the vicinity of a frontal boundary which reaches central PA by 0000 UTC and then just N of PHL by 1200 UTC where it stalls. Scattered haze is reported across PA, MD and VA lingering into the early afternoon hours.

***August 4*:** Ozone increases along a band from just north of Washington, DC to just north of New York City with widespread Code Red concentrations in a pattern characterized by re-circulation and stagnation. The cold front that reached into eastern PA on the previous day becomes stationary along a line from Portland, ME to just north of New York City and then across central PA to near Pittsburgh. This boundary washes out by 1200 UTC with surface high pressure remaining in place over WV and an ALT analyzed along the I-95 Corridor at 1800 UTC.

***August 5*:** Scattered Code Red ozone concentrations near Washington DC. The presence of significant cloud cover north of the Mason Dixon Line reduces peak ozone in that region. The frontal boundary has washed out over New England with remnants still quasi-stationary over northern PA. The next cold front reaches northwestern PA by 1200 UTC. Again there is considerable vertical shear noted by the forecast back trajectories with southerly flow at the lowest (500 m) layer.

<u>Episode of August 10-14</u>

***August 10*:** High pressure is directly over the mid-Atlantic with dew points in the mid-50's $^{\circ}$F, and clear skies. Temperatures are generally in the upper 80s across the Washington, D.C. region. With high pressure overhead, the forecast back trajectories indicate very light winds and recirculation. Highly variable ozone field with concentrations are present on August 10th in the Washington, D.C area. Scattered Code Orange peaks were reported along the I-95 Corridor. While the Dulles, Virginia (IAD) sounding at 1200 UTC did not show a very strong low-level inversion, with 950 mb temperatures only 21°C, there was a very strong cap at 805 mb with absolutely stable conditions above this level. The presence of a deep residual layer (975-805 mb) suggests

the presence of stagnation. Peak eight-hour average ozone exceedances in the Washington, DC region ranged from 87 ppbv (Arlington and Loudoun Counties, VA) to 93 ppbv (Fairfax County, Annandale, VA).

***August 11*:** Surface high pressure drops slowly southeastward across the mid-Atlantic with the center analyzed in western NC at 1200 UTC drifting to coastal SC by 1800 UTC. The upper level ridge has also moved east and is located over the mid-Atlantic at 1200 UTC. The ozone map for the Washington area shows another day of highly variable peak ozone. A peak concentration of 120 ppbv occurred along the I-95 Corridor northeast of Washington DC. Again, a very clear day in the mid-Atlantic. Winds are generally south to southwest as is reflected in the boundary layer back trajectories. The key factor driving local ozone production appears to be a very stable boundary layer. The 1200 UTC sounding at IAD shows a very strong low-level inversion from 950-900 mb with a deep residual layer beneath a continuing strong subsidence inversion, now based at 760 mb. Peak eight-hour average exceedances ranged from 88 ppbv (Prince Georges County, MD) to 106 ppbv (Washington, D.C., McMillan).

***August 12*:** The upper level ridge remains quasi-stationary with its axis over the mid-Atlantic. The center of high pressure at 850 mb is over NC/GA. At the surface, the characteristic Appalachian lee trough (ALT) is analyzed at 0000 UTC and remains in place through 1800 UTC, continuing into August 13. Clear skies remain, although haze is seen in the 1600 UTC visible image. The surface observations show a rapid and widespread decrease in visibility west and northwest of the I-95 Corridor, shifting further east by early afternoon. The 1200 UTC IAD sounding is similar to the preceding in several respects: a slightly deeper and continuing strong low level inversion, now from 975-925 mb with a strong cap at ~ 770 mb. Winds are fairly strong from the NW. This is reflected in the forecast back trajectories that show a shift to westerly transport. The upwind O3 concentrations at 1600 UTC on August 11 in the vicinity of the origin of the forecast back trajectories is enhanced, on the order of 78-86 ppbv. Ozone concentrations fall this day west of the Appalachians but increase markedly across the mid-Atlantic with widespread Code Red observations from NC to Boston. Widespread exceedances are found in the Washington area, ranging from 85 ppbv (Rockville, MD) to 114 ppbv (Arlington County, VA).

***August 13*:** Periods of calm winds are reported overnight. Significant haze has now spread all along the I-95 Corridor and remains into the afternoon hours. The regional ozone map shows an extensive episode. Skies are again clear with shallow convection developing later in the afternoon. The 1200 UTC IAD sounding showed a continuing strong low level inversion with a residual mixed layer to 850 mb ending just beneath a weak secondary inversion. The cap aloft has lifted to ~ 630 mb and the sounding is more unstable compared to previous day's between the two inversion layers. In addition to a very stable, and hazy, boundary layer, the surface analyses show that the ALT continues in place from late on August 12, to a position slightly further east at 1200 UTC and then backing west at 1800 UTC. As is typically the case, the highest ozone concentrations are

found in proximity to this boundary. Eight-hour exceedances ranged from 87 ppbv (Loudoun County, VA) to 125 ppbv (Fairfax County, Mt. Vernon, VA).

***August 14*:** Back trajectories forecast fairly fast flow along the I-95 Corridor. The increase in southerly wind component results as the upper level ridge axis finally moves offshore. On the back side of the upper level ridge, low level southerly winds increase as the Bermuda High circulation pushes maritime air northward. The haze reports corroborate a slow clean out from south to north with morning haze reported north of Washington, D.C. This episode ends in a very different manner than the standard high ozone episode. Instead of the passage of a sharp cold front, this episode ends gradually as cleaner air sweeps north, winds increase and the atmosphere steadily destabilizes. On August 15, concentrations fall across the region as low level flow becomes more southeast and the Bermuda high fills in westward. Cloud cover spreads over the region on August 16 with ozone concentration continuing to decrease. Peak eight-hour exceedances ranged from 87 ppbv (Arlington County, VA) to 101 ppbv (Fort Meade, MD).

Episode of September 9-10

Summary: A two-day ozone episode with northeasterly flow due to high pressure to the north and west and Tropical Storm Gustav to the southeast. Strong subsidence occurs over the region as Gustav approached and moves along the North Carolina coast. Northeasterly winds occurs due to clockwise flow around high pressure over the Ohio Valley and counter-clockwise flow around Gustav as it neared the Outer Banks. Highest ozone concentrations on September 9th occur in central Pennsylvania, northeast of Baltimore, near Annapolis, MD and west of Fairfax County, VA. A sharp ozone gradient was evident on the 10th with low concentrations east of a Baltimore-Rockville, MD-Fairfax City, VA line while eight-hour exceedances occurred in counties immediately west and south of Fairfax.

September 9: At 1200 UTC, Tropical Storm Gustav is southeast of Cape Hatteras, NC with high pressure was over Ohio and Indiana. Widespread surface haze observed in Ohio, Michigan, Indiana, and Illinois. Very warm air aloft over Pennsylvania and West Virginia enhanced stable atmospheric dispersion conditions. The upper air pattern indicates a large ridge over the eastern half of the US, with a closed low associated with Gustav off the southeast coast. Strong subsidence occurs over Mid-Atlantic region, centered over south-central Pennsylvania. Forecast back trajectories indicate flow from the northeast megalopolis (Philadelphia to New York City). Code Orange concentrations are observed throughout much of New Jersey, northeast Maryland, and the western Virginia suburbs of Washington, DC. Code Red was reached northeast of Baltimore. Code Green conditions occurred in coastal southern Delaware and Maryland due to the influence of clean air from Gustav.

September 10: Tropical Storm Gustav nearer Cape Hatteras with heavy precipitation along the Outer Banks. Widespread surface haze was again observed throughout the Ohio Valley into Indiana, Illinois, and Michigan. As Gustav moves closer to the North Carolina coast, the region of strong subsidence moves further west, along and to the west

of the Appalachians. Forecast back trajectories indicate the influence from Gustav as the flow was generally from the east. The maritime tropical air from Gustav reaches as far inland as Washington, D.C. but stable, continental air is quite close to the west as indicated by the 8-hour ozone peak concentration map. A very sharp ozone gradient is evident. Conditions range from Code Green to Code Red just several miles apart in Fairfax County, VA. Code Orange conditions occur west of Baltimore and in the western Virginia suburbs of DC while Code Green conditions occur along I-95 and eastward. Code Red conditions occur just west of I-95 at three Virginia locations in the Washington, D.C. region.

Appendix F-4

Modeling Domain Boundary

Appendix H-5

Horizontal Grid Definition for MM5
And
CMAQ Modeling Domain

Appendix H-6

Vertical Layer Definitions for MM5
And
CMAQ Modeling Domain

Appendix H-7

Report on the Set-up and Application of the 36 km CMAQ Model
And
The Extraction of the Boundary Conditions

Appendix H-8

MM5 Model Performance Evaluation

Appendix H-9

MM5 Model Configurations

Appendix H-10

SMOKE Processing Description and Configuration

Appendix H-11

CMAQ Configuration

Appendix H-12

CMAQ Model Performance

Appendix H-13

Additional Information on the RRF and the Modeled Attainment Test

Appendix H-14

Future Year Modeling Emissions and Controls

OTC CMAQ 12km Modeling Domain

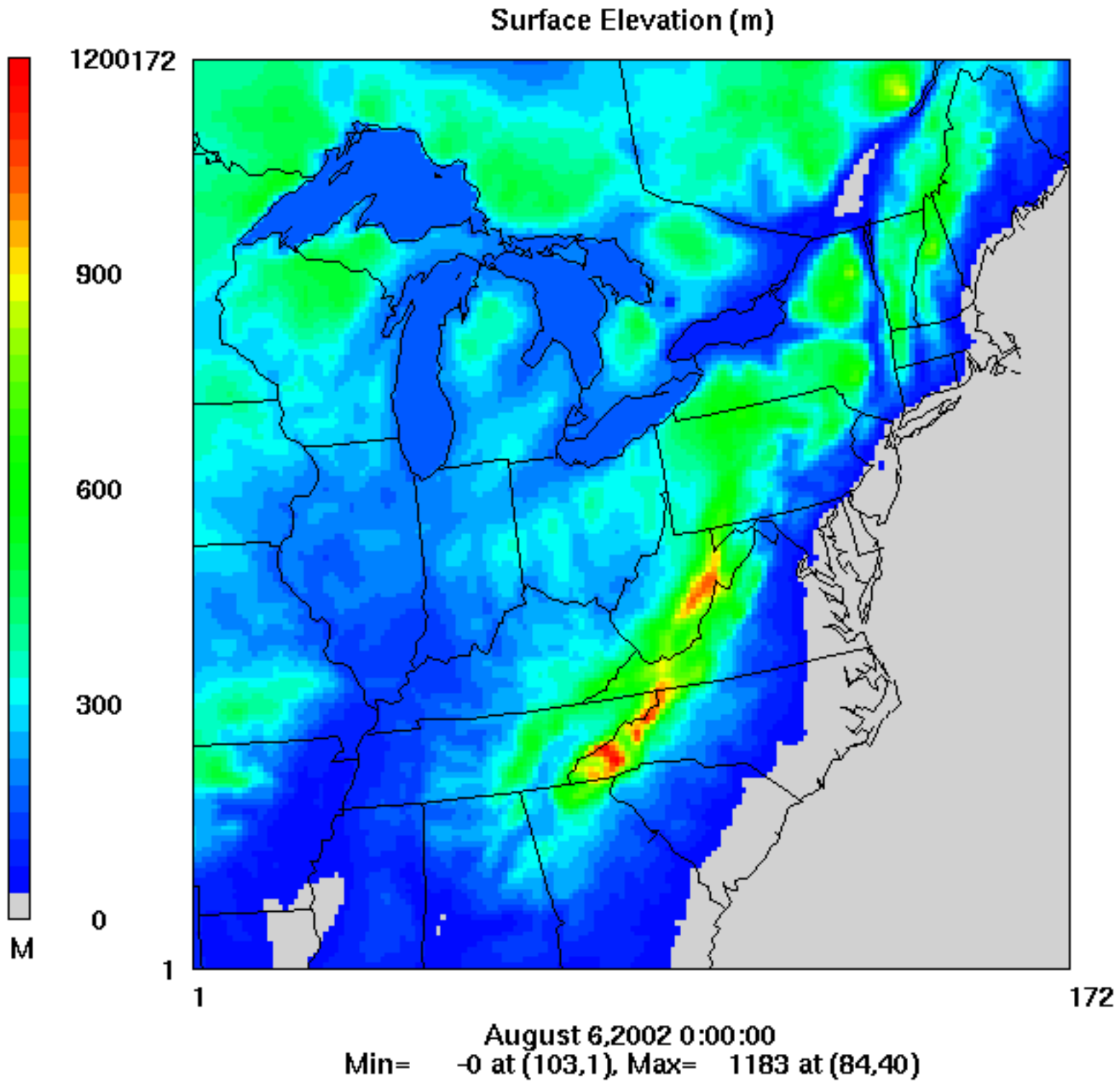

Appendix F-5
Horizontal Grid Definition for MM5 and CMAQ Modeling Domain

Table F-5-1. OTC Grid Definitions for MM5 and CMAQ

Model	Columns Dot (nx)	Rows Dot (ny)	X-Origin (km)	Y-Origin (km)
MM5 36-km	149	129	-2664	-2304
CMAQ 36-km	145	102	-2628	-1728
MM5 12-km	175	175	252	-900
CMAQ 12-km	172	172	264	-888

Appendix F-6
Vertical layer Definitions for MM5 and CMAQ Modeling Domain

Table F-6-1
OTC Vertical Layer Definition for MM5 Simulations and Approach for Reducing CMAQ Layers by Collapsing Multiple MM5 Layers

MM5					CMAQ				
Layer	Sigma	Pres(mb)	Height(m)	Depth(m)	Layer	Sigma	Pres(mb)	Height(m)	Depth(m)
29	0.000	50	18600	2145	23	0.000	50	18600	4290
28	0.040	88.5	16450	2145					
27	0.080	127.1	14300	1460	21	0.080	127.1	14300	2920
26	0.123	168.5	12800	1460					
25	0.168	211.8	11400	1200	20	0.168	211.8	11400	2390
24	0.218	260.0	10200	1200					
23	0.268	308.1	8990	934	19	0.268	308.1	8990	1870
22	0.318	356.3	8060	934					
21	0.368	404.5	7120	772	18	0.368	404.5	7120	1540
20	0.418	452.6	6350	772					
19	0.468	500.8	5580	662	17	0.468	500.8	5580	1320
18	0.518	549.0	4920	662					
17	0.568	597.1	4250	581	16	0.568	597.1	4250	1160
16	0.618	645.3	3670	581					
15	0.668	693.4	3090	532	15	0.668	693.4	3090	532
14	0.718	741.6	2560	455	14	0.781	741.6	2560	455
13	0.763	785.0	2110	388	13	0.763	785.0	2110	388
12	0.803	823.5	1720	337	12	0.803	823.5	1720	337
11	0.839	858.2	1380	290	11	0.839	858.2	1380	290
10	0.871	889.0	1090	247	10	0.871	889.0	1090	247
9	0.899	916.0	844	207	9	0.899	916.0	844	207
8	0.923	939.1	637	169	8	0.923	939.1	637	169
7	0.943	958.3	468	133	7	0.943	958.3	468	133
6	0.959	973.7	334	107	6	0.959	973.7	334	107
5	0.972	986.3	227	82	5	0.972	986.3	227	82
4	0.982	995.9	145	57	4	0.982	995.9	145	57
3	0.989	1002.6	89	40	3	0.989	1002.6	89	40
2	0.994	1007.5	48	27	2	0.994	1007.5	48	27
1	0.9974	1010.7	21	21	1	0.9974	1010.7	21	21
0	1.000	1013.24	0	0	0	1.000	1013.24	0	0

Note: Layer-top pressures assume a surface pressure of 1013.24 hPa. Layer-top heights are determined by averaging MM5 (CMAQ)-calculated layer-top heights over time (August 2002) and space (the entire 172x172 domain).

Table F-6-1
OTC Vertical Layer Definition for MM5 Simulations and Approach for Reducing CMAQ Layers by Collapsing Multiple MM5 Layers

MM5					CMAQ				
Layer	Sigma	Pres(mb)	Height(m)	Depth(m)	Layer	Sigma	Pres(mb)	Height(m)	Depth(m)
29	0.000	50	18600	2145	23	0.000	50	18600	4290
28	0.040	88.5	16450	2145					
27	0.080	127.1	14300	1460	21	0.080	127.1	14300	2920
26	0.123	168.5	12800	1460					
25	0.168	211.8	11400	1200	20	0.168	211.8	11400	2390
24	0.218	260.0	10200	1200					
23	0.268	308.1	8990	934	19	0.268	308.1	8990	1870
22	0.318	356.3	8060	934					
21	0.368	404.5	7120	772	18	0.368	404.5	7120	1540
20	0.418	452.6	6350	772					
19	0.468	500.8	5580	662	17	0.468	500.8	5580	1320
18	0.518	549.0	4920	662					
17	0.568	597.1	4250	581	16	0.568	597.1	4250	1160
16	0.618	645.3	3670	581					
15	0.668	693.4	3090	532	15	0.668	693.4	3090	532
14	0.718	741.6	2560	455	14	0.781	741.6	2560	455
13	0.763	785.0	2110	388	13	0.763	785.0	2110	388
12	0.803	823.5	1720	337	12	0.803	823.5	1720	337
11	0.839	858.2	1380	290	11	0.839	858.2	1380	290
10	0.871	889.0	1090	247	10	0.871	889.0	1090	247
9	0.899	916.0	844	207	9	0.899	916.0	844	207
8	0.923	939.1	637	169	8	0.923	939.1	637	169
7	0.943	958.3	468	133	7	0.943	958.3	468	133
6	0.959	973.7	334	107	6	0.959	973.7	334	107
5	0.972	986.3	227	82	5	0.972	986.3	227	82
4	0.982	995.9	145	57	4	0.982	995.9	145	57
3	0.989	1002.6	89	40	3	0.989	1002.6	89	40
2	0.994	1007.5	48	27	2	0.994	1007.5	48	27
1	0.9974	1010.7	21	21	1	0.9974	1010.7	21	21
0	1.000	1013.24	0	0	0	1.000	1013.24	0	0

Note: Layer-top pressures assume a surface pressure of 1013.24 hPa. Layer-top heights are determined by averaging MM5 (CMAQ)-calculated layer-top heights over time (August 2002) and space (the entire 172x172 domain).

Appendix F-7

Report on the Set-up and Application of the 36 km CMAQ Model and the Extraction of the Boundary Conditions

Development of CMAQ Boundary Conditions

One of the necessary inputs for performing CMAQ simulations is the boundary condition (BC). The past CMAQ regional photochemical modeling covering episodes relied on the use of 'clean' BCs. Recently, it has been recognized that seasonal and annual simulations, the appropriate BCs can be developed from global models (EPA, 2004). With the development and progress of global chemical transport models such as GEOS-CHEM of Harvard University (http://www-as.harvard.edu/chemistry/trop/geos/index.html) and MOZART of National Center for Atmospheric Research (NCAR) (http://www.acd.ucar.edu/science/gctm/mozart/index.php), it is possible to generate BCs for CMAQ through appropriate interpolation of the global model outputs.

In this note we describe the development of the BCs for the OTC Modeling Committee application of CMAQ at 36 km grid spacing and perform a limited comparison with the BCs reported for Visibility Improvement State and Tribal Association of the Southeast's (VISTA) modeling domain. GEOS-CHEM simulation data for 2002 were obtained through the efforts of the Northeast Consortium of Air Use Management (NESCAUM) in December 2004. The GEOS-CHEM simulation data was at the spatial resolution of 4˚ by 5˚ in the horizontal and 20 layers in the vertical extending from surface to about 100 mb. The model provides information for about 50 chemical gas and particulate matter chemical species. We utilized and modified version of the GEOS-CHEM to CMAQ interface program developed by Prof. Daewon Byun of Huston University so as to match the OTC 36 km modeling domain. To provide an added level of confidence in the development of the BCs, a comparison is performed with the BCs reported for the VISTAs 36 km modeling domain. It should be noted that the two domains differ in their definition with the OTC domain being smaller horizontally and has more layers in the vertical when compared with the VISTA domain.

Spatial patterns of Ozone and SO_4

Figure 1 displays ozone concentrations in layer 1 along the boundaries for OTC and VISTA domains at hour 15 on August 13, 2002. Although the OTC domain is slightly smaller than VISTA domain, both exhibit similar maximum concentration level of about 70 ppb. The OTC domain had slightly higher peak ozone (168 ppb) at the top of the domain along the boundaries than VISTA (see Figure 2), which has a maximum of 139 ppb. This is not unexpected since the top layer of the OTC domain is higher than VISTA domain. Figure 3 shows similar displays for SO_4 at the boundary at the lowest layer of the OTC and VISTA domains.

Averaged Ozone and SO_4 concentrations at the boundaries of the modeling domain

Table 1 lists the averaged ozone concentrations at surface and for the whole boundary layer, (OTC domain with 22 layers, and VISTA domain with 19 layers), at each one of the four boundaries. In both cases the concentrations exhibit similar pattern, with higher concentrations at south and east boundaries and low concentration in the north and west boundaries. Table 2 is similar to Table 1, except it lists SO_4 concentrations. The higher

SO_4 boundary conditions at east direction may be due to the outflow from the US continent.

Averaged Ozone and SO_4 BC vertical profiles from each of the domain

Figure 4 displays the average vertical profile of ozone concentrations at each of four boundaries. As to be expected, GEOS-CHEM yields increasing ozone concentrations with increasing altitude and this is reflected in Figure 4. Figure 5 displays the average vertical profile of SO_4 concentration at each of the four boundaries. The high SO_4 in the East direction may be due to the outflow from the US continent.

References

EPA (2004): Use of GEOS-CHEM for CMAQ Boundary Conditions, http://www.epa.gov/air/interstateairquality/pdfs/GEOSCHEMforCMAQ_Description.pdf

Table 1: The average ozone concentrations at each one of the four boundaries for the OTC and VISTA 36 km domains

Boundary	OTC (22 layer averaged)	VISTA (19 layer averaged)	OTC (surface)	VISTA (surface)
South	43.9 ppb	35.6 ppb	36.8 ppb	31.6 ppb
East	52.2 ppb	46.4 ppb	40.5 ppb	40.7 ppb
North	34.1 ppb	21.9 ppb	13.7 ppb	13.5 ppb
West	40.0 ppb	32.9 ppb	25.8 ppb	24.9 ppb

Table 2: The average SO_4 concentrations at each one of the four boundaries for the OTC and VISTA 36 km domains

Boundary	OTC (22 layer averaged)	VISTA (19 layer averaged)	OTC (surface)	VISTA (surface)
South	0.54	0.51	0.70	0.56
East	1.50	1.67	2.04	1.88
North	0.45	0.54	0.63	0.64
West	0.42	0.47	0.53	0.53

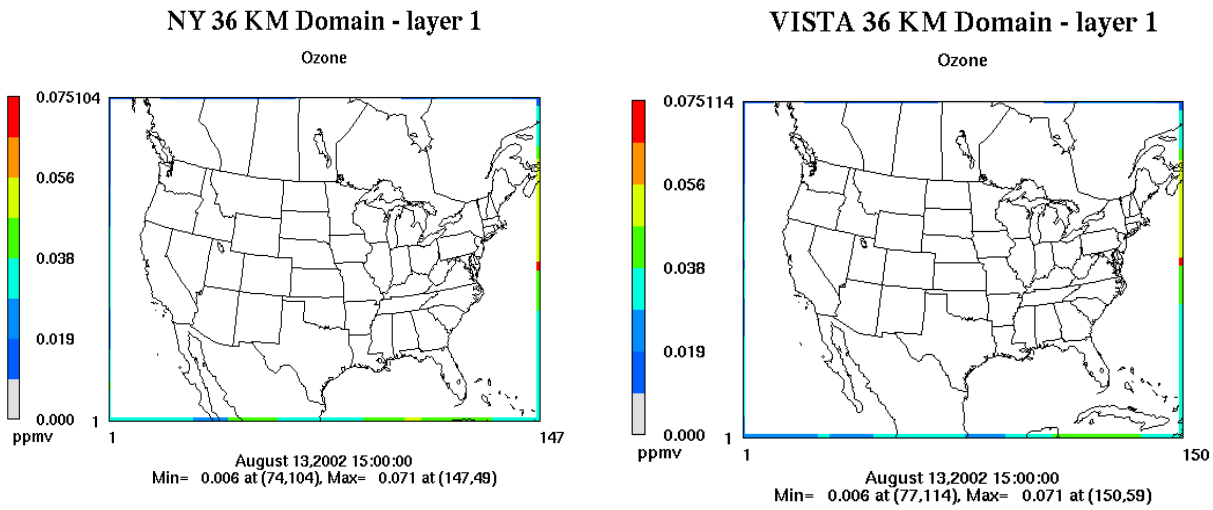

Figure 1: The lowest layer of ozone BC for OTC and VISTA 36 Km domain

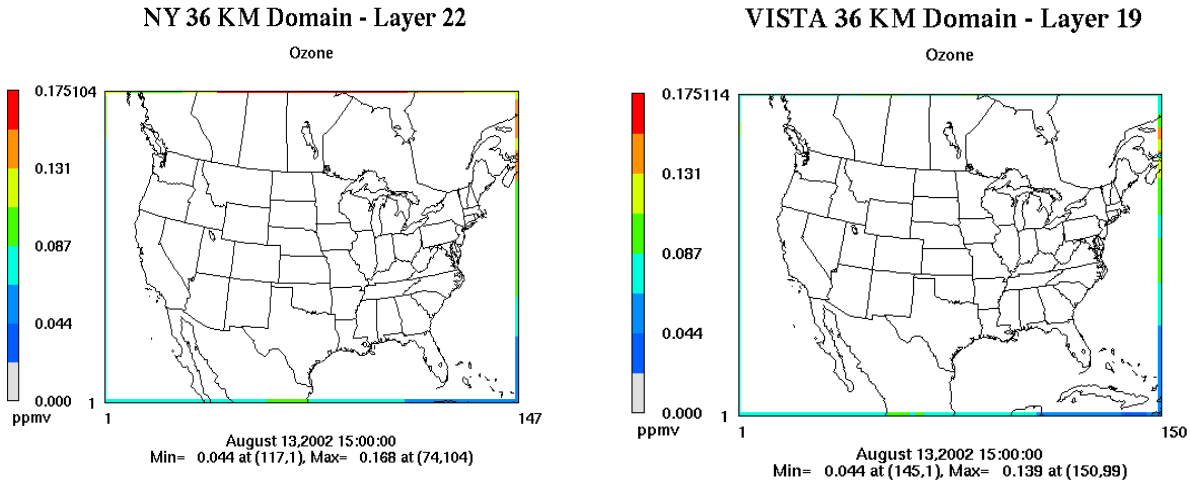

Figure 2: The top layer ozone BC for OTC and VISTA 36 Km domain

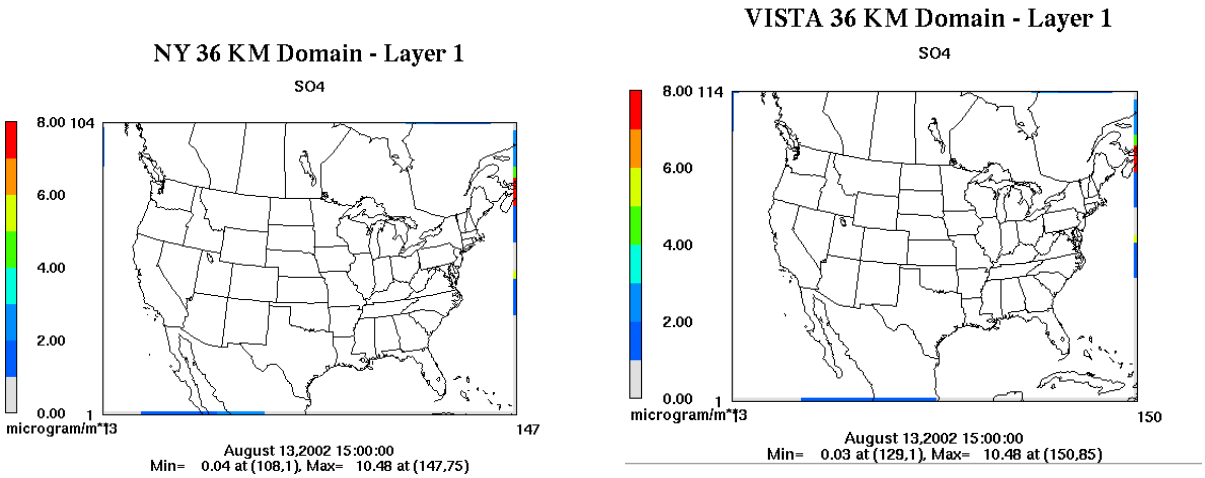

Figure 3: The lowest layer SO4 BC for OTC and VISTA 36 Km domain

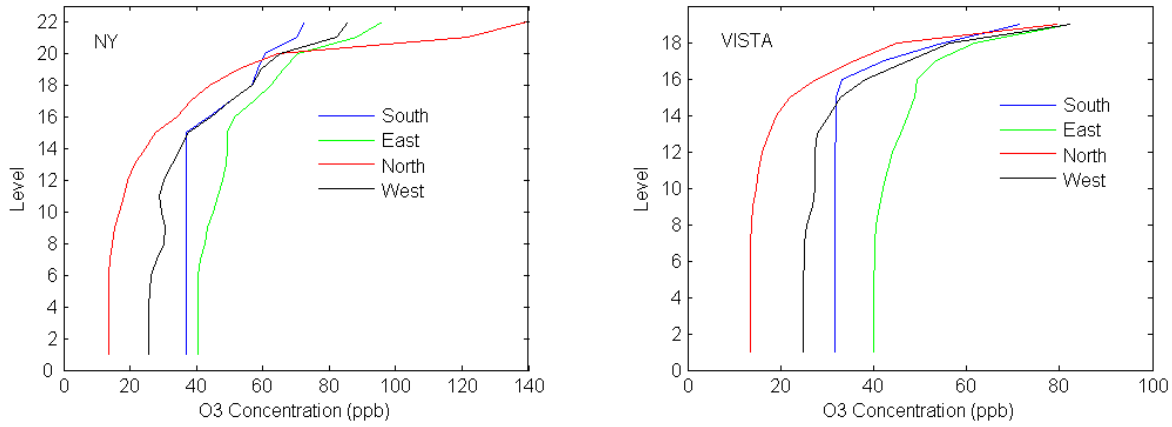

Figure 4: Averaged vertical profiles from each direction of ozone BC

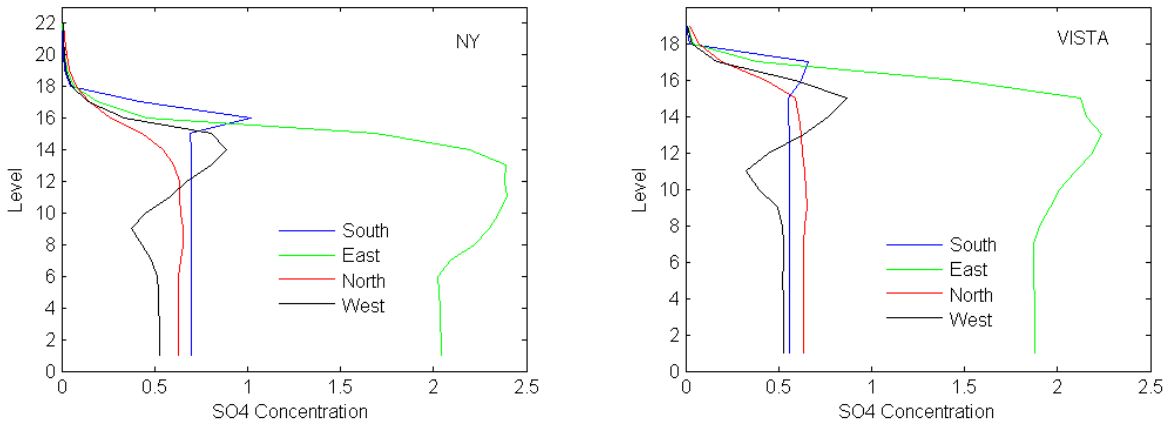

Figure 5: Averaged vertical profiles from each direction of SO4 BC

Appendix F-8

MM5 Model Performance Evaluation

March 4, 2004

Analysis of MM5 Simulations based on three PBL schemes over the eastern US for August 6 to 16, 2002

Winston Hao, Mike Ku, and Gopal Sistla
NYSDEC-DAR
Albany, NY 12233

Introduction: In a prior report[1] dated December 8, 2003, a comparison was performed between meteorological measurements and the simulated MM5 fields for August 6 to 16, 2002 based upon 3 approaches to the PBL. In this report, we provide the comparison with TDL and CASTNet measurements.

Purpose: The intent of this exercise was to investigate the response of three PBL schemes and develop a recommendation for the use of a PBL method for developing meteorological fields for the May through September of 2002, in support of air quality modeling work.

Approach: In this study, Prof. Dalin Zhang of University of Maryland, applied 3 PBL schemes for the August 6 to 16, 2002, a period in which the OTR experienced high ozone as well as particulate levels. The three schemes were (a) modified Blackadar [BL], (b) the Pleim-Xiu scheme with the soil module [PX], and (c) modified Blackadar with soil module [SSIB]. The simulated meteorological fields were compared to the measurements from TDL (NWS) and CASTNet.

Model setup: The MM5 model setup is similar to the earlier exercise of developing meteorological fields for July 1997, with the first level at 10 m. The projection for this exercise was that recommended by the RPOs, and has a spatial resolution of 12 km (see Figure 1)

Analysis: The basic approach used is to compare domain-wide averaged measurements and predictions for surface temperature, wind speed and direction, and where available with humidity. While the CASTNet sites are more representative of rural areas, the TDL are reflective of urban/suburban settings. There are 47 CASTNet and about 600 NWS sites in the TDL data set over the modeling domain.

TDL data and MM5 simulations:

Average wind speed and direction (see Figures 2a through 2c)

[1] Hao, W., Ku, M., and Sistla, G. (2002) 'Preliminary analysis of MM5 simulations for the August 6 to 17, 2002 – A status report', NYSDEC, Albany, NY 12233

Overall, the 3 PBL schemes provide good agreement with the observed average wind direction . In terms of wind speed:
BL: Under prediction of daytime maximum wind speed, but agreement with nighttime low windspeed
P-X: Systematic under prediction during daytime and over prediction in the nighttime
SSIB: Under prediction during daytime with phase lag, the predicted maximum occurring latter than the measured maximum

Temperature (see Figures 3a through 3c)

BL: Good agreement throughout the episode days
P-X: Initial over prediction of temperature minimum, and under prediction of daytime maximum
SSIB: Over prediction of daytime maximum

Humidity (see Figures 4a through 4c)

BL: While the general trend is captured during the episode, there is poor agreement between the observed and predicted diurnal patterns, with the observation showing a double peak versus one peak based on predictions.
P-X: The model yields the observed daily double peak, but with underprediction and a phase lag.

CASTNet data and MM5 simulations:

Average wind speed and direction (see Figures 5a through 5c)

All 3 PBL approaches provide good agreement with the observed average wind direction. In terms of wind speed:

BL: Wind speed over prediction during the daytime, a feature that differs from the TDL results, but good agreement with nighttime minimum
P-X: Wind speed over prediction, for both day- and nighttime hours.
SSIB: Wind speed over prediction at the start and end of the episode, and exhibiting a phase-lag of 1 to 2 hours

Average Temperature (see Figures 6a through 6c)

BL: Overall good agreement
P-X: Systematic under prediction during daytime and over prediction in the nighttime with phase lag
SSIB: Over prediction during the daytime, but good agreement during nighttime

Average Humidity

There were no data to perform this comparison, as mixing ratio cannot be estimated due to lack of station pressure.

Spatial distribution of correlation between TDL data and MM5 simulations

Wind Speed (see Figures 7a through 7c)
BL: The correlation levels are generally in the 0.7 or higher range over most portions of the domain, with lower values mainly confined to the southeastern and western parts of the domain.
P-X: The correlation levels are slightly lower compared to BL, with more stations exhibiting a correlation level of less than 0.6 in the Southeastern portion of the domain.
SSIB: The correlation levels are similar to P-X, but with increased number of stations exhibiting correlation levels less than 0.6 over the domain

Temperature (see Figures 8a through 8c)
BL: The correlation levels are generally higher (>0.97) over the northeastern portions of the domain, with the remainder of the domain exhibiting correlation levels in the range of 0.94 to 0.96
P-X: Overall the correlation levels are slightly lower than BL
SSIB: Similar to P-X, with correlation levels in the 0.95 throughout the domain

Humidity (see Figures 9a through 9c)
BL: The correlation levels over the northeast are generally higher than the rest of the domain, although most portions of the domain report correlation of 0.70 or higher
P-X: The correlation levels are comparable or slightly better than BLK
SSIB: The correlation levels are comparatively lower than the other two over the northeastern portions of the domain

Discussion and conclusions

On an overall basis, it appears that the BL scheme exhibits a better correspondence to the measured data than the other two schemes. The exception being the poor capture of the observed diurnal pattern of humidity in the case of the BL scheme. While the P-X scheme shows a better correspondence with the observed diurnal pattern for humidity, it fails to perform well for wind speed and temperature. Further work is needed to improve the performance of these methods. An examination of other studies in which the P-X scheme was applied suggests the predictive performance is similar to this study.

Other comparisons of model to observed or measured parameters such as cloud cover, precipitation, and upper air soundings/profiler network are under examination to provide a comprehensive evaluation of the meteorological model. Also, the use of the model simulated fields in air quality model and comparison to pollutant fields is also in progress.

Figure 2a MM5 Simulation - UMD BLK & TDL - Aug 6 01Z to Aug 17 00Z 2002

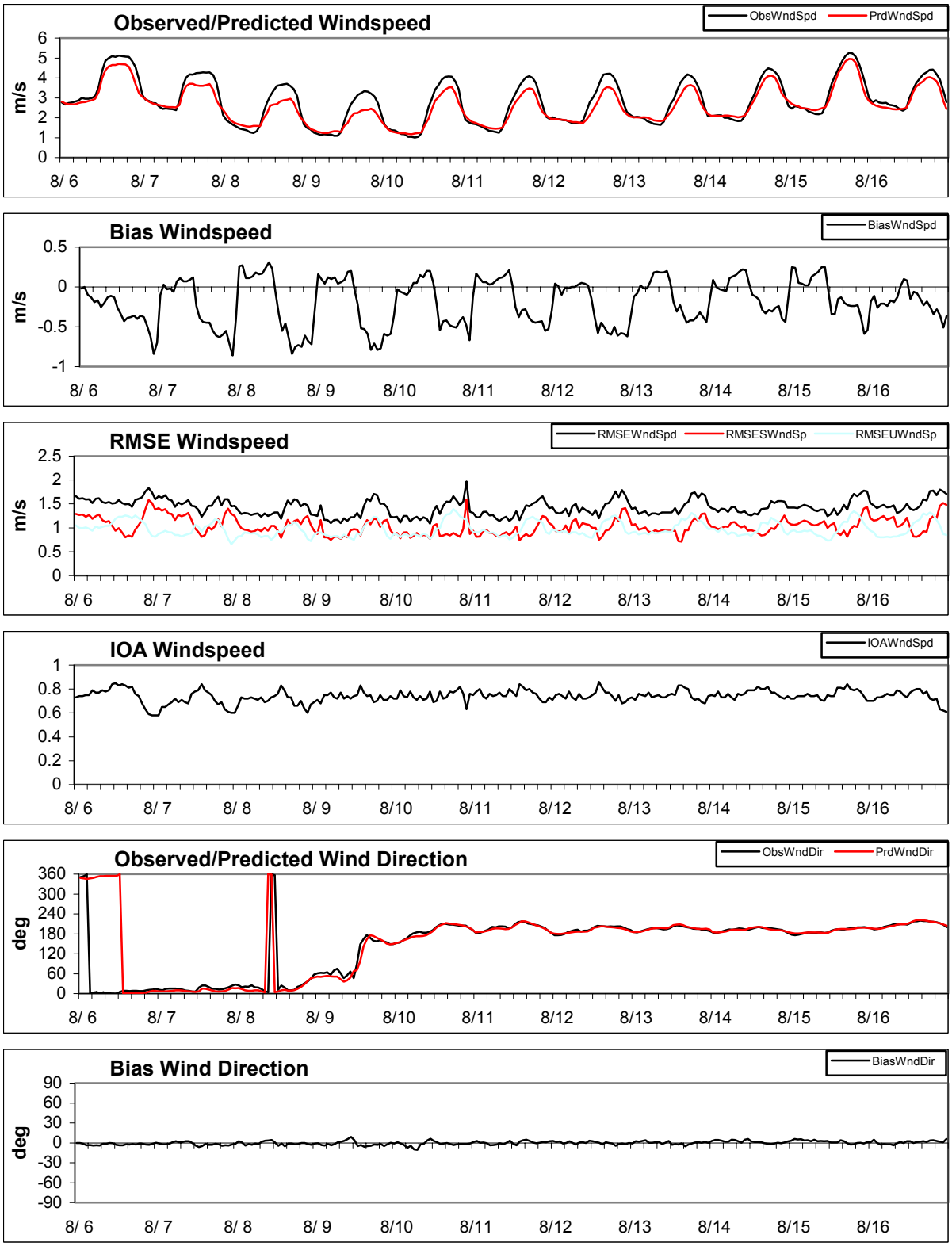

Figure 2b MM5 Simulation - UMD PX & TDL Aug 06 01Z to Aug 17 00Z 2002

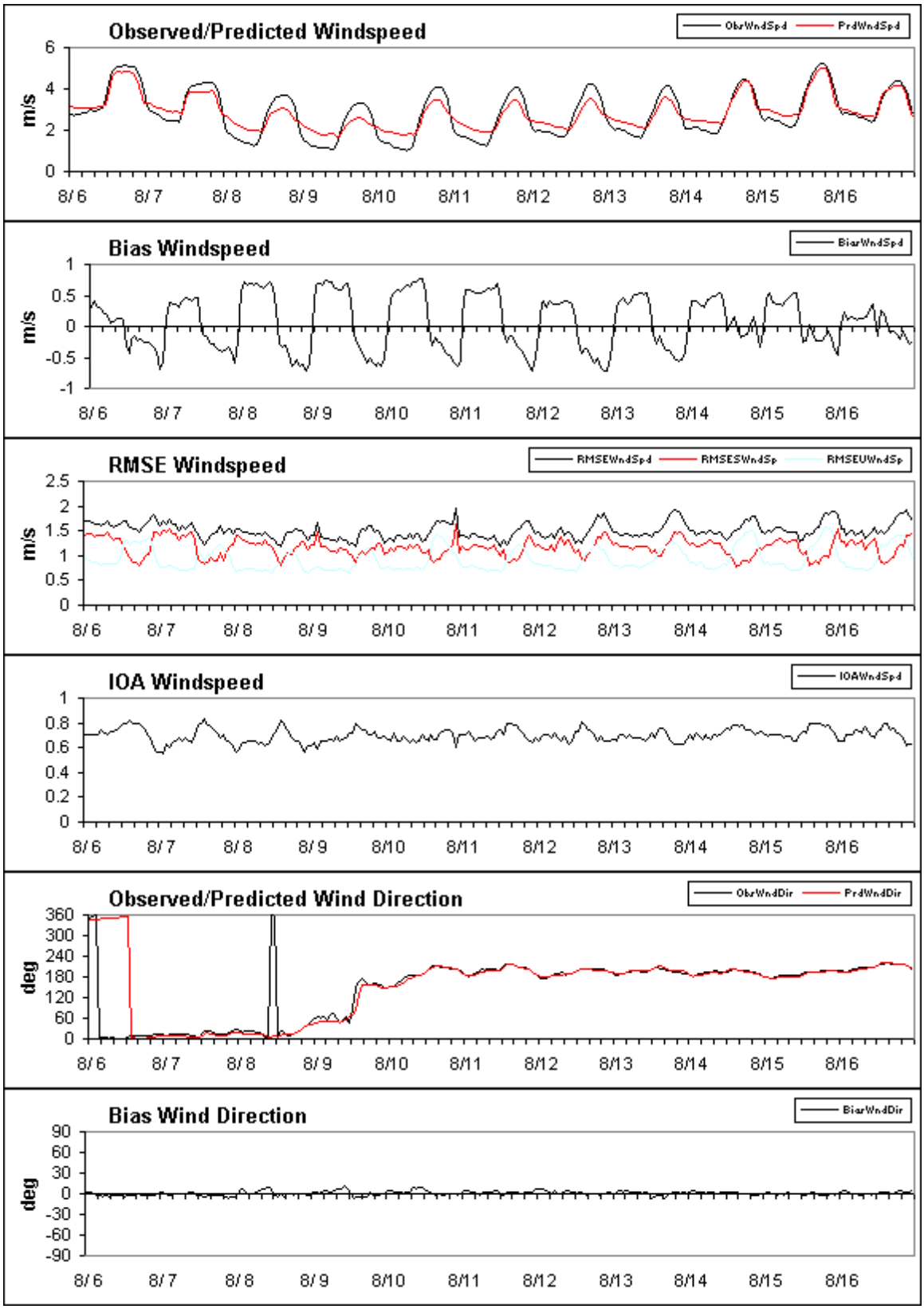

Figure 2c MM5 Simulation - UMD SSIB & TDL Aug 06 01Z to Aug 17 00Z 2002

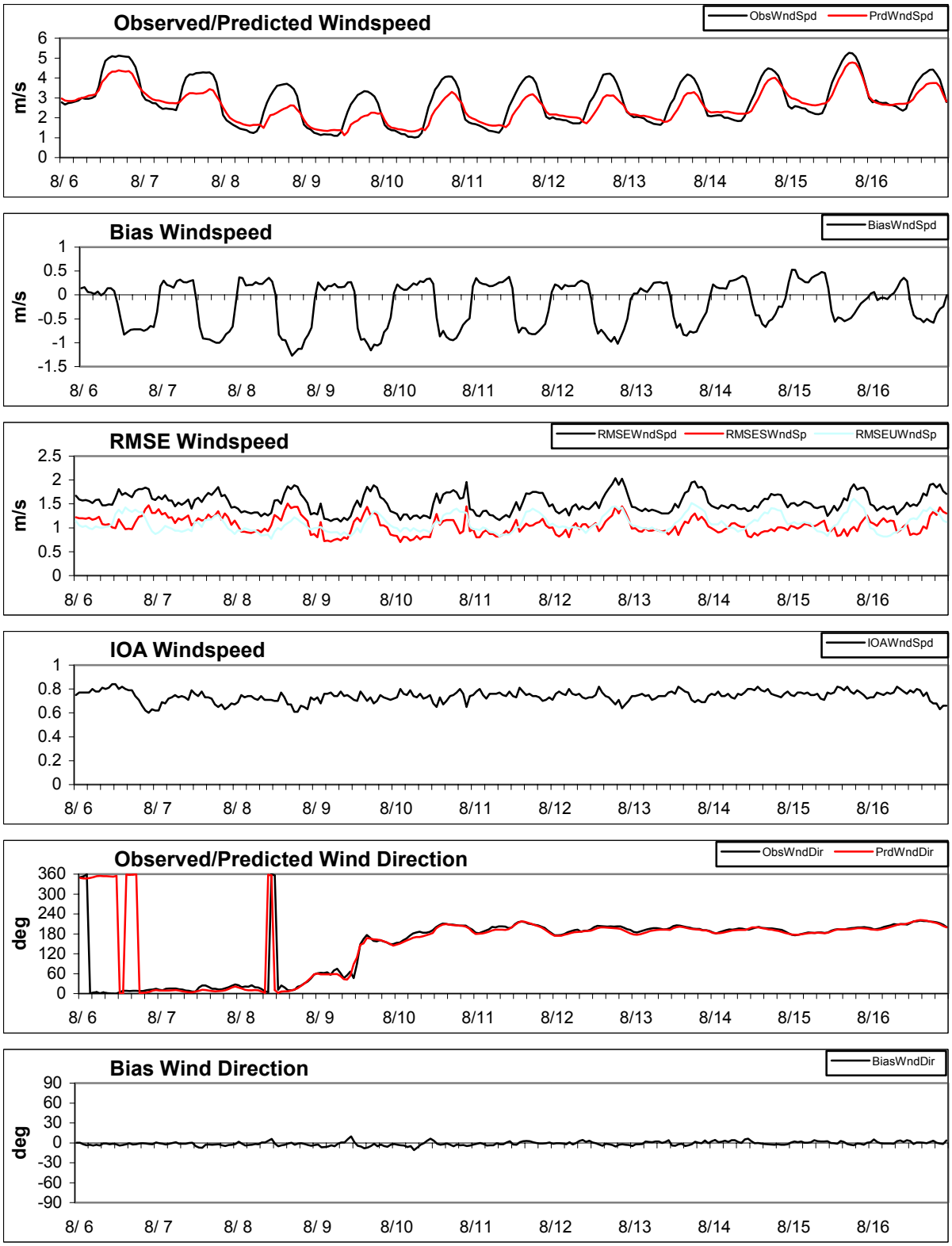

Figure 3a MM5 Simulation - UMD BL & TDL Aug 6 01Z to Aug 17 00Z 2002

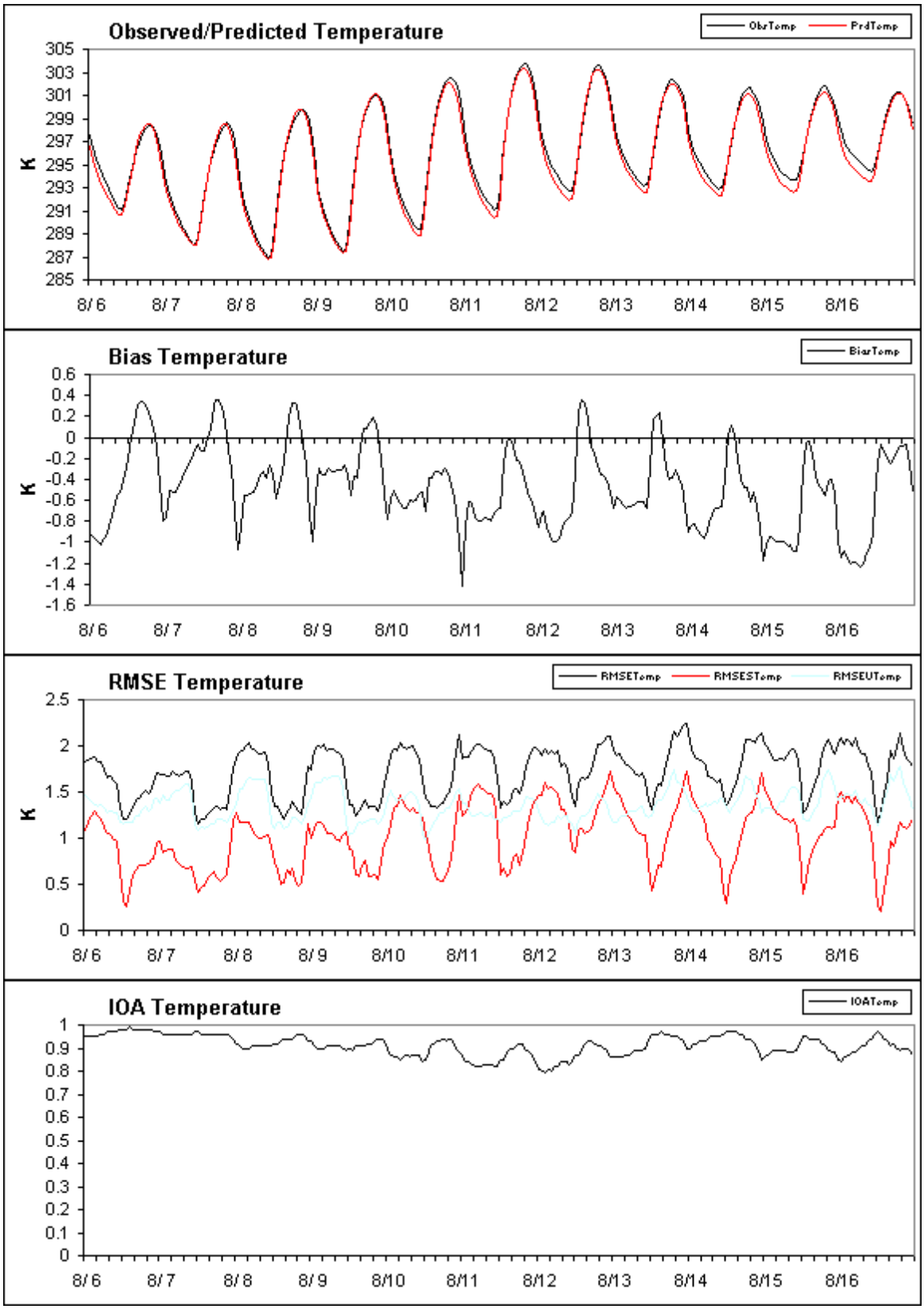

Figure 3b MM5 Simulation - UMD PX & TDL Aug 06 01Z to Aug 17 00Z 2002

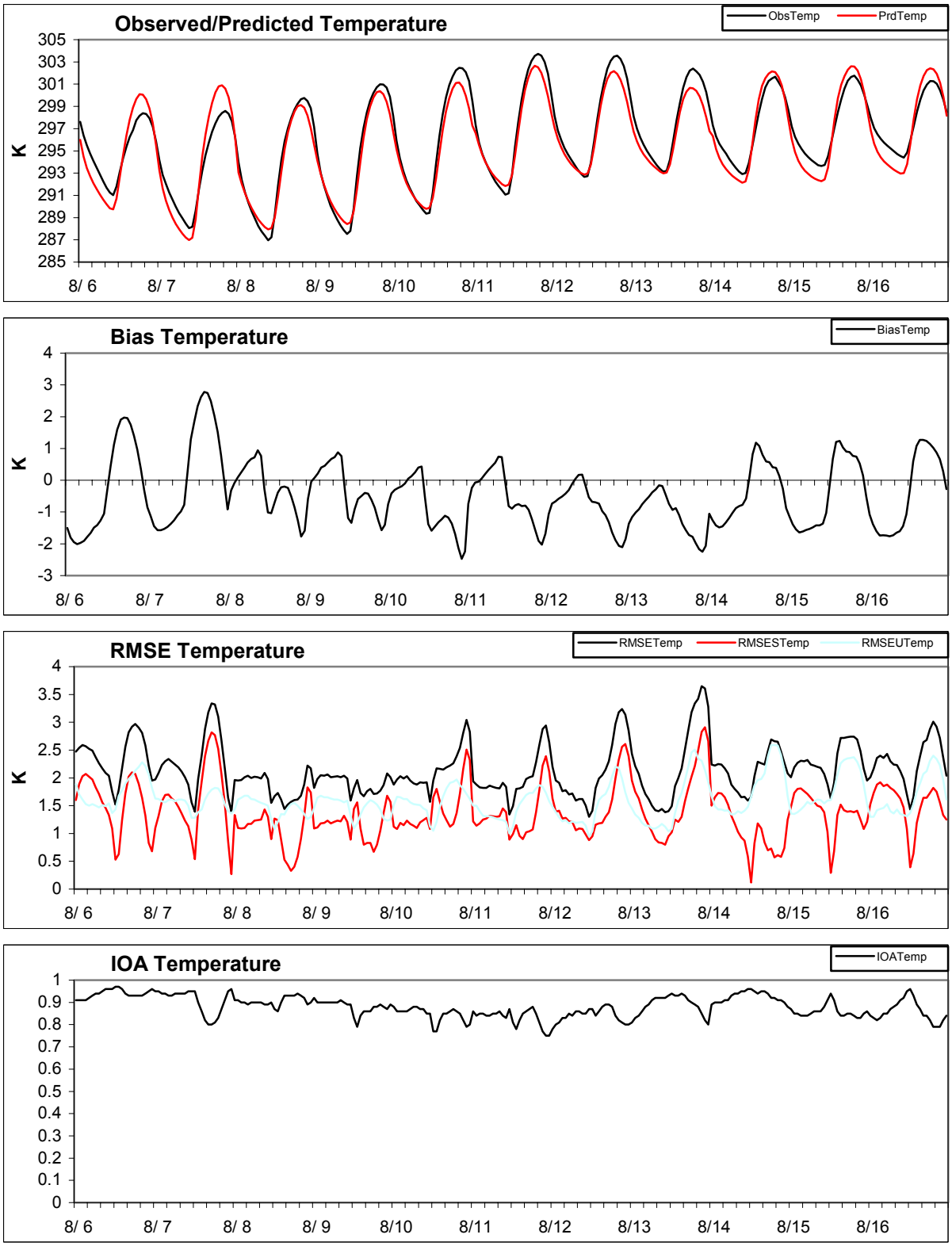

Figure 3c MM5 Simulation - UMD SSIB & TDL Aug 06 01Z to Aug 17 00Z 2002

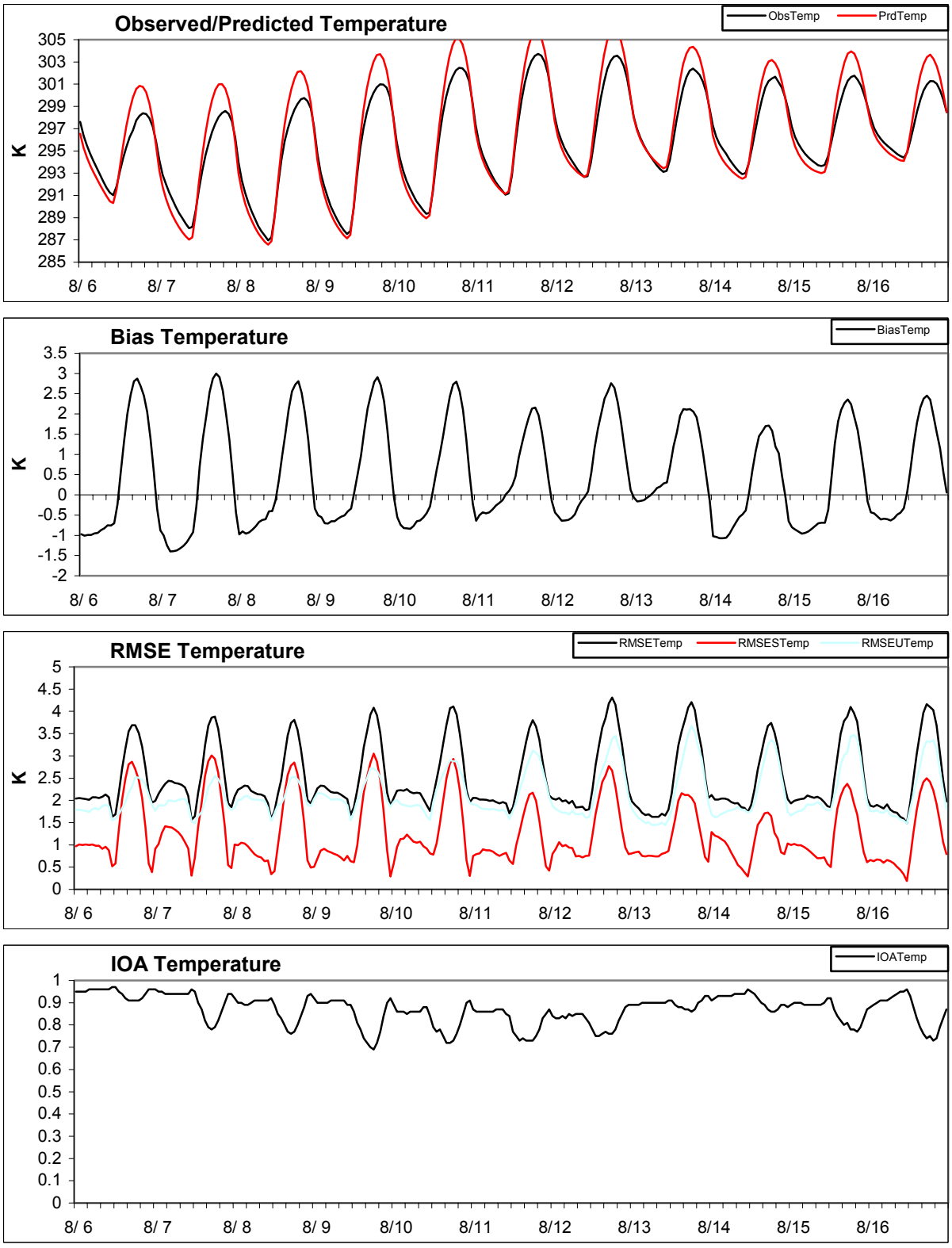

Figure 4a MM5 Simulation - UMD BL & TDL Aug 6 01Z to Aug 17 00Z 2002

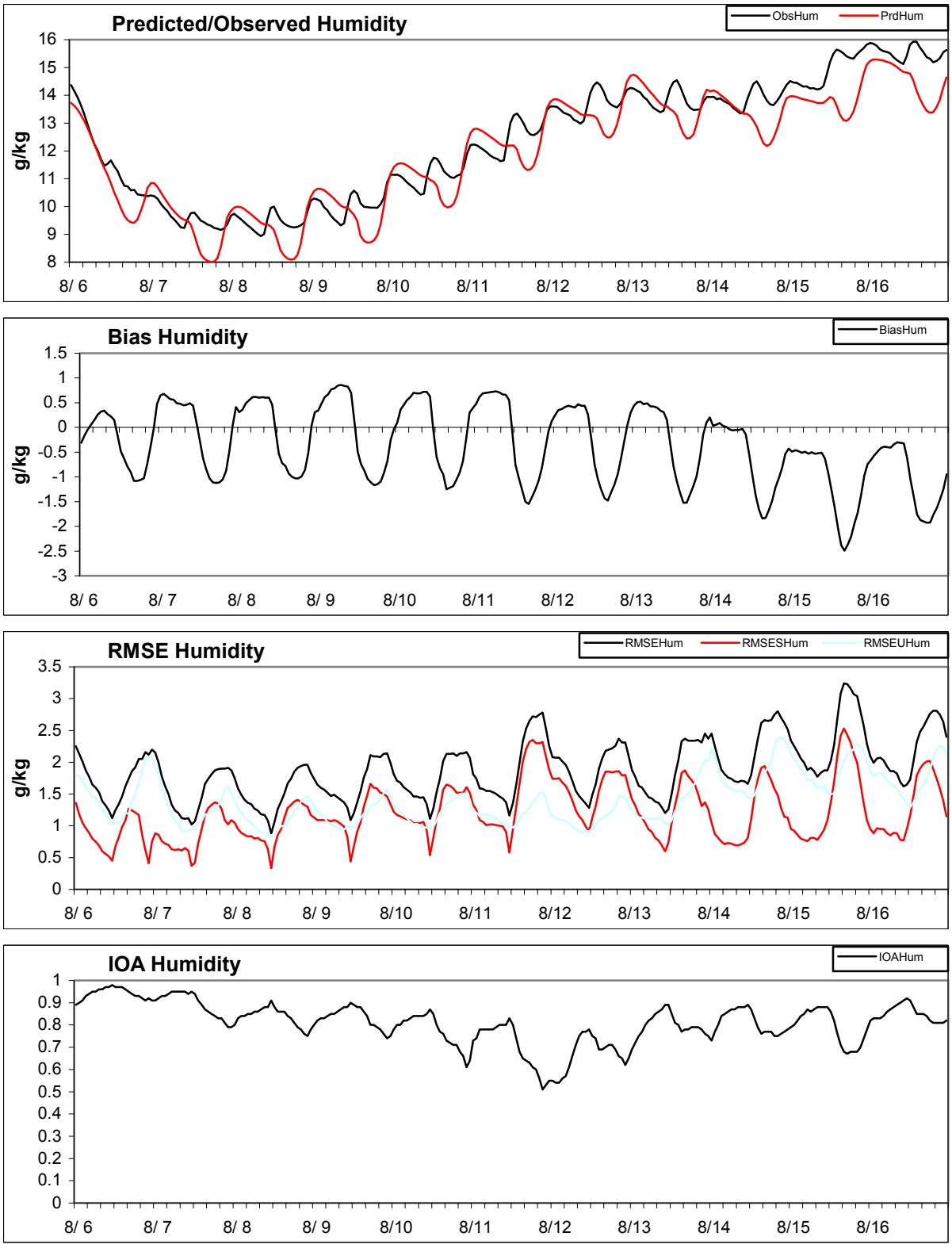

Figure 4b MM5 Simulation - UMD PX Aug 06 01Z to Aug 17 00Z

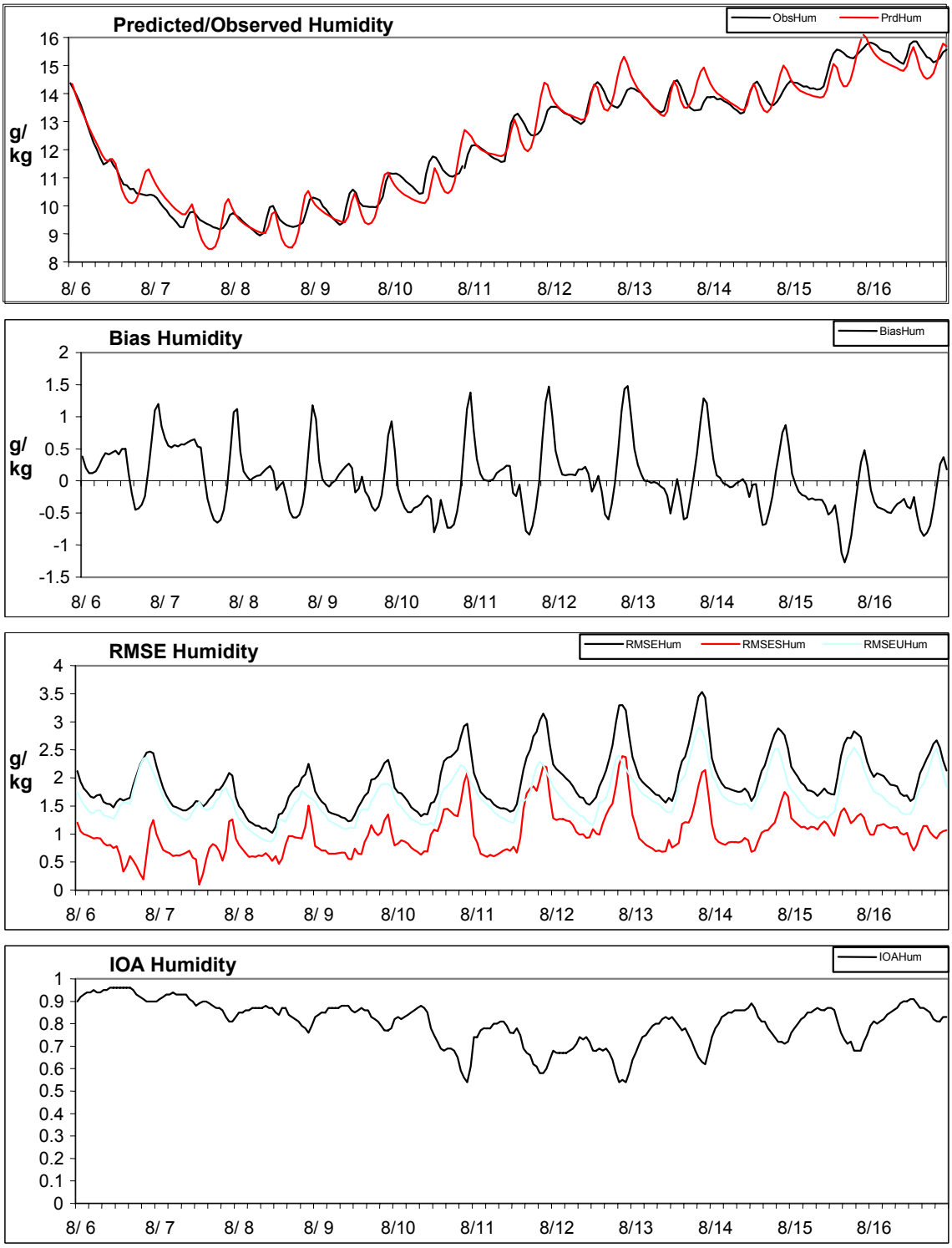

Figure 4c MM5 Simulation - UMD SSIB & TDL Aug 06 01Z to Aug 17 00Z 2002

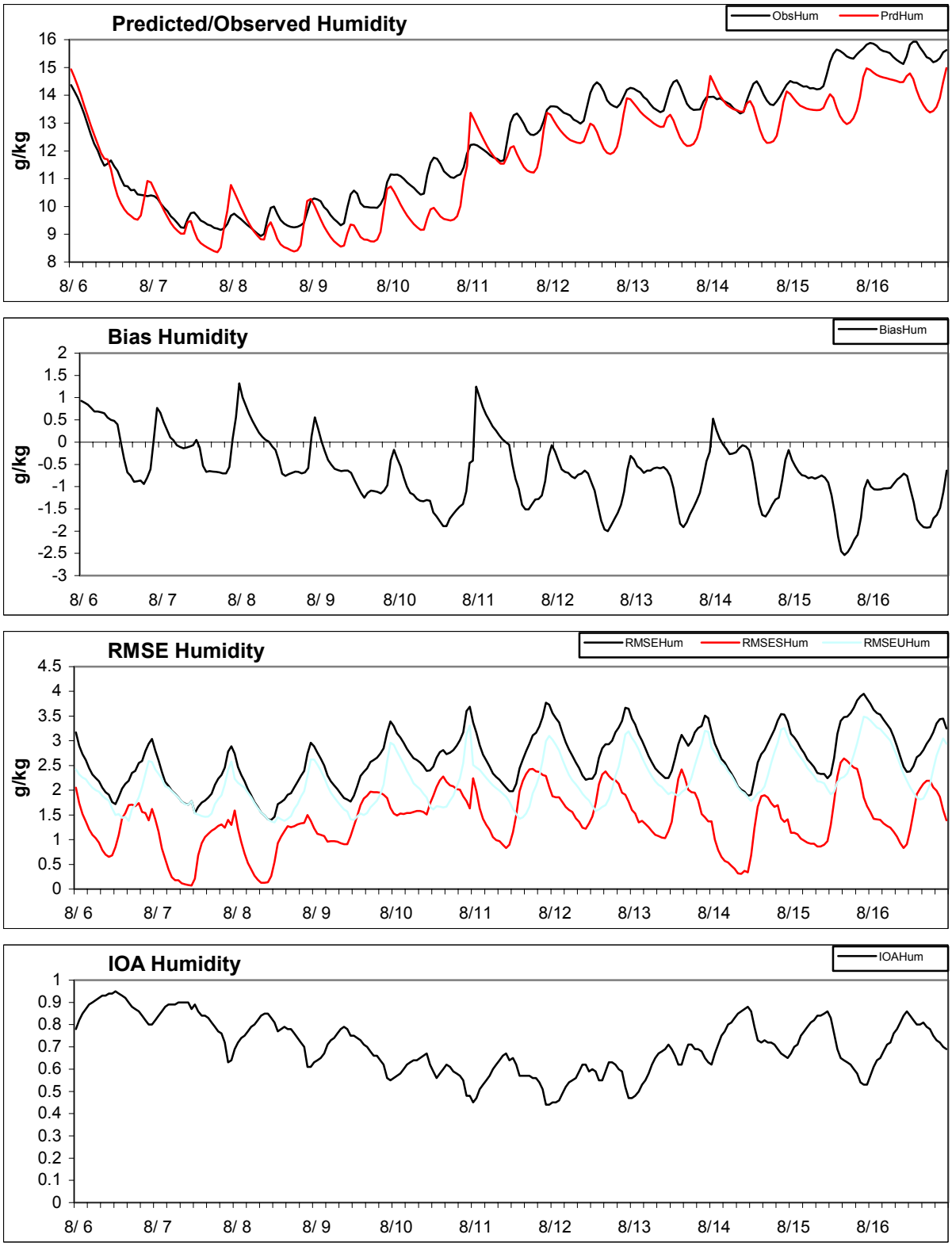

Figure 5a MM5 UMD - BL & CASTNet Aug 6 01Z to Aug 17 00Z 2002

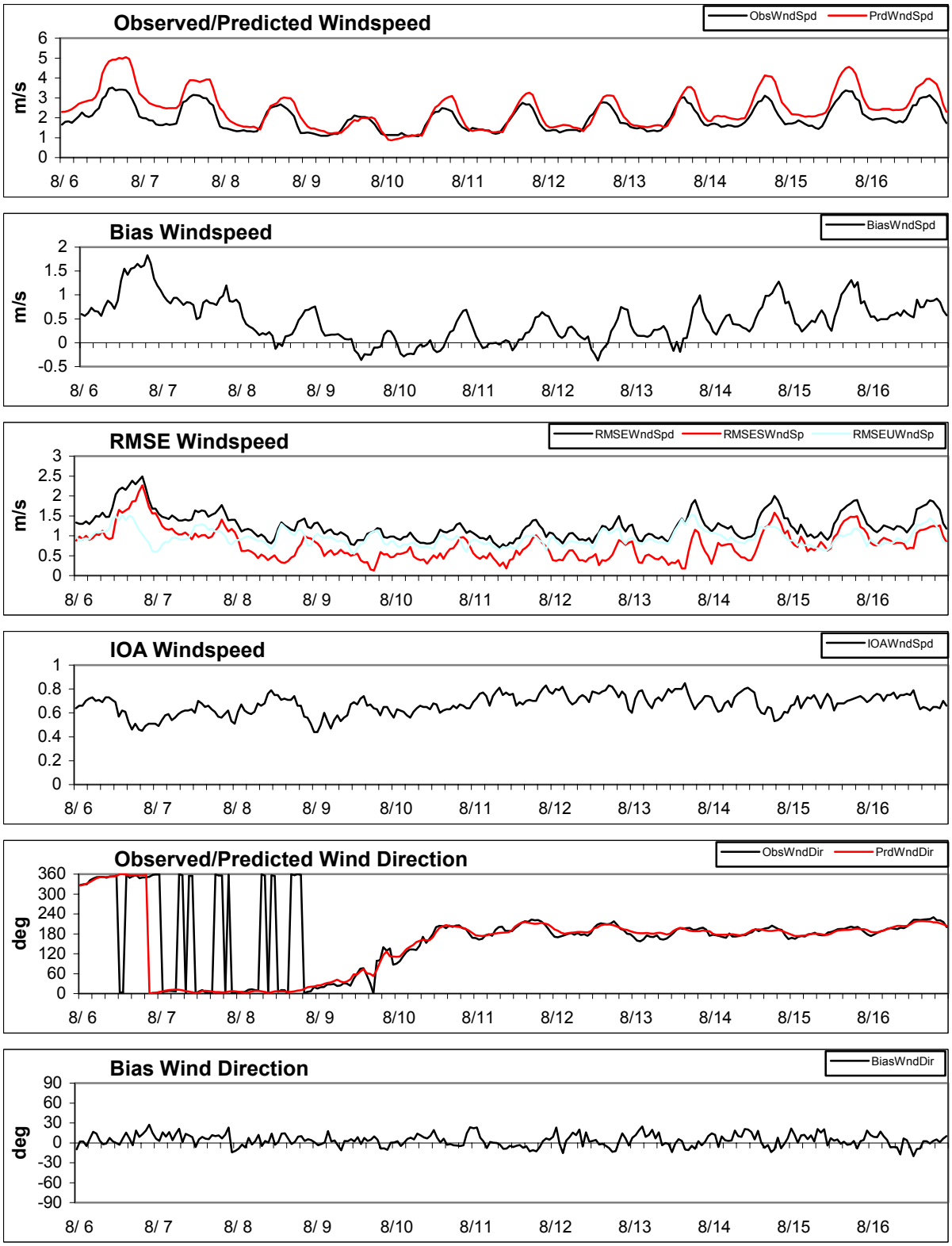

Figure 5b MM5 - UMD PX & CASTNet Aug 06 01Z to Aug 17 00Z 2002

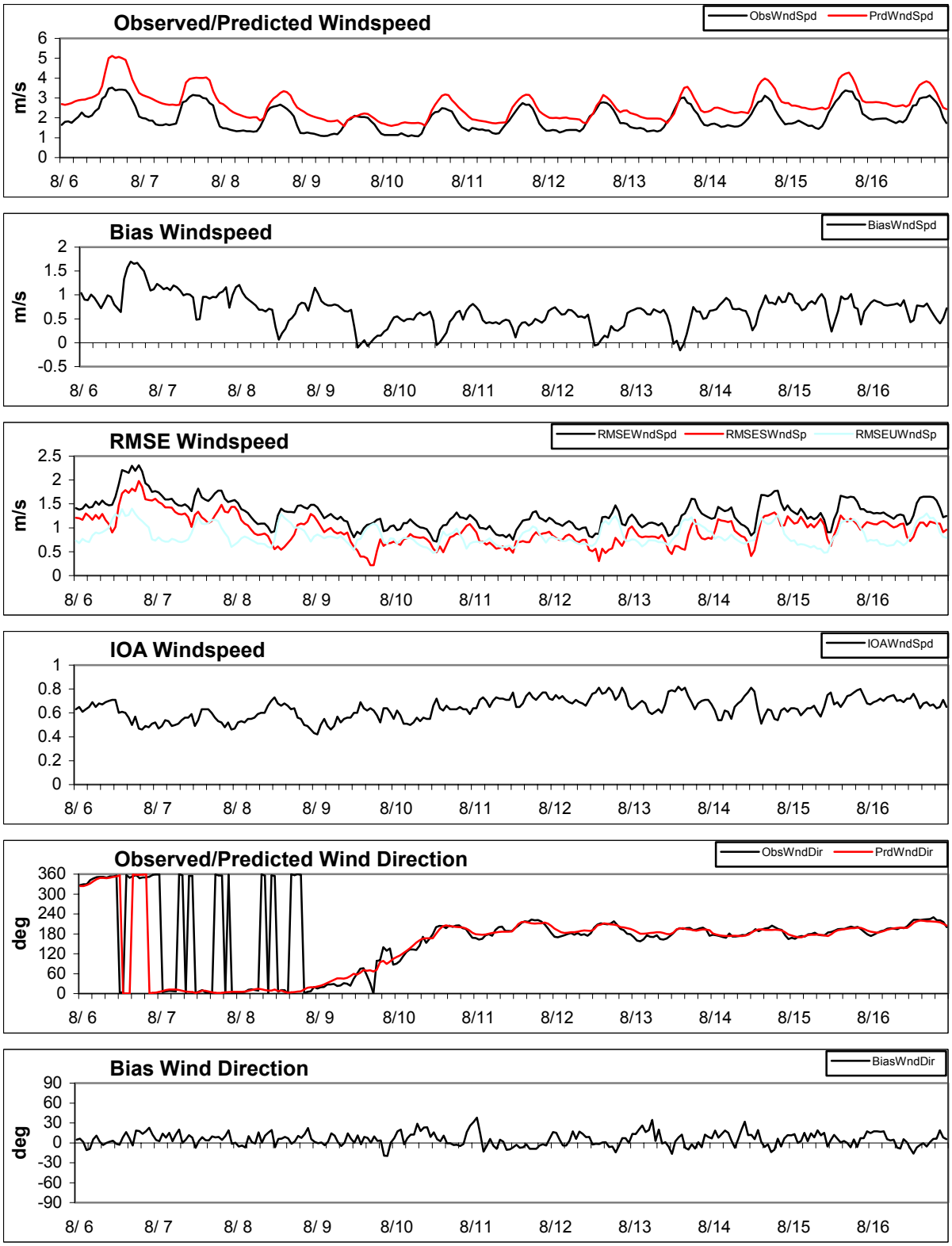

Figure 5c MM5 - UMD SSIB & CASTNet Aug 06 01Z to Aug 17 00Z 2002

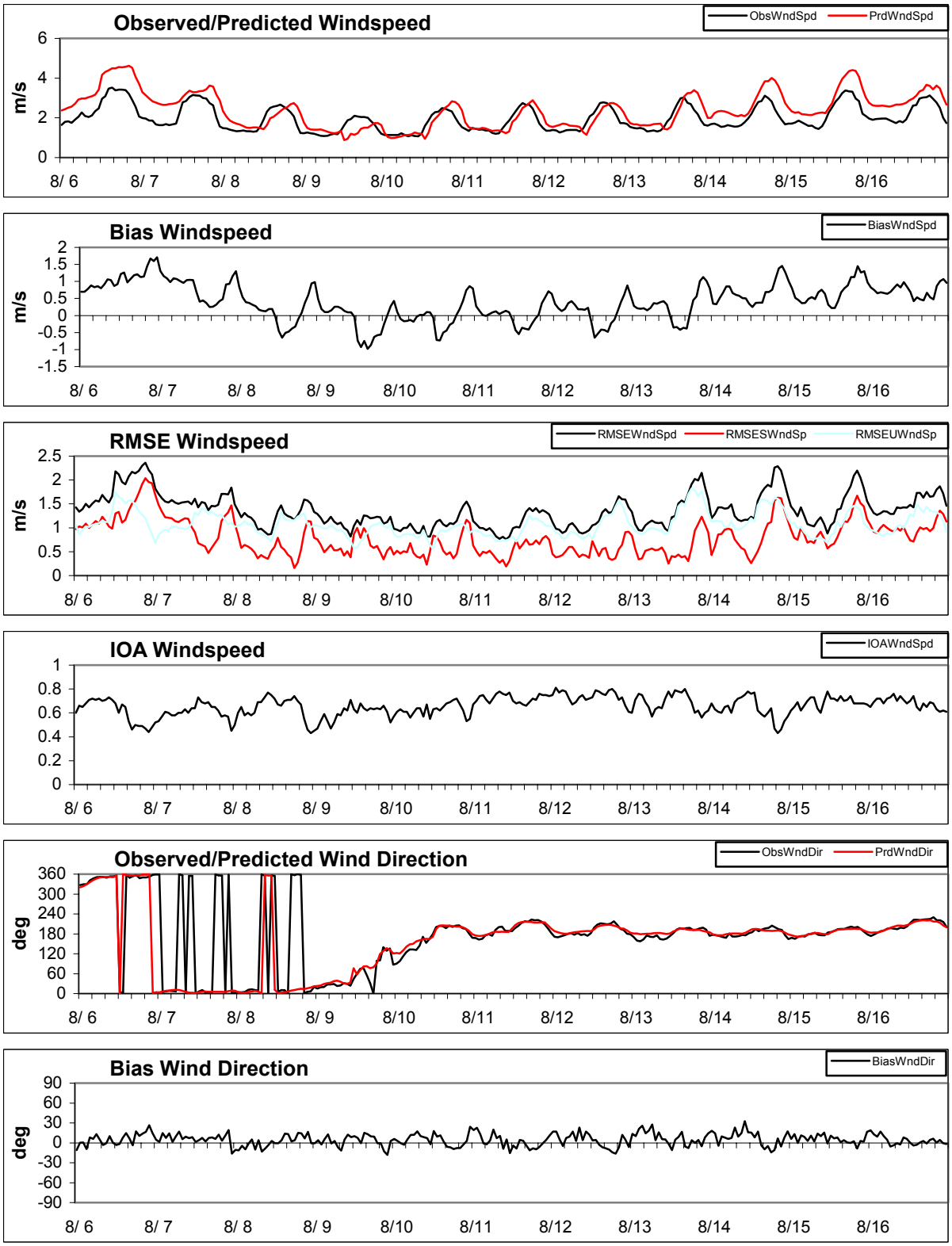

Figure 6a MM5 - UMD BL & CASTNet Aug 6 01Z to Aug 17 00Z 2002

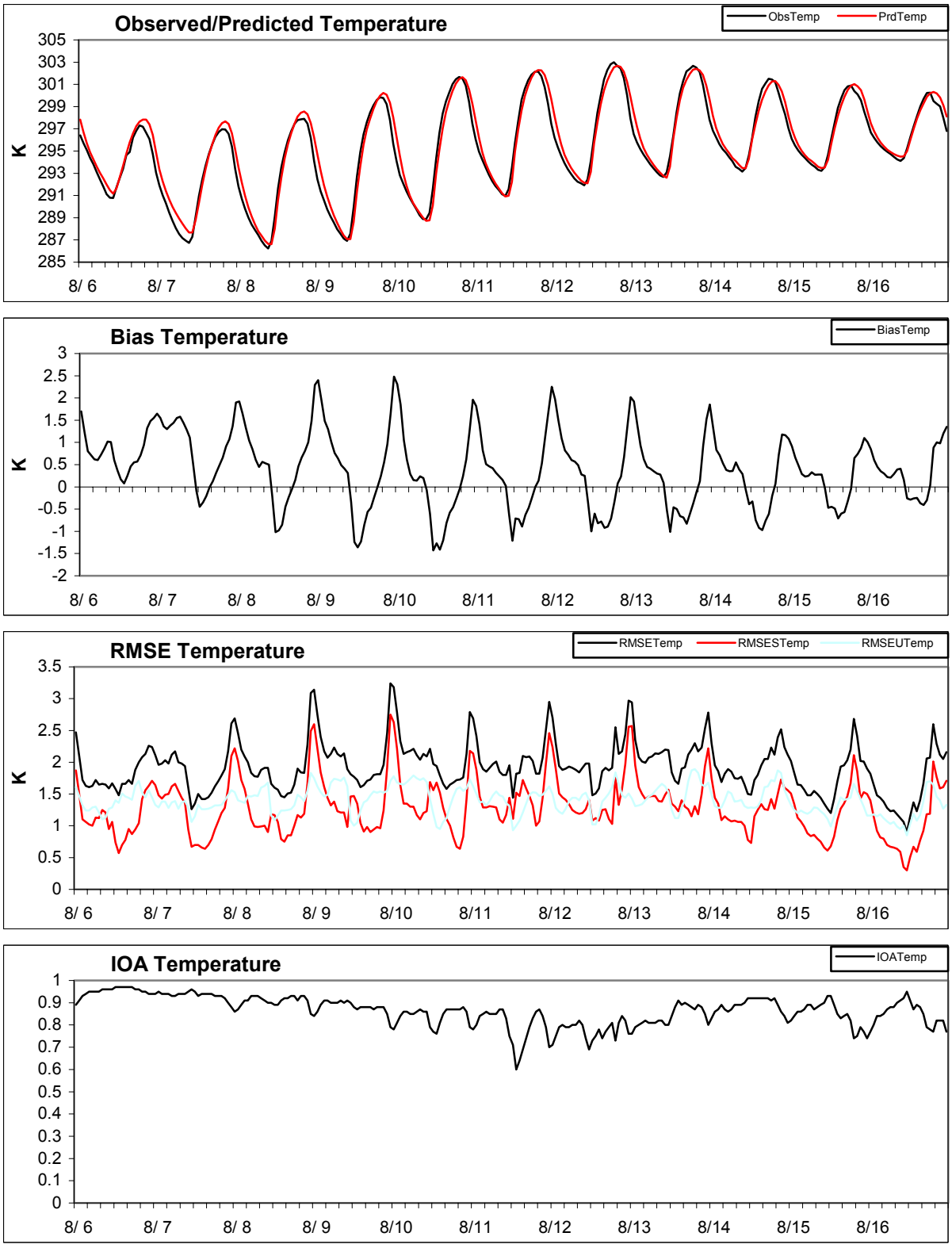

Figure 6b MM5 - UMD PX & CASTNet Aug 06 01Z to Aug 17 00Z 2002

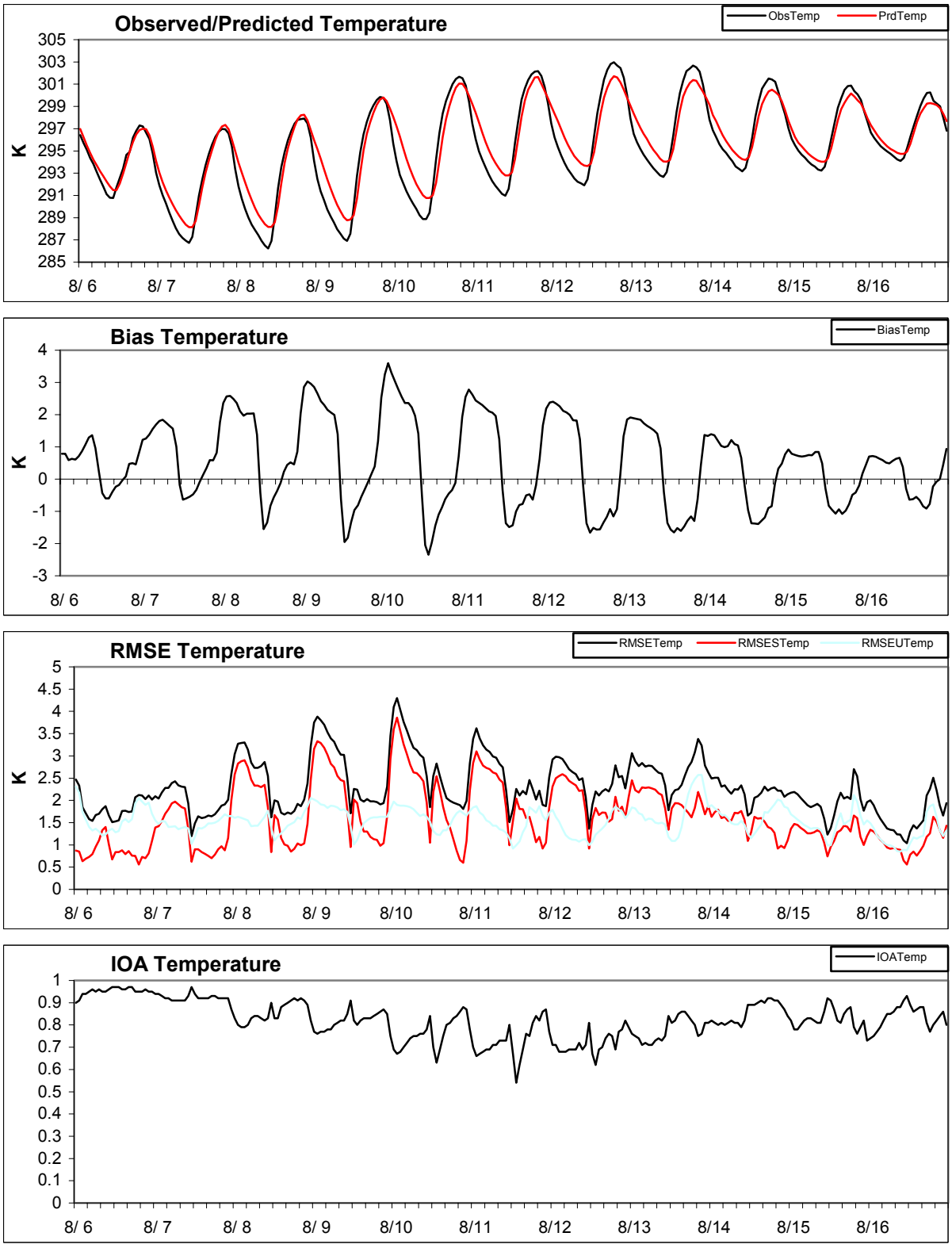

Figure 6c MM5 - UMD SSIB & CASTNet Aug 06 01Z to Aug 17 00Z 2002

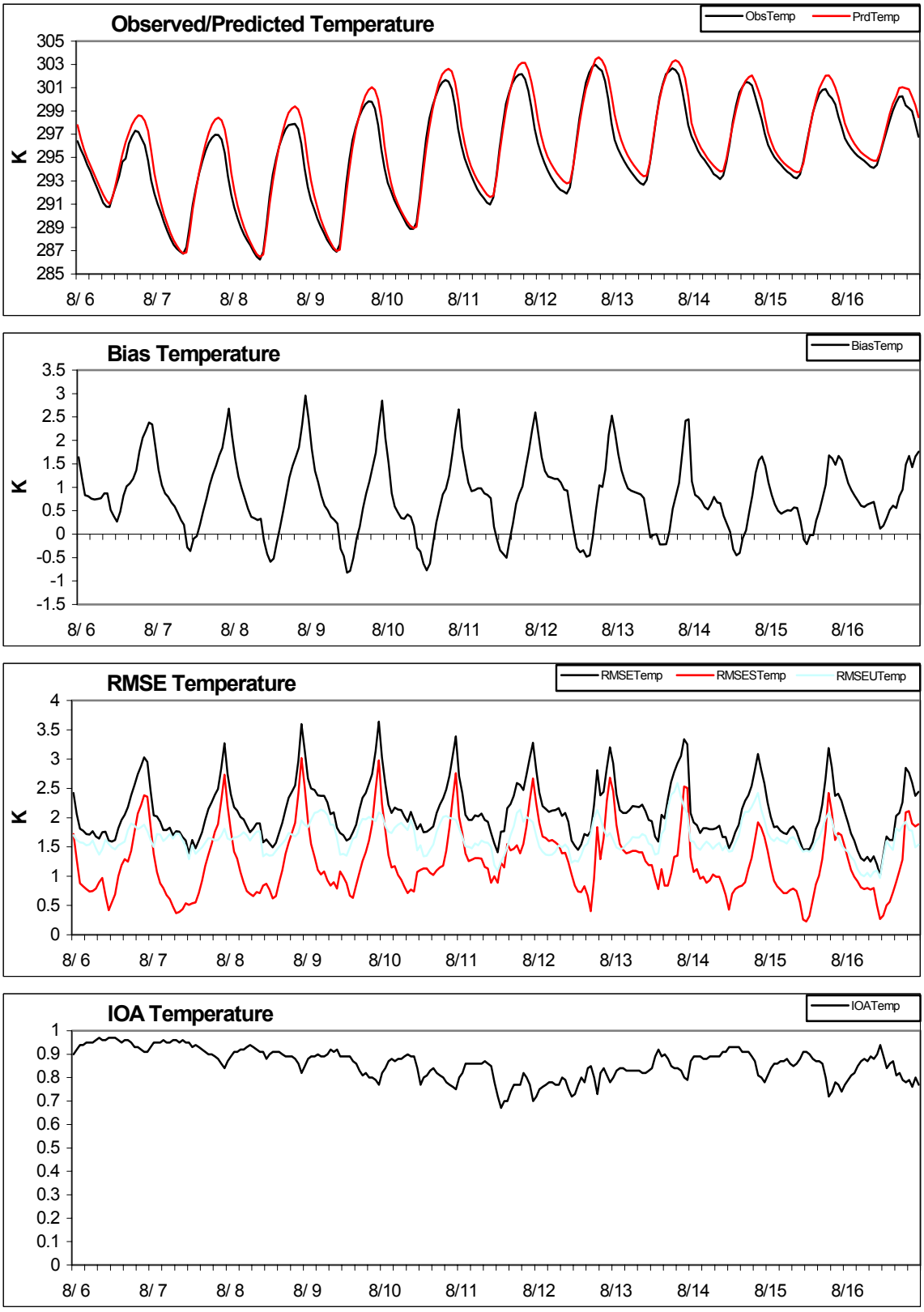

Figure 7a Spatial Correlation – Wind speed – BL & TDL

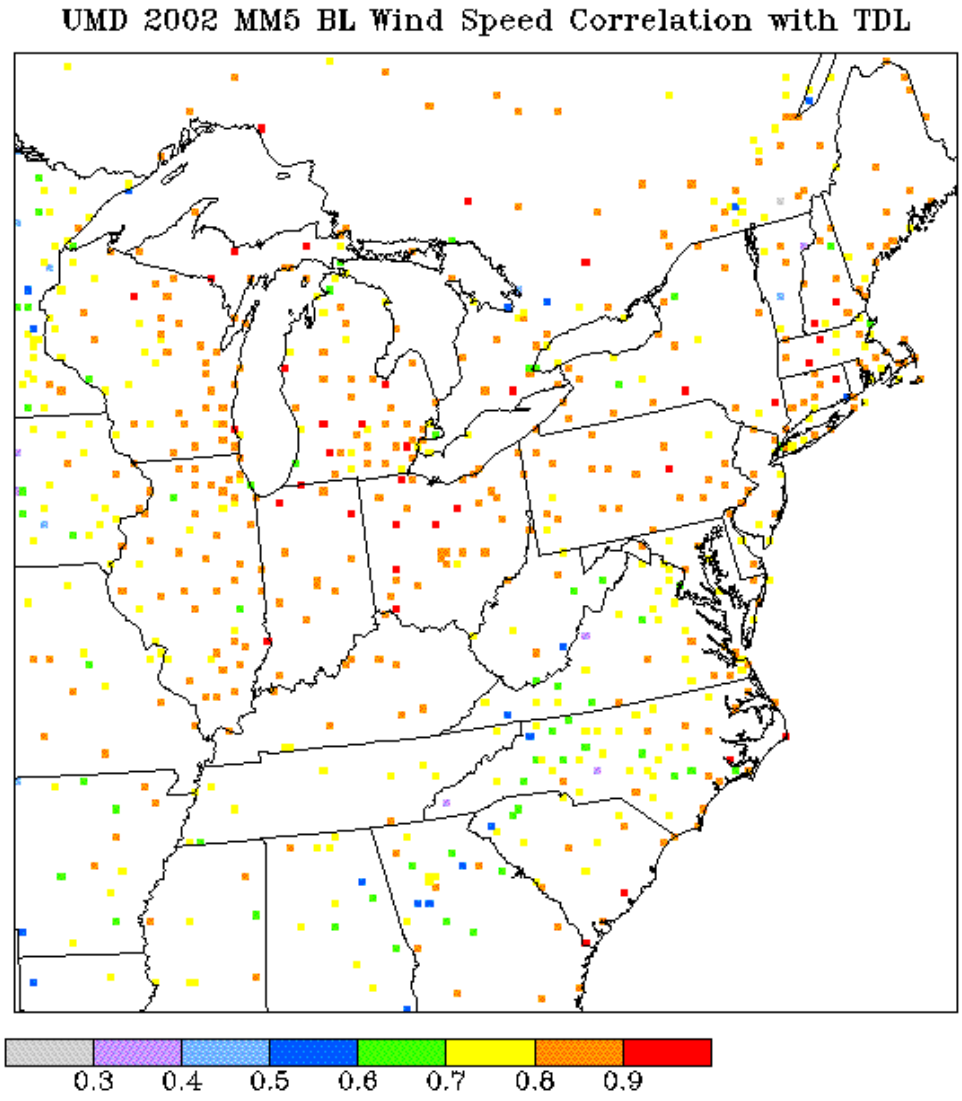

Figure 7b Spatial Correlation – Wind Speed – P-X & TDL

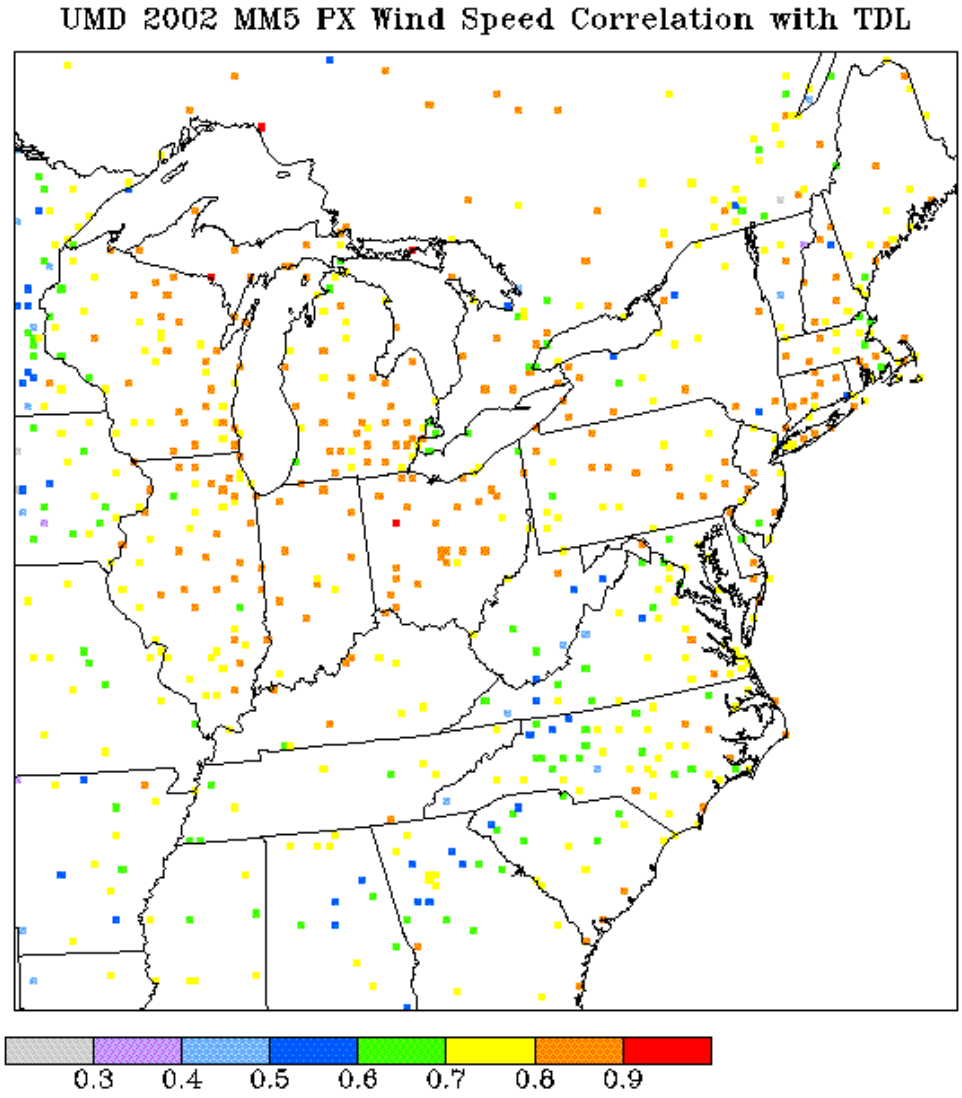

Figure 7c Spatial Correlation – Wind Speed SSIB & TDL

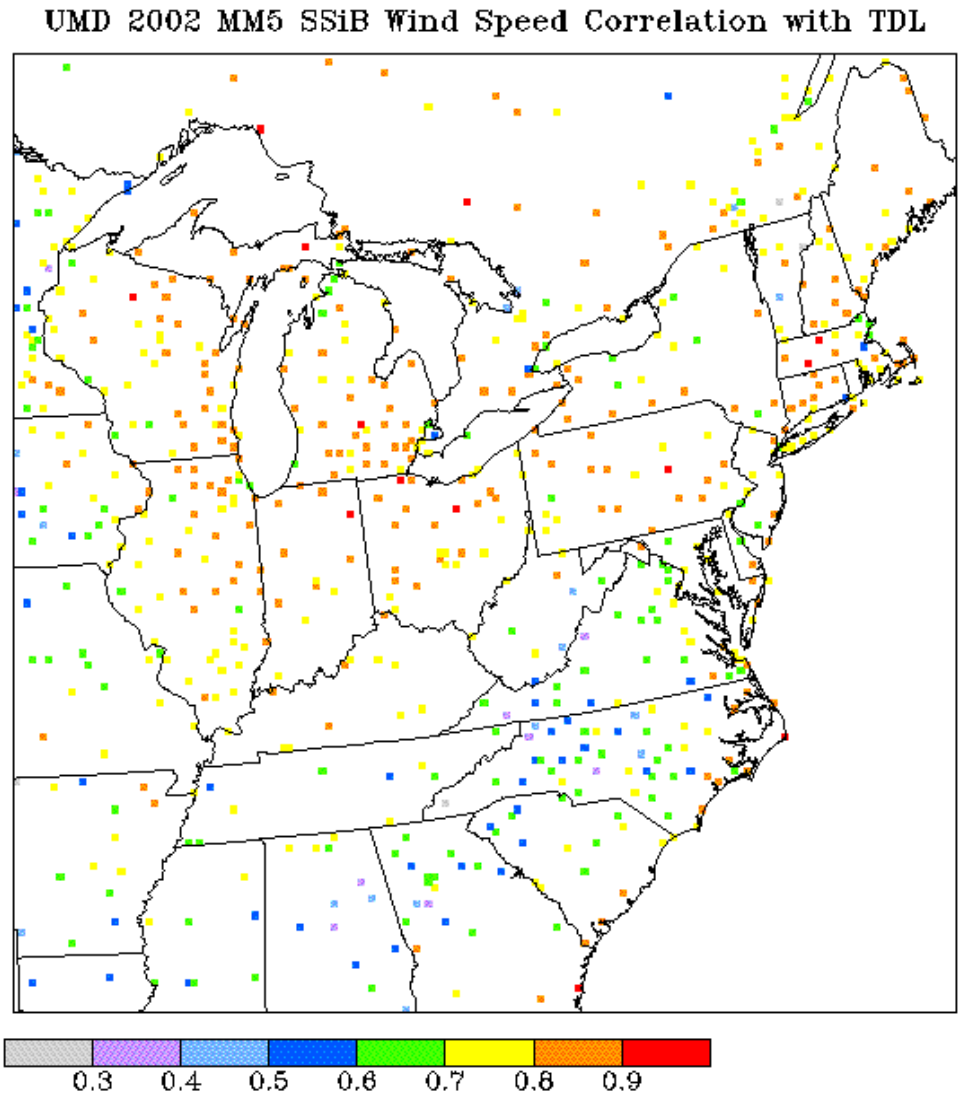

Figure 8a Spatial Correlation – Temperature – BL & TDL

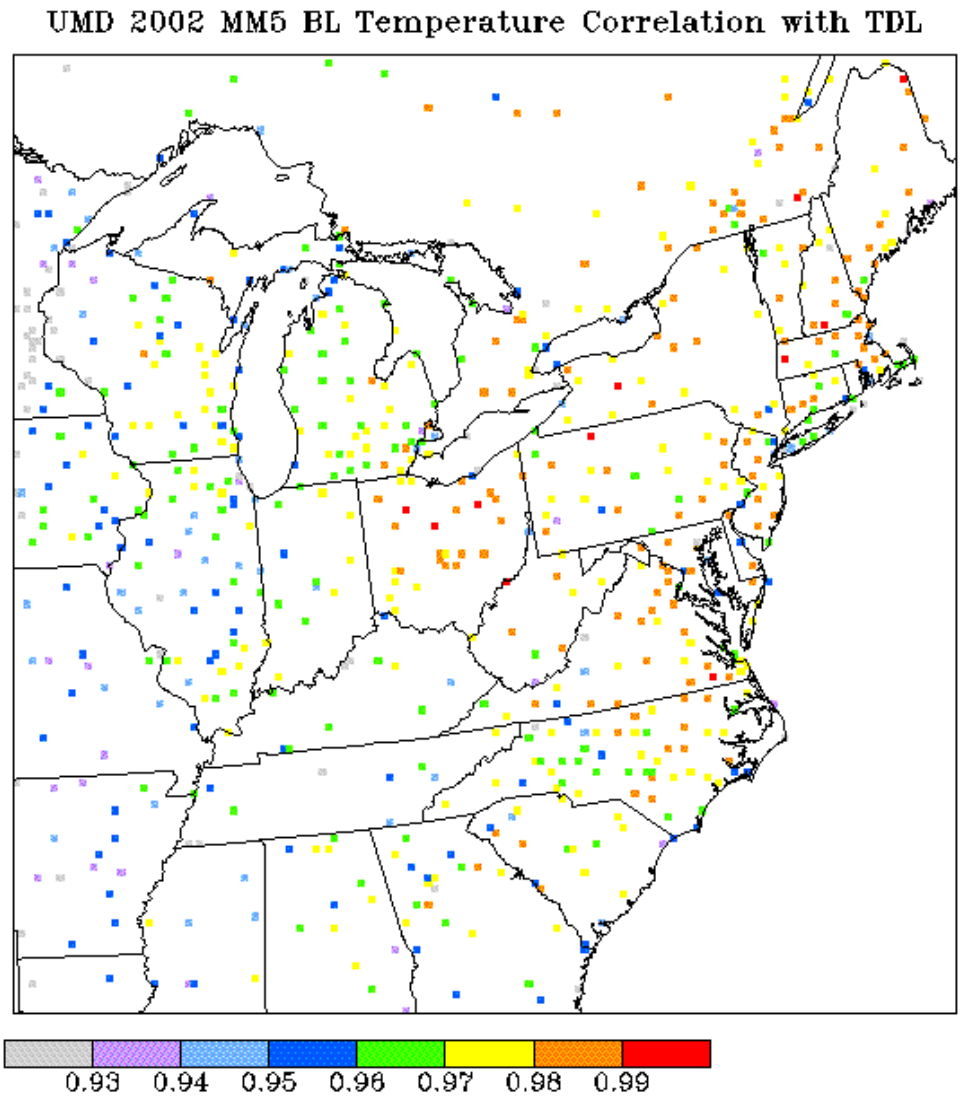

Figure 8b Spatial Correlation – Temperature – PX & TDL

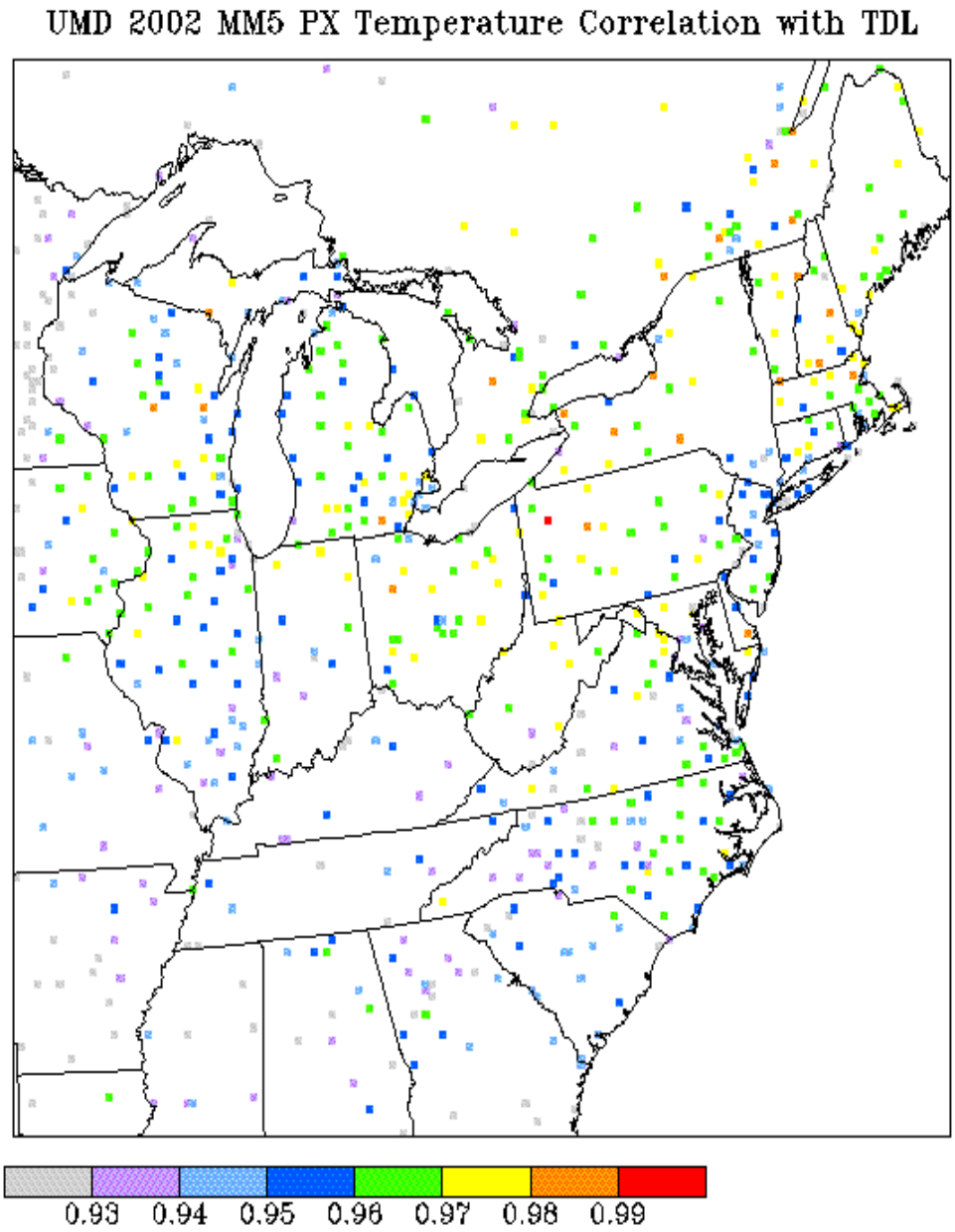

Figure 8c Spatial Correlation – Temperature SSIB & TDL

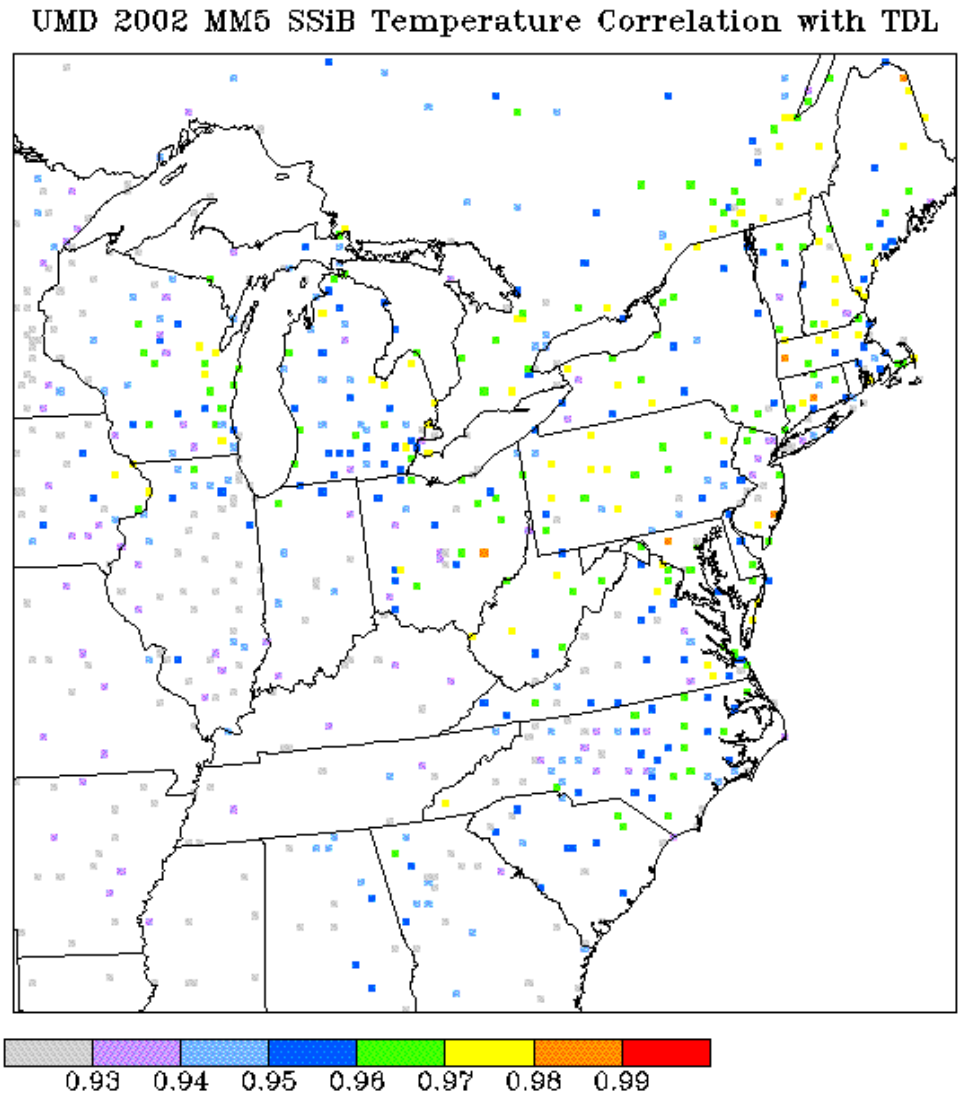

Figure 9a Spatial Correlation - Humidity BL & TDL

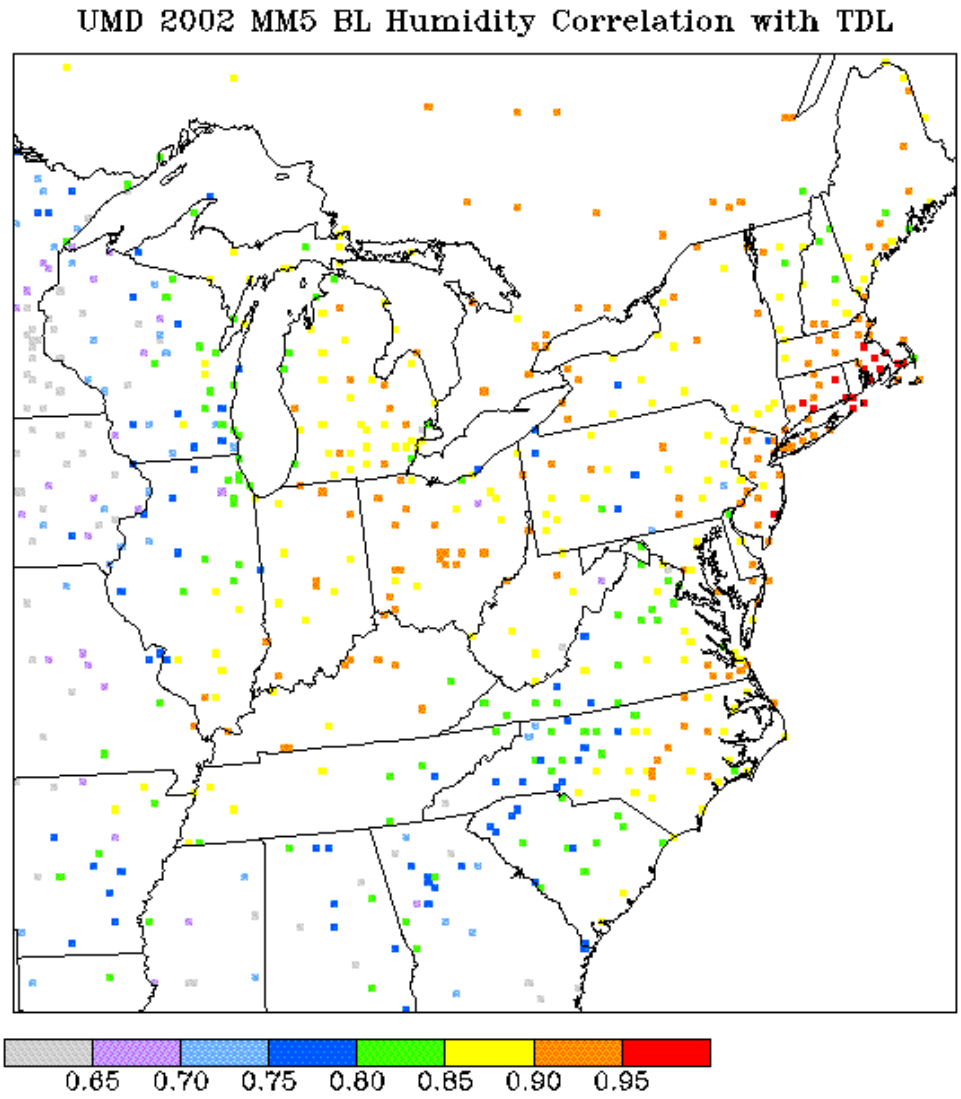

Figure 9b Spatial Correlation – Humidity PX & TDL

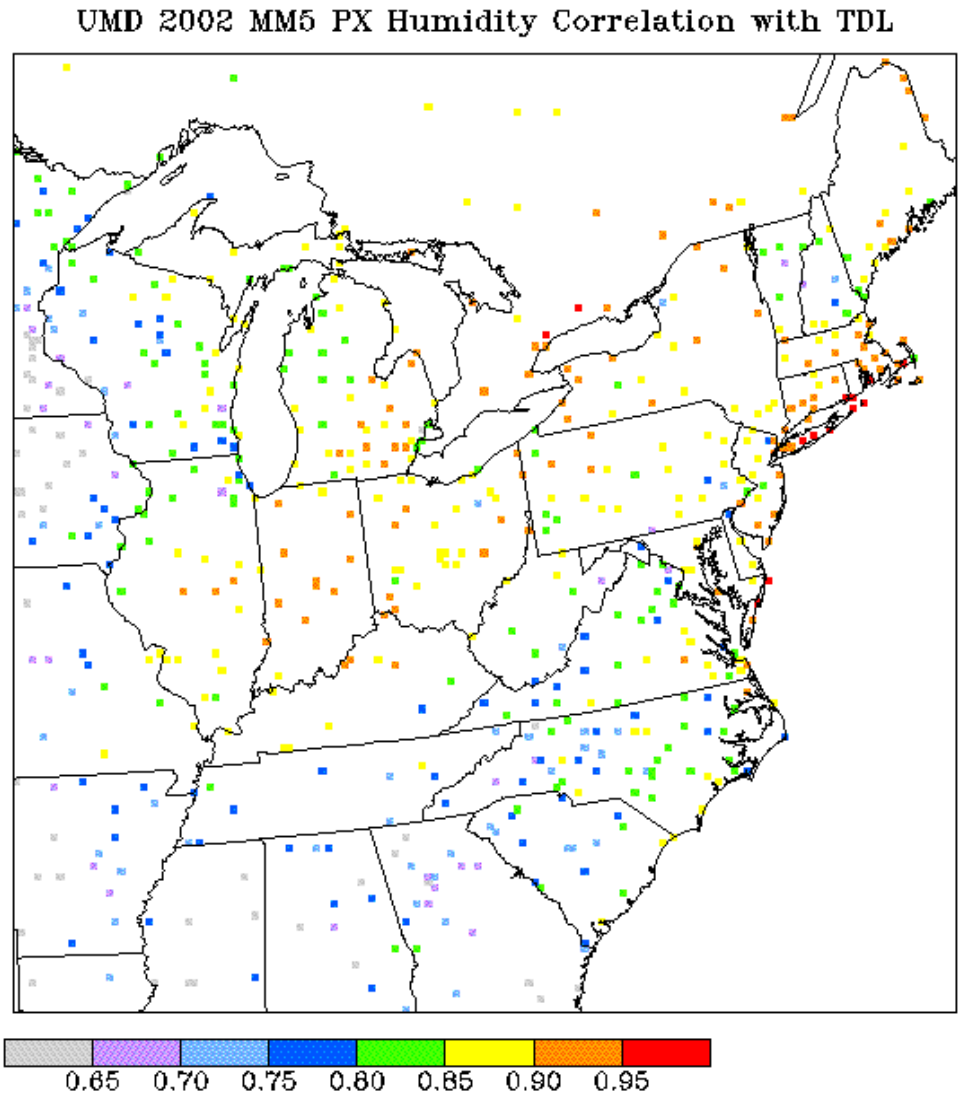

Figure 9c Spatial Correlation – Humidity SSIB & TDL

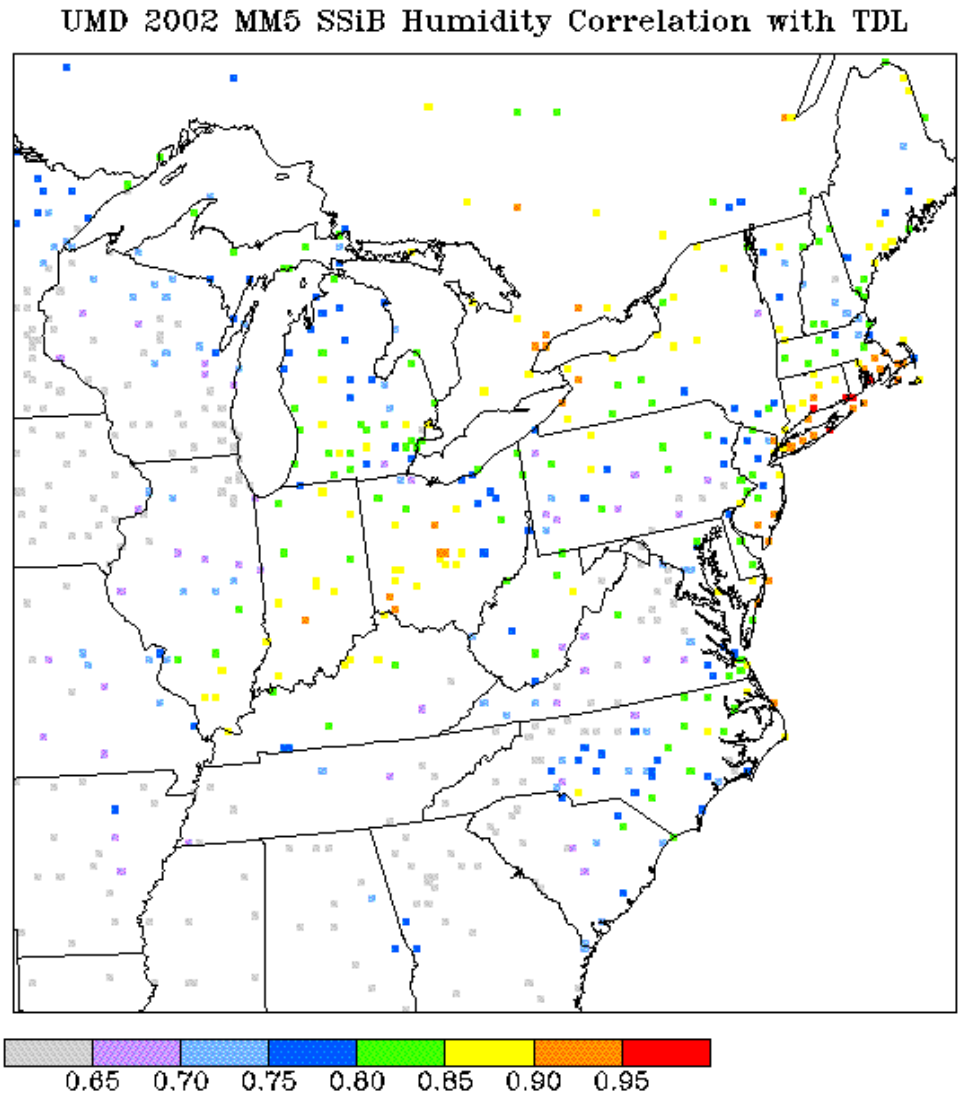

Numerical Experimental Analysis Data for the Year of 2002

Da-Lin Zhang and Shunli Zhang
Department of Atmospheric and Oceanic Science, University of Maryland
College Park, MD 20742
Tel. (301) 405-2018; Email: dalin@atmos.umd.edu

1. Introduction

A total of 128 numerical experiments, in 3-day segments, for the year of 2002 (i.e., from 0000 UTC 14 December 2001 to 0000 UTC 1 January 2003) have been conducted on our newly purchased Cluster using the nested-grid (36/12 km) Version 3.6 of the PSU/NCAR mesoscale model (i.e., MM5). The NCEP's Eta analysis with 40-km resolution was used to initialize the model integrations and specify the outmost lateral boundary conditions. To minimize the influence of model errors but retain as many mesoscale circulations as possible, the dynamical nudging or four-dimensional data assimilation (FDDA) technique was adopted to include observations of the surface winds and upper-level meteorological information. More attention was paid to the accuracy of surface winds due to their important roles in ozone transport. The model integrations were re-initialized every 3.5 days, allowing a 12-h period for the model spin-up (i.e., the first 12-h data could be truncated in the application of the datasets). Hourly model outputs were archived for the period of 12.5 months. This four-dimensional high resolution (in time and space) analysis dataset so assimilated was generated for air quality modeling and for regional haze studies. These integrations yielded a total of 830 Gbytes analysis data.

2. Model description

The Version 3.6 of MM5 with a Lambert conformal map projection, an MPP Version developed for clusters, was used for this project. The (x, y) dimensions of the coarse (36 km) and fine (12 km) mesh domains are 149 x 129 and 175 x 175, respectively. The vertical discretion uses terrain-following σ-coordinates, but the pressure at the σ-levels are determined from a reference state that is estimated using the hydrostatic equation from a given sea-level pressure and temperature with a standard lapse rate. There are 30 uneven σ levels, giving 29 layers, with higher resolution in the planetary boundary layer (PBL). The σ levels are placed at the following values:

1.000, 0.9974, 0.994, 0.989, 0.9820, 0.972, 0.959, 0.943, 0.923, 0.8990,
0.871, 0.839, 0.803, 0.763, 0.718, 0.668, 0.618, 0.568, 0.518, 0.468, 0.418,
0.368, 0.318, 0.268, 0.218, 0.168, 0.123, 0.080, 0.040, 0.00

The surface layer is defined at an altitude of about 10 m, the level at which surface winds are typically observed. The model top is set at 50 hPa with a radiative upper boundary condition. The time steps for the 36 km and 12 km resolution domains are 75 and 25 seconds, respectively.

Figs. 1 and 2 show the nested-grid (36/12 km) domain and the fine-mesh domain, respectively, that were used for this project.

Domain 1 is centered at 40^0N latitude and 97^0W longitude with a grid size of 36 km, and it covers the U.S. continents, Mexico, Canada, the Gulf of Mexico, and part of the East Pacific and West Atlantic oceans.

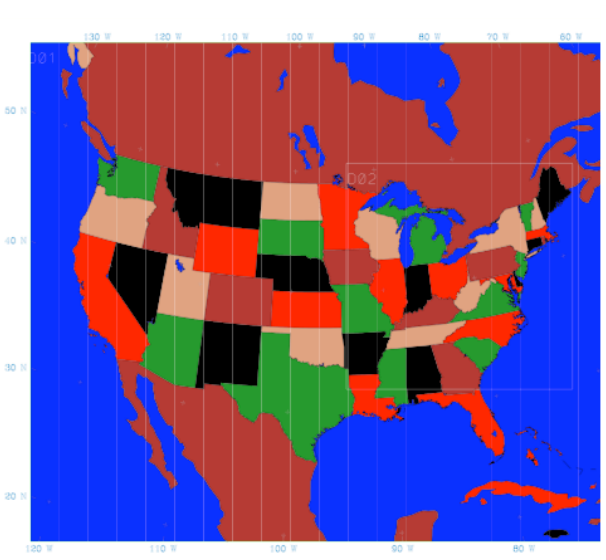

Fig. 1 The coarse-mesh (36 km) domain.

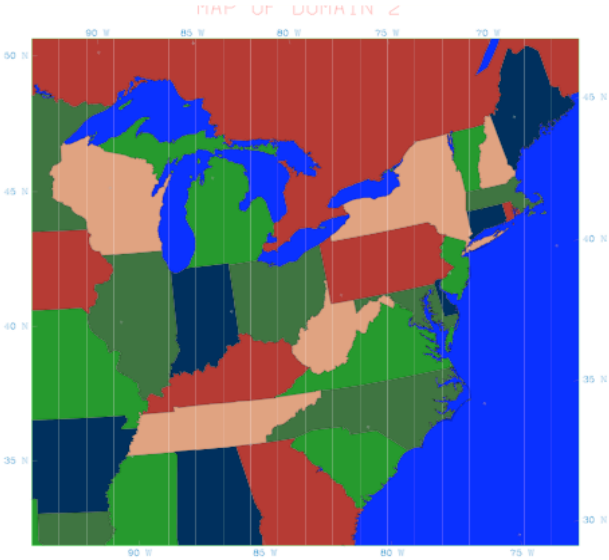

Fig. 2 The fine-mesh (12-km) domain.

Domain 2 uses a grid size of 12 km, and it covers the northeastern, central and southeastern US as well as Southeastern Canada.

The important model physics of the MM5 used for this project include:

(i) The latest version of the Kain-Fritsch (1993) convective scheme was used for both 36- and 12-km resolution domains;

(ii) An explicit moisture scheme (without the mixed phase) containing prognostic equations for cloud water (ice) and rainwater (snow) (Dudhia 1989; Zhang 1989);

(iii) A modified version of the Blackadar planetary boundary layer (PBL) scheme (Zhang and Anthes 1982; Zhang and Zheng 2004);

(iv) A simple radiative cooling scheme (Grell et al. 1997);

(v) A multi-layer soil model to predict land surface temperatures using the surface energy budget equation (Dudhia 1996).

Note that the Blackadar PBL scheme has been modified in order to reproduce the diurnal cycles of surface winds and temperatures, after performing a comparative study of the following five different PBL schemes: the Gayno-Seaman TKE scheme (Shafran et al. 2000), Burk-Thompson (1989), Blackadar (Zhang and Anthes 1982), MRF (Hong and Pan 1996), and Miller-Yamada-Jajić (Miller and Yamada 1974; Jajić 1990, 1994). These changes are given as follows (see Zhang and Zheng 2004 for more detail):

• K-coefficient is determined by the Richardson number according to Zhang and Anthes (1982), where the critical Richardson number is set to be 0.25. In addition, the mixing length is set to be the thickness of the model layer.

• Use of potential temperature rather than virtual potential temperature to calculate the bulk Richardson number Rb.

3. Nudging Processes

The MM5 provides options for nudging observations for each domain during the course of model integration (Stauffer and Seaman 1990; Stauffer et al. 1991). The Eta

analyses of upper-air winds, temperature and water-vapor mixing ratio as well as their associated surface fields, were nudged every 6 hours, and the higher-resolution surface wind field was nudged every 3 hours. While only the surface winds were nudged, their influences could be extended into the PBL (see Stauffer et al. 1991).

Based on our previous experience with many numerical experiments, the following nudging coefficients have been used:

- Upper-air wind fields: 5.0E-4 for Domain 1, and 2.5E-4 for Domain 2;
- Upper-air temperature fields: 1.0E-5 for both Domains;
- Surface winds: 5.0E-4 for Domain 1, and 2.5E-4 for Domain 2; and
- Surface temperature and moisture: not nudged due to instability consideration.

4. Model initialization

The model is initialized with NCEP's Eta model analysis (ds609.2) as a first guess that is then enhanced by observations at upper levels and the surface.

(i) NCEP's ADP global upper-air observations (NCAR archive ds353.4) are used to further enhance the upper-level Eta analysis.

(ii) The following two sets of surface observations have been introduced into the model initial state to improve the Eta analysis of surface wind fields:

- The NCEP's ADP global surface wind observations (NCAR archive ds464.0): This dataset provides 6-hourly surface observations over land (i.e., at 0000, 0600, 1200, 1800 UTC) in one stream, and 3-hourly (i.e., at 0300, 0900, 1500, 2100 UTC) over both land and ocean surfaces in another stream.
- The TDL's U.S. and Canadian surface observations (NCAR archive ds472.0): This dataset provides hourly surface observations over the U.S. and Canadian regions.

The Eta model analysis has a domain covering the entire U.S. continents with a 40-km horizontal resolution. It includes the following types of observations:

- Rawinsonde mass and wind;
- Piball winds;
- Dropwindsondes;
- Wind profiles;
- Surface land temperature and moisture;
- Oceanic surface data (ship and buoys);
- Aircraft winds;
- Satellite cloud-drift winds;
- Oceanic TOVS thickness retrievals;
- GOES and SSM/I precipitable water retrievals.

The Cressman objective analysis option was used to enhance the Eta analysis. However, we analyzed the results and found that it still could not reproduce the right diurnal cycle of surface winds and temperatures. Thus, we repeated the Cressman procedures three more times to enhance the surface analyses. Results indicate that this procedure significantly improved the results.

Note that (i) because of the initial model spin-up, we recommend that the first 12-h model integration of each run be discarded; and (ii) because the synoptic-scale upper-air winds and temperatures were nudged, the flow fields above the PBL might contain less smaller-scale features (e.g., in low-level jets, mountain-forced perturbations and etc.).

5. Data Archive

As mentioned above, we have conducted a total of 128 experiments, in 3-day segments, from 0000 UTC 14 December 2001 to 0000 UTC 1 January 2003. The following table lists the experiments and their corresponding integration periods:

Exp. #	Period	Exp. #	Period
1	00/15/12-00/18/12*01	2	00/18/12-12/21/12*01
3	00/21/12-00/24/12*01	4	00/24/12-00/27/12*01
5	00/27/12-00/30/12*01	6	00/30/12-00/02/01*02
7	00/02/01-00/05/01*02	8	00/05/01-00/08/01*02
9	00/08/01-00/11/01*02	10	00/11/01-00/14/01*02
11	00/14/01-00/17/01*02	12	00/17/01-00/20/01*02
13	00/20/01-00/23/01*02	14	00/23/01-00/26/01*02
15	00/26/01-00/29/01*02	16	00/29/01-00/01/02*02
17	00/01/02-00/04/02*02	18	00/04/02-00/07/02*02
Exp. #	Period	Exp. #	Period
19	00/07/02-00/10/02*02	20	00/10/02-00/13/02*02
21	00/13/02-00/16/02*02	22	00/16/02-00/19/02*02
23	00/19/02-00/22/02*02	24	00/22/02-00/25/02*02
25	00/25/02-00/28/02*02	26	00/28/02-00/03/03*02
27	00/03/03-00/06/03*02	28	00/06/03-00/09/03*02
29	00/09/03-00/12/03*02	30	00/12/03-00/15/03*02
31	00/15/03-00/18/03*02	32	00/18/03-00/21/03*02
33	00/21/03-00/24/03*02	34	00/24/03-00/27/03*02
35	00/27/03-00/30/03*02	36	00/30/03-00/02/04*02
37	00/02/04-00/05/04*02	38	00/05/04-00/08/04*02
39	00/08/04-00/11/04*02	40	00/11/04-00/14/04*02
41	00/14/04-00/17/04*02	42	00/17/04-00/20/04*02
43	00/20/04-00/23/04*02	44	00/23/04-00/26/04*02
45	00/26/04-00/29/04*02	46	00/29/04-00/02/05*02
47	00/01/05-00/04/05*02	48	00/04/05-00/07/05*02
49	00/07/05-00/10/05*02	50	00/10/05-00/13/05*02
51	00/13/05-00/16/05*02	52	00/16/05-00/19/05*02
53	00/19/05-00/22/05*02	54	00/22/05-00/25/05*02
55	00/25/05-00/28/05*02	56	00/28/05-00/31/05*02
57	00/31/05-00/03/06*02	58	00/03/06-00/06/06*02
59	00/06/06-00/09/06*02	60	00/09/06-00/12/06*02
61	00/12/06-00/15/06*02	62	00/15/06-00/18/06*02
63	00/18/06-00/21/06*02	64	00/21/06-00/24/06*02
65	00/24/06-00/27/06*02	66	00/27/06-00/30/06*02

67	00/30/06-00/03/07*02	68	00/03/07-00/06/07*02
69	00/06/07-00/09/07*02	70	00/09/07-00/12/07*02
71	00/12/07-00/15/07*02	72	00/15/07-00/18/07*02
73	00/18/07-00/21/07*02	74	00/21/07-00/24/07*02
75	00/24/07-00/27/07*02	76	00/27/07-00/30/07*02
77	00/30/07-00/02/08*02	78	00/02/08-00/05/08*02
79	00/05/08-00/08/08*02	80	00/08/08-00/11/08*02
81	00/11/08-00/14/08*02	82	00/14/08-00/17/08*02
83	00/17/08-00/20/08*02	84	00/20/08-00/23/08*02
85	00/23/08-00/26/08*02	86	00/26/08-00/29/08*02
87	00/29/08-00/01/09*02	88	00/01/08-00/04/09*02
89	00/04/09-00/07/09*02	90	00/07/09-00/10/09*02
91	00/10/09-00/13/09*02	92	00/13/09-00/16/09*02
93	00/16/09-00/19/09*02	94	00/19/09-00/22/09*02
95	00/22/09-00/25/09*02	96	00/25/09-00/28/09*02
97	00/28/09-00/01/10*02	98	00/01/10-00/04/10*02
99	00/04/10-00/07/10*02	100	00/07/10-00/10/10*02
101	00/10/10-00/13/10*02	102	00/13/10-00/16/10*02
103	00/16/10-00/19/10*02	104	00/19/10-00/22/10*02

Exp. #	Period	Exp. #	Period
105	00/22/10-00/25/10*02	106	00/25/10-00/28/10*02
107	00/28/10-00/31/10*02	108	00/31/10-00/03/11*02
109	00/03/11-00/06/11*02	110	00/06/11-00/09/11*02
111	00/09/11-00/12/11*02	112	00/12/11-00/15/11*02
113	00/15/11-00/18/11*02	114	00/18/11-00/21/11*02
115	00/21/11-00/24/11*02	116	00/24/11-00/27/11*02
117	00/27/11-00/30/11*02	118	00/30/11-00/03/12*02
119	00/03/12-00/06/12*02	120	00/06/12-00/09/12*02
121	00/09/12-00/12/12*02	122	00/12/12-00/15/12*02
123	00/15/12-00/18/12*02	124	00/18/12-00/21/12*02
125	00/21/12-00/24/12*02	126	00/24/12-00/27/12*02
127	00/27/12-00/30/12*02	128	00/30/12-00/02/01*03

The datasets listed above include the MM5 outputs from Domain 1 (36 km) and Domain 2 (12 km), the analysis data used for FDDA, and initial and lateral boundary conditions. If necessary, any of the experiments listed above could be re-run. The MM5 outputs include the three-dimensional fields of temperature, horizontal winds, vertical motion, pressure perturbations, moisture, cloud water/rain water/ice water/snow water mixing ratio, and radiation tendency; and the two-dimensional fields of the map-scale factor, longitude and latitude, Coriolis parameter, land use category, terrain height, PBL depth, accumulated convective/non-convective precipitation, surface sensible/latent heat flux. A FORTRAN program to read the datasets has also been included.

6. Acknowledgments

This project was funded by Maryland's Department of Environment (MDE) and Northeast States for Coordinated Air Use Management, Inc. (NESCAUM). New York State Department of Environmental Conservation (NYDEC) has evaluated the MM5's performance with TDL and CASTNet measurements for the summer-season episodes of 6 – 16 August 2002 before the production of a complete 5-month simulation from 1 May to 30 September 2002. Similarly, NESCAUM evaluated the MM5 simulations of 23 – 29 January 2002 before the simulation of the winter-season episodes and the remaining annual model simulations. We are very grateful to Gopal Sistla, Mike Ku, and Winston Hao of NYSDEC, and Shan He and Gary Kleiman of NESCAUM for their careful evaluations of the MM5 performance.

References

Burk, S. D., and W. T. Thompson, 1989: A vertically nested regional numerical weather prediction model with second-order closure physics. *Mon. Wea. Rev.,* **117,** 2305–2324.

Dudhia, J., 1989: Numerical study of convection observed during the winter monsoon experiments using a mesoscale two-dimensional model. *J. Atmos. Sci.,* **46,** 3077–3107.

Grell, G. A., J. Dudhia, and D. R. Stauffer, 1995: A description of the fifth-generation Penn State/NCAR Mesoscale Model (MM5). NCAR Tech. Note NCAR/TN-398 1 STR, 122 pp.

Hong, S.-H., and H.-L. Pan, 1996: Nonlocal boundary layer vertical diffusion in a medium-range forecast model. *Mon. Wea. Rev.,* **124,** 2322–2339.

Jajić, Z. I., 1990: The step-mountain coordinate: Physical package. *Mon. Wea. Rev.,* **118,** 1429-1443.

——, 1994: The step-mountain Eta coordinate model: Further development of the convection, viscous sublayer and turbulent closure schemes. *Mon. Wea. Rev.,* **122,** 927-945.

Kain, J.S., and J.M. Fritsch, 1993: Convective parameterization for mesoscale models: The Kain-Fritsch scheme. Cumulus Parameterization. *Meteor. Monogr.*, **46**, Amer. Meteor. Soc., 165-170.

Mellor, G. L., and T. Yamada, 1974: A hierarchy of turbulence closure models for planetary boundary layers. *J. Atmos. Sci.,* **31,** 1791–1806.

Shafran, P.C., N.L. Seaman, and G.A. Gayno, 2000: Evaluation of numerical predictions of boundary layer structure during the Lake Michigan ozone study. *J. Appl. Meteor.,* **39,** 412-426.

Stauffer, D. R., N. L. Seaman and F. S. Binkowski, 1991: Use of four-dimensional data assimilation in a limited-area mesoscale model. Part II: Effects of data assimilation within the planetary boundary layer. *Mon. Wea. Rev.*, **119**, 734-754.

Stauffer, D. R. and N. L. Seaman, 1990: Use of four-dimensional data assimilation in a limited-area mesoscale model. Part I: Experiments with synoptic-scale data. *Mon. Wea. Rev.*, **118**, 1250-1277.

Zhang, D.-L., 1989: The effect of parameterized ice microphysics on the simulation of vortex circulation with a mesoscale hydrostatic model. *Tellus*, **41A**, 132-147.

——, and R. A. Anthes, 1982: A high-resolution model of the planetary boundary layer—Sensitivity tests and comparisons with SESAME-79 data. *J. Appl. Meteor.,* **21,** 1594–1609.

——, and W.-Z. Zheng, 2004: Diurnal cycles of surface winds and temperatures as simulated by five boundary-layer parameterizations. *J. Appl. Meteor.,* **43**, 157-169.

TSD-1a

Meteorological Modeling using Penn State/NCAR 5th Generation Mesoscale Model (MM5)

Bureau of Air Quality Analysis and Research

Division of Air Resources

New York State Department of Environmental Conservation

Albany, NY 12233

March 19, 2006

Meteorological Modeling using Penn State/NCAR 5th Generation Mesoscale Model (MM5)

Version 3.6 of MM5 was used to generate annual 2002 meteorology for the OTC modeling work. Prof. Dalin Zhang of the University of Maryland performed the MM5 simulations in consultation with NYSDEC staff. The model was applied in Lambert conformal map projection and utilized MPP Version developed for clusters. The two-way nested domain consisted of coarse (36km) and fine (12km) mesh corresponding to 149x129 and 175x175 grids, respectively, in this application (see Figure 1).

The Lambert projection used in this work followed the Regional Planning Organization (RPO) national domain setup with the center at (40°N, 97°W) and parallels at 33°N and 45°N. Map projection parameters in reference to the projection center point are as follows: Southwest corner for the 36 km grid is at (-2664km, -2304km) and the northeast corner at (2664km, 2304km). In the case of the 12km grid, the southwest corner is at (252km, -900km) and the northeast corner at (2340km, 1188km). In the vertical direction, the terrain following σ-coordinate system was used with the pressure at each σ-level determined from a reference state that is estimated using the hydrostatic equation from a given sea-level pressure and temperature with a standard lapse rate. There are 30 unevenly spaced σ levels, giving 29 vertical layers, with higher resolution within the planetary boundary layer (PBL). The σ levels are:

1.0000, 0.9974, 0.9940, 0.8980, 0.9820, 0.9720, 0.9590, 0.9430, 0.9230, 0.8990,

0.8710, 0.8390, 0.8030, 0.7630, 0.7180, 0.6680, 0.6180, 0.5680, 0.5180, 0.4680,

0.3680, 0.3180, 0.2680, 0.2180, 0.1680, 0.1230, 0.0800, 0.0400, 0.0000

The surface layer was set at about 10m, the level at which surface winds were typically observed, and the model top was set at 50hPa with a radiative top boundary condition. The time steps for the 36km and 12km domains were 75 and 25 seconds, respectively.

The important model physics options used for this MM5 simulation include:

- Kain-Fritsch (1993) convective scheme for both 36- and 12-km domains
- Explicit moisture scheme (without the mixed phase) containing prognostic equations for cloud water (ice) and rainwater (snow) (Dudhia 1989; Zhang 1989)
- Modified version of the Blackadar planetary boundary layer (PBL) scheme (Zhang and Anthes 1982; Zhang and Zheng 2004)
- Simple radiative cooling scheme (Grell et al. 1994)
- Multi-layer soil model to predict land surface temperatures using the surface energy budget equation (Dudhia 1996)

Note that the Blackadar PBL scheme has been modified in order to correct the phase shift of surface wind speed and temperature diurnal cycle, following a study that compared five different PBL schemes: the Gayno-Seaman TKE scheme (Shafran et al. 2000), Burk-

Thompson (1989), Blackadar (Zhang and Anthes 1982), MRF (Hong and Pan 1996), and Mellor-Yamada-Jajic (Mellor and Yamada 1974; Jajic 1990, 1994). The details of the study can be found at Zhang and Zheng (2004).

Nudging Processes

The MM5 provides options for nudging observations for each domain during the model integration process (Stauffer and Seaman, 1990; Stauffer et al. 1991). The Eta analyses of upper-air winds, temperature and water-vapor mixing ratio as well as their associated surface fields were used for nudging every 6 hours, and the Eta surface wind fields blended with surface wind observations were used to nudge every 3 hours. While only the surface winds were nudged, their influences could extend into the PBL as well (see Stauffer et al. 1991). Based on UMD's prior experience in numerical experiments, the following nudging coefficients have been used:

- Upper-air wind fields: 5. 0E-4s^{-1} for Domain 1 (36km), and 2. 5E-4s^{-1} for Domain 2 (12km);
- Upper-air temperature fields: 1.0E-5s^{-1} for both Domains;
- Surface winds: 5. 0s^{-1}E-4s^{-1} for Domain 1, and 2.5E-4s^{-1} for Domain 2; and
- Surface temperature and moisture: not nudged due to instability consideration.

ASSESSMENT

This assessment covers the period of May through September 2002.

National Weather Service (NWS) and CASTNet data – Surface temperature, Wind Speed, and Humidity

NWS (TDL) and CASTNet (www.epa.gov/castnet/) surface measurements of temperature, wind speed, and humidity (note there were no humidity measurements for CASTNet) were used to compare with the MM5 outputs. The evaluation was performed with METSTAT program developed by Environ Corporation (www.camx.com/files/metstat.15feb05.tar.gz) When comparing to NWS data, the METSTAT interpolates the first layer MM5 (at 10m height) temperature and humidity data to a height of 2m, the level that corresponds to the NWS measurement of these parameters. However, no such interpolation was made for wind speed and direction. In the case of CASTNet surface measurements, no such changes were needed as CASTNet data were reported at a height of 10m. In this analysis, no exclusion was made for calm conditions. The reported calm winds (zero wind speed measured) were treated as is in this evaluation effort. The METSTAT calculated standard statistical measures – average, bias, error and index of agreement between the measured and predicted parameters.

Figure 2 displays the temperature and wind speed comparison of MM5 and measured data from NWS and CASTNet networks for August 2002. MM5 performance for both in magnitude and diurnal timing, temperature can be considered to be quite good for both NWS and CASTNet data, while MM5 underpredicted NWS and overpredicted CASTNet

daytime wind speed, respectively. It should be pointed out that there are differences in how the meteorological information is collected and reported by the two networks as well as in MM5. The CASTNet measurements are based on hourly averaged wind speed while NWS reports 2min average at 10min before the hour, whereas MM5 predictions are reflective of the last time-step of the hour of computation. Interestingly, MM5 appears to track quite well the nighttime minimum wind speed for both networks. In the case of humidity (not shown), MM5 tracks the NWS observed humidity trend well, but MM5 missed the observed semi-diurnal cycles. Comparisons for the five months including bias and root mean square error from both NWS and CASTNet are available on request from NYSDEC.

The above assessment is based on domain-wide averages to provide an overall response of the model over the five months. Another way of assessing the model is to examine the degree of correlation between the measured and predicted parameters. Figures 3a and 3b displays such a comparison for wind speed and temperature, respectively, for the NWS hourly data covering the period of May through September 2002. For the NWS data, the correlations are in the range from 0.7 to 0.8 for wind speed, above 0.96 for temperature, and in the range of 0.8 to 0.9 for humidity. CASTNet data (not shown) also exhibit similar correlation. These correlations indicate that MM5 simulation has captured both the diurnal and synoptic scale variations. Detailed plots of this comparison are available on request from NYSDEC.

Vertical Profiler – Winds

The Wind-Profiler network measurements along the U. S. East Coast (www.madis-fsl.org/cap) were used to evaluate the vertical profiles from MM5. There are twelve wind-profiler measurement stations from which data were available for comparison. For convenience of comparison, the wind-profiler measurements were interpolated to the MM5 vertical levels. The approach used was simple interpolation between two adjacent wind-profiler layers to the MM5 vertical level, and was limited to that reported by the profiler measurement. The focus of the comparison was to assess if MM5 was able to capture the measured vertical structure, and for this we used the observed Low Level Jet (LLJ) as an indicator. The comparison was performed for June, July and August 2002. In general it is found that MM5 captures the profiler measured vertical wind field structure reasonably well. Figure 4 displays an example of the MM5 and wind profiler comparison for the August 2002 episode at Richmond, VA and Concord, NH. MM5 predicted weaker LLJ winds compared to those based on the wind-profiler measurements. The detailed plots of this comparison are available on request from NYSDEC.

Cloud Cover – Satellite cloud image

Cloud information derived from satellite image data (www.atmos.umd.edu/~srb/gcip/webgcip.htm)were used to assess the MM5 prediction of cloud cover. The 0.5^{o} by 0.5^{o} resolution of the satellite data were interpolated into the 12km MM5 grid for comparison. The MM5 total cloud fraction was estimated by MCIP based on the MM5's low cloud, middle cloud and high cloud predictions. In general,

MM5 captured the satellite cloud pattern well but underestimates the satellite cloud fraction (see Figure 5 as an example). Part of problem may due to the coarse resolution of the satellite cloud data.

Precipitation comparison

The monthly total observed precipitation data were constructed from 1/8-degree daily precipitation analysis data (http://data.eol.ucar.edu/codiac/dss/id=21.093 produced by Climate Prediction Center, based on 7,000-8,000 hourly/6-hourly gauge reports and radar). The MM5 monthly total precipitation was estimated from the MM5 predicted convective and non-convective rainfall and summed up for each month. In general, MM5 captured the observed spatial patterns in May and September, but no so well for June, July and August (See Figure 6), perhaps reflective of the summertime convective rain activities not captured by MM5. Detailed plots of this comparison are available on request from NYSDEC.

Calm Conditions

Calm conditions are defined as observed wind speed of zero knots and wind direction as 0^{o}. It would be useful to assess how MM5 performs under observed calm conditions, because of potential pollutant buildup that could occur under such conditions. Table 1 lists the summary of the percentage of calm condition at each hour for the August 2002 from the NWS data within the 12km domain. It is apparent from the Table that the calm conditions occur primarily during the night and early morning hours, from 23Z (7 p.m. EDT) to 15Z (11 a.m. EDT) with a peak at 10Z (6 a.m. EDT). To assess MM5 performance, the observed and MM5 predicted wind speeds were divided into calm and non-calm according to observed wind speed. Figure 7 displays such a comparison of the MM5 predicted wind speed to the observed wind speed under the calm and non-calm conditions for the month of August 2002. For the "calm" group, the average wind speed for MM5 varies from 1 m/s during the night and early morning hours and over 1.5 m/s during the day. MM5 is over-predicting during observed calm wind conditions. There are local minima every 3 hours, due to the surface observed wind speed nudging in MM5. In contrast under the non-calm conditions, MM5 underpredicts by about 0.5 m/s for all hours with noticeable local maximum happening at the nudging hours. The MM5 nudging process would pull predictions toward the measured data, while the underprediction of MM5 for the non-calm conditions may due to the adopted PBL scheme in this simulation.

Summary

In this study, we performed an assessment of the MM5 simulation to real-world data, both at the surface level as well as in the vertical. While there are no specific recommended procedures identified for this assessment, similar approaches have been used elsewhere (Dolwick 2005, Baker 2004, and Johnson 2004). Traditionally, the NWS surface measurements are used for such a comparison. Since NWS data had been used through nudging processes in developing the MM5 simulation, the comparisons should

not be far removed from each other. In this study, we extended the evaluation by using CASTNet measurements that were not used in the MM5 simulations. Thus comparison with CASTNet data provides for an independent assessment and should complement the comparison with NWS data. We also compared the MM5 results with the wind profiler data and cloud data derived from satellite images to diagnose if the MM5 simulation is yielding the right type of dynamics in the vertical. The analyses shows that in general, the performance of the MM5 is reasonable both at the surface and in the vertical, thereby providing confidence in the use of these data in the CMAQ simulations.

References

Baker, K. 2004: www.ladco.org/tech/photo/photochemical.html

Burk, S. D. and W. T. Thompson, 1989: A vertically nested regional numerical weather prediction model with second-order closure physics. Mon. Wea. Rev., 117, 2305–2324.

Dudhia, J., 1989: Numerical study of convection observed during the winter monsoon experiments using a mesoscale two-dimensional model. J. Atmos. Sci., 46, 3077–3107.

Dudhia, J., 1996: A multi-layer soil temperature model for MM5. Preprints, 6th Annual MM5 Users Workshop, Boulder, CO.

Dolwick, P. 2005:
http://cleanairinfo.com/modelingworkshop/presentations/MPE_Dolwick.pdf

Grell, G. A., J. Dudhia , and D. R. Stauffer 1994: A description of the fifth-generation Penn State/NCAR Mesoscale Model (MM5). NCAR Tech.Note NCAR/TN-398 1 STR, 122 pp.

Hong, S.-H., and H.-L. Pan, 1996: Nonlocal boundary layer vertical diffusion in a medium-range forecast model. Mon. Wea. Rev., 124, 2322–2339.

Jajic, Z. I., 1990: The step-mountain coordinate: Physical package. Mon. Wea. Rev., 118, 1429-1443.

Jajic, Z. I., 1994: The step-mountain Eta coordinate model: Further development of the convection, viscous sublayer and turbulent closure schemes. *Mon. Wea. Rev*., 122, 927-945.

Johnson, M. 2004: www.ladco.org/tech/photo/photochemical.html

Kain, J.S., and J.M. Fritsch, 1993: Convective parameterization for mesoscale models: The Kain-Fritsch scheme. Cumulus Parameterization. Meteor. Monogr., 46, Amer. Meteor. Soc., 165-170.

Mellor, G. L., and T. Yamada, 1974: A hierarchy of turbulence closure models for planetary boundary layers. J. Atmos. Sci., 31, 1791–1806.

Shafran, P.C., N.L. Seaman, and G. A. Gayno, 2000: Evaluation of numerical predictions of boundary layer structure during the Lake Michigan ozone study. J. Appl. Meteor., 39, 412-426.

Stauffer, D. R., N. L. Seaman and F. S. Binkowski 1991: Use of four-dimensional data assimilation in a limited-area mesoscale model. Part II: Effects of data assimilation within the planetary boundary layer. Mon. Wea. Rev., 119, 734-754.

Stauffer, D. R. and N. L. Seaman, 1990: Use of four-dimensional data assimilation in a limited-area mesoscale model. Part I: Experiments with synoptic-scale data. Mon. Wea. Rev., 118, 1250-1277.

Zhang, D.-L., 1989: The effect of parameterized ice microphysics on the simulation of vortex circulation with a mesoscale hydrostatic model. Tellus, 41A, 132-147.

Zhang, D.-L, and R. A. Anthes, 1982: A high-resolution model of the planetary boundary layer-sensitivity tests and comparisons with SESAME-79 data. J. Appl. Meteor., 21, 1594–1609.

Zhang, D.-L, and W.-Z. Zheng, 2004: Diurnal cycles of surface winds and temperatures as simulated by five boundary-layer parameterizations. J. Appl. Meteor., 43, 157-169.

Table 1 Measured calm and non-calm occurrences over the modeling domain during August 2002 based on NWS data

Hour	#Non-Calm	#Calm	#Total	% Calm
00Z	18209	3924	22133	17.7
01Z	16531	6026	22557	26.7
02Z	15604	6929	22533	30.8
03Z	14983	7245	22228	32.6
04Z	14309	7540	21849	34.5
05z	14073	7735	21808	35.5
06Z	13934	7949	21883	36.3
07Z	13792	8040	21832	36.8
08Z	13542	8273	21815	37.9
09Z	13542	8385	21927	38.2
10Z	13708	8591	22299	**38.5**
11Z	14139	8693	22832	38.1
12Z	15297	7690	22987	33.5
13Z	17336	5192	22528	23
14Z	18522	3439	21961	15.7
15Z	18755	2617	21372	12.2
16Z	19169	2015	21184	9.5
17Z	19555	1617	21172	7.6
18Z	19982	1430	21412	6.7
19Z	20149	1389	21538	6.4
20Z	20565	1288	21853	5.9
21Z	20518	1383	21901	6.3
22Z	20672	1556	22228	7
23Z	20231	2292	22523	10.2

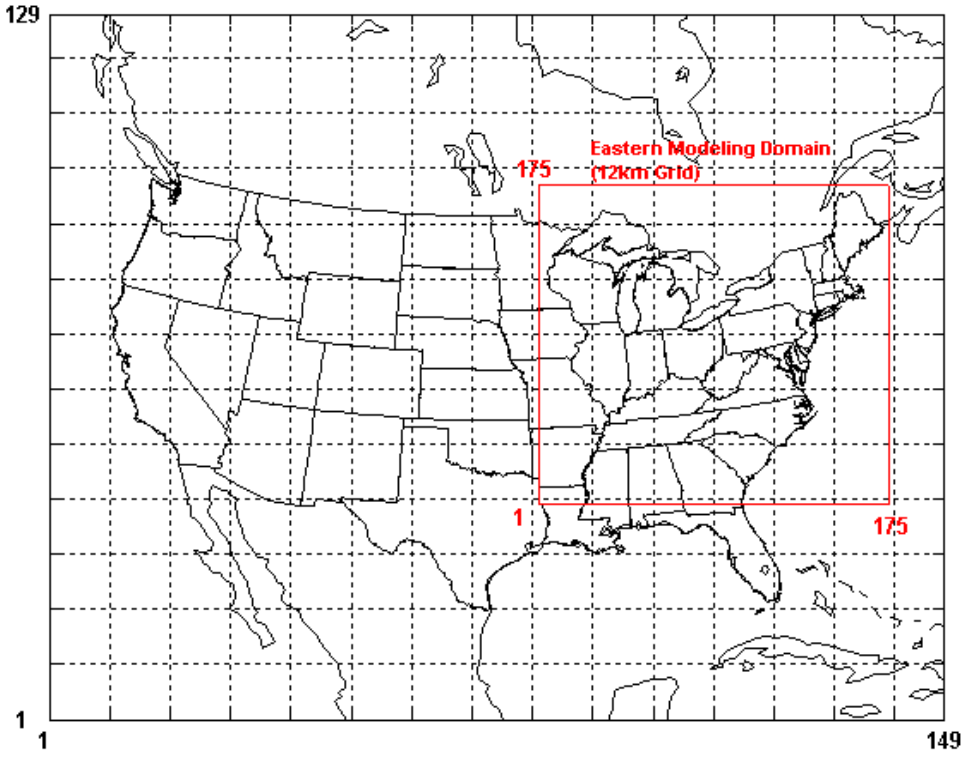

Figure 1: OTC MM5 modeling domain with areal extent of 12km and 36km grids

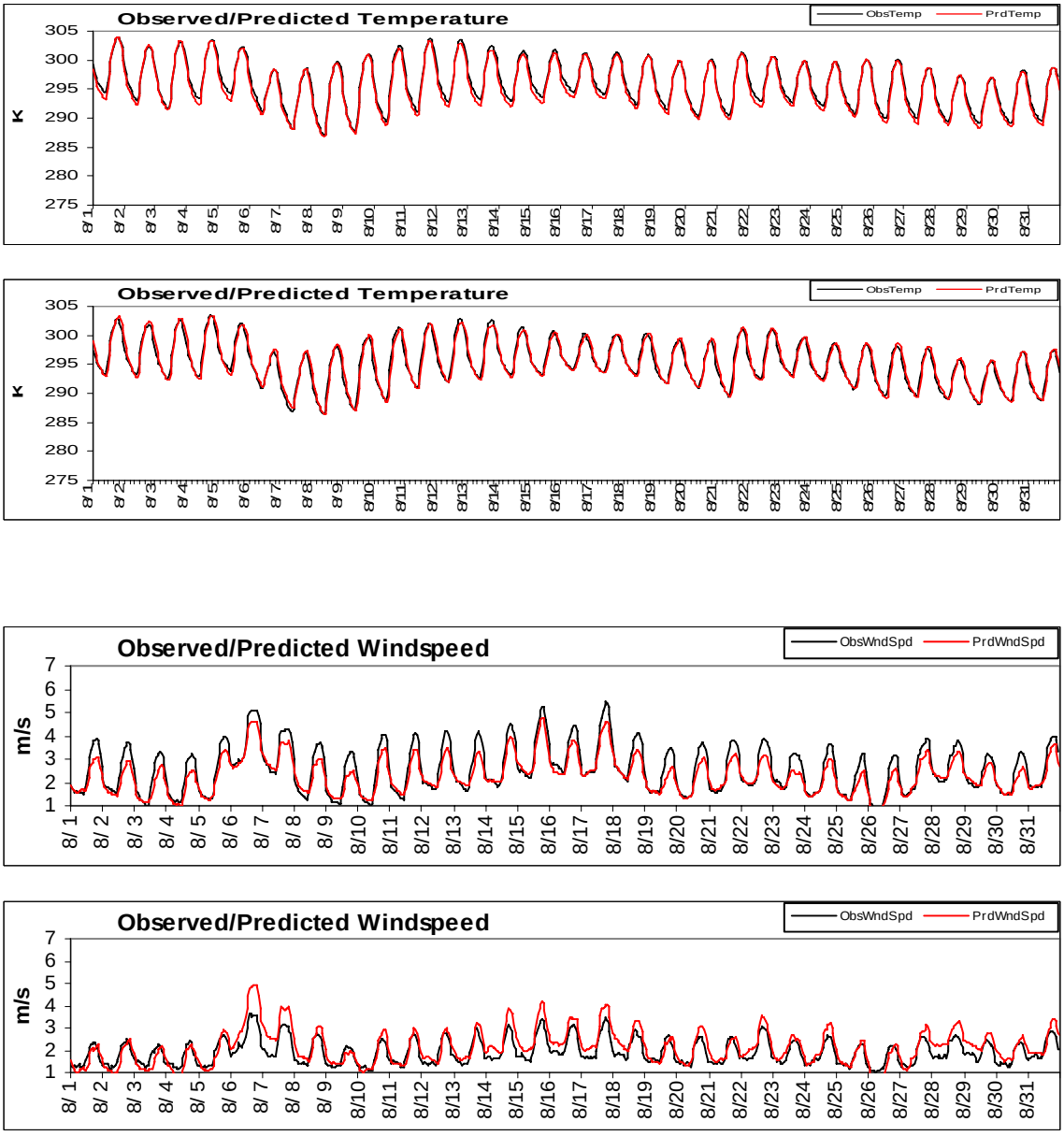

Figure 2: Temperature and Wind speed comparisons for August 2002. In each case the upper panel corresponds to comparison between MM5 and NWS data and the lower panel between MM5 and CASTNet data.

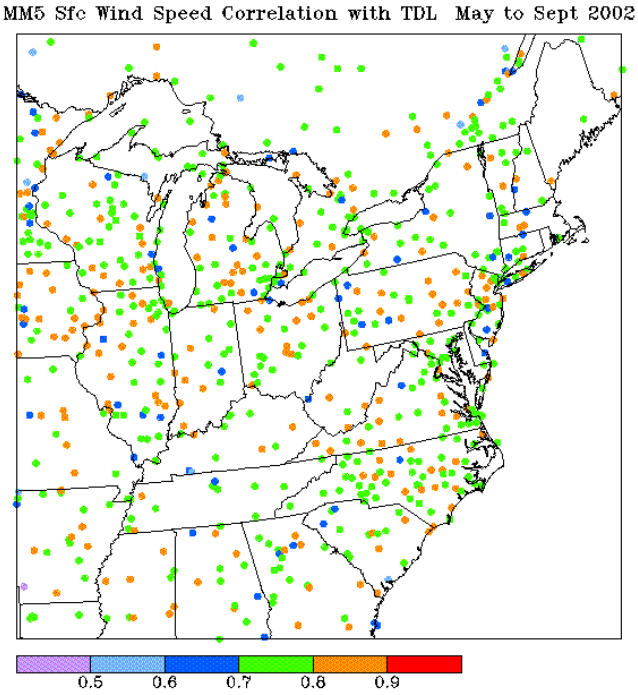

Figure 3a: Spatial correlation estimates between MM5 and NWS data for wind speed from May to September 2002

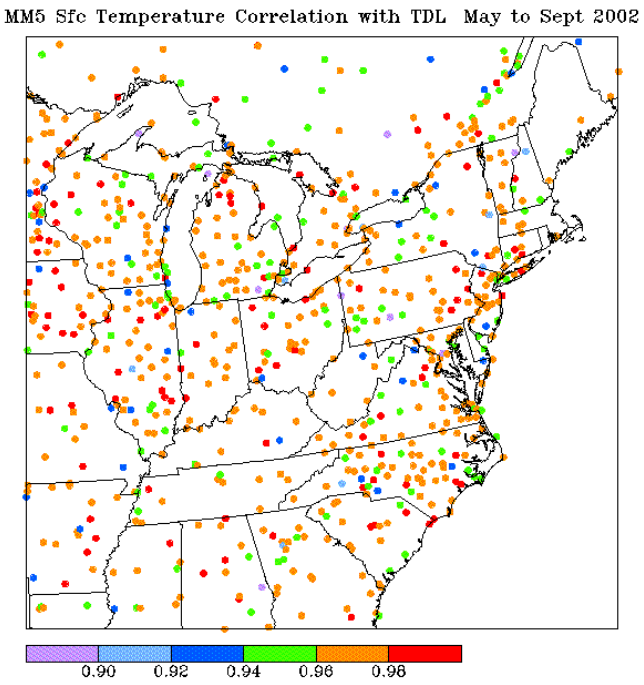

Figure 3b: Spatial distribution of correlation coefficients for Temperature between MM5 and NWS data from May to September 2002.

Richmond, VA

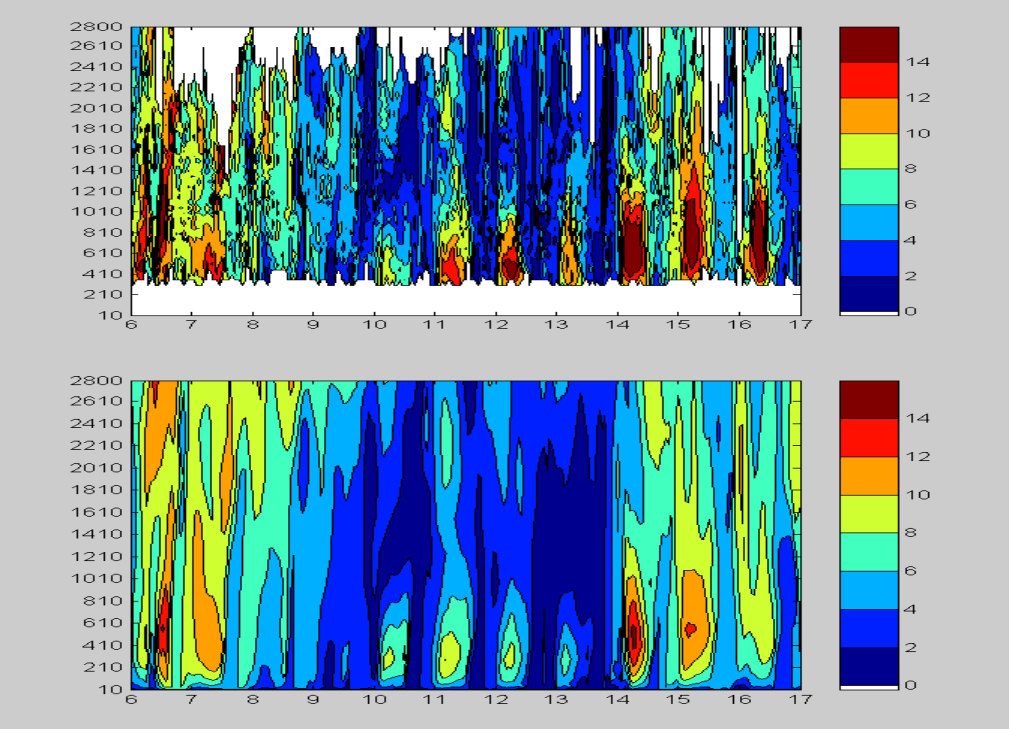

Concord, NH

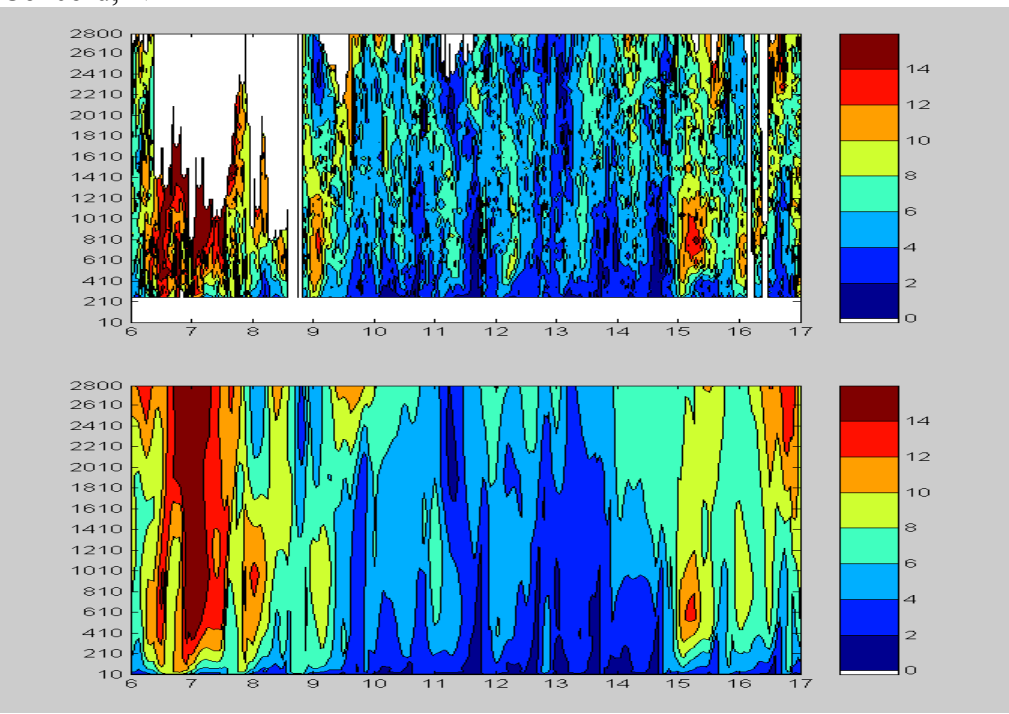

Figure 4: MM5 and Wind profiler comparison for August 6 to 17, 2002 at Richmond, VA and Concord, NH. The upper and lower panes at each station are for MM5 and profiler, respectively. The abcissa represents day and the ordinate the height (m).

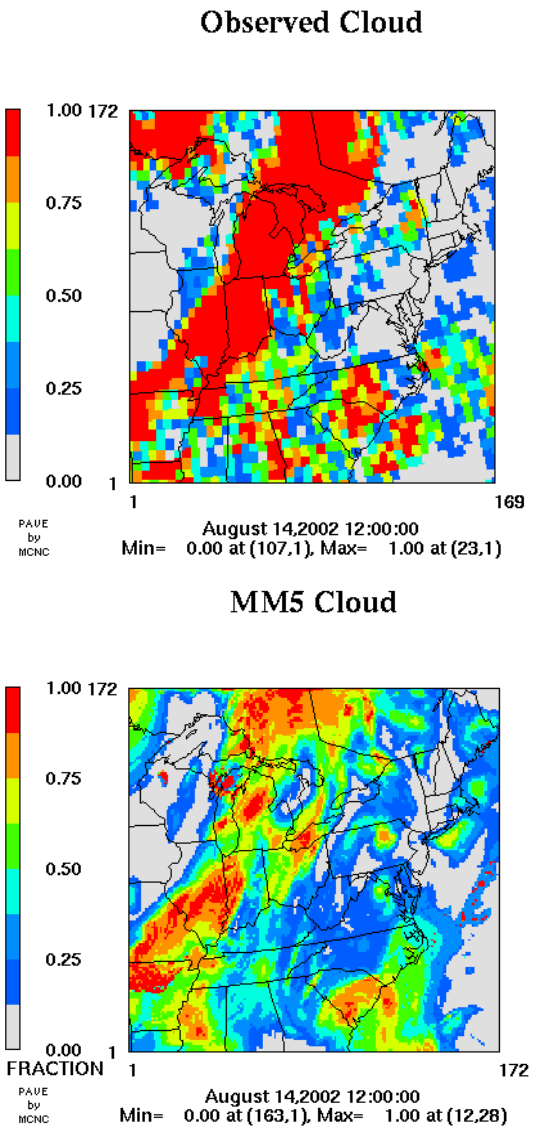

Figure 5: MM5 and Satellite cloud images for August 14, 2002 at 0700 EST

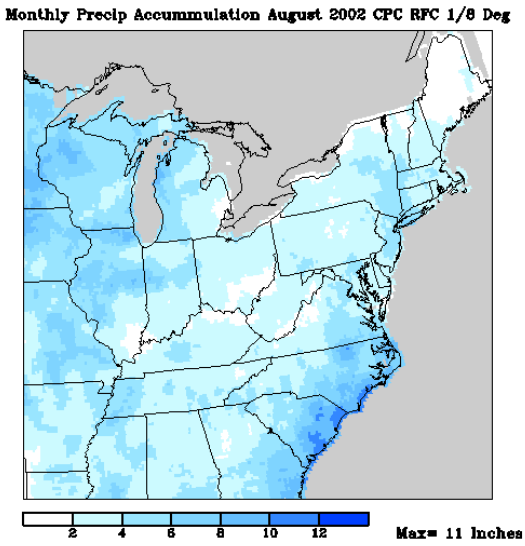

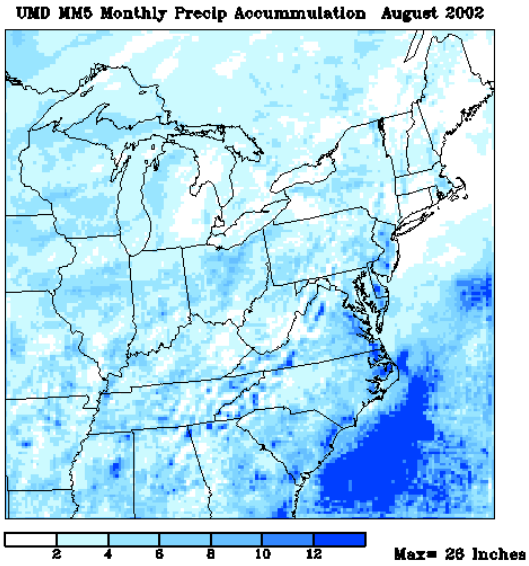

Figure 6: MM5 predicted and measured precipitation over the domain for the month of August 2002

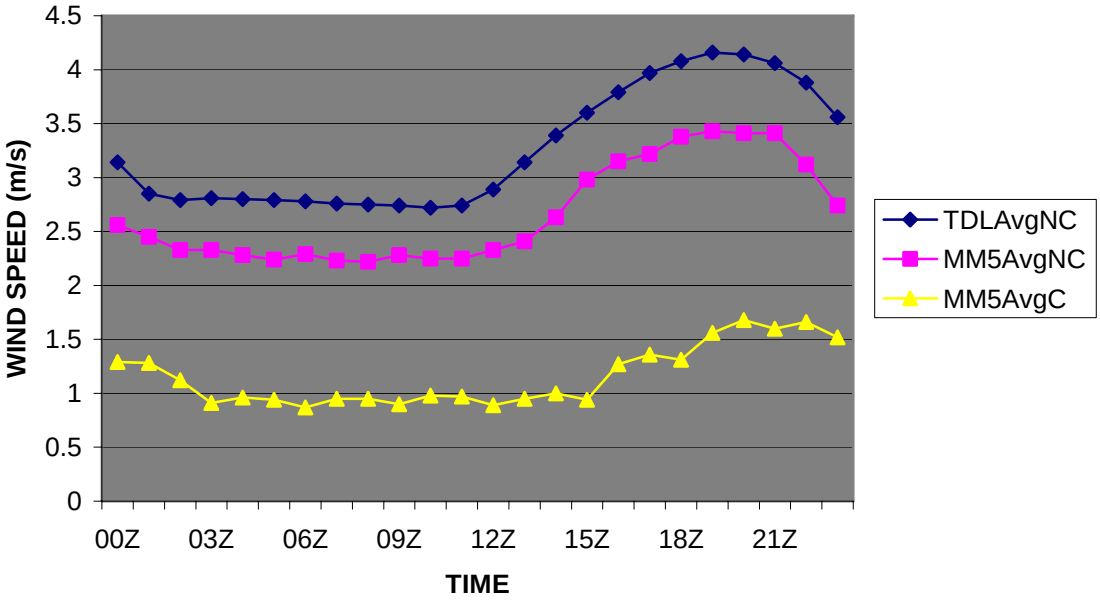

Figure 7: Comparison of averaged wind speed between MM5 and observed under calm (C) and non-calm (NC) conditions.

Appendix F-9

MM5 Model Configurations

Table F-9-1. OTC MM5 Meteorological Model Configuration

Science Options	Configuration	Details/Comments
Model Code	MM5 Version 3.6	
Horizontal Grid Mesh	36km/12km	
36-km grid	149x129 cells	
12-km grid	175x175 cells	
Vertical Grid Mesh	29 layers	
Grid Interaction	No feedback	Two-way nesting
Initialization	Eta first guess fields/LittleR	
Boundary Conditions	Eta first guess fields/LittleR	
Microphysics	Simple Ice	
Cumulus Scheme	Kain-Fritsch	36km/12km grids
Planetary Boundary Layer	High-resolution Blackadar PBL	
Radiation	Simple cooling	
Vegetation Data	USGS	24 Category Scheme
Land Surface Model	Five-Layer Soil model	
Shallow Convection	None	
Sea Surface Temperature	Do not update SST	
Thermal Roughness	Default	
Snow Cover Effects	None	
4D Data Assimilation	Analysis Nudging: 36km/12km	
Integration Time Step	75 seconds	
Simulation Periods	2002	
Platform	Linux Cluster	Done at UMD

Appendix F-10

SMOKE Processing Description and Configuration

TSD-1b

Processing of Biogenic Emissions for OTC / MANE-VU Modeling

Bureau of Air Quality Analysis and Research
Division of Air Resources
New York State Department of Environmental Conservation
Albany, NY 12233

September 19, 2006

Biogenic emissions for the time period from January 1, 2002 – December 31, 2002 were calculated by NYSDEC using the Biogenic Emissions Inventory System (BEIS) version 3.12 integrated within SMOKE2.1. General information about BEIS is available at http://www.epa.gov/AMD/biogen.html while documentation about biogenic emissions processing within SMOKE2.1 is available at http://cf.unc.edu/cep/empd/products/smoke/version2.1/html/ch06s10.html and http://cf.unc.edu/cep/empd/products/smoke/version2.1/html/ch06s17.html . Note that the SMOKE documentation refers to BEIS3.09 and has not yet been updated for BEIS3.12. This affects the number of species modeled as well as the use of different speciation profiles. However, the general processing approach has not changed from BEIS3.09 to BEIS3.12. In short, this processing approach is as follows and was utilized by NYSDEC for its biogenic emission processing for 8-hr ozone and $PM_{2.5}$ modeling:

1. **Normbeis3** reads gridded land use data and emissions factors and produces gridded normalized biogenic emissions for 34 species/compounds. The gridded land use includes 230 different land use types. Both summer and winter emissions factors for each species/compound are provided for each of the 230 land use types. On output, **Normbeis3** generates a file `B3GRD` which contains gridded summer and winter emission fluxes for the modeling domain that are normalized to 30 °C and a photosynthetic active radiation (PAR) of 1000 µmol/m^2s. In addition, gridded summer and winter leaf area indices (LAI) are also written to `B3GRD`.

2. **Tmpbeis3** reads the gridded, normalized emissions file `B3GRD` and meteorological data from the MCIP-processed MM5 meteorological fields generated by the University of Maryland for MANE-VU/OTC modeling. Specifically, the following MM5/MCIP meteorological variables are used by **Tmpbeis3** to compute hour-specific, gridded biogenic emissions from the normalized emission fluxed contained in `B3GRD`: layer-1 air temperature (“TA”), layer-1 pressure (“PRES”), total incoming solar radiation at the surface (“RGRND”), and convective (“RC”) and non-convective (“RN”) rainfall. Additionally, the emissions for the 34 species/compounds modeled by BEIS3.12 are converted to CO, NO, and the CB-IV

VOC species utilized in CMAQ via the use of the BEIS3.12-CB-IV speciation profile. In adition, an optional seasonal switch file, `BIOSEASON`, was utilized to decide whether to use summer or winter emissions factors for any given grid cell on any given day. This file was generated by the SMOKE2.1 utility **Metscan** based on MM5 layer-1 air temperatures to determine the date of the last spring frost and first fall frost at each grid cell. Summer emission factors are used by **Tmpbeis3** for the time period between the last spring frost and first fall frost at any given grid cell, and winter emission factors are used for the remaining time period. Documentation for the **Metscan** utility is available at http://cf.unc.edu/cep/empd/products/smoke/version2.1/html/ch05s07.html . An animated GIF file showing the `BIOSEASON` file used by NYSDEC can be found at ftp://ftp.dec.state.ny.us/dar/air_research/chogrefe/biog_reports/b3season_movie.gif

3. For reporting purposes, the hourly, speciated, gridded emissions were aggregated to the county level for each day. For any given grid cell, emissions are distributed among the counties intersecting this grid cell in proportion to the area of each of these counties within the grid cell. The area gridding surrogates needed for this aggregration are based on a file obtained from EPA via http://www.epa.gov/ttn/chief/emch/spatial/new/bgpro.12km_041604.us.gz followed by windowing for the MANE-VU/OTC modeling domain.

Table 1 County and State totals of estimated biogenic emissions (tpy)

State	FIPS	County	NO [TPY]	CO [TPY]	VOC [TPY]
Connecticut	009001	Fairfield	52	894	7150
	009003	Hartford	88	915	8537
	009005	Litchfield	98	1261	12221
	009007	Middlesex	54	615	5587
	009009	New Haven	80	876	7544
	009011	New London	74	906	8960
	009013	Tolland	55	651	5999
	009015	Windham	60	772	8019
Connecticut		**TOTAL**	560	6889	64017
Deleware	010001	Kent	308	1354	15912
	010003	New Castle	143	875	8834
	010005	Sussex	539	2045	21595
Deleware		**TOTAL**	990	4274	46342
DC	011001	Washington	30	150	1726
DC		**TOTAL**	30	150	1726
Maine	023001	Androscoggin	35	885	8204
	023003	Aroostook	741	15531	140877
	023005	Cumberland	49	1298	11528
	023007	Franklin	72	3269	32111
	023009	Hancock	66	2950	27090
	023011	Kennebec	73	1425	12849
	023013	Knox	30	689	6680
	023015	Lincoln	32	849	8072
	023017	Oxford	79	3224	34189
	023019	Penobscot	211	7249	63128
	023021	Piscataquis	146	8638	80748
	023023	Sagadahoc	37	526	4504
	023025	Somerset	173	8413	77850
	023027	Waldo	57	1833	18125
	023029	Washington	144	6459	58678
	023031	York	73	1698	15571
Maine		**TOTAL**	2018	64936	600203
Maryland	024001	Allegany	63	661	8664
	024003	Anne Arundel	79	945	12786
	024005	Baltimore	166	847	8102
	024009	Calvert	59	798	10048
	024011	Caroline	202	648	7907

	024013	Carroll	189	822	7853
	024015	Cecil	86	654	10093
	024017	Charles	78	1079	15042
	024019	Dorchester	134	829	10337
	024021	Frederick	204	1123	10964
	024023	Garrett	102	930	11391
	024025	Harford	141	911	9053
	024027	Howard	75	562	4460
	024029	Kent	177	498	4761
	024031	Montgomery	134	813	6786
	024033	Prince Georges	87	732	10214
	024035	Queen Annes	222	684	7146
	024037	St Marys	99	886	10793
	024039	Somerset	58	498	5796
	024041	Talbot	131	495	5225
	024043	Washington	112	781	7538
	024045	Wicomico	124	796	10304
	024047	Worcester	158	1121	13079
	024510	Baltimore	54	235	1762
Maryland		**TOTAL**	2934	18350	210104
Massachusetts	025001	Barnstable	261	668	5905
	025003	Berkshire	73	1182	11029
	025005	Bristol	107	753	7142
	025007	Dukes	115	252	1728
	025009	Essex	55	794	7128
	025011	Franklin	61	1031	9424
	025013	Hampden	51	904	9201
	025015	Hampshire	61	820	7056
	025017	Middlesex	68	1085	11630
	025019	Nantucket	56	159	1362
	025021	Norfolk	49	615	5513
	025023	Plymouth	170	1197	11876
	025025	Suffolk	26	177	1351
	025027	Worcester	103	1955	23612
Massachusetts		**TOTAL**	1257	11594	113957
New Hampshire	033001	Belknap	25	693	6915
	033003	Carroll	40	1512	14981
	033005	Cheshire	49	1019	10099
	033007	Coos	72	3239	33668
	033009	Grafton	91	2442	23151
	033011	Hillsborough	48	1337	14503
	033013	Merrimack	48	1314	13566
	033015	Rockingham	39	1120	10080
	033017	Strafford	25	686	6617
	033019	Sullivan	45	943	8314
New Hampshire		**TOTAL**	482	14306	141894

New Jersey	034001	Atlantic	135	1225	18890
	034003	Bergen	37	239	2455
	034005	Burlington	151	1827	25255
	034007	Camden	68	491	7751
	034009	Cape May	90	566	7763
	034011	Cumberland	122	773	10699
	034013	Essex	57	199	1831
	034015	Gloucester	119	556	8444
	034017	Hudson	26	125	701
	034019	Hunterdon	81	706	5743
	034021	Mercer	85	475	4889
	034023	Middlesex	98	456	5267
	034025	Monmouth	125	1152	15423
	034027	Morris	63	604	7288
	034029	Ocean	128	1871	27063
	034031	Passaic	41	339	3841
	034033	Salem	123	535	8304
	034035	Somerset	49	518	5548
	034037	Sussex	67	718	7768
	034039	Union	21	168	2191
	034041	Warren	125	517	4505
New Jersey		**TOTAL**	1813	14058	181618
New York	036001	Albany	59	730	6253
	036003	Allegany	129	1218	9526
	036005	Bronx	25	100	657
	036007	Broome	107	879	7861
	036009	Cattaraugus	148	1654	13540
	036011	Cayuga	227	986	7928
	036013	Chautauqua	202	1260	8144
	036015	Chemung	88	521	3911
	036017	Chenango	149	1120	7833
	036019	Clinton	138	1631	13341
	036021	Columbia	96	896	8484
	036023	Cortland	101	616	4280
	036025	Delaware	133	1672	13435
	036027	Dutchess	90	1096	10288
	036029	Erie	165	1127	6898
	036031	Essex	94	2547	20888
	036033	Franklin	228	2337	17197
	036035	Fulton	90	764	5275
	036037	Genesee	201	645	3993
	036039	Greene	47	886	8182
	036041	Hamilton	78	2092	16056
	036043	Herkimer	175	1783	12846
	036045	Jefferson	251	1754	12503
	036047	Kings	15	60	309

	036049	Lewis	154	1693	12116
	036051	Livingston	222	888	6048
	036053	Madison	149	1049	7528
	036055	Monroe	223	990	6237
	036057	Montgomery	106	579	4715
	036059	Nassau	81	408	2859
	036061	New York	16	76	473
	036063	Niagara	335	940	5182
	036065	Oneida	214	1515	10021
	036067	Onondaga	171	929	6259
	036069	Ontario	178	767	6024
	036071	Orange	110	1065	13024
	036073	Orleans	195	635	3314
	036075	Oswego	119	1277	7911
	036077	Otsego	157	1190	7958
	036079	Putnam	32	473	5243
	036081	Queens	20	105	543
	036083	Rensselaer	96	894	7316
	036085	Richmond	47	173	1292
	036087	Rockland	26	300	4006
	036089	St. Lawrence	376	3876	28960
	036091	Saratoga	76	1125	9010
	036093	Schenectady	39	377	3032
	036095	Schoharie	95	737	5496
	036097	Schuyler	87	438	3193
	036099	Seneca	127	438	3305
	036101	Steuben	267	1475	12085
	036103	Suffolk	368	1328	12886
	036105	Sullivan	76	1325	12538
	036107	Tioga	102	730	5400
	036109	Tompkins	96	576	4128
	036111	Ulster	82	1493	15714
	036113	Warren	46	1396	11568
	036115	Washington	183	1109	8355
	036117	Wayne	270	920	5940
	036119	Westchester	35	549	5347
	036121	Wyoming	194	720	3813
	036123	Yates	107	507	4017
New York		**TOTAL**	8313	63436	492483
Pennsylvania	042001	Adams	186	892	8926
	042003	Allegheny	182	948	6727
	042005	Armstrong	108	940	9955
	042007	Beaver	69	600	4895
	042009	Bedford	128	1249	14127
	042011	Berks	280	1377	14146
	042013	Blair	91	729	7579
	042015	Bradford	224	1265	9423

042017	Bucks	144	954	8399
042019	Butler	149	1032	8602
042021	Cambria	128	805	6545
042023	Cameron	25	627	7563
042025	Carbon	53	585	8121
042027	Centre	158	1344	16886
042029	Chester	264	1176	10474
042031	Clarion	85	848	10743
042033	Clearfield	149	1368	13267
042035	Clinton	71	1230	18191
042037	Columbia	106	802	9080
042039	Crawford	204	1297	10839
042041	Cumberland	193	816	9505
042043	Dauphin	116	799	8502
042045	Delaware	35	410	3250
042047	Elk	49	949	8921
042049	Erie	199	1107	8273
042051	Fayette	156	1087	9277
042053	Forest	26	577	7122
042055	Franklin	271	1057	10296
042057	Fulton	93	744	9341
042059	Greene	91	830	6966
042061	Huntingdon	135	1093	12606
042063	Indiana	144	1078	9156
042065	Jefferson	101	865	7362
042067	Juniata	79	588	8263
042069	Lackawanna	58	586	5569
042071	Lancaster	464	1299	9565
042073	Lawrence	114	503	3755
042075	Lebanon	155	623	5827
042077	Lehigh	149	594	6040
042079	Luzerne	75	1013	13215
042081	Lycoming	152	1457	16633
042083	Mc Kean	57	1044	7113
042085	Mercer	175	865	7114
042087	Mifflin	107	620	7508
042089	Monroe	75	773	8856
042091	Montgomery	106	812	6736
042093	Montour	85	321	3306
042095	Northampton	144	506	4416
042097	Northumberland	92	570	6340
042099	Perry	113	804	10216
042101	Philadelphia	29	194	1420
042103	Pike	37	757	9946
042105	Potter	89	1129	9027
042107	Schuylkill	123	1050	15001
042109	Snyder	88	538	6373
042111	Somerset	221	1251	11228

	042113	Sullivan	45	684	5112
	042115	Susquehanna	126	978	6448
	042117	Tioga	176	1313	10942
	042119	Union	71	541	6435
	042121	Venango	72	855	9086
	042123	Warren	76	1031	7352
	042125	Washington	166	1068	7429
	042127	Wayne	89	862	5954
	042129	Westmoreland	199	1297	10589
	042131	Wyoming	60	551	4634
	042133	York	366	1393	12758
Pennsylvania		**TOTAL**	8645	59945	585271
Rhode Island	044001	Bristol	40	90	441
	044003	Kent	41	328	3471
	044005	Newport	37	183	1646
	044007	Providence	39	591	6901
	044009	Washington	54	572	6775
Rhode Island		**TOTAL**	211	1764	19233
Vermont	050001	Addison	186	922	6274
	050003	Bennington	43	896	7349
	050005	Caledonia	58	1149	10239
	050007	Chittenden	74	606	3633
	050009	Essex	61	1315	11795
	050011	Franklin	208	971	5927
	050013	Grand Isle	50	490	3506
	050015	Lamoille	36	727	5627
	050017	Orange	57	1182	10120
	050019	Orleans	120	1570	12842
	050021	Rutland	102	1257	9867
	050023	Washington	47	1099	9502
	050025	Windham	42	1232	10898
	050027	Windsor	57	1330	10796
Vermont		**TOTAL**	1142	14745	118376
Virginia	051001	Accomack	187	959	9472
	051003	Albemarle	140	1246	12533
	051005	Alleghany	35	522	7369
	051007	Amelia	70	915	10717
	051009	Amherst	80	905	10823
	051011	Appomattox	76	830	10447
	051013	Arlington	17	64	531
	051015	Augusta	135	1049	13291
	051017	Bath	46	771	11636
	051019	Bedford	189	1279	13052
	051021	Bland	41	515	7097
	051023	Botetourt	74	780	10211

051025	Brunswick	98	1458	18254
051027	Buchanan	32	722	9557
051029	Buckingham	76	1287	18830
051031	Campbell	112	1078	12933
051033	Caroline	73	1173	16020
051035	Carroll	132	634	6885
051036	Charles City	93	415	4711
051037	Charlotte	84	1219	14277
051041	Chesterfield	69	802	10686
051043	Clarke	56	369	4009
051045	Craig	39	538	7314
051047	Culpeper	105	894	10720
051049	Cumberland	56	814	10677
051051	Dickenson	20	550	6910
051053	Dinwiddie	82	1207	16511
051057	Essex	58	671	7403
051059	Fairfax	111	533	5538
051061	Fauquier	150	1166	14084
051063	Floyd	47	593	6493
051065	Fluvanna	54	775	10756
051067	Franklin	119	1297	15933
051069	Frederick	64	588	8798
051071	Giles	38	508	4918
051073	Gloucester	32	510	5945
051075	Goochland	47	670	10392
051077	Grayson	60	627	8260
051079	Greene	57	434	5727
051081	Greensville	63	735	9009
051083	Halifax	201	1852	22730
051085	Hanover	91	950	12493
051087	Henri	81	427	5468
051089	Henry	59	805	9772
051091	Highland	44	608	8579
051093	Isle Of Wight	178	813	8049
051095	James City	41	314	3989
051097	King And Queen	77	673	7615
051099	King George	62	540	6111
051101	King William	102	712	7846
051103	Lancaster	33	311	3669
051105	Lee	97	680	7221
051107	Loudoun	137	942	8999
051109	Louisa	78	1142	16780
051111	Lunenberg	88	1108	13611
051113	Madison	70	598	7305
051115	Mathews	27	367	4025
051117	Mecklenburg	145	1478	18507
051119	Middlesex	42	480	5561
051121	Montgomery	70	501	5366

051125	Nelson	67	979	12465
051127	New Kent	35	600	8240
051131	Northampton	90	263	2019
051133	Northumberland	88	778	9298
051135	Nottoway	74	894	10670
051137	Orange	98	759	8265
051139	Page	77	540	6705
051141	Patrick	75	884	10255
051143	Pittsylvania	203	1806	22102
051145	Powhatan	47	675	10194
051147	Prince Edward	69	942	12042
051149	Prince George	73	572	6484
051153	Prince William	38	718	10979
051155	Pulaski	61	450	6510
051157	Rappahannock	61	521	7141
051159	Richmond	63	383	4548
051161	Roanoke	63	427	5278
051163	Rockbridge	101	813	9710
051165	Rockingham	189	1020	12959
051167	Russell	56	703	7975
051169	Scott	95	753	9943
051171	Shenandoah	117	757	10570
051173	Smyth	78	603	7159
051175	Southampton	177	1306	15588
051177	Spotsylvania	46	911	12575
051179	Stafford	27	637	8344
051181	Surry	85	784	10024
051183	Sussex	102	1267	16362
051185	Tazewell	77	639	7477
051187	Warren	44	438	6310
051191	Washington	142	632	6822
051193	Westmoreland	101	777	9357
051195	Wise	35	462	5685
051197	Wythe	109	596	7803
051199	York	35	271	3423
051510	Alexandria	38	145	1065
051515	Bedford	22	101	604
051520	Bristol	37	135	1220
051530	Buena Vista	6	43	381
051540	Charlottesville	18	98	528
051550	Chesapeake	71	666	8477
051560	Clifton Forge	27	61	436
051570	Colonial Heights	35	88	662
051580	Covington	24	114	1605
051590	Danville	55	343	3405
051595	Emporia	19	234	3300
051600	Fairfax	18	96	1518
051610	Falls Church	16	98	1120

	051620	Franklin	66	142	1041
	051630	Fredericksburg	14	250	3012
	051640	Galax	45	94	519
	051650	Hampton	24	127	1112
	051660	Harrisonburg	73	143	746
	051670	Hopewell	26	79	711
	051678	Lexington	8	62	620
	051680	Lynchburg	45	250	2135
	051683	Manassas	17	86	743
	051685	Manassas Park	17	50	268
	051690	Martinsville	19	190	1625
	051700	Newport News	63	231	2187
	051710	Norfolk	42	197	2692
	051720	Norton	13	120	1305
	051730	Petersburg	58	171	1419
	051735	Poquoson	17	122	1351
	051740	Portsmouth	34	285	3215
	051750	Radford	27	76	609
	051760	Richmond	29	239	3517
	051770	Roanoke	33	91	770
	051775	Salem	14	61	568
	051790	Staunton	69	205	1550
	051800	Suffolk	118	964	11269
	051810	Virginia Beach	186	924	8724
	051820	Waynesboro	43	120	895
	051830	Williamsburg	3	38	446
	051840	Winchester	42	117	772
Virginia		**TOTAL**	9267	80615	981848

TSD-1c

Emissions Processing for 2002 OTC Regional and Urban 12km Base Year Simulation

Bureau of Air Quality Analysis and Research
Division of Air Resources
New York State Department of Environmental Conservation
Albany, NY 12233

March 19, 2007

Overview

All emissions processing for the revised 2002 OTC regional and urban 12 km base case simulations was performed with SMOKE2.1 compiled on a Red Hat 9.0 Linux operating system with the Portland group fortran compiler version 5.1. The emissions processing was performed on a month-by-month and RPO-by-RPO basis, i.e. SMOKE processing was performed for each month for each of the RPOs (MANE-VU, VISTAS, CENRAP, MRPO) individually as well as for Canada. For each month/RPO combination, a separate SMOKE ASSIGNS file was created, and the length of the episode in each of these ASSIGNS files was set to the entire month. Also, as discussed in Section 3, there was no difference between "episode-average" temperatures and "monthly-average" temperatures for the Mobile6 simulations that used the option of temperature averaging.

This document is structured as follows: A listing of all emission inventories is given in Section 2, organized by RPO and source category. Section 3 discusses the Mobile6 processing approach employed for the different RPOs, while Section 4 describes the processing of biogenic emissions with BEIS3.12. Finally, Sections 5 through7 describe the temporal allocation, speciation, and spatial allocation of the emissions inventories, respectively.

1. Emission Inventories

1.1 MANE-VU

Version 3 of the MANE_VU inventory was utilized to generate CMAQ-ready emissions. This emissions inventory data were obtained from the MANEVU archive in April 2006.

1.1.1 Area Sources

- Files: MANEVU_AREA_SMOKE_INPUT_ANNUAL_SUMMERDAY_040606.txt and MANEVU_AREA_SMOKE_INPUT_ANNUAL_WINTERDAY_040606.txt prepared by PECHAN, downloaded from **ftp.marama.org** (username mane-vu, password exchange)
- Fugitive dust correction: This was applied as county-specific correction factors for SCC's listed at http://www.epa.gov/ttn/chief/emch/invent/index.html#dust; the correction factor file gcntl.xportfrac.txt was obtained from EPA's CAIR NODA ftp site http://www.airmodelingftp.com (password protected).; this adjustment was performed using the SMOKE programs cntlmat and grwinven to generate an adjusted IDA inventory file used for subsequent SMOKE processing

1.1.2 Nonroad Sources

- File: MANEVU_NRD2002_SMOKE_030306 prepared by PECHAN; downloaded from **ftp.marama.org** (username mane-vu, password exchange)

1.1.3 Mobile Sources

- VMT/Speed: MANEVU_2002_mbinv_02022006_addCT.txt prepared by PECHAN and NESCAUM; downloaded from http://bronze.nescaum.org/Private/junghun/MANE-VU/onroad_ver3_update/MANEVU_V3_update.tar

1.1.4 Point Sources

- Files: MANEVU_Point_SMOKE_INPUT_ANNUAL_SUMMERDAY_041006.txt and MANEVU_Point_SMOKE_INPUT_ANNUAL_WINTERDAY_041006.txt prepared by PECHAN were downloaded from **ftp.marama.org** (username mane-vu, password exchange)
- Fugitive dust correction: This was applied as county-specific correction factors for SCC's listed at http://www.epa.gov/ttn/chief/emch/invent/index.html#dust; the correction factor file gcntl.xportfrac.txt was obtained from EPA's CAIR NODA ftp site http://www.airmodelingftp.com (password protected).; this adjustment was performed using the SMOKE programs cntlmat and grwinven to generate an adjusted IDA inventory file used for subsequent SMOKE processing
- Corrected the omission of 2,100 tons/year VOC emissions from several point sources in NJ. NJDEP provided updated IDA files on June 30 that were used for modeling.

1.2 CENRAP

The inventory data were obtained from the CENRAP ftp site in March 2006 and reflect version BaseB of the CENRAP inventory.

1.2.1 Area Sources

- Files:
  - CENRAP_AREA_SMOKE_INPUT_ANN_STATES_081705.txt
  - CENRAP_AREA_MISC_SMOKE_INPUT_ANN_STATE_071905.txt
  - CENRAP_AREA_BURNING_SMOKE_INPUT_ANN_TX_ NELI_071905.txt
  - CENRAP_AREA_MISC_SMOKE_INPUT_NH3_MONTH_{MMM} _072805.txt where {MMM} is JAN, FEB, … DEC
  - CENRAP_AREA_SMOKE_INPUT_NH3_MONTH_{MMM} _071905.txt where {MMM} is JAN, FEB, … DEC
- Fugitive dust correction: This was applied as county-specific correction factors for SCC's listed at http://www.epa.gov/ttn/chief/emch/invent/index.html#dust; the correction factor file gcntl.xportfrac.txt was obtained from EPA's CAIR NODA ftp site http://www.airmodelingftp.com (password protected).; this adjustment was performed using the SMOKE programs cntlmat and grwinven to generate an adjusted IDA inventory file used for subsequent SMOKE processing
- Note about area and nonroad source SMOKE processing for the CENRAP region: All area source inventories (both annual and month-specific) were processed in

one step through SMOKE. SMK_AVEDAY_YN was set to N, so seasonal profiles were used to apportion the annual inventories numbers by month. This setting was also used for the nonroad processing performed in a separate step. This was necessary since the month-specific files had zero in their 'average-day' column and the annual total column reflects the "monthly emissions as annual totals" as per header line. Therefore, seasonal profiles are used to apportion both the annual and month-specific files. As described below, we utilized the temporal profiles and cross-reference files generated by CENRAP. However, we did not verify that this approach indeed leads to the intended monthly allocation of ammonia and nonroad emissions.

1.2.2 Nonroad Sources

- Files:
  - CENRAP_NONROAD_SMOKE_INPUT_ANN_071305.txt
  - CENRAP_NONROAD_SMOKE_INPUT_MONTH_{MMM}_071305.txt where {MMM} is JAN, FEB, … DEC

1.2.3 Mobile Sources

- VMT/Speed files:
  - mbinv02_vmt_cenrap_ce.ida
  - mbinv02_vmt_cenrap_no.ida
  - mbinv02_vmt_cenrap_so.ida
  - mbinv02_vmt_cenrap_we.ida

1.2.4 Point Sources

- File: CENRAP_POINT_SMOKE_INPUT_ANNUAL_DAILY_072505.txt
- Fugitive dust correction: This was applied as county-specific correction factors for SCC's listed at http://www.epa.gov/ttn/chief/emch/invent/index.html#dust; the correction factor file gcntl.xportfrac.txt was obtained from EPA's CAIR NODA ftp site http://www.airmodelingftp.com (password protected).; this adjustment was performed using the SMOKE programs cntlmat and grwinven to generate an adjusted IDA inventory file used for subsequent SMOKE processing.

1.3 VISTAS

All VISTAS emission files were obtained from the Alpine Geophysics ftp site. They reflect version BaseG of the VISTAS inventory with the exception of fire emissions which reflect BaseF and BaseD. These files were downloaded between February and August, 2006.

1.3.1 Area Sources

- Files:

    - arinv_vistas_2002g_2453922_w_pmfac.txt
    - ida_ar_fire_2002_vistaonly_basef.ida
- Note: the header lines of these files indicate that the fugitive dust correction was already applied, so no further correction was performed.

1.3.2 Nonroad Sources

- Files:
    - nrinv_vistas_2002g_2453908.txt
    - marinv_vistas_2002g_2453972.txt

1.3.3 Mobile Sources

- VMT/Speed file: mbinv_vistas_02g_vmt_12jun06.txt

1.3.4 Point Sources

- Files:
    - Annual:
        - egu_ptinv_vistas_2002typ_baseg_2453909.txt
        - negu_ptinv_vistas_2002typ_baseg_2453909.txt
        - ptinv_fires_{MM}_typ.vistas.ida where {MM} is 01, 02, 03, etc. depending on the month; these annual point fire files were generated as part of the VISTAS BaseD inventory and were obtained in January 2005
    - Hour-specific:
        - pthour_2002typ_baseg_{MMM}_28jun2006.ems where {MMM} is jan, feb, mar, etc.
        - pthour_fires_{MM}_typ.vistas.ida where {MM} is 01, 02, 03, etc. depending on the month; these hourly point fire files were generated as part of the VISTAS BaseD inventory and were obtained in January 2005
- Note: No fugitive dust correction was performed for these files.

1.4 MRPO

MRPO emissions for SMOKE modeling were generated by Alpine Geophysics through a contract from MARAMA to convert the MRPO BaseK inventory from NIF to IDA format. The files were downloaded from the MARAMA ftp site **ftp.marama.org** (username mane-vu, password exchange) between April and June 2006.

1.4.1 Area Sources

- Files:
    - Annual:
        - arinv_mar_mrpok_2002_27apr2006.txt
        - arinv_other_mrpok_2002_20jun2006.txt
    - Month-specific:

        - arinv_nh3_2002_mrpok_{mmm}_3may2006.txt where {mmm} is jan, feb, etc.
        - dustinv_2002_mrpok_{mmm}_23may2006.txt where {mmm} is jan, feb, etc.
- Fugitive dust correction: This correction was performed only to the arinv_other_mrpok_2002_20jun2006.txt file using county-specific correction factors for SCC's listed at http://www.epa.gov/ttn/chief/emch/invent/index.html#dust; the correction factor file gcntl.xportfrac.txt was obtained from EPA's CAIR NODA ftp site http://www.airmodelingftp.com (password protected).; this adjustment was performed using the SMOKE programs cntlmat and grwinven to generate an adjusted IDA inventory file used for subsequent SMOKE processing.
- Note about area source SMOKE processing: SMOKE processing was performed separately for the annual and month-specific files. For the annual inventory processing, SMK_AVEDAY_YN was set to N, so seasonal profiles were used to apportion the annual inventories numbers by month. For the month-specific inventory processing, this variable was set to Y so that no seasonal profiles would be applied and the inventory numbers in the 'average day' column would be used. To save a SMOKE processing step, the annual "marine" inventory "arinv_mar_mrpok_2002_27apr2006.txt" was processed together with the annual "other area source" inventory "arinv_other_mrpok_2002_20jun2006.txt" even though it technically is part of the nonroad inventory.

1.4.2 Nonroad Sources

- Files: nrinv_2002_mrpok_{mmm}_3may2006.txt where {mmm} is jan, feb, etc.

1.4.3 Mobile Sources

- VMT/Speed file: mbinv_mrpo_02f_vmt_02may06.txt

1.4.4 Point Sources

- Files: ptinv_egu_negu_2002_mrpok_1may2006.txt
- Fugitive dust correction: This correction was performed only to the arinv_other_mrpok_2002_20jun2006.txt file using county-specific correction factors for SCC's listed at http://www.epa.gov/ttn/chief/emch/invent/index.html#dust; the correction factor file gcntl.xportfrac.txt was obtained from EPA's CAIR NODA ftp site http://www.airmodelingftp.com (password protected).; this adjustment was performed using the SMOKE programs cntlmat and grwinven to generate an adjusted IDA inventory file used for subsequent SMOKE processing.

1.5 Canada

1.5.1 Area Sources

- File: AS2000_SMOKEready.txt obtained from ftp://ftp.epa.gov/EmisInventory/canada_2000inventory
- Fugitive dust correction: We applied "divide-by-four" correction for SCC's listed at http://www.epa.gov/ttn/chief/emch/invent/index.html#dust; this adjustment was performed outside SMOKE with in-house Fortran programs. No county/province-specific correction factors were available for Canada

1.5.2 Nonroad Sources

- File: NONROAD2000_SMOKEready.txt obtained from ftp://ftp.epa.gov/EmisInventory/canada_2000inventory

1.5.3 Mobile Sources

- File: MOBILE2000_SMOKEready.txt obtained from ftp://ftp.epa.gov/EmisInventory/canada_2000inventory
- Fugitive dust correction: applied "divide-by-four" correction for SCC's listed at http://www.epa.gov/ttn/chief/emch/invent/index.html#dust; this adjustment was performed outside of SMOKE with in-house Fortran programs. No county/province-specific correction factors were available for Canada.

1.5.4 Point Sources

There has long been difficulty in obtaining an up-to-date Canadian criteria emissions inventory for point sources. This is due largely to confidentiality rights afforded to Canadian facilities. Thus far, the most recent inventory of Canadian point sources is rooted in the 1985 NAPAP data and is close to two decades old. Because there are a number of high emitting industrial facilities in southern Canada it is of particular importance to have a reasonably accurate inventory of these sources especially when modeling air quality over the Northeast and Midwest United States. Toward this end, an effort was made to obtain more recent Canadian point source data and incorporate it into an inventory database, which could then be used for the 2002 OTC air quality modeling.

Perhaps the most accurate and publicly accessible source of Canadian pollutant data is now available from the National Pollutant Release Inventory (NPRI) database. This database contains 268 substances. Facilities that manufacture, process or otherwise use one of these substances and that meet reporting thresholds are required to report these emissions to Environment Canada on an annual basis. The NPRI data are available at Environment Canada's website and can be found at the link http://www.ec.gc.ca/pdb/npri/npri_home_e.cfm. The page hosts an on-line search engine where one can locate emissions by pollutant or location. In addition, the entire database is available for download as an MS Access or Excel file. The NPRI database contains

numerous pages with a rather comprehensive list of information. Detailed information is available about each facility, including location, activity and annual emissions. In addition, facilities having stacks with a height of 50 meters or more are required to report stack parameters.

Unfortunately, one of the limitations of the NPRI database for modeling purposes is that the data are only available at the facility level. Emissions models require process level information, so in order to use this data, a few generalizations had to be made. Each facility has a Standard Industrial Classification (SIC) code associated with it; however, emissions models require Source Classification Codes (SCC's). SCC's are of critical importance as the emissions models use these codes for assignment of temporal and speciation profiles. SIC codes describe the general activity of a facility while SCC codes describe specific processes taking place at each facility. While no direct relationship exists between these two codes, a general albeit subjective association can be made.

For the purposes of creating a model-ready inventory file it was necessary to obtain the whole NPRI database. After merging all the necessary components from the NPRI database required in the SMOKE inventory file, the SIC code from each facility was examined and assigned an SCC code. In most cases, only a SCC3 level code was assigned with confidence. While this is admittedly a less than desirable process, it does allow for the use of the most recent emissions from the NPRI database to be used in modeling. Furthermore, having some level of SCC associated with these emissions will ensure that they will be assigned a temporal and speciation profile by the model, other than the default. Once the model-ready inventory file was developed, it was processed through SMOKE.

2. Mobile6 Processing

2.1 MANE-VU

2.1.1 Mobile6 input files

- Month-specific input files were prepared by PECHAN and NESCAUM and were downloaded from http://bronze.nescaum.org/Private/junghun/MANE-VU/onroad_ver3_update/MANEVU_V3_update.tar
- Added the line "REBUILD EFFECTS :0.10" to each file before the SCENARIO record to override the Mobile6 default setting of 0.9 (90%) for the "chip reflash" effectiveness

2.1.2 SMOKE/Mobile6 auxiliary files

- SMOKE/Mobile6 auxiliary files were prepared by PECHAN and NESCAUM and were downloaded from http://bronze.nescaum.org/Private/junghun/MANE-VU/onroad_ver3_update/MANEVU_V3_update.tar

2.1.3 Temperature averaging

- Following the setting in the MANEVU_2002_mvref.txt files, the following procedures were used by SMOKE for temporal and spatial temperature averaging in the calculation of emission factors:
    - Spatial averaging: temperatures were averaged over all counties that share a common reference county (i.e. Mobile6 input file)
    - Temporal averaging for May – September emissions processing: no temporal averaging was used, i.e. day-specific temperatures were used to calculate emission factors for each day.
    - Temporal averaging for non-summer-months emissions processing: Temporal averaging over the duration of the episode (i.e. the entire month, see introduction) was used, i.e. monthly average temperatures were used to calculate the emission factors.

2.2 CENRAP

2.2.1 Mobile6 input files

- Mobile6 input files for the CENRAP region for January and July were contained in the files central_M6_{MMM}.zip, north_M6_{MMM}.zip, south_M6_{MMM}.zip, west_M6_{MMM}.zip where {MMM} is either jan or jul. July input files were used for April – September processing, while January input files were used for the remaining months
- All files were downloaded from the CENRAP ftp site in March 2006.

2.2.2 SMOKE/Mobile6 auxiliary files

- SMOKE/Mobile6 auxiliary files were contained in the files central_M6_RD.zip, north_M6_RD.zip, south_M6_RD.zip, and west_M6_RD.zip. The SMOKE MCREF, MVREF, and MCODES files were contained in the file MOBILESMOKE_Inputs.zip. The MCREF and MVREF files were combined for the different regions (“central”, “east”, “west”, “north”)
- All files were downloaded from the CENRAP ftp site in March 2006.

2.2.3 Temperature averaging

- The following procedures were used by SMOKE for temporal and spatial temperature averaging in the calculation of emission factors according to the setting in the mvref files:
    - Spatial averaging: no spatial averaging of temperatures, i.e. the temperatures for the reference county is used to calculate emission factors for all counties that share this reference county (i.e. Mobile6 input file)
    - Temporal averaging: Temporal averaging over the duration of the episode (i.e. the entire month, see introduction) was used, i.e. monthly average temperatures were used to calculate the emission factors.

2.3 VISTAS

2.3.1 Mobile6 input files

- Month-specific Mobile6 input files were obtained from the Alpine Geophysics ftp site in July 2006. They reflect version BaseG of the VISTAS inventory.

2.3.2 SMOKE/Mobile6 auxiliary files

- SMOKE/Mobile6 auxiliary files utilized were obtained from the Alpine Geophysics ftp site in July 2006. They reflect version BaseG of the VISTAS inventory.

2.3.3 Temperature averaging

- The following procedures were used by SMOKE for the temporal and spatial temperature averaging in the calculation of emission factors according to the setting in the mvref_baseg.36k.ag.txt file:
    - Spatial averaging: temperatures averaged over all counties that share a common reference county (i.e. Mobile6 input file)
    - Temporal averaging: Temporal averaging over the duration of the episode (i.e. the entire month, see introduction) was used, i.e. monthly average temperatures were used to calculate the emission factors.

2.4 MRPO

2.4.1 Mobile6 input files

- Month-specific Mobile6 input files for SMOKE modeling were generated by Alpine Geophysics through a contract from MARAMA. They are based on version BaseK of the MRPO inventory. The files were downloaded from the MARAMA ftp site **ftp.marama.org** (username mane-vu, password exchange) in May 2006.

2.4.2 SMOKE/Mobile6 auxiliary files

- SMOKE/Mobile6 auxiliary files for SMOKE modeling were generated by Alpine Geophysics through a contract from MARAMA. They are based on version BaseK of the MRPO inventory. The files were downloaded from the MARAMA ftp site **ftp.marama.org** (username mane-vu, password exchange) in May 2006.

2.4.3 Temperature averaging

- The following procedures were used by SMOKE for the temporal and spatial temperature averaging in the calculation of emission factors according to the setting in the mvreg_mrpo_basek.txt file:
    - Spatial averaging: temperatures averaged over all counties that share a common reference county (i.e. Mobile6 input file)

- Temporal averaging: Temporal averaging over the duration of the episode (i.e. the entire month, see introduction) was used, i.e. monthly average temperatures were used to calculate the emission factors.

3. Biogenic Emission Processing

Hourly gridded biogenic emissions for the 12 km and 36 km modeling domains were calculated by BEIS3.12 through SMOKE, using MCIP-processed MM5 fields for temperature ("TA", layer-1 temperature), solar radiation ("RGRND"), surface pressure ("PRES"), and precipitation ("RN" and "RC"). A 'seasonal switch' file was generated by the SMOKE utility metscan to determine whether winter or summer emission factors should be used for any given grid cell on any given day. Winter emission factors are used from January 1st through the date of the last frost and again from the data of the first frost in fall through December 31st. Summer emission factors are used for the time period in between. This calculation is performed separately for each grid cell.

4. Temporal Allocation

4.1 MANE-VU

4.1.1 Area and nonroad sources

- Generated as part of the MANE-VU version 1 inventory
- amptpro.m3.us+can.manevu.030205.txt
- amptref.m3.manevu.012405.txt
- downloaded from **ftp.marama.org** (username mane-vu, password exchange) in January 2005

4.1.2 Mobile sources

- MANEVU_2002_mtpro_02022006_addCT.txt
- MANEVU_2002_mtref_02022006_addCT.txt
- prepared by PECHAN and NESCAUM and downloaded from http://bronze.nescaum.org/Private/junghun/MANE-VU/onroad_ver3_update/MANEVU_V3_update.tar

4.1.3 Point Sources

- Based on the same files as for the MANE-VU area and nonroad temporal files listed above, but added the CEM-based 2002 state-specific temporal profiles and cross-references for EGU sources for the MANE-VU states that were generated by VISTAS for their BaseD modeling and obtained in February 2005.
- No CEM-based hour-specific EGU emissions were utilized

4.2 CENRAP

The following temporal profiles and cross-reference files were used:

- Area and nonroad sources:
  - amptpro.m3.us+can.cenrap.010605_incl_nrd.txt
  - amptref.m3.cenrap.010605_add_nh3_and_nrd.txt
- Mobile sources:
  - mtpro.cenrap.v3.txt
  - mtref.cenrap.v3.txt
- Point sources:
  - ptpro.{QQ}.cenrap_egus_cem.00-03avg.121205.txt where {QQ} is Q1 for January/February/March, Q2 for April/May/June, etc.
  - ptref.{QQ}.cenrap_egus_cem.00-03avg.121205.txt where {QQ} is Q1 for January/February/March, Q2 for April/May/June, etc.
- All files were downloaded from the CENRAP ftp site in March 2006.

4.3 VISTAS

The following month-specific temporal profiles and cross-reference files were used:

- Area and nonroad sources:
  - atpro_vistas_basef_15jul05.txt
  - atref_vistas_basef_15jul05.txt
- Mobile sources:
  - mtpro_vistas_basef_04jul05.txt
  - mtref_us_can_vistas_basef_04jul05.txt
- Point sources:
  - ptpro_typ_{MMM}_vistasg_28jun2006.txt where {MMM} is jan, feb, mar, etc.
  - ptref_typ_vistas_baseg_28jun2006.txt
- These files were obtained from the Alpine Geophysics ftp site. They reflect version BaseG of the VISTAS inventory for the point source allocation files and version BaseF for the area, nonroad, and mobile source allocation files. These files were downloaded between February and July, 2006.

4.4 MRPO

The following month-specific temporal profiles and cross-reference files were used for all source categories:

- amptpro_typ_us_can_{MMM}_vistas_27nov04.txt where {MMM} is jan, feb, mar, etc.
- amptref_2002_us_can_vistas_17dec04.txt
- These files were obtained from VISTAS in January 2005 and reflect their BaseD modeling. No updated temporal profiles or cross-reference files were developed for use with the MRPO BaseK inventory.

4.5 Canada

For Canada, the SMOKE2.1 default temporal profiles and cross-reference files (amptpro.m3.us+can.txt and amptref.m3.us+can.txt) were utilized.

5. Speciation

The same speciation profiles (gspro.cmaq.cb4p25.txt) and cross-references (gsref.cmaq.cb4p25.txt) were utilized for all regions and all source categories. Different versions of these files were obtained (SMOKE2.1 default, EPA-CAIR modeling, VISTAS, CENRAP and MANE-VU) and compared. After comparing the creation dates and header lines of these files, it was determined that the EPA-CAIR and MANE-VU files had the most recent updates, and consequently the final speciation profile and cross-reference files used for all regions and source categories was based on the EPA-CAIR files with the addition of MANE-VU specific updates.

6. Spatial Allocation

6.1 U.S.

The spatial surrogates for the 12km domain were extracted from the national grid 12km U.S. gridding surrogates posted at EPA's website at
http://www.epa.gov/ttn/chief/emch/spatial/newsurrogate.html
The gridding cross-references were also obtained from this website, but for the processing of MANE-VU area source emissions, MANE-VU specific cross-reference entries posted on the MARAMA ftp site were added.

6.2 Canada

The spatial surrogates for Canadian emissions for the 12km domain were extracted from the national grid 12km Canadian gridding surrogates posted at EPA's website at
http://www.epa.gov/ttn/chief/emch/spatial/newsurrogate.html
The gridding cross-references were also obtained from this website.

Reference:

Pechan: (2006) Technical Support document for 2002 MANE-VU SIP Modeling inventories, version 3. Prepared by E. H. Pechan & Associates, Inc. 3622 Lyckan Parkway, Suite 2005, Durham, NC 27707.

TSD-1d

8-h Ozone modeling using the SMOKE/CMAQ system

Bureau of Air Quality Analysis and Research

Division of Air Resources

New York State Department of Environmental Conservation

Albany, NY 12233

February 1, 2006

Air Quality Modeling Domain

The modeling domain utilized in this application represented a sub-set of the inter-RPO's continental modeling domain that covered the entire 48-state region with emphasis on the Ozone Transport Region. The OTC modeling domain at 12km horizontal mesh is displayed in Figure 1 is part of the 36km continental domain that is designed to provide boundary conditions (BCs). The particulars of the two modeling domains are:

The 36km domain covered the continental US by a 149 by 129 mesh in the east-west and north-south directions, respectively. The domain is based on Lambert Conformal Projection with the center at (97ºW 40ºN) and parallels at 33ºN and 45ºN. As evident from Figure 1, the 12km domain utilized in this analysis covers most areas of the eastern US and has 172 by 172 mesh in the horizontal. Both domains utilize 22 layers in the vertical extending to about 16km with 16 layers placed within the lower 3km.

Photochemical Modeling -- CMAQ

The CMAQ (version 4.5.1) with CB4 chemistry, aerosol module for $PM_{2.5}$ and RADM cloud scheme was utilized in this study. Photochemical modeling was performed with the CCTM software that is part of the CMAQ modeling package. Version 4.5.1 of this modeling software was obtained from the CMAS modeling center at http://www.cmascenter.org. The following module options were used in compiling the CCTM executable:

- Horizontal advection: yamo
- Vertical advection: yamo
- Horizontal diffusion: multiscale
- Vertical diffusion: eddy
- Plume-in-Grid: non operational
- Gas phase chemical mechanism: CB-4
- Chemical solver: EBI
- Aerosol module: aero3
- Process analysis: non operational

The following computational choices were made during compilation:

- Compiler version: PGI 6.0
- Fortran compiler flags:-Mfixed -Mextend -Bstatic -O2 -module ${MODLOC} -I.
- C compiler flags: -v -O2 -I${MPICH}/include
- IOAPI library: version 3.0
- NETCDF library: version 3.6.0
- Parallel processing library version: mpich 1.2.6
- Static compilation on 32-bit system

The following choices were made for running the executable:

- Number of processors: 8
- Domain decomposition for parallel processing: 4 columns, 2 rows
- Number of species written to the layer-1 hourly-average concentration output (ACONC) file: 39 (O3, NO, CO, NO2, HNO3, N2O5, HONO, PNA, PAN, NTR, NH3, SO2, FORM, ALD2, PAR, OLE, ETH, TOL, XYL, ISOP, ASO4I, ASO4J, ANO3I, ANO3J, ANH4I, ANH4J, AORGAI, AORGAJ, AORGPAI, AORGPAJ, AORGBI, AORGBJ, AECI, AECJ, A25I, A25J, ACORS, ASEAS, ASOIL)
- Each daily simulation was performed for 24 hours starting at 05:00 GMT (00:00 EST)

The following postprocessing steps were performed using utility tools from the "ioapi" software package obtained from http://www.baronams.com/products/ioapi/AA.html#tools:

- Extract and combine the following species for each hour for the first 16 model layers from the full 3-D instantaneous concentration output file: O3, CO, NO, NO2, NOY_1 (*=NO + NO2 + PAN + HNO3*), NOY_2 (*=NO + NO2 + PAN + HNO3 + HONO + N2O5 + NO3 + PNA + NTR*), HOX (*=OH + HO2*), VOC (*=2*ALD2 + 2*ETH + FORM + 5*ISOP + 2*OLE + PAR + 7*TOL + 8*XYL*), ISOP, PM2.5 (*=ASO4I + ASO4J + ANO3I + ANO3J + ANH4I + ANH4J + AORGAI + AORGAJ + 1.167*AORGPAI + 1.167*AORGPAJ + AORGBI + AORGBJ + AECI + AECJ + A25I + A25J*), PM_SULF (*=ASO4I + ASO4J*), PM_NITR (*=ANO3I + ANO3J*), PM_AMM (*=ANH4I + ANH4J*), PM_ORG_SA (*=AORGAI + AORGAJ*), PM_ORG_PA (*=1.167*AORGPAI + 1.167*AORGPAJ*), PM_ORG_SB(*=AORGBI + AORGBJ*), PM_ORG_TOT (*=AORGAI + AORGAJ + 1.167*AORGPAI + 1.167*AORGPAJ + AORGBI + AORGBJ*), PM_EC (*=AECI + AECJ*), PM_OTH (*=A25I + A25J*), PM_COARS (*=ACORS + ASEAS + ASOIL*), SO2, HNO3, NH3, H2O2
- Extract all species for all model layers for the last hour of each daily instantaneous concentration output file to enable "hot" restarts of modeling simulations
- Create daily files of hourly running-average 8-hr ozone concentrations with time stamps assigned to the first hour of the averaging interval

The following files are archived on LTO2 computer tapes (each tape holds approximately 200 Gb of data) for each day:

- Aerosol/visibility file
- Layer-1 hourly-average concentration output file (contains 39 species)
- Dry deposition file
- Wet deposition file
- Extracted 16-layer species file
- Restart file (last hour of full 3-D instantaneous concentration file)
- Hourly 8-hr concentration file

Photolysis Rates

One of the inputs to CMAQ is the photolysis rates. In this study, photolysis rate lookup tables were generated for each day of 2002 with the JPROC software that is part of the CMAQ modeling package. This software was obtained from the CMAS modeling center at http://www.cmascenter.org. Rather than using climatological ozone column data, daily ozone column measurements from the NASA Earthprobe TOMS instrument were downloaded from ftp://toms.gsfc.nasa.gov/pub/eptoms/data/ozone/Y2002/ and used as input to the JPROC processor. It should be noted that TOMS data were missing for the time period from August 3 – 11, 2002. The missing period was filled as follows-- TOMS data file for August 2 was used as JPROC input for August 3rd through August 7th, and the TOMS data file for August 12th was used as JPROC input for August 8th through August 11th.

Boundary Conditions (BCs)

The boundary conditions for the 12km grid were extracted from the 36km CMAQ simulation. The 36km simulation utilized boundary conditions that were based on a one-way nest approach to GEOS-CHEM global model outputs (Moon and Byun 2004, Baker 2005). As stated above, the intent of the 36km CMAQ simulation was to provide the BCs for the 12km model that would be more reflective of the emissions and meteorology rather than to use either clean or arbitrary pollutant fields. Also, in this study the CMAQ simulations utilized a 15-day ramp-up period, thereby minimizing the propagation of the boundary fields into the areas of concern. A report on the setup and application of the 36km CMAQ and the extraction of the BCs is available from NYSDEC.

Meteorological data

The meteorological data for this study was based on MM5 modeling (see Meteorological Modeling, 2007). The MM5 fields are then processed by MCIP version 3.0, a utility available as part of the CCTM software from CMAS Modeling Center (see http://www.cmascenter.org) to provide CMAQ model-ready inputs.

Emissions

The emissions data for 2002 were generated by individual states within the OTR and were assembled and processed through the Mid Atlantic Northeast Visibility Union (MANE-VU), a Regional Planning Organization (RPO). These emissions were then processed by NYSDEC using SMOKE processor to provide CMAQ compatible inputs (Anthro-Emissions 2006). The 2002 emissions for the non-OTR areas within the modeling domain were obtained from the corresponding RPOs and were processed using SMOKE, in a manner similar to that of the OTR.emissions. Details of this processing are outlined in the report (Pechan 2007), and the hourly biogenic emissions (Bio-Emissions, 2006)

CMAQ simulations

CMAQ simulations were performed using the one-way nesting approach in which we perform the continental CMAQ simulation at 36km grid spacing. For this simulation we utilized clean initial conditions with boundary conditions extracted from the simulation of GEOS-CHEM global chemical model. The interface program used in this application was developed by University of Huston (Moon and Byun 2004), which was applied to obtain hourly 36km boundary concentrations from GEOS-CHEM outputs. The CMAQ 36km simulation was initiated from December 15, 2001 with the first 15 days as spin up period and terminated on December 31, 2002. The simulation utilized the 2002 emissions data available from the RPOs and 2002 MM5 meteorological fields developed by the University of Maryland (TSD-1a). The hourly boundary fields for the 12km CMAQ domain were obtained by application of BCON program to the 3-D concentration fields generated by the 36km CMAQ simulation.

The 12km simulations for both base and future year were assigned the boundary conditions based on the 36km CMAQ simulation and clean initial conditions. The simulation period covered was from April 15 through September 30, with the first 15 days of April set as ramp-up or spin-up period and that only data from May 1 through September 30 were used in the analysis. Details on CMAQ setup and run scripts are available from NYSDEC.

References

Baker, K.: (2005) http://www.ladco.org/tech/photo/present/ozone.pdf

Moon, N. and D. Byun: (2004) A simple user's guide for "geos2cmaq"code: Linking CMAQ with GEOS-CHEM. Version 1.0. Institute for Multidimensional Air quality Studies (IMAQS), University of Houston, Houston TX.

Meteorological Modeling: (2007) Meteorological Modeling using Penn State/NCAR 5th Generation Mesoscale Model (MM5). TSD-1a

Pechan: (2006) Technical Support document for 2002 MANE-VU SIP Modeling inventories, version 3. Prepared by E. H. Pechan & Associates, Inc. 3622 Lyckan Parkway, Suite 2005, Durham, NC 27707.

Bio-Emissions: (2006) Processing of Biogenic Emissions for OTC/MANE-VU Modeling. TSD-1b

Anthro-Emissions: (2006) Emission Processing for the Revised 2002 OTC Regional and Urban 12 km Base Case Simulations. TSD-1c

Figure 1 Display of 36- and 12km air quality modeling domains.

Appendix F-11

CMAQ Configuration

Table F-11-1. OTC CMAQ Air Quality Model Configuration

Science Options	Configuration	Details/Comments
Model	CMAQ Version 4.5	
Horizontal Grid Mesh	36km/12km	
36-km grid	145x102 cells	
12-km grid	172x172 cells	
Vertical Grid Mesh	22 Layers	
Grid Interaction	One-way nesting	
Boundary Conditions	GEOS-CHEM	
Emissions		
Baseline Emissions Processing	SMOKE (Version 2.1) model configuration	MM5 meteorology input to SMOKE & CMAQ
Sub-grid-scale Plumes	No Plume –in-Grid (PinG)	
Chemistry		
Gas Phase Chemistry	CBM-IV	
Aerosol Chemistry	AE3/ISORROPIA	
Secondary Organic Aerosols	Secondary Organic Aerosol Model (SORGAM)	
Aerosol Mass Conservation Patch	Yes	Schell et. al., (2001)
Cloud Chemistry	RADM-type aqueous chemistry	Includes sub-grid cloud processes
N_2O_5 Reaction Probability	0.01-0.001	
Meteorological Processor	MCIP Version 3.0	
Horizontal Transport		
Eddy Diffusivity Scheme	K-theory with Kh grid size dependence	Multi-scale Smagorinsky (1963) approach
Vertical Transport		
Eddy Diffusivity Scheme	K-theory	
Diffusivity Lower Limit	Kzmin = 1.0	
Planetary Boundary Layer	No Patch	
Deposition Scheme	M3dry	Directly linked to Pleim-Xiu Land Surface Model parameters
Numerics		
Gas Phase Chemistry Solver	Euler Backward Iterative (EBI) solver	Hertel et. Al. (1993) EBI solver ~2x faster than MEBI
Horizontal Advection Scheme	Piecewise Parabolic Method (PPM) scheme	
Simulation Periods	2002	
Platform	Linux Cluster	

Table F-11-1. OTC CMAQ Air Quality Model Configuration

Science Options	Configuration	Details/Comments
Model	CMAQ Version 4.5	
Horizontal Grid Mesh	36km/12km	
36-km grid	145x102 cells	
12-km grid	172x172 cells	
Vertical Grid Mesh	22 Layers	
Grid Interaction	One-way nesting	
Boundary Conditions	GEOS-CHEM	
Emissions		
Baseline Emissions Processing	SMOKE (Version 2.1) model configuration	MM5 meteorology input to SMOKE & CMAQ
Sub-grid-scale Plumes	No Plume –in-Grid (PinG)	
Chemistry		
Gas Phase Chemistry	CBM-IV	
Aerosol Chemistry	AE3/ISORROPIA	
Secondary Organic Aerosols	Secondary Organic Aerosol Model (SORGAM)	
Aerosol Mass Conservation Patch	Yes	Schell et. al., (2001)
Cloud Chemistry	RADM-type aqueous chemistry	Includes sub-grid cloud processes
N_2O_5 Reaction Probability	0.01-0.001	
Meteorological Processor	MCIP Version 3.0	
Horizontal Transport		
Eddy Diffusivity Scheme	K-theory with Kh grid size dependence	Multi-scale Smagorinsky (1963) approach
Vertical Transport		
Eddy Diffusivity Scheme	K-theory	
Diffusivity Lower Limit	Kzmin = 1.0	
Planetary Boundary Layer	No Patch	
Deposition Scheme	M3dry	Directly linked to Pleim-Xiu Land Surface Model parameters
Numerics		
Gas Phase Chemistry Solver	Euler Backward Iterative (EBI) solver	Hertel et. Al. (1993) EBI solver ~2x faster than MEBI
Horizontal Advection Scheme	Piecewise Parabolic Method (PPM) scheme	
Simulation Periods	2002	
Platform	Linux Cluster	